

WAITE INSTITUTE  
9.7.90  
LIBRARY

INVESTIGATIONS OF FERRICRETES AND WEATHERED ZONES  
IN PARTS OF SOUTHERN AND SOUTHEASTERN  
AUSTRALIA - A REASSESSMENT OF  
THE 'LATERITE' CONCEPT

ROBERT P. BOURMAN

B.A. (Hons), M.A., Dip. Ed., Dip.T.

Submitted in fulfilment of the  
requirements for the degree of

**Doctor of Philosophy**

in the  
Department of Soil Science,  
Waite Agricultural Research Institute,  
University of Adelaide.

Submitted: May, 1989.

**" Only by prolonged and rigorous attention to the processes involved in the formation of the different forms of laterite, and by precise definition of the end products of such processes, will any real progress be made in the perplexing study of laterite."**

**Paton and Williams (1972)**

## TABLE OF CONTENTS

	Page
<b>Table of Contents</b>	<b>i.</b>
<b>List of Figures</b>	<b>vii.</b>
<b>List of Plates</b>	<b>ix.</b>
<b>List of Tables</b>	<b>xiv.</b>
<b>Abstract</b>	<b>xvi.</b>
<b>Statement of originality</b>	<b>xix.</b>
<b>Acknowledgements</b>	<b>xx.</b>
<b>Published papers submitted in support of the Degree</b>	<b>xxi.</b>
<b>CHAPTER 1: AIMS, TERMINOLOGY, METHODOLOGY, CLASSIFICATION AND AGE INDICATORS.</b>	
1.1 Introduction	1
1.2 Background	3
1.3 Aims	5
1.4 Terminology	6
1.5 Classification of ferricretes	8
1.6 Methods	9
1.6.1 Field investigations	9
1.6.2 Laboratory analyses	10
1.6.2.1 X-ray diffraction	10
1.6.2.2 X-ray fluorescence	12
1.6.2.3 Micro-morphology	12
1.7 Age indicators	12
<b>CHAPTER 2: REGIONAL GEOLOGY, GEOMORPHOLOGY AND CLIMATE OF SOUTHERN SOUTH AUSTRALIA</b>	
2.1 Geology and geomorphology	14
2.1.1 Introduction	14
2.1.2 Precambrian and Cambrian	14
2.1.3 Ordovician to Permian	15
2.1.4 Permian	15
2.1.5 Mesozoic	16
2.1.6 Tertiary	17
2.1.6.1 Faulting in the Mount Lofty Ranges	18
2.1.7 Quaternary	20
2.2 Climate	21
2.3 Palaeoclimates	22
<b>CHAPTER 3: LITERATURE REVIEW</b>	
3.1 Review of 'Laterite' studies in southern South Australia in relation to the international 'Laterite' literature	25
3.1.1 Introduction	25
3.1.2 General Review of South Australian Literature	25
3.1.3 Detailed Literature Review	29
3.1.3.1 Early Geological Studies	29
3.1.3.2 Pedological studies	31
3.1.3.3 Later Geological Investigations	39
3.1.3.4 Stratigraphic Approach to Investigations of 'Lateritic' Materials	48
3.1.3.5 Geomorphological investigations	52
3.1.4 Summary and Conclusions	63

3.2	Discussion of recent International views on 'Laterite' classification and formation	65
3.2.1	Chemical classification of Schellmann (1981)	65
3.2.2	An Assessment of 'Relative' and 'Absolute' Accumulations	66
3.2.3	'Laterite' formed by Chemical Diffusion	67
3.2.4	Residuum Theory of McFarlane	68
3.2.5	French Workers	69
3.3	Review of the Pathways of Formation and Transformation of Iron and Aluminium Oxides and Oxyhydroxides	70
3.3.1	Iron oxide minerals	71
3.3.1.1	Goethite	71
3.3.1.2	Hematite	72
3.3.1.3	Maghemite	73
3.3.1.4	Green rust	74
3.3.1.5	Lepidocrocite	74
3.3.1.6	Ferrihydrite	75
3.3.2	Aluminium oxide minerals	75
3.3.2.1	Gibbsite	75
3.3.2.2	Boehmite	76
3.3.2.3	Corundum	76

#### CHAPTER 4: FERRUGINOUS AND BLEACHED MATERIALS IN THE MOUNT LOFTY RANGE PROVINCE AND ADJACENT BASINS

4.1	Introduction	77
4.2	The High Level Summit Surface	77
4.2.1	Ferricretes	79
4.2.1.1	Nodular, Pisolitic and Vermiform Ferricretes	79
4.2.1.1.1	Spring Mount-Mount Cone area	79
4.2.1.1.2	Parawa Plateau area	81
4.2.1.1.3	The Summit Surface of Kangaroo Island	82
4.2.1.2	Ferricreted Sediments	85
4.2.1.2.1	Glen Shera Plateau	85
4.2.1.2.2	Cut Hill Road, Kangarilla	86
4.2.1.2.3	Knott Hill	87
4.2.1.2.4	Parawirra	87
4.2.1.2.5	Humbug Scrub	87
4.2.1.3	Ferricreted Bedrock	88
4.2.1.4	Slabby ferricretes	88
4.2.1.4.1	Chandlers Hill	88
4.2.1.5	Vesicular to Massive Ferricretes	90
4.2.1.5.1	Peeralilla Hill	90
4.2.1.5.2	Anstey Hill Iron Mine	92
4.2.1.5.3	Kangaroo Island summit surface	93
4.2.1.5.4	Almanda Hill	93
4.2.2	Ferruginised Channel Fill Materials	94
4.2.2.1	Mount Desert area	94
4.2.2.2	Pottery Road	96
4.2.2.3	Clarendon-Kangarilla Road Cut	96
4.2.2.4	Chapel Hill, near Echunga.	98
4.2.2.5	Blackwood Rail Cutting	98
4.2.3	Ferruginised Bedrock Mottled Zones	100
4.2.3.1	Range Road Cuttings near Willunga Hill	100
4.2.3.2	Mottled zone on Willunga Hill	101
4.2.3.3	Other summit surface localities in S. M. L. Ranges	101
4.2.3.4	Mottled materials in hills near Kapunda	102

4.2.3.5	Upland Surface of the East Mount Lofty Ranges	104
4.2.4	Pisoliths	105
4.2.4.1	Mid North area	106
4.2.5	Bleached Bedrock	107
4.2.5.1	Longwood Quarry	107
4.2.6	Weathered zones beneath the summit surface	108
4.2.6.1	Willunga Hill Borehole	108
4.2.6.2	Parawa Plateau	111
4.2.6.2.1	Chemistry of borehole samples	112
4.2.6.2.2	Mineralogy of borehole samples	114
4.2.6.2.3	Summary and Discussion	116
4.3	Lower Level Landsurfaces marked by Ferricretes, Pisoliths and other Ferruginised Weathered Zones	119
4.3.1	Ferricretes	119
4.3.1.1	Vermiform and Pisolitic Ferricretes	119
4.3.1.1.1	The Mount Taylor Plain	119
4.3.1.1.2	Cape Borda	123
4.3.1.2	Ferricreted Sediments	123
4.3.1.2.1	Green Hills Surface	123
4.3.1.2.2	Waitpinga area	124
4.3.1.2.3	Upper Hindmarsh Valley & Myponga Basin	126
4.3.1.2.4	Yundi road cutting	127
4.3.1.2.5	Tookayerta Toposequences	128
4.3.1.2.6	Tookayerta Quarry	129
4.3.1.2.7	Finniss Quarry	130
4.3.1.2.8	The Gun Emplacement	130
4.3.2.2.9	The Bremer Valley	136
4.3.2.2.9.1	'Lucernbrae' Ferricrete	137
4.3.2.2.9.2	Ferricrete down valley from the Early Miocene shoreline	139
4.3.2.2.9.3	The Compton Conglomerate	140
4.3.1.3	Vesicular Ferricrete	141
4.3.1.3.1	Mount Compass bog iron ore deposits	141
4.3.1.3.2	Kangaroo Island	141
4.3.2	Mottled Zones	141
4.3.2.1	Willunga Scarp Bench	141
4.3.2.2	Happy Valley Reservoir Overflow Channel	144
4.3.3	Pisoliths	146
4.3.3.1	Waitpinga area	146
4.3.3.2	The basalt surface of the Gap Hills	146
4.3.3.3	Cape Borda	148
4.4	Ferruginised Materials from Basins within and marginal to the Ranges	149
4.4.1	Downfaulted Mottled and Weathered Permian Sediments in coastal cliffs near Kingscote, Kangaroo Island	151
4.4.2	Pleistocene Sediments	156
4.4.2.1	Mottled 'Kurrajong' Formation sediments	156
4.4.2.1.1	Sellicks Creek	157
4.4.2.1.2	Other scarp foot environments	157
4.4.2.2	Hallett Cove	157
4.4.2.3	Redbanks, Mid North	158
4.4.2.4	Bow Hill, Murray Basin	158
4.4.2.5	Ochre Cove/Ochre Point	159
4.4.2.6	Kangaroo Island	160

4.4.3	Conclusion	163
4.5	Recent and Continuing Iron Mobility	163
4.5.1	Fisherman Bay	163
4.5.2	Boinkas of the Murray Basin	164
4.5.3	Mount Compass 'Coffee Rock'	165
4.5.4	Kangaroo Island	166
4.6	Age of the summit surface and its associated 'laterite'	168
4.6.1	Mid North area	168
4.6.2	Kangaroo Island	169
4.6.3	South Mount Lofty Ranges	169
4.6.4	Oxygen isotope analyses	170
4.6.5	Discussion	171
4.7	Conclusions	171
CHAPTER 5: A SYNTHESIS OF GENERALISATIONS DERIVED FROM INVESTIGATIONS OF FERRICRETES AND OTHER FERRUGINOUS AND WEATHERED MATERIALS		
5.1	Introduction	174
5.2	Categories of Ferricretes	174
5.3	Macroscopic and mesoscopic features of ferricretes	176
5.3.1	Ferricreted bedrock	176
5.3.2	Ferricreted sediments	176
5.3.2.1	Ferricreted clastic sediments	176
5.3.2.2	Ferricreted organic sediments	176
5.3.2.3	<i>In situ</i> oxidation of 'primary' iron-rich minerals	176
5.3.3	Complex ferricretes	177
5.3.3.1	Pisolitic ferricretes	177
5.3.3.2	Nodular ferricretes	177
5.3.3.3	Slabby ferricretes	177
5.3.3.4	Vermiform ferricretes	177
5.4	Bulk Chemistry of Ferricrete Categories and Types	177
5.5	Bulk Mineralogy of Ferricrete Categories and Types	178
5.6	Reconstructed Environments during Ferricrete Formation	179
5.6.1	Ferruginised bedrock (ferricretes and mottled bedrock)	179
5.6.2	Ferricreted sediments	181
5.6.2.1	Ferricreted clastic sediments	181
5.6.2.2	Ferricreted organic sediments	182
5.6.3	Complex Ferricretes	183
5.6.3.1	Pisolitic ferricrete	183
5.6.3.1.1	Pisoliths	184
5.6.3.1.2	Origin of maghemitic pisoliths	187
5.6.3.1.3	Heating experiments	189
5.6.3.2	Nodular ferricrete	190
5.6.3.3	Slabby ferricrete	191
5.6.3.4	Vermiform Ferricrete	192
5.7	Modern Iron Oxide Mobility	194
5.8	Conclusions	195

## CHAPTER 6: FERRICRETES, IRON-MOTTLED AND WEATHERED MATERIALS ON EYRE PENINSULA.

6.1	Introduction	197
6.2	Previous Investigations	197
6.3	Investigations of this thesis	198
6.3.1	Northern Eyre Peninsula	198
6.3.1.1	Summit surface sites	198
6.3.1.1.1	Weathered and iron-mottled profiles	198
6.3.1.1.1.1	Blue Range	198
6.3.1.1.1.2	Glenville Etch Surface	199
6.3.2	Low Level Weathered and Iron Mottled Zones	200
6.3.2.1	The Corrobinnie Depression	200
6.3.2.2	Weathering on Mount Cooper	206
6.3.2.3	Point Labatt	206
6.4	Southern Eyre Peninsula	207
6.4.1	Weathered and Mottled Bedrock Zones	207
6.4.1.1	Coastal Cliffs at Sleaford Bay	207
6.4.1.2	Quarry near railway crossing on Sleaford Mere	208
6.4.1.3	Lincoln Highway several km north of Tumby Bay	209
6.4.1.4	Quarry north of Koppio in the Tod River Valley	209
6.4.1.5	Road Cutting on Flinders Highway W. of Pt Lincoln	210
6.4.1.6	Road cutting on Tumby Bay - Cummins Road	210
6.4.1.7	Cutting east of tower on Tumby Bay-Cummins road	212
6.4.2	Pisolitic and Nodular Ferricretes	212
6.4.2.1	Quarry north of Koppio in the Tod River Valley	213
6.4.2.2	Vanilla Conservation Park	214
6.4.2.3	Tod River Reservoir Road	214
6.4.2.4	Knott Hill	215
6.4.2.5	Yallunda Flat	215
6.4.3	Ferruginised sediments	216
6.4.3.1	Vesicular ferricrete	216
6.4.3.2	Ferricreted sediments in palaeochannel deposits	216
6.5	Discussion and Conclusions	217

## CHAPTER 7: FERRICRETES, FERRUGINOUS AND WEATHERED ZONES OF THE WESTERN OTWAY BASIN

7.1	Introduction	221
7.2	Discussion of various forms of ferruginisation	222
7.2.1	The Dundas 'Laterite'	222
7.2.2	Pebble Point Formation	227
7.2.3	The Compton Conglomerate and equivalents	229
7.2.4	Ferruginisation affecting other materials in Otway Basin	230
7.3	Conclusions	233

## CHAPTER 8: A REAPPRAISAL OF THE SYDNEY 'LATERITES'.

8.1	Introduction	236
8.2	Previous investigations	236
8.3	Investigations of this Thesis	237
8.3.1	Field Relationships	237
8.3.2	Chemistry and Mineralogy	239
8.3.3	Micromorphology	241
8.4	Discussion	243
8.5	Conclusions	248

<b>CHAPTER 9. FERRICRETES WITH ASSOCIATED VOIDAL CONCRETIONS IN THE TELFORD BASIN.</b>		
9.1	Introduction	251
9.2	Geological Background of the Telford Basin	251
9.3	Macromorphology of the Ferricrete Concretions and their Field Relationships	252
9.4	Chemistry and Mineralogy of the Concretions	253
9.5	Ferricrete and Voidal Concretion Formation	253
9.6	Conclusions	257
<b>CHAPTER 10: AN ASSESSMENT OF THE 'LATERITE' CONCEPT</b>		
10.1	Findings Related to Ferricrete Formation from Investigations of this Thesis	259
10.2	Modes of Ferricrete Formation in areas studied	261
10.2.1	Oxidation of pre-existing iron minerals to form ferruginised sediments	261
10.2.2	Ferricretes as detritus	261
10.2.3	Ferricretes formed by the ferruginisation of pre-existing bedrock and sediments	262
10.2.4	Continual weathering and erosion model, preferred for ferricrete formation on the summit surface of Fleurieu Peninsula	263
10.3	Summary and Conclusions	267
	<b>Figures</b>	<b>270</b>
	<b>Plates</b>	<b>330</b>
	<b>Appendices - Tables</b>	<b>384</b>
	<b>References</b>	<b>478</b>

I request that my thesis not be available for photocopying as there are areas of the thesis which have not yet been published.

Photocopying of this theses is ~~allowed~~ unless the author has entered into an official contract with the University embargo-ing the use of this thesis. No such contract has been entered into as at 3 July 1990.

E. RANDVA  
(Authorized Copyright Officer  
- WHITE LIBRARY)



## LIST OF FIGURES

- Figure 1.1 Sketch of 'Normal or standard laterite profile' of Stephens (1946).
- Figure 2.1 Geological map of South Australia.  
 Figure 2.2 Generalised Geological Time Scale (After Barker, 1986)  
 Figure 2.3 Geological provinces of southern South Australia (After Ludbrook, 1980).  
 Figure 2.4 Permian sedimentary basins of South Australia (After Wopfner, 1970).  
 Figure 2.5 Rainfall and temperature maps of South Australia.
- Figure 3.1 Location map of sites discussed in Chapter 3.  
 Figure 3.2 Inset of Figure 3.1, Mount Lofty Ranges.  
 Figure 3.3 Chemical pathways postulated for the formation and transformation of iron oxides (Schwertmann & Taylor, 1987).
- Figure 4.1 Map of distribution of ferricretes studied in the Mount Lofty Ranges.  
 Figure 4.2 Map of distribution of ferricretes studied on Kangaroo Island.  
 Figure 4.3 Schematic cross-section through the South Mount Lofty Ranges showing the relationships of different types of ferricretes to topography and geology.  
 Figure 4.4 Spur-line profile through the Spring Mount-Upper Hindmarsh Valley-Mount Cone area showing relationships of ferricretes to Tertiary limestone.  
 Figure 4.5 Triangular diagram of samples from the Mount Cone-Spring Mount area.  
 Figure 4.6 Triangular diagram of Parawa Plateau and Kangaroo Island summit surface samples.  
 Figure 4.7 Triangular diagram of iron-impregnated sediments from the summit surface.  
 Figure 4.8 Sketch of Chandlers Hill section.  
 Figure 4.9 Triangular diagram of slabby ferricretes.  
 Figure 4.10 Cross section through Peeralilla Hill.  
 Figure 4.11 Triangular diagram of vesicular ferricretes.  
 Figure 4.12 Triangular diagram of Anstey Hill samples.  
 Figure 4.13 Triangular diagram of channel fill and associated materials.  
 Figure 4.14 Triangular diagram of mottled zone samples.  
 Figure 4.15 Triangular diagram of Mid North samples.  
 Figure 4.16 Triangular diagram of East Mount Lofty Ranges samples.  
 Figure 4.17 Triangular diagram of Willunga Hill borehole samples.  
 Figure 4.18 Triangular diagram of Willunga Hill borehole samples with bases.  
 Figure 4.19 Chemical ratios down the Willunga Hill borehole.  
 Figure 4.20 Variations in bulk mineralogy down the Willunga Hill borehole.  
 Figure 4.21 Variations in mineralogy of <2 micron clay fraction down the Willunga Hill borehole.  
 Figure 4.22 Distribution of auger holes on the Parawa Plateau of Fleurieu Peninsula in relationship to bedrock geology.  
 Figure 4.23 Generalised variations in chemistry and mineralogy beneath the Parawa Plateau.  
 Figure 4.24 Section across the Mount Taylor Plain, Kangaroo Island.  
 Figure 4.25 Triangular diagram of samples from the Mount Taylor Plain.  
 Figure 4.26 Cross section through Waitpinga, Green Hills to Upper Hindmarsh Valley (After Bourman, 1973).  
 Figure 4.27 Triangular diagram of iron-impregnated clastic sediments.  
 Figure 4.28 Graphs showing variations in chemistry in the toposequences in the Tookayerta Creek valley.  
 Figure 4.29 Map of Bremer valley area showing distribution of ferricretes in relationship to Tertiary limestones.  
 Figure 4.30 Long section through the Bremer valley showing the relationship of ferricretes to Tertiary limestones.  
 Figure 4.31 Triangular diagram of Bremer River valley samples.  
 Figure 4.32 Triangular diagram of samples from the Kingscote cliffs, Kangaroo Island.

### List of Figures (cont.)

- Figure 4.33 Diagram illustrating the lower ages of rocks and sediments affected by mottling, bleaching and diffusely iron-impregnated materials and overlain by ferricretes and pisoliths. Where possible the upper age limits of these features are indicated by arrows.
- Figure 4.34 Location map showing Fishermans Bay and Hatta Lakes.
- Figure 4.35 Geological map of Fishermans Bay area.
- Figure 5.1 Triangular diagram showing three different categories of ferricretes.
- Figure 5.2 Triangular diagram of bulk chemistry of all types of ferricretes.
- Figure 5.3 Triangular diagram showing mean plot of ferricrete types and their ranges.
- Figure 5.4 Triangular plot of of pisolitic ferricretes and individual pisoliths.
- Figure 5.5 Triangular diagram showing variations in ferricrete mineralogy.
- Figure 5.6 Triangular diagram of Schellmann (1981) showing different degrees of 'lateritisation'.
- Figure 6.1 Location map of study sites on Eyre Peninsula.
- Figure 6.2 Triangular diagram of samples from the Blue Range and from the so-called Glenville Etch Surface of Twidale *et al.* (1976).
- Figure 6.3 Triangular diagram of samples from the Corrobinnie Depression (weathered basement rocks and Garford Formation sediments).
- Figure 6.4 Triangular diagram of pisolitic ferricretes from the Corrobinnie Depression.
- Figure 6.5 Triangular diagram of ferricretes from the Corrobinnie Depression.
- Figure 6.6 Triangular diagram of samples from Mount Cooper.
- Figure 6.7 Location map of ferricrete sites studied in southern Eyre Peninsula.
- Figure 6.8 Triangular diagram of samples from the Sleaford Bay area.
- Figure 6.9 Triangular diagram of samples from the Lincoln Highway.
- Figure 6.10 Triangular diagram of samples of weathered and mottled bedrock from the Koppio Quarry site.
- Figure 6.11 Triangular diagram of samples from road cuts on the Tumby Bay-Cummins Road.
- Figure 6.12 Triangular diagram of ferricrete samples from Koppio Quarry site, Tod River Valley, Wanilla Conservation Park, Knott Hill and Yallunda Flat.
- Figure 7.1 Location of the Otway Basin.
- Figure 7.2 Location of sample sites in the western Otway Basin.
- Figure 7.3 Location of sample sites in the Casterton area.
- Figure 7.4 Triangular diagram of samples from the western Otway Basin.
- Figure 8.1 Geology of the Sydney area (After Faniran, 1971).
- Figure 8.2 Location of study sites in the North Sydney area (After Hunt *et al.*, 1977).
- Figure 8.3 Triangular diagram of samples from the North Sydney area.
- Figure 9.1 Location and geology of the Telford Basin.
- Figure 9.2 Triangular diagram of samples from the Telford Basin.
- Figure 10.1 Sketches of 'Standard or normal Laterite Profile' and 'Deep Weathering' with the development of mottled and bleached zones.
- Figure 10.2 Sketches of simple types of ferricretes, showing their environments of formation, macro-morphology, chemistry and mineralogy.
- Figure 10.3 Sketches of simple ferricretes (continued) and sketches of complex types of ferricretes, showing their environments of formation, macro-morphology, chemistry and mineralogy.

## LIST OF PLATES

- Plate 2.1 Reverse fault near Cambrai on the eastern side of the Mount Lofty Ranges, exposed in a scarp foot valley.
- Plate 3.1 Oblique aerial view of Witton Bluff, south of Adelaide.
- Plate 3.2 Contorted and convoluted ferruginous sandstone unit of Pleistocene age in Witton Bluff.
- Plate 4.1 General view of the summit surface of the South Mount Lofty Ranges and the Willunga escarpment looking southeast from near Clarendon.
- Plate 4.2 Vermiform ferricrete showing tubule structures filled with light-coloured clays.
- Plate 4.3 Pisolitic ferricrete illustrating discrete pisoliths set in ferruginous matrix material.
- Plate 4.4 Block of nodular ferricrete, with large nodule right of centre outlined by fracture.
- Plate 4.5 Sectioned boulder of vesicular ferricrete, showing small cavities that were originally filled with clay-rich materials.
- Plate 4.6 Blocks of slabby ferricrete separated by clay-rich material exposed in road cut on Chandlers Hill.
- Plate 4.7 Block of iron oxide-impregnated sandstone.
- Plate 4.8 Bedrock impregnated with iron oxides.
- Plate 4.9 View across the Upper Hindmarsh Valley from Spring Mount northwards towards Mount Cone
- Plate 4.10 Small mesa sporadically capped with nodular ferricrete east of Mount Cone.
- Plate 4.11 Eastward view from Mount Cone of the small mesa sporadically mantled with nodular ferricrete.
- Plate 4.12 Photomicrograph in ordinary light of vermiform ferricrete from the summit surface of Kangaroo Island.
- Plate 4.13 Photomicrograph of vermiform ferricrete from summit surface of Fleurieu Peninsula.
- Plate 4.14 Photomicrograph of vermiform ferricrete showing islands of clay and quartz grains surrounded by interstitial goethite and gibbsite.
- Plate 4.15 Photomicrograph of poorly sorted coarse sandy sediment, in which the sub-angular quartz grains are cemented by a dark ferruginous matrix.
- Plate 4.16 Photomicrograph of quartzose sediment with complex semi-opaque matrix of hematite and clays connecting poorly sorted, angular, shard-like and embayed quartz clasts.
- Plate 4.17 Hematite as small crystals with red internal reflections in incident polarised light.
- Plate 4.18 Photomicrograph of weathered bedrock, showing quartz grains aligned as in a metasandstone with an iron oxide matrix consisting of masses of hematite in yellowish clay and goethite mixture.
- Plate 4.19 Photomicrograph of clay-rich sediments with scattered quartz grains impregnated by iron oxides, which consist of fine equigranular hematite crystallites.
- Plate 4.20 View of scrape on Peeralilla Hill showing ferruginous crust of vesicular ferricrete and light-coloured materials in left foreground that include calcite and barite.
- Plate 4.21 Closer view of ferricrete at Peeralilla Hill showing structures which dip to the south.
- Plate 4.22 Photomicrograph of calcite material underlying ferricrete on Peeralilla Hill.
- Plate 4.23 Photomicrograph of vesicular ferricrete from Mount Compass.
- Plate 4.24 Photomicrograph of vesicular ferricrete from Mount Compass showing presumed organic matter replaced by iron oxides.
- Plate 4.25 Photomicrograph of vesicular ferricrete from Peeralilla Hill (BOU 12) showing linear voids.

### List of Plates (cont.)

- Plate 4.26 Photomicrograph of vesicular ferricrete from Peeralilla Hill, showing cell-like structures.
- Plate 4.27 Palaeochannel on summit surface near Mount Desert cut into weathered and iron mottled Kanmantoo Group metasedimentary rocks and exposed by road construction.
- Plate 4.28 Unconsolidated pisoliths with goethitic rinds occurring on weathered bedrock near Parawa.
- Plate 4.29 Resin impregnated slab of pisolitic ferricrete from the Parawa Plateau.
- Plate 4.30 Hammer head marks contact of base of channel filled with ferruginous detritus and underlying weathered Cambrian metasedimentary rocks.
- Plate 4.31 Resin impregnated slab of channel fill material extracted from above the erosional contact shown in Plate 4.32.
- Plate 4.32 Resin impregnated slab of materials across the contact of the underlying weathered bedrock and the base of the channel fill.
- Plate 4.33 Microphotograph of well-rounded sandstone sediment with a clay matrix partly replaced by iron oxides, particularly along fractures in the matrix.
- Plate 4.34 Section in road cut near Clarendon, showing angular unconformity with ferruginised pebbles, grits and sands of Eocene age overlying weathered and partly kaolinised Precambrian metasiltsstones.
- Plate 4.35 Ferruginised and cross-bedded fluvial North Maslin Sand sediments exposed in a road cutting on the south side of the Onkaparinga Gorge.
- Plate 4.36 Section exposed in the Blackwood railway cutting showing partly weathered Precambrian rocks at the base, which become more intensively weathered and mottled immediately below the unconformity, which is overlain by a sandy sediment with dense hematitic mottles.
- Plate 4.37 Section in road cutting on Range Road near Willunga. Large purplish hematitic mottles occur at the base. Towards the surface the mottles have become isolated and smaller, with goethitic rinds.
- Plate 4.38 Hematitic mottles in Precambrian metasiltsstone bedrock in abandoned road cutting near Willunga Hill.
- Plate 4.39 Photomicrograph of ferruginised bedrock, which displays a metamorphic structure, with angular embayed quartz grains and large unaltered micas.
- Plate 4.40 Photomicrograph of coarse schistose metasediment impregnated with iron oxides.
- Plate 4.41 Hematitic mottled zone in Precambrian bedrock, near Kapunda, Mid North.
- Plate 4.42 Strongly mottled zone in Precambrian bedrock south of Kapunda in Mid North. Mottles are dominantly hematitic and show a vertical orientation.
- Plate 4.43 Photomicrograph of hematitic mottle from weathered bedrock zone south of Kapunda.
- Plate 4.44 Coarsely mottled zone exposed in road cutting near Mount Torrens. Purple coloured iron oxides are hematitic and orange-yellow colours are goethitic.
- Plate 4.45 Bleached and kaolinised Precambrian Aldgate sandstone exposed by quarrying at Longwood.
- Plate 4.46 View south across the Mount Taylor Plain from the summit surface of Kangaroo Island.
- Plate 4.47 Photomicrograph of complex polygenetic pisolith with earlier generation yellow pisoliths with gibbsite rinds, within clast with series of complex laminated rinds.
- Plate 4.48 Complex goethite-rich pisoliths with quartz clasts up to grit size, in clay matrix replaced by iron oxide.
- Plate 4.49 Photomicrograph of a sandy sediment with an intergranular matrix of opaque hematite and goethite.
- Plate 4.50 Photomicrograph of ferruginised quartzose sediment, with large rounded quartz and rock fragments with fine angular and smaller grains cemented with iron oxides.
- Plate 4.51 Road cutting near Yundi, with surface ferricrete dipping below the surface towards the far left of the section.

### List of Plates (cont.)

- Plate 4.52 Photomicrograph of bedded sandy sediment, in which the larger grains are sub-rounded and silt-sized grains angular and shard-like cemented dominantly by goethite with minor hematite.
- Plate 4.53 View to the northeast of ferricrete-capped Gun Emplacement on the margin of the Eden escarpment.
- Plate 4.54 Variably iron-stained and bleached sediments of possible Eocene age, which underlie the Gun Emplacement.
- Plate 4.55 Sandy sediments underlying the Gun Emplacement containing clasts of quartz and small ferruginous pisoliths and fragments.
- Plate 4.56 Northwestern edge of Gun Emplacement showing goethite-impregnated sands with pisolith structures overlain by fanglomerate material displaying dominantly hematite-rich mottles.
- Plate 4.57 View of the Bremer scarp looking east from Mount Barker.
- Plate 4.58 Bench on the Willunga escarpment at approximately 160 m asl underlain by mottled sandy sediments.
- Plate 4.59 Section approximately 4 m deep exposed in the overflow channel of the Happy Valley reservoir. Tertiary sediments with goethitic mottles are overlain by a dark grey to black Vertisol.
- Plate 4.60 Road cutting on the Victor Harbor-Cape Jervis road west of the Waitpinga road, exposing pisoliths at a depth of about 1 m in sandy sediments.
- Plate 4.61 Photomicrograph of former aeolian sandy sediment impregnated with iron oxides (dominantly goethite).
- Plate 4.62 Photomicrograph of matrix material shown in Plate 4.63, illustrating colloform structures developed by the successive pulses of iron oxides into the intergranular spaces.
- Plate 4.63 Contact between Jurassic basalt and underlying bleached Permian glaciogene sediments in the Old Government Quarry, Kingscote, Kangaroo Island.
- Plate 4.64 Ferruginous mottles in sea cliff eroded in Permian glaciogene sediments near jetty, Kingscote, Kangaroo Island.
- Plate 4.65 Structure at the cliff base near the Kingscote jetty with an alunite core and a rim of iron oxides.
- Plate 4.66 Convoluted ferricrete in coastal cliff at Kingscote, formed by the iron oxide-impregnation of Permian ice-contact glaciogene sediments.
- Plate 4.67 Close-up of clay clasts incorporated into sandy sediments in a pro-glacial environment.
- Plate 4.68 Photomicrograph of ferruginised Eocene limestone.
- Plate 4.69 Photomicrograph of ferruginised Eocene limestone.
- Plate 4.70 Eroding mottled zone in Pleistocene sediments at Hallett Cove, forming a lag of ferruginous clasts at the surface.
- Plate 4.71 Section of mottled Pleistocene sediments at Redbanks on the Light River, Mid North.
- Plate 4.72 Variably weathered and ferruginised Precambrian basement rocks of Brachina Formation overlain by Pliocene and Pleistocene sediments at Ochre Cove.
- Plate 4.73 Road cutting near 'Yorke Farm' on the Kingscote-Penneshaw road. Weakly iron-mottled sandy sediments occur at the base of the section, succeeded by a carbonate-rich horizon on which the modern soil with ferruginous pisoliths occur.
- Plate 4.74 View of ferruginous Pleistocene sediments exposed in the coastal cliffs at Redbanks, Kangaroo Island.
- Plate 4.75 View of peritidal environment at Fishery Bay. Calcareous Pleistocene sediments (cliff) and iron oxide precipitation (foreground).
- Plate 4.76 Spodosol with well developed pipy Bh and BHir horizons, with a deeper Bhir horizon (placic horizon or 'coffee rock') and a pronounced bleached A2 - horizon exposed in sand quarry near Mount Compass.
- Plate 4.77 Photomicrograph of spodic horizon at Mount Compass.
- Plate 4.78 Saline seepage zone in the Middle River catchment area, Kangaroo Island. Ferrihydrite has precipitated at the sites of piezometers.
- Plate 4.79 Photomicrograph of core of incipient pisolith in seepage zone of Tin Hut Creek.

### List of Plates (cont.)

- Plate 5.1 Pronounced undulating stoneline of ferruginous pisoliths at the top of the B-horizon in a soil profile near Craighburn in the Mount Lofty Ranges.
- Plate 5.2 Photomicrograph of intergranular void between skeleton quartz veins in a ferruginised sediment.
- Plate 5.3 Photomicrograph of portions of two complex pisoliths.
- Plate 5.4 Photomicrograph of pisolith with core of ferruginised metasandstone.
- Plate 5.5 Photomicrograph of pisolith consisting of alternating but irregular bands of quartz grains and iron oxides.
- Plate 5.6 Vermiform ferricrete in 'Laterite Quarry' near Ione, California, showing a pronounced horizontal orientation.
- 
- Plate 6.1 Profile showing calcareous earth overlain by red soil with ferruginous pisoliths on the Blue Range, Eyre Peninsula.
- Plate 6.2 General view from Mount Nield of area mapped as Glenville etch surface by Twidale *et al.* (1976).
- Plate 6.3 Weathered and bleached Precambrian gneissic bedrock with coarse hematitic mottles in the Corrobinnie Depression, overlain by weathered and ferruginised Eocene sediments of the Garford Formation.
- Plate 6.4 Closer view of hardened dense mottles shown in Plate 6.3.
- Plate 6.5 Closer view of section exposed in the weathered and ferruginised Garford Formation sediments shown in Plate 6.3.
- Plate 6.6 Ferricrete crust at top of section shown in Plate 6.5, showing voids in crust, some of which are occupied by light-coloured clay-rich materials.
- Plate 6.7 Ferricrete (BOU 573) formed in claypan near Pinjarra dam in the Corrobinnie Depression.
- Plate 6.8 Bleached weathering profile preserved on Mount Cooper, a granitic inselberg in western Eyre Peninsula.
- Plate 6.9 Bleached and mottled gneissic bedrock exposed in the lowest 4 m of the coastal cliffs at Point Labatt, Eyre Peninsula.
- Plate 6.10 Weathered, bleached and iron-mottled Precambrian rocks exposed in coastal cliffs at Sleaford.
- Plate 6.11 Accumulation of ferruginous pisoliths in small channel cut in weathered Precambrian basement rocks in coastal cliffs at Sleaford Bay.
- Plate 6.12 Surface lag of ferruginous pisoliths above weathered Precambrian bedrock at Sleaford Bay.
- Plate 6.13 Pisolitic ferricrete overlying weathered and iron-stained basement rocks in coastal cliffs at Sleaford Bay.
- Plate 6.14 Mottled and bleached boulders of sandstone and grit on the Lincoln Highway.
- Plate 6.15 Quarry in light-coloured, weathered and slightly iron-stained bedrock in the Tod River valley near Koppio, Eyre Peninsula.
- Plate 6.16 Intricately iron-stained kaolinised bedrock exposed in quarry shown in Plate 6.15.
- Plate 6.17 Mottled, bleached and weathered bedrock overlain by and impregnated with calcium carbonate.
- Plate 6.18 Weathered, bleached and iron-mottled Precambrian bedrock exposed by a road cut on the Tumby Bay-Cummins road.
- Plate 6.19 Ferruginised channel fill material occupying palaeochannel cut in underlying weathered and mottled basement rocks in the same area as Plate 6.18.
- Plate 6.20 Yellow soil containing ferricrete fragments on the flank of Knott Hill.
- Plate 6.21 Pisolitic ferricrete at Yallunda Flat, Eyre Peninsula.
- Plate 6.22 Strongly ferruginised fluvial sediments occupying palaeochannel eroded in weathered and bleached Precambrian basement rocks near Yallunda Flat.

### List of Plates (cont.)

- Plate 7.1 Headwall of landslide on southern edge of 'Noss Mesa' at 150 m asl, near Casterton.
- Plate 7.2 Landslide headwall on the northern margin of "Noss Mesa" near Casterton, revealing bleached and mottled zone overlain by the modern soil profile.
- Plate 7.3 Photomicrograph of massive ferricrete (BOU 201) shown in Plate 7.1.
- Plate 7.4 Photomicrograph of mottle (BOU 208) from the section illustrated in Plate 7.2.
- Plate 7.5 Section at Killara Bluff: bleached Late Cretaceous Otway Group metasediments overlain by ferruginised Pebble Point Formation.
- Plate 7.6 Close-up view of ferruginous rhizomorphs formed towards the base of the Pebble Point Formation.
- Plate 7.7 Compton Conglomerate of Oligocene age exposed in Allen's Quarry near Mount Gambier.
- Plate 7.8 Photomicrograph of ferruginised quartzose sediment from Coleraine.
- Plate 7.9 Photomicrograph illustrating crystals of iron oxides in a clay matrix.
- Plate 7.10 Weathered zone exposed by road cut in the partly ferruginised Hamilton basalt near Branhholme, Victoria.
- Plate 7.11 Photomicrograph of pisolith formed from weathering and erosion of the Hamilton basalt.
- 
- Plate 8.1 Photograph of Site 1 at Terrey Hills quarry. Hematitic pisoliths with no surface rinds overlain by hematite-rich pisoliths with pronounced goethitic rinds.
- Plate 8.2 Photograph of Site 2, Terrey Hills quarry, where mottled and vermiform ferricrete is overlain by pisoliths.
- Plate 8.3 Close view of vermiform ferricrete at base of section shown in Plate 8.2.
- Plate 8.4 Photograph and sketch of section examined at Site 3 in Terrey Hills quarry.
- Plate 8.5 Photograph and sketch of section at Site 4 in the Terrey Hills quarry.
- Plate 8.6 Photograph and sketch of section exposed at Site 5 in Terrey Hills quarry.
- Plate 8.7 Photograph of indurated detrital ferricrete containing boulders and clasts of varying characters.
- Plate 8.8 Boulder of vesicular ferricrete incorporated into detrital ferricrete.
- Plate 8.9 Unconformity between detrital ferricrete and *in situ* Hawkesbury Sandstone exposed in road cutting on the Mona Vale road.
- Plate 8.10 Bedrock structures in the Hawkesbury Sandstone in road cutting in the Ku-ring-gai Chase National Park.
- Plate 8.11 Hawkesbury Sandstone with bed desilicified and weathered.
- Plate 8.12 Ferruginous and magnetic clasts lying on the ground surface in Ku-ring-gai Chase National Park.
- Plate 8.13 Section exposed in Terrey Hills quarry illustrating modern soil overlying what appears to be an older lithified soil.
- Plate 8.14 Photomicrograph of the complex rind of a pisolith incorporating zones of laminated microcrystalline brown goethite and yellowish gibbsite, lenses of quartz clasts and concentric fractures lined with opaque maghemite.
- Plate 8.15 Photomicrograph of complex pisolith in polarised incident light, showing details of outer zone of rind of pisolith.
- Plate 8.16 Ferrihydrite precipitated in drainage ditch in Ku-ring-gai Chase National Park.
- 
- Plate 9.1 One of a series of cuestas formed by differential erosion of ferricrete with associated voidal concretions in the Telford Basin.
- Plate 9.2 Voidal concretion approximately 30 cm across showing layers dominantly of hematite, goethite and lepidocrocite.
- Plate 9.3 Concretion broken open to reveal a clay core.
- Plate 9.4 *In situ* concretion with core closely packed with clays and gypsum.
- Plate 9.5 Skin of secondary iron oxides around core of unweathered sideritic siltstone in Upper Series overburden beds
- Plate 9.6 Concretion with outer layer of dark-coloured hematite, intermediate layer of yellow-orange iron oxides and core of partly weathered sideritic siltstone.

### LIST OF TABLES

Table	3.1	Ferruginous and bleached weathering zones and palaeosols (Firman, 1981).
Table	4.1	Chemistry and mineralogy of samples from Mount Cone area.
Table	4.2	Chemistry and mineralogy of samples from Spring Mount area.
Table	4.3	Chemistry and mineralogy of samples of summit surface (Parawa and Kangaroo Island).
Table	4.4	Chemistry and mineralogy of samples of summit surface iron-impregnated sediments.
Table	4.5	Chemistry and mineralogy of samples of ferruginised bedrock (Mid North) and slabby ferricretes (Chandlers Hill).
Table	4.6	Chemistry and mineralogy of samples of Peeralilla Hill (Sandy clays and vesicular ferricretes) and Mt Compass (vesicular ferricrete).
Table	4.7	Chemistry and mineralogy of samples from Anstey Hill iron mine.
Table	4.8	Chemistry and mineralogy of samples of summit surface vesicular ferricretes.
Table	4.9	Chemistry and mineralogy of samples from summit surface palaeochannels
Table	4.10	Chemistry and mineralogy of samples from palaeochannels.
Table	4.11	Chemistry and mineralogy of samples of Tertiary sediments.
Table	4.12	Chemistry and mineralogy of samples of mottled zones, Range Road.
Table	4.13	Chemistry and mineralogy of samples of Mount Lofty Range Province bedrock mottled zones.
Table	4.14	Chemistry and mineralogy of samples of mottled zones in the Kapunda area.
Table	4.15	Chemistry and mineralogy of samples from the Mid North (Black Hill area).
Table	4.16	Chemistry and mineralogy of samples from the East Mt Lofty Ranges.
Table	4.17	Chemistry and mineralogy of samples from the North M.L.Ranges (pisoliths), Longwood (bleached bedrock) and Para Reservoir (hematitic quartzite).
Table	4.18	Chemistry of samples from the Willunga Hill borehole.
Table	4.19	Ratios of Fe/Ti, Fe/Al, Si/Al and K/Al; Willunga Hill Borehole.
Table	4.20	Chemistry and mineralogy of unweathered bedrock samples underlying the Parawa Plateau.
Tables	4.21-4.50	Chemistry and mineralogy of Parawa Plateau Boreholes RBA-1 to RBA-30.
Table	4.51	Chemistry and mineralogy of samples from the Mount Taylor Plain area.
Table	4.52	Chemistry and mineralogy of samples of ferruginised quartzose sediments from the Green Hills area.
Table	4.53	Chemistry and mineralogy of samples of ferruginised quartzose sediments from the Waitpinga Creek area.
Table	4.54	Chemistry and mineralogy of samples of ferruginised quartzose sediments and vesicular ferricrete from the Waitpinga Beach area.
Table	4.55	Chemistry and mineralogy of samples of ferruginised quartzose sediments from lower level surfaces in the Mount Lofty Ranges.
Table	4.56	Chemistry and mineralogy of samples of ferruginous quartzose clastic sediments of the Tookayerta toposequences.
Table	4.57	Chemistry and mineralogy of ferruginised glaciogene sediments from the Tookayerta and Finnis quarries.
Table	4.58	Chemistry and mineralogy of ferruginised sediments from the Gun Emplacement.
Table	4.59	Chemistry and mineralogy of samples from the Bremer Valley.
Table	4.60	Chemistry and mineralogy of samples of mottled sediments.
Table	4.61	Chemistry and mineralogy of samples of low level pisoliths.
Table	4.62	Stratigraphy of weathered, ferruginised and bleached materials.
Table	4.63	Chemistry and mineralogy of samples from the Kingscote Cliffs (K.Is.).
Table	4.64	Chemistry and mineralogy of samples from the Kingscote Cliffs (K. Is.).
Table	4.65	Chemistry and mineralogy of samples of iron-mottled and bleached Pleistocene sediments.
Table	4.66	Chemistry and mineralogy of samples of ferruginous mottles from Pleistocene sediments in scarp foot positions.
Table	4.67	Chemistry and mineralogy of samples from Ochre Cove and Ochre Point.
Table	4.68	Chemistry and mineralogy of samples from the Ochre Cove/Ochre Point area.



### List of Tables (cont.)

- Table 4.69 Chemistry and mineralogy of samples of Pleistocene sediments from Kangaroo Island.
- Table 4.70 Chemistry and mineralogy of samples of iron-impregnated Holocene sediments.
- Table 4.71 Chemistry and mineralogy of samples of modern iron precipitates.
- Table 5.1 Classification of ferricretes.
- Table 5.2 Mean chemical analyses (XRF) of major ferricrete types.
- Table 5.3 Chemistry and mineralogy of samples of pisoliths, vermiform and pisolitic ferricretes.
- Table 6.1 Chemistry and mineralogy of samples from the Blue Range, Eyre Peninsula.
- Table 6.2 Chemistry and mineralogy of samples from the 'Glenville Etch Surface', Eyre Peninsula.
- Table 6.3 Chemistry and mineralogy of samples (Corrobinnie Depression) of unweathered, bleached & mottled gneissic bedrock.
- Table 6.4 Chemistry and mineralogy of samples (Corrobinnie Depression) of Garford Formation (bleached and mottled materials).
- Table 6.5 Chemistry and mineralogy of samples (Corrobinnie Depression) of ferricretes on the Garford Formation.
- Table 6.6 Chemistry and mineralogy of lacustrine ferricretes (Corrobinnie Depression).
- Table 6.7 Chemistry and mineralogy of pisolitic ferricretes (Corrobinnie Depression).
- Table 6.8 Chemistry and mineralogy of pisolitic ferricretes ( Corrobinnie Depression).
- Table 6.9 Chemistry and mineralogy of weathered samples from Mt Cooper, Eyre Peninsula.
- Table 6.10 Chemistry and mineralogy of mottled bedrock Sleaford area, Eyre Peninsula.
- Table 6.11 Chemistry and mineralogy of pisoliths and pisolitic ferricrete from the Sleaford area, Eyre Peninsula.
- Table 6.12 Chemistry and mineralogy of mottled materials on Lincoln Highway, Eyre Peninsula.
- Table 6.13 Chemistry and mineralogy of samples of weathered, mottled and bleached bedrock from the Koppio Quarry and Flinders Highway.
- Table 6.14 Chemistry and mineralogy of samples of mottled zones from the Tumby Bay-Cummins road cuts.
- Table 6.15 Chemistry and mineralogy of samples from a weathered profile in the Tumby Bay-Cummins Road cut, near tower.
- Table 6.16 Chemistry and mineralogy of samples from the Koppio Quarry area, Eyre Pen.
- Table 6.17 Chemistry and mineralogy of samples of ferricretes from Tod River Valley.
- Table 6.18 Chemistry and mineralogy of samples from Knott Hill and Yallunda Flat, Eyre Peninsula.
- Table 7.1 Chemistry and mineralogy of samples from the Western Otway Basin.
- Table 7.2 Chemistry and mineralogy of samples from the Western Otway Basin.
- Table 7.3 Chemistry and mineralogy of samples from the Western Otway Basin.
- Table 7.4 Chemistry and mineralogy of samples from the Western Otway Basin.
- Table 8.1 Chemistry and mineralogy of samples from the Sydney area.
- Table 8.2 Chemistry and mineralogy of samples from the Sydney area.
- Table 8.3 Chemistry and mineralogy of samples from the Sydney area.
- Table 8.4 Chemistry and mineralogy of samples from the Sydney area.
- Table 9.1 Chemistry and mineralogy of samples from the Telford Basin.

## ABSTRACT

A review of the local literature on materials described as 'lateritic' in southern South Australia reveals much confusion about the identification, nature, age and formation of 'laterite'. However, the pedogenic model of the 'normal laterite profile' (Stephens, 1946), with genetically associated horizons of 'laterite', mottled and pallid zones, has dominated interpretations of 'lateritic' materials. According to this model 'laterite' developed on 'peneplain' surfaces in the Tertiary, under humid tropical climates, both through downward leaching and upward movement of dissolved iron and aluminium oxides, by capillarity and associated fluctuating water tables. There have been few attempts to apply alternative models of 'laterite' formation, such as those involving landscape downwasting.

This thesis investigates 'laterite' (here termed 'ferricrete'), and weathered, mottled and bleached zones of the regolith, by utilising a multi-faceted approach that involved field investigations of the relationships of these to each other, to geology, geomorphology, topography, pedology, and where possible, to hydrology. Laboratory work on samples of the ferricretes and associated materials was undertaken to determine their chemical and mineralogical compositions and micromorphological characteristics.

The major area of study has been the South Mount Lofty Ranges, both on the mainland and Kangaroo Island, where three major types of ferricretes were identified, namely, ferricreted bedrock, ferricreted sediments, which include both clastic quartzose sediments and organic materials (vesicular ferricrete), and ferricretes of complex sedimentary and pedogenic origins. Among the complex types several varieties have been noted that include pisolitic, nodular, slabby and vermiform ferricretes. Laboratory analyses of these different varieties of ferricretes allow them to be distinguished on the combined bases of bulk chemical and mineralogical composition and degree of aluminium substitution in the crystal structure of goethite, which is the most common iron oxide in the ferricretes studied. These factors probably reflect environmental conditions during their formation and subsequent transformations. These findings are generally supported by micromorphological and limited microprobe studies as well as by considerations of synthesis experiments on the pathways of formation of iron and aluminium oxides as reported in the literature.

Ferricretes in the areas studied all appear to be younger than the immediately underlying 'companion materials' of Stephens (1971), rather than being of the same age and monogenetically related to them. Diverse forms of ferricrete appear to have developed in different environments through the operation of a range of processes. For example, some ferricretes have formed by the *in situ* weathering transformation of pre-existing minerals such as siderite, pyrite and glauconite to secondary iron oxides such as goethite, hematite and lepidocrocite. Some other ferricretes developed as a result of the accumulation and iron oxide cementation of iron-rich materials such as pisoliths and fragments of mottles, transported into relatively low topographic points. Other types have formed by the precipitation of ferrous iron from solutions, dominantly forming goethite, filling voids or replacing interclast clays in pre-existing porous clastic and/or organic sediments. Such ferricretes formed in localities such as low angle valley sides, valley bottoms and swamp, lacustrine or peritidal environments.

So-called 'laterite profiles' are typically incomplete vertically, and there is no convincing evidence for the former existence of extensive and continuous ferricretes over 'peneplained' surfaces in the regions studied. Here, weathering and erosion appear to have affected a landscape of greater relief than the equivalent modern landscape, with salients of resistant bedrock protruding above differentially weathered and ferruginised undulating landsurfaces. Some profiles are actually sedimentary sequences, which might simulate the 'normal laterite profile', and some include calcareous horizons and channel fill deposits that demonstrate multigenetic origins for the profiles. Many profiles lack ferricrete crusts, and this was widely interpreted in the past as evidence for truncation of the profile, but the view expressed here is that the crust may never have been present. Under some conditions, lags of hardened mottles accumulated at the surface during landscape downwasting and have been indurated to form a ferricrete younger than the underlying weathered and mottled material. Many alleged fossil bleached sandy 'lateritic' A-horizons are actually modern soils or the result of aeolian activity.

Chemical analyses of both surface and sub-surface samples of mottled zone materials suggest that the mottles developed by the weathering of bedrock under the influence of ground water, leading to the release of iron from the bedrock and its concentration as hematite in mottles, probably via the mineral, ferrihydrite. Some borehole data suggest that weathering has led to the detailed and local concentration of iron oxides, but has not resulted in massive vertical translocations of iron oxides.

There is limited evidence for the *in situ* formation of pisoliths in the study area; the majority of them are interpreted to have developed by the breakdown, transport and pedogenetic modification of former ferricretes and/or ferruginous mottles. Even where there is evidence of sub-surface *in situ* pisolith formation, pisoliths at the surface have distinctively different physical, mineralogical and chemical characteristics. Bushfires are important in influencing these changes.

Evidence from the Mount Lofty Ranges suggests that there are similar types of ferricretes on both upland and lower level surfaces. Particularly on the latter they can be dated relatively with respect to rocks and sediments of known ages. In some cases the occurrence of ferricretes has facilitated better palaeogeographic reconstructions as some represent iron oxide-impregnated sandy Tertiary shoreline sediments, preserved well above the level of the associated submarine fossiliferous limestones. Consequently, the locations of these palaeoshorelines can be determined more precisely. Rocks and sediments ranging in age from the Precambrian to the Holocene display different degrees of weathering and ferruginisation, suggesting iron mobilisation and precipitation over immense periods of geological time up to and including the present. These data confirm the interpretation of weathered zones and ferricretes as complex polygenetic features, developed and modified over long spans of time, and cannot simply be interpreted in terms of inheritance from discrete ancient weathering events of short duration. Consequently it is impossible to generalise with respect to a particular time of 'lateritisation', or to associate ferricretes unequivocally with past humid tropical climates. The character of any ferricrete reflects the integrated effects of continual weathering and erosional processes, active to the present day, so that the preservation of ancient pristine ferricretes in the current landscape is unlikely.

The findings generated from investigations in the Mount Lofty Ranges were tested and extended by studies on Eyre Peninsula, the western Otway Basin, the North Sydney area and in the Telford Basin of the Flinders Ranges. In many cases re-interpretations of previous studies by other workers in these areas have been made.

**This thesis contains no material which has been accepted for the award of any other degree or diploma in any University and to the best of the candidate's knowledge and belief, the thesis contains no material previously published or written by another person, except where due reference is made in the text of the thesis**

**Signed:**

**Robert P. Bourman**

## ACKNOWLEDGEMENTS

I wish to express my sincere gratitude to my supervisors, Dr. Tony Milnes and Professor Malcolm Oades for their guidance, assistance and encouragement in carrying out this research.

Special thanks go to the Soils Division of CSIRO at Adelaide for access to laboratory facilities, where the majority of the analytical work was carried out. In particular I would like to thank Dr. Keith Norrish, Dr. Rob Fitzpatrick and Dr. Reg Taylor for discussions on various aspects of the study. John Pickering and Graham Riley (CSIRO Soils) provided guidance in the initial stages of XRD work, as did Dr. David Lewis (Waite Institute), and Heinz Konczalla (CSIRO Soils) prepared some of the thin sections. Dr. Neville Alley, Dr. Colin Murray-Wallace and Sally Phillips provided some of the samples for analysis, and Neville Alley and Dr. Nick Harvey commented on the text of the thesis.

John Keeling and Greg Drew of the S.A. Department of Mines and Energy provided samples from drilling programs and access to field sites respectively.

Mr G.C. Thorpe of Kangarilla Drilling Pty Ltd provided samples from a borehole on the plateau surface near Willunga.

Malcolm Wright (CSIRO Soils Division) provided valuable assistance on soil descriptions and classification.

John Coppi (CSIRO) and Derek Lambert (SACAE) assisted with their photographic expertise, and Michael Tscharke and Judy Laing drafted many of the diagrams.

I am indebted to my employer, the SACAE for allowing me to carry out the project, and to Samantha for her continued good humour, interest, encouragement and support.

**Published papers in support of the Degree**

BOURMAN, R.P., MILNES, A.R. & OADES, J.M. (1987): Investigations of ferricretes and related surficial ferruginous materials in parts of southern and eastern Australia. *Z.Geomorph. N.F. Suppl.-Bd.* 64: 1-24.

MILNES, A.R., R.P. BOURMAN & R.W. FITZPATRICK (1987): Petrology and mineralogy of 'laterites' in southern and eastern Australia and South Africa. *Chemical Geology.* 60: 237-250.

MILNES, A.R., R.P. BOURMAN & K.H. NORTHCOTE (1985): Field relationships of ferricretes and weathered zones in southern South Australia: a contribution to 'laterite' studies in Australia. *Aust. J. Soil Res.* 23: 441-465.

## CHAPTER 1: AIMS, TERMINOLOGY, METHODOLOGY CLASSIFICATION AND AGE INDICATORS.

### 1.1 Introduction

Duricrusts such as silcretes, calcretes and ferricretes have long been of interest to pedologists, as they commonly form parts of soil profiles; and to geomorphologists and geologists, primarily because of their perceived roles in landscape reconstruction as morpho- and pedo-stratigraphic markers, and as ostensible indicators of climatically controlled pedological and geomorphic processes. However, until the nature and origin of these duricrusts are better understood, many of the conclusions drawn from these investigations must remain speculative. The diversity of scientific disciplinary groups operating from different points of view has so far failed to provide acceptable solutions to many of the problems related to the origins and ages of duricrusts. In many instances the special interests and purposes of the investigators have influenced the resulting interpretations.

Ferruginous duricrusts have commonly been referred to as 'laterite' in the global literature, and this custom persists (e.g. Ogura, 1987; Herbillon & Nahon, 1987; McFarlane, 1987) despite calls by some for the abandonment of the term, especially as 'laterite' has been applied to such a diverse range of indurated and unconsolidated materials (Hemming, 1968). There have been many reviews of the extensive literature on 'laterite', including those of Prescott & Pendleton (1952), Alexander & Cady (1962), Sivarajasingham *et al.* (1962), Maignen (1966), Faniran (1969), Paton & Williams (1972) and McFarlane (1976). The paper by Paton & Williams (1972) is particularly significant in that it questions many of the long held views about the nature of 'laterite' and the conditions of its formation. In particular, they considered that a tropical climate is not necessary for 'laterite' to form, that pedogenic 'laterite' is younger than the weathered rock beneath it, that the influence of lithology and relief on weathering may be more important than climate and so they concluded that relic 'laterites' are poor palaeoclimatic indicators.

Furthermore, they concluded that the use of 'laterite' as a morphostratigraphic marker is suspect. However, this work appears to have been largely ignored. For example, an overview of the majority of papers presented at Lateritisation Processes Conferences in India at Trivandrum in 1979, Brazil (Melfi &



Carvalho, 1983), and Tokyo (Ogura, 1987) and the First International Conference on Geomorphology at Manchester (McFarlane, 1987) suggests that most workers consider 'laterites' to be the products of chemical weathering of rocks on planation surfaces in tropical environments (30° N to 30° S) and that where they occur beyond these limits, there are implications of climatic change and/or continental drift.

It also appears that there has been too much emphasis on attempts to define 'laterite' at the expense of detailed and systematic investigations of weathered and ferruginised materials, independently of perceptions coloured by the traditional views concerning their nature and conditions of formation. In a recent endeavour to define 'laterites', Schellmann (1981) regarded them as the 'products of intense subaerial rock weathering, the Fe- and/or Al-contents of which are higher than in merely kaolinised parent rocks'. He suggested that they consist predominantly of kaolinite, goethite, hematite, gibbsite and quartz. Furthermore, he presented a triangular diagram with  $\text{Fe}_2\text{O}_3$ ,  $\text{Al}_2\text{O}_3$  and  $\text{SiO}_2$  at the apices to illustrate the progressive 'lateritisation' of different types of rocks on the basis of their chemical compositions. This approach led Banerji (1981) to conclude that if a material does not display "incongruent dissolution of kaolinite to gibbsite", then it cannot be called 'laterite'. On this criterion, he commented that huge expanses of 'ferruginous duricrust' in West Africa should not be regarded as 'laterite'. However, there are various inadequacies in the scheme proposed by Schellmann (1981), which will be discussed later in this thesis. Moreover, the view expressed by Banerji (1981) has not been adopted by the vast majority of workers studying 'laterite' (M.J. McFarlane - *pers. comm.*). Aleva (1983) attempted to describe and classify the wide range of structural features, textures, void geometry, and coatings on 'lateritic' materials, using non-genetic terms, to provide IGCP-129 with a means of communicating on 'laterite' textures. However, many of his terms were genetic, which was one of the reasons why they were not adopted (M.J. McFarlane - *pers. comm.*).

Recently studies have been undertaken to date 'laterites' in Australia and elsewhere using palaeomagnetic techniques (e.g. Schmidt & Embleton, 1976; Idnurm & Senior, 1978; Schmidt *et al.*, 1976) and these studies tend to support concepts of distinct periods of climatically controlled regional 'lateritisation'.

Some of the results have considerable error ranges, however. For example, the Canaway Profile in Queensland was dated at  $30 \text{ Ma} \pm 15 \text{ Ma}$  (Idnurm & Senior, 1978). Moreover, the results are not always reliable, sometimes displaying conflicts with stratigraphic evidence.

The vast majority of studies on 'laterite' emphasise only one approach to their investigation, which often leads to unreliable conclusions and highlights the need for integrated interdisciplinary investigations. In this thesis 'ferricretes', commonly referred to in the local and international literature as 'laterites', are investigated by a multi-faceted approach that involves geologic, stratigraphic, geomorphic, hydrologic and pedologic field studies integrated with laboratory investigations incorporating micromorphological, mineralogical, chemical and micro-chemical analyses of samples.

## 1.2 Background

Regolith materials commonly referred to as 'laterite' in southern South Australia have long been recognised throughout parts of the Mount Lofty Ranges, Kangaroo Island and Eyre Peninsula (See Fig. 3.1). A review of previous studies related to these materials, is detailed in Chapter 3, and reveals the following points:-

- \* Confusion and lack of consistency about the nature of materials called 'laterite', these varying from superficially iron-stained sediments, without associated profile differentiation, to iron-mottled and kaolinised bedrock with associated profile differentiation.
- \* A lack of clear definition by many workers with respect to what they mean by the term 'laterite'.
- \* An implied or specified association of 'laterite' with 'deep weathering' by most previous workers.
- \* An absence of detailed and systematic studies. Many have been merely coincidental to other geological investigations, and others have been very broad scale geomorphic reports that involved inter-regional correlations based on the use of 'laterite' as morpho-stratigraphic markers and indicators as palaeosols.
- \* The shackling effect on landscape interpretation of the model of the 'normal laterite profile', which implies the original occurrence of a complete profile including ferruginous, mottled and pallid materials

having developed by the *in situ* weathering of regolith materials. The absence of ferruginous and/or mottled zones has been explained by various degrees of truncation of an original and complete profile.

- \* The association of 'laterite' development with humid, tropical conditions on 'peneplains' close to base level (sea level). These implied associations have often led to the use of circular arguments relating climate, topography and 'laterite'. Thus the present distribution of 'lateritic materials' on upland areas has been explained by the dissection of formerly continuous 'laterite' after disruption and uplift by faulting.
- \* Very few studies involving detailed chemical, mineralogical and micromorphological analyses.
- \* The recognition of different types of 'lateritic' fabrics, but with no discussion on their significance.
- \* Suggestions of the age of 'laterite' formation varying from the Mesozoic to the present.
- \* Quite unwarranted correlations of 'lateritic' materials between remotely spaced locations, based on relatively superficial observations such as the shape, size and colour of iron oxide mottles.
- \* The unreliability of palaeomagnetic data and other age dating associations such as palaeoclimatology (e.g. McGowran, 1979a; 1979b) in demonstrating the timing of 'lateritisation'.
- \* The promulgation of the view that 'laterite' of great antiquity persists in pristine form in the contemporary regolith.

Nevertheless, there have been some innovative works of their time related to 'laterite' and landscape evolution including those of Teale (1918), Fenner (1930), Glaessner (1953b), Bauer (1959), Lang (1965), Wopfner (1972a) and Alley (1977) (See Chapter 3).

In view of the historical background of studies on 'laterite' in southern South Australia it was decided to carry out detailed field studies investigating vertical and lateral variations in weathering profiles and ferruginous crusts with respect to topography, hydrology, geology and stratigraphy. Within this region there is a considerable variety of ferruginous materials that occur in different parts of the landscape, and which sometimes exhibit specific relationships to rocks and sediments of established ages. Laboratory investigations were

undertaken in order, more fully, to characterise the chemical, mineralogical and micromorphological constitutions of the various 'lateritic' materials.

During investigations of 'ferricrete' in southern South Australia the occasions arose to examine alleged 'laterite profiles' on a 'classic peneplain' in western Victoria, and 'laterites' in the Sydney area of N.S.W., where previous intensive investigations have been carried out. Studies in these two areas provided opportunities to test and extend some of the ideas that had been developed from the enquiries in southern South Australia. Ferricretes from the Triassic Telford Basin of the Flinders Ranges were also investigated as they are markedly different from all other ferricretes encountered, and they contain distinctive voidal concretions.

### 1.3 Aims

The aims of this thesis are:-

- \* To describe the occurrence and field relationships of strongly coloured ferruginous (ferricretes, mottles, pisoliths, nodules, geodes, voidal concretions) and bleached materials, particularly with respect to each other and to their geological and geomorphological settings.
- \* To characterise the chemical and mineralogical compositions of these materials in the laboratory, in order to assess any relationships between their field situations and mineralo-chemical compositions.
- \* To examine the mechanisms of iron redistribution with respect to both the materials themselves, and the broader landscapes in which they occur.
- \* To assess concepts of 'ferricrete' genesis in the light of information about the occurrence, distribution and characteristics of ferruginous and bleached materials and mechanisms of weathering and iron transport. Specifically, to test the validity of the application of the 'Normal laterite profile' to explanations of so-called 'lateritic' materials.

In South Australia, in particular, the concept of the 'Normal/ Classic/ Standard laterite profile' has dominated interpretations of landform and pedogenic development (See details in Chapter 3). The 'standard laterite profile' (Figure 1.1) in South Australia has been used in a narrow genetic sense in that it implies monogenetic *in situ* formation, largely by isovoluminous

weathering, at a particular time on a 'peneplain' surface under humid tropical conditions. Under this view the present distribution of 'lateritic materials' has been explained by the variable dissection of formerly continuous 'laterite' profiles. This particular view of 'laterite' development has been discarded in some parts of the world. However, it has been widely and recently used in South Australia as well as being a favoured model among modern French workers.

Many workers, world wide, have associated the development of ferricretes with 'deep weathering', without specifically stating whether the term refers simply to the physical depth of weathering, to the degree of weathering or to a combination of both. Work carried out for this thesis suggests that many so-called 'deep weathering profiles' in South Australia have been simply leached of iron and still contain many weatherable minerals such as feldspars, micas, barite and calcite, while the clays may include smectite, vermiculite, interstratified clays, and chlorite. If the weathering has been pervasive one should expect the elimination of the weatherable minerals, the domination of the clays by kaolinite and perhaps some evidence of the destruction of kaolinite. There are many problems and hazards associated with using mineralogical criteria in this fashion, but it represents a first approximation of defining 'deep weathering' more precisely.

#### **1.4 Terminology**

The terms 'laterite' and 'laterite profile' have been widely used both in the local and international literature to describe a variety of materials, including the original Buchanan (1807) 'laterite', ferruginous zones in weathering profiles (Stephens, 1946; Connah & Hubble, 1960), complete profiles (Walther, 1915) and ferruginised, mottled and bleached rocks, sediments and soils. Consequently, much confusion has arisen from the use of this term, particularly as it has genetic connotations. It would be impossible to dispose of the term completely, however, as it is so firmly entrenched in the literature as demonstrated at recent international conferences. Furthermore, in review, it is not always possible to use an appropriate substitute term, because authors do not always make clear the nature of the material they describe as 'laterite'.

Some of the other terms that have been used to describe ferruginous materials in southern South Australia include 'ortstein', 'ferruginous duricrust', 'duricrust', 'ironstone', 'indurated zones', 'ironstone gravels' and 'ferricrete'. All may have had particular meanings in the context of the specific investigations in which they were used, but are difficult to transfer out of context.

Problems of terminology have perennially beset studies of 'laterite' (McFarlane & Sombroek, 1984), and these remain unresolved, there being no internationally accepted range of terms to describe 'lateritic' textures and structures. Until there is an accepted international terminology, it is incumbent upon individual workers to provide detailed descriptions and photographs of the materials being studied, and, where possible, associated micromorphological, chemical and mineralogical data. In this thesis, iron-cemented and indurated continuous crusts and horizons are referred to as 'ferricretes' (Lampugh, 1902) without genetic connotations. Iron cemented materials that do not form pronounced indurated crusts and horizons will be referred to as ferruginised materials. Where the term 'laterite' is mentioned in reference to its use by other workers, it will be placed in quotation marks. Iron-depleted and iron-mottled materials will be referred to as bleached and mottled zones respectively. In this thesis, individual ferruginous sub-spherical bodies will be referred to as ooliths (0.25 - 2 mm in diameter) (Pettijohn, 1957), pisoliths (>2 mm - 5 mm), nodules (>5 mm up to 3 cm) and concretions (> 3 cm in diameter). There is no connotation of genesis intended in this terminology, which refers only to size variations.

Throughout this thesis the term 'ferruginous' is used in a general sense to describe materials in which secondary iron oxides are prominent (as opposed to siliceous or calcareous), the presence of which gives a red or rusty colour. It is an umbrella term, which can be used to describe a wide range of materials including ferricretes, pisoliths, nodules, mottles, pipestems, iron-impregnated sediments, sediments comprising iron-rich clasts derived from prior ferricretes or iron-mottled zones mottles, but not necessarily cemented together by iron oxides. It also includes sediments with iron-rich clasts derived from sources such as pyrite, siderite and glauconite. The term 'ferruginised' is used to describe materials that have been impregnated with, and indurated by,

iron oxides, and include ferricretes of various types, indurated ferruginous sediments, mottles, concretions and pisoliths, which do not form continuous crusts.

### 1.5 Classification of ferricretes

Various types of ferricretes have been recognised during the course of this study and these include 'ferricreted bedrock', 'ferricreted sediments' (both distinguished by their parent materials), and 'complex and composite ferricretes', which have a complex parentage.

- i. *Ferricreted bedrock* comprises iron-indurated bedrock and can be recognised as such by the preservation of distinctive metamorphic structures and minerals in the bedrock of the Mount Lofty Range Province specifically, and elsewhere by the preservation of structures in bedrock whether it be metamorphic, sedimentary or igneous in character. The fabric of the ferricrete is the same as that of the original bedrock material, which is commonly more consolidated than sediments.
- ii. *Ferricreted sediments* consist of iron oxide-impregnated and indurated sediments (clastic quartzose and organic sediments). Ferricreted sediments bear unconformable relationships to the underlying bedrock materials. The ferricreted sediments have been subdivided into:
  - a. Ferricreted clastic sediments, such as sands and gravels, display the fabrics of the original sedimentary structures and can include blocks of reworked ferricrete (Detrital ferricrete).
  - b. Ferricreted organic sediments, which consist of organic sediments impregnated by chemically precipitated iron oxides (bog iron ores). Such vesicular to massive ferricretes contain numerous small cavities that are usually filled with clays, but where these have been washed out the small vesicles or voids are very prominent.
  - c. Ferricreted shales. In this case iron- rich sediments containing siderite, glauconite and pyrite have been

weathered *in situ*, giving rise to very distinctive ferricretes with large voidal concretions

- iii. '*Complex and composite ferricretes*' have a complex origin and cannot be assigned to a single parent material. They include the following types:-
- a. Pisolitic ferricrete consists of individual pisoliths, many of which display multiple and complex rinds, cemented together to form a coherent rock-like mass .
  - b. Nodular ferricrete, which is similar to pisolitic ferricrete, except that the individual clasts are larger than pisoliths and rinds are generally thin or absent .
  - c. Slabby ferricrete that consists of horizontally disposed plate-like masses of ferricrete up to several cm thick and separated by clays.
  - d. Vermiform ferricrete, which contains sinuous worm-like channels, often infilled with light coloured clays that contrast strongly with the surrounding iron-rich material, and give a very distinctive character to the ferricrete.

Further detail on the classification of ferricretes is presented in Chapter 5.

## 1.6 Methods

Investigations for this thesis involved roughly equal amounts of field and laboratory work.

### 1.6.1 Field investigations

Where field samples were collected, assessments were made of the site geology, including the nature of the parent materials in which the ferruginous and bleached materials occur, as well as their profile distributions, including soils, and spatial arrangements. Detailed observations were made in road cuttings, quarries and other artificial exposures, wherever possible, and sub-surface samples were obtained from augering and drilling of water bores. In natural landscapes relationships were difficult to determine and observations were often restricted to superficial surface outcrops and float materials. At particular sites, relationships to fossiliferous sediments such as Tertiary limestones were determined. Positions in the landscape, in both relative and



absolute senses were also noted. Attempts were made to sample materials to cover the range of variation at exposures, so that sub-sampling could be carried out in the laboratory if required. After preliminary laboratory analyses some sites were revisited for more detailed sampling. Photographs were taken of sampling sites in the field in order to relate the sample to its field location. Sites investigated have been located by six figure map references on 1:50 000 map sheets for southern South Australia. Where soil profiles were examined in association with ferricretes or other ferruginous materials, they were classified according to the scheme of Northcote *et al.* (1975).

### 1.6.2 Laboratory analyses

Slabs of coherent ferricretes were cut using a diamond saw and the characteristics and relationships of their constituents were noted after examination using a hand lens and/or a binocular microscope to provide initial micromorphological data. All samples were air dried and sub-samples sufficiently large to cover the range of within-sample variation were ground either in a Siebtechnik ring and puck mill, for well indurated samples, or with an agate mortar and pestle, for less indurated samples.

#### 1.6.2.1 X-ray diffraction

The ground powders were pressed on filter paper into aluminium holders to produce randomly oriented powder samples for X-ray diffraction. When only small amounts of sample were available for analysis, acetone slurries of the samples were smeared thinly on the surface of either glass or aluminium plates. Whenever comparisons between samples were made, they were prepared in a uniform fashion. All samples were analysed in a Philips PW/710 diffractometer using cobalt radiation, automatic divergence slits and a graphite monochromator. For the majority of samples analysed, the scan speeds were  $1^{\circ}2\theta$  per minute through an angular range of  $2^{\circ}2\theta$  to  $75^{\circ}2\theta$ . For more detailed investigations much slower rates of  $0.25^{\circ}2\theta$  per minute were used. Mineral identification was carried out using powder diffraction data given in Brindley & Brown (1980) or in the JDPCS Powder Diffraction File cards and books.

For analysis of the clay mineralogy of selected samples, the  $<2$  micron clay fraction was separated following dispersion of 20 gm of the sample in a 10 ml

concentrated sodium hexametaphosphate - sodium hydroxide solution by shaking for 10 minutes. The dispersed sample was placed in a 400 ml measuring cylinder and paddled until suspended. After 16 hours settling at 20° C, 20 ml of suspended sample was drawn off from a point 20 cm below the water surface, to collect the <2 micron clay fraction. The sample was then concentrated by centrifuging, and subsequently sucked under vacuum onto porous ceramic plates, resulting in the accumulation of a thin oriented clay coating. The clay coatings were washed repeatedly with distilled water, saturated with MgCl<sub>2</sub>, washed repeatedly to remove excess chloride, saturated with glycerol and allowed to air dry. These samples were run in the diffractometer through the range from 2° 2θ to 20° 2θ and the clay mineralogy determined using diffraction data (Brindley & Brown, 1980). Cation exchange capacities were also calculated on <2 micron clay fractions sedimented onto ceramic plates and saturated with BaCl<sub>2</sub>. C.E.C's were determined to assist the semi-quantitative calculation of clay mineral abundance (Norrish & Pickering, 1983). Powder X-ray photographs were taken of the residual samples to assess total mineral contents.

Estimations of the relative contents of iron (goethite, hematite and maghemite) and aluminium (gibbsite) oxides and hydroxides in bulk samples of ferricretes were derived from peak intensities of selected characteristic lines on X-ray diffractometer traces. The following lines were chosen to minimise interference effects from overlapping lines:- goethite (110), hematite (110), maghemite (220) and gibbsite (002). The very weak goethite (101) line, which coincides with the hematite (110) line was ignored. However, the main maghemite peak coincides with the hematite (110) line, and where there were high contents of maghemite, the relative proportions of maghemite and hematite were derived by comparison of hematite (012) line (relative intensity 30) with the maghemite (220) line (relative intensity 30). The author is aware that this method of assessing mineral abundance is semi-quantitative at best. However, tests were carried out on various mixtures of synthetic minerals, which suggest that the data have a reasonable degree of acceptability. Moreover, Coventry *et al.* (1983) demonstrated, by comparison with standards, that peak heights, especially where crystallinity varies little, are reliable indicators of mineral abundance when dealing with naturally occurring iron oxides. In samples examined for this thesis, usually the relative iron oxide

contents were quite marked so that the dominant iron oxide could be determined easily. In some cases, the peak areas were compared to determine relative abundances, but invariably for the samples analysed, these corresponded reasonably closely to the peak heights. The degree of aluminium substitution in the goethite structure was calculated using the methods of Norrish & Taylor (1961) and/or Schulze (1984).

#### *1.6.2.2 X-ray fluorescence*

Approximately 1.5 g of the ground samples were placed in ceramic crucibles of known weight, weighed and ignited in a furnace at 1000° C for 60 minutes, after which ignition losses were calculated following cooling in a desiccator and reweighing. 0.28 g of the ignited samples were mixed with 1.5 g of a lithium tetraborate-lanthanum oxide flux, heated in platinum crucibles and fused into glass buttons following the method of Norrish & Hutton (1969). These were placed in a Philips PW 1400 X-ray Spectrometer and analysed for eleven major elements, using algorithms developed by Dr. K. Norrish for correcting for X-ray absorption and interference. In order to make comparisons between samples on the basis of chemical data, the major elements Fe, Si and Al were calculated as oxides and normalised to 100% to allow them to be plotted on triangular composition diagrams.

#### *1.6.2.3 Micro-morphology*

Sub-samples of poorly consolidated materials were impregnated with polyester resin using the techniques of Cent & Brewer (1971). Thin sections were subsequently prepared from these materials and from consolidated samples, using standard techniques. In some cases, polished thin sections were prepared of the same samples for electron-probe microanalysis (Long, 1977). Descriptions of thin sections were made using a general terminology rather than the scheme proposed by Brewer (1964).

### **1.7 Age indicators**

The ages of ferricretes and other ferruginous and weathered materials examined in this thesis are best derived from noting their relationships to each other and to rocks and sediments of known ages. Generally the different phases of iron and aluminium oxides reflect the environments in which they formed, rather than the ages of the ferricrete or ferruginous material.

However, there are some phases, which, in conjunction with other data, may be useful as indicators of relative ages in the study areas. These are discussed at various locations through the thesis.

For example, many of the oldest and most complex ferricretes display higher total iron contents than do similar younger ferricretes and older ferricreted sediments invariably contain higher hematite contents than do equivalent younger ferricretes; hematitic mottles appear to have been largely inherited from previous environments in the zone of water table fluctuation and are currently transforming to goethite under the current weathering conditions; although maghemite can form via a number of mechanisms, strongly maghemitic pisoliths almost certainly formed at or near the surface, under the effects of burning by bushfires, and where they are currently at depth it is implied that they have been transported and buried; and pisoliths with multiple complex rinds and mixed core materials imply a long history of evolution and transport in the landscape.

## CHAPTER 2: REGIONAL GEOLOGY, GEOMORPHOLOGY AND CLIMATE OF SOUTHERN SOUTH AUSTRALIA

### 2.1 Geology and geomorphology

#### 2.1.1 Introduction

A brief resume of the regional geology and geomorphology of southern South Australia is presented here to provide a framework and background for a more detailed examination of ferricrete development. Figure 2.1 is a map of the surface geology of the State prepared by the South Australian Department of Mines and Energy, and is presented here with permission of the Director-General. A generalised geological time scale (Figure 2.2), showing absolute ages is also included.

#### 2.1.2 Precambrian and Cambrian

The main geological provinces of southern South Australia are shown in Figure 2.3. The oldest of these, the Gawler Craton, is an eastern extension of the Westralian Shield, which consists of a complex series of Precambrian crystalline intrusive and extrusive igneous rocks, together with a sequence of variably metamorphosed rocks. The rocks of the stable Gawler Craton are 2700 Ma to 1450 Ma old (Parker *et al.*, 1985), and include the Sleaford Complex, the Hutchison Group, the Corunna Conglomerate and the Pandurra Formation. Inliers of these ancient rocks underlie, and occur within and on the margins of the Adelaide 'Geosyncline', as the Denison, Mt Painter and Willyama Blocks. They also underlie the Cainozoic Eucla, Murray, Otway and Duntroon Basins. The rocks of the Gawler Craton record several orogenic and metamorphic events.

The Adelaide Geosyncline, now occupied by the site of the upland areas of Kangaroo Island and the Mount Lofty and Flinders Ranges, including parts of the Olary Upland, formed in Late Precambrian times (Preiss, 1987). Extensive basaltic extrusions accompanied initial rifting and subsidence. A sedimentary succession in excess of 24 km in thickness, comprising largely shallow water, marine and glaciogenic sediments and derived from the higher areas of the Gawler Craton, accumulated in the gradually subsiding 'geosyncline'. Sedimentation occurred from the Late Precambrian into the Cambrian and included the Burra, Callana, Umberatana, Wilpena (Late Precambrian) and

the Normanville and Kanmantoo (Cambrian) Groups. An unconformity occurs at the base of the Cambrian sequences. The Burra Group includes the Skillogalee Dolomite with well preserved stromatolites, an extensive record of Late Precambrian glaciation (Sturt Tillite) occurs in the Umberatana Group, and the Wilpena Group contains the Ediacara fauna, fossils of soft-bodied organisms. The Cambrian Groups contain trilobites in shales and *Archaeocyatha* in limestones, and the Kanmantoo Group includes sediments deposited as deep sea fans.

During the Delamerian Orogeny (Thomson, 1969) of Late Cambrian and Early Ordovician age (480 - 500 Ma ago), the sediments of the geosyncline were subjected to compressive tectonic forces that resulted in folding, faulting, intrusion of granitic rocks (e.g. Encounter Bay Granites) and variable metamorphism. These forces culminated in the formation of a vast fold mountain range, the Delamerides (Daily *et al.*, 1976), which probably extended into the then juxtaposed Antarctic continent.

### **2.1.3 Ordovician to Permian**

For the next 250 Ma the geological record is sparse, and the area was probably subjected to prolonged erosion, during which the Delamerides were eroded to expose granites that had been emplaced at depths of 10 km (Milnes *et al.*, 1977). Ordovician fossils were recently identified from strata in the Warburton Basin in the north of the state (Cooper, 1986), but Ordovician deposits are unknown in the south. No Devonian sediments have been identified in southern South Australia, but the occurrence of reworked Devonian micro-fossils on Yorke Peninsula (Harris & McGowran, 1971) and beneath the Murray Basin (N.F. Alley - *pers. comm.*) suggests their former presence here.

### **2.1.4 Permian**

The next major geological event was that of extensive glaciation during the Permian, some 270 Ma ago. There is some controversy concerning the nature of the glaciation (Bourman, 1987), but the major direction of ice movement across southern South Australia was from the southeast towards the northwest. Striations on granite at Port Elliot demonstrate that the granite was exposed prior to or during the Permian ice advance (Milnes & Bourman, 1972).

During the Permian, much of South Australia was affected by glacial processes. However, the present distribution of Permian glacial sediments is restricted in the south to the Renmark Trough (underlying the Murray Basin) and the Troubridge Basin, where many surface exposures occur, and to sub-surface occurrences in the Cooper, Arckaringa and Pedirka Basins in the north of the State (Fig. 2.4). Sedimentation at this time occurred largely in intracratonic basins under stable conditions. Late Permian units in these basins include marine shales and freshwater sediments with some coals, reflecting deglacial and post-glacial conditions (Wopfner, 1972b). Permian glacial palaeo-topography can be recognised in places, having been exhumed following uplift and erosion. Glacigenic sediments of the Cape Jervis Beds (Ludbrook, 1967), include lodgement tills, flow tills, ice-contact, fluvio-glacial, glacio-lacustrine and glacio-marine deposits (Alley & Bourman, 1984). The Permian glacial sediments are non-lithified, which suggests that they have never been deeply buried.

### 2.15 Mesozoic

During the Triassic and Jurassic the entire land mass of the State stood above sea level so that only fluvial and lacustrine sediments were deposited. In the north, Wopfner (1972b) suggested that a deeply weathered and kaolinised regolith developed on a senile landscape throughout this time. During the Jurassic, large scale downwarping led to the formation of the major sedimentary basins of South Australia and culminated in the Cretaceous with marine incursions. Coal measures were deposited in several small intramontane basins (Telford, Springfield and Boolcunda Basins) during the Late Triassic to Middle Jurassic in the Flinders Ranges. These freshwater fluvio-lacustrine conditions also favoured the development of sideritic and pyrite-rich horizons within the sediments.

Fluvial Late Jurassic kaolinitic sandstones and conglomerates (Algebuckina Sandstone) were deposited on weathered Permian sediments and Precambrian bedrock on the western margin of the Eromanga Basin. Fluvial sediments of Mesozoic age are not known from the south of the state, but basalts of Jurassic age (Daily *et al.*, 1974) on Kangaroo Island and in the Polda Trough (Milnes *et al.*, 1982) were possibly extruded in response to stresses related to the separation of Australia from Antarctica about 165 Ma ago

(Ludbrook, 1980). Wopfner (1970) suggested that diastrophism in the Permo-Devonian may have been the first indication of the impending separation, which culminated in the Late Jurassic and Cretaceous.

Major Jurassic sedimentation occurred in the Great Artesian Basin in the north of the State, but in the south, Jurassic sediments were restricted to lignitic clays in the Poldia Basin (Harris, 1964). Cretaceous strata occur extensively in the Great Artesian Basin and underlie parts of the Murray and Eucla Basins and the Gambier Embayment in the southern section of the State.

### 2.1.6 Tertiary

Most of the southern part of the State remained above sea level throughout the Mesozoic, when the landsurface was subjected to prolonged weathering and erosion (Milnes *et al.*, 1985). Throughout the Tertiary, reactivated faults resulted in the further uplift of the denuded Delamerides to form the Mount Lofty - Flinders Ranges. Upland areas of the Eyre Peninsula were also uplifted at this time. Compensating subsidence produced the adjacent Murray, St Vincent, Pirie-Torrens and Uley-Wanilla-Cummins Basins and accentuated the Eucla Basin. Initially freshwater sediments were deposited in basins within and marginal to the ranges overlying weathered basement rocks. Later marine sedimentation occurred in the marginal basins.

The Murray Basin is a broad, shallow basin occupied by Tertiary marine sediments and separated from the Gambier Embayment of the Otway Basin by the Padthaway Ridge. There were several marine incursions into the Murray Basin in the Tertiary, reaching a maximum in the Middle Miocene, after which there was a major regression due to tectonic uplift and eustatic sea level changes as ice accumulated in Antarctica. Sediments related to the maximum transgression occur within intramontane basins of the Mount Lofty Ranges such as the Upper Hindmarsh Valley and the Myponga Basin (see Fig. 3.2), and provide evidence of the timing of the tectonic uplift of the ranges (Lindsay, 1986). Parts of the plateau surface of the ranges, particularly on Kangaroo Island, were submerged at the maximum extent of the Miocene seas. A limited marine transgression in the Pliocene resulted in the deposition of marine sediments along the valley of the River Murray.



The succession of Tertiary sediments in the St Vincent Basin is broadly similar to that in the Murray Basin. Terrestrial freshwater sediments (North Maslin Sands) initiated deposition in the Middle Eocene, and these were followed by the marginal marine South Maslin Sands and later marine sediments including the Port Willunga Formation of Late Eocene to Oligocene age. As in the Murray Basin, the marine transgression during the Pliocene was not extensive. The Late Pliocene Hallett Cove Sandstone occurs at levels up to 30 m asl (above sea level) in the St Vincent Basin. Exposures of limestone east of Hallett Cove and up to 100 m asl have been regarded by some workers as equivalent to the Hallett Cove Sandstone (Twidale *et al.*, 1967), but they may be considerably older. Sediments equivalent to the Hallett Cove Sandstone include the Dry Creek Sands. On Kangaroo Island, Milnes *et al.* (1983) recorded an Early Pliocene marginal marine transgression succeeded by a widespread advance of the seas in the Late Pliocene.

The Tertiary was thus a period of considerable geological change as differential and episodic tectonism led to the broad scale development of uplands and plains. Weathered landsurfaces were uplifted, thus initiating dissection and the stripping of previously deposited sediments by streams, which cut gorges and deposited widespread channel and lacustrine sediments throughout the Mount Lofty Ranges and large areas of Eyre Peninsula (Binks & Hooper, 1983). These sediments and events, together with deposits of several marine transgressions, provide opportunities for dating landsurfaces and ferricretes.

#### *2.1.6.1 Faulting in the Mount Lofty Ranges*

There has been considerable debate about the nature and timing of the faulting that is responsible for the basic character of the present Mount Lofty Ranges. Twidale & Bourne (1975a), for example, considered that there is no direct evidence of the time when faulting was initiated in the Mount Lofty Ranges. However, parts of the ranges have been terrestrial environments since the Permian glaciation (Milnes *et al.*, 1985) so that the ranges have been relatively high points for a long time. Furthermore, Glaessner (1953b) provided evidence that lignitic and other Eocene sediments appeared to have had their deposition controlled by pre-existing fault scarps. There is also evidence demonstrating the existence of a pre-Oligocene fault-controlled valley (the Bremer Valley) within the eastern section of the Mount Lofty Ranges (Fig. 4.29). It provided an

avenue for various marine incursions during the Tertiary, so that faulting almost certainly occurred in pre-Oligocene times.

It appears that different faults (see Fig. 4.29) have displayed different degrees of fault activity. For example, the Bremer Fault has probably not been active throughout the Tertiary, and there is minimal displacement of Pleistocene sediments across the site of the Clarendon-Ochre Cove Fault at Ochre Cove (Ward, 1966). Near Hackam the same fault has displaced probable Early Pliocene deposits only a small amount (Stuart, 1969). On the other hand there is clear evidence of dislocated Middle Pleistocene sediments on the Willunga Fault at Sellicks Beach (Campana & Wilson, 1955; May & Bourman, 1984), and on the Milendella Fault (Plate 2.1) on the eastern margin of the Mount Lofty Ranges (Mills, 1965).

Mills (1965) believed that displacement on the Milendella fault since 'pre-Tertiary peneplanation' is of the order of 335-366 m, of which he attributed 250 m to Early Tertiary to Miocene faulting and 60-90 m to Miocene to Pleistocene faulting. Twidale & Bourne (1975a) preferred to explain the occurrence of Tertiary limestone on the eastern margin of the Mount Lofty Ranges, at elevations up to 160 m asl as the result of eustatically controlled high Tertiary sea levels. However, the identification of the distinctive Lower Miocene marine foraminifer, *Lepidocyclina* (Lindsay, 1986) in limestone collected by the author from the Bremer Valley, within the Mount Lofty Ranges, at an elevation of approximately 170 m asl has facilitated the more precise dating of geologic and geomorphic episodes in the Eastern Mount Lofty Ranges. Taking into account the environmental restrictions of *Lepidocyclina*, Lindsay (1986) concluded that there has been minimum uplift of the ranges relative to the Murray Basin (Lindsay & Giles, 1973) of at least 100 m, since the Middle Tertiary, and possibly much more. More recently, Bourman & Lindsay (1989) reported the occurrence of diagnostic foraminifera in samples of limestone dragged up in the fault zone of the Milendella Fault, illustrating that the limestone is from the lower part of the Early Miocene Mannum Formation (about 20 Ma). This determination adds credence to the view of Mills (1965) that the position of the limestone on the escarpment is due to tectonic uplift of 60 - 90 m since the Miocene. Without denying the evidence for eustatic influences in the Tertiary (e.g. Vail & Hardenbol, 1979) it is clear that post Middle Miocene faulting is far more

significant in the evolution of the East Mount Lofty Ranges than suggested by Twidale & Bourne (1975).

The interpretation adopted here is that the Eastern Mount Lofty Ranges were in existence prior to the Tertiary, that there was marked reactivation of uplift in the late Early Miocene, with a cumulative amount of uplift since that time in excess of 100 m. The remainder of the uplift must have occurred prior to that time. This interpretation thus largely accords with that of Mills (1965) except that it envisages a greater period of time over which the post-Early Miocene uplift occurred.

Most investigators have followed the work of Sprigg (1945; 1946) who considered that the Tertiary faults were mainly normal faults occurring along the sites of ancient Palaeozoic thrust faults. However, where there are clear exposures, some of the faults are an expression of compressive forces, such as on the Milendella Fault (Plate 2.1) (Mills, 1965) and on the Clarendon-Ochre Cove Fault (Inset in Fig. 4.29), where it was intersected by tunnelling operations (Gibson, 1963). Furthermore, Glaessner (1953b) presented evidence of flexuring of the Precambrian basement and adjustments in the overlying Tertiary sediments at Sellicks Beach, rather than clear cut faulting, and he attributed the development of the Mount Lofty Ranges to compressive forces, a view favoured by the author.

### **2.1.7 Quaternary**

During the Pleistocene, extensions and retreats of glaciers, mainly in the Northern Hemisphere, were accompanied by glacio-eustatic sea level fluctuations. The earliest Pleistocene marine sediments in the south of the State are the Burnham Limestone and the Point Ellen Formation (Ludbrook, 1983). During the majority of the Pleistocene Period, shorelines stood below modern sea level. However, excursions of up to 6 m above the present shoreline occurred during Late Pleistocene interglacials. The marine Glanville Formation and equivalents are widespread around the coastline of South Australia and indicate the level of the sea during the Last Interglacial some 120 ka ago. During the Pleistocene, calcareous sand dunes were swept inland from the coastline. These dunes were later consolidated to form extensive calcarenites with associated calcretes and palaeosols broadly termed the

Bridgewater Formation. On Eyre Peninsula there is a complex mix of aeolian deposits of diverse ages (Milnes & Ludbrook, 1986), but in the southeast of the state tectonic uplift of the coastal plain has led to the separation of more distinct beach/dune barrier systems (Cook *et al.*, 1976). Subsequent coastal erosion of the consolidated dune complexes has formed spectacular cliffed shorelines on Eyre and Yorke Peninsulas.

Inland large areas of the State were covered by desert sand dunes during this time, when clay pans and salinas also formed. Climatic change, tectonic activity and glacio-eustatic sea level fluctuations resulted in the development of cut-and-fill alluvial sequences along drainage lines and the widespread deposition of terrestrial sediments. Episodic volcanism in the Late Pleistocene and Holocene resulted in the formation of volcanic cones and ash deposits near Mount Gambier in the southeast of the State (Sheard, 1983).

Most recently, the impacts of European settlement on the region have caused changes related to mass movements and fluvial, aeolian and coastal erosion and deposition (Bourman & Harvey, 1986).

## **2.2 Climate**

Often 'laterite' formation has been associated with distinctive seasonally humid tropical climatic regimes and used as a palaeoclimatic indicator. A brief summary of the present climate of South Australia is presented here to provide a background, against which local ferricrete formation and can be assessed. A detailed account of the South Australian climate is presented in Gentilli (1972).

The southern part of South Australia has a 'Mediterranean' type of climate with warm-to-hot, dry summers and cool-to-mild, wet winters (May to August). The majority of rainfall is associated with the eastward passage of unstable, moist airstreams. Occasional thunderstorms in summer also occur. The northern part of the State is affected by semi-arid to arid climatic conditions. Most rainfall here results from summer incursions of moist tropical air, the remnants of tropical cyclones.

The mean annual rainfall of South Australia (Figure 2.5a) shows that the highest rainfall occurs in the far south of the State, with a northward extension of higher rainfall corresponding to the central uplands of the Mount Lofty and Flinders Ranges, which also act as rain-shadows for localities to their east.

Figures 2.5b and 2.5c illustrate the mean annual temperatures for summer (January) and winter (July). Summer temperatures are lowest near the coastline and in the higher altitudes of the ranges. Frosts can occur in many areas of the state in winter, but snowfalls are very rare and are confined mainly to the central uplands.

### 2.3 Palaeoclimates

Evidence for climatic change in southern South Australia is considerable but of variable reliability. Firman (1981) reported pre-Permian remnants of weathering but the vast majority occupy time since the Permian.

During the *Permian* South Australia was affected by climatic conditions that favoured the development and maintenance of extensive glaciation. Following this, Late Permian coal beds in the Cooper Basin have been equated with a temperate to subtropical and moist climate (Daily *et al.*, 1974). This climatic phase was succeeded by aridity during the *Early Triassic* (Wopfner, 1972).

During the *Mesozoic* the Mount Lofty Range Province stood above sea level and was subjected to prolonged weathering and erosion. *Late Triassic to Middle Jurassic* freshwater fluvio-lacustrine sediments containing numerous coal seams were deposited in the Telford, Springfield and Boolcunda Basins of the Flinders Ranges (Parkin, 1953; Playford & Dettmann, 1965; Townsend, 1979). Palynological evidence indicates that some of the coal seams formed in swamps covered by vegetation of low diversity and that climate may have been warm temperate with a variable rainfall regime (Hos, 1977; 1978). *Late Jurassic* lignitic sediments have also been described from the Poldia Basin of Eyre Peninsula (Harris, 1964).

Various lines of evidence including deep sea cores, palaeobotany and foraminifera have been tendered to demonstrate climatic change throughout the Tertiary (Galloway & Kemp, 1981; McGowran, B. (1977, 1979a, 1979b; Kemp,

1981; Alley, 1977; Truswell & Harris, 1982; Lindsay, 1976), although there are many uncertainties and inconsistencies. The following is a general summary of Tertiary climates.

Climates in southern South Australia during the *Early and Middle Eocene*, derived from pollen spectra, appear to have been warm and temperate with a very high rainfall (Alley, 1977). Using marine planktonic faunas, Lindsay (1976) suggested that South Australia experienced warm, if not tropical, climatic phases during the *Middle and Late Eocene, Late Oligocene to early Middle Miocene* and the *Middle Miocene*.

During the *Early Miocene* the seas were warm relative to the present time and the preceding cool *Oligocene* (Galloway & Kemp, 1981) and generally climates were warm and wet (Alley, 1977) until the *Middle Miocene* when temperatures dropped. Temperate rainforest communities dominated the vegetation of coastal South Australia at this time, but grasslands also developed in the *Early Miocene* suggesting seasonality in the rainfall. In the *Late Miocene* temperatures rose to drop dramatically in the *latest Miocene*.

The *Early Pliocene* (5.9 to 4.3 Ma) was marked by warming, with wet conditions and persistent rainfall, followed by marked cooling and subsequent fluctuations throughout the *Late Pliocene* and *Pleistocene*. Lindsay (1976) considered that the *Early and Late Pliocene* were characterised by relatively warm and transgressive conditions. During the *Quaternary* there were numerous climatic fluctuations accompanying glaciation and deglaciation elsewhere in the world. Climate in the *Early and Middle Pleistocene* appears to have been dominantly dry (Galloway & Kemp, 1981), with some relatively moist periods during interglacials.

If one follows the view of Dury (1971) that humid tropical climates are necessary for the development of 'deep lateritic weathering' there are many times during the *Mesozoic* and *Tertiary* when 'lateritisation' may have occurred in southern South Australia. In particular, for middle latitude locations, he favoured the view of 'lateritisation' during the *Eocene* and *Middle Miocene*. However, some other workers (e.g. Paton and Williams, 1971) do not follow the view that 'lateritisation' is intimately related to tropical climates, but

may occur under various climatic regimes given suitable bedrock and drainage conditions. Furthermore, there are almost intractable problems in equating specific weathering profiles with precise climatic periods. After reviewing palaeoclimatic evidence, Twidale (1983) concluded that climatic conditions suitable for duricrusting occurred for at least 60 Ma and possibly for 200 Ma. Palaeomagnetic dating of weathered landsurfaces covers periods of millions of years and the error range of the dating may be so great that it may be more realistic to think in terms of continually operating weathering processes, which may occur more rapidly under certain climatic regimes.

## CHAPTER 3: LITERATURE REVIEW

### 3.1 Review of 'Laterite' studies in southern South Australia in relation to the international 'Laterite' literature

#### 3.1.1 Introduction`

Since the first description of 'laterite' by Buchanan (1807), who regarded it as a geological stratum, many concepts of 'laterite' genesis have been postulated. These include volcanic and marine modes of origin, both of which have been readily dismissed as universal mechanisms of 'laterite' genesis. Other models proposed have involved lacustrine origins (Fermor, 1911), and biological (termite) influences. 'Lake laterites' or chemical deposits of 'bog iron ore' have been described from various areas of the world, including Australia (Christian & Stewart, 1946; Prescott & Pendleton, 1952; White, 1954). Generally termites have been assigned only minor roles in 'laterite' formation, perhaps assisting oxidation of iron oxides (McFarlane, 1976), but some workers such as Machado (1983a, 1983b) are adamant that the Buchanan 'laterite' and associated pisoliths owe their origins to termite activity.

Two basic theories of 'laterite' genesis involving 'laterite' as a precipitate or as a residuum became established. The formation of 'laterite as a precipitate (Maclaren, 1906; Simpson, 1912; Walther, 1915; Campbell, 1917; Woolnough, 1927), involved 'laterite' constituents being introduced in solution, replacing minerals weathered out from the original rock. 'Laterite' formation as a residuum involved the differential mechanical accumulation of hydrated iron and aluminium oxides consequent upon the removal of silica and bases in solution (Holland, 1903). However, many contradictory statements about the genesis of 'laterite' have prevailed throughout the Twentieth Century.

#### 3.1.2 General Review of South Australian Literature

Numerous papers and theses report evidence relevant to understanding the characteristics, ages and origins of ferruginous crusts, ferruginous horizons, mottled zones and 'deep' weathering that in the South Australian literature have rather loosely been called 'laterite'. Different workers have commonly had varying views on the nature of 'laterite' and many generalisations have been drawn from isolated lines of evidence that relate to the timing of weathering and the ages of landsurfaces on which the 'laterites' rest. At times



unwarranted and extensive extrapolations have been made on the assumption that ferruginous crusts and weathering profiles provide reliable morpho-stratigraphic markers. Other arguments have been tendered that relate 'laterite' formation with humid-tropical climates (e.g. McGowran, 1979a).

An attempt has been made to place weathering zones and ferruginous crusts within a stratigraphic framework (e.g. Firman, 1981), but to date there has been no systematic attempt to categorise them utilising chemical and mineralogical data that may provide bases for more reliable identification and correlation.

Three main groups of workers have been involved in 'laterite' studies in South Australia, pedologists, geomorphologists and geologists. The early work on 'laterite' in southern South Australia was carried out by geologists, who regarded 'laterite' as a *rock* and equated it with 'Desert Sandstone' (silcrete) or a series of terrestrial deposits referred to as 'Upland Miocenes'. Following overseas work, which associated 'lateritic crusts' with weathering profiles (Walther, 1889; Maclaren, 1906), this concept was extended to the Australian continent by Simpson (1912) and Walther (1915), who developed some of the descriptive terminology of 'laterite profiles' such as *Fleckenzone* (mottled zone) and *Bleichzone* (pallid zone). At this time the surface indurations of 'laterite' were regarded as efflorescences of iron and aluminium oxides precipitated from evaporated soil solutions brought to the surface by capillarity processes from the underlying water table. A tropical climate with pronounced wet and dry seasons, such as that of Darwin, was considered ideal for the formation of 'laterite' by this mechanism (Walther, 1915). This allegedly resulted in the reversal of soil A and B-horizons, with the surface 'laterite' being the illuvial B-horizon and the underlying iron-depleted clay being the eluvial A-horizon. Thus, this model required the cogenetic formation of the complete 'laterite profile'. Woolnough (1927), who thought that 'laterite' formation required impeded drainage on 'peneplained' surfaces under seasonally dry humid tropical climatic conditions, apparently followed this view.

However, Prescott (1931) questioned the efficacy of capillary uplift from positions deep below the surface and pointed out that the distribution of salt, calcium carbonate and gypsum in soils highlighted the dominance of

downward leaching in soil development, except in waterlogged environments. Thus the view was preferred that podzolisation was the 'normal process of soil formation' in the tropics, and that the 'laterite' horizon represented the illuvial B-horizon of fossil podzols, many orders of magnitude greater than modern soils. Furthermore he considered that the occurrence of 'laterites' in arid areas pointed to their fossil character, rather than to capillary uplift induced by intense evaporation. The iron and aluminium oxides were implied to have derived from the overlying bleached A-horizons, which, in some instances may have provided an insufficient source, as was found in Africa by Du Bois & Jeffrey (1955), who found it necessary to postulate additional inputs of iron from aeolian dust. However, it was not realised that the column of saprolite consumed to yield the residuum could not be adequately assessed without identifying and utilising an appropriate resistant index (McFarlane, 1976). Whitehouse (1940) accepted that the ferruginous zone was originally an illuvial B-horizon of a fossil podzol but considered that on a planation surface there would also be accessions of iron oxides from below, both by upward water table movements and from capillary rise of iron oxides in solution.

Subsequently, in South Australia the majority of work on 'laterite' was undertaken by pedologists. For example, Stephens (1946) stressed the dynamic nature of 'lateritic' materials when he associated the dissection of an original and fossil podzolic 'laterite profile' with pedogenic processes operating both on the eroded profile and the detritus transported from the profiles. This approach was followed by contemporary pedologists such as Northcote (1946), Northcote & Tucker (1948) and Rix & Hutton (1953). Nevertheless, the podzolic origin of 'laterite' was not universally accepted by all workers. For example, Hallsworth & Costin (1953) considered that the upper podzolised layers characterising topsoils of southern Australian 'laterites', rather than being parts of original 'laterite profiles', were the result of 'strongly podzolising' climates after 'lateritisation'. However, Prescott & Pendleton (1952) maintained that on the sand plains of Western Australia, relic podzolic soils with ironstone gravels were acid despite the current low rainfall. They reaffirmed their view that 'laterite' was essentially the exposed illuvial horizon of an ancient soil.

Bauer (1959) disagreed with Prescott & Pendleton (1952) and considered that 'laterites' may form wherever the soil is subjected to wetting and drying, facilitating the migration of ferrous iron towards the surface during waterlogging and conversion to the more stable ferric iron upon desiccation. He believed that this could occur within a few centuries and that 'lateritic materials' might be currently forming in southern Australia.

Nevertheless, the majority of workers in southern South Australia have followed the view of 'laterite' as a fossil pedogenetic feature, part of the 'normal laterite profile' as espoused by Stephens (1946). Views such as those of Holland (1903) and King (1962) have largely been ignored. The former believed that 'laterites' formed via the differential mechanical accumulation of hydrated iron and aluminium oxides after the removal of silica and bases in solution and the latter considered that 'laterites' in Australia displayed the 'ultimate state of pedalfers development', that they are residual in origin and that all but the most insoluble constituents have been removed. Furthermore, theories that involve the accumulation of 'laterite' as a mechanical residuum during landscape reduction (Trendall, 1962; de Swardt, 1964 and McFarlane, 1971; 1976) have not been considered at all.

Geologists such as Sprigg (1946) accepted Prescott's view of 'laterite' development as the result of podzolic pedogenic processes, as did many geomorphologists (e.g. Brock, 1964). However, the majority of geologists and geomorphologists lacked the pedological expertise to interpret different 'lateritic' materials, and distinctively different materials were often regarded as equivalents (Horwitz, 1960; Crawford, 1959) leading to the allocation of spurious ages for the 'laterites'. Many geological studies obviously were concerned with 'laterite' in only a very incidental fashion, and almost any iron-rich horizon was regarded as 'laterite' (e.g. Glaessner, 1953a; Olliver, 1964), and some seemed to consider it as a rock unit (Major & Vitols, 1973). On the basis of much equivocal evidence, the tectonic behaviour of parts of the Mount Lofty Ranges in relation to the ages of 'lateritisation' (e.g. Horwitz, 1960) have been implied by various workers.

Geomorphologists have been little concerned with the genesis of 'laterite' in South Australia. Their work has been largely involved with using 'laterite' as

a morphostratigraphic marker and palaeoclimatic indicator in dating landforms and in developing denudation chronologies.

Throughout the South Australian literature, following the work of Stephens (1946), runs the thread of the 'normal laterite profile', which has influenced palaeo-climatic and palaeo-environmental reconstructions in a detrimental fashion. Only rarely have studies departed from this restrictive model.

### **3.1.3 Detailed Literature Review**

In the following detailed review, studies have been subdivided under headings of early geological studies, pedological investigations, later geological work, stratigraphic investigations and geomorphological studies. Where more than one line of investigation has been used the paper has been discussed under the heading of the dominant approach taken. Localities referred to in this review are shown on Figs 3.1 and 3.2.

#### **3.1.3.1 Early Geological Studies**

The term 'laterite' has been in the scientific literature since the early 19th century (Buchanan, 1807). David (1887) discussed the origin of 'laterite' in the New England district of New South Wales in the late 19th century, but he did so without reference to Buchanan's work, and the term did not appear in the South Australian literature until more than 100 years after its first usage (Teale, 1918). Nevertheless, features regarded by later workers as 'laterite' had been discussed by earlier workers under labels such as 'Desert Sandstone' and 'Upland Miocenes'.

For example, *Tate (1879)* regarded 'evenly-bedded sandrock, mottled clayey sands and ironstone conglomerates', occupying flat-topped points on the Adelaide foothills and within the ranges up to 290 m asl, as 'Upland Miocenes' and correlatives of terrestrial clays (now known to be of Pleistocene age) that overlie fossiliferous limestone at Adelaide. Similar beds with 'silicified tree stems' were identified as 'gold drifts' in intramontane basins and valleys within the Mount Lofty Ranges. The 'Upland Miocenes' were considered to be terrestrial equivalents of the Tertiary limestones that border the Mount Lofty Ranges. Tate attributed the discontinuous distribution of the 'Upland Miocenes', separated by deep ravines, to extensive denudation after uplift of the

ranges. More recent work has demonstrated that the sediments regarded by Tate (1879) as of Miocene age actually vary in age from the Pleistocene through to the Eocene. Furthermore, the limestone exposed in the city of Adelaide is now known to be of Late Pliocene age rather than Miocene as assumed by Tate.

The 'Desert Sandstone' of the northern part of South Australia, currently known as silcrete, was interpreted by Tate (1879) as an extensive lacustrine deposit, contemporary with the river gravels and sands of the 'Upland Miocenes' in the Mount Lofty Ranges. Thus silcrete and 'laterite' were not distinguished and they were both considered to be geological deposits or rocks.

Whereas Tate (1879) grouped sediments within the ranges and on their flanks as equivalent 'Upland Miocenes', *Benson (1906)* separated them into two groups, with an older Miocene series capping hills, overlooking deeply incised gorges in the ranges, and continuous with other gravels in the Barossa Valley. A second series, younger than the Miocene, was mapped flanking the western escarpment of the Mount Lofty Ranges. These were regarded as sediments produced by streams flowing down the fault block and along the scarp foot. The summit surface of the Mount Lofty Ranges was interpreted as an Early Tertiary differentially uplifted and dissected 'peneplain, surmounted by monadnocks' such as Mount Lofty, Mount Barker and Mount Gawler (*Benson, 1911*).

*Mawson (1907a)* extended the 'peneplain' concept to Eyre Peninsula where he described 'peneplains' in the Port Lincoln area at about 100 m and 6 m above sea level. He equated mottled clay beds underlying the lower surface with freshwater Miocene beds near Adelaide. Consequently he correlated this stage of 'peneplanation' with the Miocene 'mid-level plane so strongly marked in the hills near Adelaide.' *Mawson (1907b)* also described a large saucer-shaped body of bog iron ore, with a maximum thickness of 10 m, forming a flattish-topped hill about 200 m asl at Wadella Springs near Tumby Bay on Eyre Peninsula. After observing contemporary precipitation of iron oxides and gypsum from emerging spring waters, he concluded that the large bog iron ore deposit had originated from spring waters, with iron sulphate having derived from the oxidation of underlying pyrite bodies. Thus Mawson had observed and explained the occurrence of a distinctive type of ferricrete (vesicular ferricrete).

*Woolnough (1927)*, who had widespread experience of 'duricrust' in Australia regarded the 'Upland Miocenes' of South Australia as 'veritable Duricrust albeit of somewhat aberrant type'. He drew similarities between ferruginous cappings in the Mount Lofty Ranges with examples in Western Australia, and regarded some of the ferruginous materials on highland areas near Adelaide as "thoroughly typical 'lateritic' crusts". He suggested that the distribution of remnants of the terrestrial 'Upland Miocenes' agreed completely with the physiographic conditions postulated for 'Duricrust' formation, and that the ferruginous surface of much of the 'Mount Lofty Plateau' was underlain by highly decomposed arenaceous rocks, similar to those related to 'Duricrust'.

'Laterite', 'Upland Miocenes' and 'Desert Sandstone' were thus considered as contemporary and equivalent 'duricrusts', resting on weathered rock materials (*Woolnough, 1927*). He further postulated that they had formed in the Miocene on a continental 'peneplain' with sluggish surface drainage accentuated by marked seasonal rainfall. They were thus interpreted as the result of prolonged chemical weathering during the late stages of the 'cycle of erosion' (*Davis, 1909; 1920*). This essentially followed the view of 'laterite' as a capillary efflorescence as espoused by *Simpson (1912)* and *Walther (1915)*.

The view of 'ironstone' formation as lacustrine (e.g. *Fermor, 1911*) or swamp deposits on a 'peneplain' surface close to sea level, with the water table close to the ground surface was suggested by *Segnit (1937)*. After investigations in the Mount Lofty Ranges he noted the occurrence of three types of 'ironstone' cappings on high level ground and slopes. The first two types were thought to have formed via *in situ* weathering on a swampy 'peneplain surface' near to sea level, with angular quartz fragments having derived from the disintegration of quartz veins. The third type was interpreted as iron-cemented alluvial deposits. *Segnit (1937)* claimed that stream and swamp junctions were marked by 'ironstone cappings' displaying a progressive lateral transition from angular to well-rounded clasts.

### 3.1.3.2 Pedological studies

Investigations of 'laterite' were taken up by pedologists when *Teale (1918)* studied soils and forestry in the South Mount Lofty Ranges. He made some

extremely perspicacious comments on the nature and formation of ferruginous materials and his work represents the most comprehensive, detailed and objective discussion of iron oxides among all of the early investigators, drawing conclusions from his own careful observations. Teale (1918) interpreted the summit surface of the ranges as dislocated and eroded remnants of a former extensive 'peneplain'. He used the term 'ironstone' to describe ferruginous materials, which were noted to affect all materials except alluvium. They were categorised into four main types:-

- i. Sporadic occurrences of loose, concretionary gravels, occurring independently of geology, in deposits up to a metre thick ('pisolithic laterite' of McFarlane, 1976). Rarely was it noted to have been cemented into a hard deposit.
- ii. Limited patches of iron-cemented sands and gravels in generally unconsolidated sediments.
- iii. Ferruginised Cambrian and Precambrian slates and quartzites occurring on ridges and slopes. These were noted to display the effects of oxidation and impregnation by 'limonite' and manganese oxides converting them into impure 'ironstones' with an 'open and loose nature'.
- iv. Restricted occurrences of 'lateritic ironstone', and aluminous and argillaceous 'limonite', forming hard sheets at or near the surface.

Teale (1918) concluded that the formation of the different phases of 'ironstone' were related as they depended upon ferruginous rock or subsoil for a source of iron; that they required similar conditions for dissolving iron, largely by organic acids; and that a hot season was required to 'pump the iron salts' up to the surface, to achieve the oxidation and precipitation of 'limonite'. He noted that thick and extensive ferruginous clay subsoils restricted downward movement of solutions, preventing leaching and ensuring an abundant supply of soil water for local iron solutions to be precipitated at the surface during dry seasons.

The interpretation of 'laterite' as the B-horizon of a fossil podzolic soil was pursued by *Prescott (1931)* in view of evidence of leaching in 'laterite profiles', and this became the most pervasive view on 'laterite' formation in South

Australia. Many soils associated with 'uplifted peneplains' in Australia were noted to contain concretionary 'ironstone gravels', attributed by Prescott (1934) to former wetter periods when waterlogging of soils and shallow water tables were more common than at present. Many of the gravels were noted to be associated with 'ironstone duricrusts' or 'laterite cappings'. Samples of gravels separated from soils in Western Australia and South Australia were analysed to determine their chemical compositions. The analyses were interpreted to demonstrate the concretionary character of the 'ironstone gravels' as they presumably contained material from the soil in which they were assumed to have developed. For the South Australian samples the  $\text{Fe}_2\text{O}_3$  contents varied from 54% to 34.7%, MnO was very low,  $\text{Al}_2\text{O}_3$  varied from 2.0% to 9.2% and  $\text{TiO}_2$  from 0.1% to 0.4%. The ignition losses on these samples were low, averaging 3.1%. These results are compatible with analyses of ferruginous pisoliths presented in this thesis, and the low ignition losses suggest that the dominant iron oxide minerals present were hematite and maghemite.

The view of 'laterite' as the indurated, iron-rich B-horizon of a fossil, podzolic soil profile was championed by *Stephens (1946)*, who summarised general views on the form and age of 'laterite' in Australia. He noted many relic formations of massive 'laterite' and unconsolidated 'lateritic gravels' on dissected tablelands, some of which he thought had been associated with Tertiary lake formations. The possible age of the 'lateritisation' was also discussed. Whitehouse (1940) had considered that all 'laterites' in Australia developed contemporaneously in a pluvial period of 'peneplanation' in the Pliocene whereas Woolnough (1927) had suggested a Miocene age for the 'lateritisation'. However, Bryan (1939) using palaeontological work of Hills (1934), favoured the Pliocene, and suggested two periods of 'laterite' formation corresponding with two postulated precipitation maxima in the Pliocene.

A dynamic pedological model of soil formation, subsequent upon dissection of the 'lateritic' regions in South Australia, was presented by *Stephens (1946)*. He argued that different parent materials were available for soil formation depending upon the degree of dissection of the 'original 'laterite profile', or the nature of the derived sediments. *Stephens* regarded 'laterite' as a pedogenic material and suggested that ferruginous concretionary gravels accumulated in



the soil profile in the zone of oscillating seasonal water table as a result of alternating reducing and oxidising conditions. He associated the water table fluctuations with a low relief and a humid climate. Under these conditions the concretionary gravels were assumed to form an indurated horizon by their progressive union and enlargement. Later uplift and dissection of the landscape was postulated to explain the 'laterite' mantling remnants of former 'peneplains'. Thus it is apparent that Stephens (1946) envisaged sources of iron both from the overlying leached A-horizon and from iron-depleted and weathered bedrock below, as did Whitehouse (1940). He noted that Marbut (1932) and others used the term 'laterite' to describe highly ferruginous and aluminous soils of similar chemical but different physical and pedogenic characteristics to what he considered to be 'true laterite', although Thorp (1941) was attributed with partly rectifying this misuse.

The 'normal laterite profile' (Fig. 1.1) was envisaged as essentially a podzol with A, B and C horizons of eluviation, illuviation and weathering, with an accessory 'laterite horizon' usually above a clayey B-horizon. Occasionally several 'lateritic horizons' were noted in one profile. Complete profiles were considered to have a grey organic A1-horizon and a bleached, ash-like A2-horizon virtually free of organic matter. Nodular, massive or pisolitic 'lateritic' gravel was noted to occur in the A or B horizons. The B-horizon consisting of mottled grey, brown and red kaolinitic clay was described as passing down into a lighter coloured C-horizon reticulately mottled with red. At depth white kaolinised rock retaining original parent bedrock structures and fabrics was recorded.

Stephens believed that the 'normal laterite profile' was restricted to southern Australian occurrences: in Queensland 'laterite' was thought to occur as an horizon in red-earth profiles (Bryan, 1939; Whitehouse, 1940), which also contained silicified zones, suggesting that the required complete removal of dissolved silica had not occurred. Soils developed on 'laterite profiles', variably dissected, were described by Stephens and in some cases he perceived that erosion of finer soil particles caused the 'ironstone gravels' to sink as the soil collapsed imperceptibly, producing, in extreme cases, a surface pebble pavement of nodular and pisolitic 'laterite'. Remnants of 'lateritic' tablelands with steep sides and sharp breakaway edges with superficial remnants of the

A-horizon were described from various locations in southern Australia. On Eyre Peninsula alluvial gravels, now stranded 60 m above valley floors, were reported to be incorporated into the matrix of the 'laterite'. However, he believed that the exposure of C-horizon kaolinitic clay is rare in South Australia.

The model presented by Stephens has considerable merit in that it emphasises the dynamic nature of landform change and pedogenesis. However, its dependence on the widespread occurrence of a former 'normal laterite profile' related to former regional water table fluctuations, is unrealistic and has led to simplistic explanations of landscape development. Furthermore there are various objections to the view that the original 'laterite' is the illuvial horizon of a fossil podzolic soil.

Widespread 'lateritic' soils on the 'elevated peneplain' of Kangaroo Island, the Mount Lofty Ranges, Yorke Peninsula and Eyre Peninsula were reported by Crocker (1946), who observed that they contained considerable percentages of loose and indurated 'lateritic ironstone gravels'. Some of these gravels were considered to have formed *in situ*, but on dissected marginal slopes secondary origins for them were suggested. Crocker (1946) followed the view of Prescott (1931) that 'laterite' is the fossil illuvial horizon of a tropical Pliocene podzolic soil. Thus he reiterated then current thoughts about 'laterite' and further promulgated the association of 'laterite', 'peneplains', tropical climates and the Pliocene (or Tertiary), thereby setting the stage for the generation of circular arguments and conclusions based on little objective evidence.

The pedogenic origin of 'laterite' was further propounded by Northcote (1946) and Northcote & Tucker (1948). These workers mapped and described a soil unit, the *Eleanor Sand*, which occurs on small, slightly elevated portions of the 'lateritic' plateau of Kangaroo Island, and was regarded as a relic 'laterite profile' of Pliocene age. According to Northcote (1946) the profile conformed to the 'normal laterite profile' of Stephens (1946). Crocker (1946) had commented that 'lateritic residuals' on Kangaroo Island were covered by grey and white siliceous sands derived from resorted A-horizons, originally developed on Pleistocene coastal calcareous sand dunes. However, Northcote (1946) claimed that the constant ratio of coarse to fine sand throughout the profile indicated

that it had formed *in situ* and that the surface had not received accessions of wind-blown sand. Consequently he regarded the Eleanor Sand as a relatively undisturbed fossil soil with a 'lateritic horizon' developed *in situ* and preserved on an 'uplifted peneplain'.

*Rix & Hutton (1953)*, who carried out a soil survey in the South Mount Lofty Ranges, also regarded the summit surface as a block-faulted, uplifted and dissected 'peneplain'. They followed *Sprigg (1946)*, considering that by Early Tertiary times Precambrian rocks had been reduced to a base surface, subsequently buried by a Tertiary lacustrine and marine 'covermass'. The soil pattern suggested to them that a further cycle of erosion had removed the greater part of the 'covermass', leaving isolated areas of varying extents thereby creating a new 'peneplain', with remnants of Tertiary deposits preserved in topographic lows. They postulated 'lateritisation' of soils on the 'peneplain', prior to major faulting and dissection, concurring with *Whitehouse (1940)* that there had been contemporaneous 'laterite' formation throughout Australia in the Pliocene. Residual 'lateritic' soils were only mapped on hill summits and spurs so they suggested that erosion had removed most of a 'lateritic sandplain' following uplift and dissection.

The dominant factor influencing soil formation was attributed to earlier 'lateritisation' of the area. 'Lateritised' and relic 'lateritic podzolic soils' were noted to occur at levels in the landscape in accordance with the dips of the various fault blocks. One of the soils, the *Yaroona Gravelly Sand*, they regarded as an original 'laterite profile' (See Plate 4.36). This profile was described as a massive band of 'laterite' 22-30 cm thick, containing water-washed grits, gravels and sands, unconformably overlying kaolinised Precambrian shales. *Rix & Hutton* maintained that other residual podzols in the area exhibited profiles of ferruginous, mottled and pallid zones, overlying unweathered country rock, as the generally accepted order expected in 'laterite profiles'. It is clear that these workers were strongly influenced in their interpretations by the 'normal laterite profile' model of *Stephens (1946)* and they presented a convoluted explanation of an anomalous 'laterite profile', the *Yaroona Gravelly Sand* profile. It is actually a geological sequence of Precambrian rocks weathered in pre-Tertiary times, overlain by gravels, grits and sands of Eocene age (*Mawson, 1953*), that were deposited in a former

stream channel. Subsequently these sediments were silicified in places and superficially stained red by small amounts of iron oxides, introduced by groundwaters. A thin grey soil with pisoliths occurs at the surface. The above example demonstrates how complex deductive arguments, within the framework of the model of the 'normal laterite profile', were used to introduce events, for which there was no evidence, in order to 'explain' apparently aberrant observations. Despite this, these workers produced a detailed soil map to provide a 'springboard' for later workers.

*Lang (1965)* reported on soils and geomorphology of the Yundi area within the South Mount Lofty Ranges. His work represents a departure from that of many earlier workers as he invoked different types of weathering, erosional and sedimentary influences to explain the current landscape, and he envisaged 'lateritisation' and 'duricrust' formation proceeding over long periods of time, on landscapes of variable relief and positions above sea level.

Lang followed Hallsworth & Costin (1953), restricting the term 'laterite' to crusts associated with well-differentiated profiles allegedly formed by *in situ* relative accumulation of iron oxides. 'Ortstein' was used to describe crusts developed by laterally derived absolute accumulations. Where 'ortstein' crusts formed above weathered profiles, and simulated *in situ* weathering profiles they were called 'duricrusts'. Lang considered that 'laterites' on the oldest surfaces were only occasionally developed from materials recognisable in the pallid zone, and he assumed that a discontinuous layer of Tertiary sediments overlay older rocks throughout the 'lateritic area'.

The geomorphic and soil history of the area was outlined as follows:-

- i. A pre-Tertiary peneplain of low relief, covered with mixed terrestrial deposits, was uplifted in pre-Miocene times.
- ii. Subsequently, erosion re-excavating Permian valleys was accompanied by 'lateritisation'.
- iii. 'Lateritisation' continued during the Lower Miocene when a marine transgression entered the adjacent Myponga and Upper Hindmarsh Valleys.
- iv. Soils with duricrusts developed in the Early Pliocene during a postulated low sea level.

- v. The Late Pliocene witnessed instability following growing aridity that led to the dissection of soils with duricrusts and there was the development of a series of fans of mixed 'lateritic' material graded to 180 m asl.
- vi. Further periods of instability occurred in the Quaternary.

Additional comments on 'laterite' were made by *Ward (1966)*, who was, however, primarily concerned with Quaternary stratigraphy and soils in his study of the area south of Adelaide. He described flat surfaces preserved on the crests and gentle back slopes of the western blocks of the Mount Lofty Ranges as relics of a pre-deformational Mount Lofty 'peneplain', mantled by 'deep weathering' and 'laterite'. He believed that the 'peneplain' was not of the same age everywhere, but was no younger than the Early Pliocene. Relationships between soil morphologies and degrees of 'lateritisation' of materials were noted, as were well-developed 'lateritic mottled zones' formed beneath surfaces attributed to the Late Pliocene, Early Pleistocene and Late Pleistocene.

*Maud (1972)*, who extended the work of *Lang (1965)* described surface occurrences of 'massive and pisolitic ironstones', regarded as accumulations of iron oxides, formed in fossil soil profiles by 'lateritisation' processes on a 'peneplain' surface. The accumulation of iron and aluminium oxides was attributed either to the removal of silica and bases (concentrating by loss = relative accumulation) or their accumulation from outside sources (absolute accumulation). He also followed the suggestion of *Hallsworth & Costin (1953)* that only soils displaying 'ironstones' overlying mottled and pallid zones should be regarded as 'laterites'. He considered that the surface occurrences of 'ironstone' reflected various phases in weathering and erosional history from the Mesozoic through until the Recent. Scattered erosional remnants of 'laterite' were thought to be extant in the modern landscape, surviving above the level of Miocene limestones that had been deposited in partly exhumed glacial valleys. This suggested that the 'laterite' surface was being destroyed in the Miocene, which it pre-dated. *Maud (1972)* suggested that faulting and tilting of the 'lateritised' surface had occurred earlier than the Pliocene age favoured by *Sprigg (1942)*. According to *Maud* the 'lateritised' surface antedated the major period of diastrophism and he equated it with the Australian Surface of *King (1962)*.

'Lateritised' surfaces occurring across infilled glacial valleys were correlated with the summit surface despite their lower landscape positions. Gentle non-tectonic inclinations of 'ironstone' cappings were regarded as original valley morphologies, and Maud concluded that the original erosion surface was one of considerable relief.

Maud (1972) noted that although 'laterite profiles' were typically thick, with well developed mottled and pallid zones, 'laterite' horizons were rare, which he attributed to erosional truncation of the profile. Well developed 'lateritic ironstones' on Permian glaciogene sediments were explained by the concentration of iron oxides from lateral sources, whereas thinner crusts on pre-Permian rocks were ascribed to *in situ* weathering losses of silica and bases. Furthermore, he believed that outcrops of 'lateritic ironstone' at various levels in the landscape were relics of a number of periods of 'lateritisation', affecting alluvial sediments, including reworked crusts, on former broad valley floors. He suggested that the 'ironstone' terrace remnants varied in age from Pliocene for the highest to Recent for the lowest. These valley 'ironstones' were described as forming parts of typical 'laterite' profiles, with bleached, though rarely kaolinised, pallid zones. Following landscape rejuvenation and lowering of the water table, Maud (1972) believed that the zones of iron-enrichment had irreversibly hardened into 'lateritic ironstones'. He also argued that the process of iron oxide-enrichment of sediments is currently proceeding on broad valley floors, and does not depend upon a climate any different to that of today.

### 3.1.3.3 Later Geological Investigations

Basically, the contributions of geologists to 'laterite' studies in South Australia have not been concerned with understanding the genesis but rather with the age of 'laterite' as an aid to interpreting geological history.

According to *Sprigg (1945)* 'laterite' in the Mount Lofty Ranges formed on both a Precambrian and Cambrian bedrock 'undermass' and an 'overmass' of Tertiary limestones and lacustrine sediments. He assigned its formation to a humid pluvial period in the Pleistocene. He considered it unwise to associate 'laterite' formation with 'peneplanation', which implied formation over a very long period, whereas he believed that 'lateritisation' occupied only a relatively

short time span. This interpretation has important implications for landscape evolution as 'laterite' formation would first require the development of an extensive planation surface.

Sprigg (1946) concurred with the interpretations of Prescott (1931) and Crocker (1946) concerning 'laterite' genesis. He was thus able to imply that faulting and uplift of former low-lying, undulating surfaces had occurred after 'laterite' formation, indicating land movements of between 180 m and 300 m. Similarities between mottled zones of 'laterite' of the ranges and mottled Pleistocene clays of the gulf lowland prompted Sprigg (1946) to correlate the two disparate occurrences. As the mottled clays are of demonstrable post-Lower Pliocene age, 'lateritisation' was regarded to be of Pleistocene age, but older than the 'Kosciusko' epoch of block faulting.

Sprigg (1945) was critical of the 'double peneplanation' theory of Fenner (1930; 1931). However, subsequently Sprigg (1946) made the observation that the widespread occurrence of 'laterite' over the Mount Lofty Ranges presented a potent argument in favour of this theory.

A detailed stratigraphic study by *Glaessner (1953b)* and *Glaessner & Wade (1958)* on the western margin of the Mount Lofty Ranges allowed them to suggest several periods of 'lateritisation', provide information on the character and timing of tectonic activity and to elucidate aspects of landscape evolution. Rocks and sediments of Precambrian, Cambrian, Permian and Tertiary ages were noted to be variably 'lateritised' or to contain blocks of 'laterite'. However, many of the iron oxides within these sediments and attributed to 'lateritisation' may have formed since exposure, in recent times, by oxidation of 'primary' iron minerals such as glauconite and siderite.

Contrary to much earlier work (e.g. Fenner, 1931), *Glaessner (1953b)* suggested that the tectonic framework on the western margin of the Mount Lofty Ranges was not a series of tilt blocks, but asymmetrical synclinal structures. Some interesting suggestions were made regarding Tertiary marine deposits that throw light on the evolution and weathering history of the Mount Lofty Ranges:-

- i. Some Eocene marine sediments formed a shoreline near the foot of the present ranges, implying the existence of pre-Eocene fault scarps.
- ii. The marine fossiliferous Port Willunga Beds transgressed into the ranges but there is no evidence that they ever completely covered them. Instead the transgression appears to have been restricted to structurally-controlled lows within the ranges, thereby casting doubt on the 'double planation' hypothesis of Fenner (1930; 1931).

Summaries of the Tertiary geology of the marginal basins of the Mount Lofty Ranges involving faulting, weathering and marine incursions provide a valuable framework within which the processes of weathering and ferricrete formation can be viewed, but it is unfortunate that the authors apparently had the view that all occurrences of iron oxides provided evidence for 'lateritisation'. For example, they considered that a 'lateritic profile', modified by later subsidence, occurs in a coastal headland (Witton Bluff) south of Adelaide (Plate 3.1). However, there is no unequivocal 'laterite' profile on Witton Bluff, but there is a stratigraphic sequence of Early Tertiary sediments overlain by Quaternary units that include a distinctive iron-impregnated sandy sediment with pronounced intra-formational slumping (Plate 3.2). These workers considered that there were at least two periods of 'lateritisation', one in pre-Tertiary times and one of post-Eocene age, which is a similar interpretation to that of Campana (1955).

Further geological work was carried out by *Aitchison et al. (1953)*, who reported Early Tertiary lacustrine mottled sands, argillaceous sandstone and clays occurring sub-horizontally on a pre-Tertiary erosion surface in the Adelaide area. Lignitic clays, brown coals and gravel beds were also reported in association with the Early Tertiary sediments. Outcrops of mottled sandstone and rare white clay in the northeastern foothills were also thought to be of Early Tertiary age. They reported that the southerly tilting of the Para Block had brought the Early Tertiary sediments close to the surface on the western side of the block. A few outliers of 'lateritised' Early Tertiary sediments were reported in the Mount Lofty Ranges and in the southern hills. *Aitchison et al. (1953)* considered that in the Middle Tertiary the Early Tertiary sediments were



downfaulted and overlain by marine sandy limestones, sandstones and marls. They suggested that the Tertiary sediments had suffered faulting, being dragged up against the main western escarpment of the Mount Lofty Ranges (Eden Fault).

In the southern part of the Mount Lofty Ranges, *Campana & Wilson (1955)* identified a planation surface at levels up to 420 m asl, as a pre-Tertiary 'peneplain', uplifted during Tertiary and Quaternary times and deeply dissected by subsequent cycles of erosion. They described the plateau remnants as being generally covered by a 'leached residual lateritic soil', which was attributed to (?)Pliocene to Recent weathering.

*Campana (1955)* extended his studies to the north when he described the geology of the area near Gawler in the North Mount Lofty Ranges. He noted a 'leached lateritic soil' overlying gneisses, schists and several areas of Tertiary fluvial deposits that rest on a pre-Tertiary weathered erosion surface. He reported several layers of gravels and coarse sands cemented by iron oxides within the Tertiary sediments. Tertiary sediments within the ranges were distinguished according to their lithologies, and near the western margin of the ranges, comparable deposits containing littoral marine fossils were considered to be of Lower Miocene to Upper Oligocene age. Those within the ranges were described as fluvial-deltaic sediments, containing silicified tree trunks, carbonaceous remains of fossil wood and leaf impressions. Campana's mapping of the Tertiary (Lower Eocene) strata in this area indicated that deposition occurred in a system of lakes and rivers on a weathered surface of moderate relief, above which ridges of harder rocks projected. After deposition of the non-marine strata, Campana considered that they and older rocks had been subjected to widespread 'lateritisation' during the period of time between the Lower Eocene and the Miocene.

The sequence outlined above by Campana (1955) illustrates pre-Tertiary weathering and bleaching of basement rocks, the deposition of Tertiary terrestrial sediments over a dissected landscape, differential ferruginisation of suitable host rocks and the inhibition of this by marine submergence.

Working on Fleurieu Peninsula, *Crawford (1959)* identified 'laterite' capping Wilson Hill at 320 m, around which an area was mapped as the lower part of a 'laterite profile' developed on Kanmantoo Group metasedimentary rocks. The occurrence of areas of 'hard laterite' at lower elevations (100 m asl), on quartzose sediments, was interpreted as indicating a very irregular original 'lateritised' surface of Late Tertiary age. Subsequently, Bourman (1973) demonstrated that the two occurrences were distinctively different and probably of two different ages.

While carrying out regional geological investigations on Yorke Peninsula, *Crawford (1965, pp 39-41)* described Pleistocene deposits, exposed in the sea-cliffs at Ardrossan, as mottled dark red to olive green argillaceous sediments [The 'Ardrossan Clays and Sandrock' of Tepper (1879)]. He suggested that the mottling could be due to 'lateritisation', with the upper indurated zone having been removed by erosion and the pallid zone occurring sub-surface. However, he noted that fresh felspar gravel in the mottled material argued against 'lateritic' weathering. Consequently, an alternative explanation of mottling produced by alternate wetting and drying in an environment of low relief was also suggested. *Crawford (1965)* obviously considered 'laterite' within the framework of the 'standard laterite profile', and attempted to fit his observations into it by postulating the erosional removal of an upper indurated zone. He did, however, also consider a more realistic alternative explanation for his observations.

After investigations on Fleurieu Peninsula (*Horwitz, 1960*) and in the Mid North (*Horwitz, 1961*), Horwitz discussed evidence relating to the nature and age of 'laterite'. This evidence suggested two major periods of 'lateritisation', one in the pre-Eocene and another in the Pliocene. He reported 'glazed pisolites, pebbles and limonite pisolites' beneath Oligo-Miocene limestones and within basal Early Tertiary conglomerates. Subsequently, wherever surfaces with similar 'glazed pisoliths' were noted, he assigned them to the pre-Tertiary. However, the correlation of ferruginous materials, which superficially appear similar, must be approached with caution. For example, one surface carrying alleged Early Tertiary pisoliths could not have developed until post-Miocene times (Bourman, 1973). Moreover, the occurrence of pisoliths in reworked Early Tertiary sediments is not a critical indicator of

their maximum possible age. They may be of variable ages, or be older clasts reincorporated into younger sediments. In addition, it appears that some of these pre-Eocene ferruginous materials represent the transgressive marine *Compton Conglomerate* (Oligocene) of the Murray Basin (Ludbrook, 1961; Lindsay & Williams, 1977), and do not relate to exposure in a terrestrial environment.

The evidence presented by Horwitz for major 'lateritisation' in the Pliocene is also equivocal. In the intramontane Upper Hindmarsh Valley of Fleurieu Peninsula over 150 m of cross-bedded and mottled brown ferruginous sands, capped by a crust of 'limonite'-cemented gravels were reported. By extrapolation these were considered to overlie fossiliferous Early Miocene limestones. The sands were thus tentatively assigned to the Pliocene. Horwitz also considered that these 'lateritised' Pliocene sands were continuous with 'limonite'-cemented gravels' on the high plateau. Thus he assigned them to the same Pliocene age. Brock (1964; 1971) questioned the contemporaneity of the high-level and low-level crusts and Bourman (1969; 1973) highlighted their different characters and suggested that the higher crust was of pre-Miocene age and the lower one of Pliocene age.

*Johns (1961a)* reported on the preservation of 'fossil laterites' and 'lateritic gravels and conglomerates', in many cases at high levels, over large tracts of central and southern Eyre Peninsula, particularly in the Lincoln Uplands. During presumed humid pluvial conditions of the Pliocene, poorly drained soils were considered to have been leached, leading to the accumulation of iron oxides and the *in situ* formation of 'laterite'. He conjectured that most of the sediments deposited on the coastal plains and the Central Basin were materials resorted from the uplands so that their soils carry 'pisolitic' or massive 'ironstone' gravels. Johns believed that during 'lateritisation' the previously 'peneplained basement rocks' underwent deep weathering, ferruginisation and kaolinisation. In particular, weathered schists, were noted to grade up into reddish-brown clayey rocks with pebbly concretions, merging upward into 'ironstone crusts'. Lithological variations in the basement rocks were thought to have had no influence on the final product of weathering. He believed that low relief and high tropical temperatures had favoured the removal of silica, with seasonal oscillations of the water table

leading to the concentration of iron oxides. He held the view that much of the Lincoln Uplands is still obscured by 'laterite', a formerly continuous mantle now partly stripped following regional uplift, drainage rejuvenation and erosion.

*Johns (1961b)* considered that the accordance of summit levels in the eastern Mount Lofty Ranges represented a base-levelled terrain of Pliocene age, carrying sporadic occurrences of ferruginous grits and 'laterites'. He believed that previously continuous 'ironstone' cappings of Pliocene or post-Pliocene age have been largely removed by erosion. The best exposures of 'ironstones' were reported from "Lucernbrae" where deposits about 1 m thick were noted to mantle Kanmantoo Group metasedimentary rocks.

At various locations within and on the margins of the Mount Lofty Ranges, Tertiary sediments, variably weathered and ferruginised, have been reported to contain 'laterite'. For example, at Happy Valley, *Olliver (1964)* described a sequence of Eocene marine Blanche Point Marls and North Maslin Sands overlain by Pliocene freshwater sands and clays capped and preserved by a 'lateritic' horizon at about 200 m asl. The so-called 'laterite' was a band of iron-impregnated sandy sediment. Similar occurrences were described in many sand quarries in Tertiary sands in the Adelaide region by *Olliver & Weir (1967)*.

*Harris & Olliver (1964)* reported on palynological analysis of organic material preserved in "coal balls" exposed in quarry faces in Tertiary sands in the Barossa Valley. The basal Tertiary unit was described as a 'lateritic' sand and gravel overlain by laminated silty and sandy clays, and was considered to be of Lower Tertiary age. The clays were considered to be capped by an upper 'laterite'. Previously the sands had been assigned to the Eocene (*Glaessner, 1955*) or Pliocene (*Hossfeld, 1949*), but *Harris & Olliver (1964)* suggested that the microfloras indicated a Miocene or possibly a Lower Pliocene age for the sediments.

Working on the summit surface of northwestern Kangaroo Island, *Major & Vitols (1973)* described a 'massive rock composed of pebble-sized pisolites of maghemite and limonite and fine-grained quartz sand cemented by limonite'. This crust was noted to be up to 1 m thick, but nowhere was a complete

'laterite' profile exposed. The crust was overlain by white, fine-grained quartz sand and underlain by mottled yellow and red clay or rocks of the weathered Kanmantoo Group metasediments. The crust was noted only as boulders, where ripped up by ploughs, and was not observed as a massive sheet. Loose 'pisolites' mixed with white or yellow sand were recorded on the margins of the inland plateau. An aeolian calcarenite (Middle Pleistocene Bridgewater Formation) was thought to overlie the 'pisolites', and elsewhere blocks of ferruginous 'pisolite' were noted to overlie marine limestone of probable Late Pliocene age, suggesting that the ferruginous 'pisolites' were of Late Pliocene or Early Pleistocene age.

Wopfner (1972a) carried out a rare analytical investigation of mottled materials that in other contexts have been referred to as 'lateritic'. He discussed maghemite in mottled Cainozoic sediments at Hallett Cove, where both 'primary' and reworked maghemite were identified. He considered that maghemite was a climatic indicator and presented opportunities for correlation of Cainozoic sediments. Maghemite was reported from two locations within the sediments:

- i. In conspicuous red mottles within medium grained white sandstone, small amounts (2%) of maghemite were noted, with the concentration of maghemite within the mottles used as evidence for *in situ* formation.
- ii. In a reworked conglomeratic horizon containing maghemitic sub-rounded 'ironstone' pebbles.

Wopfner reported identical mottled profiles from the Mid North and the South East regions of South Australia, where mottled profiles were reported to be capped by brown ferruginous and maghemitic crusts. He claimed that the profiles and the crusts are genetically related so that the Hallett Cove example is a stripped maghemite profile, with the conglomerate reworked from an original *in situ* crust.

The suggestion was made that the maghemite had originated by thermal dehydration of lepidocrocite formed by oxidation under fluctuating water table levels and warm climatic conditions. He concluded that lepidocrocite and goethite may have formed as gels that were subsequently dehydrated and

crystallised as maghemite and hematite under conditions of low relief, warm climate and heavy seasonal rainfall.

Iron-stained rounded quartz grains and 'ferruginous pellets' were reported from within a fossiliferous marine limestone of probable Upper Eocene age (*Bourman & Lindsay, 1973*), intersected in a drill hole at -36 m underlying part of the Waitpinga Creek drainage basin, and at an elevation of about 60 m asl. This observation was interpreted as indicating the development of 'lateritisation', or at least ferruginisation, prior to the Eocene.

*Robertson (1974)* reported on an 18 m exposure of 'deeply weathered' Adelaidean metasedimentary rocks in the central section of the South Mount Lofty Ranges at about 450 m asl. The rocks were noted to have been kaolinised and to contain some concentrations of iron oxides, irregularly infilling joints and fractures, and forming liesegang rings. Some ferricrete fragments were observed on top of an adjacent hill and the weathered material was interpreted as part of a 'Tertiary laterite profile'.

*Daily et al. (1974)* claimed that evidence on Kangaroo Island enabled direct and precise dating of the 'laterite' developed on the uplifted plateau summit surface of the Mount Lofty Ranges. They described Kangaroo Island as a dissected, tilted and block-faulted plateau with a caprock of 'laterite', in places, breached by faults. Adjacent lowlands were noted to be essentially coincident with Permian glaciogene sediments that were also 'lateritised' and overlain by basalt of Jurassic age.

The 'lateritic' capping of the summit plateau surface of Kangaroo Island was described as part of a 'laterite profile' and they explained the lack of a complete 'laterite profile' in the Late Palaeozoic sediments beneath the basalt by erosion of the ferruginous horizons prior to the basalt extrusion. No evidence of 'deep weathering' on the basalt was observed during their investigations. Consequently, they ruled out the possibility of the basalt surface being an etch surface.

They concluded that as the basalt is of Middle Jurassic age, then both the 'laterite' and the summit surface must be older. The 'laterite' was regarded as

an indicator of a humid tropical climate and as a reliable morphostratigraphic marker. Using stratigraphic and palaeoclimatic evidence they decided that the summit surface was eroded and 'lateritised' during the Late Triassic, Early Jurassic, or both. Support for this conclusion was derived from evidence of warm, humid conditions associated with the Triassic flora of Leigh Creek, in the Flinders Ranges, and evidence of tectonism and uplift of a deeply weathered kaolinised zone during the Mid-Jurassic, which had led to the development of the Polda Basin on Eyre Peninsula and the extrusion of the Kangaroo Island basalt.

A Middle to Late Tertiary age for the 'lateritised' surface was preferred by Northcote (1979), who considered that the correlation of the summit surface weathering with that beneath the Jurassic basalt was unresolved.

*Schmidt et al. (1976)* presented palaeomagnetic evidence that required sub-basaltic weathering during a Late Oligocene to Early Miocene period of dominant 'lateritic' weathering. Idnurm & Senior (1978) suggested that during this period Australia experienced a major 'lateritic' weathering event, when there was synchronous remagnetisation for perhaps all of Australia's 'laterites'.

*Daily et al. (1979)* did not dismiss this possibility, but quoted evidence from the basins marginal to the Mount Lofty Ranges demonstrating 'deep lateritic weathering' of pre-Eocene age, and suggested that a Mid-Tertiary weathering event might have been superimposed on the earlier weathering profile.

*Milnes et al. (1982)*, on the other hand, pointed out some of the deficiencies in the arguments presented for sub-basaltic weathering. For example, they considered that the preservation of the sharp contact at the sole of the basalt, the absence of leaching or kaolinisation of the basal basalt, and the fact that the basalt everywhere is largely unweathered, favoured a pre-basaltic age for the weathering.

### **3.1.3.4 Stratigraphic Approach to Investigations of 'Lateritic' Materials**

*Firman (1967a; 1967b; 1976; 1981)* attempted to place weathered zones and palaeosols within a stratigraphic framework. For example, he gave formal

status to ferruginised clastic sediments and bedrock weathering profiles consisting of 'sesquioxides of iron' and forming 'ironstone crusts', by introducing the name, *Yallunda Ferricrete*. The *Yallunda Ferricrete* was reported to exceed 1 m in thickness in its type area at high levels over the interfluves of the Lincoln Uplands (Eyre Peninsula) and on remnants of old high surfaces elsewhere. The term 'ferricrete' was used to describe ferruginous layers and crusts both independent of and in association with weathered profiles. He considered that the original materials, now 'ferricreted', have separate lithostratigraphic status and that continuous sheet ferricrete has both rock and soil stratigraphic status.

Ferricretes in various stratigraphic situations were recorded by Firman (1967b), including ferricrete above and below Lower Tertiary sediments in the Barossa Valley, as well as ferricretes in the highlands of the Mount Lofty Ranges and the Lincoln Uplands. He also suggested that there were equivalents of upland ferricretes in the sedimentary succession of the Murray Basin. These included oolitic siderite-rich sediments and 'laterite' in the Lower Pliocene Bookpurnong Beds, as well as ferruginous beds and cappings in the Upper Pliocene Parilla Sand near the Victoria-South Australia border. Some of the ferricretes discussed above, however, have resulted from the relatively recent oxidation of pre-existing iron-rich sediments containing glauconite and siderite. Consequently they cannot be used as reliable soil stratigraphic markers.

Firman (1976) considered that during the time between the Permian and the Early Tertiary, some 200 Ma, the Mount Lofty Range was a land mass experiencing prolonged weathering and erosion, so that by Early Tertiary times a subdued and 'deeply weathered' landscape had developed. Associated bleached profiles were considered to have originated in the Mesozoic.

A range of different ages of weathering and 'lateritisation' was reported:-

- i. Decomposed, bleached or mottled bedrock underlying Eocene sediments in the Adelaide region was ascribed to pre-Tertiary weathering.
- ii. An alleged 'laterite profile' developed in Eocene gravelly sands was used to indicate post-Eocene weathering.



- iii. Silicified and ferruginous zones in Early Pleistocene sediments were noted to overlie older bleached zones and to have alleged equivalents in 'laterite profiles' in the adjoining uplands.
- iv. Ferruginisation in carbonaceous and pyritic Eocene sediments was attributed to recent exposure and oxidation.

Following investigations in the Great Australian Basin province in South Australia, Firman (1981) described a series of weathering zones and palaeosols of various ages. The work was carried out in the north of the State but correlations were made with weathering profiles in the south. This review will consider only those palaeosols related to 'deep weathering' and ferruginisation. These are summarised in Table 3.1, with respect to their recognised weathering characteristics and ages. Thus Firman observed weathering, bleaching, cementation, concretions, mottling and irregular masses of iron oxides affecting materials ranging in age from the Proterozoic to the Pleistocene. The two most common types of ferruginous materials noted were mottles, which sometimes graded into younger ferruginous crusts containing clasts.

He believed that the classic 'laterite profile' of massive, vesicular, cellular or concretionary 'ironstone' overlying mottled and pallid zones actually contained layers formed in different ways at different times, with the profile being as old as the first weathering of the parent rock.

Weathering profiles were thus regarded as assemblages showing weathering and diagenesis of different ages. For example, the bleached zone of the *Arckaringa Palaeosol* was not considered to have been genetically associated with younger ferruginous zones, but to have preceded the development of mottles and ferricretes. He ascribed bleaching to early cool climates and ferruginisation to tropical conditions. This view is at variance with much earlier work, which favoured the contemporaneous formation of complete 'laterite profiles'.

The work of Firman marks a pronounced departure from all previous investigations and is commendable in that it attempts to establish stratigraphic

Table 3.1 Ferruginous and Bleached Weathering Zones and Palaeosols postulated by Firman (1981)

Weathering Zone or Palaeosol	Weathering Characteristics	Suggested Age
<i>Ancient Weathering</i>	Exhumed weathering	Proterozoic
<i>Playfair Weathering Zone</i>	Large irregular red, yellow and white patches, up to 10 m across and 100 m deep. Best developed on fine-grained rocks. Coarse rocks show little alteration. Occurs in road cut at Kapunda	Middle to Late Palaeozoic
<i>Mesozoic Weathering</i>	White bleached. Oldest bleached zones, superimposed on older weathering. Affects Precambrian rocks in Blackwood railway Cutting	Permian to Jurassic
<i>Post-Winton Formation Weathering</i>	Pale grey, purple, brown, strong red, green, yellow weathering colours. In places obliterated by younger bleached zones.	Mesozoic
<i>Arckaringa Palaeosol</i>	White, bleached (with younger mottles and ferruginous stains, e.g. of San Marino Palaeosol)	Pre-Tertiary Superimposed on older Mesozoic weathering
<i>San Marino Palaeosol</i>	Dark red ferruginous mottles up to 30 cm across (=Yallunda Ferricrete). Occurs in Tertiary sediments in Blackwood Railway Cut	Oligocene to Middle Miocene
<i>Ardrossan Palaeosol</i>	Dark red mottles in pale olive grey clayey sand. Red veining in older weathered zones	Younger than Late Pliocene
<i>Karoonda Palaeosol</i>	Thin silicified veneer of detritus with reworked clasts of Ardrossan Palaeosol. Forms caprock in 'laterite profiles' and younger than San Marino Palaeosol and Yallunda Ferricrete	Lower Pleistocene

ages for different weathering phenomena. However, the correlation of weathering events on the basis of the shape, size and colours of mottles and other weathering indicators, where there is no stratigraphic control, is fraught with hazards. Firman pointed out that some profiles have been modified by younger weathering activity, thereby obliterating the results of earlier weathering, and that similar mottling occurs in weathered profiles claimed to be of different ages. Firman takes no account of local environmental conditions, which may have favoured synchronous bleaching in one area and mottling in another. Various questions remain unanswered, such as what happened to the iron derived from the bleaching of the Arckaringa Palaeosol, where did the iron for the development of the San Marino Palaeosol come from, and how was it concentrated in discrete, but more-or-less uniformly distributed mottles within previously bleached bedrock?

### **3.1.3.5 Geomorphological investigations**

Geomorphologists, who have dominated discussions on 'laterite' in the last 25 years in particular, have been interested primarily in using it to establish denudation chronologies, to establish the ages of particular landforms and to correlate widely spaced planation surfaces.

*Fenner (1930, 1931)* presented a 'double peneplanation' hypothesis, suggested to him by Prof. D.W. Johnson, to account for the evolution of the Mount Lofty Ranges. In so doing he provided a geomorphic and tectonic framework for the use of subsequent authors. He believed that the greater part of the Mount Lofty Ranges had been stripped of an easily eroded Miocene marine 'covermass'. He saw the double planation theory as necessary to explain transverse drainage and exhumed surfaces in the ranges. He postulated that a pre-Miocene peneplain blanketed with a Miocene marine 'covermass' had been affected by block-faulting, tilting and differential uplift in the Upper Miocene or Lower Pliocene. Subsequently this irregular surface was thought to have been 'peneplained', with the older surface having been resurrected in places, from beneath the 'covermass', and a new 'peneplain' developed on both Precambrian and Miocene rocks. Pleistocene (Kosciusko Epoch) tectonism renewed erosion. Some fault blocks remained buried by Tertiary sediments and others, exhumed from beneath the 'covermass', were subjected to renewed weathering and

erosion. Fenner did not specifically discuss the timing of 'lateritisation', but by implication, it must have been of post-Miocene age.

Today it is generally agreed that the Mount Lofty Ranges were not totally immersed by the Miocene seas, so that the 'double planation' theory cannot be accepted in its entirety. However, large areas of the Mount Lofty Ranges and Kangaroo Island were covered by the Miocene seas at heights in excess of 200 m asl, and there is evidence that the shorelines were even higher than this. Moreover, even though the 'covermass' of marine deposits may not have totally covered the ranges, Tertiary terrestrial sediments occur extensively and at higher levels than do the marine sediments. Consequently, the 'double planation' theory has considerable merit, but it is still inadequate to account for all of the geomorphic complexities of the ranges, which have been variably exposed to continuous processes of weathering and erosion for immense periods of time.

*Bauer (1959)* addressed problems associated with 'lateritic' soils on Kangaroo Island. He noted that the Eleanor Sand regarded by Northcote (1946) as a Pliocene 'fossil lateritic soil', occurs both on a Pliocene plain of marine abrasion at 50 m to 100 m asl (Mount Taylor Plain), and on the highest portions of an undissected Tertiary plateau surface at heights up to 300 m asl. Regardless of whether the Eleanor Sand formed in two separate periods or one, *Bauer (1959)* considered that both were no older than the Early Pleistocene. *Bauer* noted that regardless of elevation the Eleanor Sand occurs on areas of low relief and poor drainage that would have suited periodic waterlogging and drying. Thus he thought that topography may have been important in assisting the formation of a distinctive soil in two differing physiographic locations.

*Bauer* questioned the view of Prescott & Pendleton (1952) that 'laterite' is an exposed podzolic illuvial horizon of Tertiary age, as he noted the occurrence of 'laterite' on presumed Pleistocene surfaces. Several anomalous 'laterite' occurrences were examined by *Bauer*, who interpreted them to favour *in situ* 'laterite' formation although Northcote (*pers. comm.* to *Bauer*) suggested that the 'ironstones' had been derived by transport and could not have formed *in situ* because of the small amounts of associated clays. However, *Bauer (1959)*

doubted this explanation on age and topographic grounds. Subsequent work (Milnes *et al.*, 1982) revealed that the critical limestones used by Bauer (1959) to date the 'laterites' are older than he thought. Consequently, many of his objections to transported origins for the 'laterites' may be removed.

The chemistry involved in the formation of ferruginous soil horizons was discussed by Bauer. Prescott & Pendleton (1952) believed them to be the products of disintegration of Tertiary 'laterites' so that they were considered as secondary rather than primary materials. However, Bauer favoured the view that such accumulations formed where the soil was subjected to wetting and drying, with ferrous iron migrating upward during waterlogging and being converted to stable ferric iron in dry oxygenating periods. He also believed that this could have occurred within a few centuries. Bauer (1959) concluded that a ready source of iron was available from decomposing country rock and that the temperature regime was not too low to inhibit the reduction, migration and oxidation of iron. Thus, he considered that 'lateritic' material might be forming at present in southern Australia.

Bauer (1959) had proposed a refreshing and different view on the ages, origins and climatic environments of 'laterites' on Kangaroo Island, although his views were constricted by lack of information on the ages of limestones and the detailed characteristics of the 'lateritic' materials.

*Brock (1964; 1971)* identified remnants of an ancient landsurface on the spine of Fleurieu Peninsula covering an area of 25 km<sup>2</sup>; the remnants were described as having little relief and a capping of the 'normal laterite profile' of Stephens (1946). Several varieties of 'laterite' were recognised by Brock on Fleurieu Peninsula. 'Pisolitic laterite' associated with the Parawa High Plain was regarded as equivalent to the southern Australian 'normal podzolic laterite'. He agreed with D'Hoore (1954) that dissection of 'lateritic' terrain accompanied by lateral water movement may have redeposited iron oxides on gentle slopes to form slope cappings. Brock (1964) concluded that the Parawa High Plain developed as a 'peneplain' after a prolonged period of subaerial weathering and erosion in the Palaeozoic, culminating in a phase of crustal stability in the Mesozoic and Early Tertiary, when 'lateritisation' occurred prior to uplift and dissection of the surface.

Twidale and his co-workers have written numerous papers on 'laterite' in the upland regions of South Australia (e.g. Twidale, 1968; 1976a; 1976b; 1983); Twidale *et al.* (1976); Twidale & Bourne (1975a; 1975b); Bourne (1974)).

*Twidale (1968, p.377)* examined the traditional explanation of the summit surface of the Mount Lofty Ranges. This is that an extensive 'lateritised surface of erosion' developed in the ranges, close to regional base level in the Late Tertiary, that it was subsequently upthrust along ancient fault lines, after which it suffered dissection. He noted that a problem with this interpretation is the apparent absence of downfaulted remnants of the 'lateritised erosion surface'. While conceding that ferruginous crusts of the postulated 'laterite profile' might have been removed by sub-surface solutional processes, he also considered that the extensive landsurface may have developed in relationship to high level local base levels, one of the possibilities suggested by the work of Kennedy (1962). However, no critical evidence was presented to show that the summit surface of the Mount Lofty Ranges developed in this fashion.

Regardless of how it formed, Twidale (1968) described the summit surface of the Mount Lofty Ranges as a 'lateritised peneplain', surmounted by a few residual remnants or 'monadnocks'. He concluded that the 'deep weathering' occurred late in the Tertiary (Pliocene) and may have even continued into the early part of the Pleistocene.

*Twidale & Bourne (1975a)* investigated the geomorphic evolution of the Eastern Mount Lofty Ranges and identified a summit high plain (Tungkillo surface) at 200 - 300 m asl as an etch surface occasionally surmounted by scattered mesas or conical hills up to 10 m high and either underlain by 'lateritic weathering profiles' or capped by alluvial quartzitic gravels (Whalley surface). They believed that the scattered 'lateritic' remnants were remnants of a once-contiguous weathered surface of low relief.

The Whalley surface and its associated 'deep weathering' was considered to be of Mesozoic age by extrapolation from Kangaroo Island (Daily *et al.*, 1974). They also argued that palaeontological considerations favoured the Triassic as providing the most suitable humid, tropical climatic conditions for the

formation of 'laterite'. Twidale & Bourne agreed that the alleged ancient Whalley surface had been dislocated by faulting but could find no evidence of buried 'laterite' on the downthrown side of the Milendella fault. They explained its apparent absence by sub-surface dissolution of the iron oxides.

*Mills (1965)* had regarded the lower part of the Milendella fault scarp (eastern boundary of the Eastern Mount Lofty Ranges) to be the result of post-Miocene faulting. Miocene marine sediments perched on the fault scarp were correlated by him with Miocene strata intersected by bores under the Murray surface, and he regarded the 60 - 90 m difference in elevation to be due to post-Miocene dislocation. Mills (1965) also noted that the orientation of boulders in Pleistocene conglomerates suggested recent movement on the fault. Further indications of recent faulting came from seismic activity and the distinctness of the scarps, which suggested geological youthfulness.

While conceding these points, Twidale & Bourne (1975a) maintained that the scarps are deeply and intricately dissected, and suggested essentially an erosional origin for the lower part of the scarp. Much of the interpretation rests on the precise ages of the Miocene limestones on the Milendella scarp and those under the Murray surface. Mills (1965) believed that both were the Mannum limestone, whereas Twidale & Bourne (1975a), suggested that the limestone on the scarp may have been the younger Morgan limestone, even though no definitive evidence was available. Consequently, they suggested that the major elevational difference between the two could be attributed to eustatic rather than to tectonic effects. This conflict may be resolved only by accurate age determination of these critical deposits. The most recent work on this problem by *Lindsay (1986)* suggests that there has been at least 100 m of fault offset since the Middle Tertiary, which favours the hypothesis of Mills (1965).

*Twidale (1976a)* reviewed the character and age of the summit high plain of the Mount Lofty Ranges. He noted that many workers have considered that the surface and its carapace are of later Tertiary ages because the sediments deposited in marginal Tertiary basins indicated that there were only areas of low relief nearby during their deposition. Twidale argued that there was no evidence directly to correlate the summit surface 'laterite' with the Later Tertiary basin deposits, but that marine Eocene and Miocene sediments in

basins eroded well below the level of the summit surface on Fleurieu Peninsula suggested a pre-Tertiary age for the surface and its 'laterite'. By extrapolating from Kangaroo Island (Daily *et al.*, 1974) and palaeoclimatic evidence, Twidale favoured a Triassic age for the 'laterite'.

This remarkable alleged preservation of the summit surface for 200 Ma was thought to be due to a combination of various influences (*Twidale, 1976b*):-

- i. The recurrent uplift of the Mount Lofty Ranges, according to Twidale, resulted in postponing the ultimate degradation of the ranges by exposing new land to the area undergoing reduction. Evidence of recurrent uplift was cited to show the applicability of this hypothesis to the Mount Lofty Ranges. However, investigations presented later in this thesis demonstrate that the best preservation is in relatively lowlying points and least in areas of greatest uplift.
- ii. The development of the Mount Lofty Ranges on an anticline, the flanks of which are faulted, was used by Twidale to help to explain the preservation of the 'laterite'-capped plateau. He maintained that the bulk of the plateau is centrally located close to the resistant compressional zone of the anticline, while remnants near the western margin are buttressed by sandstone and limestone outcrops. However, the folding, which occurred in the Cambrian, was very complex and did not result in the formation of a simple anticline. Moreover, erosion of this complex structure has been so pronounced that vertical and near-vertical rock structures are exposed, and subsequent tensional faulting has occurred within the ranges (Glaessner, 1953a), so that the core of the ranges should not be considered to be in compression.
- iii. The sandy A-horizon of the 'laterite' profile was thought to have assisted palaeosurface preservation by providing an absorbent cushion to protect the underlying ferruginous horizon from rainfall. However, there are no 200 Ma old sandy A-horizons preserved in the ranges, but only modern sandy soils.
- iv. The alleged permeable and porous nature of the ferruginous crust of the 'laterite' profile, was thought to render this zone



- resistant to erosion. However, ferruginous crusts are relatively rare and discontinuous, with the thickest crusts occurring in positions well below the level of the postulated ancient surface.
- v. Gully gravure, which involves the alternation of the locus of intense erosion via the protective influence of coarse debris, was also thought by Twidale to be significant in the preservation of ancient 'laterite'-capped land surfaces. However, no specific sites were discussed by Twidale and the author has not observed the extensive operation of this process in the Mount Lofty Ranges.
  - vi. The unequal activity of rivers, which incise more rapidly than they erode laterally, was also invoked. While river incision may operate more rapidly than valley-side processes in some situations, the operation of the processes of weathering, surface wash and gullying on valley slopes and hill summits for 200 Ma would have led to considerable modification of the landscape.

Twidale (1976b) presented a model of landscape evolution involving increasing relief amplitude in order to account for the preservation of these alleged ancient palaeoforms. However, the deductive arguments presented were not supported by field evidence and it is not reasonable to accept the view that the summit surface of the Mount Lofty Ranges has survived essentially unchanged for this enormous period of time.

Younger weathering events in the Cainozoic were also reported by Twidale (1976b). For example, a weakly developed ferricrete was thought to have formed on sands in piedmont zones that would have favoured the precipitation of iron oxides. Their present positions were attributed to Late Tertiary to Early Quaternary faulting. Other ferruginised surfaces were noted to occur on Eyre and Yorke Peninsulas, at One Tree Hill and near Myponga. Some of these were believed to have derived from the disintegration of the summit surface 'laterite'.

*Twidale et al. (1976)* and *Bourne (1974)* described eight palaeosurfaces on Eyre Peninsula. Among these was an epigene surface of low relief (Lincoln surface) protected by a 'lateritic duricrust' and formed under humid tropical climatic

conditions during the Early Mesozoic. A younger surface characterised by a 'ferruginous duricrust' ascribed to the Late Tertiary was also described. These surfaces were used as evidence for the progressive exposure of inselbergs on Eyre Peninsula (*Twidale & Bourne, 1976b*).

The suggestion was made that the Lincoln surface is a 'laterite'- capped 'dissected peneplain' formerly contiguous with summit surfaces in the Mount Lofty Ranges and on Kangaroo Island and disrupted by faulting. Pedogenic accumulations of iron oxides lacking mottled and pallid zones were reported at lower elevations below relics of silcrete duricrust assigned to the Middle Tertiary, and thus were attributed to the Late Tertiary and correlated with similar ferricretes on Yorke Peninsula and in the southern Mount Lofty Ranges. The Glenville surface was also mapped in the area and was regarded as an etch plain equivalent of the 'laterite' surface.

*Twidale (1983)* published recently on the ages and significance of Australian 'laterites' and silcretes. He regarded 'laterites' and bauxites as ferruginous and aluminous members of comparable origins with similar physiographic and climatic implications, developed on contiguous land surfaces and of the same age ranges in given regions. He reproduced a map of Australia (after *Stephens, 1971*) showing a peripheral distribution of 'laterite' and an interior preservation of silcrete in arid Australia. *Young (1985)* produced a map showing a much wider distribution of silcrete than depicted on these maps, indicating that silcrete occurs within 'laterite' areas. *Twidale (1983)* considered that primary 'laterite' and silcrete are good stratigraphic markers, which can be used to date landforms and landscapes.

*Twidale* considered that the dating of 'laterite', silcrete and their associated surfaces has been confused by the assumption that all relic 'laterites' are of the same age and by the fact that primary and secondary 'laterites' have been confused (See, however, *Brock, 1964; Bourman, 1969; Forrest, 1969*). Moreover, he considered that the operation of other geomorphic activities during the period of deep weathering has been ignored (See, however, *Alley, 1973, 1977*). *Twidale (1983)* also thought that silcrete developed mainly during the Early and Middle Tertiary, forming under warm-humid to sub-humid conditions (See however, *McGowran et al., 1978*), but is today preserved in aridity.

Twidale (1983) concluded that:-

- i. During the Late Mesozoic and Tertiary much of Australia was base-levelled and this surface of low relief was deeply weathered under humid, warm conditions; 'laterite' and bauxite formed in the marginal areas with external drainage while silcrete developed in interior catchments.
- ii. The formation of the duricrust was interrupted by geologic and geomorphic events so that the duration and timing of events was not everywhere the same.
- iii. Climatic conditions for duricrusting lasted for at least 60 Ma and probably for 200 Ma.
- iv. Ferruginous and siliceous crusts are related to the same extended period of warm, humid climate but, are separated from analogous Cainozoic development by tectonic rather than by climatic events (See Alley, 1977).
- v. Duricrust cappings are excellent morphostratigraphic markers, as for example, in displaying the progressive exposure of a granite inselberg.
- vi. There are great palaeoclimatic implications, for 'laterite' implies warm, humid conditions, but according to palaeomagnetic evidence Australia was situated in high latitudes when 'laterites' allegedly formed.

*Bourman (1969; 1973)*, identified a multicyclic landscape marked by two major erosion surfaces, the Spring Mount Plateau (Mesozoic to Eocene) and the Green Hills surface (Pliocene) on Fleurieu Peninsula. The former, underlain by a 'lateritic weathering profile' consisting of pallid, mottled and ferruginous-rich zones, was mapped at an elevation of about 400 m asl. The surface was considered to have been tilted to the southeast. The second surface was interpreted as an erosional surface 170-100 m asl, and capped in places by 'ferricrete', a term used to describe iron-cemented crusts not underlain by 'deep weathering' profiles. The ferricrete on the Green Hills surface was thought to have formed from reworking of 'lateritic' material from the summit surface. Using stranded river gravels and river profiles, Bourman (1973) suggested that the base level during the development of the Green Hills surface

had been approximately 60 m asl. At this time in the Pliocene, fluvial action apparently modified a resurrected pre-Miocene erosion surface. Bourman (1973) presented evidence for two different 'ferruginous duricrusts' of two different ages on the summit surface and on the sands that overlie Miocene limestone in the Upper Hindmarsh Valley. Previously, Horwitz (1960) had regarded these crusts as contiguous and of the same Pliocene age. Bourman (1973) also suggested that 'deep weathering' had proceeded under the summit surface after uplift.

*Forrest (1969)* examined the geomorphic evolution of the Bremer Valley in the Eastern Mount Lofty Ranges and identified two erosional surfaces of low relief, which he considered had formed prior to a major marine transgression in the Miocene. Consequently, both the surfaces and their associated cappings of 'lateritic' material were interpreted as being of pre-Miocene age. 'Laterite' was categorised as 'fossil or relic', which referred to the complete 'normal laterite profile'; 'truncated', where the upper horizon was absent; 'immature', where the percentage of iron in the capping was low and the underlying bedrock was only partially weathered; 'derived', when the capping had been derived from the reworking of higher crusts and where this reworked capping rested on weathered bedrock; and 'ferricrete' where an iron-rich crust incorporated partially-rounded quartz pebbles and overlay fresh bedrock. The various landsurfaces and laterites were related to local occurrences of Miocene limestone, which *Forrest (1969)* interpreted as nearshore deposits. He considered that the Miocene sea transgressed an area with relief similar to that of today, and that 'lateritisation' of the bedrock followed the development of the Whalley Hill and Lucernbrae erosion surfaces prior to the Miocene. Another surface, an exhumed one with a remnant of derived ferricrete, and thought to have formed by stripping of the Miocene limestone cover, was considered to be of Pliocene age.

In a study of landsurface development in the Mid North of South Australia, *Alley (1973; 1977)* identified remnants of a 'laterite' surface, occurring high in the landscape but below resistant quartzite ridges. Remnants of the 'laterite' surface were noted to be most common at stream heads, but were also mapped on prominent hills that stand nearly 100 m above modern valley floors. The 'laterite' capping of angular quartz fragments set in a matrix of iron oxides

was observed to overlie severely weathered and locally kaolinitic bedrock, and to be consistently thicker on lower slopes. Sections of the 'laterite' surface were thought to have been down-faulted in the Early Tertiary and later buried by Middle Tertiary sediments. Alley (1973) regarded the 'laterite' surface to be of (?)Early to pre-Tertiary age and considered that it persisted to the Middle Tertiary in the Barossa area. A consistently lower silcrete-capped landsurface was considered to be younger than the 'laterite' surface and was ascribed a Mid-Tertiary age. Palynological data was interpreted by Alley (1977) to demonstrate that the Eocene appeared to have been warm and temperate with a very high rainfall, and that the Miocene was similar with perhaps slightly warmer temperatures and a slightly lower precipitation. The evidence that both 'laterite' and silcrete formed together for at least some time on identical strata and under similar climatic conditions was used to show that some other factor(s) must have controlled the processes of weathering. Only the base levels of erosion differed between the silcreted and 'lateritised' surfaces, according to Alley, and silcrete developed on a surface, the drainage of which flowed sluggishly into Tertiary lakes. The concentration of silica near to the landsurface was attributed to higher alkalinity, slower groundwater movement and a higher water table close to the lakes. From his studies in the Mid-North of South Australia Alley concluded that:-

- i. 'Laterite' and silcrete formed at different times but co-existed for part of the Early Cainozoic in adjacent drainage basins.
- ii. 'Laterite' and silcrete did not form co-genetically as suggested by Stephens (1971).
- iii. The view that 'laterite' is associated with tropical conditions and silcrete with aridity is not valid in the Mid-North, where both formed in similar climatic and biotic regimes; only the base levels and groundwater conditions varied.

Using chemical (Hutton, 1977), palynological and stratigraphic evidence *McGowran et al. (1978)* disagreed with Alley that 'laterite' and silcrete formed concurrently on similar rocks and under broadly similar climatic conditions from Eocene to Miocene times. However, Alley (1978) was able to rebuff the arguments presented by *McGowran et al. (1978)* and made a valuable contribution to 'laterite' genesis by highlighting the influence of local

topographic and groundwater conditions in its formation, as well as questioning climatic influences on 'laterite' and 'silcrete' development.

*King (1976)* recognised several of his world wide erosional surfaces in the Mount Lofty Ranges of South Australia. He considered that south of the Willunga Fault, 'laterite-encrusted tablelands' represented the "Moorlands" planation ('great Australian denudation cycle') of Late Cretaceous to Mid Cainozoic age, whereas north of the fault the Mount Lofty Ranges were thought to be surmounted by his "Rolling" landsurface of Miocene age that lacked a 'true laterite'. The "Widespread" landscape of Pliocene age was recognised in broad valleys and basins accordant with a Pliocene coastal plain at about 180 m asl, and the "Youngest" Cycle was related to deep valleys and gorges in the ranges.

*Twidale (1978)* criticised King's interpretation, and considered that the summit surface both north and south of the Willunga Fault was contiguous and of the same Early Mesozoic age. However, areas of 'laterite' mapped by Twidale (1978) north and west of the Willunga Fault on the Eden and Clarendon Blocks are variably covered with weathered and ferruginised Eocene to Pliocene sediments. In places these have been eroded to expose an underlying weathered pre-Tertiary surface, eroded and reweathered since exhumation (Sprigg, 1945). Consequently, the summit surface here cannot be of Early Mesozoic age. Furthermore, there may be some support for King's generalised scheme, as weathered zones have been stripped from large areas of the summit surface north of the Willunga Fault, especially in the Eastern Mount Lofty Ranges (Twidale & Bourne, 1975), allowing further erosion and the potential development of a younger surface, possibly equivalent to King's Rolling surface.

### **3.1.4 Summary and Conclusions**

Early geological workers in South Australia (Tate, 1887; Benson, 1906, 1911) regarded materials later described as Miocene 'laterite' by Woolnough (1927) as geological strata. Segnit (1937) suggested that some 'ironstones' had formed by deposition in swamps or lakes. Woolnough (1927) followed Walther (1915) in believing that 'laterite' formed on 'peneplain' surfaces as efflorescences of iron and aluminium oxides brought to the surface by capillarity during dry seasons.

Prescott (1931), on the other hand, regarded 'laterite' as the indurated iron-rich B-horizon of a fossil podzolic soil developed by leaching. This view was taken up and slightly modified by Whitehouse (1940) and Stephens (1946), who envisaged inputs of iron oxides both from above by leaching and from below by fluctuating water tables. Subsequently, the pedogenic model of the 'normal laterite profile' involving a 'laterite' horizon successively underlain by companion materials of mottled and bleached bedrock (Stephens, 1946), and developed on a pre-existing 'peneplain', has dominated interpretations of 'laterite' in South Australia. Views of 'laterite' genesis as a residuum (e.g. McFarlane, 1976) have received scant attention in South Australia, as have theories involving chemical diffusion (See Mann & Ollier, 1985). Furthermore, there have been no detailed analytical studies such as those of the French workers (e.g. Muller & Bocquier, 1986; Herbillon & Nahon, 1987). Throughout the above review numerous authors have associated 'laterite' with weathering profiles developed on 'peneplain' surfaces under humid tropical climatic conditions. The upland sites of many 'laterites' have been attributed to tectonic uplift and dissection (e.g. Crocker, 1946; Sprigg, 1946).

Evidence of former 'lateritisation' has been attributed to the occurrence of weathered, bleached and mottled bedrock as well as to ferruginous crusts. The assumption has often been made that the occurrence of part of the 'normal laterite profile', such as bleached or mottled bedrock, implies the former existence of a complete profile and its variable erosion (e.g. Robinson, 1974; Daily *et al.*, 1974, Maud, 1972). Surprisingly, often only the 'laterite' crust has been reported missing, even though this would be likely to be the most resistant part of the profile. Furthermore it has been sometimes implied that 'laterite profiles' were formerly continuous over extensive 'peneplain' surfaces (e.g. Johns 1961a; Twidale & Bourne, 1975a), that they are therefore excellent morphostratigraphic markers, that in some cases the 'laterite profiles' have been preserved in pristine form for some 200 Ma (Twidale, 1976b), and that inter-regional extrapolations can be made on the basis of such materials (e.g. Twidale, 1976b; 1983; Twidale *et al.*, 1974; Twidale & Bourne, 1975a; 1975b; Bourne, 1974). As 'laterite' formation has often been equated with humid, torrid conditions it has also been used as a palaeoclimatic indicator (McGowran, 1979a), although some workers (e.g. Bauer, 1959; Maud, 1972) considered that current climatic conditions may be suitable for its formation.

Iron oxide-impregnated sediments of various ages have been described as 'laterite' by various workers including Rix & Hutton (1953), Glaessner (1953b), Glaessner & Wade (1958), Crawford (1959), Olliver (1964), Olliver & Weir (1967), whereas some others have referred to them as 'ortstein' (Lang, 1965; Maud, 1972) or as 'ferricrete' (Firman, 1967a; Bourman, 1969; 1973).

Some exceptions to the views of 'laterite' being a fossil soil profile formed on 'peneplains' under tropical climatic conditions have been put forward by Bauer (1959) and Alley (1977), but these views, though very innovative, have not proved popular.

Views on the age of 'laterite' have varied from the Early Mesozoic (Twidale, 1983; Twidale & Bourne, 1975a), Mesozoic (Brock, 1972; Daily *et al.*, 1974), Mesozoic to Eocene (Bourman, 1969, 1973; Brock, 1974), pre-Tertiary (Glaessner, 1953a; Glaessner & Parkin 1958; Campana, 1955, Horwitz, 1960), pre-Eocene (Bourman & Lindsay, 1973; Alley, 1973), post-Eocene (Glaessner & Parkin, 1958; Campana, 1955), pre-Miocene (Maud, 1972; Forrest, 1969), Miocene (Woolnough, 1927, Lang, 1965), Pliocene (Whitehouse, 1940; Northcote, 1946; Stephens, 1946; Crocker, 1946; Rix & Hutton, 1953; Crawford, 1959; Horwitz, 1960; Johns, 1961a, 1961b; Olliver, 1964; Harris & Olliver, 1964; Major & Vitols, 1973; Twidale, 1968), Plio-Pleistocene (Fenner, 1930, 1931), Pleistocene (Sprigg, 1945; Bauer, 1959; Crawford, 1965) to the Recent (Campana & Wilson, 1955).

The above summary highlights the diversity of interpretations concerning the nature of 'laterite', its age, processes of development and the topographic and climatic requirements for its formation. A pathway to the solution of these divergences of opinion about 'lateritic' materials in South Australia requires detailed and multi-faceted studies, towards which this thesis is contributing.

### **3.2 Discussion of recent International views on 'Laterite' classification and formation**

#### **3.2.1 Chemical Classification of Schellmann (1981)**

One of the most recent classifications of 'laterite' is the chemical classification of Schellmann (1981), discussed in Chapter 5. It developed as the culmination of discussions of the International Geological Correlation Program No.129 and



was accepted by the French workers, Herbillon & Nahon (1987), particularly as they claimed that it accommodates the concepts of 'relative' (accumulation of  $\text{Fe}_2\text{O}_3$  and  $\text{Al}_2\text{O}_3$  with loss of  $\text{SiO}_2$  and bases) and 'absolute' (imports of  $\text{Fe}_2\text{O}_3$  and/or  $\text{Al}_2\text{O}_3$ ) accumulations (D'Hoore, 1954), regarded in the French literature as the key geochemical processes leading to the formation of 'laterite'. However, they pointed out that there are difficulties in determining which elements have been mobilised when applied to actual chemical data from 'laterite profiles'. They also stated that the Schellmann chemical classification is independent of genetic interpretations. However, as Schellmann claimed that 'laterites' are the products of intense subaerial weathering, the position of samples in his triangular diagrams should reflect the effects of weathering intensities on the underlying bedrock. Furthermore, they approved of Schellmann's scheme because it applies equally well to unconsolidated materials as to hard or soft iron crusts, with all types being regarded as being influenced by 'laterization' processes. However, this writer considers that the indiscriminate application of 'laterite' to such a diverse range of materials is turning the clock back. Many earlier workers (e.g. Marbut, 1932; Thorp, 1941; Pendleton & Sharasuvana, 1946; Hemming, 1968) were aware of the confusion generated by such an approach, which should be avoided at all costs. Furthermore, ferricretes may have formed in various ways, they may not be genetically related to the underlying bedrock, and they do not simply reflect the intensity of weathering, so that the chemical classification of Schellmann is of little value.

### **3.2.2 An Assessment of 'Relative' and 'Absolute' Accumulations'.**

A widely followed subdivision of 'laterites' is that attributed to D'Hoore (1954), who distinguished between relative and absolute accumulations of iron and aluminium oxides. The former involves both the interpretation of ferricrete as a chemical precipitate in co-genetic relationship to parts of a weathering profile, and its interpretation as a residuum of weathering, in which relatively immobile constituents accumulate near the surface through the depletion of the more mobile elements. The model of absolute accumulation involves both the physical and chemical derivation of iron and aluminium oxides from higher lateral sources, such as pre-existing ferricretes, and their concentration and cementation in lower parts of the landscape. Although one of the above mechanisms may be dominant in the development of iron and

aluminium oxide-enrichment in ferricretes, in reality, both modes of enrichment may occur. McFarlane (1971; 1976) pointed out that both *in situ* and detrital 'laterites' involve elements of both absolute and relative accumulations. Furthermore, in many cases distinguishing *in situ* and detrital laterite and bauxite becomes merely an academic exercise (Plumb & Gostin, 1973). The use of the terms 'absolute' and 'relative' accumulation at a micro-scale (e.g. Brewer, 1964; Muller & Bocquier, 1986) further confuses the issue. As both detrital and *in situ* influences affect the vast majority of ferricretes at various scales, the subdivision of D'Hoore (1954) may often only apply to the operation of the dominant process.

Some confusion also seems to apply to the use of the term *in situ*. The term means 'in its original position', but some workers would consider that a ferricrete formed by landscape downwasting, probably involving components of both vertical and lateral movement of clasts, had formed *in situ*. It would be better to regard ferricretes formed in this way as residual or sedentary rather than *in situ*. Technically, *in situ* weathering should apply only to isovoluminous weathering.

### 3.2.3 'Laterite' formed by Chemical Diffusion

Mann & Ollier (1984) suggested that the upward chemical diffusion of ferrous iron in solution from a bedrock weathering front, through deeply weathered profiles, followed by oxidation and precipitation of ferric oxyhydroxides at the water table could account for occurrences of ferruginous duricrusts above tens to hundreds of metres of pallid zone clay. There is no doubt that the change to oxidising conditions above the water table, or immediately below it, where fresh and oxygenated water might occur, would have led to the oxidation and precipitation of ferrous iron, but there is no necessity to invoke ionic diffusion for the operation of these processes. This model implies the development of both the pallid zone and the ferricrete by the one integrated process. They dismissed the role of lateral accession of iron oxides because of the widespread occurrence of ferricretes on interfluves. Furthermore, they claimed that the depletion of the pallid zone could account for the quantity of iron in the ferricrete, and concluded that chemical diffusion is the most important chemical process involved in ferricrete formation.

The operation of this model of ferricrete formation requires very special conditions, including the widespread occurrence of stagnant groundwater, conditions that would be difficult to achieve. The lack of detailed topographic descriptions, together with the absence of data on the chemical, mineralogical, hand specimen and micromorphological characteristics of the ferricretes involved in the study makes the model difficult to assess. It may have limited relevance in particular sites. However, other models of landscape and 'laterite' development can account for the widespread occurrence of 'laterite' on interfluves.

### 3.2.4 Residuum Theory of McFarlane

The residuum theories of Trendall (1962) and de Swardt (1964) that required landsurface reduction were criticised on various grounds by McFarlane (1976), who presented a compromise geomorphic model of 'laterite' formation. In this model, original iron precipitates were believed to have formed in the narrow fluctuating range of a groundwater table, which fell as the landsurface was lowered. This groundwater 'laterite' was thought to have developed as a mechanical residuum during late stages of landscape downwasting. With the cessation of downwasting and stabilisation of the water table, the residuum was thought to have been hydrated to form massive 'laterite', having the appearance of a 'true precipitate' (McFarlane, 1976). Vertical lowering of the landsurface was postulated to have allowed its entire coverage with laterite', and a sinking water table obviated the need for 'impossibly large water table fluctuations', such as those postulated by de Swardt (1964) and Trendall (1962). It also associated 'laterite' formation with an original surface of some relief, although its ultimate development was coupled with very low relief. No iron was considered to have been derived from the underlying pallid zone, which McFarlane (1971) suggested had developed by leaching through the permeable *in situ* 'laterites' after uplift and incision of the 'laterite'.

Butt (1982) has applied the model of landscape downwasting to a discussion of weathering profiles in the Australian context. He considered that weathering profiles have developed progressively, with horizons having formed from progenitors that resemble those currently beneath them.

### 3.2.5. French Workers

The contributions of French workers to investigations of 'laterite' have been summarised recently in a paper by Herbillon & Nahon (1987). From West Africa they described a typical 'laterite profile', which had a succession of six layers, recognised in most profiles, that displayed an increase in  $\text{Fe}_2\text{O}_3$  from the bottom to the top. The observation was made, however, that the total thickness of each 'laterite' formation and the relative importance of each layer within the same profile was widely variable even in limited restricted areas, and as with examples from South Australia, some profiles were not capped with crusts. The lower horizons were noted to preserve bedrock textures and weathering was considered to have been isovoluminous. The mottled zone was considered to have formed with the absolute accumulation of iron in kaolinised bedrock involving the epigenetic replacement of kaolinite by hematite. The formation of mottles was considered to have occurred isovoluminously as ghosts of entire kaolinite booklets were observed within the hematite, and the precipitation of iron and the dissolution of kaolinite were considered to be the result of two coupled reactions. Soft nodular and hard nodular iron crusts were described in the upper part of the profile that involved the transformation of "soft yellow plasma into 'pisolites'". The hard nodular iron crust was characterised by an increase in hematite content and size of nodules, with a decrease in porosity. Goethitic rinds were noted on hematite nodules in the upper few cm of the hard crust. Iron oxides throughout the profile were noted to be variably Al-substituted, but generally increasing in degree of Al-substitution towards the top (hematite 4-7%; goethite varied from Al-poor in soft domains up to 21% in the cortex of pisoliths) and kaolinite in near-surface material was noted to be less crystalline and more iron-rich than kaolinite lower in the profile.

The profiles studied appear to have been specifically selected as ideal profiles and the others ignored, thereby biasing their samples towards an 'ideal profile'. Furthermore, the variations in Al-substitution discussed above suggest that the upper part of the profile has developed by surface transformations, perhaps involving lateral transport. Specifically, the development of highly Al-substituted goethite in the cores of pisoliths would require the dissolution of pre-existing iron oxides and reprecipitation to

facilitate the incorporation of Al into the goethite structure. Subsequently, rinds of different character have developed around this cortex material.

### **3.3 Review of the Pathways of Formation and Transformation of Iron and Aluminium Oxides and Oxyhydroxides**

The formation of the various secondary iron and aluminium minerals is influenced by factors such as temperature, moisture, pH and Eh (Schwertmann & Taylor, 1987) and thus their occurrences may provide insights into environmental conditions prevailing during their formation or transformation. Furthermore, the degree of crystallinity of the various Fe-oxide minerals (as indicated by the broadening of XRD peaks) and the degree of Al-substitution in the crystal structure of goethite (as illustrated by XRD lines shifts), may reflect current environments as well as also elucidating palaeoenvironmental conditions (Fitzpatrick, 1987).

The following is a review of current views on conditions of formation of iron and aluminium minerals as presented by Schwertmann (1985), Schwertmann & Taylor (1987), Taylor (1987), Fitzpatrick (1987), Hsu (1977) and Milnes & Farmer (1987). Throughout this thesis the term 'oxide' is used for brevity but also includes oxyhydroxides and hydrated oxides. Secondary iron oxides are very simple chemical compounds, but the arrangement and packing of their components affect their mineral forms (Evans, 1964). It is relatively easy to synthesise the various Fe-oxides found in soils and sediments at pH7 and ambient temperatures, both from Fe(II) and Fe(III) solutions. Generally, Fe(II) is much more readily mobilised than is ferric iron. At pH values observed in nature, concentrations of Fe(III) in solution rarely exceed one part per million. However, Fe(III) as ferrihydrite can also be mobilised readily. The major iron oxides encountered in this investigation include goethite, hematite, lepidocrocite, maghemite and ferrihydrite.

In oxygenated environments Fe(III) hydrolyses to form iron oxides of low solubility. This process is irreversible, but Fe(III) can be remobilised through complexation by organic ligands, by reduction in microbial-induced oxygen deficient anaerobic environments or by dissolution under acidic soil conditions. Thus iron oxides of varying solubilities can be remobilised to form new phases, although ferrous iron is more readily mobilised than is ferric

iron. The chemical pathways postulated for the formation and transformation of soil iron oxides are illustrated in Fig. 3.3, reproduced from Schwertmann & Taylor (1987).

### 3.3.1 Iron oxide minerals

#### 3.3.1.1 *Goethite* ( $\alpha$ -FeOOH)

Goethite is a widespread, yellow-brown coloured iron oxide in soils and weathering environments. It is the most stable phase, possibly due to the presence of isomorphously substituted Al, and it is commonly associated with other less stable iron oxides. Goethite from aerobic tropical environments is generally poorly crystalline due to high rates of Al-substitution, but where formed under reducing environments, such as peat swamps, produces relatively sharp XRD peaks. It displays high Al-substitution when derived from highly weathered, acid and leaching environments, particularly where precipitated close to its source. In gibbsitic, highly desilicified environments, goethite is commonly highly Al-substituted, up to a maximum of 33 mole %. The higher Al-substitution in goethites from acid soils may reflect higher solution of Al with decreasing pH. On the other hand goethite displays low substitution in materials formed in weakly acid and reductomorphic environments, particularly where there is migration of iron to environments low in available Al (e.g. calcareous weathering environments). Some aluminium substituted goethites in modern soils may be inherited from former climatic regimes.

Conditions that favour the formation of goethite include low temperatures, high water activity and high organic contents, and its formation is maximised at a pH of 4. Synthesis experiments show that where Al ions are present goethite formation by oxidation of Fe(II) solutions is favoured over both lepidocrocite and magnetite. In synthesis experiments, small amounts of Al have been shown to suppress goethite in favour of hematite formation (Schwertmann, 1985). However, highly Al-substituted goethite occurs in nature, so that the effect of Al may be over-ridden by other variables such as time, temperature, organic matter and pH.

Goethite has been demonstrated to form through nucleation and crystal growth via solution from the species  $[\text{Fe}(\text{OH})_2]^+$  and  $[\text{Fe}_2(\text{OH})_4]^{2+}$  monomers derived

from any source. In cool climates, goethite may also form via solution from ferrihydrite. In reductomorphic environments (hydromorphic soils) goethite may be found in association with lepidocrocite, having formed from Fe(II) or Fe(III) in solution. Goethite formation is favoured by higher partial pressures of CO<sub>2</sub>, and by increased rates of oxidation as well as by the presence of Al in the system. Goethite can also form from lepidocrocite via dissolution and reprecipitation, but only very slowly. Organic matter and high moisture contents may control mineralogical transformations of hematite-rich to goethite-rich material through dissolution and reprecipitation.

### 3.3.1.2 Hematite ( $\alpha$ -Fe<sub>2</sub>O<sub>3</sub>)

Hematite is bright red to purple in colour, and can contain substituted Al in its structure up to approximately 12 mole%. Hematite is more stable in environments with comparatively low water activity and several publications report strong climatic influences on the hematite:goethite ratio. There is a tendency for hematite to be dominant in warmer, humid regions and goethite to be more dominant under more temperate humid conditions (Fitzpatrick, 1987). Other factors that influence the goethite:hematite ratio are the moisture status and organic content of the environment, which in turn can be affected by factors such as topography and depth in the profile. Generally hematite formation is maximised at a pH of 7-8, and is favoured by high temperatures, dry conditions, lack of organic matter, and a high rate of release of Fe(II) (Schwertmann & Taylor, 1987; Taylor, 1987; Fitzpatrick, 1987). It has also been noted that small amounts of Al suppress goethite over hematite formation when formed from ferrihydrite.

Although hematite formation and preservation is favoured by warm conditions, small amounts of hematite has also been reported from cold climes (R.W. Fitzpatrick-*pers. comm.*). The common key factors appear to be the formation of ferrihydrite, via rapid release of Fe(III), and its crystallisation to hematite, which requires low moisture and organic matter concentrations and dehydration conditions. Ferrihydrite is thus considered to be a necessary precursor of hematite, which forms through aggregation and dehydration. Hematite has been noted to form under laboratory conditions by the ageing of ferrihydrite (D. Lewis, *pers. comm.*). Hematite can also form by slow

dehydration of other phases such as goethite and lepidocrocite by heating above 200° C.

### 3.3.1.3 *Maghemite* ( $\gamma$ -Fe<sub>2</sub>O<sub>3</sub>)

Maghemite is reddish-brown in colour and ferrimagnetic. In pedogenic environments it is typically concentrated in the upper layers, but it has been noted in some deeper zones as well. It has been demonstrated to form by various mechanisms:-

- i. Through derivation from lithogenic and biogenic magnetite by partial or complete oxidation of Fe(II) to Fe(III). Soil maghemites can contain up to 3% by weight of Fe(II) (or even more if associated with Ti), suggesting incomplete oxidation. Where formed by oxidation of magnetite, transitions in an isomorphous replacement series from magnetite to maghemite with inherited impurities (e.g. Ti) between the two phases may be noted. It has been demonstrated that ultrafine-grained magnetite can form organically in the biosphere (Lowenstam, 1981), both anaerobically and in the presence of oxygen (Lovley *et al.*, 1987). Furthermore, Kirschvink *et al.* (1985, p. 153) noted that extremely fine-grained magnetite is oxidised very easily to maghemite, hematite and other iron oxides, especially at elevated temperatures.
- ii. By dehydration of lepidocrocite. Heating to 300° C will dehydrate lepidocrocite to maghemite. This mechanism is thought to be of minor significance, as lepidocrocite usually forms at depth in mottles.
- iii. By heating of goethite, in the presence of combustible organic matter, at temperatures of 300 - 500° C.
- iv. By analogy with synthetic experiments, maghemite may form by the oxidation of magnetite derived via the intermediate stage of 'green rust' precipitated from Fe(II) solutions at a pH >7.
- v. By reduction-oxidation of hematite in the transient reducing environment that develops in the combustion zone in bush fires (Anand & Gilkes, 1987).
- vi. By biogenic formation in the biosphere (Lowenstam, 1981; Frankel *et al.*, 1979; Towe & Moench, 1981), although magnetite is the



primary magnetic source in biomagnetic systems (Banerjee & Moskowitz, 1985).

Al-substitution in maghemite may be inherited from oxidation of Al-rich magnetite without thermal transformation, or from Al-substituted goethite involving thermal transformation.

#### 3.3.1.4 *Green rust*

Green rust consists of dark green-blue mixed Fe(II) - Fe(III) hydroxides that in synthetic experiments are intermediate phases in the formation of common iron oxides, to which they rapidly oxidise with associated colour changes. It is postulated that green rust may cause the dark green-blue colours in reductomorphic soils (Schwertmann & Taylor, 1987).

#### 3.3.1.5 *Lepidocrocite* ( $\gamma$ -FeOOH)

As a pure mineral lepidocrocite has a dark, rich-purple colour but in soil mottles displays a distinctive orange hue. It is a metastable polymorph of goethite. Al-substitution in lepidocrocite is rare, and small amounts of Al favour the formation of goethite during the oxidation of Fe(II). In synthesis experiments goethite can form via 'green rust' from either Fe(II) or Fe(III) solutions, but lepidocrocite formation requires Fe(II) as a necessary precursor. The occurrence of lepidocrocite is thought to indicate earlier or prevailing reductomorphic conditions, where Fe(II) formed and moved to aerated sites that favoured oxidation of lepidocrocite via green rust. High water supply, low soil temperatures, low evaporation and slow water movement favour Fe(II) mobilisation, from which lepidocrocite may form through reoxidation. Lepidocrocite may form from the pseudomorphous alteration of pyrite in all climatic conditions.

Schwertmann (1985) preferred the view of two competitive processes determining the relative proportions of goethite and lepidocrocite in soils, rather than that of goethite formation from lepidocrocite. This view was favoured because the lepidocrocite-goethite transformation is very slow, and because both can be synthesised in the same system. Lepidocrocite formation is suppressed by high CO<sub>2</sub>, carbonate and Al contents.

### 3.3.1.6 *Ferrihydrite* ( $\text{Fe}_2\text{O}_3 \cdot 2\text{FeOOH} \cdot 2.6\text{H}_2\text{O}$ )

Ferrihydrite is a poorly ordered Fe(III) oxide, that structurally resembles hematite. Its poor crystallinity makes it difficult to identify by XRD. It is typically a precursor to other iron oxides, it has a colour intermediate between goethite and hematite, and occurs either as a brown gel-like precipitate or as a dark reddish brown friable crust. Ferrihydrite formation is favoured by the rapid release and oxidation of Fe(II), restricted complexation by organic matter, high pH and good aeration. The Fe(II) ions are rapidly oxidised in the presence of high concentrations of organic matter and/or silicates. These compounds indirectly favour ferrihydrite formation by hindering the formation of FeOOH phases. However, they also retard the rate of transformation of ferrihydrite to more stable phases.

### 3.3.2 Aluminium oxide minerals

Only three aluminium oxide minerals, gibbsite, boemite and corundum were identified in samples analysed for this thesis. Al-oxides in soil environments appear to be limited to warm and humid climates, particularly in wet areas with good drainage. In weatherable primary or secondary minerals trivalent Al in complex alumino-silicates is released into the soil following the breakdown of the silicate structures. The weathering products may be removed simultaneously through leaching, react together to form pedogenic clay minerals or undergo differential removal, depending on the relative solubilities of the breakdown products.

#### 3.3.2.1 *Gibbsite* ( $\gamma\text{-Al(OH)}_3$ )

Gibbsite is the most common pedogenic form of  $\text{Al(OH)}_3$  and its formation is thought to be favoured by warm conditions, high rainfall and good drainage. In nature it has been found to be typically associated with kaolinite and is claimed to be confined to highly weathered acidic soils. Its formation is thought to be accelerated by the absence of foreign ions. Gibbsite may form through the incongruent dissolution of kaolinite and the removal of Si in solution under acid leaching conditions, the microbial breakdown of kaolinite (McFarlane & Heydeman, in press) or the precipitation of Al-rich gels (Milnes & Farmer, 1987). As well as gibbsite forming from the break down of kaolinite, Si and Al can be reconstituted to form kaolinite.

### 3.3.2.2 *Boehmite* ( $\gamma$ -AlOOH)

Boehmite, which is isostructural with lepidocrocite, is not common in soils, but appears in bauxite deposits together with gibbsite, from which it is believed to form by slow partial dehydration. Temperatures in excess of 130° C are required for laboratory synthesis of boehmite from gibbsite, but in nature the presence of salts in soil solutions may facilitate partial dehydration at lower temperatures.

### 3.3.2.3 *Corundum* (Al<sub>2</sub>O<sub>3</sub>)

Corundum, which has the same structure as hematite, is the ultimate product of heating of gibbsite at 900° C, and its occurrence in soils may be related to inheritance from hydrothermal activity or heating by bushfires.

## CHAPTER 4: FERRUGINOUS AND BLEACHED MATERIALS IN THE MOUNT LOFTY RANGE PROVINCE AND ADJACENT BASINS

### 4.1 Introduction

The Mount Lofty Range Province of South Australia (Figs 4.1 & 4.2) occupies the southern portion of the Adelaide Geosyncline (Fig. 2.3) and includes Kangaroo Island, which is separated from the mainland by an exhumed and drowned Permian glacial trough. The geology of the Mount Lofty Range Province, discussed in Chapter 2, includes variably folded and faulted metamorphosed Precambrian and Cambrian rocks, intrusive granitic rocks, Permian glaciogene sediments, Jurassic basalt and Tertiary and Quaternary terrestrial and marine deposits. The majority of detailed work for this thesis has been carried out in the Mount Lofty Range Province, particularly in examining the field relationships of ferricretes and weathered zones. Some of the ferruginous zones including ferricretes have been dated relatively with respect to rocks and sediments of known ages.

Bulk chemical and mineralogical data are presented in tabular form as appendices, but only those data considered relevant to the genesis of the materials will be discussed in the text. For example, many samples display high SiO<sub>2</sub> contents that reflect inherited quartz, which was largely inert (as indicated by thin section observations), during ferricrete formation, whereas secondary iron and aluminium oxides were active components during its development.

### 4.2 The High Level Summit Surface

When viewed from a great distance the modern summit surface of the Mount Lofty Ranges appears as a remarkably level and continuous surface (Plate 4.1) and has been widely interpreted in the past as an uplifted erosion surface or 'peneplain' capped by a fossil 'laterite profile', variously considered to be of Pleistocene (Horwitz & Daily, 1958), Pliocene (Horwitz, 1960), Early Tertiary (Glaessner & Wade, 1958) or Mesozoic (Daily *et al.*, 1974) ages. Twidale (1983) believed that parts of the summit surface have been preserved in pristine form throughout 200 Ma of exposure to epigene processes. However, the planate nature of the summit surface is more apparent than real, for when examined in detail it displays considerable relief amplitude, and in some areas evidence of Tertiary topography similar to, if not more accentuated than, that of today.

Only very restricted areas are occupied by level to gently undulating topography.

The general summit elevations of the Mount Lofty Ranges vary between about 420 m and 150 m, with occasional points underlain by resistant quartzite bedrock standing up to 50 m higher. Investigations of this thesis revealed that there is not only great variety in the topography of the summit surface, but that there is also considerable diversity in the character of the weathered zones and ferruginised horizons resting on and underlying the surface (Fig. 4.3), and that these are of different origins and ages, reflecting evolving environmental conditions during their formation.

During field investigations various types of weathered and ferruginised materials were identified on and beneath the summit surface. The types of ferricretes encountered include:-

- i. *Vermiform ferricrete*, which contains sinuous worm-like channels, often infilled with light coloured clays that contrast strongly with the surrounding iron-rich material, and give a very distinctive character to the ferricrete (Plate 4.2).
- ii. *Pisolitic ferricrete* that consists of individual pisoliths, many of which display multiple and complex rinds, cemented together to form a coherent rock-like mass (Plate 4.3).
- iii. *Nodular ferricrete*, which is similar to pisolitic ferricrete, except that the individual clasts are larger than pisoliths and rinds are generally thin or absent (Plate 4.4).
- iv. *Vesicular to massive ferricrete*, which consists of a dense, massive iron oxide-rich material containing numerous small cavities that are usually filled with clays, but where these have been washed out the small vesicles or voids are very prominent (Plate 4.5).
- v. *Slabby ferricrete* that consists of horizontally disposed plate-like masses of ferricrete up to several cm thick and separated by clays (Plate 4.6).
- vi. *Ferricreted sediments*, which consists of iron oxide impregnated and indurated sediments, in which original sedimentary materials, fabrics and structures have been preserved (Plate 4.7). In some instances the sediments can be recognised as occupying former fluvial channels.

- vii. *Ferricreted bedrock*, which can be recognised as such by the preservation of metamorphic and sedimentary structures (Plate 4.8) and distinctive minerals. The last two types of ferricretes (ferricreted bedrock and ferricreted sediments) in the Mount Lofty Ranges can be distinguished in exactly the same way as metamorphic rocks and sediments can be differentiated.

Other ferruginous and weathered materials associated with the summit surface include ferruginised mottled zones in both sediments (channel fills) and basement rocks, bleached and weathered bedrock and loose pisoliths at or near the surface. The summit surface will be discussed under headings of the dominant natures of the ferricretes and other ferruginised and ferruginous and weathered materials studied, the distributions of which are shown on Figures 4.1, 4.2 and 4.3. Locations of sites discussed are given with alphanumeric grid references.

#### 4.2.1 Ferricretes

##### 4.2.1.1 *Nodular, Pisolitic and Vermiform Ferricretes*

###### 4.2.1.1.1 *Spring Mount-Mount Cone area (J29)*

This area is among the highest in the ranges where ferricretes are well developed, and has been exposed to subaerial processes of weathering and erosion over long periods of geological time. The landsurface is approximately 400 m asl and is underlain by weathered materials up to 69 m thick (Bourman, 1973). The area has been exposed to the terrestrial environment since the Permian glaciation (Milnes *et al.*, 1985). The summit surface stood above the influence of the high Miocene sea level in the area, evidence of which occurs up to 230 m asl in the Upper Hindmarsh Valley and 235 m asl in the Myponga Basin (Furness *et al.*, 1981). The relationships between the various types of ferricretes and Tertiary fossiliferous limestone, which crops out in the vicinity, are illustrated in cross section in Figure 4.4.

The ferricretes have only a sporadic distribution. More commonly there is only a thin surface layer of pisoliths in and below the A-horizon of the soil, which directly overlies weathered and mottled bedrock. Where ferricrete does occur it occupies gently sloping to undulating sections of the high level surface. The crusts occur over a variety of materials that include weathered bedrock.

Mount Cone (Willunga MR 783802) proper stands above the general level of the summit surface (Fig. 4.4; Plate 4.9); it is composed of Precambrian gneiss that has been weathered and partly ferruginised, but the original gneissic bedrock structures are clearly evident in hand specimen. The mineralogical composition of this rock, which includes large amounts of muscovite and feldspar (BOU 301) as shown in Table 4.1 (Appendix I), reflects its bedrock character. Approximately 1 km east of Mount Cone is a near level surface that is partially capped by a *nodular* variety of ferricrete and forms a small mesa (Plate 4.10). The chemistry and mineralogy of this material (BOU 303) is quite different from that of the weathered bedrock of Mount Cone, as it has twice the  $\text{Fe}_2\text{O}_3$  content, less  $\text{SiO}_2$  and higher  $\text{Al}_2\text{O}_3$  (Fig. 4.5). The mineralogical contrast is also very marked, with BOU 303 having a high concentration of gibbsite, goethite and hematite and a small amount of maghemite, while the ferruginised bedrock of Mount Cone (BOU 301) is dominated by muscovite and quartz with smaller amounts of kaolinite, feldspar, hematite and goethite. The ferricrete on the small mesa (BOU 303) is composed of weathered material and/or soil in which there is no evidence of original bedrock structures. Both the chemical (Fig. 4.5) and mineralogical compositions of the nodules (BOU 423) and the matrix material (BOU 424) of this ferricrete are similar, suggesting essentially an *in situ* mode of formation.

If it is the case that these two contiguous areas have been exposed to similar extended periods of weathering, and there is no evidence that this is not the case, then why should there be such marked contrasts in their physical, chemical and mineralogical characteristics? The answer almost certainly lies in local variations in topography and drainage. The nodular ferricrete has developed essentially in a local environment where there was the accumulation of materials weathered and eroded from higher surrounding areas such as Mount Cone. This material was subjected cumulatively to far more extensive weathering than the bedrock at Mount Cone, where fresher rock was perpetually subjected to exposure at the surface.

On the western flank of the mesa carrying the nodular ferricrete there is a sharp break in slope, at the base of which ferricrete boulders of *vesicular* character (BOU 302) occur. This ferricrete differs markedly from the nodular variety on the mesa, displaying a very high total  $\text{Fe}_2\text{O}_3$  content with a dominance of goethite, and minor amounts of hematite. This accumulation of iron oxides occurred at a point about 10 m below the level of the mesa (Plate

4.11) partially capped by the nodular ferricrete, and demonstrates the progressive development and modification of the present summit surface. It also illustrates the close proximity of different types of ferricretes that have different physical, chemical and mineralogical characteristics (Fig. 4.5), depending on variations in local environments.

On the Spring Mount Plateau (Bourman, 1973) at the Spring Mount Trig. (Willunga MR 767753) some of the ferricrete (BOU 370) (Table 4.2; Fig. 4.5) has a similar nodular morphology to that on the small mesa near Mount Cone. Other ferricrete at Spring Mount is of a *vermiform* type (BOU 366), and on the surfaces of isolated boulders of vermiform ferricrete there are secondary accumulations of laminated iron oxides (BOU 309) forming thin rinds. These probably indicate a later phase of iron oxide precipitation affecting a pre-existing ferricrete. Both the vermiform and nodular types at Spring Mount contain gibbsite, but the laminated coatings on isolated boulders do not.

#### 4.2.1.1.2 Parawa Plateau area (F32)

On the summit surface at about 360 m asl near Parawa (Torrens Vale MR 604613), sporadic masses of *pisolitic* to *vermiform* ferricrete occur. In some places the ferricrete forms the margins of breakaways. Occasional shallow quarries, surface scrapes and road cuts indicate that it is up to 80 cm thick and overlies weathered materials. However, these exposures also demonstrate the non-continuous nature of the ferricrete. The outer surfaces of the ferricrete in this area sometimes have the appearance of pisolitic ferricrete, but the body of the ferricrete masses invariably display vermiform fabrics superimposed on fragmental and pisolitic structures. Furthermore, glazed goethitic coatings form thin rinds on some exposed surfaces. These observations suggest complexity in the formation of the ferricretes. Analyses of samples of vermiform ferricretes from this locality (BOU 18, BOU 21, BOU 339, BOU 343) (Table 4.3) all show similar  $\text{Fe}_2\text{O}_3$ ,  $\text{SiO}_2$  and  $\text{Al}_2\text{O}_3$  contents (Fig. 4.6) and distinctive mineral assemblages including, goethite, gibbsite, hematite, micas and kaolinite, as well as discrete maghemite clasts. The common occurrence of high proportions of gibbsite in these crusts corresponds to analyses of samples from the Mount Cone-Spring Mount area, and favours the view of protracted weathering having affected these high areas. Both kaolinite and gibbsite infill tubules in the distinctive vermiform ferricrete.



Thin section examination of vermiform ferricretes reveals patches of iron oxides and zones of light coloured clays (kaolinite and gibbsite) infilling the intervening areas (Plate 4.12). The iron-rich zones comprise vague bands and glaebules that, in places, contain very fine quartz grains. Laths of mica, or pseudomorphs after mica, occur in the matrix. They do not display a preferred orientation as would be expected if the sample was of *in situ* basement rock, but their presence suggests that they have derived from pre-existing bedrock. There is a tendency for the micas to be aligned parallel to the surface coating but to be randomly dispersed elsewhere (Plate 4.13). The thin section observations suggest that the material could represent a palaeosol. In places the ferricrete has a detrital appearance and contains small clasts of maghemite.

Even on this pronounced plateau surface (the Parawa Plateau; Brock, 1964; 1971) the thickest development of vermiform ferricrete occurs on low angle slopes away from the plateau summit, rather than on the summit itself. This is taken to indicate preferential enrichment and accumulation of iron oxides in locally favourable situations, rather than the uniform development of ferricretes over extensive areas. In a drilling program on the summit surface in this area (Keeling, 1985), 30 boreholes were sunk into the weathered clays underlying the plateau but not one intersected ferricrete. The ferricrete crusts are thus relatively rare and sporadic, even on a surface which might be regarded as owing its preservation to a ferricrete capping (see for example, Twidale, 1983).

It has been demonstrated that the summit surface of Fleurieu Peninsula has been exposed to terrestrial conditions for a very long period of geological time (Milnes, *et al.*, 1985). The chemical, mineralogical and micromorphological characteristics of the nodular, pisolitic and vermiform ferricretes associated with this landsurface reflect the effects of protracted exposure to subaerial processes. They are not unmodified, ancient crusts preserved throughout 200 Ma of epigene attack as has been suggested by Twidale (1976; 1983). On the contrary, the evidence indicates the operation of continual weathering and erosion and the progressive development and modification of these ferricretes.

#### *4.2.1.1.3 The Summit Plateau Surface of Kangaroo Island*

Pisolitic to vermiform ferricrete occurs over many areas of the summit surface of Kangaroo Island. Bauer (1959) mapped the *Eleanor Sand*, which includes

pisolitic to vermiform ferricrete, on remnants of the undissected plateau up to 275 m asl (Fig. 4.2). The Eleanor Sand on the upland plateau surface of Kangaroo Island was described by Northcote (1946) as a relic of 'lateritisation', a fossil Pliocene soil exhibiting the 'normal laterite profile' of southern Australia (Stephens, 1946).

The following is a profile description of the Eleanor Sand:-

*A1 horizon* : 0-10 cm of non-wetting, organic-rich, slightly loamy sand with a 2.5 Y 3/1 colour.

*A2 horizon* : 10-35 cm bleached coherent but brittle sand with rare maghemitic gravels. Colour 10YR 5.5/2 (moist); 10YR 8/2 (dry).

*B1 horizon* : Massive sandy clay with ferruginous gravels at 35 cm. Mottle-free. Colour 10YR to 2.5Y 6/4

*B2 horizon* : Mottled, gravel-free clay. Main colour 2.5Y 7/3 with mottles (7.5YR 5/8), overlying 30 cm of consolidated gravels in matrix of slightly loamy sand, forming sheet 'laterite' (ferricrete). Colour 10YR to 2.5Y 6/4.

*Classification:* Dy 5.84 (with sheet 'laterite').

In places the pisoliths in the B2 horizon are cemented together to form a continuous pisolitic to vermiform ferricrete crust, and this ferricrete can grade laterally into unconsolidated pisoliths.

It should be noted that the full profile of the Eleanor Sand ranges over only 2 m (Northcote, 1946), and its associated ferricrete, which is only about 30 cm thick, probably developed as a pedogenic horizon having concentrated in preferred parts of the landscape. This profile is not compatible with the thick vermiform ferricrete on parts of Fleurieu Peninsula, although it has been equated with such by some workers (e.g. Twidale, 1983). Northcote & Tucker (1948) mapped the 'lateritic plateau' of Kangaroo Island on the occurrence of the Eleanor Sand, which allegedly provided the detritus for younger soils such as the Seddon Series. In places, however, the Eleanor Sand occurs below the level of the soil it is alleged to have contributed to. For example, it occurs at an elevation of about 80 m asl north of Murray Lagoon as well as on the high plateau surface at up to 260 m asl (See Fig.4.2). The chemical and mineralogical compositions of a typical sample (BOU 101) of vermiform ferricrete from the Eleanor Sand is shown in Table 4.3. In thin section BOU 101

appeared as segregations with coatings displaying complex iron-aluminium phases. Islands of clay and quartz surrounded by goethite are interpreted as the result of the preferential penetration of a soil or sediment by iron oxides. The thin section also shows that the fabric of the crust is a fine-grained material with wisps of parallel bedding, and in places these have been removed to produce cavities. Minerals in this sample include gibbsite, goethite, kaolinite, hematite and maghemite, which are distinctive of vermiform ferricretes.

Fossiliferous Early Miocene limestones have been reported within the dissected part of the 'lateritic' plateau of Kangaroo Island by Milnes *et al.* (1983), at "Willandra" (Fig. 4.2) about 10 km southeast of the Parndana township at about 125 m asl (Seddon MR 097300). The limestone caps at least three small unweathered bedrock knolls, which are surrounded by weathered and mottled bedrock and discontinuous exposures of vermiform ferricrete. The resistance of the unweathered bedrock highs may account for the preservation of the limestone. The relationships between the ferricrete and limestone are not clear but the absence of ferricrete fragments in the limestone favours the view that ferricrete formation has taken place after the deposition of the limestone, possibly in the Late Miocene and Pliocene. Thin sections of the vermiform ferricrete (Plates 4.12 and 4.14) show that it appears to be formed of discrete bodies or segregations with concentric layers, but the main difference between the segregations and the matrix is that the segregations contain more iron oxide. Minerals identified in this sample (BOU 126) (Table 4.3) included goethite, gibbsite and small amounts of maghemite (detected by a magnet). The presence of smectite and only small amounts of kaolinite suggest that the ferricrete has not been affected by intensive weathering, or neoformed smectite has resulted from a later phase of resilication.

A short distance away from the limestone-capped ridge is a limestone-free hillock at a slightly higher elevation. This carries a brown sandy soil mantle up to 40 cm thick, with a surface and near surface accumulation of pisoliths that are strongly magnetic (BOU 130) (Table 4.3). Examination in thin section reveals that some of these are complex pisolith-in-pisolith structures with silt-sized quartz occurring around the edges of some of the pisoliths, the cores of which contain coarser quartz fragments. Generally the pisoliths have a sandy quartz grain framework impregnated with iron oxides. Often the cores are of hematite and maghemite with thin rims of goethite and clays containing

gibbsite. The presence of gibbsite and the complex character of the pisoliths suggest that they have had a long history of evolution and were probably derived from pre-existing ferricretes.

The field and laboratory evidence suggests that the limestone was once more extensive than at present, and following the marine regression, pisoliths from higher ground were transported onto the limestone surface. Lowering of the limestone surface by weathering and erosion led to the stranding of the pisoliths above the general level of the surrounding landscape, which underwent further lowering, and subsequently a sporadic vermiform ferricrete developed around the flanks of the limestone knolls. In view of the suggested tectonic tilting of the summit surface of Kangaroo Island (Northcote & Tucker, 1948) it is not possible to be certain of the complete former extent of Early Miocene limestone over the present summit surface of Kangaroo Island, and it is possible that even higher Middle Miocene sea levels existed on Kangaroo Island as on the mainland (Lindsay, 1986). See also Vail & Hardenbol (1979), Vail & Mitchum (1979) and Vail *et al.* (1977), who suggested even higher Tertiary sea levels, in the Late Miocene, of which no evidence has yet been located in South Australia. Regardless of this, large areas of the modern summit surface have developed only after the erosion of the Early Miocene limestones. This is reflected in the development of the Eleanor Sand, allegedly a 'fossil laterite profile' (Northcote, 1946), on it. Moreover, the characteristics of the weathering profiles on the summit surface are quite different to those under the basalt near Kingscote (See section 4.3.1.1.1 The Mount Taylor Plain), so that the correlation of the two by Twidale (1983) is unwarranted.

Sporadic outcrops of vesicular ferricrete (bog iron ore) occur on the plateau, and elsewhere accumulations of pisoliths rest directly on weathered basement rocks. Hence the character of the ferruginous materials on the plateau surface is very variable, suggesting great complexity in the development of part of the summit surface of Kangaroo Island.

#### **4.2.1.2 Ferricreted Sediments**

##### **4.2.1.2.1 Glen Shera Plateau**

The Glen Shera Plateau (Willunga MR 798874) forms a distinctive topographic unit capped, in places, by a thick ferricrete crust at about 350 m asl (Fig. 4.1; J28). It was regarded by Maud (1972) as part of the original high plateau surface, although it is underlain by relatively soft Permian glacial

sediments. He considered that the surface displayed the character of a broad open valley contiguous with the summit surface. This interpretation may not be unreasonable, because the highest surrounding country only extends up to about 400 m asl.

Unfortunately, there is no direct indication of the age of the surface forming the Glen Shera Plateau. Remnants of a former high level broad valley floor extend to the southwest from the Glen Shera Plateau following the line of a tributary of the modern Myponga River. This could represent the remnants of a pre-Tertiary drainage line. However, the Tertiary seas in this area extended at least up to 235 m asl and possibly up to 300 m asl so that the valley may have developed in relationship to this base level during the Tertiary.

In hand specimen the ferricrete that underlies the Glen Shera Plateau appears to have formed via the impregnation of sand-sized quartzose sediments by iron oxides. It has the same fabric as the underlying, unconsolidated Permian sediments. This interpretation is confirmed by chemical and mineralogical analyses (BOU 306) (Table 4.4; Fig. 4.7) as well as thin section observations. The  $\text{Fe}_2\text{O}_3$  content of 12% is accounted for by a dominance of goethite and minor hematite. No gibbsite was detected, and the small amount of  $\text{Al}_2\text{O}_3$  (1.63%) determined could be present in kaolinite, which was identified by XRD. In thin section the sample is a poorly sorted coarse sandy to gritty sediment, consisting of sub-angular quartz grains in a dark ferruginous groundmass. In this, scattered fine hematite crystallites occur in clay patches that occupy voids (Plate 4.15).

#### *4.2.1.2.2 Cut Hill Road, Kangarilla (Fig. 4.1; L23)*

At an elevation of about 380 m on the Cut Hill Road (Noarlunga MR 891084) on the modern summit surface, sporadic blocks of ferricrete occur (BOU 57) (Table 4.4). The ferricrete is essentially a sandstone, with some larger quartzose clasts, cemented by iron oxides. This is reflected in the dominance of  $\text{SiO}_2$  (70.4%) and  $\text{Fe}_2\text{O}_3$  (23.06%), with only a small amount of  $\text{Al}_2\text{O}_3$  (1.72%) (Fig.4.7).

By extrapolation from the regional geology and shallow exposures, the ferricrete overlies weathered Precambrian metasedimentary rocks. The dominant minerals are quartz, reflecting its origin as a quartzose clastic sediment, with hematite as the main iron oxide and a lesser amount of goethite. Maghemite was only detected by magnetic response. The relatively high concentration of hematite is typical of many high level ferruginised

sediments within the Mount Lofty Ranges. For example, a ferricrete on the flanks of Mount Gawler (540 m asl) (Onkaparinga MR 016487) at an elevation of some 410 m asl, displays similar proportions of hematite and goethite (BOU 397) (Table 4.4).

#### *4.2.1.2.3 Knott Hill (Fig. 4.1; L25)*

At Knott Hill (Noarlunga MR 887033) at an elevation of some 340 m asl, quartz-rich glacial sediments of Permian age have been variably ferruginised to form discontinuous ferricretes (BOU 359). The character of these ferricretes is reflected in their bulk chemistry and mineralogy (Table 4.4). At this site the ferricretes are not well developed, with iron oxides fairly uniformly dispersed throughout the porous sediments. The majority of equivalent summit surface ferricretes analysed generally display higher contents of hematite than does a sample from this locality. The higher goethite content of a Knott Hill sample may reflect dissolution of hematite and reprecipitation as goethite (Schwertmann, 1985). Conversely, original conditions during iron oxide impregnation may have favoured goethite formation. Although Knott Hill occurs on the modern summit surface, it is developed at a relatively lower elevation in easily eroded glacial sediments. The field and laboratory evidence is interpreted as signifying development of the ferricrete at Knott Hill at a later stage than that at nearby Cut Hill.

#### *4.2.1.2.4 Parawirra (Fig. 4.1; O14)*

Analyses of ferricrete sampled from the summit surface at Parawirra (Barossa MR 004627), 260-270 m asl (BOU 380) (Table 4.4) displayed constituents typical of an iron oxide-cemented quartzose sediment. In thin section the sample comprises a coarse, closely packed quartz-rich sediment with interstitial opaque iron oxides and clays containing relic mica crystals. Goethite is the dominant iron oxide mineral in the matrix: darker areas of the matrix appear hematitic, but in detail the matrix is quite complex displaying a mixture of opaque and non-opaque (silicate) crystals. The ferricreted sediment overlies mica-quartz schist Precambrian bedrock, which is not extensively weathered.

#### *4.2.1.2.5 Humbug Scrub (Fig. 4.1; O19)*

Ferricrete (BOU 4), collected from near an aircraft landing field at Humbug Scrub (MR Barossa 985501) at an elevation of 410 m asl is a sediment with quartz grains and some rock fragments set in a very dense matrix of iron oxides. This interpretation is confirmed by chemical and mineralogical

analyses (Table 4.4). This material occurs on a gently westward sloping landsurface below higher resistant salients of the ranges up to 520 m high, which carry no ferricrete. It has developed above Precambrian bedrock of the Saddleworth Formation, which consists dominantly of metasiltstones.

In thin section, the framework grains of clastic minerals, are poorly sorted (fine to coarse), angular and shard-like. Accessory minerals include tourmaline and andalusite, and there are rock fragments with micas. The matrix encompasses the detrital grains and consists predominantly of well crystallised hematite, which invades the embayed borders of individual grains of quartz and tourmaline (Plate 4.16). The hematite occurs as small crystals, which exhibit red internal reflections in incident polarised light (Plate 4.17), as well as in thin zones around voids. The angular and embayed character of the framework grains suggest that some of the sediment has developed through *in situ* breakup of larger grains. In this case there may have been partial dissolution of some of the quartz grains.

#### 4.2.1.3 Ferricreted Bedrock

There are very few ferricretes formed by the ferruginisation of bedrock (See Figure 4.1). The best example of such a ferricrete occurs in the North Mount Lofty Ranges, and appears to have developed in Precambrian metasiltstone. Here a massive ferricrete crust (BOU 386) (Table 4.5) (Fig. 4.9) occurs on a ridge at about 340 m asl, some 3 km west of Koonunga (Kapunda MR 130929; Fig. 4.1; Q8), but below the level of the high land nearby. In thin section this crust contains very angular quartz grains arranged as in metasedimentary rocks. In detail the matrix is composed of masses of hematite crystallites set in yellowish clay plus goethite. Well crystallised hematite also occurs along fractures. Small spherical bodies in the matrix appear to coalesce along fractures to form continuous mamillary textured coatings, which have laminar goethite and thin hematite rinds (Plate 4.18).

#### 4.2.1.4 Slabby ferricretes

##### 4.2.1.4.1 Chandlers Hill (Fig. 4.1; K23)

At an elevation of about 360 m asl a profile including ferricrete (Plate 4.6) has been exposed by a road cutting at Noarlunga MR 82 3144. The profile has been described and figured by Ward (1966, pp. 92-93), and is overlain by soils classified by Ward (1966) as the *Kuitpo Loamy Sand* and the *Chandler Loamy Sand* (Fig. 4.8). Quartz veins through parts of the section suggest that it has

developed through the weathering of the underlying Precambrian metasiltstone (Figure 4.9).

Samples were analysed from the B horizon of the Kuitpo Loamy Sand, and from the slabby ferricrete and its surrounding matrix below the Chandler Loamy Sand. Samples of the slabby ferricrete (BOU 20, BOU 60 and BOU 429) compared with the surrounding material (BOU 430) (Table 4.5) (Figure 4.9) have higher concentrations of  $\text{Fe}_2\text{O}_3$ ,  $\text{Al}_2\text{O}_3$  and lower  $\text{SiO}_2$ . Minerals identified in the slabby ferricrete, in decreasing order of abundance, include quartz, goethite, hematite, kaolinite, feldspar, vermiculite, anatase and a small amount of gibbsite. The enclosing material differs from the ferricrete in that kaolinite is more abundant, hematite is the dominant iron oxide, and smectite and feldspar are present. No gibbsite was identified in the matrix material. A sample (BOU 398) of the B horizon material of a yellow podzolic duplex soil [Dy2.11 (no mottles) to Dy3.11 (with mottles)] that occurs near the surface contains quartz, kaolinite, goethite, anatase, feldspar, and possibly gibbsite, all of which could have derived from the underlying materials. Thus it appears that the soil has developed on previously weathered materials.

In thin section slabby ferricrete fragments (BOU 20) are essentially clay-rich materials containing poorly sorted and scattered quartz grains varying from silt to sand-sized. Together with very fine kaolinitic clay, iron oxides (dominantly goethite) fill fracture zones and coat voids. Fine equigranular hematite occurs as crystallites in the goethite plus clay matrix, and hematite-rich zones have resulted from the coalescence of the individual crystallites (Plate 4.19). Higher concentrations of hematite than goethite are present in the incoherent material enclosing the ferricrete fragments, which may suggest that the hematite has formed at a later stage than the goethite, or that it was the dominant iron oxide formed as a result of the prevailing environmental conditions.

Downslope, the slabby ferricrete progressively dips below the land surface so that it is overlain by mottled sandy clays. During winter, a spring discharges at the ferricrete level, and it is possible that such a mechanism, operating in the past, was responsible for the lateral transport of iron oxides in solution, from points upslope, to be precipitated above the water table or impermeable zones to develop this particular type of ferricrete.



#### 4.2.1.5 Vesicular to Massive Ferricretes

##### 4.2.1.5.1 Peeralilla Hill (Fig. 4.1; K30)

At an elevation of about 290 m on the summit surface of Fleurieu Peninsula there occurs the most massive accumulation of iron oxides in the South Mount Lofty Ranges (Heath, 1962; Bourman, 1973). Superficially the mine and quarry exposures on Peeralilla Hill (Willunga MR 837717) resemble profiles described in the literature as 'lateritic', and Heath (1962) regarded the ferricrete at Peeralilla Hill as a 'more ferruginous variant of the Tertiary laterites which cap many of the hills and ridges of the Mount Lofty Ranges' and commented that the 'high alumina, water and moderate silica contents' are characteristic of 'laterite' deposits. However, close field inspection and laboratory analyses reveal that the materials comprise a stratigraphic sequence of deposits of different ages.

The thick ferricrete crust at Peeralilla Hill does not occur near the summit of the hill, but in a bedrock depression at a lower elevation (Fig. 4.10; Plate 4.20). The crust near the surface is composed dominantly of vesicular to massive ferricrete, but at depth, in places, takes on a more earthy texture, and indurated iron oxides are concentrated along steeply dipping laminar structures (10 mm thick), with intervening ferruginous clay-rich zones, that are composed of smectite, kaolinite, hematite and goethite, (Plate 4.21). The laminated structures are similar to features commonly noted in association with many karstic bauxite deposits (Prof. I. Valeton-*pers. comm.*). Large isolated blocks and boulders of vesicular ferricrete as well as smaller clasts of ferruginous material also occur within this lower zone of iron enrichment. Many ferricrete fragments and pisoliths at the surface contain maghemite, as indicated by magnetic attraction. Magnetic clasts are particularly prevalent near sites affected by burning during modern bushfires.

Sands and included pebbles and larger clasts of quartzite are exposed in a dam site to the north of the iron crust, and may be Permian glacigenic sediments. Drilling through the surface crust has established the occurrence of sandy sediments below it. A surface scrape cut through the crust (Plate 4.20) has exposed white and green, calcareous clays, and XRD analysis has revealed the presence of both barite and calcite in them (BOU 32, BOU 33) (Table 4.6) (Fig. 4.11). The white clayish sediments (BOU 33) in thin section contain rounded to sub-rounded and sub-angular quartz grains ranging from silt to sand-sized, set in a matrix of calcite plus smectite and kaolinite, which coats the grains

and fills cavities and fractures (Plate 4.22). The calcite has the form of rounded structures composed of fibrous radiating crystallites. The green coloured clays (BOU 32) consist dominantly of kaolinite and barite ( $\text{BaSO}_4$ ).

The presence of calcite and barite may argue against leaching and the operation of intensive weathering processes in the formation of the ferricrete crust, although they may have precipitated out of ground waters after the ferricrete developed. Nevertheless, the high total  $\text{Fe}_2\text{O}_3$  contents of 67.7% (BOU 10) and 69.8% (BOU 11) (Table 4.6), suggest iron oxide influx from lateral sources into a former depression. Thus the sequence at Peeralilla Hill indicates that the deposition of iron oxides here occurred in a depression in an ancient landscape. Comparison of the Peeralilla crust with samples of vesicular ferricrete (BOU 5, BOU 6) (Table 4.6; Fig. 4.11) collected from the modern valley floor at Mount Compass (MR Willunga 818861) reveals similarities in both mineralogy and chemistry (Section 4.3.1.3.1). In thin section the Mount Compass ferricrete is shown to consist principally of iron oxides with occasional sand to silt sized quartz grains. Elongated and rectilinear cavities occur through the groundmass (Plate 4.23). At high magnifications very distinctive cellular structures (Plate 4.24), represent former plant material entirely replaced by iron oxides.

Thin sections of samples of ferricrete from Peeralilla Hill reveal similar elongated rectilinear cavities (Plate 4.25), and features that generally resemble plant cells replaced by iron oxides (Plate 4.26), but these are not as clear as those in the Mount Compass samples.

The chemical, mineralogical, thin section, topographic and stratigraphic evidence favours a view that the crust at Peeralilla Hill formed essentially as a sedimentary deposit, primarily from the precipitation of iron carried in solution, but with some physical concentration of iron as well, in a depression on an old landsurface. However, since its formation and exposure the original deposit has been modified by weathering, erosion, burning, deposition and remobilisation and reprecipitation of iron oxides.

Some of the complex history of the Peeralilla Hill crust is reflected in its mineralogy. Typically iron oxides, chemically precipitated in freshwater swampy environments are composed exclusively of goethite, exhibiting low aluminium substitution (Fitzpatrick & Schwertmann, 1982), and while this is

the dominant mineral in the Peeralilla Hill crust, small amounts of hematite, kaolinite, quartz and smectite are also present. The quartz is probably detrital as may be the kaolinite and smectite, but these may also have formed by weathering of primary detrital minerals after the deposition of the sediments. Hematite is not usually associated with such 'bog-iron ore' deposits in Europe (R.W. Fitzpatrick-*pers. comm.*), and its occurrence at Peeralilla Hill may reflect slightly warmer conditions that favoured the crystallisation of some hematite from ferrihydrite that precipitated from Fe(II) influxed in solution. No maghemite was detected by XRD, but all samples showed a very slight reaction to a strong magnet. The presence of maghemite in the near surface layers could have resulted from heating by bushfires, by which process goethite can be transformed to maghemite. Microscopic examination of thin sections of the Peeralilla Hill crust provides further evidence for its complex development as small hematite pellets occur in a goethite matrix, and voids lined with crystalline goethite suggest various modifications to the crust, representing several generations of iron oxide mobility.

Despite the fact that the Peeralilla Hill crust is considered to have developed essentially by chemical precipitation of iron oxides, there had been some physical incorporation of iron-rich materials into the depression. Moreover, the crust is of some antiquity. There is no direct evidence for the age of the Peeralilla crust, nor for the origin of the calcium carbonate or barite, which underlies it. However, the surviving outcrops of Miocene limestone in the adjacent Upper Hindmarsh Valley stand only some 60 m below the ferricrete crust at Peeralilla Hill. The amount of erosion of the Miocene limestone is unknown as is the precise level to which the Miocene seas reached in this area. However, ferricrete benches near Myponga range up to 290 m asl, and they may represent former Tertiary backshore deposits, now ferricreted. Thus it is possible that the calcite is related to that former higher sea level, which would place the initiation of crust formation here into the Middle to Late Tertiary. Thus it may be younger than the higher sections of the summit surface, which were exposed to epigene processes prior to this time.

#### 4.2.1.5.2 Anstey Hill Iron Mine (Fig. 4.1; M17)

On the modern summit surface at an elevation of about 400 m at Adelaide MR 938430, iron ore has been mined in the past. Within the area of the mine, ferricretes, range from vesicular and massive 'bog-iron ore' (BOU 337, BOU 340, BOU 342), occurring in sub-surface positions in mine shafts, to iron-

impregnated sandy sediments (BOU 338, BOU 345, BOU 350, ) (Table 4.7; Fig. 4.12), collected from or near to the surface. Generally the vesicular to massive ferricretes have relatively high  $\text{Fe}_2\text{O}_3$  contents, an iron oxide mineralogy dominated by goethite, with rare hematite and no maghemite. Sample BOU 340 has a higher  $\text{SiO}_2$  content than the other samples of vesicular ferricrete, which is explained by the occurrence of secondary silica rather than by the inheritance of quartz grains. On the other hand the iron-impregnated quartzose sandy and gritty sediments generally have lower  $\text{Fe}_2\text{O}_3$  contents, greater mineralogical diversity, higher contents of hematite and occasional maghemite. The occurrence of maghemite may reflect burning during a relatively recent severe bushfire in the area. This could also be responsible for some of the hematite content.

At this site there is no evidence of a present or former 'lateritic profile'. Moreover, the mineralogy and chemistry of the ferricrete samples at Anstey Hill does not reflect intensive weathering but supports the interpretation of ferricrete formation by the ingress of iron oxides in solution into a mixed quartz-rich clastic and organic environment, under non-leaching conditions. Some later surface transformations have probably occurred through bushfires.

#### 4.2.1.5.3 *Kangaroo Island summit surface*

In some locations on the high summit surface of Kangaroo Island, such as at Stokes Bay MR 980047 at an elevation of about 180 m asl *vesicular* ferricrete occurs (Fig. 4.2), which has developed by the accumulation of iron oxides carried into a former relatively low freshwater swampy point in the topography that acted as a sink for the collection and precipitation of iron oxides. This interpretation is supported by an analysis of a sample of this material (BOU 147) (Table 4.8). The high iron content (59.3%  $\text{Fe}_2\text{O}_3$ ) and an iron oxide mineralogy dominated by goethite, with only minor hematite and no maghemite, is typical of equivalent ferricretes resulting from such chemically precipitated accumulations.

#### 4.2.1.5.4 *Almanda Hill (Fig. 4.1; L22)*

The iron bleached from bedrock at higher elevations may have provided a source for iron oxide enrichment at another occurrence of vesicular ferricrete on the summit surface, near Almanda Hill and 'Engadene' homestead (Noarlunga MR 876166), where the ferricrete has been mined. This material (BOU 353) (Table 4.8) has a vesicular macro-fabric, a high total iron content

(76.4%) and an iron oxide mineralogy dominated by goethite, with only minor amounts of hematite. Material sampled from the surface (BOU 348) contained a similar iron content, but displayed a different mineralogy dominated by hematite and maghemite. BOU 348 contains about 5% more  $\text{Al}_2\text{O}_3$ , but the kaolinite content of both samples appear similar, so that some degree of aluminium substitution may have occurred in goethite.

#### 4.2.2 Ferruginous Channel Fill Materials

Channel fill materials comprise a variety of sediments (sands, gravels, clays, pisoliths, and other ferruginous clasts) deposited in former stream channels on the summit surface. Ferricretes are not associated with these channel fills, and iron oxides in them are either concentrated into mottles or spread diffusely throughout the fill materials.

##### 4.2.2.1 Mount Desert area (Fig. 4.1; H33)

The complex development of the summit surface of Fleurieu Peninsula is further indicated near Mount Desert (Torrens Vale MR 714609), where a road cut at about 250 m asl has exposed infilled channels (Fig. 4.3; Plate 4.27). The channels have been cut into kaolinised and iron-mottled Kanmantoo Group metasedimentary rocks of Cambrian age, and are infilled with detritus that includes fragments of the bedrock mottles (BOU 422) (Table 4.9; Fig. 4.13) and pisoliths with multiple rinds that occur at the base of the channel. The palaeochannel is exposed on both sides of the road cutting thereby demonstrating that it is a true channel and not simply a basin.

The pisoliths at the base of the channel are identical in all respects to pisoliths that occur to the west of this site and at a higher elevation on the summit surface, where they form a 1 m thick deposit in conjunction with bedrock fragments and other detrital materials (Torrens Vale MR 583617) (Plate 4.28). The individual pisoliths have characteristic goethitic surface rinds (Plate 4.29). Undisturbed samples taken across the contact of the channel base and its infill (Plate 4.30) do not reveal any indication of incipient *in situ* development of pisoliths in the weathered bedrock below those in the channel (Plates 4.31, 4.32.).

The pisoliths in the channel contain maghemite. It can be speculated that perhaps the pisoliths were formerly in a surface or near surface situation, where heating in the presence of organic material can transform goethite to

maghemite. Thus the occurrence of maghemite-rich pisoliths at a depth of some 6 m below the present ground surface is interpreted as evidence for transport from a higher section of the summit surface and subsequent burial near the base of a former channel.

It is noteworthy that the mineralogy of the pisoliths varies on opposite sides of the road cut, even though they are in similar positions in the palaeochannel. Pisoliths from both sides are maghemitic, but those on the southern side are soft and have hematite as the dominant iron mineral (BOU 372), whereas those on the north are dominated by goethite (BOU 371) and are relatively hard (Table 4.9). Goethitic rinds on pisoliths are generally regarded as the result of dissolution and reprecipitation of iron oxides from the pisolith itself or the accretion of fresh layers of iron oxides on the pisolith surfaces (Schwertmann, 1985). Both of these processes are thought to occur in soil environments. Hence it is possible that the hematite-rich pisoliths were not affected by these soil processes, but it would be extremely fortuitous for these pisoliths to have accumulated exclusively in one part of the channel. Another possibility is that the hematitic pisoliths were subjected to a second period of heating after deposition in the stream channel, with heat being concentrated by the burning of a tree stump or root that only affected the pisoliths nearby. This could account for the lack of a goethite rind, which would have been transformed to hematite and/or maghemite. Alternatively, another process involving *in situ* dissolution of goethite and precipitation of hematite via ferrihydrite may have occurred locally.

Much of the channel fill material near Mount Desert appears to consist of mudflow debris as it contains coarse, angular and randomly dispersed fragments within a clay-rich matrix. The fill material has a relatively fine reticulate mottling pattern, with more goethite present than in the coarse hematitic mottling that affects the surrounding bedrock basement rocks. Uniformly mantling both the channel fill and the mottled bedrock is a yellow duplex podzolic soil (Dy2.41), which contains ferruginous, maghemitic pisoliths in its upper section.

The sequence described here illustrates the complex development of the summit surface as it provides evidence for weathering being interrupted locally by erosion, transport and sedimentation with modern soil development continuing to modify it. Consequently, it is not possible to interpret this locality

simplicistically as the mere preservation of an ancient landsurface carrying 'laterite' of Mesozoic age (See, for example, Twidale, 1983).

#### 4.2.2.2 Pottery Road (Fig. 4.1; K26)

A short distance along Pottery Road, the continuation of Pennys Hill Road (Noarlunga MR 965840) and east of the intersection of Range Road at 'The Range' settlement, a road cutting has exposed a palaeochannel on the summit surface at some 350 m asl. The channel fill material is essentially a diffusely iron-impregnated sandy sediment, which is reflected in the high silica (72.5%) content of the sample (BOU 17) (Table 4.9). As the sand-rich fluvial sediment contains kaolinite it has probably been subjected to weathering over a considerable period of time, unless the kaolinite has been inherited from pre-existing kaolinite. In thin section (Plate 4.33) the sample consists of well-rounded quartz in a clay matrix that has been partly replaced by iron oxides, with the merging of tiny hematite crystallites. The iron enrichment appears to be a single generation event as there are no complex zones or layers.

#### 4.2.2.3 Clarendon-Kangarilla Road Cut (K23)

A road cutting exposes an angular unconformable contact between weathered Precambrian metasiltstone and uniformly ferruginised gravels and sands (Plate 4.34) on the main Clarendon-Kangarilla road at Noarlunga MR 851105 approximately 250 m asl. The section here was figured and described by Rix & Hutton (1953; pp 24-25) as a soil profile they named, the *Yaroona Gravelly Sand*. The base of the section is occupied by weathered Precambrian bedrock regarded by them as the 'pallid zone' of a 'laterite profile'. The mineralogy and chemistry of a sample of this material (BOU 75) (Table 4.10) are characteristic of bleached and partly kaolinised basement rocks. However, the presence of feldspars, micas and smectite suggest that the weathering has not been complete. The weathered Precambrian bedrock is overlain by coarse gravels grading up into grits and sands, that have been variably silicified and ferruginised. A sample (BOU 74) (Table 4.10) from the hard layer immediately above the unconformity, and indicated as 'laterite' by Rix & Hutton (1953), contained only 4.32%  $\text{Fe}_2\text{O}_3$ , but is well indurated, suggesting silica as the dominant cementing agent. This suggestion is supported by the occurrence of silicified wood in the immediate area (Mawson, 1953).

Similar cemented gravels occur at various locations between here and Mount Bold (e.g. Noarlunga MR 868114) (L23) where they are at a slightly higher

elevation of 260 m. A sample of these cemented gravels (BOU 355) (Table 4.10) differed only slightly in chemical composition from sample BOU 74, containing higher  $\text{Fe}_2\text{O}_3$  contents. These gravels are also very similar to those near Echunga at the Chapel Hill (M23) gold diggings (Echunga MR 968154) at 350 m asl and on the eastern side of the Willunga Fault. They almost certainly demarcate a palaeochannel related to the ancestral Onkaparinga River.

The red ferruginous sands and grits (BOU 73) were regarded by Rix & Hutton (1953) as the 'mottled zone' of a 'laterite profile'. However, the iron oxides are uniformly distributed throughout the sediments and do not form pronounced mottles. Ferruginous pisoliths occur at the top of the section within and on the modern soil.

The age of the sediments has been established by the discovery of fossils of *Magnolia sp.* flora near their base (Mawson, 1953). The sediments have been assigned to the Eocene on this basis and may be equated with the North Maslin Sands. About 6 km to the southwest from here sediments typical of the North Maslin Sands with spectacular cross and herringbone-bedding and channel structures are exposed in a road cutting at 190 m asl (Noarlunga MR 797057) (Plate 4.35). If the gravels near Echunga are of the same age then it demonstrates the occurrence of an ancestral Onkaparinga River in the Eocene. Stuart (1969) used the informal name Bakers Gully Sands for the fluvial sediments on the northeastern margin of the Willunga Embayment. He considered that in places these beds intertongue with the basal parts of the Port Willunga Beds, but elsewhere unconformably underlie them. It appears that the age of the sands is variable, with some being younger than and resulting from the reworking of the Middle Eocene North Maslin Sands.

The interpretation assigned to the sequence described here is as follows:-

- i. Weathering involving bleaching and partial kaolinisation of the basement rocks.
- ii. Erosion of the weathered basement rocks by the ancestral Onkaparinga River in the Eocene, and the
- iii. Deposition of gravels in the base of the channel, followed by grits and sands as the channel migrated.
- iv. The variable impregnation of the permeable sediments by silica and small amounts of iron in solution, and their precipitation in preferred localities in the former channel deposits.



- v. Progressive weathering and erosion of the sediments, including soil formation and pisolith accumulation at the surface, following tectonic uplift of the area and the lateral migration of the Onkaparinga River.

This interpretation is simpler than the complex and convoluted one tendered by Rix & Hutton (1953), which involved complex modifications to hypothetical 'laterite profiles'. It is also clear that the red 'lateritic' colouring is due to the mere staining of the sediments with iron oxides. For this reason the crusts associated with this site and with the next site are not ferricretes.

*4.2.2.4 Chapel Hill, near Echunga.* (Echunga MR 968154), 350 m asl (M23). Similarities between the sequence at the Clarendon-Kangarilla road cut and that at the Chapel Hill mine (Fig. 4.1; M23) near Echunga have already been mentioned. In various diggings in the area, the contact between basal gravels and weathered bedrock has been exposed by mining for alluvial gold. The weathered bedrock (BOU 336) (Table 4.10; Fig. 4.13) contains a considerable amount of kaolinite, as well as muscovite, feldspars and smectite. No iron oxide minerals were detected by XRD as the sample contains only 1.05% Fe<sub>2</sub>O<sub>3</sub>. Minerals identified in the overlying ferruginised gravels (BOU 344) include goethite, hematite, kaolinite, smectite and possibly inherited staurolite. Red sands (BOU 346) above the gravel beds were also analysed for comparison with the Clarendon section. Again the sample contained only a small amount of Fe<sub>2</sub>O<sub>3</sub> (5.6%) despite a pronounced reddish colour. Minerals similar to those in equivalent materials near Clarendon (BOU 73) were identified in sample (BOU 346) at Chapel Hill (Table 4.10).

*4.2.2.5 Blackwood Rail Cutting (Fig. 4.1; K21)*

In the Blackwood Railway Cutting (Noarlunga MR 825214) at an elevation of some 250 - 270 m asl an unconformable contact is exposed between variably weathered, bleached and mottled Precambrian metasediments and mottled sands, gravels and clays of Tertiary age (Plate 4.36). At the surface there is a yellow ironstone gravelly acid duplex soil (Dy3.41) with ferruginous gravels concentrated in the A-2 horizon and scattered throughout the B horizon.

The Tertiary sediments here, on the Eden-Moana fault block, were regarded by Ward (1966) as equivalents of the Pliocene Seaford Formation. Previously Sprigg (1946) had correlated these beds, on the basis of lithology and

stratigraphy, with non-marine sediments now known as the North Maslin Sands. Stuart (1969) could not date these sediments, but noted that they were physically similar to fluvial sediments in the general area overlain by Pleistocene to Recent sediments. However, in view of the proximity of this site to the dated sediments at Bakers Gully, which are in a similar topographic situation, it seems likely that the beds at Blackwood are also of Eocene age. Furthermore the sediments here bear no similarities to the Seaford Formation in its type section. Nevertheless, in places, the older Tertiary sediments have been reworked to form younger Tertiary deposits, as was recognised by Sprigg (1942), and in some localities they may be difficult to distinguish one from the other.

An analysis of a dense, red to purple-coloured iron-rich mottle (BOU 56) (Table 4.11; Fig. 4.13) from the Tertiary sediments at Blackwood revealed roughly equal contents of  $\text{Fe}_2\text{O}_3$  (35.9%) and  $\text{SiO}_2$  (41.6%) with 10.31%  $\text{Al}_2\text{O}_3$  and 1.05%  $\text{MgO}$ , and the minerals identified included quartz, goethite, hematite, kaolinite, vermiculite, anatase and smectite. This analysis is quite different from that of the Seaford Formation from its type section (BOU 48, Table 4.11).

Elsewhere on the Eden-Moana fault block, west of the Blackwood exposure, bleached sands occur that may relate to reworking of the Eocene sediments. For example at the corner of Blacks Road and Glenalven Drive, Flagstaff Hill (Noarlunga MR 793187) at an elevation of 180 m asl, sandy and gravelly bleached quartzose sediments (BOU 38) occur that contain 87.8%  $\text{SiO}_2$  with <1%  $\text{Fe}_2\text{O}_3$  and 6.34%  $\text{Al}_2\text{O}_3$ . Minerals identified include quartz, anatase, kaolinite, smectite, vermiculite and mica. This sample occurs immediately above the Sturt Gorge, the base of which is some 110 m lower, and may suggest reworking of the previous cover of Eocene sediments on the fault block surface into which the Sturt River is incised. Other outcrops of this material flank Blacks Road, and small outcrops and breakaways form at the edge of the Ochre Cove fault block surface near Onkaparinga MR 784183 at 180 m asl. Here it also consists of white bleached fine sands and silts in which no bedding structures are apparent, but it does contain mottles near the surface. These are currently developing or being modified as water emerges from the seasonally saturated soil at the soil/rock junction. The mottling is dominantly of hematite transforming to goethite although some mottles are of goethite. The surface soil contains a lag of ferruginous gravels that has probably derived from the progressive exposure and breakup of the underlying mottles. At depth the

sands are coarser, unconsolidated, and more uniformly iron-impregnated. This material has strong chemical, stratigraphic and sedimentological affinities with that exposed at a lower elevation in the Happy Valley overflow channel, as described below. The field observations and analyses suggest that there has been continual weathering with recycling of iron oxides occurring, sporadically interrupted by phases of erosion and sedimentation.

### 4.2.3. Ferruginised Bedrock Mottled Zones

#### 4.2.3.1 Range Road Cuttings near Willunga Hill (Fig. 4.1; K26)

Along the Range Road north of Willunga Hill, on the summit surface at 370 m asl, road cuttings (Willunga MR 818946) have exposed weathered and mottled Precambrian bedrock. Original bedrock structures are still discernible so there is no doubt that the regolith has developed by *in situ* weathering. In cuts and quarries below the level of the Range Road both unweathered and bleached bedrock have original structures well preserved. It is possible that some of the pronounced spur-line benches that occur on the flank of the Willunga escarpment at about 300 m asl may, at least partly, owe their origins to the evacuation of weathered bedrock along the weathering front.

Large hematitic mottles exposed in the road cut (Plate 4.37) essentially have developed preferentially in meta-sandstone units of the bedrock, whereas the bleached material is dominantly weathered meta-siltstone (BOU 425) (Table 4.12; Fig. 4.14). In the upper part of the section the original bedrock structures have been destroyed to some extent by a churning process that could have resulted from wetting and drying of the near surface clay-rich zone that contains kaolinite and smectite. Relatively large, soft, purplish and hematite-rich mottles (BOU 426) occur towards the base of the section, but successively upwards through the profile the mottles take on yellower colours due to an increasing goethite content (BOU 427, BOU 428) (Table 4.12). When broken these mottles reveal hematite-rich cores with goethitic rinds that become thicker as the land surface is approached. Bedrock structures are still visible in mottles near the surface.

A stoneline of dark-coloured maghemitic pisoliths, bedrock fragments and platy yellowish goethitic fragments of former, now hardened and residual mottles occurs at the surface and in the surface soil (Dy3.41), which appears to have developed on previously weathered materials. Thus the progressive transformation of hematite-rich mottles near the base of the exposed section

can be traced upward to progressively goethite-enriched mottles that ultimately form a lag near the surface. The hematitic mottles are postulated to have formed in the zone of a former fluctuating water table, with alternating reducing and oxygenating conditions. Under reducing conditions ferrous iron could have been released from the bedrock and, as the water table fell, precipitated as the ferric oxide, ferrihydrite, which subsequently dehydrated and aged to hematite. In the study area today, under the present surface and near surface environmental conditions, hematite is apparently being transformed to goethite via dissolution and reprecipitation, as suggested by Schwertmann (1971).

No maghemite has been identified in ferruginous nodules and mottles immediately below the modern soils, but strongly magnetic pisoliths and nodules occur in and on the soil.

#### *4.2.3.2 Mottled zone on Willunga Hill (Fig. 4.1; J27).*

About 5 km southwest of the cuttings on the Range Road, along the abandoned Adelaide-Victor Harbor road (Willunga MR 801915) at approximately 350 m asl, pronounced iron mottling occurs in Precambrian metasiltstone and is exposed in a road cutting (Plate 4.38). A sample of a mottle (BOU 23) (Table 4.13) contained 38.5%  $\text{Fe}_2\text{O}_3$ , the vast majority of which occurred as hematite. A halo of goethite occurs around some of the mottles, suggesting a later phase of dissolution of the hematite and reprecipitation as goethite. In thin section the metamorphic structure of the bedrock is indicated by the preferred orientation of aligned minerals (Plate 4.39), including quartz, feldspar, chlorite and large unaltered micas. Quartz grains are angular and embayed and the fine-grained groundmass has been partly replaced with iron oxides. The preservation of unweathered minerals within this mottled zone, together with the high total iron content suggests that there has been a concentration of iron oxides in the mottles from surrounding bleached bedrock.

#### *4.2.3.3 Other summit surface localities in the South Mount Lofty Ranges with surface lags of ferruginised mottles.*

Near Ashbourne (Milang MR 983955) there is an isolated hill or mesa 350 m high that is underlain by mottled and iron impregnated Cambrian metasedimentary rocks (Fig. 4.1; N26). The total iron content of a sample of this material is high at 59.4% and the dominant iron mineral is goethite, with some hematite (BOU 19) (Fig. 4.14; Table 4.13). The high iron content suggests

that there has been accumulation of iron in this locality. However, there is no surface crust, nor was gibbsite identified in the sample.

At "Hawthorn Farm" (Echunga MR 031169) near Mount Barker (Fig. 4.1; O22), surface lag material has also developed on a hill summit some 400 m asl, again as a result of downwasting of a mottled bedrock zone. Samples of the surface lag (BOU 25) have a mineralogy similar to that at the Range Road cuttings, with goethite dominating over hematite. Samples of similar materials from other localities such as Bonython Hill (BOU 31) (Echunga MR 051109) (Fig. 4.1; O24), 440 m asl, Sellicks Hill (BOU 357) (Fig. 4.1; I28) (Yankalilla MR 713854) at 350 m asl, and 'Sundial Hill' (Echunga MR 958150) at 350 m asl (Fig. 4.1; O23), in the Mount Barker area (BOU 28) are given in Table 4.13. The last mentioned sample, in thin section shows as a coarse schistose metasediment, with much non-quartz material impregnated with iron oxides (hematite and goethite); relic porphyroblasts of metamorphic minerals and replaced micas also occur (Plate 4.40).

*4.2.3.4 Mottled materials in hills near Kapunda in the Mid North (Fig 4.1; P7)*  
Alley (1969) commented that nowhere else in the Mid North of South Australia is the summit surface, the 'ancient Mount Herbert Surface so prominent as in the hills around Kapunda'. Consequently, samples were collected from this area for detailed examination and analysis.

A weathered profile (Plate 4.41) was examined near the 'Belvidere' Trig. (Kapunda MR 073883), which is about 10.6 km south of Kapunda. The profile exposure occurs about 0.4 km east of 'Belvidere' at about 380 asl and has developed in Precambrian metasedimentary rocks. Ferruginised bedrock, in which secondary iron oxides are uniformly distributed in the bedrock, (BOU 383) (Table 4.14; Fig. 4.15) at the base of the profile contained only 15.0%  $\text{Al}_2\text{O}_3$  and 8.17%  $\text{Fe}_2\text{O}_3$ . Roughly equal amounts of goethite and hematite comprised the iron oxides present, and although some kaolinite was identified, the occurrence of feldspars, micas, smectite and randomly interstratified clays suggests that the weathering of the rock has not been intensive. A sample of a pronounced mottle (BOU 384) near the top of the hill contained far more  $\text{Fe}_2\text{O}_3$  (25.9%), less  $\text{SiO}_2$  and roughly the same amount of  $\text{Al}_2\text{O}_3$  as sample BOU 383 (Table 4.14). Moreover, the iron oxide mineralogy was dominated by hematite. No maghemite was detected either by XRD or magnetic attraction. Bleached material (BOU 391) adjoining the mottle (BOU 384) contained so little  $\text{Fe}_2\text{O}_3$

(0.6%) that no iron oxide minerals were identified by XRD. All of the ferruginised bedrock (BOU 383), bleached (BOU 391) and mottled (BOU 384) materials displayed similar chemical and mineralogical characteristics apart from  $\text{Fe}_2\text{O}_3$  contents (Table 4.14). This suggests mobilisation of inherited iron and differential concentration in favourable localities during weathering. Microscopic examination of the bleached material revealed that it is a bleached metasediment in which quartz and mica are abundant, with a conspicuous kaolinitic matrix and well crystallised muscovite lathes. Some of these have transformed to kaolinite parallel to cleavages. No ferricrete crust is associated with this profile and the preservation of the hill appears to be associated with resistance provided by the iron-enrichment and hardening of the mottles near to the surface.

The weathering pattern described above is repeated in many other hills in the area, such as Mount Allen (Kapunda MR 072057) (BOU 54) and prominent hills at MR 059011, MR 061004 and MR 116915. Mount Allen is underlain by bleached bedrock towards its base and mottled, ferruginised bedrock in its upper section. There is no crust present at the surface, where bedrock structures can be discerned. The chemistry of an iron mottle from Mount Allen (BOU 54) (Table 4.14) is dominated by  $\text{SiO}_2$  (77%),  $\text{Fe}_2\text{O}_3$  (9.14%) and  $\text{Al}_2\text{O}_3$  (7.91%), with a mineralogy that includes kaolinite, hematite, goethite, muscovite, feldspars, smectite and anatase.

At Kapunda MR 116915, about 7.5 km SSE of Kapunda township and at an elevation of approximately 320 m asl, dark ferruginous mottles, developed in Precambrian rocks have been exposed by quarrying (Plate 4.42). The chemistry and mineralogy of a sample of non-mottled weathered bedrock (BOU 389) from this site are shown in Table 4.14. Thin section examination shows that the bedrock here is a quartzose metasediment with a strong preferred orientation outlined by kaolinised micas. The iron oxide is largely goethite, but there are also abundant scattered hematite crystallites. Hematite also lines voids and channels that may be pipestems or root channels. In places the hematite is concentrated along quartz grain boundaries and local fractures and appears as scattered hematite crystallites and patches in the kaolinitic groundmass (Plate 4.43). Mottled bedrock material (BOU 388), derived from the same site, contains much more  $\text{Fe}_2\text{O}_3$  (29.5%), less  $\text{SiO}_2$  (41.8%), slightly more  $\text{TiO}_2$  and approximately the same  $\text{Al}_2\text{O}_3$  (16.4%) as the weathered bedrock (BOU 389) (Table 4.14). In contrast to the weathered bedrock, the iron oxide mineralogy of

the mottle is dominated by hematite, being roughly twice as abundant as goethite. No maghemite was detected in the mottle. Adjacent bleached bedrock material (BOU 387) contained only 0.67%  $\text{Fe}_2\text{O}_3$ . However, all of the following elements were in greater concentration in the bleached material than in the mottle:  $\text{SiO}_2$  (23%),  $\text{Al}_2\text{O}_3$  (3.46%),  $\text{TiO}_2$  (0.30%),  $\text{CaO}$  (0.03%),  $\text{K}_2\text{O}$  (0.26%),  $\text{MgO}$  (0.27%) and  $\text{Na}_2\text{O}$  (0.42%) (Table 4.14). The major variations can be accounted for by variations in  $\text{Fe}_2\text{O}_3$  contents. Higher  $\text{Na}_2\text{O}$  contents in the more permeable bleached material probably reflects the presence of ephemeral halite. Titanium was most abundant in the bleached material, next in the mottle and least in the bedrock. A speckled mottle (BOU 390) (Table 4.14) from the same site was also examined. The red speckles are due almost entirely to the presence of hematite; no goethite was detected and no maghemite was indicated by XRD, but there was a very slight reaction to a hand magnet. If there is maghemite present it may have developed as a result of biomineralisation (Kirschvink, 1985), by the dehydration of lepidocrocite or the oxidation of magnetite formed from a 'green rust' precursor (Taylor, 1987). The bleached material superficially appears to be well weathered, yet it contains smectite, mica and randomly interstratified clays.

From Black Hill, 10 km northeast of Kapunda (Kapunda MR 026063) at about 430 m asl, two weathered bedrock samples (BOU 392; BOU 394) (Table 4.15) were collected for analysis. In thin section BOU 394 showed as iron-impregnated bedrock with quartz grains of uniform size with characteristic serrated borders sitting in a complex hematitic and clay groundmass. In detail, the hematite formed crystallites in a yellow-brown clay matrix. In this sample most of the micas and feldspars have been weathered to kaolinite. An iron-rich crust (BOU 393) toward the summit of Black Hill has a high total iron content (53.3%) and a low aluminium content (4.46%). The iron oxide mineralogy is dominated by hematite, with some goethite and a small trace of maghemite detected with a hand magnet. In thin section this crust comprises scattered quartz grains and rock clasts set in a matrix in which there is a strong preferred orientation of fine quartz and replaced micas.

#### *4.2.3.5 Upland Surface of the East Mount Lofty Ranges.*

Twidale & Bourne (1975a) identified remnants of an alleged Mesozoic landsurface (Whalley Surface) standing above an etch surface (Tungkillo Surface) in the eastern Mount Lofty Ranges. They correlated the Whalley Surface with the summit surface of Kangaroo Island, which has been assigned

a pre-Jurassic age by Daily *et al.* (1974). However, at the summit of Whalley Hill proper (Tepko MR 227256) (S20) at 360 m asl there is no evidence of 'deep weathering', but there is ferruginised bedrock (BOU 356 and BOU 367) (Table 4.16; Fig 4.16). The mineralogy of these samples is consistent with slightly kaolinised and iron-impregnated bedrock. The total  $\text{Fe}_2\text{O}_3$  content varies between 21.16% and 28.54% and comprises dominantly hematite with sub-dominant goethite. The presence of micas, feldspars and smectite argues against intensive weathering. The iron-impregnated bedrock nature of this material was verified by thin section examination. Other ferruginised bedrock samples collected from about 460 m asl (BOU 381) (Tepko MR 181359) and BOU 382 (Tepko MR 182345) collected from the 'lateritised' Whalley Hill surface gave similar results (Table 4.16), apart from the absence of goethite. Where goethite was identified, it probably indicates transformation from hematite by dissolution and reprecipitation under present weathering conditions.

Near Mount Torrens (Q18) at an elevation of 490 m (Tepko MR 175396) a road cut has exposed large red mottles within pallid, bleached bedrock (Plate 4.44). The bedrock mottle (BOU 375) (Table 4.16) is comprised dominantly of  $\text{SiO}_2$  and  $\text{Fe}_2\text{O}_3$ , with a small amount of  $\text{Al}_2\text{O}_3$  and the iron mineralogy is dominated by hematite. Sporadic masses of ferricrete occur at the surface. A sample of this (BOU 360) contains more  $\text{Fe}_2\text{O}_3$ , less  $\text{SiO}_2$  and more  $\text{Al}_2\text{O}_3$  than the mottle, but it still contains mica and feldspar. The iron mineralogy is also different as goethite is more abundant than hematite in the surface material. It is suggested that the surface material has developed from the downwasting of the mottled zone, the hardening of the mottles and their accumulation as a lag at the surface as the surface has been lowered by erosion. With the progressive exposure of the mottled material it is suggested that the hematite in the hematite-rich mottles underwent progressive dissolution, reprecipitation and crystallisation as goethite.

#### 4.2.4 Pisoliths

Pisoliths at and near the surface are the most common features of the ferruginous landsurfaces in the Mount Lofty Range Province. The detailed characteristics of pisoliths are dealt with in Chapter 5. Only one area with pisoliths is discussed here as they have been used to imply the age of the summit surface of part of the Northern Mount Lofty Ranges.



#### 4.2.4.1 *Mid North area (Fig. 4.1; A1, E1).*

Horwitz (1961) mapped extensive areas of a presumed Early Tertiary to pre-Tertiary erosion surface capped with 'iron hydroxide coated pebbles and pisolites' at elevations ranging from less than 45 m to more than 220 m asl on the summit surface on the 1:63360 Wakefield Geology Sheet. The elevational variation was attributed to the relief on the original surface and its later tectonic dislocation. The ferruginous lag on the surface was equated with 'identical ferruginous material...found reworked in the basal conglomerates of Early Tertiary deposits in the Clinton area', so that the surface was assigned to the pre- and/or Early Tertiary.

No detailed mapping was carried out in this region by the author. However, it appeared that the areas of the erosion surface mapped on the Wakefield Sheet are excessive. Furthermore, no pronounced zones of weathering underlying the surface were observed during a reconnaissance investigation, but there were extensive areas underlain by calcareous material, on which, in some localities, a ferruginous lag occurred. The situation here appears to be similar to that on the Blue Range on Eyre Peninsula (see Chapter 6), where a calcareous fine-earth separates bedrock from a surface lag of ferruginous material. In both of these instances the land surfaces are probably quite young, having been engulfed or overwhelmed by aeolian transported calcium carbonate, probably during the Pleistocene.

The ferruginous lag, where observed, occurs within and on the modern soil and appears to consist dominantly of fragments of ferruginised sandstone derived from bedrock sources. This lag may have developed in a fashion akin to that described for gibber surfaces as discussed by Bourman & Milnes (1985) or have been transported laterally from higher exposures of bedrock.

Samples of the ferruginous lag were collected from north of Mount Templeton (Balaklava MR 498314) (F1) at an elevation of approximately 230 m asl and from north of Kulpara (Wakefield MR 270287) (A1) at 160 m asl. All of these ferruginous fragments, some of which were superficially glazed, consisted of sandstone, and were from exposures in the modern soil. These clasts were separated into magnetic (BOU 69) and non-magnetic (BOU 68) fractions (Table 4.17). Both the non-magnetic and the magnetic materials contained high SiO<sub>2</sub> contents (84.5% and 72.8%) reflecting the quartz-rich nature of the original material, but the magnetic clasts contained more Fe<sub>2</sub>O<sub>3</sub> (22.3% to 9.33%), and

whereas the iron minerals identified in the magnetic clasts were hematite and maghemite, the non-magnetic clasts contained hematite only. Smectite, which may have been derived from adhering soil material, was identified in both samples, but kaolinite was identified only in the non-magnetic clasts. Both samples contained anatase, but the magnetic sample had a higher  $\text{TiO}_2$  content. Relatively the magnetic clasts were enriched in  $\text{Fe}_2\text{O}_3$ ,  $\text{TiO}_2$  and  $\text{ZrO}$ , and contained less  $\text{SiO}_2$  and  $\text{Al}_2\text{O}_3$ . Goethite was not identified in either sample.

The evidence above, particularly the occurrence of calcareous material between the ferruginous clasts and the underlying bedrock, suggests that the landsurface, on which the ferruginous clasts rest, may be of quite recent origin. Although other clasts, superficially similar, may occur in the basal conglomerate of Tertiary sediments elsewhere in the region, there is no compelling evidence to suggest that they are contemporary fragments of an Early or pre-Tertiary age. Furthermore, there is no justification for correlating the surface here with that of the Mount Herbert Surface elsewhere in the Mid North.

#### **4.2.5 Bleached Bedrock**

##### *4.2.5.1 Longwood Quarry (Fig. 4.1; L22)*

On the summit surface at 430 m asl (Noarlunga MR 919181) quarrying has exposed bleached and kaolinised Aldgate Sandstone (Olliver & Nichol, 1975) to a depth of at least 30 m (Plate 4.45). Apart from rare weak mottles, the material is essentially iron-free (BOU 341) (Table 4.17). The total iron content is only 0.27% and the sample is dominated by  $\text{SiO}_2$  (81.3%) and  $\text{Al}_2\text{O}_3$  (12.52%). Not all the bases have been weathered from the rock. Despite kaolinite being the dominant clay mineral present, micas, smectite and randomly interstratified clays were also identified, as were feldspars.

Iron derived from the now commonly bleached and weathered Precambrian Aldgate Sandstone may have contributed to the development of ferricretes at lower elevations, such as near Almanda Hill (Noarlunga MR 876166) (L22) (See section on vesicular ferricretes). The original iron content of the Aldgate Sandstone was probably quite variable, but relatively low. However, some unweathered iron-rich zones (BOU 395) (Table 4.17) within the Aldgate Sandstone (BOU 395) contain up to 80%  $\text{Fe}_2\text{O}_3$ , dominantly in the form of hematite.

#### 4.2.6 Weathered zones beneath the summit surface.

The review presented in Chapter 3 reveals that many workers have regarded ferricretes as parts of monogenetic 'deeply weathered profiles' developed on 'peneplain' surfaces under conditions of 'humid tropical climates'. These conditions arguably favoured the leaching of bases and silica as the bedrock weathered, while beneath fluctuating water tables alternating reducing and oxygenating conditions caused bleaching at depth, mottling in the zone of fluctuation, and iron oxide concentration at the upper limit of fluctuation, that could be extended upward by capillarity. Such an accumulation of iron oxides was regarded as resulting from *relative* chemical accumulation.

Two areas of 'deep weathering' were studied from drill holes on the modern summit surface, one near Willunga Hill, where there is only the surface development of lags of hardened and isolated mottles, and the other on the Parawa Plateau (Brock, 1964; 1971) of Fleurieu Peninsula, where there are sporadic occurrences of pisolitic to vermiform ferricrete. In both instances undisturbed cores were not available. However, chemical and mineralogical analyses of bulk samples were undertaken.

##### 4.2.6.1 Willunga Hill Borehole

Samples were analysed from a drill hole sunk in Section 255, Hundred of Kuitpo, on the 'Broadacres' property, approximately 2 km northeast of Willunga Hill (Willunga MR 804916) at approximately 350 m asl (Fig. 4.1; J27). The hole was drilled and logged by Mr C.G. Thorpe of Kangarilla Drilling Pty Ltd, during the period 20/9/82 - 21/9/82. The following log was kindly provided:-

0.0 - 0.5 m	Top soil
0.5 - 3.0 m	White clay
3.0 - 6.0 m	Hard red clay
6.0 - 9.0 m	Hard yellow clay
9.0 - 12.0 m	Hard orange clay
12.0 - 33.0 m	Yellow shale
33.0 - 43.0 m	Grey shale
43.0 - 60.0 m	Soft slate with broken layers
60.0 - 104.0 m	Soft grey slate

Water was intersected at depths below the ground surface at:-

43.0 - 43.5 m
60.0 - 60.5 m
73.0 - 73.5 m

94.0 - 96.0 m, with a standing level of 21.2 m.

Samples were taken at 3 metre intervals down the borehole and these were sub-sampled for analysis. The chemical analyses are presented in Table 4.18 (Appendix II) and Figures 4.17, 4.18 and 4.19. The fact that the samples were bulked and taken at only 3 m intervals may have obscured detailed differences between iron-mottled and bleached zones as well as causing contamination. However, this allows an assessment of broad scale variations in a weathering profile.

The chemical composition of the samples down the borehole is remarkably constant. Plots of  $\text{SiO}_2$ ,  $\text{Fe}_2\text{O}_3$  and  $\text{Al}_2\text{O}_3$  on a triangular diagram (Fig. 4.17) fall within a very restricted range.  $\text{SiO}_2$  varies between a minimum of 58.1% at a depth of 6 m to a maximum of 66.4% at 93 m, although there is no dramatic depletion of  $\text{SiO}_2$  in the upper part, nor marked variation down the borehole, as might be expected in a 'laterite profile', in which a mottled zone is associated with an underlying pallid zone. The  $\text{Fe}_2\text{O}_3$  content is uniform throughout the profile, apart from pronounced depletion in the upper 3 m, the opposite to that expected for a 'laterite profile'. However, there is a relatively greater abundance of  $\text{Al}_2\text{O}_3$  in the upper 12 m of the profile, with a maximum of about 21% in the upper 3 m. There is minor depletion of combined bases in the upper part of the profile from 3 m (1.64%) to 18 m (2.57%), which coincides approximately with the standing level of water in the bore. Near this level there is a marked alteration in  $\text{Na}_2\text{O}$  content (0.27% to 1.16%) and  $\text{MgO}$  (0.44 to 1.89%) over a 6 m interval. Below 18 m the total base content reaches a maximum of 11.4% (75 m), within the zone of soft grey slate, which is probably bedrock. A plot of  $\text{Al}_2\text{O}_3$ ,  $\text{Fe}_2\text{O}_3$  and  $(\text{K}_2\text{O} + \text{Na}_2\text{O})$  on a triangular diagram illustrates this minor trend towards depletion of bases (Fig. 4.18). There is also a possible minor depletion of  $\text{MnO}$  and  $\text{P}_2\text{O}_5$  in the upper 15 m and 6 m respectively. Other very minor variations in the profile may relate to levels where water was intersected. There is no statistically demonstrable variation in  $\text{TiO}_2$  in the profile and ratios of  $\text{Fe}_2\text{O}_3/\text{TiO}_2$ ,  $\text{Fe}_2\text{O}_3/\text{Al}_2\text{O}_3$ ,  $\text{SiO}_2/\text{Al}_2\text{O}_3$  and  $\text{K}_2\text{O}/\text{Al}_2\text{O}_3$  are presented in Table 4.19 (Appendix II), to support the above conclusions.

Despite the fact that there are only relatively minor fluctuations in chemical composition down the profile (Fig. 4.19), the bulk mineralogy does display considerable variation (Fig. 4.20).

*Quartz* increases in abundance from the surface to a depth of 27 m after which it remains relatively constant. *Kaolinite* decreases in abundance from -3 m to -36 m. No *gibbsite* was identified in the profile. *Muscovite* increases in abundance from -3 m to a maximum at -48 m and from -51 m to -102 m maintains a fairly constant value. *Vermiculite* as a minor alteration product of chlorite is relatively uniform throughout the profile, with a maximum value at -78 m. Both alkali and plagioclase *felspars* increase in abundance from -3 m to about -39 m, similar to *muscovite*. They correlate negatively with kaolinite, suggesting that kaolinite developed from the weathering of these minerals. *Chlorite* was identified at -42 m from which level it increased to a depth of about -75 m and this is maintained to the bottom of the bore. As neither *goethite* nor *hematite* was identified below a depth of -27 m, *chlorite* is probably the main iron bearing mineral, and is clearly one of the primary minerals in the underlying Precambrian metasedimentary basement rocks. *Hematite* was only unequivocally identified in the samples from -3 m and -6 m. *Anatase* is fairly uniform in abundance throughout the profile as are relatively minor amounts of *smectite* and *randomly interstratified clays*.

The results of analysis of the <2 micron fraction are shown in Fig. 4.21. There appears to be a uniform abundance of *smectite* through the profile, an increase in *illite* abundance towards the base, high *kaolinite* content near the surface, decreasing progressively, but continuing until at least -42 m. *Vermiculite* occurs uniformly in small amounts to a depth of about 24 m, from which point on *chlorite* occurs in relatively greater abundance. The weathering profile described here displays few of the characteristics attributed to profiles developed under conditions of intensive tropical weathering. The observations that support such an assertion include:-

- i. The lack of marked profile differentiation. The relatively constant chemical composition throughout the profile suggests that there have not been pronounced vertical translocations of minerals by water table fluctuations, but largely *in situ* mineral transformations such as *felspars*, *chlorite*, and *muscovite* to *kaolinite*, *vermiculite* and iron oxides. Consequently the more iron oxide-rich samples that may represent mottles, probably developed by localised redistribution of iron.
- ii. Although there is some depletion of bases in the upper 21 m of the profile, this is by no means complete, as reflected in the

occurrence of 2:1 layer silicates such as illite, vermiculite and smectite. Kaolinite is the most abundant of the clay minerals in this section, but the identification of the others does not favour the former occurrence of intense weathering.

- iii. The absence of gibbsite in the profile, and from nearby surface samples, may indicate that there has not been the operation of intensive leaching and acid conditions.
- iv. The lack of iron concentrations in the upper section of the profile. In fact the upper 3 m is the most iron depleted of the profile. It should be noted, however, that the iron above the modern water table is in the form of hematite and goethite, whereas that below the water table occurs dominantly in chlorite.
- v. The absence of an iron-bleached 'pallid' zone beneath a 'mottled zone'.
- vi. The broad association of zones of minor variations in chemistry and mineralogy in association with present water levels and movement through the profile suggests that some of the transformations may have occurred under conditions not markedly different from those of today.

#### 4.2.6.2 *Parawa Plateau*

Thirty auger holes (RBA-1 to RBA-30) were drilled to a maximum depth of 13.5 m on the summit surface of Fleurieu Peninsula within a 10 km radius of Rapid Bay during prospecting for low alkali shale for potential low alkali cement clinker production (Keeling, 1983; 1985). Samples, which were taken at 1 m intervals down the holes, had been thoroughly mixed in the augering process. By interpolation from geological data (Mancktelow, 1979) the area drilled can be shown to be underlain by Precambrian and Cambrian bedrock. However, the majority of the bore holes occur in the weathered Cambrian Carrickalinga Head Formation (Fig. 4.22). Analyses of unweathered samples of these rock formations are presented in Table 4.20 for comparison with the weathered equivalents intersected in the boreholes Tables 4.21 to 4.50 (Appendix III). Many profiles reported in the literature are regarded as 'ideal' profiles, and have been specifically selected because they contain the expected horizons (e.g. Nahon *et al.*, 1977) or because they are exposed in cuttings. However, the profiles reported here are from drill holes bored for quite different purposes from investigating 'laterite' profiles. Furthermore, the analyses of 30 boreholes

within an area of only about 20 km<sup>2</sup> represents the most detailed investigation of 'deep weathering' in South Australia.

The possibility of carrying out a mass balance study on the chemical data from the boreholes was considered, but rejected because there can be lateral enrichment of the surface and near surface materials as well as there being differential removal by leaching, thereby reflecting the consequences of two groups of processes. Furthermore, there is a lack of a suitable resistant index. Titanium and zirconium, possible resistant indices, were discarded because of the demonstrated mobility of both of these elements (Milnes & Fitzpatrick, 1988), which renders their use hazardous. Furthermore, the lack of precision in quantifying the very small amounts of zirconium present, would also tend to negate its reliability as a resistant index.

#### 4.2.6.2.1 Chemistry of borehole samples (See Figure 4.23)

In unweathered bedrock the  $Fe_2O_3$  content varies between 2.57 - 4.81% whereas in the weathered bedrock  $Fe_2O_3$  varies from a minimum of 0.53% at a depth of 6 m in RBA-21, to a maximum of 33.07% at the top of RBA-29. Generally, however, the weathered samples are more iron-enriched than the unweathered bedrock. The  $Fe_2O_3$  content displays great variability down the profiles: some display near uniform  $Fe_2O_3$  as in RBA-1, RBA-11, RBA-22, RBA-23, RBA-30. Other profiles, however, have highly variable  $Fe_2O_3$  contents such as RBA-2, RBA-4 and RBA-5. There is a general tendency for  $Fe_2O_3$  to be concentrated in the upper parts of profiles but not consistently so. In some cases  $Fe_2O_3$  fluctuates down the profiles, as for example in RBA-2.

The  $Fe_2O_3$  content of many of the samples of weathered materials is higher than the unweathered bedrock samples, but there are some  $Fe_2O_3$ -rich sulphide-bearing metasediments in the region (Daily & Milnes, 1971), which may have contributed to the higher iron contents of the weathered rocks.

There is no significant variation in  $MnO$  contents within and between the weathered and unweathered samples. Generally, the weathered materials display enrichment in  $TiO_2$ , but there are no pronounced or consistent trends within the profiles.

Contents of  $CaO$  in the weathered materials display uniform depletion compared with unweathered rocks. Profile RBA-12 displays uniformly high

CaO contents throughout the profile, but this bore was sited on only slightly weathered bedrock of the Brachina Formation, and most samples are probably close to the analysis of unweathered bedrock of this formation. The high CaO contents of the upper portion of some boreholes were due to contamination from limestone road metal.

Weathered materials are also generally depleted in  $K_2O$ , with a more pronounced tendency for depletion in the upper 4 m to 5 m of the profiles. Analyses of fresh bedrock varied between 1.70% to 3.56% and weathered equivalents ranged between a minimum of 0.25% to a maximum of 3.89%. Profile RBA-12, essentially in unweathered bedrock, has a uniformly high content of  $K_2O$ , and RBA-20 contains the very low value of 0.04% at a depth of 4 m, but this occurs in a sandy clastic sediment overlying weathered bedrock, in which there is a markedly higher  $K_2O$  content.

The unweathered bedrock samples analysed have  $SiO_2$  contents varying between 71.8% and 77.7%, whereas the weathered samples fluctuate between extremes of 36.6% and 79%. A high  $SiO_2$  value of 92% was obtained from the upper part of RBA-20, but as mentioned above, this sample came from a quartzose sediment. Generally there are lower values for  $SiO_2$  contents in the upper portions of some of the profiles, suggesting depletion of  $SiO_2$  in these zones, but the relative abundance of  $SiO_2$  appears to decrease proportionately as total iron content increases. The apparent depletion of  $SiO_2$  probably results from dilution due to the influx of iron oxides.

Generally all weathered samples have higher  $Al_2O_3$  contents (13.26% to 27.57%) than the unweathered equivalents (10.44% to 11.45%). RBA-20 at a depth of 5 m has a very low content of 3.09%, but once again this is within a sediment overlying the weathered bedrock. In some profiles (RBA-2, RBA-8, RBA-11, RBA-15, RBA-17, RBA-24, RBA-25) there are slightly higher  $Al_2O_3$  contents in the upper parts of the profiles. However, some others (RBA-1 and RBA-22) increase with depth whereas others may display relatively uniform contents (RBA-3, RBA-4, RBA-7, RBA-16, RBA-18, RBA-19, RBA-29).

There is no pronounced or consistent trend in  $P_2O_5$  contents down the profiles and variations from unweathered samples are not significant. Unaltered bedrock contents of  $MgO$  vary between 0.64% and 1.85%, whereas the minimum



analysed in weathered materials is 0.09% with a maximum of 2.31% (RBA-15 at a depth of 11 m). Again a very low MgO content was obtained in RBA-20 at 4 m within a quartzose sediment. Overall the weathered samples are depleted of MgO compared with unweathered bedrock, with a tendency for greater depletion in the upper sections of boreholes.

Variations of 2.0% to 3.68% were noted in the  $Na_2O$  contents of unweathered bedrock, whereas weathered samples ranged between 0.01% and 1.01%, illustrating depletion of  $Na_2O$ , with some, but not all profiles, displaying greater depletion in their upper sections. No  $Na_2O$  was detected in the sandy sediment at depths of 2 m and 3 m in RBA-20. In some weathered profiles there does appear to be an enhanced concentration of  $ZrO$ .

#### 4.2.6.2.2 Mineralogy of borehole samples

The main minerals identified in samples of the weathered materials included quartz, kaolinite, gibbsite, goethite, hematite, maghemite, muscovite, feldspars, smectite, vermiculite, randomly interstratified clays and anatase. Estimated relative abundances of these minerals are presented in Tables 4.21 - 4.50 (Appendix III) and in Figure 4.23.

*Quartz* is the most common mineral present both in the samples of unweathered and weathered bedrock and probably constitutes between 40% to 50% of samples. Where no aluminium oxides, such as gibbsite, were present, an approximation of kaolinite and quartz contents was estimated by allocating relative proportions of  $Al_2O_3$  (55%) to  $SiO_2$  (45%), in line with kaolinite composition. For example, the estimate for kaolinite from RBA-1 at a depth of 1 m is: 15.72% (55% total as  $Al_2O_3$ ) + 12.90 (45% total as  $SiO_2$ ) = c. 39%. A quartz estimate can be calculated as follows: 62% (total  $SiO_2$  present) - 12.90% ( $SiO_2$  allocated to kaolinite) = c. 49.1%. This of course ignores  $Al_2O_3$  incorporated in other clays such as smectite and interstratified clays. Quartz appears to be less abundant in the upper parts of some profiles, but this relative content is also influenced by higher amounts of iron oxides. For example, in RBA-2,  $SiO_2$  content increases from 36.6% at 1 m to 47.4% at 2 m and this increase in  $SiO_2$  is compensated for by a decrease in  $Fe_2O_3$  abundance from 18.26% to 8.48%, while all other constituents remain constant. Thus the variation may not be due simply to a depletion in  $SiO_2$  but to an influx of iron oxides. Quartz peaks of the samples under discussion are similar at both 1 m and 2 m depths.

*Kaolinite* was identified in all samples, indicating transformation of minerals such as feldspars and muscovite. Where kaolinite decreases with depth, feldspar and muscovite increase. Invariably, where there is a lower kaolinite abundance near the surface, gibbsite occurs.

*Gibbsite* only occurs in the top few metres of the borehole samples and varies inversely with kaolinite abundance. This suggests that gibbsite ( $\text{Al}_2\text{O}_3 \cdot 3\text{H}_2\text{O}$ ) may have developed by the dissolution of kaolinite accompanied by the removal of silica in solution and the concentration of  $\text{Al}_2\text{O}_3$ . The occurrence of gibbsite only near the surface suggests that it forms in a zone of strong leaching under acid conditions that lead to the removal of combined silica (Hsu, 1977). McFarlane & Heydeman (*in press*) have also suggested that microbial activity may be important in the dissolution of kaolinite to form gibbsite. However, gibbsite may also form from incoming  $\text{Al}_2\text{O}_3$  solutions.

Gibbsite was identified at all borehole sites except RBA-1, RBA-12 and RBA-27. RBA-1 is situated on the plateau margin at 315 m asl and in the top 1 m contains only 4.27% more  $\text{Al}_2\text{O}_3$  than the unweathered bedrock of the Carrickalinga Head Formation sample. RBA-12, which occurs on the Brachina Formation, although slightly enriched in  $\text{Al}_2\text{O}_3$  in the upper 2 metres, has not been intensively weathered, containing high amounts of feldspar and muscovite. It also occurs towards the margin of the plateau surface at 300 m asl. RBA-27 at 322 m asl in the central part of the plateau is possibly underlain by rocks of the Backstairs Passage Formation. Other near-surface samples from RBA-28 and RBA-29 on the same rocks do contain gibbsite, although they are at elevations 10 m higher than RBA-27. However, RBA-21 (323 m) has high gibbsite contents to depths of 4 m so that elevation differences of this order may not be significant.

*Muscovite* is an important primary rock mineral. It occurs in samples from every borehole, although it may be depleted or removed from the upper 1 m to 5 m. Generally, it increases in abundance with depth to comprise very significant proportions of the samples. The formation of kaolinite has probably depended partly on the decay of muscovite, particularly by the removal of  $\text{K}_2\text{O}$ , but its continued abundance in the weathered zones suggests that the weathering has not been of extreme intensity.

*Plagioclase feldspars* occur in the unweathered bedrock samples and they have been identified in small amounts in variable parts of the weathered profiles, particularly towards their lower parts. The identification of feldspars again indicates that the weathering has not been pervasive.

*Smectite, vermiculite* and *randomly interstratified clays* were identified, although in relatively small amounts, which suggests that the weathering has not been protracted and intense, as implied by conditions of tropical weathering.

*Goethite* and *hematite* occurred in the upper sections of the profiles. There were problems of interference by kaolinite and muscovite peaks in determining the relative amounts of goethite and hematite present, and, where they could not be clearly identified, the peak height at  $38.8^\circ 2\theta$  was used to indicate a combined value. Both hematite and goethite occur at various localities in the profiles, but they are concentrated dominantly in the top two metres. No consolidated crusts were intersected in any of the drill holes, and the near-surface materials comprise unconsolidated ferruginous gravels, soils and sediments. Ferricretes do occur sporadically in the area investigated. They may have resulted from the impregnation and cementation of the unconsolidated materials similar to those intersected in the drill holes, in preferentially favourable locations.

*Maghemite* was only identified in the top part of profiles, typically in the top 1 m. Where it has been identified below this level, at up to 2 m below the surface, it may have resulted from down-hole contamination. The maghemite occurs only in ferruginous pisoliths, and because of their near surface occurrence, their maghemitic character has probably been derived from transformation of goethite resulting from surface heating by burning in the intimate presence of organic material.

#### 4.2.6.2.3 *Summary and Discussion*

Figure 4.23 is a series of generalised graphs of chemical and mineralogical variations, below the Parawa Plateau. These show relative concentrations of  $\text{Fe}_2\text{O}_3$  and  $\text{Al}_2\text{O}_3$  and depletion of  $\text{SiO}_2$  in the upper 3 m.  $\text{CaO}$  and  $\text{Na}_2\text{O}$  are uniformly depleted throughout the profiles, while  $\text{K}_2\text{O}$  and  $\text{MgO}$  are strongly depleted in their upper parts. Mineralogically, quartz is relatively depleted in the upper 4 m, to which depth the occurrences of gibbsite, goethite, hematite

and maghemite are virtually restricted. Muscovite is severely depleted in the upper 4 m and increases uniformly to a maximum at 13 m. Kaolinite is relatively low in abundance in the upper 4 m, where its content varies inversely with gibbsite.

There is no doubt that the bedrock underlying the present landsurface in the Parawa area of Fleurieu Peninsula has suffered weathering, resulting in the formation of kaolinite, smectite, randomly interstratified clays, vermiculite, gibbsite, goethite and hematite, dominantly from quartz, muscovite and feldspars. The weathering processes have led to the depletion of  $\text{SiO}_2$ ,  $\text{CaO}$ ,  $\text{K}_2\text{O}$ ,  $\text{P}_2\text{O}_5$ ,  $\text{MgO}$  and  $\text{Na}_2\text{O}$ , and the enrichment in  $\text{Fe}_2\text{O}_3$ ,  $\text{Al}_2\text{O}_3$ ,  $\text{TiO}_2$  and possibly in  $\text{ZrO}$ . Bedrock structures and quartz veins intersected in the auger holes demonstrate that the weathered materials, particularly below a depth of 2 metres, have resulted from the *in situ* transformation of pre-existing Precambrian and Cambrian bedrock. However, in the upper sections of the boreholes the presence of sediments and soils suggest accumulation from lateral sources or from landscape downwasting. The accumulation of lags of resistant iron and aluminium-rich materials (such as mottles and pisoliths) are considered to have occurred as the differentially weathered and iron-enriched basement rocks experienced down-wasting. The influence of burning at the surface has resulted in the formation of maghemite-rich nodules, clasts and pisoliths, that have been incorporated into the sporadic occurrences of ferricrete in the area. Hence the concentration of iron oxides at the surface is not interpreted as representing the upper range of water table fluctuation, but the concentrated lag of iron oxides resulting from landscape downwasting. In some instances the iron-rich mottles in the weathered bedrock appear to have developed merely by the local redistribution of iron. Elsewhere, some zones have received additional influxes of iron oxides. There is no evidence of a pronounced 'pallid zone' at the bases of the profiles, but this may reflect the fact that the auger holes only extend to depths of 13 m.

Gibbsite occurs in the upper sections of the profiles and may have formed by lateral accessions of  $\text{Al}_2\text{O}_3$  in solution (Milnes & Farmer, *in press*), by microbial dissolution of kaolinite (McFarlane & Heydeman, *in press*), or by leaching of kaolinite under acid conditions (Hsu, 1977). This transformation may have been assisted by tectonic uplift that would have encouraged vertical leaching, as has been suggested by other workers, including McFarlane (1983). In many cases, where gibbsite occurs in the upper portions of the boreholes,

$\text{Al}_2\text{O}_3$  is not enriched, but there are lower relative amounts of  $\text{SiO}_2$ . Furthermore, as gibbsite decreases in abundance with depth, both  $\text{SiO}_2$  and kaolinite increase. Consequently, gibbsite formation resulting from incongruent kaolinite dissolution appears to have taken place. Some enrichment of  $\text{Al}_2\text{O}_3$  also appears to have occurred in the upper parts of some boreholes, so that accessions of Al in solution have probably also occurred, although the original source of the Al was probably from kaolinite. Much of the gibbsite occurs in kaolinitic clays occupying tubular structures in the ferricretes, but some also occurs within individual clasts and pisoliths, and the goethite in these materials displays a high degree (up to 20 mole%) of aluminium-substitution. This suggests a long and complex history of accumulation, transportation and weathering on this land surface. This view is further supported by the occurrence of bedrock clasts, maghemitic clasts and pisoliths, and complex pisoliths and nodules displaying multiple-layered rinds within the ferricretes that also exhibit gibbsite and kaolinite filled vermiform tubules.

The intimate association of iron oxides and gibbsite in these ferricretes seems anomalous if gibbsite formation relates to strong leaching conditions. However, if the perpetually remodelled iron oxides accumulated at the surface during landscape downwasting, while gibbsite formed through leaching, the two could have become intimately mixed. Moreover, the accession of  $\text{Al}_2\text{O}_3$  in solution from lateral sources could also provide a satisfactory model for gibbsite concentration in these situations. Under favourable conditions iron-enriched soil and surface waters may have led to the concentration of iron oxides in zones of sluggish drainage, cementing the surface lags through precipitation of goethite, incorporating aluminium from gibbsitic clay into its structure, and hematite from the rapid dehydration of ferrihydrite. Thus the weathering and mottling of the basement rocks is not genetically related to the ferricrete crusts as part of a monogenetic profile, except that the previously weathered and variably ferruginised bedrock provided iron-rich clasts and other detritus through its erosion.

Theoretical solubility diagrams for quartz, gibbsite and kaolinite at ambient temperature and pressure were constructed by Gardner (1970) using thermodynamic data. From these diagrams it was concluded that gibbsite should not form from the dissolution of kaolinite unless the following conditions apply:-

- i. Quartz should be absent from the system (quartz contents >10% retard gibbsite that forms, either directly or indirectly through an intermediate amorphous stage),
- ii. the infiltrating water has a pH >4.2, and
- iii. the initial concentration of total dissolved Si is <math>10^{-0.6}</math> moles per litre.

In all cases where gibbsite was identified in the boreholes, it was associated with quartz at contents >10%, and the underlying unweathered bedrock also has high quartz contents. Gardner (1970) also pointed out that quartz can be present if coated with impermeable clay films. However, it may be that gibbsite is capable of forming in iron-rich materials without such clay coatings.

The weathered profiles described here display relatively close affinities to those described in Western Australia by Gilkes *et al.* (1973), who considered, despite some quoted evidence for transportation and reworking of the upper parts of the profiles, that they had developed by *in situ* weathering.

### **4.3 Lower Level Landsurfaces marked by Ferricretes, Pisoliths and other Ferruginised Weathered Zones**

Ferricretes, pisoliths and other ferruginised weathered materials and zones also occur at various elevations below the summit surface, where they can be more closely related to sediments of known stratigraphic ages than can their analogues on the summit surface.

#### **4.3.1 Ferricretes**

##### *4.3.1.1 Vermiform and Pisolitic Ferricretes.*

##### *4.3.1.1.1 The Mount Taylor Plain*

Further evidence on the age and development of ferricrete on Kangaroo Island is provided by an examination of the relationships between landsurfaces carrying vermiform and pisolitic ferricretes and Miocene limestones that as Mount Taylor (140 m) (Vivonne MR 852217) and Mount Stockdale (123 m) (Vivonne MR 865203) protrude prominently above the Mount Taylor Plain (50 m and 100 m asl) (Figs 4.2, 4.24 and Plate 4.46). Bauer (1959) noted that the Mount Taylor Plain is mantled by the Eleanor Sand of Northcote (1946). Samples of vermiform ferricrete (BOU 103) (Fig. 4.25; Table 4.51-Appendix IV) from the Mount Taylor Plain in thin section appear to have developed from the complex impregnation of sands by iron oxides. Segregations of iron-rich zones with

coatings are separated by a matrix of clay replaced by iron oxides. Minerals identified include quartz, gibbsite, goethite, kaolinite, illite, maghemite and anatase.

Bauer (1959), believing the limestone on the Mount Taylor Plain to be of Pliocene age, regarded the Mount Taylor Plain as a Pliocene plain of marine abrasion and consequently considered the 'laterite' on it to be of Pleistocene age. Subsequently, Milnes *et al.* (1983) demonstrated that the limestone is of (?) Early Miocene age, so that a Pliocene age for the ferricrete on the Mount Taylor Plain is probably correct. Only after the plain had been resurrected from beneath the cover of Miocene marine sediments could the ferricrete have formed on it.

The Eleanor Sand, with its associated ferricrete horizon, occurs on two landsurfaces, the summit surface (Section 4.2.1.1.3) and the Mount Taylor Plain, widely separated in elevation. However, the crusts from the two surfaces (BOU 103; BOU 101) (Table 4.51; Fig. 4.25) have very close affinities in macromorphology, micromorphology, mineralogy and chemistry. Excavations in dams reveal that mottled and weathered zones occur below the ferricrete on the Mount Taylor Plain. Moreover, there is no evidence of physical reworking of the crust here. Consequently, the ferricrete appears to have developed via *in situ* weathering or the chemical accumulation in soils and sediments of iron and aluminium oxides influxed in solution. The Eleanor Sand of the plateau surface appears to have developed in a similar fashion, but the relative timing of this development is not clear.

There is no evidence of ferricrete on the summits of Mount Taylor and Mount Stockdale, although pisoliths litter the piedmont slopes near the base of Mount Taylor. Both mounts have small summit areas and it is possible that any former ferricrete cappings have been eroded. Be this as it may, it seems that the Eleanor Sand with its associated vermiform ferricrete developed over two separate periods of time. Unlike some other areas of the summit surface (See Section 4.2.1.1.3), there is no evidence of the high parts of the summit surface in this locality having been submerged by the Miocene seas. Hence it is possible that here the higher occurrences of the main plateau are of Miocene or pre-Miocene age and the lower ones of the Mount Taylor Plain being of post-Miocene age. Alternatively, the two disparate occurrences could be of Pliocene age, with their coeval development perhaps being dependent on conditions of

subdued topography and poor drainage that provided sinks for iron and aluminium oxides.

The present maximum elevation of the Miocene limestone is 140 m asl at Mount Taylor, but considerable dissection of the limestone has occurred, so that the maximum level reached may have been well in excess of 140 m, to cover at least some parts of the modern summit surface. The Miocene limestone has largely been stripped from the Mount Taylor Plain, thereby resurrecting or exhuming a pre-Miocene surface. It is considered unlikely that the ferricrete of the Mount Taylor Plain is of pre-Miocene age and has been resurrected. Rather, the ferricrete has formed after the re-exposure of the surface. In a large excavation for a dam on the Mount Taylor Plain, weathered bedrock was exposed, but the mineralogy of this material (BOU 143) (Table 4.51) does not support intensive weathering in its development. Towards the upper part of the excavation, mottles contain maghemitic pisoliths. This mottled material had developed in the fill material of a large palaeo-channel. This could account for the occurrence of maghemitic pisoliths at depth, and also illustrates some of the possible complexity in the development of the Mount Taylor Plain.

In dissected valley slope areas intermediate between the separate topographic occurrences of the Eleanor Sand on the summit surface and the Mount Taylor Plain, reworked pisolitic ferricretes (BOU 129) (Table 4.51) do occur, as for example in the upper part of the drainage basin of the Northeast River (Grainger MR 774304) at about 220 m asl (Figure 4.2.4). Pisoliths from sample BOU 129, in thin section, display complex laminated rinds that probably reflect different environments in which they have developed (Plate 4.47). The bulk of the pisoliths is comprised of iron oxides (hematite, maghemite and goethite) cementing quartz grains. Other minerals present include gibbsite, kaolinite, smectite, vermiculite, illite and anatase.

Near the southwestern margin of the Mount Taylor Plain and close to the junction of the Northeast and Northwest Rivers (Grainger 785173) at an elevation of approximately 30 m asl, pisolitic ferricrete, probably reworked from the vermiform ferricrete of the Mount Taylor Plain, also occurs. Thin section examination of this material (BOU 136) (Table 4.51) revealed complex goethite-rich pisoliths set in a matrix of clays, which had been partly replaced by iron oxides. Complex pisolith-within-pisolith structures (Plate 4.48) indicate a



series of cycles of formation. Quartz makes up the main framework of the pisoliths with clasts up to grit size occurring. Other minerals present include goethite, gibbsite, smectite, kaolinite, anatase, and traces of maghemite and hematite. The chemical and mineralogical data of sample BOU 136 (Table 4.51; Fig. 4.25) are consistent with derivation from the Eleanor Sand of the Mount Taylor Plain. However, the pisolitic ferricrete has a higher total iron content than the vermiform ferricrete, suggesting that iron has been added to the pisoliths in soil environments.

As noted above, ferricrete does not occur on Mount Taylor and Mount Stockdale, but pisolitic ferricrete does occur in solution hollows on similar limestone at Kelly Hill Caves (Grainger MR 718164) about 10 km southwest of Mount Stockdale and at an elevation of about 50 m asl. Thin section examination of this material (BOU 107) (Table 4.51) reveals that it consists of pisoliths with coatings set in a sandy matrix with clays variably impregnated with goethite. One of the sectioned pisoliths was noted to have a clay core. Generally, however, the individual pisoliths consist of silt-size quartz set in an iron oxide matrix and have layered rinds. The pisoliths could have easily been transported from a more distant source. Mineralogically sample BOU 107 consists dominantly of quartz, goethite, gibbsite, kaolinite, feldspars, and small amounts of hematite and maghemite. As with the pisolitic ferricretes described above, that at Kelly Hills Caves has greater  $\text{Fe}_2\text{O}_3$  and smaller  $\text{Al}_2\text{O}_3$  contents than the vermiform ferricrete on the summit surface and on the Mount Taylor Plain.

Bauer (1959) found it difficult to envisage transport of pisoliths to the hill-top location above the Kelly Hill Caves, and favoured an *in situ* mode of formation for the pisolitic 'laterite' at this locality. On the other hand, Northcote (*pers. comm.* in Bauer, 1959) considered that the small amount of clay in the weathered material, in which the pisoliths occur, argued against *in situ* formation. The thin section, mineralogical and chemical evidence presented here favours the transport hypothesis. The fact that the pisoliths are discrete bodies comprised dominantly of quartz and iron oxides and that they sit in a clay-rich matrix of quite different material argues against *in situ* formation. Most importantly the presence of maghemite and gibbsite in the pisoliths, but not in the matrix, suggests that the pisoliths were formed in a different environment and were transported to this locality. The fact that the pisolitic ferricrete sits on limestone bedrock also argues against *in situ* weathering for

its formation. Its close chemical and mineralogical affinities to the vermiform ferricrete of the Mount Taylor Plain favours derivation from this source.

Bauer (1959) was restricted in his interpretation by his belief that the limestone was of Pliocene age, which required that the 'laterite' be assigned to the Pleistocene. This limited the time available for topographic modifications required to explain an apparently anomalous occurrence of 'laterite'. The reinterpretation of the age of the limestones of Mount Taylor, Mount Stockdale and the Kelly Hill Caves to a Miocene age provides much more time for landscape modification after the proposed transport of the pisoliths.

#### 4.3.1.1.2 *Cape Borda*

Ferricrete with a pisolitic to vermiform fabric (BOU 116) (Table 4.51) occurs in a roadside scrape (85 m asl) at the intersection of the Cape Borda Road and the Larrikan Lagoon Track (Borda M.R. 470423). Thin section examination reveals that it is basically a sandy sediment with angular and embayed quartz grains cemented by iron oxides. Discrete iron oxide segregations, but without well defined borders, occur within the sediment. The framework grains in the segregations and in the surrounding material are similar, suggesting *in situ* formation of the segregations. The mineralogy and chemistry of this sample fall within the field of other vermiform ferricretes. This further suggests that there have been several phases of vermiform ferricrete formation on Kangaroo Island. On the basis of its elevation and relationships to limestones nearby, this example perhaps possibly developed in the Pleistocene.

#### 4.3.1.2 *Ferricreted Sediments*

##### 4.3.1.2.1 *Green Hills Surface*

A pronounced erosion surface, the Green Hills Surface (Bourman 1969; 1973), occurs at an elevation of 100 to 150 m asl on Fleurieu Peninsula, particularly near Victor Harbor, Waitpinga and within the Inman Valley Trough. This surface lies below the level reached by the Miocene seas (Fig. 4.26), which extended up to at least 230 m asl. The surface may have developed prior to the Miocene transgression and was subsequently exhumed from beneath the Miocene limestone deposits. However, it is more likely that its present form reflects development after the regression and erosion of the Miocene limestone. Thus the preferred model implies that the current Green Hills Surface has been eroded and the ferricretes on it developed since the Miocene transgression, thereby placing its major development in the Pliocene.

At one location on the Green Hills Surface (Encounter MR 820653; Fig. 4.1; K32), quarrying revealed two zones of ferruginisation. One ferricrete is exposed at the surface, and the other occurred about 2-3 m below the surface. The quarry has subsequently been filled.

The lower ferricrete (BOU 9) (Table 4.52; Fig. 4.27) is a coarse grit to sand-sized sediment with large rounded quartz grains and rock fragments, together with fine angular grains, cemented by iron oxides (Plate 4.49). Considerable amounts of tourmaline, micas, zircon and occasional feldspars (altered to kaolinite) are also present. The matrix is complex consisting of coalesced coatings on grains with multiple layering in voids due to successive crystallisation of both hematite and goethite (See Plate 5.2). The iron mineralogy is dominantly goethite. Irregular cavities in the matrix are filled with clays and these occur mainly next to the quartz grains.

The upper ferricrete (BOU 8; BOU 311) (Table 4.52) does not appear to be as complex as the lower one. It consists of rounded to sub-rounded sand-sized and larger quartz clasts, closely packed and reasonably well sorted, set in a mottled iron oxide matrix with irregular cavities (Plate 4.50). The matrix has developed through the coalescence of coatings around grains infilling voids. In contrast to the lower ferricrete the matrix appears to be of single phase origin, although there has been some alteration of hematite to goethite. Brownish smectitic clays occur in zones distinctly separated from goethite layers, which rim the quartz clasts. The upper surface ferricrete, in contrast to the lower one, has a slight trace of maghemite, as detected by a magnet.

Both the Green Hills ferricretes consist of pre-existing quartzose sediments impregnated by iron oxides precipitated from solution. The impregnated sediments were probably fluvial sediments derived from Permian glacial deposits and developed on a former broad open valley, now by relief inversion, occurring on the summit of a ridge.

#### 4.3.1.2.2 *Waitpinga area*

In the area occupied by the drainage basin of the Waitpinga Creek, ferricrete occurs at a similar elevation (100 m) to that on the Green Hills Surface near Victor Harbor (Fig. 4.26; Fig. 4.1; I33). However, at Waitpinga the ferricrete has developed partly on a sediplain, below which drilling has demonstrated the

presence of marine fossiliferous limestone of Eocene age about 36 m below the landsurface and 60 m asl (Bourman & Lindsay, 1973). Moreover, grain size analyses of sediments surrounding parts of the Waitpinga drainage basin suggest that they are former aeolian deposits (Bourman, 1973). This area must have been below the level of the Miocene shoreline so that the landsurface here can be no older than Late Miocene to Pliocene, or of equivalent age to the Green Hills surface.

Ferricretes occur in various parts of the Waitpinga drainage basin and around its margins where former fluvial and aeolian sediments have been variably ferruginised.

Samples of ferricrete were collected where exposed by tributaries of Waitpinga Creek (Table 4.53; Fig. 4.27). In these samples  $\text{Fe}_2\text{O}_3$  contents varied from 16.41% to 52.24%,  $\text{SiO}_2$  from 66.4% to 24.6% and  $\text{Al}_2\text{O}_3$  from 4.9% to 1.1%. One sample (BOU 328) contained a high content of MnO (11.56%). The dominant iron mineral is goethite, with only one sample (BOU 328) showing an indication of maghemite by reaction to a magnet. No hematite was detected. All samples were dominated by quartz, reflecting the nature of the original sediment, and all contained traces of feldspar and smectite, which indicate that the sediments have not been subjected to intensive weathering. The ferricretes in this area are interpreted as former fluvial or aeolian sediments of probable Pliocene age that acted as sinks for iron and manganese oxides precipitated from solutions.

Near the turnoff to Waitpinga Beach (Encounter MR 736571; Fig. 4.1; I34) ferruginous crusts occur, resting on or close to unweathered or weathered Kanmantoo Group metasedimentary rocks of Cambrian age (Bourman, 1973). Samples from this locality (BOU 329, BOU 330, BOU 331, BOU 332 and 333) (Table 4.54) bear similarities to the previous samples described from the Waitpinga drainage basin, in that they are rich in quartz and contain an iron oxide cement dominated by goethite. Two samples (BOU 331 and BOU 332) have high MnO contents. Zirconium was abundant in BOU 330 and BOU 333 displayed high iron contents (64.0%) in the form of goethite and had the typical vesicular fabric displayed by chemically precipitated iron oxides replacing organic material (bog iron ores).

The above evidence points to the former occurrence of sluggish drainage on a landscape, which favoured the accumulation of iron oxides in pre-existing quartzose-and organic-rich sediments, having been derived from higher surrounding country.

#### *4.3.1.2.3 Upper Hindmarsh Valley and Myponga Basin.*

The relationships of ferricretes to Miocene limestones in the Upper Hindmarsh Valley (Fig. 4.1; J30; Fig. 4.26) were used by Horwitz (1960) to establish a Pliocene age for the 'lateritisation' of the summit surface of the Mount Lofty Ranges. He maintained that the 'laterite' of the summit surface of Fleurieu Peninsula was contiguous with lower level 'laterite' in the Upper Hindmarsh Valley, where, by extrapolation, the 'laterite' overlies limestone of Miocene age. Consequently he attributed both the summit surface and the lower level 'laterites' to the same post-Miocene or Pliocene age.

This relationship was questioned by Brock (1964; 1971) and Bourman (1969), both of whom considered that the lower level crust had formed after the withdrawal of the Miocene seas and the breakup of the high level crust. Bourman (1973) also reported upon the occurrence of ferruginous colluvial material occurring on the steep slope separating the upper and lower level ferricretes. The elevation of the Upper Hindmarsh Valley ferricrete (Willunga MR 765768) is approximately 300 m asl and its relationship to the upper level ferricrete and the Miocene limestone is illustrated in Figs 4.4 and 4.26.

In general terms, it has now been well established that continuity of 'laterite' does not necessarily indicate contemporaneity (McFarlane, 1976), which has led to misinterpretations of landscape evolution in the past.

The character of the upper level ferricrete of Spring Mount is vermiform to nodular, and has been described above. The colluvial material (BOU 369) (Table 4.55) on the steep slope flanking Spring Mount contains quartz clasts and iron oxides largely in the form of goethite with minor hematite. Small amounts of kaolinite and smectite were also detected. The mineralogy and chemistry of the colluvial material is thus quite different from the ferricrete of the summit surface (BOU 370) (Table 4.2), which suggests different modes of genesis for the two ferricretes. The colluvial material was cemented in a scarp foot situation by iron oxides derived from above.

Ferricrete in the Hindmarsh Valley overlies sands, and is of a different character to both the high level and the colluvial ferricretes. Samples BOU 307 and BOU 310 (Table 4.55) consist primarily of quartz and goethite with some hematite and kaolinite. The chemistry, mineralogy and macro-morphology of these samples suggest an origin by iron oxide impregnation of pre-existing sandy sediments. No gibbsite was detected in the lower crust but it is common in the summit surface ferricretes. Ferricrete similar to that of the Upper Hindmarsh Valley occurs a short distance away in the Myponga Basin (Fig. 4.1; I29) at a similar elevation of 300 m asl at Willunga M.R. 756088. A sample from this site (BOU 304) (Table 4.55) had a similar chemical and mineralogical composition to those in the Upper Hindmarsh Valley. An outcrop of such ferricrete at Yankalilla M.R. 703786 forms a prominent bench at about 290 m asl. It comprises goethite-impregnated sandy sediments that may mark the approximate level of a Miocene shoreline.

#### 4.3.1.2.4 *Yundi road cutting*

In a road cutting (Willunga MR 855892) near the settlement of Yundi (Fig. 4.1; K27), iron-impregnated glacial sediments have been exposed at an elevation of about 260 m asl, resting on weathered Precambrian gneissic bedrock. The ferricreted sands occur at the surface (Plate 4.51) in places, but elsewhere dip below it, where they are overlain by other fluvio-glacial sediments. The ferricrete (BOU 7) (Table 4.55) is quite hard and strongly coloured by iron oxides, but the  $\text{Fe}_2\text{O}_3$  content is only 15.75%.

Several thin sections of this material were examined and reveal its character as a bedded sandy to silt sediment in which the larger grains are sub-rounded and the silt-sized grains are angular and shard-like. These framework grains are cemented by goethite and hematite. The grains are not closely packed, but appear to 'float' within the groundmass (Plate 4.52). The majority of the grains are quartz, with occasional rock fragments and mineral grains such as tourmaline. Some grains have been corroded and etched, developing some very irregular cavities. The matrix is composed of clay and iron oxides with roughly equal amounts of hematite and goethite. Mica grains weathered to kaolinite also occur within a single stage matrix. Goethite in the matrix appears to be cryptocrystalline, whereas the hematite is not markedly crystalline.

The ferricrete at Yundi stands about 30 m above the level of valley floor of the Finnis River, and some 100 m below the modern summit surface. The ferricrete was almost certainly in a former valley floor situation when it was formed by iron oxide impregnation of a porous sandy sediment. This ferricrete stands at a higher elevation than the ferricretes described in the next section, and it is also probably older than them. This suggested age difference is reflected in mineralogy: the older ferricretes developed by iron oxide impregnation of pre-existing sandy sediments have been noted usually to contain higher amounts of kaolinite and hematite than do the younger variants.

#### 4.3.1.2.5 *Tookayerta Toposequences*

Two toposequences were examined in the Tookayerta Valley (Willunga MR 917829; 932829) (Fig. 4.1; M29). Here Maud (1972) mapped ferricretes at different levels, which he attributed to former positions of valley bottoms progressively stranded as terrace-like features after the Tookayerta Creek had cut down to new base levels. These sequences of ferricretes were examined to determine if there is any variation in the chemistry and mineralogy of the crusts of different ages, with the higher ferricretes presumably being older than the the lower ones. Both toposequences have developed in Permian fluvio-glacial sediments or their reworked equivalents. Toposequence 1 has only two ferricretes separated by about 10 m with the lower crust being about 100 m asl, whereas Toposequence 2 has seven ferricretes extending from about 150 m to 110 m asl.

The chemical compositions of the various ferricretes are shown in Table 4.56 and Figure 4.28. In Toposequence 1,  $\text{SiO}_2$  and  $\text{Al}_2\text{O}_3$  are more abundant in the bottom ferricrete than in the top one, which has a higher  $\text{Fe}_2\text{O}_3$  content.

Similar suites of minerals occur in both ferricretes crusts, viz. quartz, goethite, hematite, feldspars, kaolinite and smectite, but there is more hematite in the higher and older crust.

In Toposequence 2 there is a slight tendency for  $\text{SiO}_2$  to increase with progressively younger ferricretes and for  $\text{Fe}_2\text{O}_3$  to decrease, with the notable exception of the second lowest crust. No trend in  $\text{Al}_2\text{O}_3$  content is apparent, which varies from a maximum in the top ferricrete (7.1%) to a minimum of 1.7% in the second highest ferricrete. Minerals identified in the ferricretes are listed in Table 4.56. Goethite is the dominant iron oxide in all ferricretes, with

small amounts of hematite being identified in the two top crusts and the bottom-most one.

The variations in  $\text{Fe}_2\text{O}_3$  and  $\text{SiO}_2$  contents could be interpreted in terms of increased leaching of silica from the upper ferricretes. However, the quartz framework grains were probably inert during ferruginisation, and the decreased  $\text{SiO}_2$  contents may simply reflect higher contents of  $\text{Fe}_2\text{O}_3$ , particularly as plots of  $\text{Fe}_2\text{O}_3$  and  $\text{SiO}_2$  abundances are virtually mirror images, reflecting mutually inverse relationships.

The variations in chemistry and mineralogy cannot have significant conclusions drawn from them with respect to the relative age relationships of the ferricretes. Age variations of the ferricretes may be too minor for their chemical and mineralogical characteristics to reflect different intensities and degrees of weathering. All ferricretes here are uniformly depleted of bases. The very minor variations of  $\text{Al}_2\text{O}_3$  in the toposequences may reflect differences in the character of the original sediments, and variable degrees of iron oxide impregnation may result from differences in iron availability at the time of formation as well as the relative porosity of the host sediment and the suitability of its location to act as a sink for iron oxide accumulation.

Fundamentally, the ferricretes reflect similar conditions of iron accumulation in valley bottom or near valley bottom positions, where sandy sediments provided suitable hosts for iron oxides accessed in solution. The presence of hematite in some of the ferricretes may reflect slight variations in environmental conditions that encouraged more rapid crystallisation of precipitated ferrihydrite. The topographic relationships of these ferricretes to those of high level Miocene limestones suggest that they have all developed since the regression of the Miocene seas, probably during the Pliocene.

#### 4.3.1.2.6 *Tookayerta Quarry (Fig. 4.1 M29)*

At an elevation of about 80 m asl in the valley of the Tookayerta Creek, downstream from the toposequences described above, a quarry (Milang MR 957807) has exposed Permian fluvio-glacial sediments, in which thin veins of iron oxides have developed subsurface. The total iron content of a sample of this material (BOU 358) (Table 4.57) is 22.16%, dominantly as goethite. Although the veins of iron oxides are not very pronounced, the above example illustrates the subsurface penetration of sediments by iron in solution and their precipitation in favoured sites, probably during Plio-Pleistocene times.



#### 4.3.1.2.7 *Finniss Quarry (Fig. 4.1; N2 8)*

In another quarry nearby (Milang MR 004829) in the valley of the Finniss River at 20 m asl, more Permian fluvio-glacial sediments have been iron impregnated. Iron oxides in a sample of this material (BOU 363) (Table 4.57) are more uniformly dispersed than in the previous example, and the total iron content is only 8.39%. However, once again it demonstrates the mobility of iron-enriched groundwaters in the environment, probably during the Pleistocene.

#### 4.3.1.2.8 *The Gun Emplacement (Fig. 4.1; L19)*

The Gun Emplacement (Plate 4.53) is a small but distinctive bench on the Eden Escarpment near Anstey Hill at Adelaide MR 917419, covering an area of about 5000 m<sup>2</sup>, at an elevation of approximately 210-220 m asl. The bench consists of Tertiary sands capped by a ferricrete. Although only a very minor feature in the modern landscape, the Gun Emplacement has been investigated by many workers. Despite this, theories related to its origin and age have been, and remain, controversial.

Howchin (1931; 1933) mapped out various deposits, which he interpreted as evidence of former, north-south trending river systems in southern South Australia. He regarded the Gun Emplacement as a remnant of one of a series of three major river terraces formed on the eastern bank of the Robertstown-Noarlunga channel. Fenner (1939) pointed out difficulties involved in such an interpretation, and considered that many of the alleged meridional trending 'dead rivers' corresponded closely with deposits preserved along north-south trending fault scarps.

Fenner (1939) distinguished between the alluvial deposits that occur on the summit surface of the ranges (e.g. Clarendon-Kangarilla Road Cut near Bakers Gully) and those at the foot of the ranges (e.g. Gun Emplacement). The high plateau grits were considered to have been uplifted, broken and tilted by faulting that affected Miocene limestones elsewhere in the ranges. In some places, such as at Bakers Gully, the plateau grits were noted to contain a *Magnolia sp.* flora of pre-fault age. On the other hand, the materials of the Gun Emplacement, Golden Grove and Hope Valley were considered to post-date the faulting. The lower sands were thought to be younger because, apart from the harder iron-cemented sands of the Gun Emplacement proper, they were generally unconsolidated, incoherent and contained no fossils that could,

at that time, be ascribed definitive ages. For example, lignites, silicified wood and leaf fragments recovered from beneath the low level sands at Hope Valley could not be given specific ages. However, Fenner thought that they were of post-fault origin, possibly of Pliocene age in their lowest sections to Late Pleistocene in the upper iron-stained cappings at the Gun Emplacement. A younger age for these deposits was also favoured because the mottling in the sands resembled mottling in Pleistocene sands in Victoria. Fenner (1939) also considered that the preservation of the lower sands against erosion by tributaries of the River Torrens and Dry Creek lent credence to a Late Pleistocene to Recent age.

The older of these deposits was related to streams that meandered over an 'old pre-Miocene peneplain' and the younger to 'fault apron' material, deposited following faulting and differential uplift of the ranges, which Fenner believed commenced in early post-Miocene times. He considered that the Gun Emplacement probably represented the highest part of one of the alluvial deltas derived from the ranges to the east.

Fenner (1939) explained the alleged unique preservation of the Gun Emplacement by postulating a combination of deep and widespread fan-delta alluviation in the Pliocene and Pleistocene to cover the Para Block, and Late Pleistocene to Recent uplift of the ranges to carry the alluvial beds to a height greater than that at which they were originally deposited. It was suggested that this was followed by the almost complete destruction of the beds along the ranges.

In contrast, Miles (1952) did not distinguish the plateau sediments from those at the scarp foot. He considered that the ferruginous sands of the Gun Emplacement represented relics of an original pre-Kosciuskan Tertiary land surface (probably 'lateritised') marking the top of the original Burnside Fault block, with a vertical dislocation of at least 70 to 75 m between the Burnside and Para Blocks.

The sediments that form the Gun Emplacement were equated by Ward (1966) with the Kurrajong Formation of suggested Late Pleistocene age, and the soils developed above them were equated with those developed on the Kurrajong Formation elsewhere. Ward (1966) believed that the beds of the Gun Emplacement are more extensive than indicated by Fenner (1939), extending

from Anstey Hill to Tea Tree Gully, but he agreed that the distribution of the beds suggested deposition by streams draining from the scarps. No indications of differential tectonic movements were noted by Ward (1966), although Fenner (1939) had suggested possible general uplift of the Gun Emplacement, which Miles (1952) had regarded as a relic of an original pre-deformational Tertiary landsurface.

Firman & Lindsay (1976) and Firman (1981) equated the surface of the Gun Emplacement with that of the Karoonda Palaeosol, which has been stratigraphically associated with the Hindmarsh Clay, above the level of the mottled zone marking the Ardrossan Palaeosol, and was thus considered to be of Late Lower Pleistocene age.

The Gun Emplacement surface was described by Twidale (1976a) as a weakly developed ferricrete of possible Late Pliocene to Early Pleistocene age, formed on Eocene Sands in the piedmont zone of the Mount Lofty Ranges. Here, Twidale (1976a) argued that the concentration of moisture had favoured the precipitation of iron oxides, and recurrent tectonism was suggested to explain the present elevation of the Gun Emplacement. Twidale (1976a) misreported the work of Fenner (1939) when he stated that 'Fenner (1939) interpreted the deposits of the Gun Emplacement as alluvia of Plio-Pleistocene age. They are neither alluvial nor transported but the result of weathering.' Fenner (1939) was actually stating that he believed that the sediments on which the ferruginisation of the Gun Emplacement developed were of Plio-Pleistocene age, whereas Twidale (1976a) considered them to be of Eocene age. In fact these two workers, although travelling along different paths, arrived at the same conclusion with respect to the age of the surface and ferruginisation of the Gun Emplacement.

The lignite deposits of Hope Valley have now been equated with the Clinton Formation of Late Eocene age (Forbes, 1980), and the sands of Golden Grove, regarded by Fenner as Plio-Pleistocene materials have recently been correlated with the Middle Eocene North Maslin Sands (N.F. Alley - *pers. comm.*). However, this does not resolve the age of the sediments at higher elevations nor the age of the ferruginised surface developed on them.

If the above dates are reliable then the sands at the Gun Emplacement may be slightly younger than those at Golden Grove, although they may be

diachronous sediments of the same deposit, with deposition proceeding progressively southwards by north-south flowing streams. Although there are difficulties in detail with the dead-river hypothesis of Howchin (1931; 1933) the above suggestion of a diachronous age for the sediments, together with the widespread occurrence of fluvial deposits of presumed Tertiary age throughout and on the margins of the Mount Lofty Ranges may suggest a source of fluvial sediments from locations far to the north. Given the widespread distribution of the sands there were few higher localities within the Mount Lofty Ranges to provide source areas for the sediments.

It is currently possible to trace the variously ferruginised and bleached sands from the quarry base (Plate 4.54) up to within a few metres of the surface of the Gun Emplacement. There are no apparent marked breaks in sedimentation or disconformities suggesting that the sands towards the surface are dramatically younger than those near the base. Occasional sedimentary bands of quartz and ferruginous clasts (Plate 4.55) occur within the otherwise homogeneous and massive sandy sediment, suggesting derivation from previously ferruginised and weathered materials. Samples (BOU 347; BOU 349) (Table 4.55) of the massive and homogeneous ferruginised sands were analysed. The  $\text{Fe}_2\text{O}_3$  content of these samples is not great, varying from 1.84% to 8.03%, exclusively as goethite, with high silica contents reflecting the character of the original sediment.

In the top few metres the material takes on a different character. There is a hint of bedding and rounded to angular clasts of quartz and ferruginised bedrock (Plate 4.56) are present, especially in positions close to the scarp. There are also discrete rounded concentrations of iron enrichment and quite prominent purplish hematite-rich mottles, which become more pronounced near the scarp. In hand specimen it is difficult to decide if the pisolith-sized iron accumulations are pisoliths forming *in situ*, or if they are degrading transported pisoliths. However, thin section observations reveal the leaching of iron from the pisoliths and the movement of titanium through the sediments, which suggest that the pisoliths are degrading, transported ones. The pisoliths (BOU 373) (Table 4.58) are not very iron-rich (3.66%  $\text{Fe}_2\text{O}_3$ ) and the iron oxide is dominantly goethite. In places, ghosts of pisoliths that have been completely bleached of iron can be discerned. This near surface material is very similar to bedded sands with pisoliths (BOU 39) (Table 4.58) east of Persistence Road, Tea Tree Gully (Adelaide MR 921435) at a slightly higher elevation. Apart from

its greater iron content, this sample has a very similar chemistry and mineralogy to sample BOU 373. However, this sample also contains maghemite, which could further suggest a transported origin for the pisoliths. Thin section observations also favour the interpretation that the pisoliths are degrading transported features.

Significantly the purplish mottles that occur in the top 2 to 3 m of the sediments, in contrast to the other mottles and stainings in the deep and surface sands, have higher total iron contents (BOU 374) (Table 4.58), which consist dominantly of hematite, with traces of maghemite and goethite. The maghemite has apparently formed *in situ* at depth in the zone of ground water. Close inspection reveals that the goethite in the mottles occurs as thin halos around hematitic cores, and has probably developed by the dissolution of hematite and reprecipitation as goethite since the mottle was originally formed. Thus it appears that there is an upper colluvial mantle of material overlying older Eocene sands and that this mantle has a distinctive iron oxide mineralogy that characterises Pleistocene scarp foot sediments elsewhere on the margins of the ranges (see below, section 4.4.2.1). These sediments appear to have formed by colluviation following tectonic uplift of the ranges, with the hematitic mottles forming within the range of a fluctuating scarp foot water table.

Ward (1966) regarded this material as the Kurradjong Formation of presumed Late Pleistocene age, but in this thesis it is considered to be a facies variation (occurring in scarp foot situations) of the Ochre Cove Formation of Ward (1966), which May & Bourman (1984), on stratigraphic evidence at Sellicks Beach, placed in the Middle Pleistocene. It has a characteristic iron oxide mineralogy that is dominated by hematite, traces of maghemite and variable but small quantities of goethite. A tentative interpretation for the formation of the Gun Emplacement was presented in a report by Miss M. McBriar and Mr. G. Krieg (Bulletin, Field Geology Club, 1978; Vol. 7, No. 10). This interpretation involved:

- i. Formation of a 'laterite' layer during a still-stand in the deposition of Eocene lacustrine(?) sands.
- ii. Burial of 'laterite' layer following the renewal of deposition.
- iii. Stripping of the overlying sands exhuming the 'resistant laterite' following accelerated uplift of the ranges.

- iv. Partial burial of 'resistant laterite' by coarse conglomeratic clastic sediments derived from the Eden Block.

Although there may have been hiatuses in the deposition of the Eocene sands, it is not necessary to invoke exhumation of the Gun Emplacement surface to account for the observed data. The evidence presented above demonstrates the relative youthfulness of the surface on the Gun Emplacement, which is not as resistant to erosion as some of the ferricretes on the summit surface of the ranges. There is some doubt that the surface on the Gun Emplacement could have survived burial and exhumation. There are instances of ferruginised materials occurring in the Eocene sands proper, which suggest the occurrence of pre-Eocene ferruginisation well above the level of the present Gun Emplacement. This has been demonstrated in many of the Tertiary sediments of the basins fringing the ranges, which could account for the report of a 'large block of rock containing what was evidently laterite overlain by fanglomerate type deposits.'

Evidence of faulting occurs in the sand quarry immediately to the south of the Gun Emplacement (Twidale, 1968). Step-like remnants of the Gun Emplacement surface are perched on the escarpment at levels up to 30 m above the general elevation of the Emplacement. Consequently, it is possible that they were uplifted to this position by faulting (also suggested in Bulletin of the Field Geology Club, Vol.7, No.1). The location of the fault closer to the south-facing escarpment of the Gun Emplacement may be indicated by steeply tilted Tertiary sands, and the amount of offset of the Gun Emplacement surface is roughly the same as that indicated by monoclinial folding of the Tertiary/Precambrian unconformity noted in the excursion report mentioned above. Thus the surface of the Gun Emplacement may record evidence of two phases of uplift: one that initiated the deposition of the Middle Pleistocene ferruginised fanglomerate material at the surface of the feature, which was probably a high level hill-valley junction, and a second that led to the displacement of the deposit across the trace of the fault locality, presumably in Middle to Late Pleistocene times. There may have been earlier phases of faulting that have not been preserved as the Tertiary sands are generally poorly consolidated and would not have maintained a surface topographic expression without induration. Moreover there is probably a zone of faulting so that the suggested displacement may only reflect movement on one branch of the fault. However, there is no evidence to support the degree of dislocation of the Gun Emplacement surface to the extent

suggested by Miles (1952). Even if the sands on the higher surfaces are of the same age as those underlying the Gun Emplacement (cf Gun Emplacement sands and Bakers Gully sands), it is not possible to equate the surfaces and ferruginisation affecting them. In fact the present evidence suggests that the Gun Emplacement surface is younger and less resistant than many within the ranges. If this is the case then, the major faulting must pre-date the age of the surface on the Gun Emplacement, and it is possible that scarps may have been in existence at the time of the original deposition, suggesting the occurrence of pre-Eocene faulting.

#### *4.3.2.2.9 The Bremer Valley*

The Bremer Valley is an asymmetrical valley in the Eastern Mount Lofty Ranges (Fig. 4.29) bounded on its eastern side by a prominent escarpment, the Bremer Scarp (Plate 4.57). This is almost certainly an erosional fault-line scarp developed along an ancient fault zone (Kleeman & White, 1956), which displayed negligible movement during the Cainozoic.

In its central section the Bremer Valley, is essentially a resurrected tectonic depression of some antiquity. It has been an avenue for marine incursions into the Mount Lofty Ranges from the Murray Basin at least three times during the Tertiary (Lindsay & Williams, 1977; Lindsay, 1986) as well as being a natural locus for river erosion at various times.

Whatever its precise origin, there is little doubt that the Bremer Valley existed as a relative lowland area during the first half of the Tertiary. Lindsay & Williams (1977) described occurrences of Tertiary limestones in it at the site of an abandoned road bridge (Cross's Bridge) and in a road cut near Hartley. Forrest (1969) reported the occurrence of Tertiary limestone further up the valley. In all cases the Tertiary sediments rest directly on slightly weathered Kanmantoo Group metasedimentary rocks. In all instances bedrock structures in the weathered basement rocks are preserved, and they have not been intensely weathered. At Cross's Bridge, unweathered bedrock forms the foundation for the bridge. Hence no suggestion can be made that the weathering under the limestones is the equivalent of that on parts of the summit surface of the ranges. However, the distribution of the limestones with respect to the bedrock topography suggests that the valley was in existence prior to the transgressions.

The identification of the distinctive Lower Miocene (16 Ma) marine foraminifer, *Lepidocyclina howchini*, in limestone collected by the author from the Bremer Valley (Lindsay, 1986), within the Mount Lofty Ranges, at an elevation of approximately 170 m asl has facilitated the more precise dating of geologic and geomorphic episodes in the Eastern Mount Lofty Ranges. Specifically it throws light on geologic events such as recurrent Tertiary marine transgressions into the Bremer Valley, the timing of movement along the Bremer Fault and the general uplift of the Mount Lofty Ranges with respect to the Murray Basin, the age of ferricretes within the Bremer Valley and its general geomorphic evolution.

Various ferricretes and other ferruginous materials occur within the Bremer Valley and their relationships to Tertiary limestones are shown in Fig. 4.30.

#### 4.3.2.2.9.1 'Lucernbrae' Ferricrete (S21)

Quite extensive remnants of a ferricrete crust occur at an elevation of about 200 m asl in the Bremer Valley on the 'Lucernbrae' property (Monarto MR 213211). These were mapped as areas of 'pisolitic laterite' by Johns (1961b), but they are actually iron-impregnated quartzose sands. Forrest (1969) regarded this ferricrete as of pre-Miocene age, forming prior to the Miocene transgression. The crust at Lucernbrae is not underlain by 'deep weathering' but by slightly weathered Kanmantoo Group metasedimentary rocks.

The ferricrete at 'Lucernbrae' occurs a short distance up valley of, and about 40 m above, the *Lepidocyclina*-bearing limestone outcrop (Monarto MR 218177), although it is certain that the actual shoreline of this sea level would have stood much closer to the 'Lucernbrae' ferricrete than does the surviving limestone remnant (See Fig. 4.30). The character of the limestone deposits suggests a near-shore environment, and the tentative suggestion is made here that the ferricrete at 'Lucernbrae' comprises remnants of dune and other backshore deposits related to the former Early Miocene coastline, subsequently impregnated by iron oxides derived from sources up valley and later indurated to form a resistant ferricrete (BOU 354) (Table 4.59; Fig. 4.31). This suggestion is favoured by:

- i. The high SiO<sub>2</sub> content of the ferricrete (71.4%), which occurs primarily as quartz, although a small amount (4%) is combined with Al<sub>2</sub>O<sub>3</sub> to form kaolinite.



- ii. Thin section examination, which demonstrates the close-packed and well-sorted nature of the quartz grains. Although they are not as well rounded as might be expected for dune sands, they are of acceptable dune sand dimensions, and have been etched and embayed by post-depositional weathering processes.
- iii. The uniform nature of the ferricrete. Rare clasts of bedrock and quartz occur in the ferruginised sands, but only at their base. The clasts may have been originally derived from the underlying bedrock by Miocene shoreline processes prior to dune formation.
- iv. The dominant iron oxide of goethite with minor amounts of hematite, is characteristic of post-Middle Miocene iron-oxide impregnated sandy sediments, such as those in the Upper Hindmarsh Valley.

No obvious structures have been observed, which might suggest a dune origin, nor is any dune-like morphology preserved. However, the dune sediments would have provided an ideal sink for iron oxides carried in solution from higher ground up valley, and the presence of kaolinite probably indicates some *in situ* weathering that might have destroyed bedding structures in the sediments.

Bleached sandstone (BOU 399) (Table 4.59), occurs at the same elevation (200 m) on the surface above and to the east of the Bremer Scarp (Monarto MR 247134) (Figs 4.29; 4.30). In thin section it has a similar character in grain shape, size and sorting to the ferruginised sandstone ferricrete at 'Lucernbrae'. As it contains little  $\text{Fe}_2\text{O}_3$  and CaO it is probably cemented by silica. The main difference between the two samples (Table 4.59; Fig. 4.31) is the  $\text{Fe}_2\text{O}_3$  content. The sediment on the Monarto Block may have been less favourably placed to serve as a sink for iron oxide deposition, but it can be considered to have a similar origin as a Tertiary shoreline backshore deposit, possibly related to the shoreline that faced eastward to the Murray Basin.

If the interpretation of the 'Lucernbrae' ferricrete as an iron-indurated Tertiary backshore deposit is acceptable it means that the ferricrete originated in the Miocene or Pliocene rather than the pre-Miocene as suggested by Forrest (1969). The Miocene is considered to be the most likely time of ferruginisation in this thesis because the ferricrete downstream is very different in character and could not have developed until after the erosion of the Miocene limestone.

The recognition of possible closely linked relationships between some ferricretes and limestones, if firmly established, will facilitate the more accurate location of former Tertiary sea levels in the ranges and thereby allow more accurate palaeogeographic reconstructions of parts of the Mount Lofty Ranges. Similar relationships between Tertiary sea levels and possible ferricreted shoreline sands also occur in the Upper Hindmarsh Valley and the Myponga Basin on Fleurieu Peninsula.

During iron oxide-impregnation of the sands at 'Lucernbrae', iron would have been released from up valley, probably both from pre-existing ferricretes and bedrock. Consequently, weathering (iron depletion, kaolinisation and mottling) would have been occurring on the upland surfaces, thereby providing iron for the development of lower level ferricretes, as well as continuing to modify and develop the mozaic of weathering patterns on the summit surface.

*4.3.2.2.9.2 Ferricrete down valley from the Early Miocene shoreline (Monarto MR 223149) (S23).*

Based on the location of the Lower Middle Miocene limestone in the Bremer Valley it is apparent that a large area down valley from this site must have been covered by limestone. Hence this bedrock depression is essentially an exhumed pre-Miocene valley. No doubt it has suffered some modification since its exhumation but its basic form was established in pre-Miocene times and possibly in the Mesozoic. Furthermore, the Early Miocene seas probably stood along the line of the present Bremer scarp.

Downstream from the outcrop of Early Tertiary limestone at 170 m there is a small and isolated outcrop of ferruginised sand and grit ferricrete (BOU 378) (Table 4.59) at an elevation of 138 m, resting directly on slightly weathered basement rocks (Figs 4.29 & 4.30). It has a fairly high iron content of 36.03%, dominantly in the form of goethite. Thin section examination reveals that it is an ill-sorted quartzose sediment, with framework grit clasts being held in a matrix of silt-sized quartz and iron oxides. Dissolution channels and voids in the sediment are filled with goethitic clay. The thin section and iron oxide mineralogy suggest that the formation of this ferricrete occurred in a terrestrial environment, in channel fill material located in a former valley bottom. The area in which this ferricrete occurs would have been submerged by the Early Miocene seas and probably formed after the exhumation of the

limestone probably in the Pliocene, as suggested by Forrest (1969). This ferricrete could be regarded as a pre-Miocene and exhumed feature, but its preservation would have been extremely fortuitous, and its mineralogy does not suggest that it has undergone a period of protracted weathering.

#### 4.3.2.2.9.3 *The Compton Conglomerate*

The ferruginous Oligocene Compton Conglomerate was recognised by Lindsay & Williams (1977) in the Bremer Valley at Cross's Bridge (Monarto MR 187040) at 50 m asl, in a road cut near Hartley (Monarto MR 181051), 70 m asl, and at the 'Kalibar' railway cutting (Monarto MR 320122) at 90 m asl (Figs 4.29; 4.30). Ludbrook (1961) regarded the Compton conglomerate as representing the onset of an Oligocene marine transgression.

At Cross's Bridge (R25) zones of ferruginisation (BOU 362) (Table 4.59) occur at the contact of the Cambrian bedrock and the overlying Tertiary limestones. Thin section examination of this material reveals large muscovite flakes held in a very fine iron oxide matrix. Tiny quartz particles occur and the mica flakes are being broken apart. Kaolinite in the material has been formed from the conversion of muscovite. At the Hartley Road Cut (R25) (BOU 361) (Table 4.59) iron oxides in places form a laminated goethite-rich crust in which gypsum crystals occur.

The  $\text{Fe}_2\text{O}_3$  contents in the sites at Cross's Bridge and the Hartley Road Cut are quite high at 32.7% and 57.4% respectively and they are comprised entirely of goethite. The sample from Cross's Bridge (BOU 362) contains a greater variety of minerals, but both localities represent the transgressive phase of the Compton Conglomerate. The lack of hematite and maghemite suggests that the iron oxides were not exposed at the landsurface and were not derived from pre-existing iron in the landscape during the transgression as suggested by Johnson (1976). Maghemite, in particular, is a common iron oxide mineral on terrestrial surfaces. Ludbrook (1961) noted that possible equivalents of the Compton Conglomerate at a depth of 159.2-163.5 m in the Murray Basin comprise dark-green and black sandy clays, in which the residues after washing consist almost entirely of ovoid siderite and glauconitic pellets. Thus there is ample iron present in unweathered equivalents of the Compton Conglomerate. This suggests that the goethite in the exposed Compton Conglomerate may have derived from *in situ* weathering of the siderite and glauconite in near surface situations.

### 4.3.1.3 Vesicular Ferricrete

#### 4.3.1.3.1 Mount Compass bog iron ore deposits (Fig. 4.1; K23)

In the modern valley floor at Mount Compass are examples (BOU 5 and 6) (Table 4.4) of very highly concentrated iron oxides (68.5% Fe<sub>2</sub>O<sub>3</sub>), where they are intimately associated with peat. The characteristics of these vesicular ferricretes have been discussed in association with high level analogues at Peeralilla Hill (Section 4.2.1.5.2). All of the evidence suggests that the vesicular ferricrete at Mount Compass has formed by the replacement of peat by iron oxides carried in solution into lacustrine or swamp-like environments. It is difficult to suggest an age for this ferricrete, because, although it occurs at about 250 m asl, it is in the base of the modern valley floor and is in a subsoil position. These last two factors together with microscopic evidence of clear preservation of plant cells replaced by iron oxides suggest that the ferricrete is reasonably young. In older vesicular ferricretes the preservation of plant cells is not as pronounced as in this modern valley floor example.

#### 4.3.1.3.2 Kangaroo Island

Vesicular ferricretes have been noted in association with pronounced benches at about 100 m asl in several areas on Kangaroo Island.

## 4.3.2 Mottled Zones

### 4.3.2.1 Willunga Scarp Bench (Fig. 4.1; J27)

Ward (1966) described benches on Willunga Scarp, one of which (Plate 4.58), at an elevation of about 160 m asl, carries 'rounded cobbles and lateritized sands'. He considered these sediments to be shoreline deposits because they resemble cobbles on the modern shoreline at Sellicks Beach, because they carry 'batter marks characteristic of such stones', and because the sands are well-sorted like those on the modern beach. These sediments were equated with the Pliocene Seaford Formation (Ward, 1966) since he considered them to be similarly weathered to alluvial beds of this formation. Consequently, the bench was regarded as a stranded marine platform of abrasion of Pliocene age.

The cobbles on the bench at 160 m asl are dominantly of quartzite. There is some evidence of aboriginal occupance at this site, but the boulders are essentially *in situ* as there are many smaller pebbles that would not have attracted the attention of tool makers. Some of the smaller clasts appear to be polished and faceted and may have been derived from previously existing

Permian glaciogene sediments. There is some variation in clast lithology which could support this hypothesis.

As reported by Ward (1966) the sandy sediments are well-sorted as might be expected from a beach-dune situation and they are positively skewed, which favours a beach origin (Chappell, 1967). However, there is no definitive evidence either with respect to the age or the origin of the bench and its associated deposits. Even if the evidence favoured a marine origin for the bench, it is not necessarily of Late Pliocene-Early Pleistocene age, but may relate to earlier events.

Nearby, at Sellicks Beach, the Early Pleistocene marine Burnham Limestone outcrops only a few metres above the modern shoreline (May & Bourman, 1984). Furthermore, the Burnham Limestone and its equivalents have not been observed above the level of 50 m asl as reported by Ludbrook (1983) from Cape Jervis. Similarly, the Late Pliocene Hallett Cove Sandstone has a limited vertical distribution, and within the immediate area only reaches up to about 30 m asl. However, higher sea levels during the Miocene are well known from the Myponga Basin, where limestone occurs up to 210 m asl. Early Tertiary marine deposits have also been mapped and described in the Noarlunga and Willunga Basins by Sprigg (1942). Furthermore, sediments previously assigned to the Pleistocene (Sprigg, 1942; Ward, 1966) or the Late Pliocene (Twidale *et al.*, 1967) are possibly older, and indicate the occurrence of a shorelines up to 100 m asl either side of the Clarendon-Ochre Cove Fault near Hackham and Noarlunga. This suggests that this fault has not been markedly active since the Early Pliocene. However, there is evidence suggesting Pleistocene fault activity on the Willunga scarp (Campana & Wilson, 1955; May & Bourman, 1984), so that the features described by Ward (1966) may well relate to events during this pre-Pleistocene time. Another possibility is that the bench and its deposits could mark a former shoreline of a Tertiary lake, such as those postulated for the deposition of the deltaic and lacustrine sediments of the Highbury and Golden Grove areas to the north. Consequently, the bench and its related deposits may relate to any of these former relatively higher shorelines.

Sediments preserved on the bench at 160 m on the Willunga scarp are ferruginised (mottled) sands and may be steeply dipping (Plate 4.58) but their orientation is difficult to ascertain. Analyses of mottled and ferruginised sands

(BOU 2) (Table 4.60) from the bench at 160 m revealed that it has only small amounts of  $\text{Fe}_2\text{O}_3$  (6.11%) exclusively as hematite. Thin section examination reveals that the framework consists essentially of sub-angular to sub-rounded quartz grains, generally well sorted but with occasional larger grains. A few feldspar and composite quartz grains occur and iron oxide-rich clays provide the cement which fills the voids and coats grains. There are suggestions of colloform structures in the matrix, but the indications are of a single generation impregnation of the sediments. Some partial replacement of grains along cleavages by iron oxides has occurred and cracks in the matrix may have resulted from shrinkage after impregnation by ferrihydrite that later transformed to hematite.

Loose sands occur at the surface and undisturbed samples were obtained by augering. These sands were sieved and gave similar results to those reported in Ward (1966). However, in this thesis they are considered to have developed by weathering of underlying consolidated and mottled sandy sediments. On a bench at about 180 m asl immediately upslope from the last site isolated fragments of ferruginous conglomerate (BOU 14) (Table 4.60) occur. In thin section, rounded fragments of shale, quartzite and sandstone set in a well-sorted silty ferruginous and clay-rich matrix. Quartz muscovite, feldspars, and small amounts of anatase, goethite and hematite were identified by XRD. It appears that this conglomerate has been derived from sources at higher levels than its present situation. Its iron oxide mineralogy, which is predominantly goethite, differs from that of sample BOU 2.

The interpretation tendered by Ward (1966) for the age of the mottled sediments on the 160 m bench relies upon unproven tectonic stability of the ranges during the Late Pliocene and Pleistocene. It also requires the Seaford Formation to be of Pliocene age, whereas both Stuart (1969) and May & Bourman (1984) allocated it to the Pleistocene. Finally, it demands that the age of the shoreline facies at 100 m east of Hallett Cove be of Pleistocene age, whereas it is likely to be much older.

Although there are many possibilities, the tentative explanation favoured to account for the evidence on the bench at 160 m on the Willunga Scarp requires that:-

- i. It marks the position of a former shoreline at least as old as the Early Pliocene, with the development of shoreline sands, cobbles

and boulders reworked from pre-existing Permian glaciogene sediments.

- ii. The sediments on it were subsequently mottled, involving the formation of hematite via transformation from ferrihydrite.
- iii. It was progressively and differentially uplifted along the line of the Willunga fault zone and eroded to leave a small remnant of mottled sandy sediments.

#### *4.3.2.2 Happy Valley Reservoir Overflow Channel (Fig. 4.1; J22)*

At an elevation of about 140 m asl at Noarlunga MR 775155 the overflow channel of the Happy Valley Reservoir exposes a section of weathered and variably ferruginised Precambrian basement rocks overlain unconformably by mottled sediments. The basement rocks are kaolinised and ferruginised mainly by goethite along bedrock structures, but occasionally more hematite-rich veins cut across these structures.

The basement rocks are unconformably overlain by mottled sandy sediments (Plate 4.59), considered by Basedow (1904) to be of Tertiary age. He distinguished between an older fossiliferous marine unit, which he assigned to the Eocene, and a younger (Miocene) sandstone bearing conformable relationships to the Eocene sediments. Fossils were found in this deposit in the overflow channel but were too imperfect for specification. The mottles in this sediment are generally hematite-rich, but occasional goethitic mottles occur, and in some other exposures, this strongly mottled zone is underlain by less consolidated sands, throughout which the iron oxides are more uniformly distributed. Unlike the basement rocks, in which the clays are predominantly kaolinitic, green-coloured smectitic clays occur. These mottled sediments are in turn overlain by calcareous materials that in places contain patches of smectite and ferruginous clasts derived from the underlying sediments. A deep Vertisol has formed above this sequence.

Sprigg (1942) recognised various Tertiary to Recent sediments in the vicinity of Happy Valley. The oldest he referred to as Oligocene lacustrine sediments and stated that they could be observed in the overflow channel of the Happy Valley reservoir, unconformably overlying basement rocks, and disconformably overlain by mottled sandstone regarded by him as of Pleistocene age. From his descriptions it is apparent that the older sand beds are the Middle Eocene North Maslin Sands. Marine sediments disconformably overlying the above deposits

were regarded as of Miocene age, but now are considered to be the Blanche Point Marls of Upper Eocene age.

Detailed drilling and palaeontological investigations were carried out by Olliver (1964) in the Happy Valley area. He noted that in the northeastern portion of the Noarlunga Basin, a shallow tectonic trough is filled with Tertiary and Quaternary sediments that are thickest adjacent to the Clarendon-Ochre Cove Fault and thin to the northwest. Isolated outcrops of North Maslin Sands and Blanche Point marls were observed below younger non-fossiliferous freshwater sands and clays assigned to the Pliocene and capped by a clayey sandstone that is 'lateritic in parts'. It is clear from the cross sections presented that there had been sub-surface development of ferricrete, perhaps having formed in this position by permeation of favourable horizons by iron-rich waters. It is also apparent that the ferruginisation occurred in sediments that are younger than the Blanche Point Marls, so that they are younger than the North Maslin Sands, probably in part developing from the reworking of those deposits. Olliver (1964) assigned them to the Pliocene, as did Sprigg & Wilson (1954) and Sprigg (1942) to the Pleistocene, but they could be considerably older and may be of Miocene age, as originally suggested by Basedow.

Analysis of the Tertiary sediment (BOU 368) (Table 4.60) show that its main constituents are  $\text{SiO}_2$  (76.2%),  $\text{Fe}_2\text{O}_3$  (16.27%) and  $\text{Al}_2\text{O}$  (4.8%). Minerals identified include quartz, hematite, goethite, smectite, kaolinite, vermiculite and anatase. These analyses suggest that the sediments have not been intensively weathered. The development of these beds and the erosion surface on which they rest could relate to a shoreline at about 100 m asl that has been mapped from east of Hallett Cove to Noarlunga Trig. (Sprigg, 1942, 1945, 1961; Ward, 1965, 1966, 1967, 1968; Twidale *et al.*, 1967; Stuart, 1969). Littoral shoreline facies have been variously ascribed to the Pleistocene or to the Late Pliocene by the above workers. However, recent work (*in prep.*) suggests that they may be considerably older. Ward (1966) considered them to be of Pleistocene age because they were noted to rest on mottled sediments, which he equated with the Ochre Cove Formation of Early Pleistocene age. This interpretation was a major platform on which his general model for the evolution of the area rested. However, recent work suggests that the mottled sediments on which the shoreline facies rests could be of Lower Pliocene, or even Miocene age.



### 4.3.3 Pisoliths

#### 4.3.3.1 Waitpinga area (Fig. 4.1; J33)

On the northern margin of the Waitpinga Creek drainage basin, a road cutting on the Victor Harbor-Cape Jervis road (Encounter MR 812600) at 100 m asl, exposes a section through ferruginised aeolian sand deposits. At or near the surface is a lag of pisoliths, and, at a depth of approximately 1 m below the surface, other pisoliths occur (Plate 4.60). The soil in which the pisoliths occur is an acid duplex soil, Dy4.21.

The surface pisoliths (BOU 322) (Table 4.61) contain 44.9% Fe<sub>2</sub>O<sub>3</sub>, 41.7% SiO<sub>2</sub>, 7.96% Al<sub>2</sub>O<sub>3</sub> and had an ignition loss of 3.85%. The iron oxide mineralogy is dominated by hematite and maghemite. Small amounts of kaolinite, smectite and mixed layer clays are also present. In contrast, the pisoliths at depth (BOU 327) contained only 5.35% Fe<sub>2</sub>O<sub>3</sub>, with 75.5% SiO<sub>2</sub> and 9.1% Al<sub>2</sub>O<sub>3</sub>; the iron oxide mineralogy is principally goethite, with a small amount of hematite. Kaolinite, smectite and possibly a small amount of gibbsite are also present.

The material in which the pisoliths occur at depth is a silty sandstone that is well sorted and consists of rounded and sub-rounded grains set in a ferruginous clay-rich matrix (Plate 4.61). The pisoliths are composed of material identical to that in the bulk of the deposit, which contains some grains of tourmaline, feldspar, andalusite and polymozaic quartz grains of metamorphic origin. At higher magnifications the iron oxides display a colloform fabric that indicates multiple influxes of iron oxides into pores spaces (Plate 4.62). Some quartz grains have hematite coatings and laminated goethite and clay occur in the voids. Some fractures in the clay matrix are filled with hematite, which suggests various phases of hematite formation.

#### 4.3.3.2 The basalt surface of the Gap Hills

A pronounced surface occurs on the mesa-like Gap Hills (Fig. 4.2) of Kangaroo Island. They are underlain by basalt of Jurassic age, which in turn overlies weathered and iron mottled Permian glaciogene sediments. The hills vary in elevation from about 180 m asl in the west to 120 m asl on their eastern extremity. The absence of 'lateritic weathering' on the surface of the Gap Hills was used by Daily *et al.* (1974) as evidence in support of a pre-Jurassic age for 'lateritisation'. On the other hand, Schmidt *et al.* (1976) attributed minimal surface weathering of the basalt to pervasive sub-basaltic weathering.

Some areas of the basalt-capped Gap Hills are completely devoid of weathered debris, but on the most easterly of the basalt remnants, Rettie Bluff (Kingscote MR 530270), which is also the lowest at 120 - 140 m asl, an unconsolidated mantle, at least 3 m deep, occurs. At shallow depths in the modern yellow clay soil and littering the surface, where the white sandy A-horizon has been eroded, are maghemitic pisoliths, nodules, and larger fragments of iron-impregnated sandy and silty sediments. The pisoliths (BOU 113) (Table 4.61) contain hematite, maghemite, kaolinite, feldspars and anatase. The larger fragments of iron-rich sediments (BOU 114) (Table 4.61) include rounded pebbles, which demonstrate some degree of reworking. Other rounded clasts of materials exotic to the basalt on which they rest have been collected from the Gap Hills surface and suggest derivation from a more distant source. In thin section, the larger fragments of iron-rich sediments consist of fine, well sorted, rounded to sub-rounded quartz and occasional patches of clay that include fine quartz set within a matrix of iron oxides. The grains are not well packed, which suggests that the iron oxides have replaced a pre-existing matrix material, possibly clays. The mineralogy of sample BOU 114 differs only in relative abundances with respect to that of the pisoliths (BOU 113). It is noteworthy that goethite was not identified in either sample.

Within the upper B-horizon of the soil (BOU 117) (Table 4.61) there are dispersed fine fragments of maghemite, which can be extracted with a magnet. The mineralogy and chemistry of the soil material differs absolutely and relatively from that of the ferruginous pisoliths (BOU 113) and sediments (BOU 114). The soil contains goethite, smectite and micas, which do not occur in the other samples, as well as higher contents of kaolinite. The occurrence of smectite is reflected in the pronounced development of gilgai in places on the Gap Hills summit. Thin section examination of the soil reveals it to be a clay with patches of poorly sorted quartz sand and silt throughout. Shrinkage cracks and iron oxide grains, which are probably detrital, also occur.

White clay-rich material was recovered from the lower part of the B-horizon of the soil on the Gap Hills (BOU 149) at a depth of about 1 m. Minerals identified in this material included calcite, quartz, feldspars, smectite and kaolinite, which have probably developed by *in situ* weathering of the basalt. The iron content (6.64% Fe<sub>2</sub>O<sub>3</sub>) is probably incorporated into iron-rich layer silicates to form smectites, but there is probably another Fe phase present, which was not

identified. Small fragments of basalt occur throughout the profile and may be precursors of future pisoliths.

Thus there does not appear to be evidence of deep and extensive weathering and ferruginisation on the summit surface of the Gap Hills. However, there are additional factors, which must be considered in interpreting the nature of the Gap Hills surface. These include evidence of an Early Miocene sea level that stood in excess of 120 m asl (Milnes *et al.*, 1983), and possible tectonic tilting of the surface. At an elevation of about 100 m asl a bench carrying calcrete, incorporating fragments of basalt and ferricrete fragments occurs around many of the basalt residuals of the Gap Hills. This occurrence may relate to former higher Tertiary sea levels. The very long period of time over which the basalt surface has been vulnerable to erosion by both subaerial and marine processes highlights the simplicity of explaining its present minimal surface weathering by the concentrated operation of sub-basaltic weathering. This is particularly so as boulders and pebbles of basalt occur in limestones of Tertiary and Quaternary ages and provide direct evidence of erosion of the basalt flows.

#### 4.3.3.3 Cape Borda (Kangaroo Island)

Bauer (1959) invoked *in situ* formation of ferruginous pisoliths at Cape Borda (Borda 445420). At an elevation of about 160 m asl they infill solution hollows developed in calcrete formed on calcarenite, which he had assumed was of Pleistocene age. Northcote (*pers.comm.* in Bauer, 1959) had suggested that the paucity of clays in the hollows favoured a transported origin for the pisoliths.

Examination of these pisoliths in thin section showed that they are complex, displaying multiple surface rinds composed of iron-rich bands and quartz accumulations. These features probably reflect a long history of movement in different environments. The chemistry and mineralogy of the pisoliths (BOU 104) are shown in Table 4.61, which indicates that hematite and maghemite are the dominant iron oxides present.

The main objection of Bauer (1959) to a transported origin for the pisoliths at Cape Borda was the topographic difficulty in explaining their occurrence at 160 m asl on an isolated hill. However, the limestones on which the pisoliths rest are possibly older than Bauer (1959) thought. Consequently there may have been greater opportunities for landscape modification than Bauer (1959) envisaged. Certainly, the high iron content, the presence of maghemite, the

absence of goethite, their situation on limestone and their complex character in thin section suggest a long history in the landscape, so that the hypothesis of transportation is preferred.

#### **4.4 Ferruginised Materials from Basins within and marginal to the Ranges.**

Rocks and sediments of various ages, in basins both within and marginal to the Mount Lofty Ranges have been variably weathered, mottled and ferruginised (Table 4.62). For example, Cambrian and Precambrian basement rocks have been weathered, bleached and mottled, Jurassic basalt on Kangaroo Island has been slightly weathered and carries ferruginous pisoliths, and sediments such as Eocene fluviatile sands and gravels have been subjected to weathering and ferruginisation as have sands of Miocene and Pliocene ages. Pleistocene sediments also display pronounced mottling, some Holocene sediments have been stained with iron oxides and there is also ample evidence of iron dissolution, transportation and precipitation in the modern environment.

Ferruginous detrital material contained in terrestrial sediments derived from the ranges, as well as in marine deposits, occupying downfaulted basins on the margins of the ranges provides evidence both for pre-existing ferricretes in the ranges and for physical iron mobility in the landscape over long periods of time, as do sequences in several intra-montane basins.

Figure 4.33 summarises the lower ages of the rocks and sediments affected by weathering and iron mobilisation including mottling, bleaching, ferricrete development and pisoliths. Where there is stratigraphic control, the upper age limits to these features are indicated by arrows.

Borehole information demonstrates the presence of weathered and partly kaolinised Precambrian basement rocks underlying sediments of Eocene age in the Adelaide Plains Basin (Milnes *et al.*, 1985). Recently, preserved carbonaceous plant roots within weathered and kaolinised basement rocks have been noted in drill cores from the Adelaide Plains, where they are sharply unconformably overlain by carbonaceous Clinton Formation sediments of Eocene age (N.F. Alley-*pers.com.*). This provides sound evidence for near surface pre-Eocene weathering of the basement rocks as opposed to sub-surface, sub-Clinton Formation weathering of the basement rocks at considerable depths. Clearly the rocks were weathered in a near surface

environment as the regolith was penetrated by plant roots subsequently preserved under carbonaceous sediments. Moreover, drilling near Walker Flat in the Murray Basin (S. Barnett *-pers. comm.*) recently intersected a ferruginous horizon resting on weathered basement rocks of the Kanmantoo Group and was in turn overlain by the Ettrick Formation of Oligocene age. This again provides sound evidence for weathering preceding both downfaulting of the basin and the marine transgression responsible for the deposition of the Ettrick Formation. The weathered basement rocks are strongly bleached and kaolinised, but the ferruginous material cannot be regarded as the ferricrete of a 'laterite' profile, as the iron oxide mineralogy is exclusively goethitic and associated light-coloured material is dominantly composed of calcite. These characteristics are typical of the Compton Conglomerate, which marks the onset of a marine transgression in the Oligocene, and the presence of the overlying Oligocene Ettrick Formation supports this interpretation. Some other ferricretes, notably vesicular ferricretes, analysed for this thesis are dominated by goethite, but even these have traces of hematite. However, all samples of the Compton Conglomerate analysed for this thesis contained goethite exclusively, and were in the correct stratigraphic position to be the Compton Conglomerate. In the past the Compton Conglomerate has sometimes been mistaken for a terrestrial ferricrete (e.g. Horwitz, 1960).

Elsewhere in the Adelaide Plains Basin Eocene sediments contain detrital ferruginous nodules and fragments apparently derived from erosion of pre-existing ferruginous materials on the adjacent highlands and allude to pre-Eocene weathering and ferricrete formation (e.g. Glaessner, 1953a; Mawson, 1953; Bourman & Lindsay, 1973). Ferruginisation of Eocene sediments has also been described (Rix & Hutton, 1953; Glaessner & Wade, 1958) and this was regarded as evidence of 'lateritisation' in post-Eocene times. There is little doubt that the North Maslin Sands of Eocene age, as exposed in a quarry near Maslins Beach (Noarlunga MR 697987) have been weathered *in situ*, because clasts of kaolinitic-rich material occur within coarse gravels, grits and sands, and are most unlikely to have survived fluvial transport in their present condition.

Harris & Olliver (1964) noted ferruginisation of sediments of both pre- and post-Miocene ages in the Barossa Valley, and Pliocene ferruginisation has been attributed to ferricretes in the Happy Valley area (Olliver, 1964), in the Upper

Hindmarsh Valley (Horwitz, 1960) and on the Green Hills Surface near Victor Harbor (Bourman, 1973).

Fossiliferous Upper Pliocene marine sediments at Ochre Point have been iron-impregnated (Ward, 1966), suggesting post-Pliocene ferruginisation.

Furthermore, various Pleistocene deposits, perhaps extending to the Middle Pleistocene (May & Bourman, 1984), have been weathered and mottled. In the Willunga and Noarlunga Basins these include the Kurrajong, Seaford and Ochre Cove Formations of Ward (1966).

Some river terrace sediments of Late Pleistocene age at Victor Harbor contain thin lenses and bands of iron oxides, as do Holocene marine deposits near Yilki, also at Victor Harbor. This indicates mobility of iron in the landscape over these relatively recent times. Ferguson *et al.* (1984) described ferruginisation of Holocene sediments from iron-rich groundwaters in a peritidal environment near Port Broughton on Spencer Gulf, a process that is proceeding today.

#### **4.4.1 Downfaulted Mottled and Weathered Permian Sediments in coastal cliffs near Kingscote, Kangaroo Island.**

The most recent critical work related to the age of 'lateritisation' of the Mount Lofty Range Province summit surface in South Australia has been carried out on Kangaroo Island. In particular, the relationships between downfaulted and weathered Permian sediments and Jurassic basalt have been variably interpreted by Daily *et al.* (1974), Schmidt *et al.* (1976), Daily, *et al.* (1979), Northcote (1979) and Milnes *et al.* (1983), as reviewed in Chapter 3.

There is no complete 'normal laterite profile' exposed beneath the basalt on Kangaroo Island. In the coastal cliffs at Kingscote the basalt rests directly on cross-bedded sandy clays and clays (Plate 4.63). No mottles or crusts occur directly below the exposed base of the basalt (35 m asl) in the Old Government Quarry (Kingscote MR 391519), but at the Bluff Quarry (Kingscote MR 530370), basalt overlies mottled, weathered and ferruginised Late Palaeozoic glacial sediments at about 10 m asl. The sands in the sandy clays, collected from beneath the basalt in the Old Government Quarry (BOU 131) (Table 4.63) (Fig.4.32) consist of angular to sub-angular quartz grains, with the clay matrix containing kaolinite derived from weathering of feldspars. The sediment contains some quite fresh muscovites, while others are altered. Titanium

oxides cause darker colours in the sediment and tourmaline occurs in the sediment as do fresh opaque minerals and unsorted rock fragments. Minerals present in the bleached sediments (BOU 131) underlying the basalt contain kaolinite, but also smectite, feldspars and micas. Clay-rich sediments (BOU 127) (Table 4.63) directly under the basalt in the Kingscote cliffs consist of water-deposited mudstone with sand lenses. This sample contains similar minerals to sample BOU 131.

Once again materials regarded as being 'deeply weathered' and the pallid zone of a truncated 'laterite' profile, (Daily *et al.*, 1974) although containing some kaolinite, also display anomalous minerals such as feldspars and smectite with relatively high values of magnesium, potassium, sodium, calcium and iron.

Ferruginous mottles (BOU 108, BOU 118, BOU 125) (Table 4.63, Fig. 4.32) occur in Late Palaeozoic glaciogene sediments immediately north of the Kingscote jetty at Beare Point (Plate 4.64), but here the basalt does not directly overlie them. Thin section examination reveals that the mottles vary from close-packed silty sands with an iron oxide matrix containing clays and altered feldspar grains, to bedded sandstone comprising sub-rounded quartz grains in a clay and iron oxide matrix, in which iron has replaced the clays. Iron oxides impregnate all interstices and coat grain surfaces. The dominant minerals present are quartz, goethite, hematite, feldspars and kaolinite (Table 4.63). The iron content in the mottles varies from 6.56% to 23.47% and this is made up of variable amounts of goethite and hematite. No maghemite could be detected in bulk samples by XRD but all three reacted to a magnet, suggesting its presence in small amounts. Feldspars and smectites identified in the analyses also suggest that the material has not suffered protracted and intensive weathering. Pallid material surrounding the mottles is composed dominantly of quartz and smectite, which, with the presence of feldspars and only small amounts of kaolinite, supports the view that these sediments have not suffered intensive weathering.

The presence of maghemite and variable amounts of hematite in the mottles strongly suggests *in situ* formation via the rapid oxidation of magnetite derived from ferrous iron via green rust (Taylor, 1987), the effects of biomineralisation (Kirschvink, 1985), or from strong heating in the presence of organic matter during the extrusion of the Jurassic basalt over previously weathered and ferruginised glaciogene sediments, or from the dehydration of lepidocrocite

originally formed in reductomorphic conditions (Fitzpatrick, 1987). Maghemite occurrence is widespread in the sediments older than the Jurassic basalt, which may suggest that the weathering and ferruginisation of them pre-dated the eruption, which affected pre-existing iron oxides. Oxygen-isotope analyses of kaolinite, sampled from directly below the basalt and provided by the author for the A.N.U. Research School of Earth Sciences, suggest that kaolinisation may have occurred in the Early Mesozoic (M. Bird - *pers. comm.*) prior to the extrusion of the basalt.

There appears to be little doubt that *in situ* weathering and iron segregation have taken place in the sediments currently underlying the basalt. For example a large weathered boulder or concretion contains dominantly quartz and alunite with a trace of kaolinite in its core (BOU 105) and a distinct iron-rich rim (BOU 106) (Plate 4.65) (Table 4.63). The occurrence of alunite may imply reaction of sulphuric acid with illitic clays. In thin section the core material appears to be a mudstone, which still retains a shale fabric, with scattered fine quartz grains. In marked contrast the rim of the concretion (BOU 106) has a vastly different mineral constitution, including, goethite, hematite, feldspar and kaolin with a trace of maghemite. In thin section the rim has a similar fabric to that of the core material and there is a halo effect of  $TiO_2$  at the junction of the rim and core materials. It is doubtful that the weathered clast could have been weathered prior to transportation by Permian ice. Consequently it is suggested that the weathering and mineral segregation occurred *in situ*.

Elsewhere along the cliff-line north of the Kingscote Jetty large masses of iron-rich materials occur near the cliff base, such as BOU 119 (Table 4.64; Fig. 4.32), which is a massive boulder of iron-impregnated sediment. In thin section the boulder was noted to consist of quartz sand and finer grains set within a ferruginous matrix containing a few vesicles. Its mineralogy includes goethite, hematite and a trace of maghemite. The boulders of iron-rich material all have relatively high  $Fe_2O_3$  contents and are regarded as local concentration of iron-oxides in preferred zones.

All of the iron-rich materials sampled close to the basalt contain maghemite including BOU 115 (Table 4.64), which is from a large mass of iron-impregnated sediment slumped from the cliff face onto the beach below, at a point immediately north of the Kingscote Jetty. Thin section observations show



that the massive ferricrete is a fine silty sediment impregnated with iron oxides that form a very complex matrix. In some places box-work structures of iron appear to be replacing calcium carbonate.

On the other hand, the formation of maghemite from goethite by heating requires the presence of organic matter and temperatures of 300 - 500°C, which may not have been achieved due to the insulating effect of the sediments. Nevertheless, the heating may have been sufficient to have dehydrated lepidocrocite to maghemite and may have altered the palaeomagnetism of the pre-basaltic weathered materials, thereby negating the palaeomagnetic work of Schmidt *et al.* (1976), who attributed weathering to post-basaltic times. Additional problems facing the interpretation of Schmidt *et al.* (1976) are the occurrences of Eocene-Oligocene limestones at elevations up to 60 m asl and Early Miocene limestone up to 120 m asl on Kangaroo Island (Milnes *et al.*, 1983). Consequently the weathered zone may have been under many metres of sea at the time suggested by palaeo-magnetism for its weathering.

Where ferricretes occur within the weathered Permian glaciogene sediments they do not form part of a standard 'laterite' profile, but comprise highly contorted and convoluted masses or zones (Plate 4.66). There has been some controversy about the age and nature of these sediments. However, these zones correspond to sandier bands of relic ice-contact structures preserved from the Permian ice age some 270 Ma ago, and can be related to the removal of support for sediments deposited against and on ice during the decay of the Permian ice sheet. A glaciogenic origin for these sediments is also suggested by the presence of clay clasts in the sandy sediments (Plate 4.67). It has been suggested that these clasts may have been transported in a frozen condition and incorporated into new sediments prior to thawing, and have been recognised from other Permian glaciogene sediments in South Australia (Alley & Bourman, 1984). This explanation accounts for the anomalous disposition of fragile clay clasts in quartzose deposits. Examples of variably iron-impregnated ice-contact structures occur a few hundred metres north of the Kingscote Jetty and immediately behind the crusher at the Bluff Basalt Quarry that fronts onto the Bay of Shoals. The cross-bedded sediments that occur immediately below the basalt in the Old Government Quarry have been interpreted as fluvial deposits of various ages. However, the presence of rare clay clasts, involutions and collapse structures suggests very strongly that they are fluvio-glacial origin

and of Permian age, rather than the Tertiary and/or Mesozoic ages that have been ascribed to them by some workers.

The more porous sandy zones within the glacial sediments have served as sites for the deposition of ferrous iron from solution. Some of the upper portions of the iron-enriched zones have harder upper surfaces, which would have encouraged the lateral migration of ground waters. These iron zones superficially appear massive, tough and very high in iron content, but their total iron content can be quite small. For example, BOU 102 (Table 4.64) from such a crust contained only 10.74%  $\text{Fe}_2\text{O}_3$  predominantly in the form of goethite. Although sample BOU 106 has a high  $\text{Fe}_2\text{O}_3$  content, it is from only a very thin layer. Thin section and mineralogical data suggest the formation of the convoluted iron zones by impregnation of a dominantly sandy sediment with ferrous iron in solution. Some *in situ* weathering and rearrangement of elements within the sediments has occurred, but this cannot have been too severe as there is only a trace of kaolinite present and considerable feldspar remains. The intensity of weathering suggested by the concretion with the alunite core described above may reflect the alteration of an original sulphide-rich boulder.

In the same area, sediments younger than the Permian glacial sediments and the Jurassic basalt have also been impregnated with iron oxides. In particular, zones of the Eocene to Oligocene limestones (Milnes *et al.*, 1983) either side of the swimming pool on the Kingscote coast contain iron. These include a sandy bed of limestone about 30 cm thick and dipping at an angle of about  $30^\circ$  to the east. The top surface of this horizon corresponds to a disconformity within the Tertiary sequence (Milnes *et al.*, 1983). Thin sections suggest that there was impregnation of the limestone by iron oxides from an external source, with goethite crystals deposited within voids in calcareous fossils (Plates 4.68 and 4.69). Minerals identified in these samples (BOU 122 and BOU 137) (Table 4.64) include goethite, calcite and smectite, and total  $\text{Fe}_2\text{O}_3$  concentrations vary from 73.39% (BOU 137) to 10.52% (BOU 122). The sample with the higher iron content is much depleted in calcium carbonate, whereas the sample with the lower concentration of  $\text{Fe}_2\text{O}_3$  still contains 45.95% CaO. Unlike the iron oxides in mottles and sediments within the adjacent Permian glacial sediments, those impregnating the Tertiary limestones do not contain maghemite, suggesting that they record a younger episode of iron impregnation than those apparently heated by the basalt extrusion.

Alternatively, the varying environmental conditions in the two different sediments may have favoured the precipitation and crystallisation of different iron oxide phases.

The iron enrichment of the Eocene limestone may have occurred during the terrestrial exposure of the disconformable surface, but the possibility of submarine iron accumulation under non-depositional marine conditions should not be overlooked. A third possibility is the subsurface deposition of iron in favourable host sediments following the tectonic tilting of the beds. Whatever the process of iron enrichment it could not have taken place at least until after the deposition of the Eocene beds, but it could have occurred well after this time. Thus it is possible that the iron impregnation of the Late Palaeozoic glaciogene sediments and the Eocene to Oligocene limestones did not occur contemporaneously. In the light of the analytical data and the geological field relationships the palaeomagnetic data of Schmidt *et al.* (1976) must be regarded as equivocal.

#### 4.4.2 Pleistocene Sediments

##### 4.4.2.1 Mottled 'Kurrajong Formation' sediments

Ferruginous mottles were sampled from Pleistocene sediments mapped by Ward (1966) as the Kurrajong Formation. However, the view is followed in this thesis that the Kurrajong Formation of Ward (1966) is equivalent to the Ochre Cove Formation. Ward (1966) argued that the Kurrajong Formation was younger than the Ochre Cove Formation, citing the example of the Kurrajong Formation forming a river terrace near Aldinga and grading to a postulated shoreline younger than that to which he attributed the deposition of the Ochre Cove Formation. However, the author has been unable to locate the site of the Kurrajong Formation near Aldinga. Moreover, the sea-level scheme of Ward (1965; 1966) has been questioned by Twidale *et al.* (1967) and the timing of the suggested events may not be possible (May & Bourman, 1984).

Where the so-called Kurrajong Formation has been observed in the Willunga, Noarlunga and Adelaide Plains Basins, it has close associations with scarp foot locations along major escarpments, where it can dip westward quite steeply. The Kurrajong Formation is regarded in this thesis as a facies variant of the Ochre Cove Formation. It is essentially a colluvial or taluvial deposit that probably formed as a consequence of renewed Early-Middle Pleistocene tectonism related to the uplift of the Mount Lofty Ranges. Where exposed by

stream erosion at scarp foot locations the material may have undergone case hardening, possibly by secondary silicification in the channel floors. In places in Sellicks Creek it can be traced continuously from a hardened variety on a channel floor, to essentially unconsolidated material that closely resembles the Ochre Cove Formation nearby.

#### *4.4.2.1.1 Sellicks Creek (Fig. 4.1; I28)*

A ferruginous mottle (BOU 53) (Table 4.65) was collected from the right bank of Sellicks Creek, a short distance downstream from the main road to Myponga (Willunga 699872) from sediments considered to belong to the Ochre Cove Formation. The chemistry and mineralogy of BOU 53 are similar to that of mottles in sediments in other areas that have generally been considered to be of the Ochre Cove Formation (e.g. BOU 41) (Table 4.66). Maghemite was detected both by XRD and magnetic reaction, corroborating the work of Wopfner (1972a) at Hallett Cove. It is of some significance that the dominant iron oxides detected by XRD in Ochre Cove Formation sediments, and alleged Kurrajong Formation materials are maghemite and hematite.

#### *4.3.2.1.2 Other scarp foot environments*

Mottles (BOU 39, BOU 58, BOU 70, BOU 71, BOU 72, BOU 364) (Table 4.65) were sampled from various locations along the foot of the main escarpment backing the Adelaide Plains, from ferruginised fanglomerate materials, and all had similar chemistry and iron oxide mineralogy. These are all regarded to represent the fanglomerate facies of the Middle Pleistocene Ochre Cove Formation considered by Ward (1966) to be the Kurrajong Formation. The chemistry and mineralogy of the mottles in these sediments reflect the character of the parent materials and the iron oxides, which in turn reflect the environments of their precipitation and crystallisation.

#### *4.4.2.2 Hallett Cove (Fig. 4.1; I22)*

A thin section of a mottle (BOU 41) (Table 4.66) sampled from the Ochre Cove Formation at Hallett Cove (Plate 4.70) revealed a framework of closely packed, well rounded and slightly embayed quartz sands, set in a clay-rich matrix impregnated by hematite. At high magnification, under conditions of incident polarised light, shrinkage fractures through the clay matrix can be observed to display hematite-enriched margins that suggest zones of influx of iron into, or loss of iron from the system. Under the same optical conditions patches of opaque oxides occur within the matrix that are almost certainly maghemite.

An adjacent mottle free zone in the Ochre Cove Formation (BOU 40) (Table 4.66) in thin section appears identical to the mottled material apart from the absence of opaque iron oxides. XRD analysis revealed that the bleached sample contained more kaolin, micas and anatase than the mottle. The difference in total  $\text{Fe}_2\text{O}_3$  iron content is less than 9%.

#### *4.4.2.3 Redbanks, Mid North (Fig. 4.1;J10)*

Mottled (BOU 44) and bleached (BOU 43) (Table 4.66) samples from the Ochre Cove Formation (Hindmarsh Clay of Firman, 1967b) at Redbanks on the River Light near Mallala were also compared. The Pleistocene sediments here overlie fossiliferous Pliocene limestone (Lindsay, 1969). The framework grains of both samples were clay and silt-sized ill-sorted quartz grains with fresh micas and feldspars. The major difference between the two was the iron content. The matrix of the mottle is impregnated with iron oxides and the original clay matrix is preserved, with the fabric of the material having been little affected by the influx of iron. The mineralogy of the samples is similar except that the mottle contains hematite and maghemite.

It was noted that the ferruginised Pleistocene sediments at Redbanks (Plate 4.71) were being readily eroded as the exposed surface material (BOU 59) was puffy, with relatively coherent sediments not occurring until up to 10 cm below the surface. The iron content of this sample was too low to identify iron oxides by XRD. Apart from these iron minerals, however, the minerals identified had also been recognised in previously analysed samples of mottled and bleached sediments (BOU 43; BOU 44), but, significantly, halite was identified in the surface crust. It appears that the growth of halite crystals has contributed to the weathering and break up of the exposed surfaces at this location.

#### *4.4.2.4 Bow Hill, Murray Basin*

A thin section sample of ferruginous material collected from the Blanchetown Clay (BOU 42) (Table 4.66), the Murray Basin equivalent of the Hindmarsh Clay, revealed closely-packed, rounded to sub-angular and embayed silty sand grains forming a framework with a clay (kaolinite) and iron oxide (dominantly goethite) matrix. Glaebular concentric structures, opaque in transmitted light, possibly consisting of hematite, occur within the dominantly goethitic matrix. This sample from the Murray Basin varies from apparently equivalent Pleistocene sediments in the St. Vincent Basin in that it has a much higher

total iron content (41.31%) and goethite is more common than hematite. It does contain a small amount of maghemite.

#### 4.4.2.5 Ochre Cove/Ochre Point (Fig. 4.1; I25)

At Ochre Cove (Plate 4.72) and Ochre Point, west of Ochre Trig. (Noarlunga MR 702997), a sequence of Pleistocene sediments standing above weathered basement rocks and sediments of Pliocene age was examined. Weathered and ferruginised Precambrian bedrock (BOU 365) (Table 4.67) occurs at the base of the sequence at Ochre Point. The major constituents of the bedrock are SiO<sub>2</sub> (49.4%), Fe<sub>2</sub>O<sub>3</sub> (24.22%) and MgO (13.17%). The mineralogy of this sample, with a dominant iron oxide mineralogy of hematite, sub-dominant goethite and no maghemite is typical of weathered and ferruginised basement rocks examined in many other areas.

At Ochre Cove, tilted Tertiary limestone also occurs and this is overlain by weathered quartz-rich grits and sands (BOU 47) that occur at the base of the Pleistocene sequence and are possibly of Tertiary age. At Ochre Point the Cainozoic sequence rests directly on the Precambrian basement rocks and the base of the younger materials is marked by a hard ferruginised crust (BOU 51), up to 0.5 m thick and regarded by Ward (1966) as the equivalent of the Upper Pliocene Hallett Cove Sandstone because it grades laterally into a softer crust that contains casts of marine fossils (BOU 50) (Table 4.67). This sediment is dominated by quartz and the only iron oxide identified in it was goethite. This phenomenon has been observed with respect to many other examples of iron oxide impregnation of pre-existing sediments, especially limestones. Similar material in the same stratigraphic situation at Ochre Cove (BOU 49) has its iron oxide mineralogy dominated by goethite. No maghemite was detected by XRD but the sample reacted slightly to a magnet.

Similar mineralogical and chemical analyses were obtained for sample BOU 50 (Table 4.67), which contains casts of marine fossils. However, no microfossils were observed in thin section, and the small amount of CaO (0.07%) in the sample suggests that there has been almost complete replacement of the marine fossils by iron oxides. The weathering appears to have been isovoluminous as the integrity of the fossils has been retained, which suggests direct substitution. The sediment is revealed in thin section to consist of a closely packed, bimodal sand with coarse and gritty sub-angular to sub-rounded quartz grains set in a matrix of fine angular silt with a

ferruginous clay cement that occurs generally as coatings on quartz and represents a single phase of iron enrichment.

Standing above the ferruginised layer of probable Pliocene age are green/grey sandy clays with weak orange-coloured mottles. These sediments were assigned to the Seaford Formation by Ward (1966). This material (BOU 48) (Table 4.68) is dominated by quartz with small amounts of smectite, feldspars, kaolinite and goethite. The mottled material contains only a very small amount of  $\text{Fe}_2\text{O}_3$  (2.55%) as goethite. No maghemite was detected either by XRD or response to a magnet.

Two samples were collected from within the overlying Ochre Cove Formation at Ochre Cove, one from near the middle of the formation (BOU 46) and one near its top, just below the base of the Ngaltunga Clay (BOU 45) (Table 4.68). Sample BOU 46 consists of a silty sand set within a clay and iron groundmass. There is little  $\text{Fe}_2\text{O}_3$  in this sample (7.54%), which occurs as goethite. Sample BOU 45 in thin section showed as a closely packed bimodal sand with thin iron coatings of goethite.

Above the level of the previously described materials, pisoliths were collected from the modern groundsurface at the western end of Lennard Drive at Moana (Noarlunga MR 698005). The chemistry and mineralogy of these pisoliths (BOU 334), which are shown in Table 4.68, are typical of many surface or near surface occurrences, particularly with respect to the presence of hematite and maghemite.

#### *4.4.2.6 Kangaroo Island*

As well as there being Cambrian, Late Palaeozoic and Tertiary rocks affected by weathering and ferruginisation on Kangaroo Island, there are also Pleistocene sediments that have been variably ferruginised and mottled.

Where the main Kingscote-Penneshaw road crosses the Cygnet Fault scarp about 8 km southeast of the Kingscote Aerodrome, and near to Yorke Farm (Kingscote MR 350400) at approximately 30 m asl a composite profile is exposed in a road cutting (Plate 4.73). The base of the section is composed of mottled clayey sands, which superficially resemble the Middle Pleistocene Hindmarsh Clay of Firman (1967b) or the Ochre Cove Formation of Ward (1966). In thin

section this sample (BOU 112) (Table 4.69) appears as a sand-sized sediment with iron oxides (goethite and hematite) replacing clay in the matrix.

The layer of mottled clayey sand is succeeded by a calcareous-rich horizon up to 1 m thick. Calcium carbonate from this zone penetrates along fissures to greater depths in the underlying mottled material. In thin section this sample (BOU 111) (Table 4.69) has a similar nature to the underlying material except that the matrix is composed of calcium carbonate (calcite) and clay. Developed over the calcium carbonate-rich layer is a yellow-coloured duplex soil (KS-Dy5.43), which contains ferruginous pisoliths (BOU 110) (Table 4.69) in the A-horizon and at the surface. In thin section the pisoliths appear as complex features with rims of different materials. Clasts of varying materials occur in the cores of the pisoliths, and iron oxides cement quartz grains in successive outer layers. Quartz, hematite and maghemite dominate the mineralogy of the pisoliths (BOU 110 and BOU 148) with other minor minerals present including feldspars, kaolinite, micas, gibbsite, smectite and anatase. The chemical and mineralogical compositions of the pisoliths reflect a long history of transport in the environment. Although the pisoliths overlie Pleistocene sediments they may have derived from older Tertiary ferricretes.

The calcareous horizon in the sequence lenses out down the slope of the hill and reappears in a similar sequence on the next hill summit to the southeast. However, the yellow duplex soil and its associated pisoliths uniformly mantle the intervening valley. The question arises as to whether the pisoliths formed *in situ*, or whether they were transported from a more distant source. A fairly extensive landsurface varying from about 90 m to 60 m asl lies south of this site on the summit of the Cygnet Fault Block and the pisoliths may have derived from this surface. It appears that the landscape about 'Yorke Farm' has suffered dissection during the Pleistocene, following uplift along the Cygnet Fault.

It is possible that the calcium carbonate material was blown into the area after the mottling of the underlying material and the formation of the pisoliths, and the pisoliths progressively migrated upward as the calcium carbonate loess accreted in the fashion described by Jessup (1960) for the formation of stony tableland soils. However, the fact that the soil and its pisoliths drape the valley where the carbonate layer has been eroded suggests that the soil and its pisoliths formed after the deposition and the dissection of the carbonate layer.



The complex internal structures of the pisoliths, their high iron contents, and incompatibilities of the pisoliths and the underlying materials, mineralogically and chemically, suggest derivation from a more distant source. It is possible that ants may have brought ferruginous fragments up to the surface, even through the carbonate layer, and were transformed into pisoliths in the soil, but most evidence favours a lateral source for them. The identification of gibbsite in them strongly favours derivation from older more severely weathered parts of the landscape. In some respects this situation of mottled bedrock overlain by calcareous sediments on which ferruginous pisoliths rest is similar to the situation on the Blue Range on Eyre Peninsula (Section 6.3.1.1.1.1) and on the hills to the south of Lochiel (Section 4.2.4.1) in the Mid North of the State.

The fact that the pisoliths mantle the soil over a variety of relief attests to the physical mobility of pisoliths, which are very widespread over much of the Kangaroo Island landscape. Lateral physical translocation of individual pisoliths over the landscape, especially after fire or other degradation of vegetation, which could include climatically-induced deterioration appears to have been extremely significant in explaining the present distribution of many ferruginous pisoliths.

Other Pleistocene deposits, both iron-mottled and calcareous occur along the coast at Redbanks (Kingscote MR 460416) (Plate 4.74) at elevations from sea level to about 15 m asl. The ferruginous mottled material (BOU 123) (Table 4.69) in thin section appears as sandy and gritty unsorted grains of quartz with a clay matrix impregnated by iron oxides. Some biogenic material, probably wood, has been transformed into iron oxides and silica. The clay matrix is mixed intimately with iron oxides. Although the mottle had a red pigmentation, the sample contained only 2.9%  $\text{Fe}_2\text{O}_3$ , and no iron oxide minerals could be identified by XRD. This demonstrates the small amount of iron oxides, particularly hematite, required to pigment some materials. The composition of an adjacent bleached sample (BOU 139) (Table 4.69) is very similar to that of the mottle (BOU 123), with the  $\text{Fe}_2\text{O}_3$  content variation being 1.77%. The occurrence of smectite, illite and feldspar, with only a small percentage of iron oxides, suggests that the sediments have not been intensely weathered and ferruginised. Moreover, the physical and chemical composition of these mottles do not equate with mottles developed in older materials such as those in the Permian glaciogene sediments at Kingscote.

Within the iron-mottled Pleistocene sediments at Redbanks, reworked pisoliths have been buried along with quartz clasts and grits. Thin section examination reveals that these are reworked, complex pisoliths (BOU 132 and BOU 121) (Table 4.69), with variable matter in their cores such as metamorphic rock fragments and clasts of clay and iron oxides. The cores are rimmed with several laminae of iron oxides (hematite, maghemite and goethite) and fine quartz grains.  $\text{Fe}_2\text{O}_3$  contents vary from 7.7% to 33.8%. The presence of multiple rinds and maghemite suggests some antiquity in the pisoliths and that they occupied a surface or near surface position prior to transport and burial within the Pleistocene sediments at Redbanks.

#### **4.4.3 Conclusion**

An assessment of evidence from the basins thus supports the view that there has been long and probably continual, but variable, chemical or physical mobility of iron in the landscape, and precipitation or clastic deposition of it in preferred localities over great periods of geological time. This evidence suggests that the present landscape should be viewed within a framework of a complex series of geological and geomorphic events on which the imprints of continual weathering have been superimposed, rather than within one requiring discrete episodes of climatically controlled 'lateritisation'.

#### **4.5 Recent and Continuing Iron Mobility**

Not only is there evidence of iron enrichment having occurred at various times in the past within and on the margins of the Mount Lofty Range Province, but iron mobilisation and precipitation are still active today in various locations.

##### **4.5.1 Fisherman Bay**

Ferguson *et al.* (1984) reported 'high concentrations of goethite, limonite and iron sulphides and lesser concentrations of hematite and ferromanganese oxides forming in Holocene carbonate sediments in the peritidal zone of Fisherman Bay, a hypersaline marine embayment on the semi-arid northeast shore of Spencer Gulf, South Australia', where a 'lens-shaped deposit of ferric oxyhydroxides' occurs. From this site (Figs. 4.34, 4.35; Plate 4.75) samples were collected of fragments of a biscuit-like crust at the surface (BOU 84), from an underlying hard and continuous crust about 20 cm thick (BOU 85), and from a soft rich red clay (BOU 86) under the crust (Table 4.70).

Minerals identified in the surface material (BOU 84) included gypsum, quartz, halite, aragonite, pyrite and small amounts of smectite and kaolinite. The  $\text{Fe}_2\text{O}_3$  content of 22.71%, the lack of clearly identifiable iron oxide minerals and very broad peaks in the diffractogram suggest the presence of ferrihydrite. The high ignition loss (26.78%) and the apparently unreliable total of 94.8% suggest a high loss of  $\text{SO}_2$  from the sample during ignition, as both gypsum and pyrite occur in the sample. The material comprising the hard, continuous subsurface crust (BOU 85) contains quartz, hematite, goethite, ferrihydrite, rozenite, anhydrite, smectite, kaolinite, feldspar, and randomly interstratified clays. It has higher  $\text{Fe}_2\text{O}_3$  (36.15%) and  $\text{SiO}_2$  (46.1%) contents than BOU 84 and a much lower ignition loss. Minerals identified in the underlying red clays included quartz, hematite, kaolinite, micas, feldspar, smectite, randomly interstratified clays, anatase and possible griegite.

These analyses provide greater detail of the mineralogical assemblage of these iron-rich deposits of the Holocene. In contrast to Ferguson *et al.* (1984), who considered that the main iron minerals present were goethite and 'limonite', the analyses presented here suggest that ferrihydrite and hematite are more dominant. This variation may simply reflect differences in sampling, but the analyses demonstrate that hematite is almost certainly currently forming in the modern environment via the dehydration and crystallisation of ferrihydrite.

#### 4.5.2 Boinkas of the Murray Basin

The widespread deposition of iron oxides along the margins of lakes or boinkas in the Murray Basin of Victoria (Fig. 4.34) has been reported by Macumber (1983). Acid groundwaters containing between 10 and 150 mg/l of Fe(II) have deposited iron oxides at the location of fluctuating lake shorelines. This deposition has been attributed to the exposure of the ferrous iron-rich spring waters to the atmosphere and the interaction of the acid-rich groundwaters with the neutral lake waters (Macumber, 1983). This worker has demonstrated the operation of these processes throughout the past 0.5 Ma of the Quaternary, and warns against interpreting these ironstone crusts as pedogenic features and confusing them with older weathering phenomena.

Four samples from the Hatta Lakes in Northwestern Victoria were analysed (Table 4.70). Recently developed and unconsolidated soft iron-rich material (BOU 61) contained hematite, jarosite, halite, feldspar, smectite and probably ferrihydrite. Consolidated pipestems (BOU 65) contained much more  $\text{Fe}_2\text{O}_3$

(28.46%), dominantly in the form of goethite, with some hematite. Samples BOU 66 and BOU 67 were collected from an 'island' above the general level of the dry lake surface, and probably represent materials deposited during a higher lake level of the Pleistocene. Purplish coloured material (BOU 67) has hematite as its main iron oxide with a trace of goethite, whereas in BOU 66 there are roughly equal amounts of goethite and hematite. There are slightly higher  $\text{Fe}_2\text{O}_3$  contents in the purple sample.

The mineralogy and chemistry of these four samples are in sympathy with their origin proposed by Macumber (1983). Halite and jarosite are typical of saline lacustrine environments, and ferrihydrite is well established as a precursor of hematite and goethite. The goethite in some samples probably resulted from the dissolution of the hematite and reprecipitation under slightly different conditions following the reduction in lake levels that stranded some of the ferruginous materials above the water levels of the modern lakes. The assemblage of clay minerals is dominated by smectite, and this, together with the presence of feldspars and micas suggest that the sediments have not been affected by intensive weathering. Only extremely minor amounts of kaolinite were identified, and these may have been inherited.

There is clear evidence that the processes of ferruginisation are proceeding in specific parts of the modern environment, under present climatic conditions. Thus care must be taken not to confuse the results of this mode of iron enrichment with other mechanisms, nor to equate it with 'lateritisation' or tropical climates. Careful examination and analyses of older analogous crusts by using landscape reconstruction and mineralogical and chemical criteria should help to avoid these pitfalls.

#### **4.5.3 Mount Compass 'Coffee Rock' (Fig. 4.1; K28)**

In a sand quarry near Mount Compass (Willunga MR 825857) there are Spodosols (Podzols) with well developed pipy Bh and Bhir horizons (Plate 4.76). The soil has developed on Permian glaciogene or reworked glaciogene sediments and at the base of the quarried material numerous exotic pebbles occur. Chemical analysis of a sample of the placic Bhir horizon (indurated 'coffee rock') (BOU 1) (Table 4.71) reveals that it is almost totally composed of  $\text{SiO}_2$  (94.3%), with only small amounts of  $\text{Al}_2\text{O}_3$  (1.8%) and  $\text{Fe}_2\text{O}_3$  (0.65%). It was difficult to identify minerals other than quartz, but very small amounts of feldspar and kaolinite may be present. In thin section the indurated material is

composed dominantly of fine, single grain sand or silt-sized, sub-angular quartz grains and larger rounded quartz and metamorphic rock fragments, together with occasional tourmaline, zircon and rutile grains, set in a reddish matrix. The sediment is thus bimodal and is also well-packed. These size and sorting characteristics probably reflect derivation from glacial deposits. Thin brown-yellow coloured mixtures of organic material (sometimes in colon-shaped clumps), clay and possibly iron oxides coat individual grain surfaces and form bridges across voids between quartz clasts (Plate 4.77).

Although this particular example contains very little iron, it provides an example in a modern soil of profile differentiation and the establishment of a framework within which further iron enrichment could occur. At the base of the quarry floor, in the Permian glacial sediments (C-horizon), pronounced occasional zones of iron enrichment (e.g. 52.1%  $\text{Fe}_2\text{O}_3$ ) occur that have formed geodes (BOU 16) (Table 4.71). The minerals identified in this sample include goethite and hematite with small amounts of kaolinite and micas. This occurrence of differential iron enrichment suggests the former presence of iron oxides influxed in solution and precipitated in favourable situations.

Some of the low-lying swampy country in the same area is underlain by clays where the water table is within 1 m of the surface, and in this environment, quite pronounced mottling by iron oxides (dominantly goethite and lepidocrocite) can be detected (Fitzpatrick & Schwertmann, 1982). This again suggests active iron mobilisation and precipitation under modern physical and climatic conditions.

#### **4.5.4 Kangaroo Island**

While carrying out hydrological investigations on the plateau of Kangaroo Island, Hartley (1981) noted that the water table in the weathered zone of the plateau surface commonly fluctuates seasonally between a depth below the surface of 3 m in winter and 9 m in summer. Moreover, there is a considerable amount of salt in the profile, some of which may be inherited from former Tertiary high sea levels, but large volumes of which have been derived as cyclic salts from the sea via rainfall. An average amount of 300 kg/ha/pa of salt has been measured by analysis of rainwater on the plateau (Hartley, 1981). Since the area has been cleared of vegetation, the water table has risen, bringing stored salts closer to the surface and initiating saline seeps (Plate 4.78). Holes were augered below the water table on both the plateau and in the seepage

zones in order to monitor water levels and water chemistry (Hartley, 1981). Piezometers located at a depth of a couple of metres in seepage zones on the margins of the plateau were found to be covered with ferrihydrite when removed. It seems that descending saline waters have leached iron out of the weathered bedrock underlying the plateau surface and this iron has been re-precipitated in the saline seepage zones.

Pallid material (BOU 140) (Table 4.71) from under the plateau surface was analysed and minerals present included kaolinite, muscovite, feldspars, smectite and vermiculite. Chemically this bleached material is composed principally of  $\text{SiO}_2$  (76.4%),  $\text{Al}_2\text{O}_3$  (14.16%),  $\text{K}_2\text{O}$  (1.93%) and  $\text{Fe}_2\text{O}_3$  (1.48%). Material collected from a depth of 1 m in the seepage zone (BOU 141) (Table 4.71) displays a greater diversity of minerals, including kaolinite, gibbsite, ferrihydrite, anatase, possible hematite, micas, smectite and feldspars. These two analyses revealed that there is an increase in total iron oxide content and  $\text{TiO}_2$  at the seepage zone, that there is more kaolinite in the upper plateau material without any free aluminium oxides, but that at depth there is gibbsite. There is a higher  $\text{Al}_2\text{O}_3$  content in the seepage zone, which occurs partly as gibbsite. The aluminium may have migrated in solution to the seepage zone in the same fashion as has the iron. This could also be reflected in the variations in  $\text{SiO}_2$  between the two sites.

Ferruginous sludge (BOU 142) (Table 4.71) was collected from a tributary creek of the Middle River drainage system. The sludge had been recently deposited by a slightly higher flow stage. Minerals identified in this modern stream deposit by XRD included feldspars, smectite and kaolinite. XRF analysis demonstrated a high  $\text{Fe}_2\text{O}_3$  content of 28.97% although no goethite or hematite could be identified by XRD. The iron present was largely in the form of the very poorly crystalline ferrihydrite. Small amounts of maghemite which were probably derived from a pre-existing source, were detected with a hand magnet. A point of interest is the high total  $\text{Fe}_2\text{O}_3$  content, which at 28.97% is many times higher than apparently iron-rich crusts and prominent mottles, some of which have total iron contents well below 10%.

Small pisoliths and incipient pisoliths (BOU 133) (Table 4.71) were collected from a periodically active seepage zone on the margins of Tin Hut Creek, a tributary of the Cygnet River, at about 230 m asl (Stokes Bay MR 866367). These appeared as segregations of iron within sandy sediments. In thin

section the incipient pisoliths had various cores including metamorphic rock fragments, biogenic material (Plate 4.79) and sandy clays impregnated with iron oxides. Simple rims consist of sandy clays variably impregnated with iron oxides. Minerals identified in these segregations included quartz, goethite, feldspars, kaolinite, vermiculite and smectite. Maghemite could not be detected either by XRD or with a magnet. This, together with the absence of hematite and thin section data, which reveal the nature of the original cores around which the pisoliths have developed, and their simple non-complex character suggests that they have formed *in situ* by the segregation of iron oxides, precipitated from ground waters, around various nuclei.

Thus there appears to be evidence of modern chemical iron mobility and precipitation in various seepage zones and drainage lines on Kangaroo Island. There is also clear evidence demonstrating the ease with which pisoliths can be moved physically in the landscape. This is provided by the rapid transport of pisoliths from ferricrete used in the construction of a car park at Remarkable Rocks. Within a short time after the original construction of the car park, pisoliths had been washed almost down to sea level.

#### **4.6 Age of the summit surface and its associated 'laterite'**

As discussed in the review (Chapter 3) on 'laterite' studies in southern South Australia, a variety of ages have been attributed to 'lateritisation' of the summit surface, often on scanty and equivocal evidence. Some of the more critical evidence for the age of the summit surface and its associated 'laterite' will now be considered.

##### **4.6.1 Mid North area.**

Part of the summit erosion surface in the North Mount Lofty Ranges was tentatively equated with the Mount Herbert Surface by Alley (1969). Horwitz (1961) had correlated pisoliths on this surface with apparently equivalent pisoliths at the base of Early Tertiary sediments. On this basis the summit surface was assigned to the pre-Tertiary and Early Tertiary. This age was also favoured by Alley (1969), as downfaulted areas, regarded as equivalent to the Mount Herbert Surface, were presumed, in places, to be buried under Middle and Upper Eocene sediments and elsewhere to predate a silicified surface of Miocene age. The occurrence of pre-Tertiary weathered bedrock is well documented in many areas of southern South Australia, but evidence presented in this chapter demonstrates the relatively youthful age of the

current summit surface, so that the buried and exposed landsurfaces cannot be regarded as of equivalent ages.

#### 4.6.2 *Kangaroo Island*

Investigations of relationships of weathered zones to Jurassic basalt (Daily *et al.*, 1974) on Kangaroo Island concluded that 'laterite' on the summit surface of Kangaroo Island, regarded as equivalent in age to the summit surface on the mainland, predates the Middle Jurassic Wisanger Basalt.

Schmidt *et al.* (1976) favoured sub-basaltic weathering to account for their palaeomagnetic data, which suggested that 'lateritisation' was of post-Jurassic age and was probably related to a Late Oligocene to Early Miocene weathering event. However, Milnes *et al.* (1982), presented convincing field evidence for pre-Jurassic weathering and a former high Early Miocene sea level that could explain the paucity of weathering on the basalt surface.

#### 4.6.3 *South Mount Lofty Ranges*

In some localities on the spine of Fleurieu Peninsula such as at Spring Mount, Mount Cone and the Parawa area, the summit surface appears to have stood above the highest levels reached by the Tertiary seas, so that the surface is potentially of some antiquity, and has been subjected to weathering and erosion during and since the Mesozoic. Some other areas of the present summit surface were submerged by marine or terrestrial sediments that in turn became affected by the processes of weathering, ferruginisation and erosion. In some localities the older weathered surface has been exhumed from beneath Tertiary sediments. Consequently the age of the summit surface is extremely variable. Even where some relics of Mesozoic weathering may persist in the modern landscape, the evidence presented suggests that weathered and mottled zones have progressively been affected by various degrees of landscape downwasting so that it is most improbable that Mesozoic landforms survive as has been claimed by Twidale (1976). It is also probable that Mesozoic weathering only persists where it has been protected by burial. Moreover, more recent soils are superimposed on inherited weathering so that the sandy A-horizons of current duplex soils cannot be regarded as parts of original 'laterite profiles' (e.g. Twidale, 1976).



#### 4.6.4 Oxygen isotope analyses

As part of a co-operative project with Mr. M.J. Bird of the Research School of Earth Sciences at A.N.U. analyses of stable oxygen isotope compositions of kaolinite from various weathered zones in South Australia have been undertaken. The application of the oxygen isotopic compositions of minerals in weathered zones is considered to be primarily dependent upon groundwater composition and temperature conditions during weathering. Some workers claim that original  $^{18}\text{O}/^{16}\text{O}$  ratios in some weathering minerals, particularly kaolinite and gibbsite, are retained over time (Lawrence & Taylor, 1971; Yeh & Savin, 1976) so that the isotopic compositions of these minerals should reflect the composition of water during their formation and, indirectly, the prevailing climatic conditions. Factors such as altitude, latitude and the evolution of the current atmospheric distributions of oxygen and hydrogen isotopes are considered important in influencing the interpretation of the data derived from weathered zones. Bird (*in prep.*) is developing an empirical oxygen isotope curve from analyses of weathered zones of established ages in order to date weathered zones where there are no other indications of their ages.

Oxygen isotope data with a range of values from +11.5‰ to +14‰ derived from kaolinite in sediments underlying Jurassic basalt at Kingscote on Kangaroo Island suggest that weathering occurred in the Early Mesozoic. In contrast, data derived from weathered bedrock on the exposed summit surface of Kangaroo Island, is distinctively different (+18‰ to +20‰) and compatible with results obtained from Mid Tertiary kaolinites elsewhere in Australia (Bird, *in prep.*). Analyses of kaolinite samples (values +19.4‰ to +20.4‰) from the summit surface on Fleurieu Peninsula also suggest that the kaolinisation is of Middle Tertiary age, and on this basis cannot be equated with the weathering beneath the basalt on Kangaroo Island, as has been done by Twidale (1983).

Analyses of kaolinite samples from successively lower levels in the RBA-3 auger hole on the Parawa Plateau suggest that the age of kaolinite formation decreases with depth (Bird, *in prep.*). Kaolinite derived from depths in excess of 13 m may demonstrate even younger ages for kaolinisation at these levels. This recognition of possible younger kaolinite at depth may support the suggestion by Bourman (1973) that weathering under the present summit surface may have continued after, and have been facilitated by, the uplift of the Mount Lofty Ranges. Furthermore, evidence supporting the view that rejuvenation re-

instates weathering has been marshalled by McFarlane (1976) from observations in Uganda.

#### **4.6.5 Discussion**

The evidence presented in this chapter suggests that there is great variety in the nature and age of the summit surface of the Mount Lofty Range Province, and that each area of the summit surface requires detailed assessment in order to elucidate its evolution. No simple generalisations can be deduced from the evidence currently available. Furthermore, data presented in this thesis suggest that the summit surface has developed as a consequence of continually operating processes of weathering, erosion, transportation and sedimentation over a long time period, beginning in pre-Tertiary times. These processes resulted in ferricrete formation in discrete preferred localities and the ferricretes are not mono-genetically related to the underlying weathered zones as parts of 'laterite profiles'. Everywhere they are considered to be younger than the immediately underlying weathered bedrock materials. This model of development is preferred over the alternative interpretation that this area is underlain by an ancient monogenetic 'lateritic' weathering profile largely preserved in its present form since the Mesozoic, and that the present sporadic distribution of ferricrete reflects differential erosion of a former continuous sheet of ferricrete.

#### **4.7 Conclusions**

The above information summarises data revealing great variability in the distribution of ferricretes throughout the present landscape and variations in their characters expressed in macro-, meso- and micro-morphologies, mineralogical and chemical compositions and their relationships to current and former environmental conditions. It also illustrates the great range of time over which iron oxide mobilisation, physical and chemical transport, precipitation and induration have occurred, with these processes currently operating in parts of the modern landscape. Consequently it is difficult to generalise on a particular time of 'lateritisation', for there is evidence of various ages of weathering and ferruginisation, with continual weathering and other processes leading to the modification of weathered and ferruginous materials.

The model of the 'normal laterite profile', which has been adhered to in the majority of South Australian studies, at least since the work of Stephens (1946),

is untenable. So-called 'laterite profiles' are incomplete, lacking one or more of the predicted zones. There is no convincing evidence for former continuous ferricrete crusts mantling extensive areas of previously 'peneplained' surfaces. In contrast, weathering and erosion in the Mount Lofty Ranges appear to have occurred in a landscape of considerable relief, with salients of resistant hills and ridges protruding above an undulating landsurface that was differentially weathered and ferruginised. Thus the view that the absence of crusts over mottled zones reflects erosion of the original complete profile is not accepted here. Rather, where associated with iron mottled and iron depleted materials, surficial iron-rich crusts appear to have formed through the physical residual accumulation of iron oxides associated with the general lowering of the landscape and their chemical and physical modification, transformation and cementation during landscape downwasting.

Ferricrete crusts on the summit surface of the Mount Lofty Range Province are currently discontinuous and it is unlikely that they were ever continuous, but formed only where depressions and low angle slopes, drainage and groundwater conditions favoured the accumulation of iron and aluminium oxides in ancient depressions, host sediments and soils. By analogy with evidence from the marginal basins and lower level ferricretes, the summit surface ferricretes developed in discrete areas and express the results of continually operating weathering processes.

There are insurmountable problems in explaining the character of the weathered and ferruginised summit surface of the Mount Lofty Range Province in simple terms of preservation of the results of Mesozoic weathering as has been postulated by Twidale (1983). Not only is the evidence for this age equivocal with respect to the relationships between the weathered material underneath the Jurassic basalt at Kingscote, and the weathering on the summit surface, but other stratigraphic evidence demonstrates that much of the present summit surface must be younger than the Early Miocene. Furthermore, the evidence presented of physical and chemical reworking of ferricrete materials and continuously operating processes of weathering, transformations and ferruginisation, over vast periods of geological time, and through to the present, show that the view of the preservation of ferricretes for some 200 Ma of epigene exposure is untenable and unnecessary.

The evidence of a variety of ferricretes of different origins and ages throughout the Mount Lofty Range Province demonstrates the simplistic character of this interpretation; some features regarded as 'laterite' are stratigraphic sequences, others relate to land surface lowering and the formation of lags of hardened mottles, others to the physical and chemical reworking of pre-existing iron-rich materials. While there may be pallid and mottled materials and crusts formed in preferred topographic and groundwater situations, they do not occur within the framework of the classic 'laterite' profile. Thus the correlation of erosion surfaces on the sole basis of superficial evidence of 'lateritisation', even within the same region, is likely to be unreliable.

## CHAPTER 5: A SYNTHESIS OF GENERALISATIONS DERIVED FROM INVESTIGATIONS OF FERRICRETES AND OTHER FERRUGINOUS AND WEATHERED MATERIALS

### 5.1 Introduction

The findings derived from field and laboratory investigations reveal weathered and/or ferruginous materials occurring on landsurfaces exposed to weathering processes for variable periods of time. These range from parts of the long exposed summit surface down to recently formed modern valley floors. Moreover, rocks and sediments, varying in age from the Precambrian to the Holocene, display variable degrees of weathering, iron bleaching, mottling and iron-enrichment, illustrating iron mobilisation throughout immense periods of geological time including the present. In some instances, the nature of the secondary iron minerals, and the recognition of the secondary aluminium mineral, gibbsite, as well as the presence of layer silicate minerals may give clues to the relative ages and conditions of formation of the ferricretes.

In carrying out investigations of ferricretes and mottled and weathered zones in the Mount Lofty Range Province, various categories and types of ferricretes have been recognised and described in Chapter 4 on the basis of field relationships and macro- and meso-morphology. With associated laboratory data given in Chapter 4 it has become evident that many ferricretes have distinctive physical and chemical characteristics, which coincide with their geomorphic situations and so possibly reflect environmental conditions during their formation or transformations.

The generalisations enunciated in this chapter have been derived essentially from studies in the Mount Lofty Range Province, as detailed in Chapter 4. Other areas in southeastern Australia were subsequently investigated to test and extend the ideas generated: the results of these studies are presented in Chapters 6, 7, 8 and 9.

### 5.2 Categories of Ferricretes

Three broad *categories* of ferricretes have been recognised, initially on the basis of reconnaissance studies of ferricrete samples from Australia and southern Africa (Milnes *et al.*, 1987). These are:-

- i. Ferricreted bedrock,

- ii. Ferricreted sediments. These comprise iron oxide-impregnated and indurated sediments, that include clays, silts, sands, grits, gravels, as well as organic deposits, and
- iii. Ferricretes of complex sedimentary and pedogenic origin.

Geochemical work presented here has demonstrated that these three categories can be broadly differentiated on the basis of bulk chemical composition. Plots of normalized values for  $\text{Fe}_2\text{O}_3$ ,  $\text{SiO}_2$  and  $\text{Al}_2\text{O}_3$  on a triangular composition diagram (Fig. 5.1) illustrate this. The chemical compositions of the various ferricretes are strongly influenced by the nature of the original materials prior to iron-impregnation. All of the ferricretes sampled are iron-impregnated materials of one sort or another and do not simply represent the chemical accumulation of the less soluble residuum of weathering.

*Ferricreted bedrock* occupies a composition range intermediate between  $\text{Fe}_2\text{O}_3$  and  $\text{SiO}_2$ , and compared with the ferricreted sediments are somewhat enriched in alumina. *Ferricreted sediments* display a broad range of chemical compositions varying from silica-rich to silica-poor types, but they are generally depleted in alumina. In marked contrast, the *complex ferricretes* are characterised by comparatively high concentrations of alumina, with roughly equal concentrations of  $\text{SiO}_2$  and  $\text{Fe}_2\text{O}_3$ .

These three broad categories of ferricrete have also been shown to display mineralogical differences, especially with respect to iron and aluminium oxides. *Ferricreted sediments* are dominated by goethite, with only minor hematite, *ferricreted bedrock* by hematite, and *complex ferricretes* by gibbsite and a greater iron oxide diversity that includes hematite, goethite and maghemite.

Within some of these broad classes, various *types* of ferricretes can be further distinguished, primarily upon the basis of their macroscopic and mesoscopic features (Bourman *et al.*, 1987), recognised initially during field studies. Using a terminology adapted from that used by McFarlane (1976) various types include massive to vesicular ferricretes, pisolitic ferricretes, nodular ferricretes, slabby ferricretes and vermiform ferricretes. This basic classification of ferricretes is summarised in Table 5.1, and in Section 1.5.

In view of the known transformation pathways of Fe and Al-oxides, reviewed in Chapter 3, it was decided to investigate the possibility that the different chemical and mineralogical characteristics of the ferricretes may reflect the physical and chemical environments during their formation and subsequent transformation.

### **5.3 Macroscopic and mesoscopic features of ferricretes**

**5.3.1 Ferricreted bedrock** and mottled bedrock zones commonly exhibit structures inherited from the host rock, and so may be clearly identified in the field. Bedding, jointing, cleavage, quartz veins and metamorphic and tectonic structures, as well as the presence of distinctive minerals, usually reveal the original nature of the material. In some instances, where inherited structures or fabrics are not conspicuous, examination of thin sections facilitates the recognition of the original bedrock character of the ferruginised material. Understanding the geological history of the area surrounding the ferricrete can also assist in interpreting the character of the iron-impregnated material.

**5.3.2 Ferricreted sediments** also commonly display a range of distinctive macro- and meso-scopic features, some of which directly reflect the nature of the original sediment.

**5.3.2.1 Ferricreted clastic sediments** can be readily identified by the abundance of skeleton grains or clasts of quartz and rock fragments. Some sediments such as Permian glaciogene deposits display distinctive structures such as clay clasts and involutions in ice-contact deposits. Isolated concretionary structures or geodes particularly derived from Permian glaciogene sediments, have sometimes resulted from iron-impregnation of inherited sedimentary structures. Ferricreted sediments include *detrital ferricretes* developed from reworking and cementation of pre-existing ferricretes, sediments and weathered bedrock.

**5.3.2.2 Ferricreted organic sediments** with rare clastic components are dense and particularly iron-rich, and characteristically contain irregular vesicles often clay-filled. These ferricretes are *vesicular to massive* in hand specimen.

**5.3.2.3** In some instances ferricretes have formed essentially *in situ* by the near surface oxidation of 'primary' sedimentary iron-rich minerals such as

glauconite and siderite incorporated within original limestones, sandstones or mudstones.

### 5.3.3 Complex ferricretes

*5.3.3.1 Pisolitic ferricretes* comprise coherent crusts consisting of individual pisoliths cemented together by iron oxides. Non-cemented rounded to sub-rounded pisoliths commonly form discrete ironstone gravels as stonelines in soils throughout large areas (Plate 5.1). The adjective *pisolithic* (McFarlane, 1976) has been used to describe relatively thick, loosely packed pisoliths that are not cemented together, but which may be precursors of future pisolitic ferricretes.

*5.3.3.2 Nodular ferricretes*, as described in this thesis, contain rounded glaeboles, larger than pisoliths and up to 3 cm in diameter, without multiple surface rinds, surrounded by a matrix similar in composition to that of the nodules.

*5.3.3.3 Slabby ferricretes* consist of horizontally to sub-horizontally disposed plate-like slabs of ferricrete up to several centimetres thick comprising indurated masses of iron and aluminium oxides separated by softer clay-rich materials.

*5.3.3.4 Vermiform ferricretes* display very distinctive light-coloured and soft clays filling tubule structures penetrating the crusts.

## 5.4 Bulk Chemistry of Ferricrete Categories and Types

Bulk samples of all ferricretes and ferruginous materials were analysed by XRF and the results have been plotted on ternary compositional diagrams (Fig. 5.2), with the apices representing 100%  $\text{Fe}_2\text{O}_3$ ,  $\text{Al}_2\text{O}_3$  and  $\text{SiO}_2$  respectively.

These apices represent iron oxides, gibbsite and quartz respectively, with kaolinite occupying a position intermediate between  $\text{Al}_2\text{O}_3$  and  $\text{SiO}_2$ . There are insufficient numbers of some types of ferricretes to allow reliable conclusions to be drawn from the data, but it is clear that many types of ferricrete occupy discrete compositional fields.

The composition field of *ferricreted sediments* encompasses two fabric types. These include iron-impregnated clastic sediments that tend to be enriched in silica due to high contents of inherited quartz and other minerals; and



ferruginised organic sediments, with a characteristic *vesicular to massive fabric*, that are highly enriched in iron due to low contents of inherited clastic minerals. All ferricreted sediments have low  $\text{Al}_2\text{O}_3$  contents. The ternary plot of chemical composition of ferricretes with associated *voidal concretions* from the Telford Basin near Leigh Creek (Chapter IX), falls within the range of *massive to vesicular ferricretes*.

*Ferricreted bedrock (and ferruginised bedrock mottles)* occupy a relatively broad field of chemical composition (Figs 5.1, 5.2, 5.3). Overall there is a tendency for higher concentrations of  $\text{Al}_2\text{O}_3$  in ferruginised bedrock compared with the ferruginised sediments.

Amongst the *complex ferricretes*, those with a vermiform fabric and three samples of nodular type have a somewhat smaller range of composition than the ferruginised sediment and bedrock ferricretes, and are consistently higher in  $\text{Al}_2\text{O}_3$ . *Pisolitic ferricretes* have a wide compositional range, evidently reflecting variations in chemical compositions of both the constituent pisoliths and the matrix material, which invariably contains clays, and, in many examples, gibbsite. The compositions of pisolitic ferricretes and individual pisoliths separated from soil gravels and pisolitic ferricretes are plotted in Fig. 5.4 for comparison. Generally the pisolitic ferricretes are more highly enriched in  $\text{Al}_2\text{O}_3$  than the individual pisoliths. Four samples of *slabby ferricrete* plotted have a fairly wide compositional range, but with relatively higher  $\text{Al}_2\text{O}_3$  contents. Average major element contents of the various ferricrete fabric types are listed in Table 5.2.

### 5.5 Bulk Mineralogy of Ferricrete Categories and Types

Estimations of the relative contents of iron oxides (goethite, hematite and maghemite) and aluminium oxide (gibbsite) in bulk samples of the various ferricrete types, were derived from peak intensities of selected characteristic lines on XRD traces (See Methods section).

The estimated abundances were plotted on a triangular diagram in terms of normalised values for hematite, goethite and maghemite + gibbsite (Fig. 5.5). The combined value of maghemite + gibbsite placed at one corner of the diagram tends to accentuate differences between the various complex ferricretes. It is not common in these samples to find high contents of gibbsite and maghemite in the one sample. Consequently, the positions of vermiform

and nodular types are dictated by relatively high gibbsite contents, whereas the isolated pisoliths are commonly free of gibbsite but contain significant maghemite. The wide mineralogical composition range of the pisolitic ferricretes, compared with that of the individual pisoliths, is probably controlled by the composition of the matrix, and in particular by variable amounts of goethite and gibbsite. This diagram illustrates a clear demarcation between hematite-rich ferricreted bedrock and goethite-rich ferricreted sediments. Both of these ferricrete categories are free of gibbsite and only contain traces of maghemite. Furthermore, differences in the relative proportions of hematite and goethite easily separate iron impregnated clastic sediment ferricretes from massive to vesicular ferricretes, which comprise high total contents of goethite.

The mineralogical data also distinguish various types of complex ferricretes. For example, vermiform and nodular types are significantly depleted in hematite relative to pisolitic ferricretes and samples of isolated pisoliths are dominated by hematite.

## **5.6 Reconstructed Environments during Ferricrete Formation**

A combination of the geologic, geomorphic, pedologic and hydrologic relationships of the various ferricretes, in conjunction with their chemical and mineralogical compositions and macro-, meso- and micro-morphological characteristics, facilitates reconstruction of environmental conditions pertaining at the times of the formation of the different ferricretes.

### **5.6.1 Ferruginised Bedrock (Ferricreted and mottled bedrock)**

In the Mount Lofty Ranges there are limited examples of ferricretes formed directly by the surface weathering and ferruginisation of bedrock. These ferricretes invariably contain higher  $\text{Fe}_2\text{O}_3$  contents than the equivalent unweathered bedrock, which suggests local iron enrichment of the bedrock by iron influxed in solution, probably from lateral sources, as the ferricretes occur in relatively lower parts of the landscape (e.g. ferruginised bedrock ferricrete at Koonunga, Section 4.2.1.3).

Masses of iron-rich bedrock litter the surface above mottled zones of weathered saprolite, in a variety of geomorphic situations in southern South Australia. These have been likened by some workers to dissected 'laterite' crusts but they are actually lags of hardened iron mottles that originally formed subsurface,

under past soil and groundwater conditions, and now have accumulated at the surface following landscape downwasting and erosional removal of softer bleached material. The *in situ* ferricreted bedrock and the lags of ferruginised bedrock mottles display similar mineralogies, both being dominated by hematite. Ferruginised bedrock mottles are considered here because, in some instances, they have been precursors of ferricrete development.

At Mount Torrens (Section 4.2.3.1), in an upland situation, large mottles of hematite-impregnated bedrock are exposed in a road cut and a short distance upslope, masses of iron-rich materials litter the surface. The mineralogy of the loose iron-rich clasts is dominated by hematite but small amounts of goethite are also present. The total iron content of the surface lag materials is greater than that of the ferruginised bedrock mottles in the weathered profile. In thin section, primary rock structures and metamorphic minerals preserved in the lag material are similar to those in the mottles. The presence of goethite in the surface material can be explained by dissolution of hematite and reprecipitation as goethite (Schwertmann, 1971) under chemical conditions appropriate to the contemporary soil-weathering environment.

At 'The Range' (Willunga Scarp) hematite-rich mottles occur, preferentially developed in metasandstone intervals within the Precambrian bedrock (Section 4.2.3.2). The large, soft, dominantly hematitic, red to purple-coloured mottles occur at the base of the section. Proceeding upwards the mottles become yellower in colour due to increasing goethite contents. When examined in section they reveal a hematitic core with a goethitic rind. In immediate subsurface horizons of the soil these mottles still display hematitic cores and retain bedrock structures. A pronounced stoneline of maghemitic pisoliths with goethitic rinds occurs in the surface soil horizon. These, together with fragments of quartzite bedrock and ferruginised bedrock mottles also form a lag at or near the surface. Generally there is an increase in total iron content towards the surface as well as an increase in the abundance of goethite. The observation of goethite rinds associated with segregations which became landsurface-related has been made by other workers elsewhere including Schwertmann (1971) and McFarlane (1976).

In these instances it appears that weathering and erosion are transforming a pre-existing hematitic mottled zone into increasingly goethitic-coated hardened mottles that eventually form stonelines and surface lags. All of the observed

phenomena can be explained in terms of downwasting and transformation of mottled material, a transformation that is proceeding under current conditions. There is no evidence of a former crust, and it is unnecessary to postulate the former existence of one. The mottling of the bedrock almost certainly developed *in situ* probably as a result of weathering and groundwater movement that led to the mobilisation of iron within the bedrock, and its concentration as mottles as discussed by McFarlane (1976). As the iron oxide mineralogy of the mottles is dominantly hematite, they probably formed in the zone of a fluctuating water, in which reducing and oxidising conditions alternated. Under reducing conditions Fe(II) could have been released from 'primary' iron minerals, and precipitated and crystallised to hematite via its precursor ferrihydrite to be concentrated in mottles under oxidising conditions during lower water table levels. The hematite mottles have probably been inherited from former periods of weathering.

Evidence from a deep bore (Section 4.2.6.1) favours the view that simple and local iron redistribution within the weathered bedrock is responsible for the mottling, and that the weathering here has not been intensive as feldspars, micas, and 2:1 layer silicate clays comprise important components of the material. Maghemite formation by surface heating of goethite is the likely process responsible for the magnetic character of many of the surface pisoliths, particularly as there is no evidence of magnetite in the parent bedrock, lepidocrocite in the mottles, or maghemite below the surface soil.

## **5.6.2 Ferricreted sediments**

The character of ferricretes developed through iron-impregnation of various sediments depends on the nature of the original sediment as well as the physical and chemical conditions during the impregnation. For example, the impregnation of sandy sediments gives rise to ferricretes with quite low total iron contents. On the other hand, ferricretes formed by the impregnation of organic sediments, that can be completely replaced with iron oxides, forms dense, iron-rich materials.

### **5.6.2.1 Ferricreted clastic sediments**

A considerable variety of sediments impregnated by iron oxides has been recognised and these include ice-contact sediments of Permian age, former valley bottom deposits of Tertiary age, Cainozoic limestones, former backshore (beach-dune) deposits related to higher Tertiary sea levels, and colluvial

material. Iron oxides fill the interstices of some sediments, with colloform structures demonstrating successive pulses of iron oxides into the intergranular voids of sandy sediment. In some cases these occur as alternating laminar deposits of hematite and goethite (Plate 5.2). In other instances iron oxides have replaced pre-existing mineral phases, and have infilled hollows formed by the solution of calcite. Generally goethite is the dominant iron mineral involved, displaying minor aluminium substitution (1-4 mole%). It has been noted that the amount of hematite present in iron-impregnated sandy sediments, although typically minor, may reflect age differences; older ferricretes characteristically display higher hematite contents than younger ones. The low degrees of Al-substitution in these ferricretes suggests little availability of Al in the environment at the time of impregnation. This favours the view of impregnation in a moist environment in which temperature influences are not critical and a lack of acid leaching conditions. The higher hematite contents of older ferricretes may reflect an aging effect or warmer conditions during impregnation.

Geomorphic reconstructions (Bourman, 1973; Maud, 1972) suggest that many of the sediments were iron-impregnated while in former valley bottoms or relatively low-lying points in the relief, including sub-surface situations, where iron oxides carried in solution by percolating waters were deposited. Today these ferricretes occupy a range of topographic locations varying from the summit surface to modern valley floors.

#### 5.6.2.2 *Ferricreted organic sediments*

The iron impregnation of former organic-rich sediments such as peats has given rise to distinctive ferricretes with *vesicular to massive* fabrics. These display very high total iron contents and an iron oxide mineralogy dominated by goethite, which displays an extremely low degree of aluminium substitution (<1 mole%). Very small amounts of hematite can occur in these materials, but no gibbsite has been detected in them.

These massive to vesicular ferricretes that resemble the bog-iron ores of Europe (Hurlbut, 1959) occur in a variety of situations and in deposits that range widely in size. They occur on parts of the present summit surface of the uplands such as Peeralilla Hill (Fleurieu Peninsula), near Longwood, on Kangaroo Island and in modern valley floors such as at Mount Compass, in sites where there is evidence for former iron sources at higher elevations in the landscape. They

occur in areas that can be reconstructed as locations of former sluggish drainage such as lakes and swamps. In thin sections of vesicular ferricretes, plant fragments replaced by goethite are conspicuous and occur in a finely crystalline matrix of goethite and kaolinite. Distinctive rectilinear voids are common, and there are small but rare quartz grains. The identification of organic matter, now ferruginised, apparently favours the formation of goethite from ferrihydrite as opposed to hematite (Schwertmann, 1985). This may also help to explain their low degree of aluminium substitution, as the organic matter may 'fix' any free aluminium available for incorporation into the goethite crystal structure (Oades & Tipping, 1988). Small amounts of hematite have been detected in vesicular crusts, unlike the bog iron ore deposits of Europe, which contain no hematite. This may reflect minor environmental differences such as temperature conditions during their formation, as warmer temperatures encourage hematite crystallisation from ferrihydrite. Generally the environmental conditions postulated for the formation of *vesicular ferricrete* favour goethite formation as summarised in Section 3.3.1.1.

The intimate association of vesicular ferricrete with calcite and barite at Peeralilla Hill is interesting but not critical with respect to the origin of the ferricrete. The presence of calcite and barite could argue against a residuum leaching origin for the iron oxides in these situations and could suggest that the iron-enrichment has occurred via lateral transport of iron ( $\text{Fe}^{2+}$ ) in solution and its precipitation in areas of former sluggish drainage. The occurrence of barite ( $\text{BaSO}_4$ ) implies the operation of sulphuric acid weathering, which probably derived from adjacent pyrite-rich sediments. However, it is possible that the barite and calcite did not form coevally with the ferricrete, but formed during a later phase of weathering.

### **5.6.3 Complex Ferricretes**

#### **5.6.3.1 Pisolitic ferricrete**

Pisolitic ferricretes have the widest range of distribution in the landscapes of southeastern Australia, varying from locations near sea level to parts of the present high level summit surface. They are regarded as the indurated equivalents of pisolithic gravels [the 'pisolithic laterites' of McFarlane (1976)], which are common and widespread components of many contemporary soils in southern South Australia and occur over a diverse range of materials. A key to the origin of pisolitic ferricrete is held in understanding the nature and origin of the individual pisoliths.

#### 5.6.3.1.1 *Pisoliths*

A considerable controversy concerning the origin of pisoliths relates to whether they have formed *in situ* or whether they have been transported to their present locations. Many French workers, such as Tardy & Nahon (1985) and Muller & Boquier (1986), follow the view that pisoliths have formed *in situ* and that their progressive formation can be traced from sub-surface zones or horizons within the profile through to the surface. Despite careful examination of profiles in the study area, no such progressive sub-surface development of pisoliths has been observed.

In the areas studied in southern Australia many of the pisoliths have complex and multiple rinds. Such pisoliths occur in the base of channel fill materials on the summit surface of Fleurieu Peninsula (Section 4.2.2.1) and clearly have been deposited here following transport. These pisoliths are identical with those occurring in pisolithic gravels at a higher elevation on the summit surface. Resin-impregnated samples of weathered materials ranging through from bedrock to channel fill deposits containing pisoliths have been slabbed and examined closely. There is no indication of structures resembling pisoliths in the weathered bedrock material below the channel fill (See Plates 4.31 and 4.32), supporting the view that they have been transported.

Prescott (1934) considered that the chemical compositions of ferruginous pisoliths demonstrated their formation in the soils in which they currently occur, although he did not spell out the reasons for this conclusion. Typically, the pisoliths examined in this thesis are markedly different in characteristics from the surrounding matrix (e.g. Plate 5.3). Furthermore, the pisoliths can contain minerals not occurring in the surrounding matrix. For example, pisoliths from a yellow podzolic soil at Mount Barker (BOU 29) contained the minerals gibbsite, hematite, maghemite, kaolinite and a small amount of goethite, whereas the soil material (BOU 30), contained only goethite and kaolinite (Table 5.3-Appendix V). Thus the pisoliths are interpreted as clastic components different from the materials in which they are found. However, they have been commonly modified in these environments particularly by the accretion of rinds on their surfaces from the surrounding soil materials, but also by other processes. Some pisoliths contain fragments of bedrock in their cores (BOU 121) encapsulated by rinds of iron oxide indurated soil-like material (Plate 5.4).

In many instances, pisolith gravel horizons occur on a variety of parent materials, including calcareous clays and sediments that could not have provided the source material for the pisoliths. For example, complex pisoliths with multiple rinds (Plate 5.5) occur on Pliocene calcarenite at Cape Borda, Kangaroo Island. Pisoliths containing gibbsite, goethite, hematite and maghemite overlie calcareous Pleistocene sediments near Yorke Farm on Kangaroo Island, and pisoliths also occur above fine, calcareous earths that overlie weathered bedrock on the Blue Range, Eyre Peninsula, and in the Hills near Kulpara and Lochiel in the Mid North of the State. It is possible that ants can transport fragments of iron-rich material from mottled materials that underlie calcareous fine earths and sediments, and may be partly responsible for the enrichment of iron in the pisoliths.

The vast majority of pisoliths examined in this study appear to be transported types, having formed by the erosion of pre-existing ferricretes or iron-mottled zones, their downslope movement under the influence of sedimentary processes, and their continual modification by pedogenesis. Only two situations were observed where pisoliths may be forming *in situ* in subsurface situations.

Incipient pisoliths may be forming in seepage zones where iron-rich waters emerge at the surface. Thin sections of such pisoliths from seepage zones on Tin Hut Creek, Kangaroo Island revealed that iron oxides had impregnated and encapsulated nuclei comprising fragments of bedrock and biogenic material. Other possible *in situ* pisoliths occur in sandy soils at depths of approximately 1 m in a road cut near Waitpinga. These pisoliths typically have much lower total iron contents than surface pisoliths, and goethite is the dominant iron mineral present. To be certain of the *in situ* formation of pisoliths at depth they should not be associated with stone lines or other material such as clasts that might indicate transport and reworking. Thin section examination shows that the fabrics of the *in situ* pisoliths and the surrounding matrix materials from the Waitpinga area are identical with the pisolith, simply being marked by greater concentrations of iron oxides, and in this sense are small versions of iron-rich mottles. However, once at the surface or in the near-surface soil environment such pisoliths appear to undergo transformations that lead to higher total iron contents and transformations in iron mineralogy from goethite to dominantly hematite and maghemite.



McFarlane (1976) distinguished soil pisoliths from groundwater pisoliths, but no evidence of groundwater pisoliths (i.e. sub-surface pisoliths in weathered parent material displaying progressive development and organisation towards the surface) was noted in the areas investigated for this thesis. The situations examined suggest that the pisoliths in the soils are the same as those in pisolitic ferricretes.

The abundance of hematite and maghemite in the pisoliths of soil gravels and in the pisolitic ferricretes contrasts strongly with the dominance of goethite in soils of the region. Both maghemite and hematite are known to form readily in pedogenic environments by the heating of goethite in the presence of organic matter during bushfires (Schwertmann, 1985). The mixture of magnetic and non-magnetic pisoliths (the magnetic character being a direct indicator of maghemite content) in the soil gravels suggests a long history of landscape development as the pisoliths probably variably transformed during transport from different parts of the landscape. Milnes *et al.* (1985) described a series of depositional multiple laminar rinds on pisoliths, usually composed of goethite, with occasional gibbsite, incorporating individual quartz grains or lenses between them as evidence of their accretionary origin. They suggested that deposition of the laminae and incorporation of the quartz occurred in a succession of pedogenic environments, consistent with a long history of exposure, transportation and weathering. No evidence of the groundwater pisoliths of McFarlane (1976) was noted in the study area. The majority of the pisoliths studied appear to have formed by the physical breakup of pre-existing ferruginous materials (ferricretes, mottles, etc) and their modification by transport and weathering in surface or near surface environments. Even if some of the pisoliths were generated in groundwater zones they have been so modified subsequently that it is impossible to trace them back to this possible source.

Individually the pisoliths that have been analysed display high total iron contents, and an iron oxide mineralogy dominated by hematite and maghemite. Maghemite may occur in the body of the pisolith but more commonly is observed in outer concentric layers. Pisoliths have cores of different materials, including fragments of former ferricretes, iron-mottles and bedrock clasts. In most pisolitic ferricretes the inter-pisolith matrix is significantly different in mineralogical and chemical composition from that of

the pisoliths (Fig. 5.5), suggesting different environments of formation for the pisoliths and matrix materials.

Work reported by Herbillon & Nahon (1987) from West Africa, supports the notion of near-surface mineralogical transformations of pisoliths. They noted that goethite from soft yellow domains of their 'typical' Diouga 'laterite profile' are Al-poor, but that goethite from the cortex of 'pisolites' may be aluminium-substituted up to 21 mole%. This variation implies dissolution of pre-existing iron oxides and reprecipitation as goethite to allow the incorporation of Al into the goethite structure.

#### 5.6.3.1.2 *Origin of maghemitic pisoliths*

Various modes of formation of maghemite have been suggested (Schwertmann & Taylor, 1987; Fitzpatrick, 1987; Kirschvink, 1985; see review in Chapter 3) but in the vast majority of cases that have been investigated in this thesis, maghemitic pisoliths, it appears, have either been exposed at the surface or have been close to the landsurface and have been subjected to strong heating by burning. This is suggested by the following evidence:-

- i. Maghemitic pisoliths typically appear in surface or near-surface positions except where it can be demonstrated on other grounds that they have been transported and buried below younger sediments.
- ii. In such cases examined, maghemite is restricted to the pisoliths, and does not occur within the surrounding matrix, which would be expected if the maghemite had precipitated from iron-rich solutions or had been the result of biomineralisation. Traces of maghemite have been identified in ferruginous mottles at depth in Pleistocene sediments at Hallett Cove (Wopfner, 1972a) and elsewhere. In these instances it must have formed *in situ* from iron solutions, possibly by the dehydration of lepidocrocite originally crystallised at depth in mottles. However, the amount of maghemite present in the mottles is extremely small, relatively to the surface pisoliths, and can only be detected by reaction to a magnet. Some maghemite in pisoliths may be inherited from such mottles or more diffuse biomineralogical sources, but additional maghemite would be required to achieve the abundances observed in many pisoliths.

- iii. Maghemite most commonly occurs as a rim on the pisoliths. Occasionally, maghemite does occur in fractures in the body of pisoliths, apparently having formed from gels. However, this mode of occurrence may be quite rare. Sometimes the cortex of a pisolith is comprised of maghemite, which may suggest derivation from magnetite or accretion around a small pisolith affected by burning.
- iv. There is widespread evidence of fires in the Australian environment at appropriate temperatures (Raison, 1979) to lead to the development of maghemite by this process.
- v. Other minerals such as boehmite, corundum and rutile, that may form from the heating of other minerals, have been identified in pisoliths from Eyre Peninsula and the Sydney area. Once again, temperatures of up to 900° C have been measured in bushfires (Raison, 1979) and these are sufficient to explain the observed transformations. Similar conclusions were reached by Anand & Gilkes (1987).
- vi. Some non-magnetic pisoliths contain only hematite as an iron oxide, and it may be the case that heating will lead to the transformation of maghemite to hematite. Banerjee & Moskowitz (1985) noted that maghemite inverts to hematite by heating at temperatures above 350° C, but in heating experiments described below transformations did not occur with temperatures below 550° C.
- vii. Had all of the maghemite formed from gels or as a result of biomineralisation, then it should be more uniformly distributed through profiles, yet, typically it is restricted to pisoliths and is rarely present in matrix material.

Corundum, rutile, maghemite and small amounts of kaolinite and gibbsite were identified in surface pisoliths (BOU 412) from the Terrey Hills quarry site (Chapter 8). If the pisoliths had been heated to 900° C to form corundum, then there should be no gibbsite, kaolinite or maghemite present. However, the amounts of these last three minerals are quite small, and may represent additions to the pisoliths after the strong burning that caused the formation of corundum, or incomplete and uneven heating of the pisoliths. This suggestion is compatible with the multilayered and concretionary nature of these and many other pisoliths, that indicate long and complex histories of their

development. This point is further illustrated by the observation that some other pisoliths contain goethite, and this is commonly in the form of yellow rinds that have developed from the dissolution of hematite and/or maghemite and the reprecipitation of goethite on the surface of the pisoliths, or from the accretion of additional goethite from the surrounding soil (McFarlane, 1976). Some outer rinds of goethite consist of cemented quartz grains that may have derived from the soil environment in which the pisolith was encapsulated.

In places relatively thick lags of pisoliths, which have accumulated at or near the surface, form deposits of pisolithic gravels, and appear to be forerunners of detrital pisolitic ferricrete. These materials are regarded as secondary or reworked accumulations. In appropriate parts of low angle slopes or in depressions, where conditions may have favoured lateral percolation of iron-rich solutions, such pisolithic soil materials may have been cemented by the deposition of new generation iron oxides, dominantly as goethite, to form detrital pisolitic ferricretes. Elsewhere, the gravels may have persisted in an unconsolidated form being available for subsequent erosion and reworking.

#### *5.6.3.1.3 Heating experiments*

Some simple laboratory experiments were carried out to test the mineral transformations suggested by the influences of heat. Both intact and ground maghemitic pisoliths were used. After heating at 600° C for 1 hour, pisoliths, which originally reacted strongly to a magnet, displayed no reaction. Thus their ferri-magnetism had been destroyed by heating. Brindley & Brown (1980) consider that this transformation, which produces hematite, can occur at much lower temperatures, but, in all cases examined, temperatures of 550 - 600° C were required.

A heating experiment was also carried out on a sample of pisolitic ferricrete from the Terrey Hills quarry site. Minerals identified in an unheated, air-dried sub-sample of this ferricrete (BOU 404) included, in decreasing order of abundance, gibbsite, quartz, hematite, goethite, maghemite, kaolinite, anatase and some randomly interstratified clays. After heating at 200° C for 1 hour, the same minerals were identified, except that the main goethite peak was lower and broader. At 210° C the minerals remained the same but some of the gibbsite peaks had weakened and broadened. Both the gibbsite and goethite peaks disappeared after heating at 400° C. At 500° C the kaolinite peaks began to reduce and at 550° C they had disappeared, while the maghemite peak had

reduced. The maghemite peaks disappeared completely at 575° C, leaving only quartz, hematite and anatase as crystalline minerals. This remained the same through 600° C to 800° C, although some diasporite possibly appeared at 700° C. At 900° C corundum appeared as an important constituent and rutile possibly appeared also. It is not possible to determine if rutile was synthesised by heating, or if it was present throughout, with its identification depending on chance preferred orientations in the pressed samples. Anatase did appear to reduce at this temperature, but the main anatase line was obscured by the corundum peak.

Thus it appears that strong heating at temperatures up to 900° C, and these temperatures are not unknown from bushfires (Raison, 1979), can cause various mineral transformations. These include the destruction of goethite, gibbsite, kaolinite and maghemite, and the formation of boehmite, diasporite(?), corundum and rutile(?). Furthermore, with appropriate organic contact, maghemite can form from goethite and/or lepidocrocite with heating by bushfires between 300° C and 500° C (Fitzpatrick, 1987). Hence these transformations may act as indicators of various ranges of heating experienced.

In the sites investigated, roughly half of the pisoliths are magnetic and half are not, which suggests that the maghemitic pisoliths are not simply preferential survivors. Comparisons of magnetic and non-magnetic ferruginous pisoliths reveal that the magnetic ones typically contain higher contents of  $\text{Fe}_2\text{O}_3$  and  $\text{TiO}_2$ . Iron oxide minerals identified in the magnetic pisoliths include dominantly hematite and maghemite, with some goethite on occasions. Non-magnetic pisoliths may contain only hematite or hematite and goethite. Those with hematite only may have been affected by very strong heating that transformed all pre-existing iron oxide minerals to hematite. On the other hand, those with combinations of maghemite, hematite and goethite have probably been affected by heating at lower temperatures in the presence of organic material, with the goethite forming by reprecipitation of iron oxides derived by dissolution of maghemite and hematite.

#### 5.6.3.2 *Nodular ferricrete*

This variety of ferricrete comprises glaebules that are larger than pisoliths, have an earthen appearance, and are less dense than pisoliths, which dominantly have burnished and metallic-like surfaces. Nodular ferricrete can

occur in similar topographic situations and, in some places, contiguously with both pisolitic and vermiform ferricretes on high level surfaces with gentle slopes. The nodules and the surrounding matrix do not display significant differences in composition and the nodules do not exhibit complex multiple surface rinds that usually indicate long histories of weathering and transportation. The simpler form of the nodular ferricretes suggests that weathering in place has been important in their formation. The nodular crusts contain goethite which is highly Al-substituted (20 mole%), indicating, as in the case of the pisolitic and vermiform types, ample availability of aluminium in the environment due to the presence of clay minerals during its formation. The abundance of gibbsite in nodular ferricretes is interpreted as reflecting the occurrence of an acid, leaching and freely draining environment.

#### 5.6.3.3 *Slabby ferricrete*

Masses of slabby ferricrete, which commonly occur within mottled clay materials on present high level surfaces, and typically near the margins of breakaways, such as at Chandlers Hill (Section 4.2.1.4.1). Slabby ferricretes are similar in chemical composition to vermiform and nodular types. However, they have a mineralogical composition intermediate between that of ferruginised bedrock ferricretes and ferruginised sediment ferricretes. In thin sections, the slabby ferricretes examined are essentially clay-rich material impregnated by iron oxides. Scattered fine crystals of hematite occur throughout the clay matrix and, in places, have aggregated to form hematite-rich zones. Goethite, with negligible aluminium substitution, is dispersed within the clay matrix and may also occur as void goethans. The common clastic quartz grains are up to sand-size and are poorly sorted.

The formation of slabby ferricretes appears to be related to precipitation of iron oxides by laterally moving sluggish ground waters near the surface of a fluctuating soil water table. Upslope from slabby ferricretes, weathered material is often iron-depleted, and may have provided the iron oxides for the development of the slabby ferricretes. Sub-horizontal patterns of iron-mottling are seen in many subsoil horizons and sedimentary sequences in the region, and support the view that slabby ferricretes formed within the regolith. The occurrence of minor gibbsite in these materials probably reflects lateral migration of aluminium gels, in the same fashion as postulated for iron oxide migration.

#### 5.6.3.4 Vermiform Ferricrete

The dominant feature of vermiform ferricretes is the presence of clay-filled, anastomosing tubules. These ferricretes have been observed to occur on flat to gently sloping and undulating surfaces in present upland situations. In the Mount Lofty Range Province they are found not only on the summit surface in discrete locations ranging between 270 - 400 m above sea-level, but also on intermediate plains 100-150 m above sea-level. Landscape reconstructions (Bauer, 1959; Brock, 1971; Bourman, 1973) suggest that these were formerly low-angle, intermediate slopes in environments of subdued relief. Under these conditions it is postulated that relatively poor lateral drainage facilitated the accumulation of iron oxides to cement surface lags. These lags consist of pisoliths, weathered bedrock and ferruginous clasts and isolated and hardened mottles that had accumulated at the surface following downwasting of a previously weathered and mottled zone containing iron segregations. The dominance of goethite with a high degree of aluminium substitution in vermiform ferricretes suggests that the iron oxides impregnated former clay-rich weathered materials, including soils. However, the tubular structures, which characterise these ferricretes, appear to be dissolution features infilled mainly with clay minerals dominated by gibbsite. In combination, these features point to the polygenetic development of the vermiform ferricretes. Evidence from analysis of borehole samples suggests that abundant gibbsite has formed largely from the disassociation of kaolinite, and interpreted as an indicator of a highly weathered, acid environment where free drainage promoted intense leaching. On the other hand there has also probably been the precipitation of gibbsite from aluminium-rich solutions derived from lateral sources.

Vermiform structures have been noted to affect a variety of materials. On Kangaroo Island they have developed in a quartzose sand, both on the summit surface and on the lower Mount Taylor Plain. This last surface is of post-Miocene age and it is possible that parts of the summit surface of Kangaroo Island are of a similar age. Other vermiform structures have been noted in ferricretes near Robertson (BOU 213) and Nowra (BOU 215) on the east coast of New South Wales where they have formed in sandstone bedrock. These two occurrences are widely separated in elevation on erosion surfaces of vastly different ages (Dr. R.W. Young - *pers.comm.*) yet they have identical chemical and mineralogical compositions, which suggests that local environmental conditions may be significant determinants of their characteristics. Similar

tubular channels filled with clays and gibbsite occur in many of the varieties of complex ferricretes.

In thin section, samples of vermiform ferricretes reveal patches of iron-enrichment, and zones of infillings of layer silicate minerals and gibbsite. Non-oriented micas and pseudomorphs after mica occur in the matrix, suggesting weathering from a pre-existing rock lag derived from metamorphic bedrock, with the fabric in places resembling a hardened soil. No clear pisolithic structures are apparent, perhaps partly reflecting the dissolution of pre-existing pisoliths by subsequent processes.

The best developed and most complex vermiform crusts in the Mount Lofty Range Province occur on Fleurieu Peninsula at an elevation of about 350 m asl on a landsurface that has been exposed to subaerial weathering and erosion throughout and since the Mesozoic. The occurrence of vermiform fabrics may suggest the transformation of the crusts essentially by *in situ* weathering, combined with landscape downwasting. Generally the apparently older vermiform crusts have higher iron and aluminium contents and commonly contain maghemite.

The dominant attitude of the vermiform structures varies. The majority observed in this study were oriented in a vertical sense, suggesting downward leaching processes. However, some display a strong horizontal orientation (Plate 5.6) perhaps indicating lateral groundwater movement. It is of interest that the clays in the horizontal tubules are dominantly kaolinitic (Ione 7, Table 5.3), with little gibbsite, whereas those in the vertical tubules contain much more gibbsite.

The vermiform fabric may represent a special form of degradation of many ferricretes through dissolution of original matrix material and subsequent illuviation of iron and aluminium oxides and clays. In some cases the tubule structures are not well developed, and the original fabric of the ferricrete can be identified. In extreme cases, original pisoliths, nodules and bedrock structures have been essentially destroyed. Some tubules have been filled with hematite; most are lined with goethite and filled with kaolinitic clays and gibbsite. In many localities, ants have colonised the clay-filled channels and have developed extensive galleries. However, it is not suggested that they are responsible for the original formation of the tubules. Furthermore, no evidence



of the role of termite activity in ferricrete genesis, as suggested by Machado (1983a, 1983b), was found during investigations for this thesis.

The evidence presented here suggests that the tubular structures have been a late stage alteration superimposed on pre-existing weathered and ferruginised materials. These had apparently accumulated as complex lags of previously developed ferruginous mottles, variably bleached and kaolinised bedrock, unweathered bedrock fragments and maghemitic clasts and pisoliths formed at the surface and subsequently reincorporated into the lag materials resulting from landscape reduction. These were subsequently cemented in preferred localities by remobilisation of iron and aluminium oxides derived both from local and lateral sources.

Thus a combination of field and laboratory data points to the polygenetic development of vermiform ferricretes, with their character interpreted to imply variations in hydrological conditions consequent upon geomorphic changes. The initial accumulation of iron oxides, physically and chemically, is taken to imply slow downwasting of a subdued landscape with a relatively high water table, followed by dissolution, mineral transformations and illuviation of clays under more freely draining conditions consequent upon lowered water tables that accompanied uplift and incision.

### **5.7 Modern Iron Oxide Mobility**

Under current climates, that vary from Mediterranean to semi-arid, iron-rich sludge-like material occurs in creeks and in seepage zones in upland parts of the Mount Lofty Ranges and Kangaroo Island, in peritidal environments such as that near Fisherman Bay, South Australia and in groundwater salinas (boinkas) in northwestern Victoria (Macumber, 1983), as discussed in the previous chapter. The iron is largely in the form of ferrihydrite, though small amounts of maghemite have been detected in material collected from Kangaroo Island. High salinities are commonly associated with these environments. Iron oxide accumulations in specific environments such as those discussed here may represent analogues of precursors of some types of older ferricretes. Moreover, current iron oxide mobility and precipitation locally may be modifying and transforming pre-existing ferricretes.

## 5.8 Conclusions.

The studies described above demonstrate the variable nature of ferricretes that in the past have been broadly grouped together as 'laterite' by many previous workers. The use of macro-fabrics as a basis for field classification of ferricretes and as a guide in reconstructing past environments of formation, appears to be justified by data from laboratory studies of mineralogy, chemistry and micro-morphology.

Thus the ferricretes reported here do not indicate various stages in either the development or dissection of a monogenetic 'normal laterite profile', but rather a variety of regolith materials and sedimentary deposits differentially weathered and impregnated by iron and aluminium oxides in response to developing local environmental conditions over various periods of time, in places extending back into the Mesozoic. Mineralogical data derived from bleached and iron-mottled zones do not display evidence of pervasive weathering and kaolinisation, generally attributed to the processes of 'lateritisation', but suggest the occurrence of zones of superficial weathering, effected by groundwaters, and reflected in the leaching of iron oxides from rocks and sediments and its redeposition elsewhere.

The clear demonstration of iron mobility and precipitation in modern weathering environment highlights the futility of a tacit acceptance of the association of iron-rich crusts, regarded as evidence of 'lateritisation' by many previous workers in South Australia, with humid tropical climates. Furthermore it points to the dangers inherent in using ferricretes as morphostratigraphic markers.

The classification of ferricretes presented here is not intended to be definitive, but it is capable of accepting new categories when relevant field and laboratory data are available. The integrated investigative approach outlined here demonstrates inadequacies in single line approaches, such as that of Schellmann (1981), who categorised 'laterites' by their degree of 'lateritisation' as indicated by their positions on ternary chemical composition diagrams (e.g. Fig. 5.6). For example he considered that samples with high iron and/or aluminium were 'strongly lateritised', yet samples of bog-iron ore (BOU 5, BOU 10, BOU 11) and ferricretes with associated voidal concretions (BOU 88) also occupy this field and need not be related to the processes of 'lateritisation' of Schellmann (1981). High concentrations of alumina in ferricretes observed on

surfaces exposed to subaerial processes for various periods of time may reflect local bedrock and/or topographic influences that favour leaching rather than indicating severe weathering. Furthermore, ferricretes studied in this thesis do not appear to be mono-genetically related to the underlying bedrock, so that the identification of the unweathered bedrock does not ensure that the overlying ferricrete developed from it by *in situ* weathering. Many ferricretes contain transported materials, which locally may display high iron and alumina contents that were derived from elsewhere, and in the case of complex pisolitic and vermiform ferricretes the problem of distinguishing transported and local components may be intractable.

## CHAPTER 6: FERRICRETES, IRON-MOTTLED AND WEATHERED MATERIALS ON EYRE PENINSULA.

### 6.1 Introduction

After developing various generalisations following field and laboratory investigations of ferricretes and weathered zones in the Mount Lofty Range Province, an examination of apparently equivalent materials was undertaken in several other areas (Chapters 6, 7, 8 and 9), including sites on Eyre Peninsula, to evaluate the hypotheses generated. For example, to see if different forms of ferricrete and iron mottling displayed distinctive chemical and mineralogical compositions that could be related to their environments of formation, to see if there was evidence of continuous iron mobility throughout geological time up to and including the present, and to see if alleged monogenetic 'laterite profiles' were stratigraphic sequences or incomplete profiles. Furthermore, the extended investigations provided the opportunity to assess previous research carried out in these areas. No exhaustive mapping or sampling program was undertaken because of time constraints. However, careful examination of field relationships of ferricretes and other ferruginous materials was made at selected sites prior to collection of samples for laboratory investigations. Emphasis was placed on the comparison of ferruginous and weathered materials with those described from the Mount Lofty Ranges. The sites investigated on Eyre Peninsula can be discussed conveniently under the regions of Northern and Southern Eyre Peninsula.

### 6.2 Previous Investigations

A summary of previous investigations of 'laterites' and ferricretes on Eyre Peninsula by Mawson (1907a; 1907b), Stephens (1946), Crocker (1946), Johns (1961a), Firman (1967a; 1967b), Bourne (1974), Twidale *et al.* (1974), Twidale & Bourne (1975b) and Twidale (1976a; 1976b; 1983) is reviewed in Chapter 3.

### 6.3 Investigations of this thesis

#### 6.3.1 Northern Eyre Peninsula

##### 6.3.1.1 Summit surface sites.

##### 6.3.1.1.1 Weathered and iron-mottled profiles.

##### 6.3.1.1.1.1 Blue Range

The summit surface of the Blue Range (Fig. 6.1) was described by Bourne (1974) and Twidale *et al.* (1976) as the most northerly occurrence on Eyre Peninsula of a postulated Mesozoic 'true laterite' surface, regarded by them as equivalent to summit surfaces on the Lincoln Uplands of southern Eyre Peninsula, Kangaroo Island and the Mount Lofty Ranges. However, exposures in dam sites and soil pits on the Blue Range (Hincks MR 063402) reveal no continuous 'laterite' profile beneath the summit surface. Near horizontal Precambrian metasediments have been bleached and mottled, but the mottles are merely superficial stains of iron oxides. For example, bedrock mottles (BOU 526 and BOU 527) (Appendix VI - Table 6.1) (Figure 6.2) contained only 2.14% and 1.75% Fe<sub>2</sub>O<sub>3</sub> respectively, and the presence of muscovite, smectite and feldspars in the samples argues against the operation of intensive weathering in their formation. Tabular blocks of iron-stained and iron-impregnated sandstone litter the surface in places and may superficially resemble a crust, but they are actually remnants of flat-lying strata within the Precambrian bedrock. The indurated metasandstone layers (BOU 525) contain 22.59% Fe<sub>2</sub>O<sub>3</sub>, but little Al<sub>2</sub>O<sub>3</sub>. Quite clearly these ferruginous sandstone slabs were pre-existing sedimentary horizons within the Precambrian bedrock and were particularly susceptible to impregnation by iron oxides. On the other hand, the underlying superficially weathered and mottled materials are fine-grained metasediments.

Especially apparent, fringing the highest sections of the Blue Range upland, are bleached Precambrian metasediments that are overlain by up to 2 m of a calcareous fine earth (Plate 6.1), which, in turn, is overlain by a sandy grey soil containing fragments of ferruginised sandstone bedrock and glazed pisoliths. These pisoliths are of two distinct sizes. Both have similar mineralogy although the smaller ones (BOU 529) have a more strongly glazed appearance and contain more Fe<sub>2</sub>O<sub>3</sub> and more maghemite than the larger ones (BOU 528) (Table 6.1; Figure 6.2).

The calcareous fine-earth material that separates bedrock from the overlying pisoliths may not provide a complete blanket over the Blue Range, although it could have been leached or washed from some of the upper slopes; certainly it penetrates well into the underlying weathered bedrock.

The well-sorted and small purplish-black pisoliths (BOU 529) form an almost continuous lag over the highest areas of the summit surface where they are underlain by the calcareous fine-earth. The calcium carbonate is probably of Quaternary age and aeolian origin (Milnes & Ludbrook, 1986) and the pisoliths could have moved progressively to the surface with successive accretions of calcium carbonate in the fashion described by Jessup (1960) and Chartres (1983) to account for the formation of desert pavements. An important alternative process involving biological influences is currently operating as ants are carrying small pisoliths from depth to the modern ground surface. These pisoliths may have originated as fragments of mottled bedrock carried to the surface by ants. The pisoliths are extremely magnetic, well-sorted and glazed, which suggests modification in a near surface environment.

#### 6.3.1.1.2 *Glenville Etch Surface*

Two sites on the Glenville Surface mapped by Twidale *et al* (1976) were examined. Mount Nield was regarded by Twidale *et al.* (1976) as part of the Glenville Etch Surface (their Figure 7, page 39) (Fig. 6.1) (Plate 6.2) where 'there is iron-oxide accumulation in former scarp-foot zones.' However, Mount Nield (Mangalo MR 407745) is a quartzite peak and no indications of iron enrichment could be found during field investigations here.

In road cuttings approximately 2 km north of Mount Nield weathered and mottled bedrock is exposed, but this weathering has developed in sulphide-rich metasediments. The rocks contain pseudomorphs of pyrite and there is no justification for attributing the weathering to the Mesozoic. Analyses were made of slightly weathered bedrock (BOU 524) and oxidised bedrock from the road cutting (BOU 530) (Table 6.2; Figure 6.2). The oxidised bedrock contains 23.72% Fe<sub>2</sub>O<sub>3</sub> and in addition to containing pyrite, was comprised of quartz, goethite, kaolinite and smectite. In this general locality there are several blocks of ferruginised fault breccia, which were probably impregnated by iron released from sulphide-rich zones. Nearby, mica-schist bedrock at the surface

is unweathered (BOU 523). At this locality there is little evidence to support the etch surface interpretation of Twidale *et al.* (1976).

## 6.3.2 Low Level Weathered and Iron Mottled Zones

### 6.3.2.1 *The Corrobinnie Depression*

The Corrobinnie Depression is a linear lowland which extends in a northwesterly direction for about 200 km from near Kimba on Eyre Peninsula (Fig. 6.1). Bourne (1974) considered that it follows a prominent fracture zone because of its linearity, its conformity to the regional tectonic pattern and its modern seismic activity. She suggested that it may have originally been a graben or fault-angle depression subsequently modified by denudation thereby destroying its original form. The transformation of the tectonic fault feature was considered to have occurred as a result of run-off from the Gawler Ranges, or by the pronounced weathering of the underlying granitic bedrock, or a combination of the two. Subsequently, Barnett (1978) and Binks & Hooper (1984) demonstrated that the Corrobinnie Depression is a large Tertiary palaeochannel, although it could be structurally guided.

The Depression stands at a maximum of 30 m below the level of the surrounding plains at an elevation of approximately 100 m asl. Many salinas occur within the Depression, the largest being about 6 km<sup>2</sup> in area. Halite crusts occur over saline muds and islands and bordering cliffs are composed of dolomitic silts and silicified dolomite of lacustrine origin (Bourne, 1974).

Spectacularly mottled and kaolinised bedrock and ferricrete crusts occur within the Corrobinnie Depression. For example, approximately 25 km north of Wudinna, near the margin of a salina, natural erosion has exposed weathered and mottled Precambrian gneissic bedrock. Dark hematitic mottles up to 30 cm across occur within the bedrock (Plate 6.3), in which primary bedrock structures are readily apparent. However, the total iron content of the coarse mottles (BOU 508) is only 4.93% and that in the bleached zones (BOU 509) (Table 6.3; Fig. 6.3) is approximately 1.8%, so that the marked variation in physical character depends on only a few percent of Fe<sub>2</sub>O<sub>3</sub>. The Fe<sub>2</sub>O<sub>3</sub> in the bleached zone may have been present in minerals other than the secondary iron oxides, and insufficient in quantity to be detected by XRD. The dominant iron mineral in the mottles is hematite, with some goethite. Kaolinite is the

dominant secondary mineral in the bleached rock. Both the bleached and mottled areas contain halite, and while this may have been derived from the nearby salina, it may also indicate stored salt in the weathered profile (Gunn, 1985), and the salt may have been important in promoting the weathering processes.

Unweathered gneissic bedrock (BOU 518) (Table 6.3; Fig. 6.3), collected from salients of unweathered rock nearby, contained 3.75%  $\text{Fe}_2\text{O}_3$ , so it appears that the mottling process in this situation did not require inputs of iron from external sources, but merely a relocation of iron within the bedrock during weathering.

Comparisons of the unweathered, mottled and bleached bedrock provide some interesting data apart from the small variations in total iron content. The  $\text{SiO}_2$  content of the unweathered bedrock (BOU 518) is considerably greater than the mottled (BOU 508) and bleached (BOU 509) materials, which have similar  $\text{SiO}_2$  contents. Depletion of bases within the weathered materials is also apparent; for example the CaO content of the unweathered bedrock is 1.19% whereas that of the mottled material is 0.03% and that of the bleached material is 0.02%. Similarly there is a decrease in  $\text{K}_2\text{O}$  from 5.36% (unweathered) to 1.13% (mottled) and 1.48% (bleached). Surprisingly, there is an increase in MgO from 0.47% (bedrock) to 0.75% (bleached) to 1.04% (mottled). There has also been a general increase in  $\text{Al}_2\text{O}_3$  content upon weathering from 12.87% (bedrock), to 17.05% (mottled) and 23.84% (bleached), largely reflected in the content of kaolinite in the bleached and mottled zones. No gibbsite was detected in the mottled and bleached materials so that the alumina present is presumed to be combined form with  $\text{SiO}_2$  largely as kaolinite. MnO, CaO,  $\text{K}_2\text{O}$ ,  $\text{SiO}_2$ ,  $\text{P}_2\text{O}_5$  and ZrO have all been depleted in the weathering process, whereas  $\text{TiO}_2$ ,  $\text{Al}_2\text{O}_3$  and MgO have increased in concentration.

Other related samples of weathered and iron-mottled gneiss (BOU 519) collected 21.2 km east of Kimba (Barna MR 533356) at 220 m asl and (BOU 521) from 30 km east of Kyancutta (Koongawa MR 777307) (Table 6.3; Fig. 6.3) displayed similar relatively low iron contents and depletion of bases, although once again both  $\text{K}_2\text{O}$  and MgO were higher than would be expected from severely weathered bedrock.



The similarity in total iron content between unweathered, mottled and bleached zones suggests that there has not been a major influx of iron oxides from an external source to provide for the mottling in the fashion implied by the work of Firman (1981). Rather it appears that there has merely been a relocation of the original iron within the bedrock as weathering proceeded. Within the zone of mottling there appears to have been contemporary iron mobilisation from pre-existing hematitic mottles into adjacent areas as goethite (Plate 6.3), suggesting that the iron mottles may have considerable age ranges with contemporary processes modifying them.

At a slightly higher level in the section exposed, the iron content increases markedly. At the surface, dense mottles, the distribution of which is controlled by bedrock structures, have a vesicular or slag-like appearance (Plate 6.4). They have an iron content of 41.55% (BOU 517) (Table 6.3; Fig. 6.3), which suggests accession from a more distant source. The  $K_2O$ ,  $MgO$  and  $Na_2O$  contents are much less than the coarsely mottled material, suggesting greater weathering effects. Furthermore, the  $SiO_2$  content is 4.4% less and the  $Al_2O_3$  content has decreased from 17.05% to 2.34%. The dominant iron mineral in the aligned mottles is hematite. The diffractogram suggested that a trace of maghemite occurs in this sample, and this was verified by reaction to a magnet. The absence of goethite and the occurrence of maghemite in association with a large hematite content suggests the possibility of marked iron enrichment in these zones together with surficial modification, perhaps by baking associated with fire. The vesicular macro-fabric of BOU 517 is in sympathy with concentrations of iron oxides having been introduced in solution. The dense and aligned mottles occur on a stripped unconformable surface between the Precambrian basement rocks and the Tertiary Garford Formation (M. Benbow - *pers. comm.*), and the contact may have favoured the ingress of iron oxides, which were later modified after exposure to atmospheric processes. The base of the low cliff at this site marks the position of the unconformity between the mottled basement rock and overlying weathered clay-rich sediments (Plate 6.5). The contact between the two is quite sharp. In turn the clays are overlain by a ferricrete crust. As stated above, the sediments overlying the coarsely mottled basement rock may represent the Eocene Garford Formation, a palaeochannel deposit (Benbow & Pitt, 1978). The

clays in these light-coloured sediments (BOU 510) (Table 6.4; Figure 6.3) directly overlying the mottled bedrock consist dominantly of kaolinite, but also contains unweathered minerals. Overlying the bleached clay-rich zone is a ferricrete, which consists of yellow (BOU 511) and red (BOU 512) coloured iron oxides (goethite and hematite) with clays occupying voids within the ferricrete (Plate 6.6). The total iron content of the ferricrete is 24.82% with 35.3%  $\text{SiO}_2$  and 21.29%  $\text{Al}_2\text{O}_3$ . The hematite-rich sections of the ferricrete crust have a higher  $\text{Fe}_2\text{O}_3$  content than the goethitic sections. The clays (BOU 513) within voids in the ferricrete display a similar mineralogy to those underlying the crust suggesting differential iron-oxide impregnation of a clay-rich sediment. Greater relative amounts of  $\text{TiO}_2$  in the clays than the crust proper may support the view of iron influx into the crustal material.

An iron-rich mottle (BOU 516) (Table 6.4; Fig. 6.3) collected from a position 2 m below the surface of the low cliff was also analysed. Field observations together with the chemistry and mineralogy of the mottle suggest that it is an iron oxide impregnated sandy sediment occurring within a fine-grained deposit, suggesting lithological control in the development of the mottle.

At the surface a variety of ferricretes occurs including an iron-impregnated sandy sediment ferricrete (BOU 514) and a pisolitic ferricrete (BOU 515) (Table 6.5; Figure 6.4) with similar mineralogy and chemistry. Although maghemite could not be clearly identified by XRD, both samples reacted to a magnet, suggesting its presence. A third variant of the surface ferricrete, a fragmental type (BOU 505) was separated into matrix material (BOU 506) and fragments (BOU 507) (Table 6.5; Fig. 6.4). Both have similar mineralogy although the relative proportions of the minerals varied. For example, there was more hematite, kaolinite and anatase present in the fragments than in the matrix and more quartz and goethite in the matrix. The iron content of the matrix (50.71%) is greater than that of the fragments (35.47%). As suggested by magnetic reaction, the fragments contain maghemite, whereas the cementing matrix does not. Similar fragmental ferricrete (BOU 588) (Table 6.5; Fig. 6.4) collected from a second exposure of the Garford Formation within the Corrobinnie Depression returned almost identical chemical and mineralogical analyses.

The field and analytical evidence from this site suggests that there has been local redistribution of iron oxides (as with the large hematitic mottles in the Precambrian basement rocks), ingressions of iron-rich solutions (as at the exposed unconformity and in some of the surficial iron-impregnated sandy and gritty sediments), and the physical accumulation of surficial angular fragments and rounded pisoliths. The profile described here is a composite one involving Precambrian basement rocks and Tertiary (Eocene(?)) sediments variably weathered and iron-enriched, further illustrating the complex and polygenetic nature of such weathering profiles.

Several other samples collected for the author from the Corrobinnie Depression by Dr. N.F. Alley of the South Australian Department of Mines and Energy were also analysed. The occurrence of jarosite, alunite and smectite in a ferricrete (BOU 573) (Table 6.6; Fig. 6.4) overlying unconsolidated sand in a clay pan bottom (Plate 6.7) 10 km northwest of Pinjarra Dam (Figure 6.1) is compatible with the accumulation of iron from groundwaters within a lacustrine environment. Reddish-purple sandy clay with yellow streaks (BOU 587) (Table 6.6; Fig. 6.4) recovered from below the level of the above ferricrete also contained minerals such as natro-jarosite, alunite and barite(?) compatible with a lacustrine origin for the iron accumulation. Sample BOU 579 (Table 6.6; Fig. 6.4), an iron-impregnated gritstone also contains jarosite and alunite and may have had a lacustrine origin. It appears very likely that within the Corrobinnie Depression the presence of lakes and sluggish drainage of former Tertiary palaeochannels favoured the accumulation of iron oxides and this could account for the sporadic distribution of ferricretes in the area rather than assuming that it is due to the differential erosion of more or less continuous ferricrete crusts.

Other samples of pisolitic ferricrete including (BOU 582) were collected from a near-surface position and resting on or incorporated within the sediments of the presumed Garford Formation of the Corrobinnie Depression were also analysed (Table 6.7). Bulk chemical and mineralogical analyses of this sample (BOU 582) revealed similar compositions to sample (BOU 515) (Table 6.5; Fig. 6.4), which was collected from a similar stratigraphic and landscape position. Pisoliths of sample BOU 582 occurred both in iron-rich matrix material and in bleached clays. The pisoliths were hand-separated from the matrix and both

were analysed separately to try to determine whether the pisoliths were significantly different in composition and thus likely to have been transported and incorporated into the matrix material at a later date.

In all samples analysed the pisoliths displayed different mineralogical compositions and iron and titanium contents to those of the surrounding matrix materials. For example pisoliths (BOU 583) separated out of BOU 582 (Table 6.7; Fig. 6.5) contained hematite, kaolinite, maghemite and anatase, with an iron content of 30.26% and  $\text{TiO}_2$  content of 1.24%, whereas the iron-rich matrix (BOU 584) contained dominantly goethite with only minor hematite, kaolinite, smectite, feldspar and anatase, with no maghemite detected either by XRD or by magnetic susceptibility. The iron content of the matrix is considerably less at 19.94% as is the  $\text{TiO}_2$  content of 0.68%. Similar relationships exist between BOU 574 (iron-rich pisoliths) and BOU 575 (iron-rich matrix). Part of the matrix in which the pisoliths (BOU 583) occurred was iron depleted (BOU 585) (Table 6.7; Fig. 6.5), which further demonstrates the diverse origins of the pisoliths and their matrixes. Pisoliths (BOU 576) within a matrix of bleached clays (BOU 577) displayed even greater differences in chemistry and mineralogy (Table 6.8; Fig. 6.5).

In all cases the pisoliths contain more iron, dominated by hematite and maghemite, whereas the main iron mineral in the iron-rich matrix material is goethite. Where maghemitic pisoliths are found at depth it is likely that they have been incorporated into the matrix material after being at the surface. However, the possibility of pisolith formation *in situ* at depth should not be discounted totally as discrete nodules of pallid material occur within a bleached matrix in BOU 586 (Table 6.8; Fig. 6.5). It is also possible that this situation could have arisen as a result of the total bleaching of pisolitic ferricrete, the interpretation that is favoured in this thesis. In some situations both iron-rich and iron-depleted pisoliths can occur juxtaposed within a bleached matrix. The evidence presented above suggests that regardless of where the pisoliths originally formed they spent some time at the surface, undergoing modifications, before being reincorporated into younger sediments.

### 6.3.2.2 *Weathering on Mount Cooper*

Small pockets of weathered materials occur on the porphyry bedrock of Mount Cooper (Venus MR 704470) at 200 m asl on Eyre Peninsula (Plate 6.8). Four samples were analysed to examine the progression of weathering through from unweathered porphyry bedrock (BOU 500) (Table 6.9; Fig. 6.6), to slightly weathered, brownish bedrock with an intact bedrock fabric (BOU 504), to weathered and bleached bedrock (BOU 503), and to severely weathered and mottled bedrock (BOU 501). The variation in iron content is only minor. With greater weathering the contents of MnO, CaO, K<sub>2</sub>O, P<sub>2</sub>O<sub>5</sub>, MgO, and Na<sub>2</sub>O generally decrease and there is an increase in ZrO in the weathered mottle, in which there has also been a marked increase in Al<sub>2</sub>O<sub>3</sub> and a decrease in SiO<sub>2</sub>.

The dominant minerals in the unweathered bedrock (BOU 500) are feldspars, quartz and micas, with some smectite. In the slightly weathered brownish bedrock (BOU 504) with intact fabric, quartz, feldspars, smectite, micas, tourmaline and smectite occur. The weathered, bleached sample (BOU 503) is dominated by quartz and feldspars, with some smectite and kaolinite. On the other hand, the weathered mottle (BOU 501) contains large amounts of kaolinite, reflected in the marked increase in Al<sub>2</sub>O<sub>3</sub> (combined with SiO<sub>2</sub> as there is no free aluminium present). Smectite and hematite are also present.

These analyses demonstrate that care is required in attributing 'deep weathering' involving kaolinisation to materials that may simply be bleached of iron.

### 6.3.2.3 *Point Labatt*

Twidale *et al.*, (1976) considered that there are no remnants of a former regolith at the base of the high aeolianite cliffs at Point Labatt. However, such a weathered zone does occur (Plate 6.9) (Milnes *et al.*, 1985). A kaolinised and mottled zone, developed in granite, is overlain by a sedimentary iron-rich crust at the modern shoreline, at the foot of precipitous coastal cliffs that are essentially formed of aeolianite of the Bridgewater Formation. The crust overlying the mottled material is an ironstone gravelly crust formed of nodules and pisoliths with poorly developed rinds set in a sandy matrix, which is less iron-rich than the nodules, and contains some clay and fine silt. Titanium is present in the matrix, which may be silicified (Milnes *et al.*, 1985). The above

provides an example of a bedrock weathered profile overlain by a sedimentary ferricrete close to present sea level.

## 6.4 Southern Eyre Peninsula

### 6.4.1 Weathered and Mottled Bedrock Zones

The so-called 'laterite' of Southern Eyre Peninsula, characterised by 'deep weathering' and mottling has been confined essentially to the high sections of the Lincoln Uplands by Johns (1961b), Firman (1967) and Twidale *et al.* (1976). However, apparently similar occurrences have now been located varying in elevation from sea level to the summit surface (Fig. 6.7).

#### 6.4.1.1 Coastal Cliffs at Sleaford Bay

In the coastal cliffs of Sleaford Bay (Sleaford MR 655417), Precambrian metasediments and granites have been weathered and ferruginised (Plate 6.10). In contrast to the view of Johns (1961b) there appear to be strong lithological controls imposed on weathering and mottling of bedrock in detail. Analyses of mottled granite bedrock (BOU 534) (Table 6.10; Fig. 6.8) revealed a chemistry and mineralogy typical of such material, being generally depleted of bases, but not totally kaolinised and with hematite being the dominant iron oxide. The bleached section (BOU 535) of this weathered zone differs from the mottle (BOU 534) primarily in its lower  $\text{Fe}_2\text{O}_3$  content and higher  $\text{TiO}_2$  abundance. Mulcahy (1960) noted similar higher titanium contents in the bleached zones in Western Australia. Mottled gneissic bedrock (BOU 537) from the same weathered zone displayed similar relationships to adjoining bleached material (BOU 538) (Table 6.10; Fig. 6.8).

In places the weathered and mottled basement rocks are directly overlain by calcrete that contains abundant pisoliths; elsewhere carbonate has been leached down into the weathered zone where the calcrete has been eroded and the surface is mantled with glazed pisoliths (Plates 6.11; 6.12). The iron oxide mineralogy of these near-surface pisoliths (BOU 536) (Table 6.11; Fig. 6.8) is dominated by hematite and maghemite with typically high  $\text{Fe}_2\text{O}_3$  contents (42.69%).

The pisoliths are sometimes overlain by a thin sandy soil, which superficially might be interpreted as a fossil 'lateritic' A-horizon. However, it seems clear

that the sand has derived from the nearby beach as a result of aeolian activity. Cliff-top dunes occur in the area, and in one locality sand can be traced continuously from the back beach up the cliff face to the cliff top.

At a point along the cliff top, as far as the road extends, there is a small valley cut into the weathered zone that has been filled with pisoliths which are hardening and cementing to form a detrital pisolitic crust of recent age (Plate 6.13). This pisolitic crust (BOU 532) (Table 6.11; Fig. 6.8) at the top of the cliffs contains quartz, kaolinite, hematite, possible gibbsite, smectite, goethite and anatase. Surprisingly no maghemite was detected by XRD but a powdered sample showed a very slight reaction to a magnet. A seepage spring-line occurs at the base of the sandy soil overlying the pisolitic crust in winter (observed on 14/8/84) and is probably assisting cementation of the pisoliths. Similar seepage phenomena were noticed in many localities throughout the Lincoln Uplands. Below the accumulation of pisoliths a pronounced quadrangular bleaching pattern, possibly following old root zones in part, occurs. However, the incipient pisolitic ferricrete is clearly much younger than the underlying weathered zone.

Pisoliths also occur on a surface lower than the crust at the cliff top. This observation suggests complex reworking and modification of the weathered profile and demonstrates its polygenetic character. Crusts in these situations may be quite young, if indeed they are not currently forming.

A short distance away at the intersection of the Sleaford Bay and Sleaford Mere (Sleaford MR 657425) roads, a conglomeratic and pisolitic ferricrete (BOU 533) (Table 6.11; Fig. 6.8) has been exposed in a scrape for road metal. It is overlain by calcrete and recent dune sand. This ferricrete, which stands at about 30 m asl contains 18.71%  $\text{Fe}_2\text{O}_3$  and 8.66%  $\text{Al}_2\text{O}_3$  but is dominated by  $\text{SiO}_2$  (67.2%), which probably reflects the quantity of quartz-rich clasts in it.

#### *6.4.1.2 Quarry near railway crossing on Sleaford Mere Road fronting embayment of Port Lincoln Proper (Jussieu MR 748517).*

Quarrying at this site has exposed weathered and mottled Archaean bedrock, which, in turn, is overlain by younger mottled sands and clasts. These composite weathered zones are overlain by calcium carbonate-rich

deposits, which have been washed into the underlying weathered material. This site is close to the shoreline and stands only about 10 m above sea level.

#### *6.4.1.3 Lincoln Highway several kilometres north of Tumby Bay.*

At an elevation of about 70 m asl grits and sands on the eastern side of the Lincoln Highway (Butler MR 137153) display weathering and prominent dark red mottles (BOU 567) and yellow ferruginous stainings (BOU 568) (Plate 6.14) (Table 6.12; Fig. 6.9). The dominant iron mineral in the red mottles is hematite and that in the yellow mottles, goethite. Both samples contain abundant quartz and lesser amounts of hematite, goethite, kaolinite and smectite. The red mottled sample contains more  $\text{Fe}_2\text{O}_3$  (11.64%) than the yellow sample (8.69%). All other elements have similar abundances in the two samples.

A short distance south of the previous site on the eastern side of the highway (Butler MR 124129) other exposures of weathered and mottled zones have been exposed by road-making. A block containing a red hematitic mottle (BOU 569) set in a matrix of goethite (BOU 570) and bleached material (BOU 571) (Table 6.12; Fig. 6.9) was collected. It had a close resemblance to material collected in the Corrobinnie Depression [Samples BOU 512 (red), BOU 511 (yellow) and BOU 513 (bleached material) (Table 6.4)]. Samples BOU 569, BOU 570 and BOU 571 may have suffered greater weathering than those in the Corrobinnie Depression as they contain more kaolinite. There is a large variation in iron content between the three samples at 47.22% (red mottle), 16.54% (yellow matrix) and 1.38% (bleached matrix). The matrix material contains more  $\text{TiO}_2$  (1.29%-bleached; 1.73%-yellow) than the red mottle at 0.11%. The bases are generally depleted in all samples apart from  $\text{Na}_2\text{O}$ , probably occurring as halite, which is present in all samples probably as an addition to the original bedrock after weathering.

#### *6.4.1.4 Quarry 3.2 km north of Koppio in the Tod River Valley (Koppio MR 785930)*

Quarrying has exposed kaolinised and mottled bedrock in the Tod River Valley and here it extends virtually to the base of the modern river valley (Plate 6.15). The weathering front is quite irregular, however, as a short distance upstream from the quarry salients of unweathered granite crop out in the valley floor. The weathered zone displays both bleaching and mottling, with intricate



weathering patterns occurring in the granitic bedrock (Plate 6.16). The clays in this weathered granite (BOU 544) (Table 6.13; Fig. 6.10) consist dominantly of kaolinite, with smaller amounts of smectite. Only 0.61%  $\text{Fe}_2\text{O}_3$  remains in the sample and all bases have been severely depleted.

There is little variation in the chemistry and mineralogy of the mottled (BOU 541) and bleached (BOU 542) (Table 6.13; Fig. 6.10) sections of weathered metasediments at the same location. Muscovite was only detected in the bleached zone and hematite in the mottled material. The difference in iron content between the mottle (1.91%) and the bleached zone (0.72%) is only very minor, demonstrating that under some conditions only small amounts of secondary iron oxides can effect a strong pigmentation influence.

#### *6.4.1.5 Road Cutting on Flinders Highway immediately west of Port Lincoln (Lincoln MR 717597)*

Weathered bedrock displaying structures and quartz veins exposed in a road cutting at about 80 m asl carries dense, indurated hematitic mottles (BOU 555) set in a bleached matrix (BOU 556) (Plate 6.17). This mottled zone has been mantled with calcium carbonate that has been leached into the weathered zone. At the surface a red soil has developed over the calcium carbonate substrate. The soil carries ferruginous maghemitic pisoliths on and just below its upper surface.

The mottled material (BOU 555) (Table 6.13; Fig. 6.10) has a high  $\text{Fe}_2\text{O}_3$  (50.65%) content and consists dominantly of hematite with minor goethite. The bleached areas (BOU 556) contain calcite, quartz, muscovite, smectite, and kaolinite. The bleached material contains far more calcium and magnesium than the mottle, which probably reflects the greater permeability of the bleached material to the influx of calcium carbonate.

#### *6.4.1.6 Road cutting on Tumby Bay - Cummins Road*

In this, the first major road cutting along the road from Tumby Bay to Cummins (Koppio MR 705826), coarsely mottled Precambrian bedrock has been exposed (Plate 6.18) at about 170 m asl. Tourmaline-rich fault(?) breccia and quartz veins occur throughout the section. The mottles appear to have hardened and concentrated at the surface to form a crust-like lag. The

mottling pattern has been broadly controlled by bedrock structures and in places the character of the mottling can vary with subtle variations in lithology. In detail, however, the mottles seem to have developed independently of bedrock structures. The top of the profile is draped with calcium carbonate in a shallow surface depression. In turn, this carbonate is overlain by ferruginous maghemitic pisoliths.

Purple-coloured mottles (BOU 559) and intervening bleached zones (BOU 560) (Table 6.14; Figure 6.11) developed in Precambrian gneiss were found to have characteristics and relationships resembling other similar materials, with iron oxide abundance being the major difference. However, the bleached material had higher contents of  $\text{TiO}_2$  (1.66% to 0.68%),  $\text{K}_2\text{O}$  (3.00% to 1.32%) and  $\text{MgO}$  (0.51% to 0.25%). These differences may suggest that there has been, on the one hand, movement of iron from the bleached rock to the mottles and greater retention of the above elements in the bleached areas. Proportional corrections to the chemical composition of the bleached material by assuming simply a loss of iron support the above interpretation.

Sporadically throughout the weathered zone there are zones enriched in iron that take the form of vesicular masses resembling bog-iron ore (BOU 561) (Table 6.14; Fig. 6.11). These contain up to 78.6%  $\text{Fe}_2\text{O}_3$  dominantly in the form of goethite, with some hematite. Such concentrations have probably resulted from the deposition of iron introduced in solution at a late stage in the weathering process. Elsewhere it has been noted that this form of iron-enrichment has occurred by the replacement of organic material with iron oxides, and this may also be the case here.

A second mottle (BOU 562) and an adjoining bleached zone (BOU 563) were also analysed revealing a similar variation in mineralogy and chemistry as with the previous samples BOU 559 and BOU 560 (Table 6.14; Fig. 6.11). The mottle is less iron-rich than BOU 559 but the relationships of  $\text{TiO}_2$ ,  $\text{K}_2\text{O}$ ,  $\text{MgO}$  and  $\text{ZrO}$  between the mottled and bleached materials are similar. The bleached zone also contained halite, which has been noted in a wide variety of weathering profiles.

This cutting at approximately 230 m asl is lower than the summit surface, and similar mottled material is exposed east of the cutting at considerably lower levels, suggesting that the weathering took place over an irregular surface, or the weathered land surface has been offset by earth movements since the major weathering occurred.

#### 6.4.1.7 Cutting east of tower on Tumby Bay-Cummins road (Koppio MR 877984)

As at the previous site coarse red hematitic mottling occurs with variations largely reflecting bedrock structures and lithologies, although coarser mottles invariably occur at changes in slope. A palaeochannel filled with alluvial deposits occurs in the weathered bedrock (Plate 6.19) and both the bedrock and the sediment are mantled with a yellow podzolic soil. A coarse red mottle (BOU 566) at the base of the profile displays characteristic chemistry and mineralogy (Table 6.15) (Fig. 6.11). The chemistry and mineralogy of crust-like material (BOU 565) collected from half way up the slope above the cutting suggests that it derived from minor modification of a former *in situ* mottle. A ferricrete fragment (BOU 564) was collected from the top of the landsurface above the cutting at about 300 m asl. This sample shows an increase in  $\text{Fe}_2\text{O}_3$  to 47.73%, a marked decrease in the proportion of  $\text{SiO}_2$  to 15.7% and a slight increase in  $\text{Al}_2\text{O}_3$  to 18.58%. Furthermore, goethite is the dominant iron oxide in this sample, whereas hematite dominated in BOU 566 and BOU 567. These analyses are compatible with the view that the crust-like material has derived from the hardening and weathering modification of fragments of mottles that formed a surface lag consequent upon the erosional lowering of the land surface. There is a similar increase in goethite and a decrease in hematite from depth to the surface at this site as at the Range Road cuttings on the summit surface of the South Mount Lofty Ranges (Chapter 4), and further illustrates the progressive transformation of inherited hematite to goethite by dissolution and reprecipitation.

#### 6.4.2 Pisolitic and Nodular Ferricretes

Several ferricretes have already been mentioned in the context of mottled profiles, but others occur where the underlying material is not exposed. Where crusts do occur they are not continuous. Furthermore, in contrast to the assertion of Johns (1961a), there is no evidence that the crust remnants ever

were continuous, particularly in view of the observation that they appear to relate to former depressions in the landscape. Nowhere were crusts observed to be developed by *in situ* weathering. In places hardened mottles form a lag at the surface to form a crust-like mantle. Elsewhere surficial sandy and gritty sediments possibly indicating former valley floor levels have been impregnated by iron oxide cement. Pisoliths have been cemented together to form pisolitic crusts and conglomeratic ironstone crusts that display a nodular and blocky habit have formed in a similar fashion.

#### 6.4.2.1 Quarry 3.2 km north of Koppio in the Tod River Valley (Koppio MR 785930).

The weathered and mottled zone that extends down to the valley floor and which has been discussed above is overlain by a pisolitic ferricrete crust (BOU 539) (Table 6.16; Fig. 6.12) that mantles a steep slope at about 170 m asl and forms a minor breakaway. It currently occurs high up on the modern valley side slope, but may have been originally deposited in a near valley base environment. Minerals identified in this ferricrete include hematite, quartz, kaolinite, gibbsite, maghemite, anatase, vermiculite and boehmite. It contains a high Fe<sub>2</sub>O<sub>3</sub> content of 56.9%, and only 14.3% SiO<sub>2</sub>, the majority of which is probably combined with Al<sub>2</sub>O<sub>3</sub> (24.86%) as kaolinite although both gibbsite and boehmite are present. The identification of boehmite in this sample is significant. It is well known that maghemite may form during burning in the presence of appropriate organic matter by the transformation of goethite or lepidocrocite (Fitzpatrick, 1987), and strong heating is suggested by the high maghemite content of this sample. However, the transformation of gibbsite to boehmite by high temperatures achieved during bushfires has not been extensively recognised, although it may be relatively common (Fitzpatrick, 1987).

Higher up the slope at about 230 m asl another breakaway edge occurs. It is formed of ferruginous material that superficially resembles a ferricrete crust. However, the ferruginous material is inherited from ancient iron-rich rocks, Precambrian hematitic quartzites (BOU 540) (Table 6.16; Fig. 6.12). No maghemite was unequivocally detected by XRD, but the sample reacted to a magnet, so that maghemite can be assumed to occur. Analysis of an

unweathered sample of hematitic quartzite (BOU 543) (Table 6.16; Fig. 6.12) revealed similar constituents to BOU 540 but a lower  $\text{Fe}_2\text{O}_3$  content.

The hematitic quartzites have doubtlessly provided sources of iron for some of the ferricretes, but care is required in distinguishing the inherited iron-rich zones from younger crusts that have developed as a result of iron-enrichment induced by more recent weathering. For example, an outcrop of hematitic quartzite occurs in a road cutting down valley from the quarry near the modern valley floor: the presence of bedrock structures, however, allows it to be distinguished as an inherited iron accumulation zone.

#### *6.4.2.2 Wanilla Conservation Park (Wanilla MR 653773) at 190 m asl.*

A pisolitic to nodular ferricrete occurs in the Wanilla Conservation Park well below the level of the summit surface on modern valley sides. The chemical analysis of this ferricrete (BOU 549) (Table 6.17; Fig. 6.12) is typical of complex pisolitic ferricretes. Significantly, the mineralogy of this sample includes gibbsite, boehmite and a small amount of maghemite as suggested by magnetic reaction. The presence of boehmite once again suggests that individual ferruginous and aluminous clasts have been affected by strong heating by bushfires in the past.

#### *6.4.2.3 Tod River Reservoir Road*

The ferricretes on the Tod River Reservoir Road (Koppio MR 755828) occur on the edge of a low angle slope at 160 m asl well below the summit surface. The crust (BOU 545) (Table 6.17; Fig. 6.12) consists of iron-cemented bedrock fragments, pisoliths and blocky nodules. The minerals identified in the ferricrete include goethite, gibbsite, quartz, hematite, kaolinite and anatase. The ferricrete is comprised dominantly of 35.21%  $\text{Fe}_2\text{O}_3$ , 21.3%  $\text{SiO}_2$  and 25.49%  $\text{Al}_2\text{O}_3$ %. Other samples of the same crust (BOU 547 and BOU 548) had similar mineralogy and chemistry even though they appeared to have been heated by recent fires. No maghemite was detected in either sample by XRD but BOU 547 displayed reaction to a magnet. A ferruginous conglomerate at a lower level down the slope (BOU 546) appeared to have been derived by reworking from the higher crust. The iron content of the lower ferricrete at 10.24% is much less than the higher one and it is of note that hematite is the dominant iron oxide with no goethite being detected, and that it contains no gibbsite. The variations

in mineralogy between the samples may reflect either slightly different environments of formation and/or different times of formation, with the time variation representing a period during which the modification of one to the other may have occurred. The difference in chemistry and mineralogy may reflect variations in weathering, with the higher ferricrete being subjected to longer periods of leaching resulting in the formation of greater amounts of kaolinite and gibbsite. Alternatively, sufficient heating by bushfires could help to explain the observed differences.

#### 6.4.2.4 *Knott Hill*

Nodular ferricrete with a blocky character occurs sporadically on the summit surface of the Lincoln Uplands and on the northern flank of Knott Hill (Koppio MR 765869) on a low angle slope, below the summit surface at 190 m asl.

Massive nodular ferricrete (BOU 551) (Table 6.18; Fig. 6.12) contains goethite, hematite, quartz, gibbsite, kaolinite and anatase, with a chemical composition dominated by  $\text{Fe}_2\text{O}_3$  (35.63%),  $\text{SiO}_2$  (22.1%), and  $\text{Al}_2\text{O}_3$  (24.79%). A shallow road cut downslope from the massive ferricrete revealed a texture contrast soil formed of a sandy A-horizon with pisoliths overlying a clay-rich B-horizon containing blocks of mottled bedrock incorporated within the clay matrix (Plate 6.20). The blocks of mottled bedrock resemble those in the hardened crust. Combinations of the chemical and mineralogical compositions of the isolated nodules (BOU 550) and the enclosing soil materials (BOU 552) (Fig. 6.12) could give rise to a ferricrete closely resembling BOU 551 if cemented by additional iron and aluminium oxides. Thus the present soil containing detrital clasts of bedrock mottles and/or ferricrete fragments could represent the precursor of a new crust forming today on a low angle slope. Water was passing through the upper part of the soil when the field observations were made during winter so that it is clear that the iron-rich soil is subjected to seasonal wetting and drying, which may be important in causing aluminium and iron-enrichment and soil-hardening.

#### 6.4.2.5 *Yallunda Flat*

Near Yallunda Flat (Koppio MR 805895) a massive pisolitic ferricrete crust occurring near the base of the modern valley floor (Plate 6.21) has been exposed by quarrying. It appears to continue to higher points to the northeast. The mineralogy and chemical composition of this ferricrete (BOU 572) is shown in

Table 6.18 and is characteristic of many pisolitic crusts that have formed by the physical accumulation of pisoliths in lowlying positions in the landscape and their subsequent cementation by iron oxides introduced by iron-enriched waters. Firman (1967) defined the '*Yallunda Ferricrete*' as occurring on interfluves. However, most commonly there are no ferricretes on interfluves but they are best developed in relatively low, or formerly low positions in the landscape, as is the case in the example described above.

### 6.4.3 Ferruginised sediments

#### 6.4.3.1 *Vesicular ferricrete*

Isolated blocks of ferricrete displaying a vesicular to massive structure, with high  $\text{Fe}_2\text{O}_3$  contents as goethite have been noted within various weathered and mottled zones, indicating the influx of iron oxides in solution into weathered zones, probably containing organic material.

Although not investigated, ferricrete resembling vesicular bog-iron ore has been reported from the Wadella Springs area about 11 km W.N.W. of Tumby Bay by Mawson (1907b). It occurs as a large ore body on a flat-topped hill about 215 m asl. Mawson (1907b) described the ferricrete as 'large masses of solid limonite, breaking with a varnish-like fracture, set in a matrix of an impure earthy variety.' He also noted the contemporary precipitation of iron oxides and calcium sulphate in association with the springs, and suggested that the bog-iron ore deposits had originated in this way. The description provided accords with the view that the ferricrete here is a vesicular type, composed dominantly of goethite and formed by the influx of iron-rich waters into a former fresh-water swamp environment where the iron oxides replaced and precipitated around organic material.

#### 6.4.3.2 *Ferricreted sediments in palaeochannel deposits*

At a number of localities in the Lincoln Uplands, cut-and-fill structures, probably representing Tertiary palaeochannels, have been exposed in road cuts. For example, a few km west of Port Lincoln (Lincoln MR 717597) at 80 m asl, iron-indurated, coarse, poorly rounded gravels and sands occupy former valleys cut into weathered and mottled basement rocks (Plate 6.22), and, in places have been cemented to form ferricretes. The fill material is weathered and mottled as well as the basement, but the weathering has probably affected

the basement rocks and the fill material at different times as clasts of the older mottled materials occur in the channels. Rhizomorphs occur in the gravel fill suggesting a former vegetation cover. The fluvial fill is overlain by a carbonate blanket with a continuous gravel layer at its base. A Mollisol has developed on the carbonate and pisoliths occur at the soil surface.

Other channels are exposed in road cuts on the Tumby Bay-Cummins Road. The first major road cutting nearest to Tumby Bay exposes channel fills of basal coarse debris, which does not appear to have travelled far. This fines upwards to grits and sands which are capped by a yellow podzolic soil, which is in turn mantled by pisoliths. There are strong hematitic mottles in the weathered basement rocks whereas the mottles in the fill material are more goethite-rich. These variably weathered and ferruginised channel fills near or on the modern summit surface have analogues in the Southern Mount Lofty Ranges (Chapter 4). On Eyre Peninsula they have been uncritically included with other varieties of ferricrete as the *Yallunda Ferricrete* by Firman (1967; 1981).

## 6.5 Discussion and Conclusions

The field and laboratory investigations reported here further confirm the interpretation of weathered zones and ferricretes as complex, polygenetic features that cannot be simply interpreted in terms of inheritance from ancient weathering events. Weathered profiles and their relationships to younger deposits, including calcareous blankets, fluvial fills, and soils with ferruginous lags, demonstrate the progressive, continual and polygenetic development of the profiles and of the current land surface.

Furthermore, these investigations highlight hazards in utilising them to date various landsurfaces, particularly where they have been used to correlate landsurfaces inter-regionally. Some apparently 'deeply weathered zones' and ferruginous crusts may have developed quite recently through the weathering of sulphide-rich rocks, or be iron-rich zones inherited from Precambrian bedrock. This may have led to the unwarranted recognition of the Glenville Etch Surface. Furthermore, the great variability in the depth of weathering and the irregular nature of the surface over which the weathering proceeded, makes the task of identifying etch surfaces extremely difficult. The intimate



association of carbonate with ferruginous weathered zones and ferruginous pisoliths indicates great complexity, reworking and modification of older weathered profiles. For example, the pisolith-mantled summit surface on Blue Range, regarded by Twidale *et al.* (1976) as the most northerly remnant of the Lincoln Surface and underlain by so-called 'true laterite' cannot have been preserved from the Mesozoic. The sequence on the Blue Range of a mottled zone overlain by a calcareous fine earth, capped by a mantle of pisoliths resembles profiles in the North Mount Lofty Ranges and Pleistocene sequences on Kangaroo Island (Chapter 4). Thus the present summit surface of the Blue Range is more likely to be of Pleistocene than Mesozoic age. Furthermore, the sandy surface horizon cannot be regarded as a fossil illuvial 'laterite' horizon preserved from the Mesozoic because it overlies carbonate material that is most likely of Quaternary age. It is also likely that alleged fossil 'lateritic' A-horizons described elsewhere (Twidale, 1976b; 1983) are related to modern soils or to recent aeolian activity.

The presence of calcareous deposits topping many weathered zones also demonstrates that large areas of the weathering profiles on the Lincoln Surface of Twidale *et al.* (1976) cannot be of Mesozoic age, as do the occurrences of coarse gravels, grits and sands occupying channels cut into the weathered and mottled zones of the Lincoln Uplands. Variations in the weathering and mottling patterns in the underlying bedrock, channel fills and modern land surface demonstrate the effects of continuous weathering and modification of the surface of the uplands. Twidale *et al.* (1976) considered that conditions were suitable for duricrust formation during the Tertiary yet they ignored the potential for modification of their postulated ancient Mesozoic summit surface during this time. Complex deductive arguments have been marshalled to account for the preservation of an ancient summit surface on the uplands of southern South Australia (Twidale, 1976b) but none of the evidence presented reflects the real field situations. In fact, the preservation of stranded river gravels over deeply weathered bedrock within the ranges clearly demonstrates erosion and reworking of parts of the alleged Mesozoic landsurface. At this stage it is not possible to demonstrate just how much modification has occurred.

Weathered profiles affecting bedrock occur from the summit surface to the modern shoreline in several localities around the Eyre Peninsula coastline. This reflects the considerable relief over which the continual weathering occurred; it cannot relate to a 'peneplain' surface close to a regional base level. Twidale *et al.* (1977) noted weathered zones close to the modern shoreline, but did not relate them with the upland 'laterite' weathering because "there is no sign of a ferruginous capping or pronounced horizon development within the gneiss". Consequently, the weathered zones near the shoreline were attributed to the Plio-Pleistocene. Furthermore, they commented that no remnants of a former regolith had been found at Point Labbat, yet here there is a well developed bleached and mottled zone overlain by a ferruginous sedimentary crust. The profile is preserved beneath extensive aeolianite deposits. Moreover, the observations from Sleaford Bay reveal weathering exposed in coastal cliffs of similar character to that exposed in the Lincoln Uplands.

None of the ferricretes observed on Eyre Peninsula in the course of this investigation appeared to be mono-genetically related to the underlying bedrock as part of a 'standard laterite profile'. The crusts comprise a series of derived pisolitic, conglomeratic, blocky and nodular crusts as well as iron-impregnated sediments. These occur at various levels in the landscape, and they may not represent former geomorphic events or regional landsurfaces, but local slope and groundwater conditions. For example, a pisolitic crust appears to be in the process of cementation close to sea level at Sleaford Bay, and a blocky and nodular crust could be developing currently on the northern flank of Knott Hill, high in the uplands.

Pisoliths are very widespread and many of them may have formed from the disintegration of erosionally exposed mottles and modification in near-surface environments. However, the ferricrete crusts are not regionally continuous, as suggested by Johns (1961b), nor is it likely that they ever were. The various crusts discussed above appear to have formed in favourable topographic situation at a variety of times in the past, and in the very recent past, or even at present, crusts appear to have formed or be forming at very different locations ranging from near sea level to near the summit surface. Consequently, these crusts may have no status for litho-stratigraphic, soil stratigraphic (Firman, 1967; 1981) and landsurface correlation (Twidale *et al.*, 1976).

The interpretations presented here differ significantly from those of previous workers, and this may partly reflect the different purposes and methods of earlier investigators. For example, Johns (1961b) was concerned with regional geological mapping, Firman (1967) was seeking soil stratigraphic units, and Twidale *et al.* (1976) with dating and correlating landsurfaces.

## CHAPTER 7: FERRICRETES, FERRUGINOUS AND WEATHERED ZONES OF THE WESTERN OTWAY BASIN

### 7.1 Introduction

Weathering and ferruginisation affect a wide variety of rock types and sediments of different ages in various topographic situations in the western part of the Otway Basin (Fig. 7.1) (Gibbons & Gill, 1964; Gibbons & Downes, 1964; Kenley, 1971; Kenley, 1975; Abele *et al.*, 1976). In particular, Cainozoic marine sediments and basalts that have been dated by palaeontological or radiometric techniques, provide a stratigraphic framework within which the processes of weathering and ferruginisation can be examined.

Gibbons & Downes (1964) carried out a land systems analysis of southwestern Victoria in which they distinguished various types of weathering and iron enrichment. They considered that climatic conditions during Miocene and Pliocene times may have been suitable for the development of 'laterite', which they regarded as a terrestrial formation, since the land surface would have been exposed during those times (Marker, 1959). They noted that the undissected surfaces of the Dundas Tableland and the Brim Brim Plateau (Fig. 7.2) are remarkably flat and capped by 'laterite'. Following Hallsworth & Costin (1953) they contrasted 'laterite' displaying a characteristic pattern of successively deeper horizons of iron enrichment, and mottled and pallid zones with 'ortstein', which they regarded as a pisolitic, laminated or massive formation of iron and manganese oxides and hydroxides, without aluminium, and without underlying mottled and pallid materials. 'Laterite' was restricted by them to the Dundas Tableland and the Brim Brim Plateau and was noted to have formed over a variety of materials including granites, shales, slates, tillites, Cretaceous Otway Group Beds and thin cappings of Tertiary sands and gravels. 'Ortstein' was characteristically found in association with the Cobbobboonee Basalt and swamps or valley floors of the Heywood and Greenwald Land Systems. 'Deep kaolinitic weathering' was observed to be restricted to the Hamilton Basalt. Kenley (1975) noted that as well as deep 'lateritic' soils occurring on the tablelands, they also cap Tertiary sediments that underlie basalts in the northern part of the Otway Basin.

The tablelands within the Otway Basin have been described as 'classic examples of peneplains' capped by 'standard laterite profiles' (Kenley, 1975). Consequently, the western part of the Otway Basin was selected as an area of study to assess variations in the chemistry and mineralogy of ferruginised materials that might have been identified as 'laterite', and developed in host rocks and sediments of different ages in varying parts of the landscape, and to evaluate the formation of so-called 'laterite profiles' in the light of the re-evaluation of the South Australian occurrences.

## **7.2 Discussion of various forms of ferruginisation**

### **7.2.1 The Dundas 'Laterite'**

Abele *et al.* (1976) stated that resistant 'laterite' up to 10 m thick caps remnants of plateaus throughout the Dundas Tablelands and the Merino Dissected Tablelands. 'Laterite' was categorised by them as massive zones of ironstone underlain by mottled and leached (pallid) sub-zones, differing pedologically and morphologically from soils developed on basalts to the south. They noted a uniform occurrence of the 'laterite' on various Palaeozoic rocks and Lower Cretaceous Otway Group sediments in the central part of the tablelands, while towards the west the host rocks were observed to be flat-lying Tertiary sediments, dominantly marls and limestones of the Heytesbury Group, and quartzose sediments of the Dorodong Sand.

They followed Gill (1958; 1964) in regarding the 'lateritisation' as occupying an extensive period of time, before ending in the Early Pliocene prior to the extrusion of the Hamilton-Branxholme Basalts. These, where undissected, were reported to carry kaolinitic soil profiles, more than 10 m thick, which resemble 'laterite', and to have a reddened friable upper surface. Previously Kenley (1971) had thought that 'lateritisation' may have extended to Middle Pliocene to Late Pliocene times in the Dundas area, and suggested that the process may have continued to affect some areas not protected by the sea until the Early Pleistocene.

Kenley (1975) regarded the 'laterite'-capped Dundas and Merino Tablelands, including the Dergholm Platform, as preserved remnants of an erosion and weathering landsurface developed between Lower Cretaceous and Middle Pliocene times, and described the surface as 'a classical example of a

penneplain - the theoretical end product of the normal cycle of erosion'. He maintained that the 'laterite' shows very little apparent lateral change across a wide variety of host rocks and considered that the deep 'laterites' developed on a low-lying 'penneplain' surface under climatic conditions that favoured a marked seasonal rise and fall of the water table.

Within the area of the Dundas Tableland Kenley *et al.* (1964) mapped two types of 'laterite' of two different ages on the Casterton 1:63360 Geological Map Sheet (Fig. 7.3). For example, about 3 km north of Casterton the Noss Road cuts across a mesa (hereafter called the 'Noss Mesa') mapped as being underlain by Otway Group (formerly Merino Group) sediments of Lower Cretaceous age, and sediments of the Heytesbury Group (formerly Glenelg Group) of Miocene to Oligocene age, above which the Dorodong Sands of Early Pliocene to very Late Miocene age occur. The last named sediments occur at the surface at an elevation of about 150 m asl and are described as basal quartz sands, gravels, clays and ironstones that are generally poorly bedded and possess a well developed 'lateritic' soil profile. According to Kenley (1971), these sediments in outcrop are characteristically deeply ferruginised and locally are the main host rocks of the Dundas 'laterite' capping. The major period of 'lateritisation' was considered to have occurred after the deposition of the Dorodong Sands.

About 3 km west of the Noss Mesa, at approximately 180 m asl a second and allegedly younger 'laterite' has been mapped (Fig. 7.3) as developed on undifferentiated host rocks; it is described as consisting of iron-rich, mottled and leached zones of a fossil 'lateritic' profile developed on several older formations. Near the 'Munthan' Homestead, within this mapped zone of younger 'laterite', a deep cutting on the Glenelg Highway (illustrated in fresh condition in Kenley, 1975, p.6), exposes faulted Otway Group sediments containing Lower Cretaceous plant fossils. According to Kenley (*pers.comm.*) a 'laterite' profile had developed, which could be traced up to the grass roots of the tableland level. Thus, at this locality at least, it appears that a weathering profile developed through *in situ* weathering in the Otway Group of sediments. However, while there is bleaching and mottling developed within the road cut, essentially in fine-grained sediments, the crust at the surface is comprised of coarse sands that make an irregular erosional contact with the underlying sediments. Consequently, while the bleaching and mottling have developed

through *in situ* weathering processes, the ferricrete has formed in a quartzose sediment (possibly the Dorodong Sand) younger than the underlying weathered and mottled fine-grained materials. It is possible that the weathering and ferruginisation occurred after the deposition of the Dorodong Sand and that the differences in character between the ferricrete and the underlying weathered bedrock could be due to lithological control. However, it is impossible to determine that this has actually occurred. In some cases there is evidence which is more suggestive of multiple weathering events. For example, reworked clasts of mottles incorporated into the overlying weathered sediment, fossiliferous unweathered younger sediments overlying older weathered bedrock, organic plant roots in the underlying bleached materials, stratigraphic evidence for multiple weathering episodes, and loading structures developed by the squeezing of the underlying pre-weathered older materials into the base of the overlying younger sediments. Consequently, until there is critical evidence available to demonstrate the synchronous weathering of the rocks and sediments of different ages, differences in weathering will be related to their stratigraphic positions.

From just north of the junction of the Glenelg Highway with the Casterton-Edenhope Road at an elevation of about 180 m asl a sample of ferricrete (BOU 222) (Table 7.1-Appendix VII) taken from this area of so-mapped 'younger laterite' is a ferruginised sandstone. This is confirmed by the high  $\text{SiO}_2$  and  $\text{Fe}_2\text{O}_3$  contents and the mineralogy of the crust, which is dominantly quartz and goethite, with minor amounts of hematite and smectite. This mineralogy is typical of many iron oxide impregnated quartzose sediments on land surfaces of some antiquity. Similar material is exposed in scrapes and dam sites on the western side of the Ferry Hills Road (Fig. 7.3). Here the impregnated sandstone displays a vermiform character in places. Moreover, recemented blocks of ferricrete and pisoliths infill depressions and hollows within the iron oxide impregnated sandstone, revealing complex weathering and reworking of the original crust. This exposure of ferricrete occurs on a gentle slope, lower than the higher parts of this surface. This observation together with the non-continuous nature of the ferricrete (none occurs in a dam excavation a short distance to the north) suggests that the crust developed preferentially in a relatively lower topographic area where iron oxides could accumulate from lateral sources.

A series of samples was collected from landslide headwalls (Plate 7.1) on the margins of the 'Noss Mesa' in the area mapped as 'lateritised' Dorodong Sand on the Casterton Geology Sheet. The Dorodong Sand (Kenley, 1971; Abele *et al.* 1976) locally carries a Late Miocene-Early Pliocene fauna near its base. In subsurface it is mainly a micaceous fine sand but in outcrops on the tablelands it is a brown ferruginous sandstone. The Dorodong Sand has been mapped to overlie the Heytesbury Group sediments, which in turn rest on the Late Cretaceous Otway Group.

These relationships are not obvious in the 'Noss Mesa' area. However, according to Kenley (*pers.comm.*) an unconformity marked by a short period of erosion can be discerned between the Dorodong Sand and the underlying Heytesbury Group in some localities, and its presence can be inferred in other places on the basis of 'laterite' lithology and stratigraphic position. Kenley (*pers.comm.*) considered that on the basis of lithology and a faint but persistent discontinuity in the 'laterite' profile, the Dorodong Sand overlies the Heytesbury Group in the 'Noss Mesa' where it caps the 'lateritised' Tertiary sequence.

Analysis of a sample of weathered Otway Group bedrock (BOU 221) (Table 7.1; Fig. 7.4), which, by extrapolation, underlie the 'Noss Mesa', shows that the materials have not been severely weathered, containing more than 14%  $\text{Fe}_2\text{O}_3$ , 2.68%  $\text{K}_2\text{O}$  and 1.68%  $\text{Na}_2\text{O}$ . Only a small amount of kaolinite was detected by XRD, and the occurrence of other minerals such as feldspars, muscovite, vermiculite, smectite and randomly interstratified clays suggests that weathering has not been intensive. Bleached material (BOU 220) (Table 7.1) was collected from the headwall scarp of the landslide (Plate 7.1), 2.2 km north of Casterton. This showed a marked decrease in the total iron content, and no iron oxides could be identified by XRD, but it contained similar contents of  $\text{CaO}$ ,  $\text{K}_2\text{O}$ ,  $\text{Al}_2\text{O}_3$ ,  $\text{MgO}$  and  $\text{Na}_2\text{O}$  as the less weathered Otway Group sediments (BOU 221). While BOU 220 has larger contents of kaolinite than BOU 221, it still contains readily weatherable minerals such as feldspars and micas as well as smectite and randomly interstratified clays. Thus this material, though bleached of iron does not fit the concept of the 'deeply weathered' pallid zone of a 'laterite profile'. Bleached material (BOU 206) from another landslide headwall (Plate 7.2) on the northern margin of 'Noss Mesa', while more



weathered than sample BOU 220, still contains unweathered micas and feldspars, with a dominant clay mineralogy of smectite and kaolinite.

Thin section examination of the pallid material (BOU 206) collected from the Burston property on 'Noss Mesa' reveals it to be a siltstone, which is markedly different in character to the iron-rich crust (BOU 201) (Table 7.2) (Plates 7.1 and 7.3), which occurs above it. The fabric of the pallid material is a very fine silt that is tightly packed and of uniform size. The major clay mineral present is kaolinite, which was probably derived by the weathering of the mudstones of the Late Cretaceous Otway Group of sediments. This thin section information supports the view that the 'laterite profile' consists of separate stratigraphic layers as suggested by Kenley (*pers. comm.*).

Samples of iron-rich mottles (BOU 202, BOU 208) (Table 7.2) collected from above the bleached material have total iron contents of 12.9% and 6.4% respectively, less than that of the partly weathered Otway Group sediments (BOU 221). Bases in the mottles are slightly more depleted than in the bleached materials. A thin section of BOU 202, collected from 4 m below the surface, revealed that it has a fine siltstone framework impregnated by iron oxides, and has a similar fabric to the underlying bleached material. The individual grains, although angular, are well-sorted (Plate 7.3), and rounded goethitic structures may be weathered biogenic glauconitic pellets. On the other hand, the mottle (BOU 208), collected from only a short distance below the surface, microscopically appears as a very ill-sorted sediment, consisting of fine to medium-coarse quartz grains set in a kaolinite-rich matrix in places and iron oxides elsewhere. Fine-grained iron oxide crystallites appear scattered throughout the matrix (Plate 7.4). Variations in these two mottles may reflect development in different sedimentary units.

The mottled material exposed in the landslide on the northern end of 'Noss Mesa' is overlain directly by the modern soil containing ferruginous and maghemitic pisoliths. However, at the site of the landslide 2.2 km north of Casterton, crust-like material occurs above the mottled sediments and below platy ironstone fragments set in a brown-coloured soil that is about 30 cm deep. Pisoliths that occur near the surface and in the modern soil react strongly to a magnet. The crust-like material (BOU 201) is friable and has an amorphous,

earthy to massive macro-fabric. Its major constituents are  $\text{Fe}_2\text{O}_3$  (35.3%),  $\text{SiO}_2$  (39.1%) and  $\text{Al}_2\text{O}_3$  (13.4%). Hematite was the dominant iron oxide detected, being twice as abundant as goethite, and no maghemite was detected either by XRD or magnetic reaction. Titanium as anatase was also shown to be present. Ferricrete (BOU 209) with a similar macro-fabric, chemistry and mineralogy was also located south of Coleraine amongst boulders of vesicular to massive goethite-rich ferricrete. Unfortunately at this site there were no exposures to allow examination of the underlying materials, but according to the mapped geology it had developed on Older Basalt.

The sample of ferricrete (BOU 201) in thin section had a very irregular, complex, clay-rich matrix that appeared to have been partly inherited and partly modified by weathering. The framework grains are unsorted, angular to very angular quartz grains, which are embayed in the quartz-rich areas. Within the matrix there are pelletal structures resembling very fine-grained clay balls without internal structure, that may represent altered crystals such as glauconite. Fossil structures that resemble tractor tyres also occur in this section. These observations may support the view that the ferricrete developed in the marine fossiliferous Heytesbury Group of sediments. Occasional glazed and strongly magnetic nodules (BOU 230) (Table 7.2) and pisoliths occur in the upper part of the crust-like material, but well below the modern soil. The presence of these maghemite-rich clasts in the crust suggests that reworking of the 'crust', including the development of a lag consequent upon downwasting of the landsurface, has occurred in the past.

Detailed examination of the two mapped 'laterites' of two different ages failed to support this interpretation, which is complicated by the fact that the alleged younger 'laterite' is higher in elevation than the older. This anomaly could be explained by faulting, however, as the Miakite Creek Fault has been mapped separating the two occurrences (Fig. 7.3).

## **7.2.2 Pebble Point Formation**

This formation represents the oldest of the Cainozoic sediments of the Otway Basin that have been affected by ferruginisation. At Killara Bluff on the valley side of the Glenelg River, 11.4 km SSW of Casterton (Fig. 7.3), Palaeocene fossiliferous marine sediments of the Pebble Point Formation rest

unconformably on the Runnymede Formation at the top of the Late Cretaceous Otway Group (formerly Merino Group) of beds (Plate 7.5) (Kenley, 1971).

At Killara Bluff the Pebble Point Formation was noted to be 16 m thick and to include two members (Kenley, 1971). The lower bed is 9.3 m thick and consists of yellow-brown ferruginous sands and thin beds of white micaceous sandy silt with occasional bands of rounded quartz gravels. Corals, pelyceps and fossil wood occur near the base of the member, and other fragmentary shells occur in the overlying beds (Kenley, 1954). The basal formation is overlain by 6.6 m of yellow-brown to dark reddish brown granular clays, sandy clays and sands with occasional white sandy silts and abundant fossils. Kenley (1971) considered that these sediments at Killara Bluff have been deeply weathered and are characterised by a 'distinctive powdery orange-brown limonite derived from the oxidation of pelletal or oolitic chamosite.' He also considered that 'lateritisation' of these beds occurred without significant volumetric alteration.

Downstream from Killara Bridge about 2 km along the Glenelg River, Kenley (1971) reported the occurrence of the Pebble Point Formation in a relatively fresh condition. Here it consists of dark-green chamositic quartz sands and oolitic and pelletal chamosite sands and glauconite with calcareous fossils. Similar unweathered 'greensand' beds have been reported from boreholes, where minor pyrite has also been recorded (Kenley, 1971).

Complex rhizomorphs and pipestems formed by iron oxides occur within the lower member of the Pebble Point Formation (Plate 7.6). Minerals identified in a sample (BOU 228) (Table 7.2) of the ferruginised Pebble Point Formation at Killara Bluff include goethite, quartz, micas, kaolinite, feldspars and vermiculite. Material from the upper part of the Killara Bluff profile, described above and illustrated in Plate 7.5 (BOU 229) (Table 7.2; Fig. 7.4) was dominated by quartz, which was only a minor constituent of BOU 228. Other minerals identified included goethite, kaolinite, feldspars, micas, smectite and vermiculite. The Dorodong Sands are mapped at the top of the Killara Bluff section (Kenley *et al.*, 1964) and the abundance of quartz in the sample is in sympathy with that interpretation. The ferruginisation of the Pebble Point Formation appears to have occurred via the release of iron oxides from local pre-existing 'primary' sources and the replacement of limestone by them.

Thus these materials are ferruginised sediments. The underlying Otway Group sediments appear unaffected by this ferruginisation, but the nearby Janjunkian Sandford Limestone of the Tertiary Heytesbury Group has been ferruginised and, in places, pisoliths contain marine fossils related to this limestone (P.R.Kenley - *pers. comm.*).

### 7.2.3 The Compton Conglomerate and equivalents

In Allen's Sand Quarry (Knight's Quarry) (Fig. 7.2), 10 km northwest of Mount Gambier, but still within the Western Otway Basin, the Compton Conglomerate of Oligocene age is exposed (Plate 7.7). Here it is about 0.6 m thick, and unconformably overlies the Eocene Dilwyn Formation. The Compton Conglomerate is an indurated conglomerate with rounded ironstone pebbles and grits, set in a goethitic matrix, and marks the base of a marine transgression (Ludbrook, 1961). Some workers (e.g. Johnson, 1976) have suggested that the ironstone pebbles were derived from weathered zones on the land as sea level rose. However, the widespread distribution of Compton Conglomerate samples with identical iron mineralogy favours the interpretation of release of iron from pre-existing iron-rich minerals to coat pebbles, fossils and other sediments in this basal conglomerate.

Minerals identified from bulk samples of the pebbles of the Compton Conglomerate (BOU 224) (Table 7.3; Fig. 7.4) from this site include goethite, quartz, kaolinite, micas and randomly interstratified clays. The sample has a high  $\text{Fe}_2\text{O}_3$  content of 53.37%, and a relatively high content of  $\text{P}_2\text{O}_5$  (1.17%). Terrestrial ferricretes are usually highly depleted in this element. The identification of only goethite in the iron oxide mineralogy of this sample favours the view of a single phase of sub-surface ferruginisation of re-existing sediments, either from iron oxides introduced in solution from outside sources, or more likely from *in situ* oxidation of inherited iron-rich minerals such as glauconite and siderite. There is no evidence for the iron oxides having developed by subaerial weathering on an exposed landsurface, or for the incorporation of pre-existing terrestrial iron oxides on a landsurface over which the sea transgressed. If either situation had been the case then the observed mono-iron oxide mineralogy would not be expected. In the examples analysed for this thesis, subaerially affected ferruginous materials invariably contain more than one type of iron oxide. For example, a short distance above

the Compton Conglomerate on the overlying Knight Group, ferruginous clasts occur, which have a diverse iron mineralogy, dominated by hematite and maghemite, with minor goethite (BOU 225) (Table 7.3). This iron oxide mineralogy is compatible with that in equilibrium with most pedogenic environments.

Material equivalent to the Compton Conglomerate, exposed in a landslide on the banks of the Crawford River (Kenley, 1971) about 20 km east of Dartmoor, also displayed an exclusive iron oxide mineralogy of goethite. Other minerals identified in this sample (BOU 226) (Table 7.3) included calcite, quartz, kaolinite and vermiculite. Furthermore, relative to subaerially developed ferruginous materials, this sample is also relatively high in  $P_2O_5$  (0.92%).

As reported in the section on the Mount Lofty Range Province (Chapter 4), analysis of two samples of the Compton Conglomerate from the valley of the Bremer River (Murray Basin) in South Australia, yielded similar results. In the past these ferruginous materials have mistakenly been related to 'lateritisation' (Kenley, 1971; Horwitz, 1960).

#### **7.2.4 Ferruginisation affecting other materials in the Otway Basin**

On the eastern side of the bridge crossing the Glenelg River at Casterton, a road cut has exposed a buried ferricrete about 1 m thick within the valley of the Glenelg River at an elevation of approximately 45 m asl. The ferricrete is formed of a mixed sediment comprised dominantly of sands, which contain transported clasts of weathered bedrock or bedrock clasts that have been weathered *in situ*. The ferricrete also appears to have been bioturbated, probably before induration, and contains pisoliths. The base of the ferricrete is softer than the top, which is overlain by a soil with a ferruginous hardpan that appears hematitic. Regardless of whether the ferricrete developed in a sediment deposited within the valley of the Glenelg River, the interpretation favoured here, or in the underlying Otway Group of sediments, it probably did not develop until after the incision of the Glenelg River, so that it can be regarded as younger than the ferricretes of the tablelands. The ferricrete was sampled at its base (BOU 223) and top (BOU 227) (Table 7.3) and it displays considerable variation in chemistry and mineralogy over very short distances.

Ferruginous materials were collected from a variety of other situations in parts of the Otway Basin. For example, on the southern border of Coleraine township, a coarse quartzose clastic iron-impregnated sediment (BOU 210) (Table 7.3) occurs on top of a pronounced escarpment. Microscopically the grains appear to be poorly sorted, angular, and, in places, embayed. Occasional altered mica patches are discernible. The framework grains are set in an iron-rich clay matrix, which contains patches of hematite granules (Plates 7.8 and 7.9). The iron-oxide mineralogy is dominated by hematite, which is more than twice as abundant as goethite. Some kaolinite was also detected. The character of the ferricrete suggests that it is of some antiquity, and it has chemical and mineralogical affinities with iron-impregnated sediments of the Dorodong Sand examined near Casterton (e.g. BOU 222).

Ferricrete (BOU 203) (Table 7.3) was also collected from within a dune immediately on the south side of Cawkers Creek where it crosses the Mount Gambier-Casterton Road (Fig. 7.2), within an area mapped as Pleistocene siliceous dune sands on the Casterton geology map sheet. This is confirmed by the dominance of  $\text{SiO}_2$  (74.1%) with only a small amount of  $\text{Fe}_2\text{O}_3$  (7.4%) and  $\text{Al}_2\text{O}_3$  (8.4%), with a mono-iron oxide mineralogy of goethite. Small amounts of kaolinite, mica and smectite were also identified in the sample, which is characteristic of relatively recent iron oxide impregnation of siliceous sediments. Thin section examination of BOU 203 revealed irregular zones of ferruginisation in a primary sediment, and various phases of iron oxide impregnation are indicated by laminar coatings of iron oxides (goethite).

Pisoliths overlying and incorporated into rocks, sediments and soils of various ages were collected from different localities in the Western Otway Basin. Pisoliths were collected from the ground surface near Tarrington, a small settlement to the east of Hamilton, and developed upon kaolinised Hamilton basalt (Gibbons & Downes, 1964) (Plate 7.10). These pisoliths (BOU 204) (Table 7.4; Fig. 7.4) appear to have developed essentially from the weathering of fragments of basalt. The major oxides in these pisoliths are  $\text{Fe}_2\text{O}_3$  (48.63%),  $\text{SiO}_2$  (19.38%) and  $\text{Al}_2\text{O}_3$  (16.21%). The presence of hematite, maghemite and goethite were identified by XRD as were kaolinite, ilmenite, illite and very small amounts of quartz. The original basalt bedrock is apparent in thin section, as ghosts of plagioclase crystals and lathe-like structures of olivines or

pyroxenes, some of which have been replaced by goethite (Plate 7.11), can be discerned. The relatively high  $\text{TiO}_2$  (1.68%) content in ilmentite also suggests fundamental derivation from a basic igneous rocks.

Pisoliths collected from near Branhholme (BOU 205) (Table 7.4) have similar chemistry and mineralogy to the Tarrington pisoliths (BOU 204). Thin section examination of BOU 205 again shows ghosts of former plagioclase laths, replaced by and coated by iron oxides (goethite) in places. BOU 205 also contained relatively high values of  $\text{TiO}_2$  (1.61%) reflecting a source from basalt.

Pisoliths (BOU 207) (Table 7.4) were also sampled from the B horizon of soil developed on the river terrace of the Surrey River near Heathmore, north of Portland, where Gibbons & Downes (1964) regarded them as ortstein of bog-iron ore origins. Hematite and maghemite were the major iron oxides identified, with smaller amounts of goethite. Quartz, gibbsite and kaolinite were also detected. Microscopically, in thin section, these pisoliths appear as rounded clasts, rich in iron oxides in which irregular grains of quartz 'float'. The chemistry and mineralogy of these pisoliths is not in sympathy with iron-rich materials that formed from the precipitation of iron oxides in freshwater lakes or swamps, which elsewhere are dominated by goethite, with little, if any hematite, and no maghemite present.

Other pisoliths were sampled from nearer the mouth of the Surrey River. These (BOU 211) (Table 7.4) have a similar chemistry and mineralogy to BOU 207. In thin section some of the pisoliths have coatings over sand to grit-sized, poorly sorted and not closely packed quartzose grains, contained within a goethite matrix, in which complex replacement has occurred. Possible algal biogenic structures have been replaced with iron oxides.

All of the four pisolith samples have high total iron contents and are dominated by hematite as the major iron oxide, with considerable amounts of maghemite and variable amounts of goethite. The so-called bog-iron ore types of pisoliths (Gibbons & Downes, 1964) cannot strictly be regarded as such, but would be more accurately described as iron oxide-impregnated quartzose sediments, that have experienced iron oxide transformations to hematite and maghemite, probably by heating in the presence of appropriate organic matter.

### 7.3 Conclusions

The following conclusions were drawn following the above examination of the field relationships, mineralogy, chemistry and micromorphology of ferruginous materials in the Western Otway Basin:-

- i. The surface of the tablelands cannot be regarded simply as as a 'peneplain', the theoretical climax of prolonged subaerial denudation. Rather, the pronounced flatness of the tablelands is apparently due to the influences of marine erosion and deposition, as indicated by the ferruginised marine beds of the Pebble Point Formation, the Heytesbury Group of sediments and the Dorodong Sands.
- ii. The range of ages of rocks and sediments affected by bleaching and ferruginisation suggests a long history of iron mobilisation and precipitation.
- iii. The ferricretes of the tablelands and other topographic situations cannot be interpreted as 'laterite' in the classic sense, because the crusts have invariably developed in sediments that are younger than the underlying mottled and bleached materials. Indisputable and complete *in situ* 'laterite profiles' have not been found by the writer in this study area. In many cases replacement of previously existing sediments by iron oxides has occurred without marked volumetric alteration, which is out of sympathy with the classic notions of the processes of 'lateritisation', which involve depletion of bases and silica.
- iv. Many different rocks, sediments and materials have been weathered and ferruginised to different degrees depending on various factors such as the source of iron-rich primary sediments, including some of the marine deposits that contain glauconite, siderite and chamosite. Most of the ferruginised limestone sediments have a mono-iron mineralogy, which suggests a simple impregnation by *in situ* transformations of pre-existing iron-rich minerals, or the ingression of ferrous iron in solution from lateral sources. The retention of CaO and



$P_2O_5$  in these sediments also argues against them being strongly influenced by terrestrial leaching environments.

- v. Bleached materials are not intensively weathered as they still contain feldspars and micas as well as including minerals such as smectites in association with varying amounts of kaolinite. Chemical analyses demonstrate that the mottled materials investigated contain relatively small amounts of  $Fe_2O_3$ . Furthermore, comparison with unweathered parent materials suggests that mottles have developed simply by the local redistribution of iron within the rock.
- vi. There are significant differences, with respect to chemical composition, between the different materials analysed such as bleached bedrock, ferruginised sandstone, ferruginised limestone (including the Compton Conglomerate), pisoliths, mottles and massive ferricrete (Fig. 7.4). These differences are even more apparent when their mineralogical compositions are also taken into account (Tables 7.1 to 7.4).
- vii. Some rocks, particularly sandstones and limestones, that are markedly iron-rich were apparently more suitable porous host rocks for impregnation by pervasive iron-enriched waters. These laterally moving waters led to the preferential development of ferricrete in discrete localities, rather than the production of a uniform blanket over the landscape.
- viii. The evidence does not favour a single or even a major period of 'lateritisation' but continuing weathering and iron mobility over a long period of time, impregnating suitable sediments in favourable situations. Elsewhere ferruginisation and weathering may have been interrupted or inhibited according to relative location to the exposed land surface, location at sites of internal or sluggish drainage that may have favoured the sporadic accumulation of iron oxides, and the operation of geological events such as submergence by the sea, which would have protected the land surface from subaerial processes of weathering and erosion.

- ix. In the sections of the Otway Basin examined, the term 'laterite' appears to have been applied widely to a variety of materials including:-
- a. those resulting from the oxidation of suitable sediments that have been exposed or brought closer to the land surface by erosion,
  - b. bleached or pallid material, whether kaolinised or not, and,
  - c. variably mottled materials and iron-impregnated sediments, some of which have relatively low total iron contents.

The interpretation of this landscape within the framework of a 'classic lateritisation' and 'peneplain' model is unacceptable in the light of the above investigations.

## CHAPTER 8: A REAPPRAISAL OF THE SYDNEY 'LATERITES'.

### 8.1 Introduction

The 'laterites' of the Sydney area have been studied by many workers over the past sixty years or so, and have been subjected to varying interpretations. After having investigated 'lateritic' materials in a variety of situations in other parts of southern Australia, those in the Sydney area were examined in order to gain experience of 'lateritic' materials that have been extensively studied and to test some of the ideas, which had developed as a result of earlier work during the preparation of this thesis. Controversial issues have arisen with respect to the origin of 'laterites' (Hunt *et al.*, 1977), particularly as a result of work carried out on the Hornsby Plateau of North Sydney (Figs. 8.1 and 8.2). For this reason efforts have been concentrated in this area, particularly at the Terrey Hills site.

### 8.2 Previous investigations

No extensive review of previous literature on the 'laterites' of the Sydney area is presented here. Such reviews are already available, such as that of Faniran (1969). The most recently published work on the Sydney 'laterites' of Hunt *et al.* (1977) diverged considerably from previous interpretations. They pointed out that most previous workers regarded the 'laterite' profiles as fossil soils formed under tropical climatic conditions during the Miocene on a 'peneplain' close to sea level, with the present sporadic distribution of 'laterite' over the area considered to have resulted from dissection of the surface after uplift.

Hunt *et al.* (1977), however, interpreted the so-called 'laterite profiles' of the Sydney area as the result of contemporary near-surface alteration of iron-rich Hawkesbury Sandstone units. They considered these contemporary processes to include the mobilisation of iron minerals as crystalline solids. The major lines of evidence used by Hunt *et al.* (1977) to substantiate their conclusions were:-

- i. The coincidence of structures in the 'lateritic profiles', especially at Terrey Hills, with structures in the Hawkesbury Sandstone.
- ii. The overlap of iron concentrations in the 'lateritic profiles' with those contained in iron-rich sequences within the Hawkesbury Sandstone. Consequently they saw no need for external sources of iron or for long distance lateral iron oxide transport.

- iii. The lack of evidence for iron-enrichment in indurated zones and impoverishment in mottled zones, and the absence of variations in aluminium and silica down the profiles.
- iv. The recognition of original sandstone fabrics in nodular indurated zones.
- v. The *in situ* formation of nodules containing maghemite within the profiles.

### 8.3 Investigations of this Thesis

The investigations reported here include examination of field relationships between different types of ferricretes, weathered Hawkesbury Sandstone and clastic deposits, together with chemical, mineralogical, micromorphological and micro-probe studies of various sections of the weathered zones.

#### 8.3.1 Field Relationships

At the Terrey Hills 'laterite' quarry site (Fig. 8.1) several variants of ferricrete fabrics occur. At the most southerly exposure of ferricrete in the quarry, cemented hematitic pisoliths without rinds (BOU 401) are overlain by cemented hematitic pisoliths with yellow surface rinds (BOU 400) (Plate 8.1), which are in turn overlain by a yellow earth. A few metres to the north of this site, cemented pisoliths (BOU 404) with rinds overlie finely mottled vermiform materials (BOU 403) (Plates 8.2; 8.3). At both of these sites fragments of strongly magnetic fine-grained material occur throughout the exposures.

Further north along the quarry wall a more complex sequence occurs. Here hardened mottles (BOU 407) are overlain by a vermiform ferricrete (BOU 406), that in turn gives way to a clastic, nodular ferricrete (BOU 408) topped by a pisolitic ferricrete (BOU 409) (Plate 8.4). Distinct segregations of strongly magnetic clasts occur throughout most of the profile. A sketch of further complicated features northward along the quarry face (Plate 8.5) reveals a lower section of semi-consolidated pisoliths and other coarse clastic material, including boulders of vesicular iron oxides resembling 'bog iron ore' (BOU 412a), superficially coated with a glaze of yellow goethitic material. The profile is capped by a ferricrete crust that varies from consolidated pisoliths (BOU 411) to fine-grained organic sediments that have been impregnated by iron oxides to produce a vesicular deposit of almost pure bog-iron ore (BOU 410). An infill of

pisoliths occurs along one of the joints in the surface ferricrete, and one of the crustal joint blocks has been intricately burrowed, displaying a myriad of biogenic trails, that have been partly infilled with secondary accumulations of iron oxides. It appears that the crust must have originally been a soil that was subsequently impregnated with iron oxides brought into the area in solution. Loose magnetic pisoliths (BOU 412) occur at the surface and within the modern soil.

At the most northerly exposure of the quarry, soft mottled material (BOU 413) at the base is overlain by a vermiform structured material, on which a hardened slabby ferricrete (BOU 414) occurs. This is in turn overlain by a clastic and nodular (BOU 415) deposit that includes variously oriented boulders of bog-iron ore, and on which rest a soft pisolitic ferricrete (BOU 416) and a hardened pisolitic ferricrete (BOU 417). The profile is topped by the modern soil (Plate 8.6). Fragments of maghemite occur throughout the full profile apart from the lowest soft mottled material.

At no place in the Terrey Hills quarry site could *in situ* Hawkesbury Sandstone bedrock be identified unequivocally. Numerous examples of ferruginous clasts and boulders occur in the quarry face (e.g. Plates 8.7 and 8.8). However, a fresh road cutting on the Mona Vale Road nearby had exposed a clear unconformable contact (Plate 8.9) visible between weathered Hawkesbury Sandstone and overlying fine-grained sediments, which contained clasts of dense magnetic material and pebbles of coarse-grained hematitic sandstone, similar to those occurring in most of the Terrey Hills site. A second unconformable contact between *in situ* bedrock and overlying ferruginous clastic sediments was observed in the quarry at Belrose that is now used as a rubbish dump.

Hunt *et al.* (1977) considered that the broad structures present in the indurated materials at Terrey Hills represented original bedrock structures of the Hawkesbury Sandstone. Certainly the lenticular structures shown in Plates 8.4 and 8.6, in broad view, resemble bedrock structures such as those exposed in road cuttings along West Head Road in the Ku-ring-gai Chase National Park (Plates 8.10; 8.11). However, it appears that the indurated materials are not superficially modified Hawkesbury Sandstone, but are weathered and iron-indurated clastic deposits of probable colluvial and detrital origins. A

distinctive feature of the weathering of the Hawkesbury Sandstone is the differential desilicification of the sandstone along more susceptible beds. For this reason, areas of the plateau summit may be composed of coherent sandstone, whereas at lower levels, beds have been preferentially weathered and removed to cause collapse of overlying strata. An excellent example of subsurface weathering and desilicification occurs at Beacon Hill, where essentially unweathered bedrock occurs near the summit, but is underlain by considerable thicknesses of weathered and iron-depleted sandstone. Prominent caves and visor structures have formed at the top of the hill as a result of differential erosion of the preferentially weathered sandstone.

In several road cuttings along the West Head Road, depressions thus formed in the sandstone have been filled with colluvial material derived from upslope. This colluvial material includes fragments of hematitic sandstone and fine-grained strongly magnetic clasts, both of which occur at the surface over many areas of the plateau in the Ku-ring-gai Chase National Park (Plate 8.12). These materials are identical to those that occur in the clastic deposits that comprise the majority of the indurated zone at Terrey Hills. Thus, while the structures present in the indurated material may not be directly inherited from the original sandstone structures, deposition of the clastic sediments may have been influenced by them, so that the clastic structures could mimick those of the original sandstone. However, it should be pointed out that the modern soils shown in Plates 8.4 and 8.6 display similar lenticular structures and there is little doubt that the soils have not been influenced by bedrock structures. Furthermore, some ferricrete structures resemble lithified soils (Plate 8.13).

### **8.3.2 Chemistry and Mineralogy**

The chemical analyses of indurated crusts, mottled zones, bleached bedrock, pisoliths and soil are shown in Tables 8.1, 8.2, 8.3 and 8.4 (Appendix VIII) and Fig. 8.3, with the detailed locations of the samples, where appropriate, being located in previous figures.

The indurated crusts, pisoliths and mottles are composed dominantly of  $\text{Fe}_2\text{O}_3$ ,  $\text{Al}_2\text{O}_3$  and  $\text{SiO}_2$  with some  $\text{TiO}_2$  present. They are well depleted of bases  $\text{CaO}$ ,  $\text{K}_2\text{O}$ ,  $\text{MgO}$ ,  $\text{Na}_2\text{O}$  and  $\text{P}_2\text{O}_5$ . Total iron content varies from 1.68% in soft mottles at the base of the most northerly section of the Terrey Hills profile to 64.05% for

bog-iron ore material. Many of the crusts vary in iron content between 20% and 40%. On the other hand, bleached Hawkesbury Sandstone from Beacon Hill (BOU 418) contained only 0.19%  $\text{Fe}_2\text{O}_3$  and a strongly coloured hematitic mottle (BOU 419), adjacent to where the bleached sample was collected, contained only 4.22%. The modern soil (BOU 405) (pisoliths excluded) contained 3.61%  $\text{Fe}_2\text{O}_3$ , 80%  $\text{SiO}_2$  and 8.5%  $\text{Al}_2\text{O}_3$ . Some samples contain relatively small amounts of  $\text{SiO}_2$  such as in the hardened mottles of sample BOU 407 (9.44%), suggesting considerable removal of silica from the profile, or that the weathering has occurred in sediments other than the Hawkesbury Sandstone. Generally there are high contents of  $\text{Al}_2\text{O}_3$  except in the bog-iron ore materials (BOU 410; BOU 412a), in the soft mottles at the base of the profile (BOU 413) and in bleached sandstone bedrock (BOU 418). In the last case there is a high  $\text{SiO}_2$  content, and the aluminium present is probably combined with silica as kaolinite.

The main minerals identified included quartz, gibbsite, hematite, goethite, maghemite, kaolinite and anatase. Gibbsite has been reported from the Hawkesbury Sandstone (Hunt *et al.*, 1977), but it occurs in such high concentrations in the iron-rich zones that it must also have developed as a result of the incongruent dissolution of kaolinite rather than being merely an original constituent of the sandstone. This view is supported by the observation that there is an inverse relationship between kaolinite and gibbsite abundances, for as the gibbsite abundance increases, the kaolinite content correspondingly decreases. Typically the high concentrations of gibbsite occur in the upper indurated crusts and decline in the lower bleached zones. Many of the samples have high  $\text{Al}_2\text{O}_3$  contents as compared with samples of Hawkesbury Sandstone, as shown in Fig. 8.3.

Variations in concentrations of minerals in pisoliths and in their surrounding matrices have also been noted. Invariably there are greater concentrations of hematite and maghemite in the pisoliths than in the matrix materials, where there are greater concentrations of gibbsite, goethite and kaolinite. Quartz concentrations can vary from sample to sample, but if there is maghemite present in the pisolitic crusts, it is present only in the pisoliths and not within the matrix.

Nodules and fragments of strongly magnetic materials occur throughout many of the profiles studied and are clasts that have been transported before being deposited within finer grained sediments above the original sandstone bedrock. Faniran (1970) studied maghemite in the Sydney 'duricrusts' and concluded that maghemite was confined to the black cores of some pisoliths and to similar materials in ferricretes. He also noted that the amount of maghemite in profiles tended to decrease from their tops to their bases, being dominantly confined to the upper indurated zones. The suggestion was made that the maghemite may have derived from magnetite in the Hawkesbury Sandstone, from siderite in the Wianamatta Shale or from basic igneous rocks.

In the course of this study, maghemite has been noted to occur within mottles and vermiform, nodular and pisolitic ferricretes. This suggests that the sediments including the maghemitic nodules have been reweathered since their transportation and deposition. The modern soil also contains pisoliths and oolites of maghemitic material and maghemitic pisoliths occur at the land surface. Some of these surface pisoliths (BOU 412) contain corundum, which could have formed as a result of heating from bushfires that transformed gibbsite into corundum. In a heating experiment gibbsite transformed to corundum at about 900° C. From experiences with natural fires, given the right conditions, temperatures of this order are not impossible (Raison, 1979).

'Bog-iron ore' sediments that display a typical vesicular structure are composed dominantly of goethite, although small amounts of kaolinite, hematite, quartz and gibbsite have also been noted. It is generally agreed that 'bog-iron ore' is a chemical deposit that suggests the area has acted as a sink for iron oxides influxed in solution at some time in the past, probably impregnating pre-existing fine soils or organic matter that had been bioturbated.

### 8.3.3 Micromorphology

In hand specimen the character of the ferruginous materials becomes clear when flat faces are produced by cutting with a diamond saw. For example, the clastic and detrital origin of some material becomes apparent, as angular to sub-rounded clasts of iron oxides that vary through various mixtures of hematite, goethite and maghemite, and fragments of hematitic sandstone,



some with yellow rinds, are set in a matrix of kaolinite and gibbsite. Similar complexities are apparent in viewing some of the pisolitic crusts. Pisoliths composed of varying cores and complex multilayered rinds are set in a matrix of gibbsite and iron oxides.

Microscopic studies reveal that the pisoliths often have hematitic cores with gibbsite in the matrix. Within the gibbsite matrix, voids and fractures have been coated with subsequent generations of hematite (Plate 8.14). Pelletal structures and oolites of gibbsite also occur within the matrix. The pisoliths do not appear to have formed *in situ*. In places virtually pure gibbsite occurs on the margins of pisoliths, suggesting either that iron has been leached from the rind or that aluminium-rich gels have crystallised as gibbsite. However, individual quartz grains in the sections do not appear to be well-rounded, so that long distant transport of them may not have occurred. This observation favours the view of the accumulation of pisoliths consequent upon landscape downwasting.

Polarised incident light reveals hematite as dark red, maghemite as black, gibbsite as yellow and mixtures of iron oxides and gibbsite as varying shades of brown. These variations in colour with changes in mineralogy have been confirmed by micro-probe analysis. Thus the distribution of minerals in the pisoliths and matrix can be mapped in this fashion, to reveal that in some pisoliths maghemite only occurs in fractures within the cores of pisoliths (Plate 8.15) and that several generations of hematite and leaching of iron oxides have occurred.

Some pisoliths reveal complex core-in-core structures, with closely packed quartz occurring in the centres of the pisoliths, whereas the rinds contain very little quartz and comprise virtually pure hematite. The lack of quartz in the rinds (Plate 5.3) is of significance to the origin of the pisoliths as the preservation of the quartz would be expected. The composition of pisolith cores is variable; some are composed largely of gibbsite and others hematite. The thickness and complexity of the rinds suggest long and complicated histories of development with layering occurring by accretion in different environments. Some smaller pisoliths display less complex structures and were probably incorporated into the ferricrete at a later stage. They are not regarded as

having formed *in situ* with the degree of complexity reflecting ageing because the pisoliths consist of materials different to that of the enveloping matrixes. Thus there appear to be pisoliths of different ages within the pisolitic crusts.

#### 8.4 Discussion

Evidence derived from field relationships, chemistry, mineralogy, macro-structures and micromorphology suggests a long and complex history of erosion, deposition and weathering, including the formation and hardening of soils, on a landscape subaerially exposed and undergoing downwasting for a long period of time that led to the accumulation of iron and aluminium oxides in favourable environments.

This conclusion is based on the following:-

- i. The abundance of gibbsite in the mottled and indurated zones. The evidence suggests that the gibbsite developed by incongruent dissolution of kaolinite, that would require protracted weathering. There appears to be an inverse relationship between the relative abundances of kaolinite and gibbsite. XRD analysis of slightly weathered Hawkesbury Sandstone from the Mona Vale Road (BOU 452) near Belrose (BOU 453: BOU 455) and Helensburg (BOU 454) (Table 8.4) has revealed the presence of quartz, kaolinite, smectite, micas, interstratified clays and feldspar. No gibbsite was detected in these samples. It is possible that the gibbsite reported from the Hawkesbury Sandstone by (Hunt *et al.*, 1977) has been derived by weathering rather than being present in the original bedrock. On the other hand, Standard (1967) did not indicate that there is any significant gibbsite content in the Hawkesbury Sandstone. Although some of the kaolinite may be detrital (Standard, 1967), its abundance suggests long periods of weathering. The greatest amounts of gibbsite and kaolinite occur within the detrital material above the weathered and kaolinised Hawkesbury Sandstone. These minerals may have derived both from the weathering of the immediately underlying sandstone and from the Wianamatta Shale.
- ii. The clastic nature of the upper sections of many profiles suggests that previously weathered materials had been eroded, transported and deposited, largely as colluvial material, probably associated with

landscape downwasting. The clastic nature of the deposit is apparent at many scales from large disoriented boulders of iron-impregnated sediments to macroscopic and microscopic clasts that rest unconformably upon weathered sandstone in which the bedding planes are still preserved.

iii. The occurrence of maghemite at depth throughout the weathered zones above the *in situ* Hawkesbury Sandstone. Faniran (1970) reported that maghemite in the Sydney 'laterites' occurs mainly in the cores of pisoliths and decreases rapidly with depth in the profiles. However, clasts composed of maghemite, hematite and small amounts of quartz and mica have been identified throughout the weathered zones above the Hawkesbury Sandstone in a variety of materials such as pisolitic ferricrete (BOU 400, BOU 401, BOU 404, BOU 409, BOU 416 and BOU 417), mottles (BOU 403, BOU 407), nodular ferricrete (BOU 408, BOU 415), vermiform ferricrete (BOU 406) and ferruginised sediment ferricrete (BOU 421). The distribution of maghemite throughout the weathered profiles may suggest that it has derived as a result of biomineralisation (Kirschvink, 1985) or from iron-rich solutions permeating through the weathered materials. While the latter mechanism may have operated in the fashion described by Schwertmann & Taylor (1987) there is ample evidence that many of the maghemitic clasts have formed elsewhere and have been transported to their present locations. Such evidence includes:-

- a. Clasts similar to those located at depth in weathered profiles occur in surface situations in the Ku-ring-gai Chase National Park.
- b. Thin section observations reveal the presence of maghemite *within* the cores of pisoliths recovered from deep locations within profiles. Other pisoliths have maghemitic rinds that almost certainly developed by the transformation of goethite by surface burning.
- c. Sources of maghemitic clasts in the Sydney duricrusts, suggested by Faniran (1970) included magnetite from within the Hawkesbury Sandstone, siderite from the Wianamatta Shales or from basic igneous rocks. Such sources would

involve physical lateral transport of maghemite. Thus it appears that these clasts have not formed *in situ* but represent transported bodies.

- d. Some of the maghemite in pisoliths probably formed at the surface as a result of heating in the presence of organic material, to later undergo transportation and burial.
  - e. Further influences of surface or near-surface modifications may be indicated by the presence of corundum in some of the maghemitic surface pisoliths. The corundum in these pisoliths (BOU 412) may have formed by the transformation of gibbsite by burning.
- iv. The presence of a complex series of mixed facies of ferricrete, including pisolitic, nodular, clastic, vermiform and vesicular types, together with soft and hard mottles, may be related to different environments. For example, vesicular structures probably result from the chemical precipitation of goethite from iron-rich waters into pre-existing fine grained or organic sediments. Pisolitic crusts may relate to former soils and in places at Terrey Hills there appears to be a succession of superimposed and hardened fossil soils, displaying biogenic structures and burrows similar to the modern soil. Clastic ferricrete material appears to relate to iron-impregnation of a colluvial mantle, and vermiform structures may reflect biogenic influences or the passage of soil or groundwater through the deposit leading to its dissolution. Hardened and soft mottles may relate to variations in seasonal water tables. All of the various ferricrete facies occur within a colluvial mantle, and within the indurated zone at the Terrey Hills site where Hunt *et al.*(1977) argued that there is clear evidence of *in situ* bedrock structures.
- v. Variations in the mineralogy and chemistry of pisoliths and their surrounding matrix materials suggest different environments of formation. Maghemite enclosed within the pisoliths suggests a near-surface formation and subsequent burial or incorporation into soils. The absence of maghemite in the matrix and the encapsulation of maghemite within pisoliths negates the significance of contemporary flushing of maghemite through the profile to concentrate it as discrete nodules.

- vi. Micromorphological studies suggest complex phases of weathering and iron mobility that are not compatible with simple *in situ* transformation. The various phases of iron mobility observed also cast doubt on the validity of palaeomagnetic dating, as does the clastic origin of the original sediments that preserve evidence of various phases of iron mobilisation and precipitation.
- vii. The occurrence of biogenic structures including burrows, trails and plant roots within the ferricretes suggests that some of the clastic materials were unconsolidated soils and weathered zones that were subsequently iron-impregnated and hardened. Coating of the indurated biogenic structures with subsequent deposits of iron oxides suggests further complexities in the development of the indurated zones.
- viii. The requirement of external sources of iron for the ferricretes. Some workers (e.g. Faniran, 1970) considered that the Hawkesbury Sandstone possesses insufficient iron for the formation of iron-cemented duricrusts and preferred iron sources from the Wianamatta Shale and the basic rocks of the area. Burgess & Beadle (1952) and Beadle & Burgess (1953) considered that the 'laterites' of the Sydney district formed from shales which may or may not remain in an unweathered condition below the 'laterite'. By examining detrital quartz from weathered Hawkesbury Sandstone and Wianamatta Shale they concluded that in most cases 'laterite' had formed from shales overlying or interbedded within the Hawkesbury Sandstone, or redistributed materials of mixed origins. They argued that the origin of 'laterite' from shales, could account for both the source of iron, as the Wianamatta Shale has a  $\text{Fe}_2\text{O}_3$  content of 5-10%, and the abundance of kaolinite in profiles. Their analytical work suggested that there were external additions of iron into the profiles from the weathering of shales and basalt flows.

On the other hand, Hunt *et al.* (1977) thought that the weathered profiles showed no evidence of iron-enrichment in the indurated zones nor depletion in the mottled zones, and claimed that as there were overlaps in the iron content of zones of the Hawkesbury Sandstone and iron-rich crusts, there was no need to invoke external

sources of iron. Chemical analyses of samples of Hawkesbury Sandstone demonstrate low total iron contents, varying from 0.32% (BOU 452) to 1.41% (BOU 453). However, all of the analyses were carried out on partly weathered sandstone, as the samples all contained kaolinite, so that iron may have already been removed from the rock. It has been suggested that bleaching rocks of iron is often a precursor of more intensive weathering (Milnes *et al.*, 1987). For example, chemical and mineralogical analyses carried out on unweathered and partly weathered bedrock has revealed that the only difference between the two was the migration of iron from the partly weathered material. A thin iron-rich crust within the Hawkesbury Sandstone (BOU 420) had an  $\text{Fe}_2\text{O}_3$  content of 19.97%, dominantly in the form of goethite with only a small amount of hematite. The iron oxides could be 'primary' minerals deposited along with the bulk of the rock, or secondary minerals introduced at a later stage during weathering processes, with the latter possibility being favoured. Standard (1967) reported sub-surface siderite contents in the Hawkesbury Sandstone of up to 4% as the main iron mineral present. As this mineral was not identified in the outcrops sampled it suggests transformation to other iron oxides, which it will do rapidly in oxidising environments. It does appear, however, that the local zones of iron enrichment, such as that at Terrey Hills, require influxes of iron oxides from outside of the immediate area, and which may have derived from a variety of sources including the Hawkesbury Sandstone, Wianamatta Shale and basic rocks. Influxes of iron oxides in solution is further suggested by the nature of some of the iron-rich clasts within the indurated zones of the profiles. If the view is followed that there was not a uniform blanket of ferricrete across a former 'peneplain' surface, but a landsurface of some relief, with only localised colluvial and chemical concentrations of iron developing in favourable environments, as the landscape suffered weathering and downwasting, then there is no requirement for vast amounts of iron. Hunt *et al.* (1977) regarded the surface on which the 'laterite' occurs as a dip slope coincident with the upper surface of the Hawkesbury Sandstone. The topography and geology of the area are compatible with this interpretation, which would also

favour the view that there has been iron and kaolinite enrichment on the Hawkesbury Sandstone from the Wianamatta Shale by weathering and erosion during landscape downwasting.

- ix. There is evidence of profile differentiation in the section at Terrey Hills. The analyses presented here appear to support the view of Hunt *et al.* (1977) that there is a fairly uniform iron content down the indurated zone of the Terrey Hills profile. The iron content varies within the range of 20% to 40% with a slight increase towards the surface. However, at the base of the most northerly outcrop at Terrey Hills, within a zone of soft mottles, there is a rapid drop in total iron content to only a few percent. Moreover, the depletion of bases and silica within the profile indicates considerable leaching of the profile. Walker (1960) noted that the present climate of the area, with a heavy rainfall, leads to long periods of intense leaching and conditions that tend to favour the removal of soil rather than its accumulation. It was also noted that modern soils show marked features of acid leaching and that most soils are acid regardless of their parent materials.
- x. There is evidence of ferrihydrite formation in the modern environment, where it forms a sludge or gel following precipitation from iron-rich waters along roadside drainage channels (Plate 8.16).

## 8.5 Conclusions

The total iron content in several weathered Hawkesbury Sandstone samples assayed at only a few percent. However, the amount of iron required for mottling is not very great; for example a sample of a strong purple hematitic mottle (BOU 419) from Beacon Hill contained only 4%  $\text{Fe}_2\text{O}_3$ . To achieve pronounced mottling all that is required is the release of iron from the original bedrock and its redistribution within the weathered bedrock. Furthermore, the evidence of vesicular bog iron ore in the Terrey Hills profile suggests that it acted as a sink for iron oxides transported in solution and that there have been local accumulations of iron derived laterally from other sources. Many of the iron-rich zones within the Hawkesbury Sandstone are quite thin and may be inadequate to produce the total amount of iron within the 'laterite' profiles, without invoking considerable lateral iron transport, or sources from formerly overlying iron-rich materials. It appears that the bands of iron within the

Hawkesbury Sandstone have been incorporated into the profiles, but dominantly as clasts rather than as the tiny flakes suggested by Hunt *et al.* (1977).

The present sporadic distribution of 'laterite' in the Sydney area does not simply reflect degrees of dissection of a former continuous and complete 'laterite weathering profile'; the weathered and iron-rich zones were not originally uniformly and completely developed, but, depending on local conditions of topography, drainage and water tables, some areas were bleached, others mottled and some acted as sinks for iron oxide accumulation to form crusts. Only in special cases might the three zones of a 'laterite profile' develop at one site, and then they need not be intimately related in a simple mono-genetic profile. Given these constraints, which appear to apply to study areas in South Australia, there is no need for vast amounts of iron to be mobilised, nor is there, by implication, need for great lowering of the landscape to account for the high concentrations of iron observed in some indurated zones.

The work of Hunt *et al.* (1977) may represent a watershed in the study of 'laterites' in Australia in that it challenged the long held model of 'laterite' formation that has restricted the advancement of understanding of these enigmatic features. Furthermore, it highlighted the importance of currently operating processes in developing and modifying iron-rich and aluminium-rich profiles. The transformation of modern ferrihydrite to hematite and/or goethite may better account for some of their observations rather than invoking the eluviation of tiny crystalline flakes of hematite and maghemite through the profiles. The fact that much maghemite is locked up in the cores of pisoliths suggests that those maghemite rich pisoliths at depth are not currently forming.

Moreover, because of the demonstrated profile complexities at various scales it is impossible to view these profiles simply as the result of superficial modification of iron-rich units within the Hawkesbury Sandstone through the operation of contemporary processes. The author is in agreement with Woolnough (1927; p. 48), who said: "Possibly there is something in the immediately underlying rocks to account for the abnormally plentiful supply of



oxides; *but I think not.*" (Author's italics). There is little doubt that contemporary processes are modifying the profiles, but the profiles also record evidence of long histories of modification and development by continually operating processes of erosion, deposition and weathering, on a landsurface that may have been of variable relief.

## CHAPTER 9. FERRICRETES WITH ASSOCIATED VOIDAL CONCRETIONS IN THE TELFORD BASIN.

### 9.1 Introduction

Conspicuous ferricrete beds formed within overburden and interburden sediments of Mesozoic coal beds in the Telford Basin (Fig. 9.1) of the Northern Flinders Ranges, were drawn to the author's attention, as they had been interpreted as palaeosols (Coffey *et al.*, 1978 - cited in Murray-Wallace, 1983). Forming significant parts of the ferricretes are strongly banded voidal concretions (Pettijohn, 1959) or 'rattling iron concretions' (Childs *et al.*, 1972). The ferricretes are resistant and comprise continuous crusts up to a kilometre long forming prominent cuestas (Plate 9.1). The ferricretes have developed by the *in situ* ferruginisation of sediments as a result of the weathering of siderite and pyrite-rich beds within the Triassic sediments. The voidal concretions comprise integral parts of the ferricretes and formed *within* them. Consequently, investigations of the detailed character of the concretions provided a satisfactory explanation for the origin of these ferricretes. Only at later stages, in some cases, have they been isolated from the ferricretes by erosion.

### 9.2 Geological Background of the Telford Basin

The intramontane Telford Basin (Fig. 9.1), which covers an area of 25 km<sup>2</sup>, is an asymmetrical syncline containing Late Triassic to Middle Jurassic freshwater fluviolacustrine sediments (Parkin, 1953; Playford & Dettmann, 1965; Hos, 1977; 1978; Townsend, 1979). These deposits comprise thin basal grits and sands overlain by a succession of carbonaceous shales and siltstones containing numerous coal seams and occasional sand beds. Palynological evidence indicates that some of the coal seams formed in swamps covered by vegetation of low diversity and that climate may have been warm temperate with a variable rainfall regime (Hos, 1977; 1978).

Pyrite is commonly dispersed throughout the coal-bearing beds and numerous pyrite-rich and siderite-rich layers also occur. Where these layers have been encountered during mining and drilling operations they have been referred to as 'hardbars'. They assume a variety of habits and their origin is problematic (Murray-Wallace, 1983). At depth the competent 'hardbars' of sideritic

siltstones are interbedded with incompetent mudstones and may have been squeezed or stretched to form boudinage structures that resemble discrete segments of detached sausage-shaped features through their inability to deform plastically and uniformly with the enveloping beds. In close proximity to the surface the 'hardbars' have been progressively weathered to form ferricretes with iron-rich voidal concretions that are intercalated with shales and sands.

It has been suggested that the ferricretes containing the concretions are palaeosols (Coffey *et al.*, 1978 - cited in Murray-Wallace, 1983), but Murray-Wallace (1983) preferred to regard them as primary sedimentary features that were transformed into ferruginous beds. Thus the development of the sub-rounded forms from rectangular blocks was believed to have occurred sub-surface, with erosion subsequently exposing them at the surface.

### **9.3 Macromorphology of the Ferricrete Concretions and their Field Relationships**

The banded ferruginous voidal concretions in the ferricretes from the Telford Basin vary considerably in character. Some have large hollow cores and consist of regularly banded ferruginous layers (Plate 9.2), and the interior hollows may be lined with inward-pointing gypsum crystals. Other hollows are filled with clays (Plate 9.3), and where gypsum also occurs in the core material, the central filling may be tightly packed (Plate 9.4). Yet others are completely filled with iron oxides. Furthermore, individual bands of iron oxides, a few centimetres thick, form oval-shaped structures, up to 15 cm across, within the weathered basement rocks of the Balcanoona Formation. These rings cut across bedding and have developed independently of it through the influx of iron oxides in solution into the bedrock. Other evidence of the former occurrence of pervasive iron-rich waters is provided by iron-impregnated biogenic materials including wood.

The concretions occur in a section of the basin where siderite and pyrite-rich 'hardbars' have been exposed at the surface. This occurs dominantly in the southern part of the basin, where there is evidence of faulting that may have been responsible for the tilting and exposure of the 'hardbars'. Recent exposures in the quarry walls and access ramps reveal that the sideritic

'hardbars' become increasingly weathered towards the surface. Layers of secondary iron oxides occur around cores of unweathered sideritic siltstone (Plate 9.5). Consequently it appears that both the weathering of the siderite, the formation of the ferricretes and their associated concretions are dependent upon exposure to the atmosphere, or to the contact with near-surface oxygenated groundwaters. Various stages in the development of the voidal concretions have thus been observed. They vary from thin surface rinds around unweathered sideritic siltstone (Plate 9.5), to thick concentric layers around partly weathered sideritic material (Plate 9.6), to cores consisting of iron-depleted clays (Plate 9.3), and to central voids without any remaining siderite (Plate 9.2).

#### 9.4 Chemistry and Mineralogy of the Concretions

Mineralogically, the concretions in the ferricretes (BOU 88) (Table 9.1) consist of roughly equal amounts of goethite ( $\alpha$ -FeOOH) and lepidocrocite ( $\gamma$ -FeOOH), with other minerals detected, in decreasing order of abundance being quartz, hematite, kaolinite, smectite and micas. Fe<sub>2</sub>O<sub>3</sub> (62%), SiO<sub>2</sub> (15%) and Al<sub>2</sub>O<sub>3</sub> (7%) dominate its chemistry. The P<sub>2</sub>O<sub>5</sub> content (1.85%) of the concretions, when compared with other ferricretes is relatively high. The concentric layers of the concretions are enhanced by distinctive colour variations, and on this basis, sub-samples were separated from the individual layers. XRD analyses of the separate layers reveal that they are dominated by hematite (dark maroon-coloured), goethite (yellow-coloured) and lepidocrocite (orange-coloured). Crystals of gypsum occupy parts of the central voids. In some concretions the cores are closely packed with gypsum and clay.

#### 9.5 Ferricrete and Voidal Concretion Formation

The field observations suggest that the ferricretes and associated voidal concretions of the Telford Basin have formed by the *in situ* weathering transformation of siderite, a process also suggested by Pettijohn (1959), Childs *et al.* (1972) and Senkayi *et al.* (1986) for similar concretions elsewhere. Siderite is stable in a reducing environment but oxidises rapidly in contact with the atmosphere or oxygen-bearing waters (Seguin, 1966). Hurlbut (1959) noted that pseudomorphs of goethite after siderite are common.

Siderite ( $\text{FeCO}_3$ ) comprises 62.1% FeO, 37.9%  $\text{CO}_2$ , 48.2% Fe and both divalent Mn and Mg may substitute for ferrous iron, while Ca may be present in small amounts (Hurlbut, 1959). Siderite is commonly associated with coal measures (see, for example, Childs *et al.*, 1972; Senkayi *et al.*, 1986), and the formation both of the coal and the siderite are associated with freshwater swamp environments (Postma, 1982). The environment of formation postulated for the formation of the coal beds of the Telford Basin (Parkin, 1953) is in sympathy with this. Senkayi *et al.* (1986) stated that when oxidised, siderite is transformed to goethite or hematite, with the alteration to hematite, probably occurring prior to the exposure of the siderite to surface weathering conditions. Senguin (1966) who studied the instability of  $\text{FeCO}_3$  in air argued that the end product of oxidation of siderite is always  $\alpha\text{-Fe}_2\text{O}_3$  (hematite) and that the rate of dissociation of  $\text{FeCO}_3$  is dominantly a function of grain size and temperature. Consequently the first stage in the formation of the concretions in the ferricrete is probably the dissociation of siderite at the boundaries of joint-bordered quadrangular blocks of siderite or siderite nodules. Thus the incipient concretion would have essentially the same dimensions as those of the original sideritic mass. Senkayi *et al.* (1986) argued for a solid solution transformation of siderite to hematite through the dissociation to FeO and subsequent oxidation to hematite as opposed to the dissolution and reprecipitation mechanism discussed by Schwertmann and Taylor (1977). In some incipient Telford Basin concretions hematite forms the outer-most layer (Plate 9.4) and does so in some fully developed concretions. However, some mature concretions have outer coatings of goethite, which may have formed by the dissolution of hematite and reprecipitation as goethite in a changed weathering environment. Senkayi *et al.* (1986) only reported hematite from the outer shell of weathering sideritic nodules, but layers of hematite have been identified at various positions within the Telford Basin concretions, including their cores. Consequently, the assertion that hematite only forms at depth and goethite only in near-surface moister environments is not supported by these observations. From some boreholes, both hematite and goethite have been identified in samples derived from considerable depths below the surface.

The formation of a very stable ferric iron layer of hematite around a sideritic mass would probably slow down the weathering of the siderite as it would inhibit the diffusion of  $\text{CO}_2$  and CO out of the siderite crystal lattice (Senguin,

1966). However, the penetration of oxygenated waters through the hematite zone could lead to the dissolution of a thin layer of siderite between the relatively insoluble ferric iron outer layer of hematite and the unweathered core of siderite, and its reprecipitation as goethite. Senkayi *et al.* (1986) argued that a surficial environment would favour the alteration of siderite to goethite but not to hematite. However, in the Telford Basin concretions there appears to be no consistent or preferential distribution of these two minerals.

Lepidocrocite also occurs as concentric layers in the voidal concretions from the Telford Basin ferricretes. This mineral was not identified in the weathered sideritic nodules described by Senkayi *et al.* (1986). Childs *et al.* (1972) identified lepidocrocite in rattling iron concretions, but neither its distribution nor its significance was discussed. Lepidocrocite occurs as dark orange layers regularly interspersed between both hematite-rich and goethite-rich layers. Goethite ( $\alpha$ -FeOOH) has hexagonal close packing as opposed to the cubic close packing of lepidocrocite ( $\gamma$ -FeOOH). There is little difference in the lattice energies of the two types of packing, and they are equally economical in filling space (Evans, 1964). It is apparent, because of the intimate association of goethite and lepidocrocite in the concretions described, that the iron minerals have formed from the same source of mobilised Fe<sup>2+</sup> in the same general environment. However, fluctuations in the detailed character of the environment must have occurred to favour the dominant formation of one oxide over the other.

Factors such as temperature, rate of oxidation, the concentration of Fe<sup>2+</sup> in solution, partial pressure of CO<sub>2</sub> and pH are important determinants of the formation of different mineral phases (Schwertmann & Taylor, 1977). Some foreign ions may inhibit the formation of certain mineral forms. For example, Al can inhibit the formation of lepidocrocite, favouring the goethite phase when an Fe(II) system is being oxidised. However, the amount of aluminium analysed in the goethite and lepidocrocite-rich layers for this thesis do not vary significantly, so that this factor may not be important in this instance. In water, lepidocrocite or goethite can form from the oxidation of green rust depending on local environmental conditions (Schwertmann & Taylor, 1977).

The formation of lepidocrocite is often associated with hydromorphy, but in the case of the voidal concretions in the ferricretes of the Telford Basin there is no need for current hydromorphic conditions as large amounts of ferrous iron in siderite are already present having been inherited from earlier reductomorphic conditions. Furthermore, the environment in which the ferricretes from the Telford Basin formed cannot be equated with a modern soil in an arid environment, but nevertheless they have formed as a consequence of weathering of inherited sideritic and sulphide-rich sediments by percolating groundwaters.

Lepidocrocite in geological environments, as opposed to soil environments, is typically very crystalline (Ramberg, 1969; Francis & Segnit, 1981). By comparison with standards, the lepidocrocite from the Telford Basin is also very crystalline with a width at half-height (WHH) of  $0.4^{\circ}2\theta$ , and a d-spacing of 6.27583 Å. The formation of well crystalline lepidocrocite may be favoured by the slow supply of  $\text{Fe}^{2+}$  and air (Fitzpatrick *et al.*, 1985).

It has been noted in certain Natal slope-gley soils by Schwertmann & Fitzpatrick (1977), that lepidocrocite and goethite may crystallise simultaneously. It is also possible that the dominant occurrence of goethite is due to the subsequent formation of goethite from lepidocrocite (Fitzpatrick *et al.*, 1985). However, in the case of the ferricrete described here, there are roughly equal amounts of goethite and lepidocrocite present, and although there is some intermixing of the minerals, they dominate in discrete zones or layers.

Siderite has a high specific gravity (3.83 - 3.88) but it is not as dense as goethite (4.37) or hematite (4.8 - 5.3). Thus during the weathering transformations of siderite to hematite and goethite, less space would be occupied. It is also significant that the total iron contents in the layers of the voidal concretions are higher than in the unweathered siderite, so that there has been a migration and concentration of iron oxides during the formation of the concretions. Moreover, during the processes of siderite weathering there would be substantial volume reductions due to the losses of  $\text{CO}_2$  and CO from the siderite. The chemical analyses show high ignition losses of sideritic-rich material (up to 30%) compared with those comprising chiefly hematite, goethite

and lepidocrocite. Consequently as the original size of the sideritic mass was fixed by the surficial transformation of siderite to hematite, the further weathering of siderite could have resulted in the ultimate development of voids, variably containing iron-depleted clays, in the central sections of the concretions. The development of small gaps between the outer shell of ferric iron and the inner ferrous iron material may have facilitated the access of circulating waters and the weathering transformations of siderite. The alternating formation of lepidocrocite, goethite and hematite is considered to reflect varying rates of oxidation of ferrous iron depending upon differing rates of oxygen supplies.

In some concretions gypsum crystals occur in the central voids, in some cases, in combination with iron depleted clays. Pyrite is present in the 'hardbars', and weathering of it would have provided sulphate to combine with the calcium held in the siderite to form  $\text{CaSO}_4$ . It is suggested that the gypsum in the cores of the concretions passed through the outer layers of the concretions in solution to crystallise slowly and form some quite large crystals in central voids.

The weathering of pyrite would have also released large amounts of ferrous iron that could account for the iron accumulations within fossil wood and the kaolinised basement rocks. This mobilisation of iron oxides may also account for variations between the layered types of voidal concretions described above.

Halite has been identified in the surface sample of a concretion and also from a deep unweathered sample, but it is suggested that halite is a relatively recent addition to the environment. Halite is common in the mine area of the Telford Basin and has been carried to considerable depths in solution along joints and other structures.

## 9.6 Conclusions

The concretions and the ferricretes described from the Telford Basin probably did not develop in a former pedogenic environment but resulted from the *in situ* weathering transformations of pre-existing siderite deposits by oxygenated groundwaters under near surface situations.



The present arid climate probably does not favour the formation of these ferricretes with the associated concretions for Senkayi *et al.* (1986) noted that a moist surficial environment led to the rapid transformation of siderite to goethite. However, Senguin (1966) concluded that temperature and grain size are the most important factors involved in the dissociation of siderite and its oxidation to form hematite. Water is important in the further weathering of the hematite-coated siderite blocks, and although rainfall is low in the Telford Basin, locally groundwaters can be quite close to the surface. For example, groundwater presents a problem for coalmining in the upper series beds, and dewatering of them is necessary before mining can proceed. Thus it is possible that weathering related to percolation by groundwaters could currently affect the development of the ferricretes. Some of the ferricretes may be relics, indicating wetter climates in the past, but their development probably does not depend on such climates. Certainly, they appear to have been modified by the current weathering regime, as many of the postulated outer layers of hematite have been transformed to goethite.

The concretions in the ferricretes have formed by the *in situ* weathering of siderite involving the progressive inward transformation of siderite to hematite, goethite and lepidocrocite and the development of central voids variably filled with detrital iron-depleted clays and gypsum that has invaded the concretion in solution. The presence of iron-sulphide ores and siderite within the overburden beds has provided an ample source of ferrous iron for subsequent precipitation in favourable locations, producing complications on the simple voidal concretions.

The ferricretes with associated voidal concretions in the Telford Basin constitute a special type of ferricrete formed through the *in situ* transformation of pre-existing ferrous iron oxides originally deposited in swampy environments. The demonstrated intimate environmental association of sideritic 'hardbars' with coal beds, both forming in freshwater swamps (Postma, 1982, 1983; Senkayi *et al.*, 1986; Childs *et al.*, 1972) and the development of distinctive ferruginous voidal concretions, within the ferricrete, from the weathering of the sideritic zones, suggests that the presence of voidal concretions may assist in preliminary prospecting for coal.

## CHAPTER 10: AN ASSESSMENT OF THE 'LATERITE' CONCEPT IN SOUTHERN SOUTH AUSTRALIA

### 10.1 Findings Related to Ferricrete Formation from Investigations of this Thesis

The investigations carried out for this thesis have demonstrated that there is great variety in the positions and relative relationships of ferricretes and mottled and pallid zones both in South Australia and some other areas of Australia. Furthermore, the investigations of this thesis demonstrate that the chemical and mineralogical characteristics of 'lateritic' materials reflect various and different modes of formation and subsequent modifications. Different facies of ferricretes have been recognised throughout the world (e.g. Pullan, 1967) and enquiries of this thesis suggest that the different ferricrete morphologies reflect environmental conditions during their formation and subsequent development. Consequently the view is taken that the detailed characteristics of the different ferricretes represent 'tape recordings' of their epigenetic histories, the unravelling of which may be accomplished by careful study of their detailed attributes.

The evidence presented suggests that there was not the development of a uniform blanket of 'laterite' over large areas, but rather that the different types of ferricretes, mottled and bleached zones developed in specific sites in response to local environmental conditions. Ferricrete crusts are relatively rare in the study areas, and are often absent above pallid and/or mottles zones, suggesting to many workers, the erosional truncation of former complete 'laterite profiles'. However, the data presented here suggest that in the greater number of cases the crusts had never developed. Wherever ferricrete crusts do occur, the evidence suggests that they did not develop as horizons in a monogenetic 'laterite profile', but are everywhere younger than the immediately underlying weathered zones, having formed in various ways by the preferential physical and/or chemical accumulation of iron and aluminium oxides in locally favourable situations .

The mobilisation and precipitation of iron and aluminium oxides over immense periods of geological time, including the present, have been demonstrated, suggesting that ferricrete formation cannot be restricted to

discrete time spans, nor can it be equated, in a restrictive sense, with humid tropical climatic conditions. There is little doubt that some ferricretes did form coevally, and that humid tropical climates may have enhanced ferricrete formation. However, the fact that different facies of ferricrete may have formed synchronously in different parts of the same landscape, and that identical ferricretes occur on landsurfaces of widely disparate ages, restricts the utilisation of ferricretes as reliable morpho-stratigraphic markers, except in the coarsest of senses. This is particularly so in the light of evidence of continual modifications of ferricretes and landsurfaces, so that they cannot be regarded simply as remnants of ancient landscapes preserved in pristine form.

No reliable indication of age appears to derive from the morphology, chemistry or mineralogy of ferricretes or their component parts, as similar ranges of weathering and ferruginous materials occur on lowland and summit surfaces. For example, pisoliths occur on many diverse landsurfaces of different ages, vesicular to massive ferricrete occurs on the the summit surface as well as on modern valley floors, and vermiform ferricrete occurs on landsurfaces widely separated in elevation and age. However, ferricretes with the greatest mineralogical diversity (e.g. hematite, goethite, maghemite, gibbsite, boehmite and kaolinite) appear to have much more complex and lengthy histories of evolution than do ferricretes and mottles with simple iron oxide mineralogies (e.g. goethite in ferruginised clastic sediments, and hematite in mottles). Gibbsite is a common constituent of complex crusts, but it has also been identified in relatively young ferricretes as well as from modern seepage zones. Its occurrence appears to reflect local environmental conditions rather than age. Although there are several possible pathways for gibbsite formation, in the majority of cases investigated, it appears to have formed from the dissolution of kaolinite, under acid weathering conditions, which mobilised aluminium in the surface horizons, and allowed precipitation in the lower, less acidic zones.

Where ferricretes are viewed holistically, within the framework of the total environment, they may be useful in local palaeogeographical reconstructions. For example, some ferricretes appear to mark the positions of former Tertiary shorelines, having apparently developed by the iron oxide impregnation of sandy shoreline sediments. Furthermore, with such ferruginised clastic

quartzose sediments, in which the iron oxide mineralogy is typically dominated by goethite, older crusts consistently display higher hematite contents than the younger ones.

## **10.2 Modes of Ferricrete Formation in areas studied**

### **10.2.1. Oxidation of pre-existing iron minerals to form Ferruginised Sediments**

In extreme cases, weathering of iron rich minerals such as glauconite, siderite, pyrite and chamosite, incorporated into various sediments such as the Pebble Point Formation of the western Otway Basin (Chapter 7) and the Compton Conglomerate and its equivalents in the Murray Basin (Chapters 4 and 7), has given rise to the ferruginisation of sediments by the isovoluminous replacement of existing minerals in oxidising environments. Such ferruginised sediments, which have commonly been mistaken for surficial pedogenic ferricretes, are characterised by an iron oxide mineralogy dominated by goethite, and this type of ferruginisation could be occurring today. Consequently it need not be related either to the operation of intensive weathering or to humid tropical climates. Other ferricretes with distinctive voidal concretions have formed in the Telford Basin (Chapter 9) by the near surface oxidation of pyritic and sideritic siltstones (Figure 10.2, No. 3). Care needs to be taken to distinguish these ferruginised sediments from surficial ferricrete crusts.

### **10.2.2. Ferricretes as detritus**

The physical erosion, transportation and deposition of pre-existing high level ferricretes, particularly by the operation of slope processes has led to the formation of some ferricretes at lower levels in the landscape (e.g. slopes of Spring Mount, Chapter 4). This mode of ferricrete formation has been recognised by many workers. In many cases detrital fragments, so derived, have been cemented by the precipitation and crystallisation of ferrous iron influxed in solution. There appears to be little controversy about the formation of ferricretes by the physical reworking of pre-existing ferricretes and the accumulation and cementation of ferruginous detritus on low angle slopes and valley bottoms at elevations below higher occurrences of ferricretes. Often the detrital character of the ferricrete is clearly apparent by inspection of hand specimens and by examining the topographic and geomorphic relationships of the different ferricretes.

As stated above, most ferricretes bear the imprints of both absolute and relative accumulations. For example, some mechanical detrital ferricrete in the Sydney area (Chapter 8) has been so modified by later weathering that the original structure of the detrital ferricrete has been largely obscured. However, combinations of detailed field, optical, mineralogical and chemical data can usually distinguish the original detrital nature of the ferricrete, as distinct from the underlying *in situ* bedrock with preserved rock structures.

### **10.2.3 Ferricretes formed by the ferruginisation of pre-existing bedrock and sediments.**

Where ferrous iron has been introduced in solution from lateral sources into pre-existing clastic and organic sediments, ferricretes with different characteristics have formed depending on the environments of deposition and the nature of the sediments involved. Such ferricretes have developed in former lakes, swamps, peat bogs, peritidal environments and valley floors. Often in these ferricretes, goethite is the dominant iron oxide, which typically displays minimal aluminium substitution in its crystal structure. These observations suggest goethite formation in wet and/or humic environments. In these instances there is no genetic relationship between the ferricrete and the underlying materials, which can include sediments and variably weathered bedrock. This process of accumulation of iron oxides from iron-rich solutions is proceeding today, in various landscapes, under current climatic conditions. Under hydrostatic pressure, continental groundwaters containing ferrous iron in solution emerges at springlines leading to the precipitation of iron oxides at the surface (Figure 10.2, No. 4 and Figure 10.3, No. 5).

Ferricreted bedrock has probably been formed in a similar fashion except that a greater proportion of the iron has been derived from the immediate parent rock. However,  $\text{Fe}_2\text{O}_3$  contents in ferruginised bedrock are consistently greater than that in the unweathered bedrock, so that there have been influxes of iron into the ferruginised bedrock, probably from lateral sources (Figure 10.2, No. 1).

#### **10.2.4. Continual weathering and erosion model, preferred for ferricrete formation on the summit surface of Fleurieu Peninsula**

The summit surface of the Fleurieu Peninsula is the area that has been studied most intensively, particularly sub-surface. Consequently it is a most appropriate area in which to assess ferricrete formation formed by the downwasting of a weathered landscape.

The evidence presented in this thesis suggests that there was not a low-lying and near level landsurface uniformly blanketed by a complete 'laterite profile'. Rather there was a landsurface of some relief, possibly even greater than some equivalent parts of the modern landscape, that led to considerable lateral variations in environmental conditions. Consequently, in some higher parts of the landscape the underlying bedrock was bleached of iron (Figure 10.1, Bleached zones), which was removed from the local environment or was accumulated in adjacent relatively low lying parts of the landscape, such as organic-rich swamps, at breaks of slopes on valley sides and in valley bottoms. The slabby ferricrete (Figure 10.3, No. 1)) occurs at plateau margins where laterally moving ground water nears the surface, leading to the precipitation and oxidation of iron carried in solution, in near-horizontal layers (See sections 4.2.1.4 and 5.6.3.3).

Elsewhere, within the zone of water table fluctuation (Figure 10.1, Mottled zone development), it is postulated that primary iron minerals within the basement rocks were degraded by weathering under reducing conditions, forming ferrous iron that was redistributed and segregated, within the weathered and partly kaolinised rock, to form ferric iron-rich mottles under oxidising conditions. These mottles were dominated by hematite formed via the dehydration of ferrihydrite. There is no doubt that the process of mottle formation can occur without physical reworking of the host material, as quartz veins and bedrock and sedimentary structures are preserved within these zones. Hence, isovoluminous weathering had occurred. Thin section observations suggest that the hematite mottles grew by the coalescence of tiny hematite crystallites, which replaced pre-existing material such as kaolinite, perhaps in the fashion suggested by Ambrost *et al.* (1986). Chemical analyses suggest that many of these weathered and mottled zones have developed through the local solution, redistribution and segregation of iron oxides,

although in some cases there may have been additional inputs of iron oxides to mottles from lateral, particularly iron-rich sources, such as pyrite beds. It is apparent that these redistributions and additions can only have taken place by processes related to water movement through the weathering zone, and may relate to regional water table fluctuations, perched water table movements, or to the slow downward seepage of surface water. Under these conditions there need be no development of a surface crust, nor do they require excessive water table fluctuations.

As surface weathering and erosion proceeded, the iron segregations, largely as hematitic mottles, were progressively exposed at the surface, where they hardened, disintegrated, and formed lags at the surface (Figure 10.1, Landscape downwasting). In favourable situations these iron-rich residua were progressively transformed to goethite by dissolution and reprecipitation, forming surface rinds on hematite-cored clasts of various sizes including pisoliths and nodules. In areas where surface slopes were too steep to favour surface accumulation, no thick residual lag formed, but only thin surface coatings of pisoliths developed, on and within soils that directly overlie the mottled material. Pisolith development in these areas occurred during the physical transport from higher areas to lower parts of the landscape. Pisolitic to nodular ferricretes (Figure 10.3, No. 2)) require the lateral physical transport of the nodules and pisoliths. The simpler character of the nodules and their similarities in chemistry and mineralogy to the surrounding matrix materials suggests the operation of less physical transport in their formation (Section 5.6.3.2).

With the progressive exposure of the relatively immobile ferric iron oxide to form lag materials, further mineral transformations are thought to have occurred, such as the transformation of hematite to goethite and the formation of maghemite by surface burning. Although ferric iron minerals (apart from ferrihydrite) are quite stable, under the conditions discussed in Chapter 3, nevertheless some may be dissolved to contribute to the cementation of the lag gravels to form a ferricrete or be removed from the immediate area to contribute to ferricrete formation at lower levels. In this fashion, by dissolution and reprecipitation, the lithification of some of the individual clasts to form pisolitic and/or nodular ferricretes may have occurred (Figure 10.3, No. 3).

Furthermore, the precipitation of the iron locally would have led to the formation of new generations of iron oxides.

As it appears that the ferricretes did not uniformly cover the landscape and as the near-surface ferricretes are not readily soluble, they could have largely survived while leaching of the underlying area could have proceeded via the circulation of sub-surface ground water. This could have led to the dissolution of kaolinite, the mobilisation of aluminium and its reprecipitation at lower levels, either as gibbsite, or within the crystal structure of synchronous generations of goethite. Thus it is envisaged that ferricrete development proceeded with further downwasting of the mottled zone, the continuing accumulation and cementation of iron-rich clasts and the provision of aluminium to be incorporated into new generations of goethite, derived from the solution of hematitic mottles. Other minerals, formed at the surface by fires, such as maghemite (from goethite), boehmite and corundum (from gibbsite), could have been incorporated into the developing ferricrete as were fragments of bedrock and quartz.

This model is a variation on the residual model of McFarlane (1976), which involved a single phase of weathering and downwasting to develop the 'laterite', with the underlying pallid zone developing by leaching through the permeable *in situ* 'laterites' after its uplift and incision. However, in the areas studied no evidence was observed of the progressive development of weathering profiles, with horizons forming from progenitors that resemble those currently beneath them. Moreover, in the South Australian situation, as well as there being evidence for the continuing modification of mottled and pallid zones under present climatic conditions, there is stratigraphic evidence for both pallid and mottled zones being older than the ferricretes. Consequently, the model of McFarlane (1976) cannot be applied unmodified to the South Australian ferricretes, although there are many points of commonality. In particular, points of agreement include the formation of mottles by local iron oxide redistribution within the saprolite, that they can form a residual lag by matrix removal associated with landscape downwasting, that the topographic relief need not be subdued for the operation of this mechanism, that pallid zones may continue to develop after uplift and that vermiform ferricrete develops across very subdued relief by the modification of former ferricretes.



Continual leaching during the downward percolation of meteoric waters has led to the partial dissolution of ferricrete and the development of vermiform structures in some of the cemented ferruginous and aluminous-rich ferricretes, and their infilling with gibbsite and kaolinitic clays (Figure 10.3, No. 3). Gibbsite not only occurs in the dissolution tubules, but also *within* pisoliths and nodules suggesting great complexity in the development of the vermiform ferricrete, by many phases of solution and precipitation of iron and aluminium oxides.

This continual model of ferricrete formation is supported by the complex nature of the ferricretes overlying weathered and mottled bedrock. Thin section observations demonstrate the intricate character of the vermiform ferricretes, which display a diverse range of minerals, and various phases of iron mobilisation and impregnation that favour the view of a long and continued history of formation and transformation. Stratigraphic evidence suggests that the summit surface of parts of Fleurieu Peninsula have been exposed to terrestrial processes during and since the Mesozoic. Thus the evidence supports the view that some ferricretes develop concomitantly with landscape evolution, and their formation is not necessarily dependent upon pre-existing planation surfaces.

The continued leaching of the underlying weathered zone is demonstrated by the concentration of gibbsite in the upper few metres of many of the profile samples from below the Parawa Plateau. The gibbsite content varies inversely with kaolinite abundance, suggesting its original source from the incongruent dissolution of kaolinite and the removal of silica from the profile. Progressive kaolinisation is also suggested by the oxygen-isotope work reported in Chapter 4. Bourman (1973) had suggested that the depth of weathering on the summit surface of Fleurieu Peninsula might suggest continuing leaching following the tectonic uplift of the area. Many of the 'deeply weathered profiles' in the Mount Lofty Ranges have been shown to be not intensively weathered as they contain variable amounts of feldspars, smectite, micas, chlorite and vermiculite.

The occurrence of ferricretes over weathered zones is quite sporadic: only in favoured situations have lags of complexly weathered iron and aluminium-

rich materials been cemented to form ferricretes. Many of the ferricretes occur on low angle slopes, which suggests lateral physical and chemical movement of ferricrete materials, as well as the residual accumulation of relatively immobile materials from overhead sources.

Other lateral variations are displayed, in which some bedrock is bleached while elsewhere it is mottled, reflecting local conditions at the time of formation. This lateral variability in weathering, bleaching, mottling and iron accumulation makes it unnecessary to postulate the former contiguous existence of complete monogenetic weathering 'laterite' profiles over extensive 'peneplain' surfaces, and obviates the need to explain present distributions in terms of variable degrees of dissection of the original profile. Furthermore, it overcomes the objections raised by some workers elsewhere of the potential deficiency of iron from pallid zones or from overhead sources.

### 10.3 Summary and Conclusions

The conclusions of this thesis are by no means definitive. In particular, few opportunities were provided for the examination of ferricretes associated with basic rocks, and it would be useful to compare ferricretes and weathered zones developed on such rocks with those reported in this study. Furthermore, current hydrological conditions appear important in developing and modifying ferricretes, and as in this study hydrological influences were largely restricted to sites examined by other workers, detailed hydrological investigations should prove fruitful. Additional data on the (palaeo-) environments of formation of ferricretes could be achieved by the further studies of Al-substitution and crystallinity of iron oxides, while the application of differential thermal analysis would allow more accurate determinations of relative iron oxide abundances, that reflect conditions during their formation. Finally, further data on the detailed processes of ferricrete formation could be achieved by additional microprobe studies and the use of scanning electron and transmission electron microscopy, in particular to investigate aluminium and silica solubility and quartz dissolution.

Nevertheless, the data collected for this thesis have allowed the identification of various types of ferricretes, bleached and mottled zones and the determination of their chemical and mineralogical compositions as well as their microscopic

characteristics, all of which have facilitated reconstructions of their modes and landscape environments of formation. These are summarised in Figures 10.1, 10.2 and 10.3 and highlight the fact that different forms of ferricrete have developed in these different environments through the operation of a range of processes. In other situations there are sedimentary sequences, which simulate so-called 'laterite' profiles, or which include calcareous sedimentary layers that demonstrate a multigenetic origin of the profile, involving processes other than those typically attributed to 'lateritisation'.

The data presented in this thesis stresses the influence of local environmental conditions in developing ferricretes and mottled and bleached zones, and that these environmental conditions can vary over reasonably short distances. Rarely is there the full vertical variation of pallid, mottled and ferricrete zones, but these zones change laterally, with some areas displaying pallid zones, others mottled zones and yet others, ferricretes.

In order to obtain more reliable interpretations of ferricretes and landscape development, an holistic approach, involving investigation of as many attributes related to ferricrete development as possible, has been adopted in this study. In contrast, studies that depend too much on only one approach, such as palaeomagnetism may ignore contradictory stratigraphic data, or geochemical studies may be carried out without an understanding of the field relationships of the ferricretes being analysed.

Ferricretes in the landscapes studied do not represent stages in the development or dissection of the 'normal laterite profile' of Stephens (1946) or the current *in situ* model of the French (Herbillon and Nahon, 1987). They are various materials, impregnated by iron oxides precipitated from percolating waters in response to local environmental conditions and have formed over a long period of time, possibly from the Mesozoic to the present. The view of 'laterite profiles' as the products of continual weathering and related processes throughout the Mesozoic and Cainozoic (Milnes *et al.*, 1985; Bourman *et al.*, 1987) has subsequently been the preferred model of landscape evolution applied to areas in Western Australia and Queensland by Ollier *et al.* (1988). Some other ferruginised materials (e.g. Compton conglomerate, voidal concretions) have been mistaken for buried pedogenic ferricretes in the past. However, the

chemical, mineralogical and stratigraphic evidence reported here should prevent future misunderstandings.

Deep pervasive weathering and kaolinisation attributed to 'lateritisation' processes do not appear to be directly associated with the formation of ferricretes, although widespread bleaching is important in providing iron oxides for ferricrete development in other parts of the landscape. These studies do not favour the view of kaolinisation occurring prior to 'lateritisation' or mottle development as suggested by Eyles (1952) and Nahon & Tardy (1987), who observed the replacement of kaolinite booklets by hematite in mottles. The view is preferred of complex synchronous weathering, bleaching, kaolinisation and ferruginous mottling of bedrock, as the data presented suggest that Fe is one of the first elements to be mobilised, and that, in many cases, it has only been redistributed in its immediate environment.

Currently, sludge-like ferrihydrite and poorly crystalline lepidocrocite occurs in creeks and seepage zones in many topographic settings in the region, including valley side slopes, peritidal environments and groundwater salinas. It has formed in many cases by precipitation from ferrous iron solutions, where pH and  $E_h$  reach appropriate values, and high salinity is frequently associated with such environments. Under such conditions ferrihydrite has the potential to impregnate pre-existing materials, and transform, in some cases, directly to hematite, or to form goethite by dissolution and reprecipitation, depending on local micro-environmental conditions.

In view of the above considerations, workers in southern South Australia, in particular, need to reassess the paradigm within which they view and interpret materials previously regarded as 'lateritic'. No longer can they simply be regarded as fossil features related solely to humid tropical climates, 'peneplains' and varying degrees of dissection.

# FIGURES

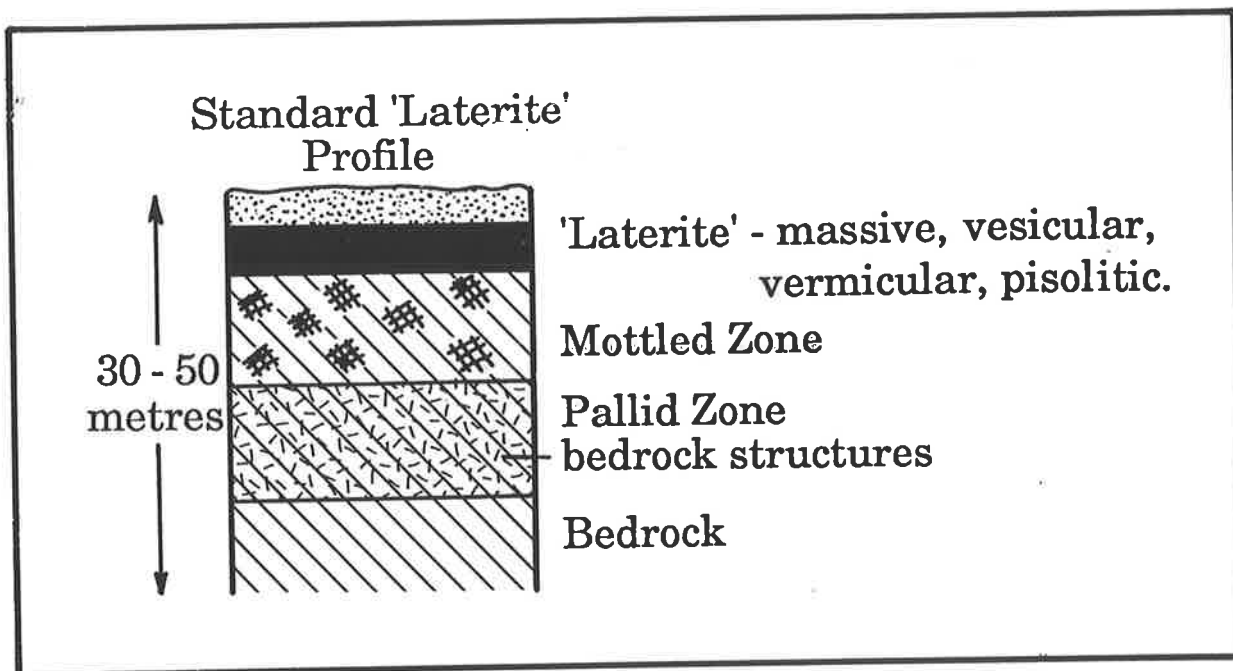


Figure 1.1 Sketch of the pedogenic model of the 'normal or standard laterite profile' incorporating a sandy, bleached A horizon above a 'laterite' horizon, successively underlain by companion materials of mottled and bleached bedrock (Stephens, 1946), considered to have developed on a 'peneplain', under humid tropical conditions.

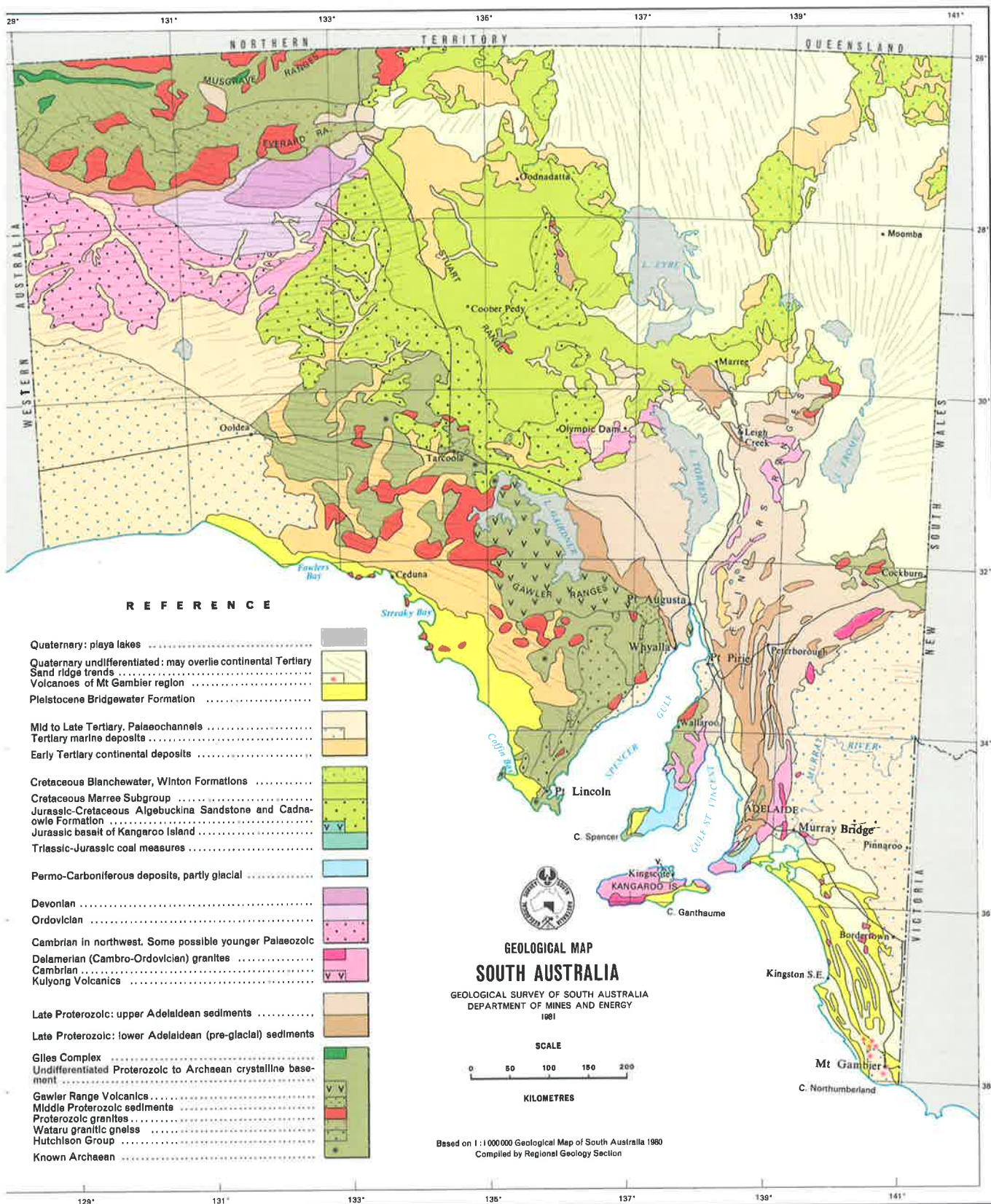


Figure 2.1 Geological map of South Australia.

GEOLOGICAL TIME SCALE				
Era	Period	Epoch	Years before present	
CENOZOIC	QUATERNARY	Holocene	10 ka	
		or Recent		
		Pleistocene		
	TERTIARY	_____		2 Ma
		Pliocene		5-7 Ma
		Miocene		26 Ma
		Oligocene		38 Ma
		Eocene		54 Ma
		Palaeocene		65 Ma
	MESOZOIC	CRETACEOUS	Late	100 Ma
Early			136 Ma	
JURASSIC		_____	195 Ma	
TRIASSIC		_____	225 Ma	
PALAEOZOIC	PERMIAN	_____	280 Ma	
	CARBONIFEROUS	_____	345 Ma	
	DEVONIAN	_____	395 Ma	
	SILURIAN	_____	440 Ma	
	ORDOVICIAN	_____	500 Ma	
	CAMBRIAN	_____	570 Ma	
ARCHAEAN	EARLY - Adelaidean	_____	2500 Ma	
	MIDDLE	_____	_____	
	LATE	_____	_____	
PRE-CAMBRIAN	_____		Formation of Earth 4 600 Ma	

Ma=mega-anna (million years); ka=kilo-anna (thousand years)

Figure 2.2 Generalised Geological Time Scale (After Barker, 1986).



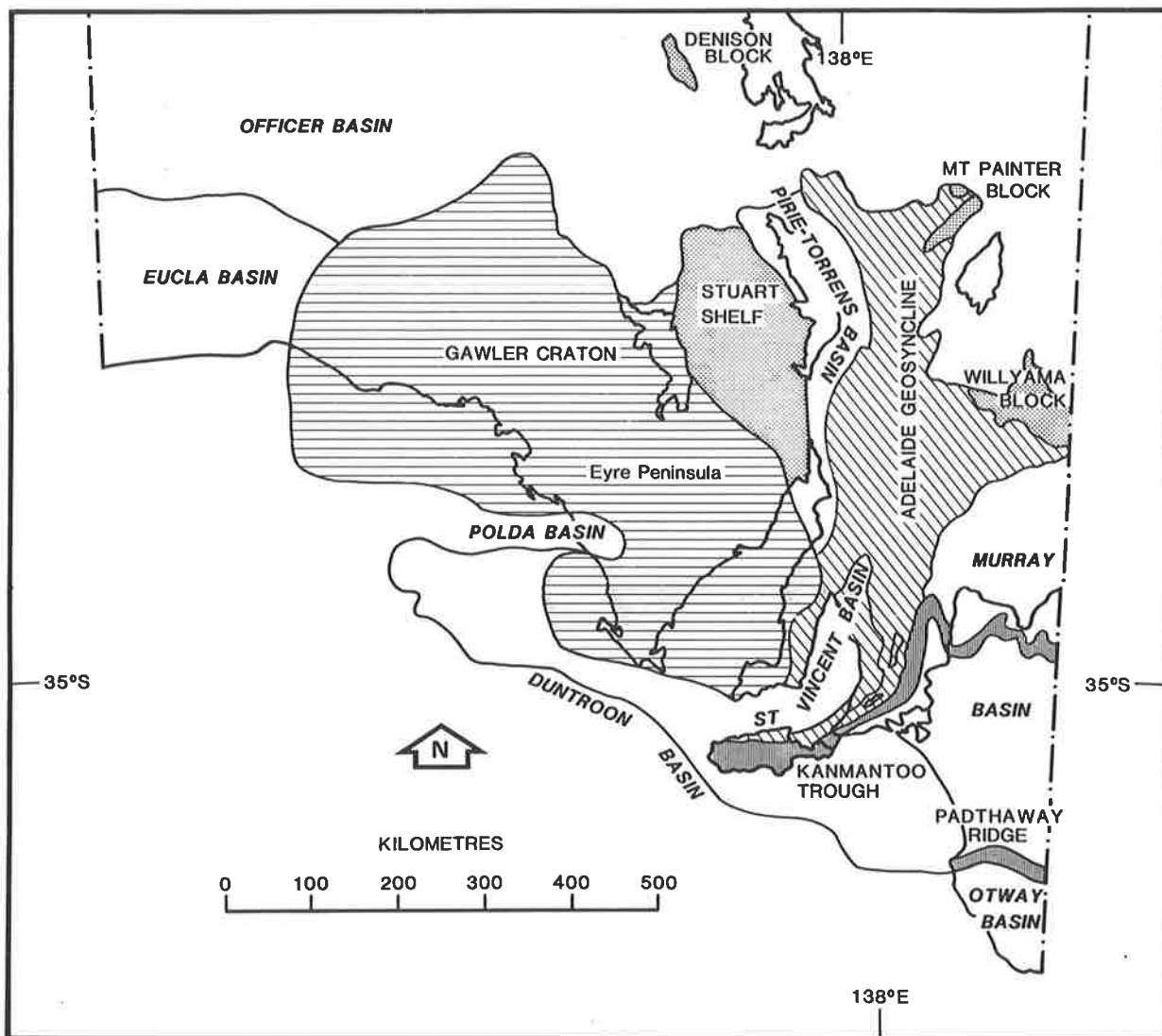


Figure 2.3 Geological provinces of southern South Australia (After Ludbrook, 1980).

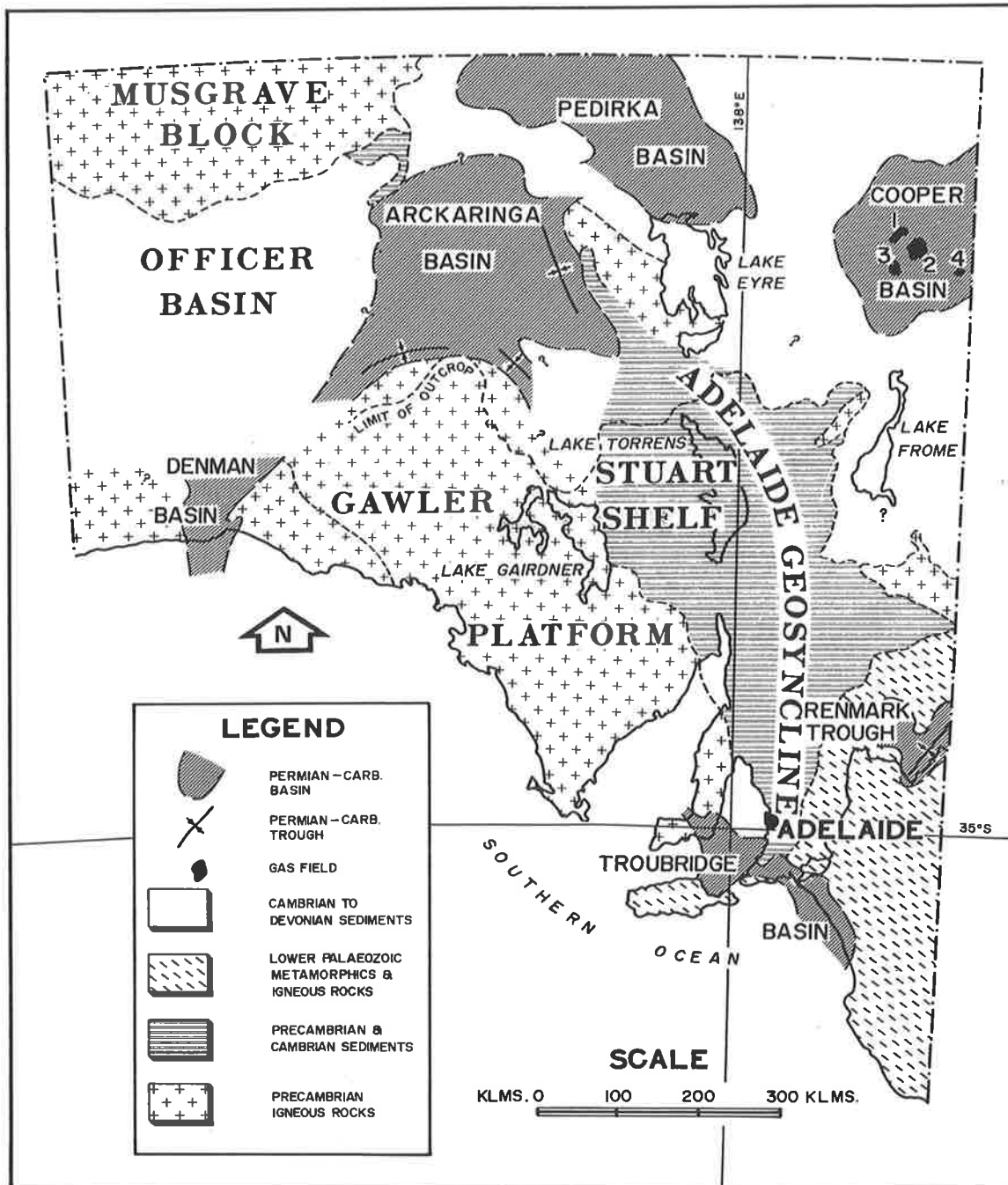


Figure 2.4 Permian sedimentary basins of South Australia (After Wopfner, 1970).

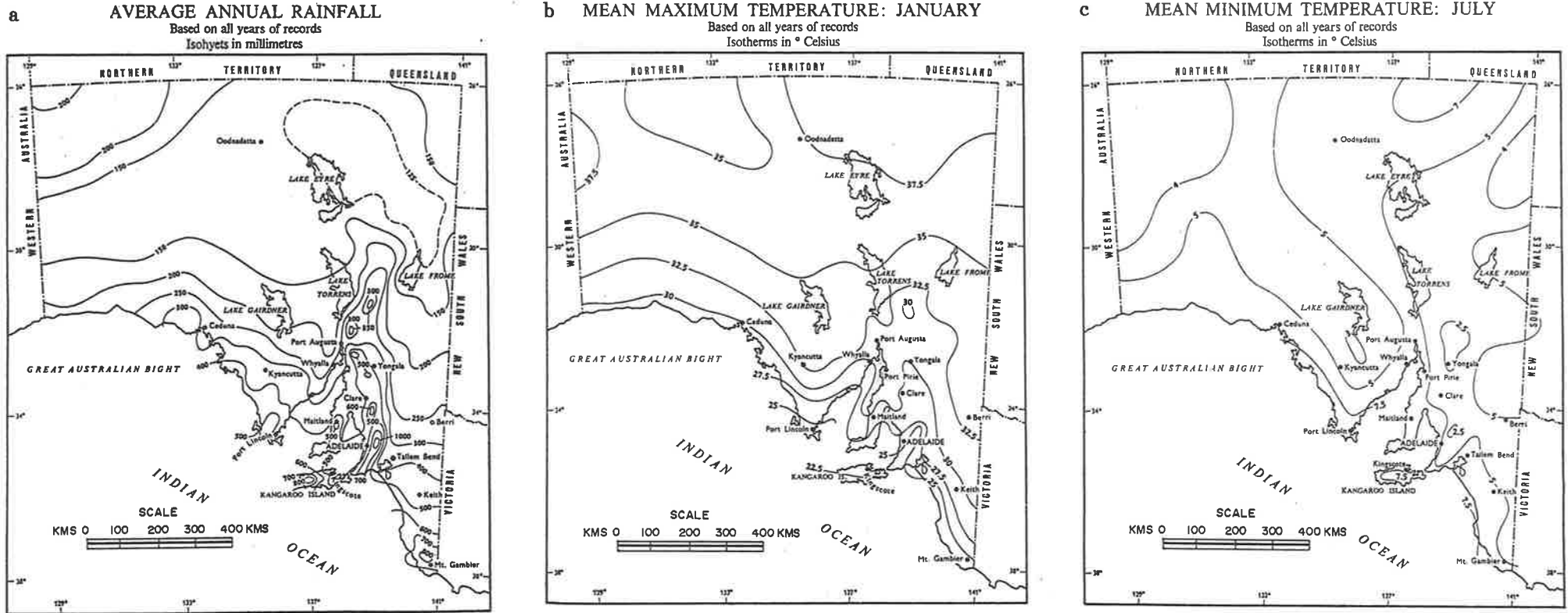


Figure 2.5 Rainfall and temperature maps of South Australia (Source: S.A. Year Book).

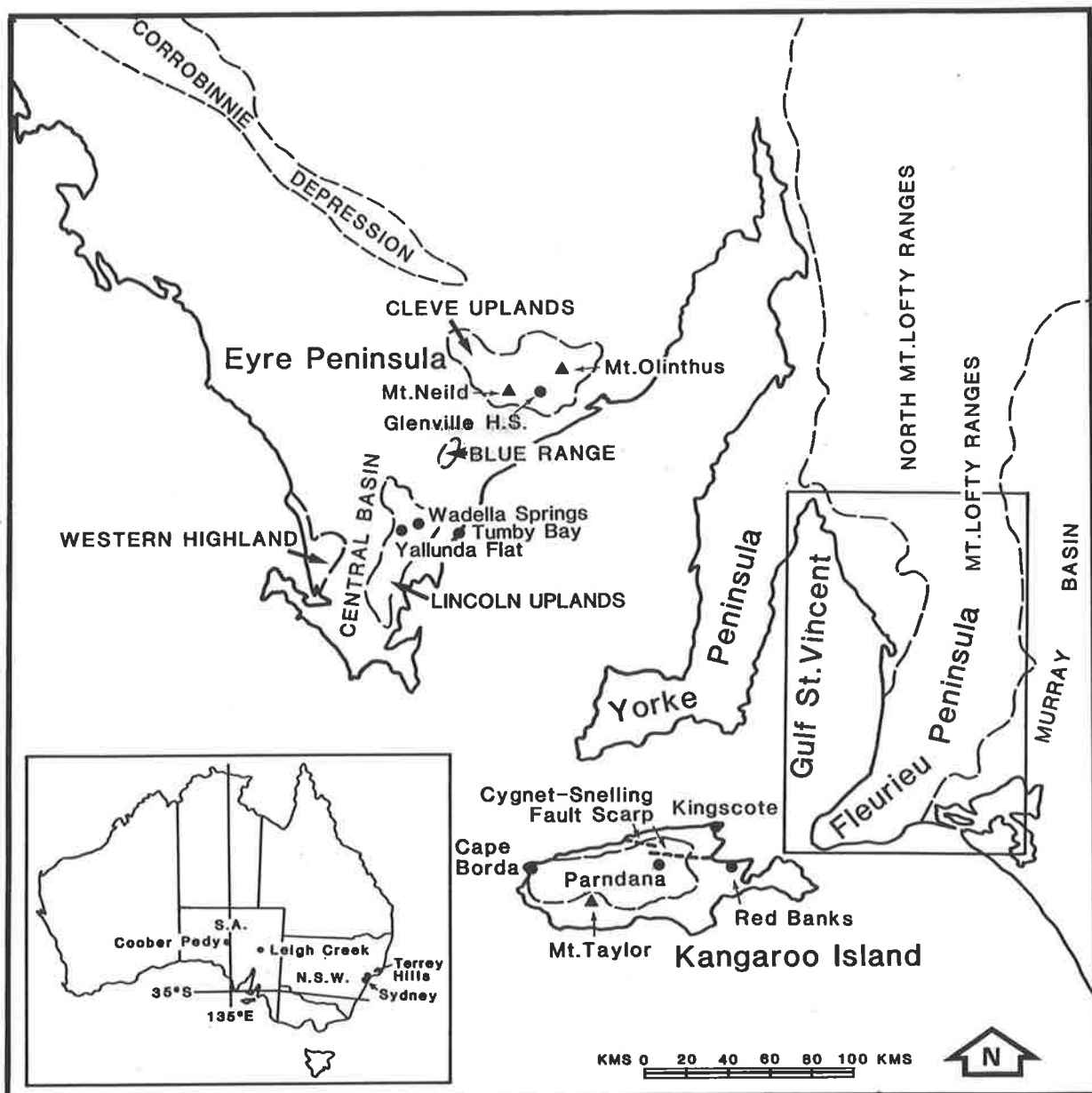


Figure 3.1 Location map of sites discussed in Chapter 3.

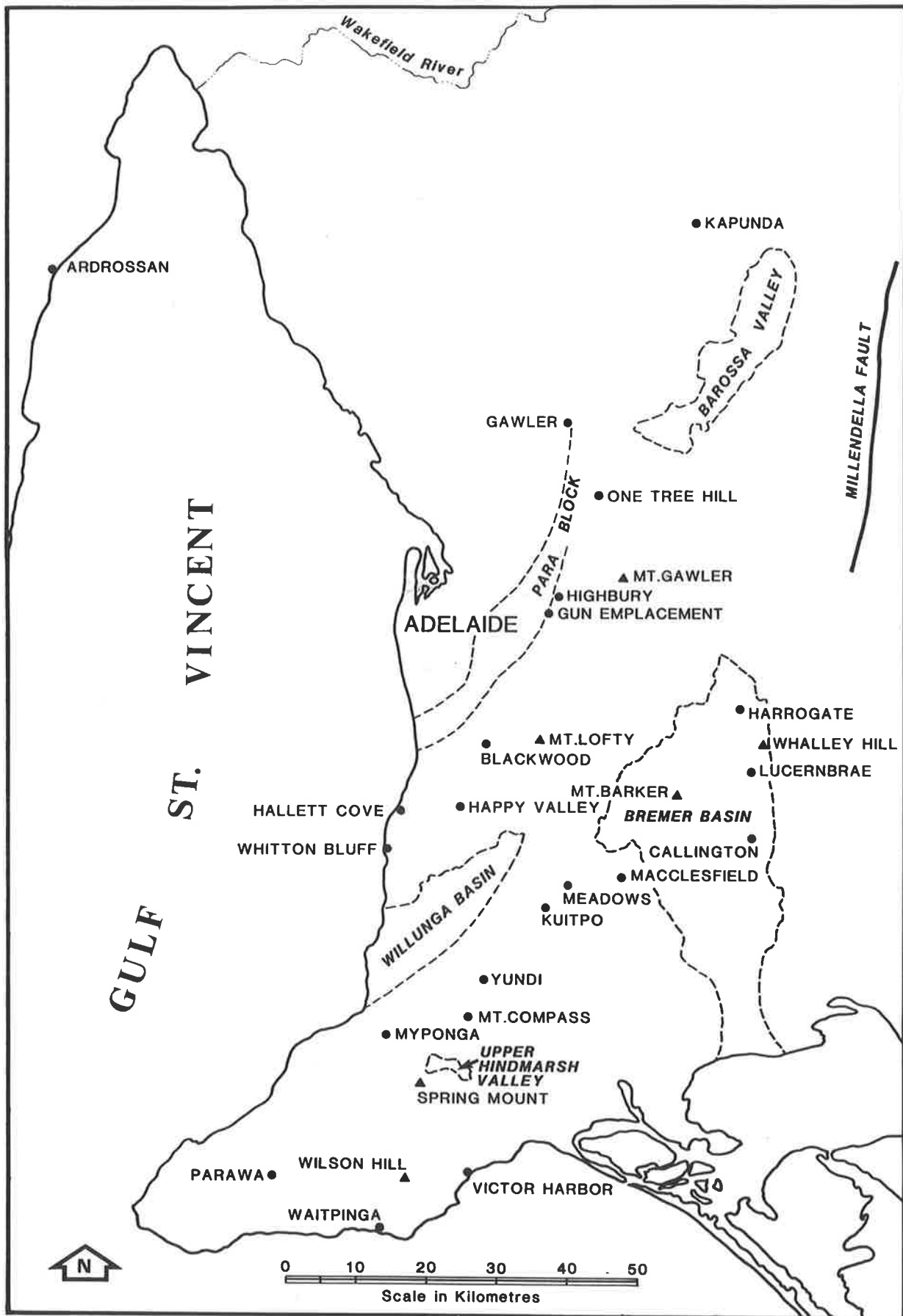


Figure 3.2 Inset of Figure 3.1, Mount Lofty Ranges.



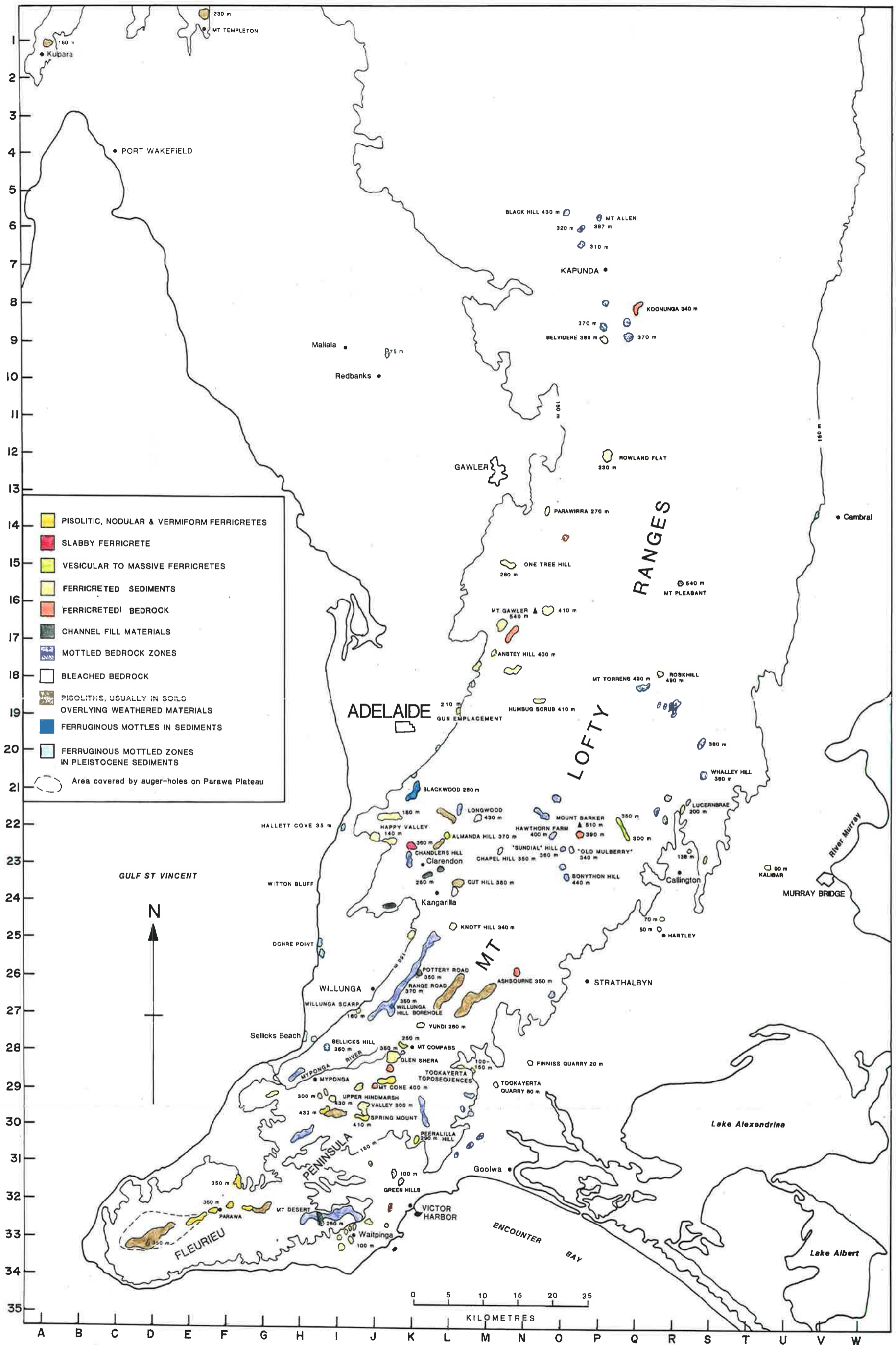


Figure 4.1 Map showing distribution of ferricretes studied in the Mount Lofty Ranges.

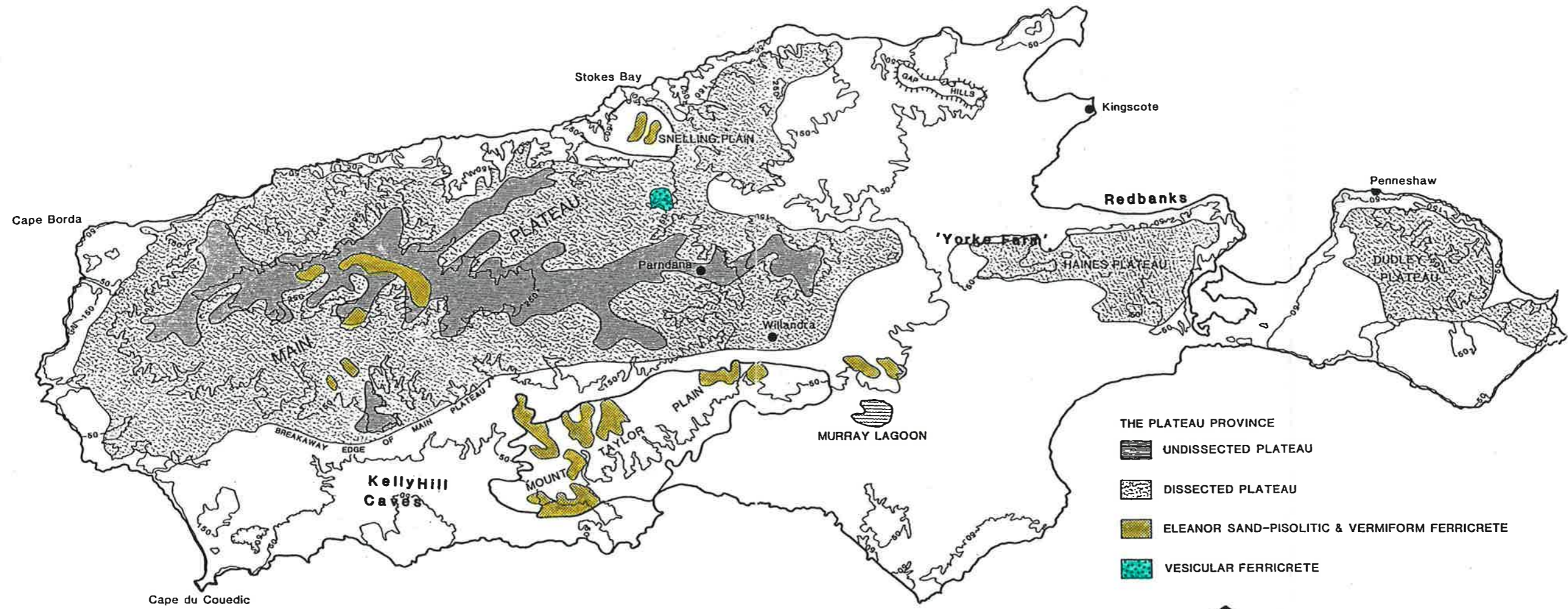


Figure 4.2 Map showing distribution of Eleanor Sand on Kangaroo Island.

AFTER BAUER (1959)



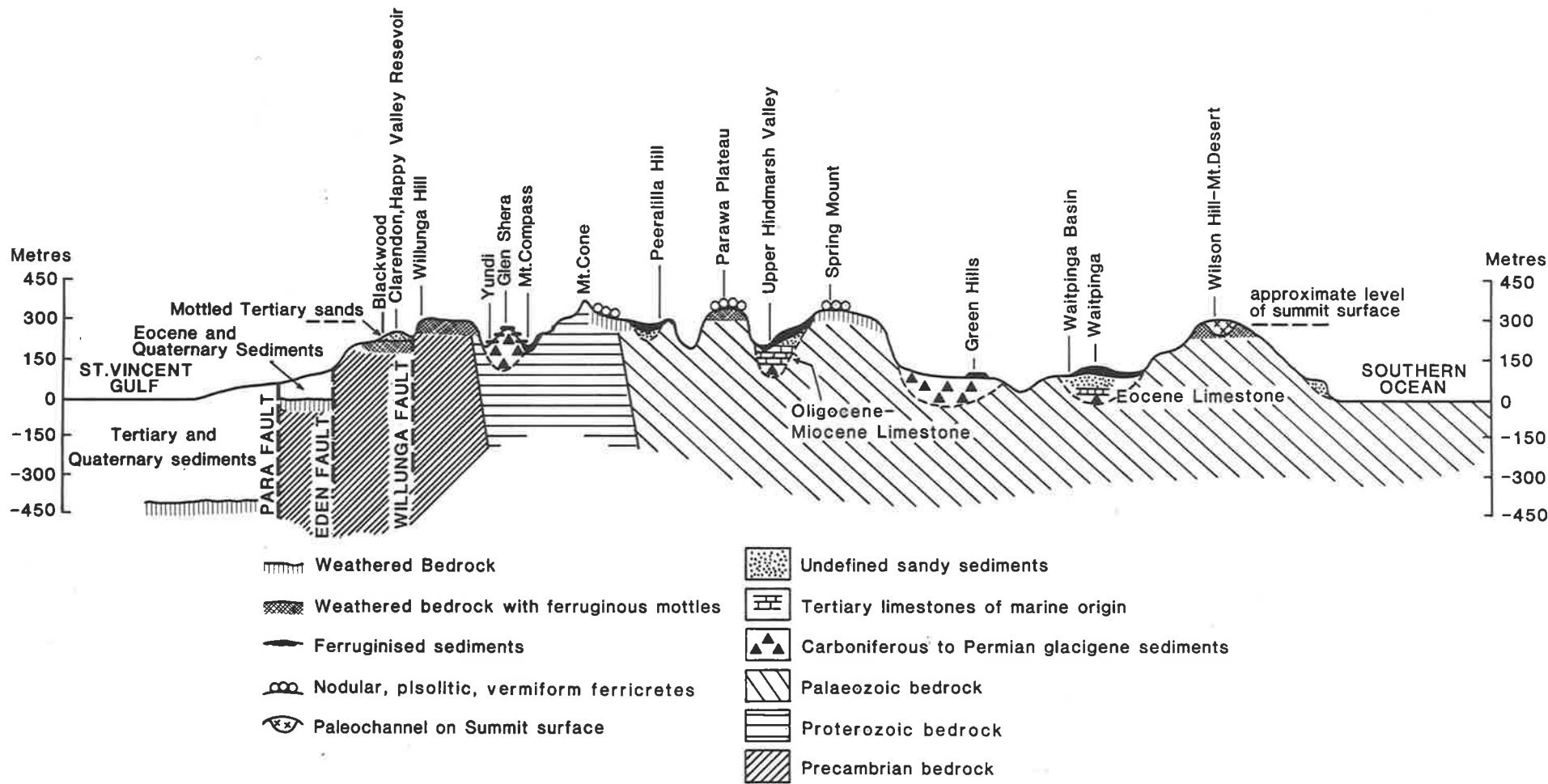


Figure 4.3 Schematic cross-section through the South Mount Lofty Ranges showing the relationships of different types of ferricretes to topography and geology.

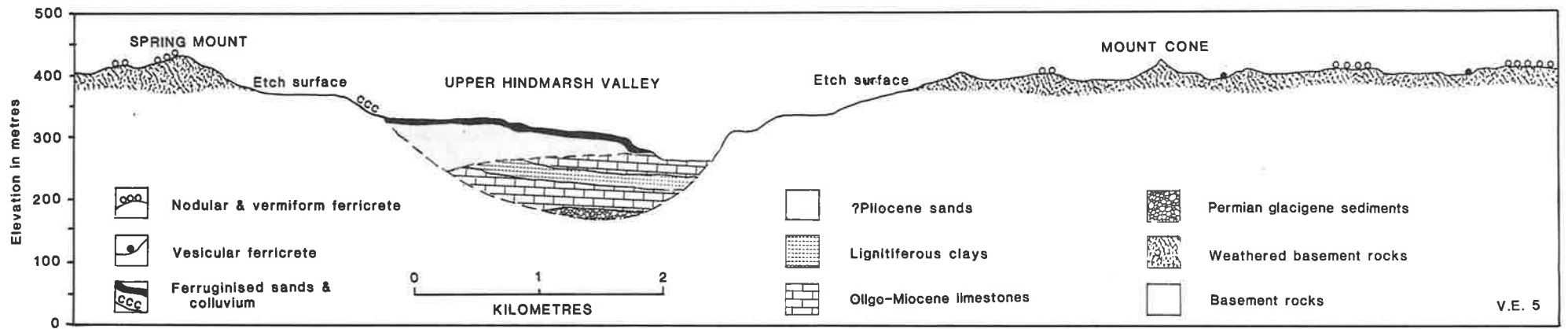


Figure 4.4 Spur-line cross-section through the Spring Mount-Upper Hindmarsh Valley-Mount Cone area showing the relationships of ferricretes to Tertiary limestone.

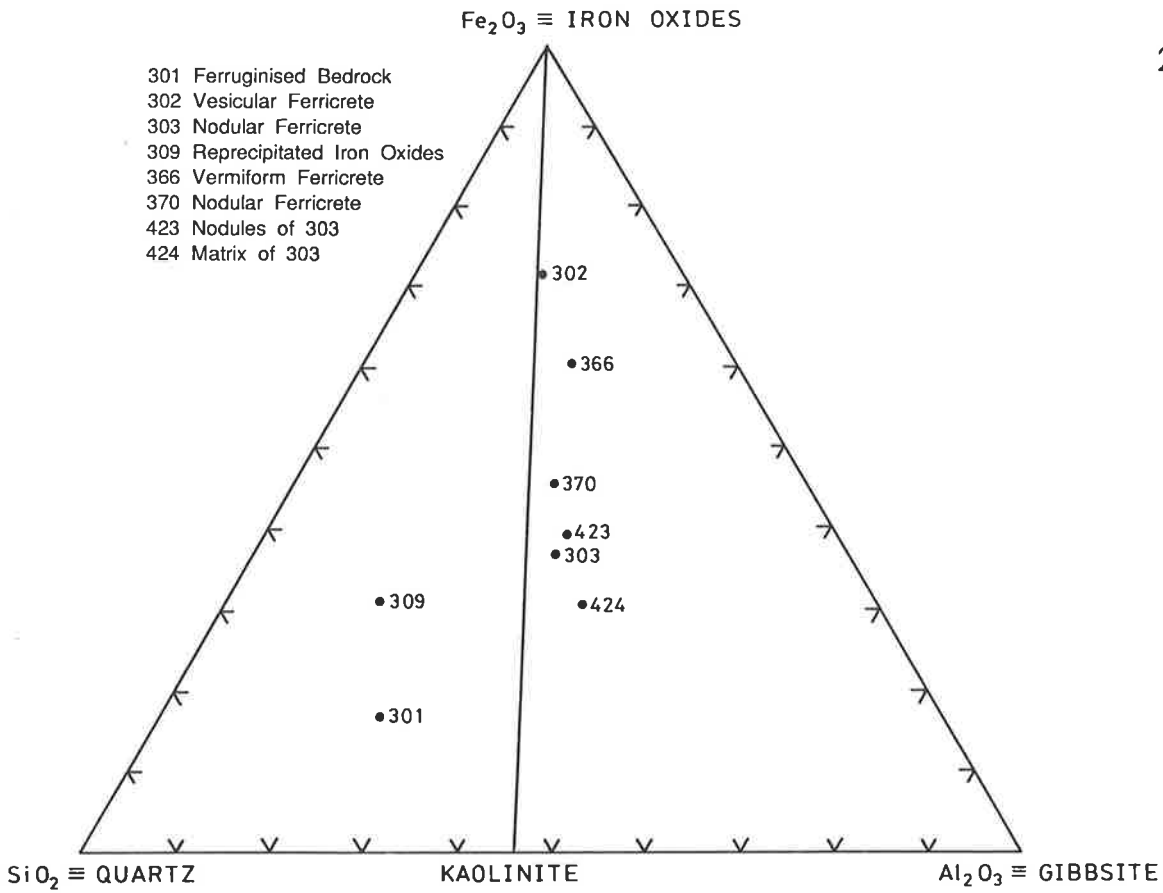


Figure 4.5 Triangular diagram of samples from the Mount Cone-Spring Mount area.

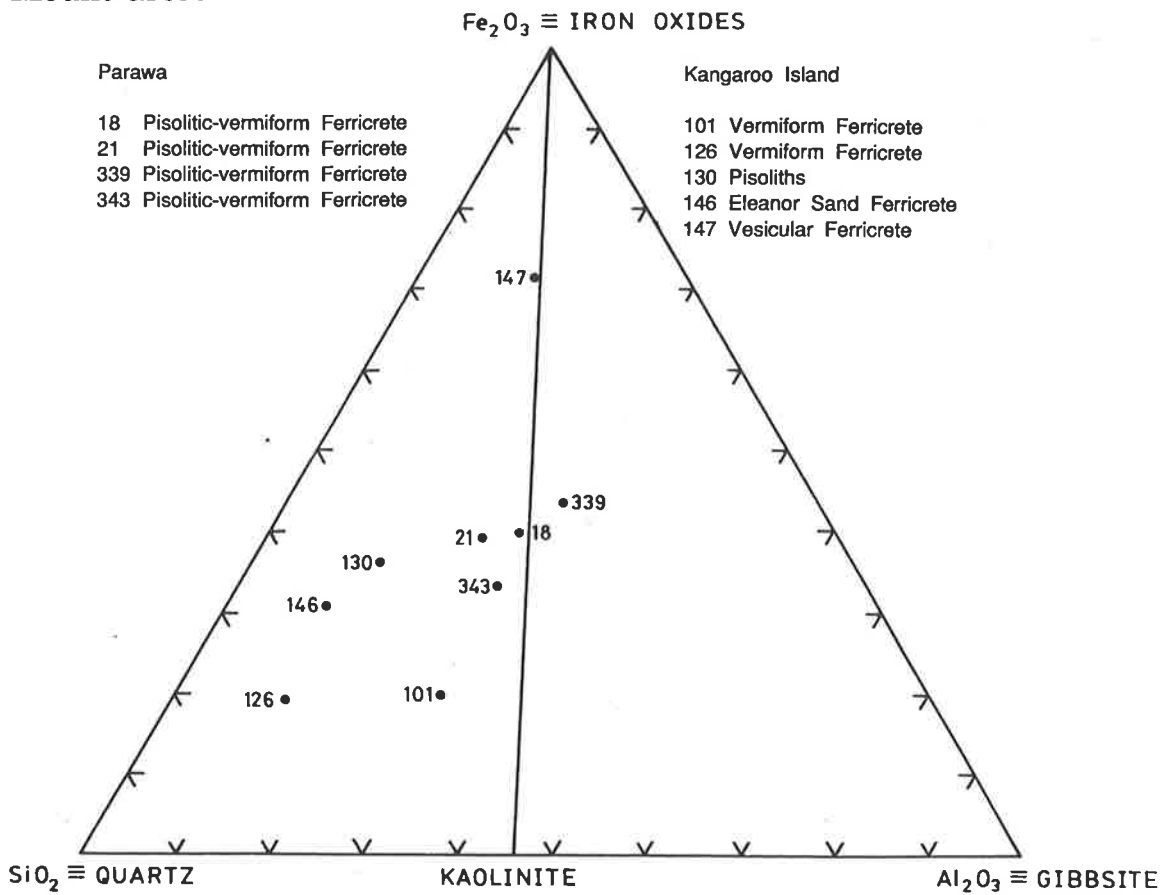
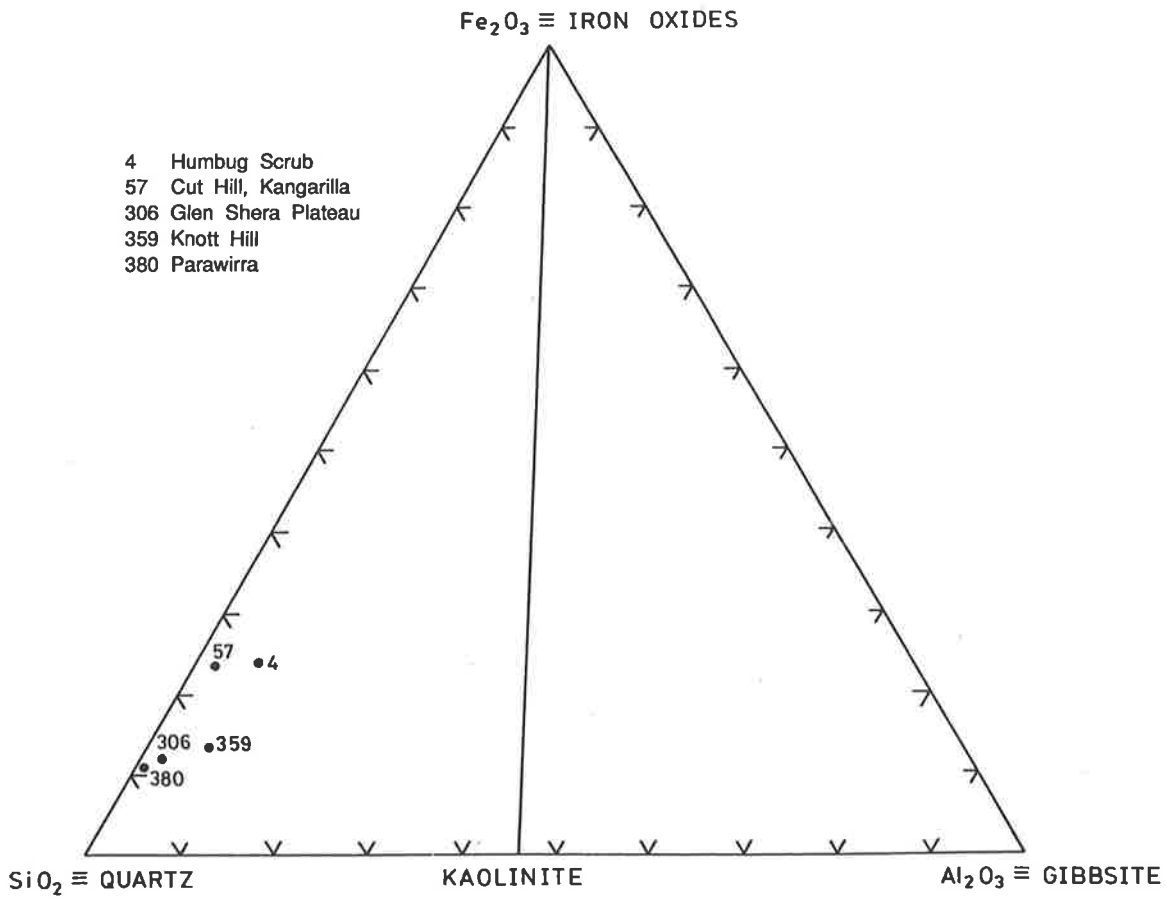


Figure 4.6 Triangular diagram of Parawa Plateau and Kangaroo Island summit surface samples.



**Figure 4.7** Triangular diagram of iron-impregnated sediments from the summit surface

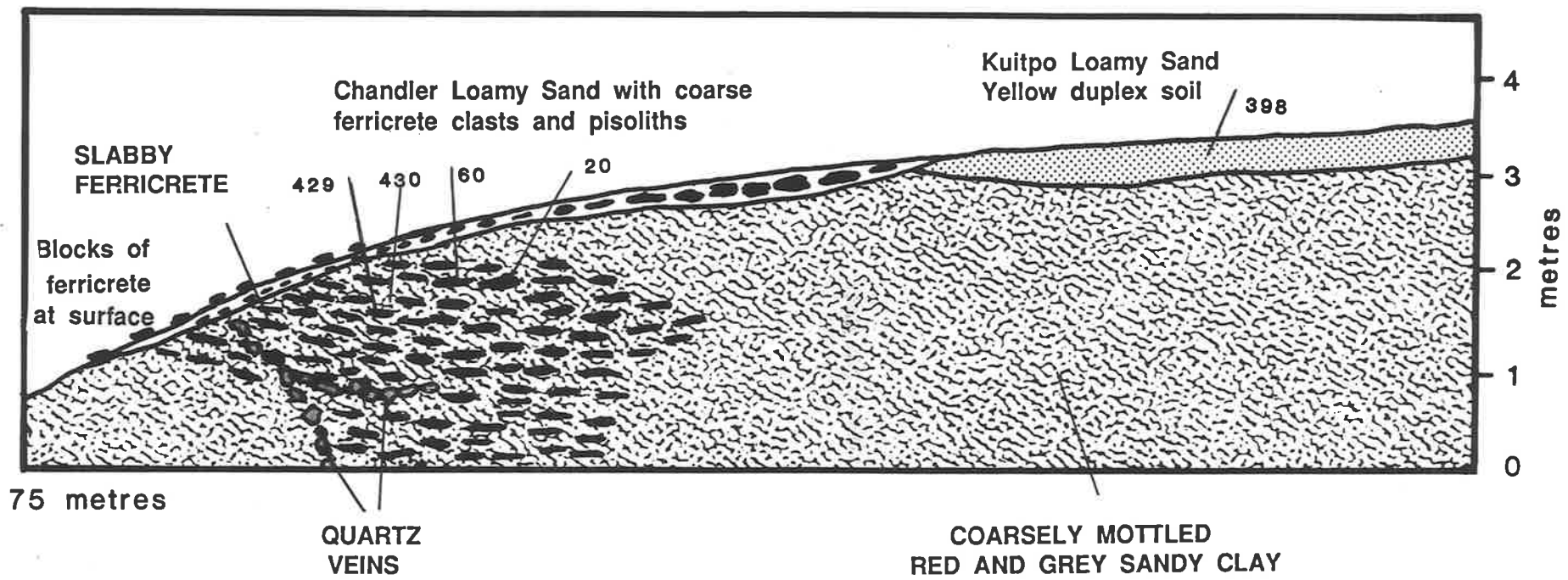


Figure 4.8 Sketch of Chandlers Hill section.

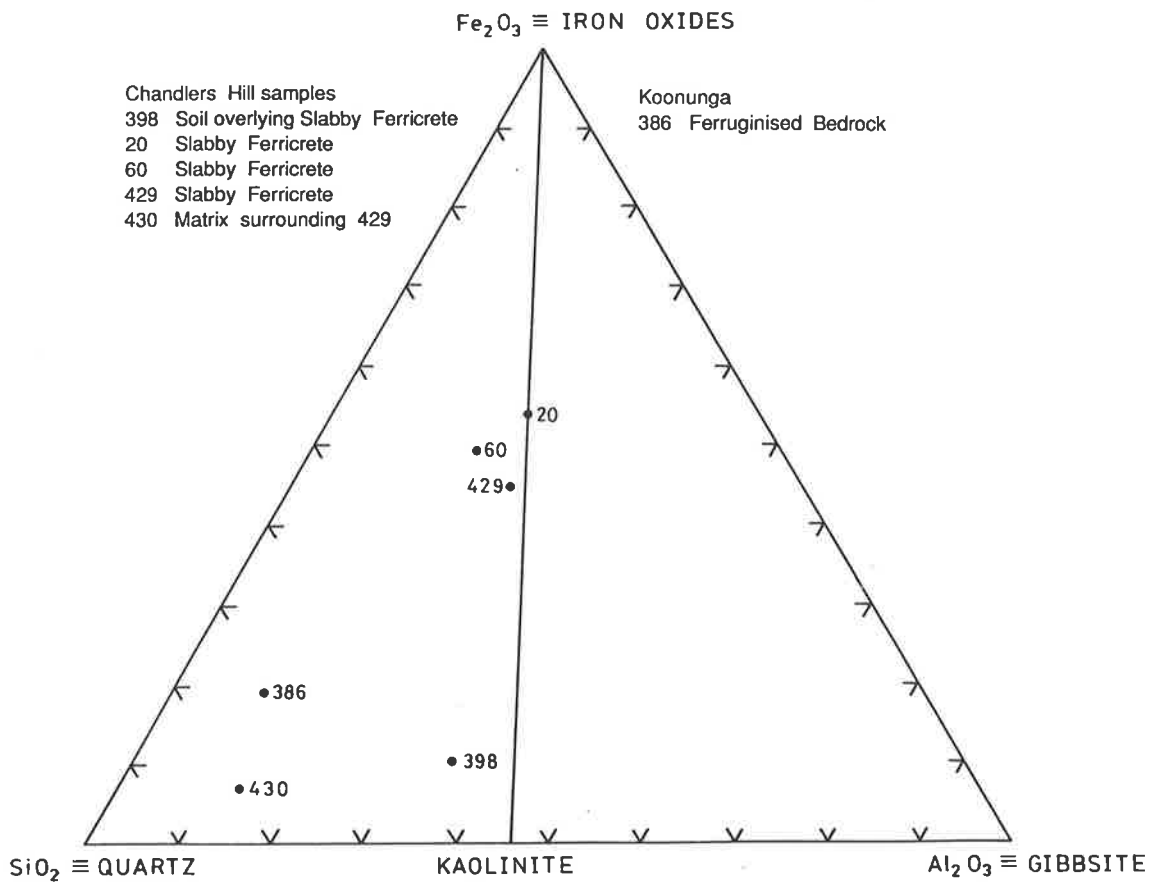


Figure 4.9 Triangular diagram of slabby ferricretes.

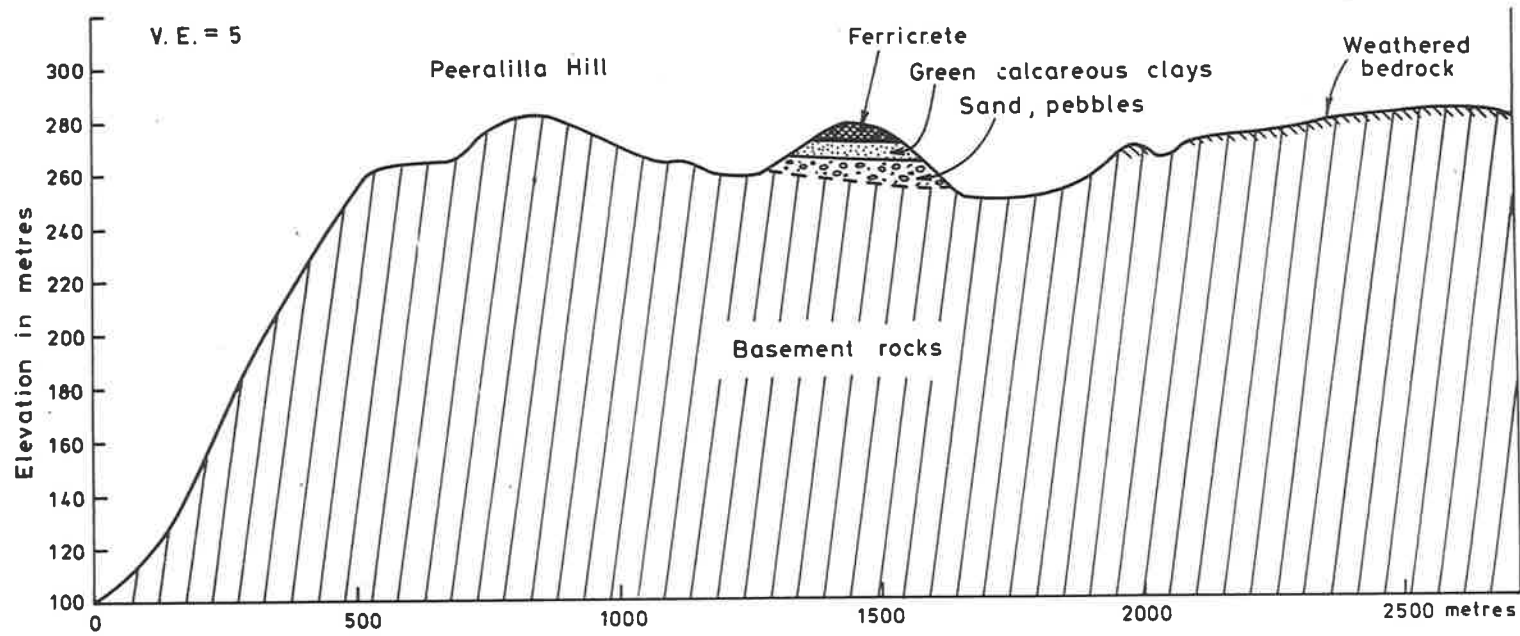


Figure 4.10 Cross section through Peeralilla Hill.

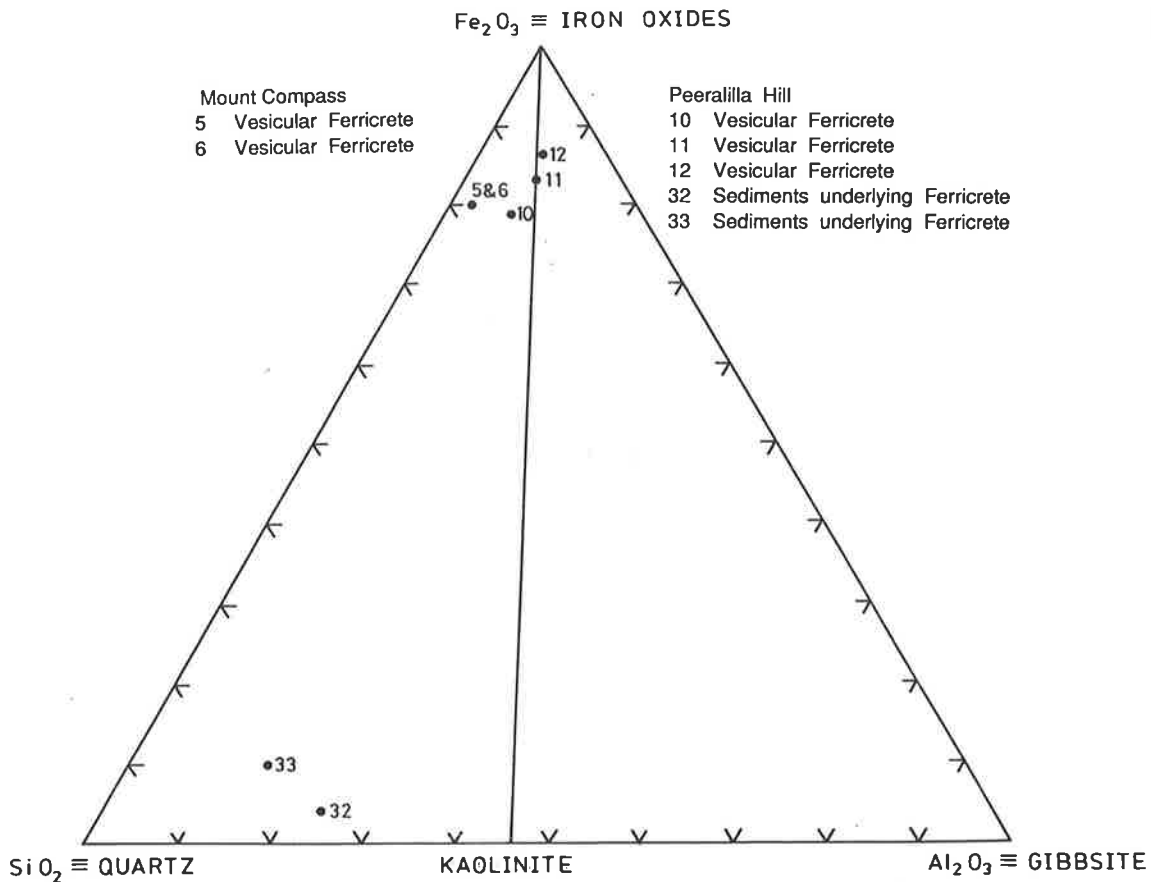


Figure 4.11 Triangular diagram of vesicular ferricretes (Mount Compass and Peeralilla Hill) and sediments underlying Peeralilla Hill ferricretes.

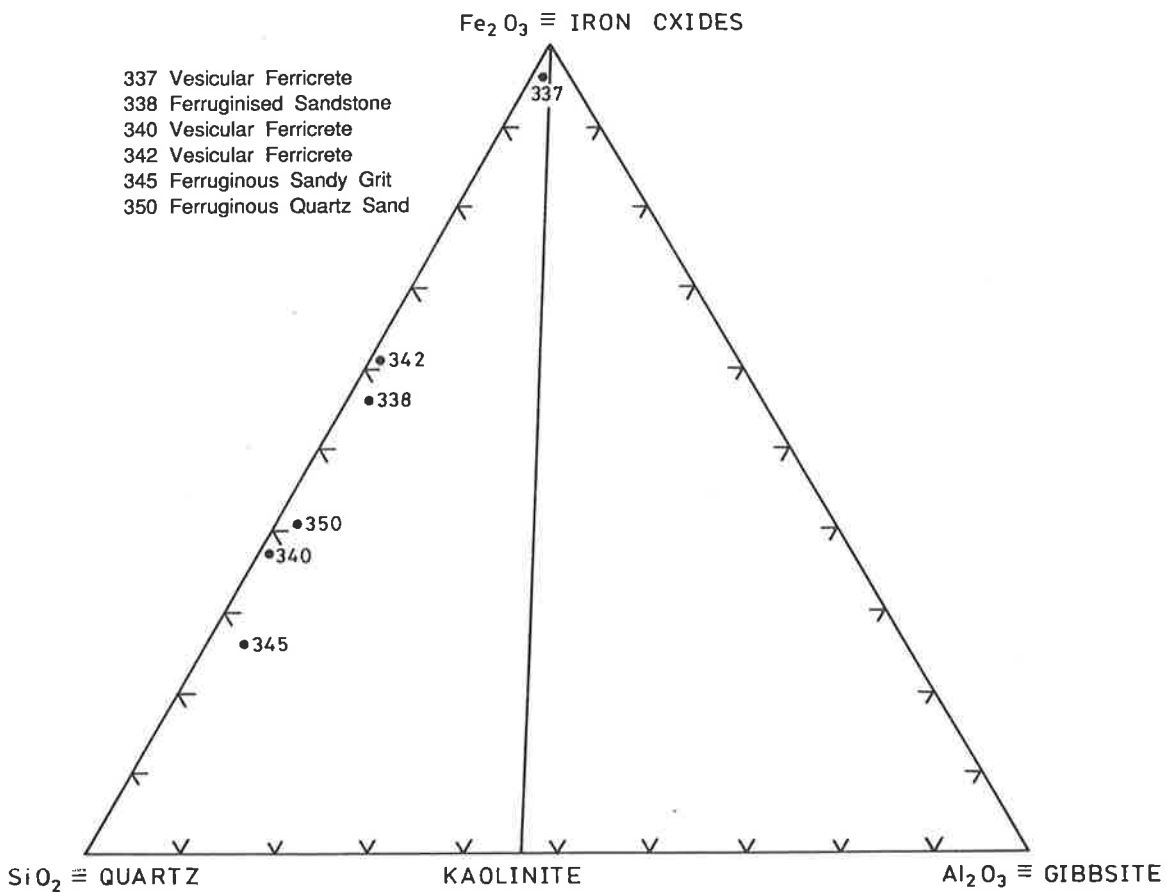


Figure 4.12 Triangular diagram of samples collected from Anstey Hill iron mine.



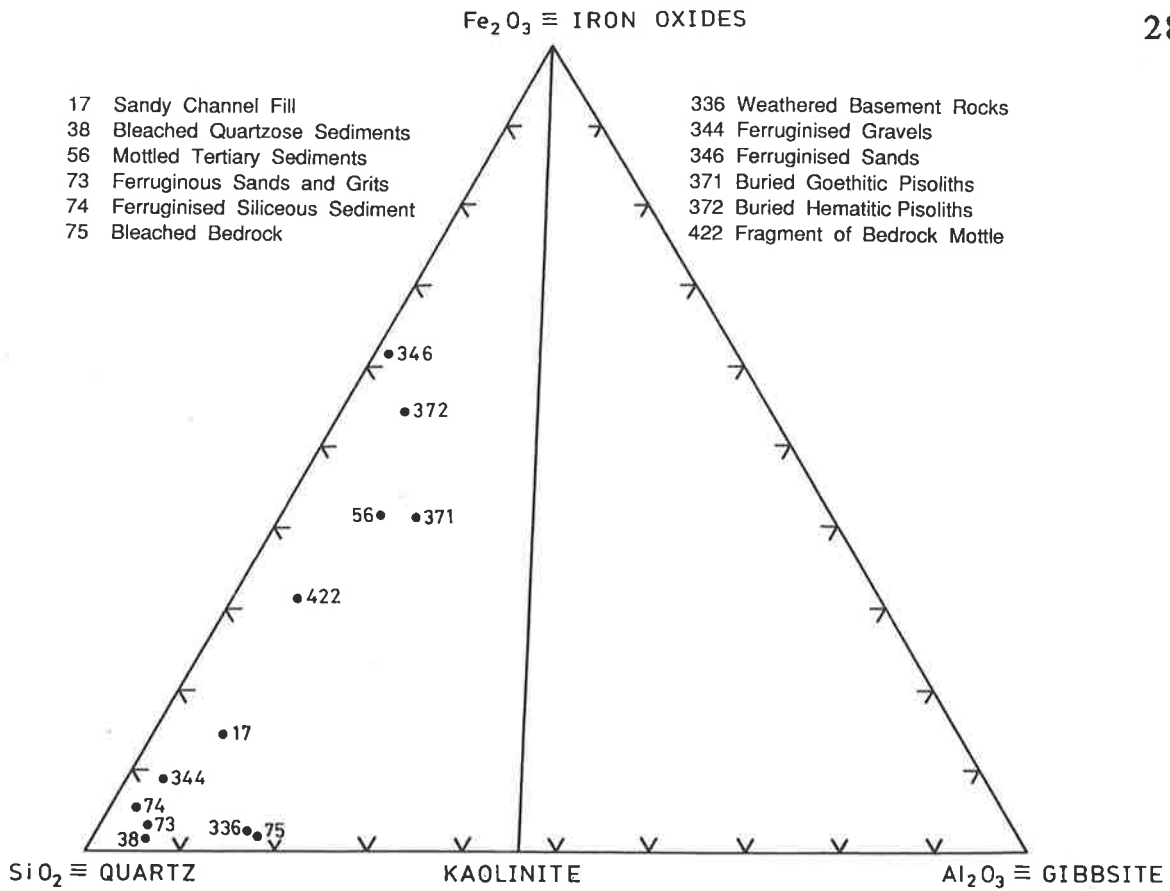


Figure 4.13 Triangular diagram of channel fill and associated materials.

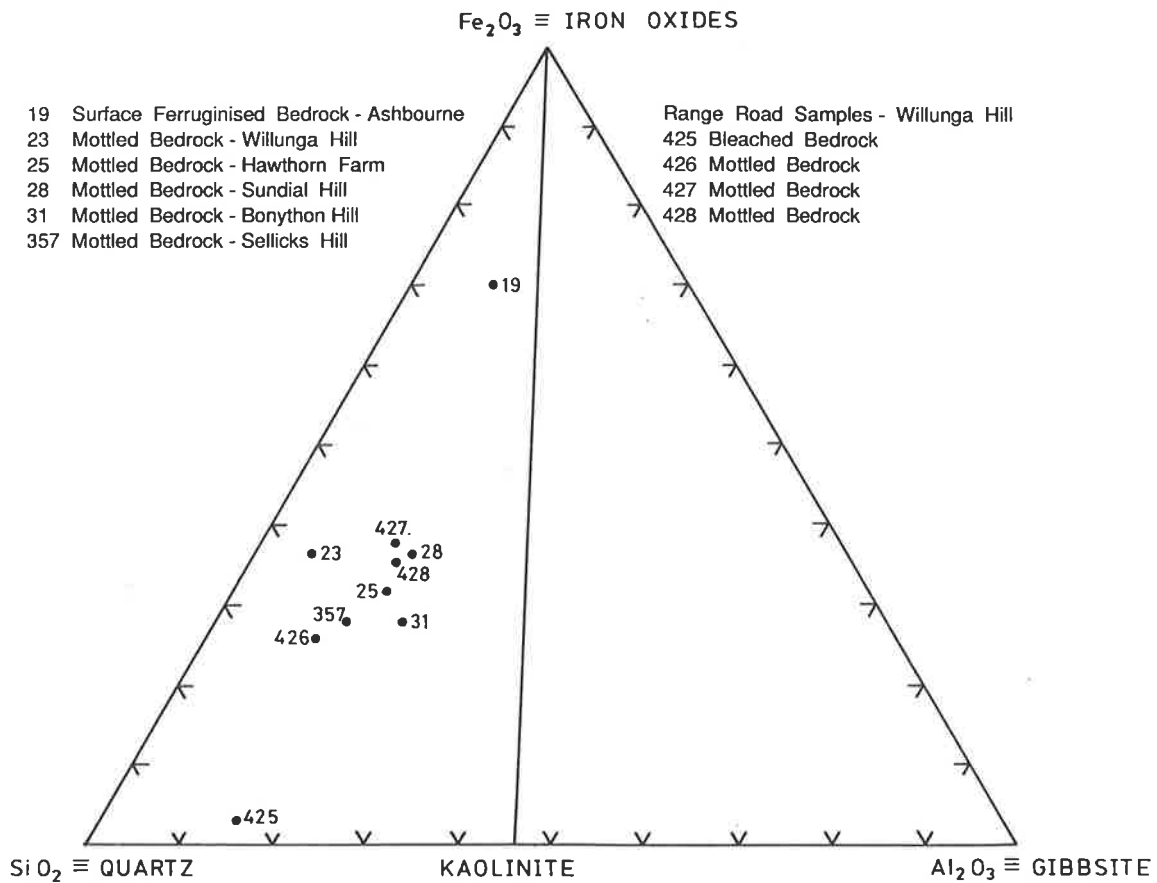
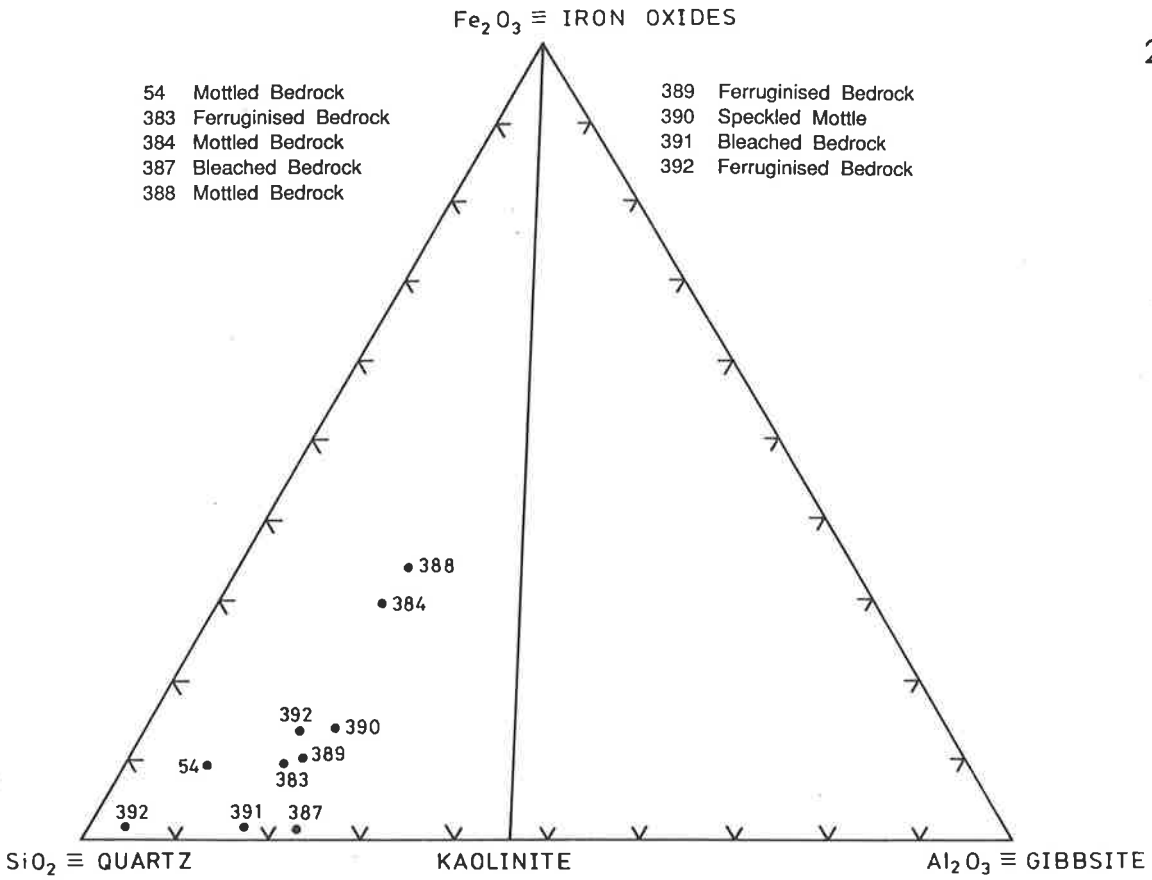
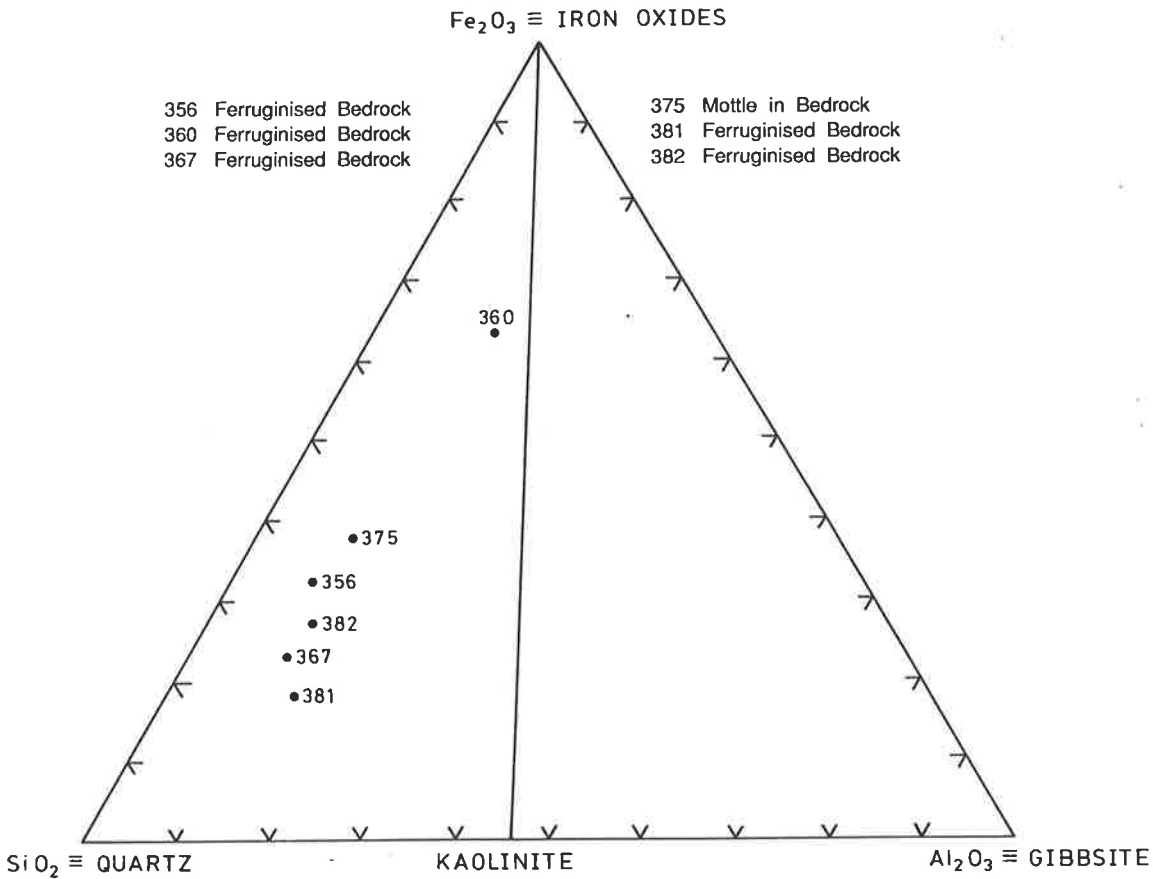


Figure 4.14 Triangular diagram of mottled zone samples.



**Figure 4.15** Triangular diagram of Mid North samples: mottled and bleached bedrock.



**Figure 4.16** Triangular diagram of ferruginised bedrock and bedrock mottles, summit surface, East Mount Lofty Ranges samples.

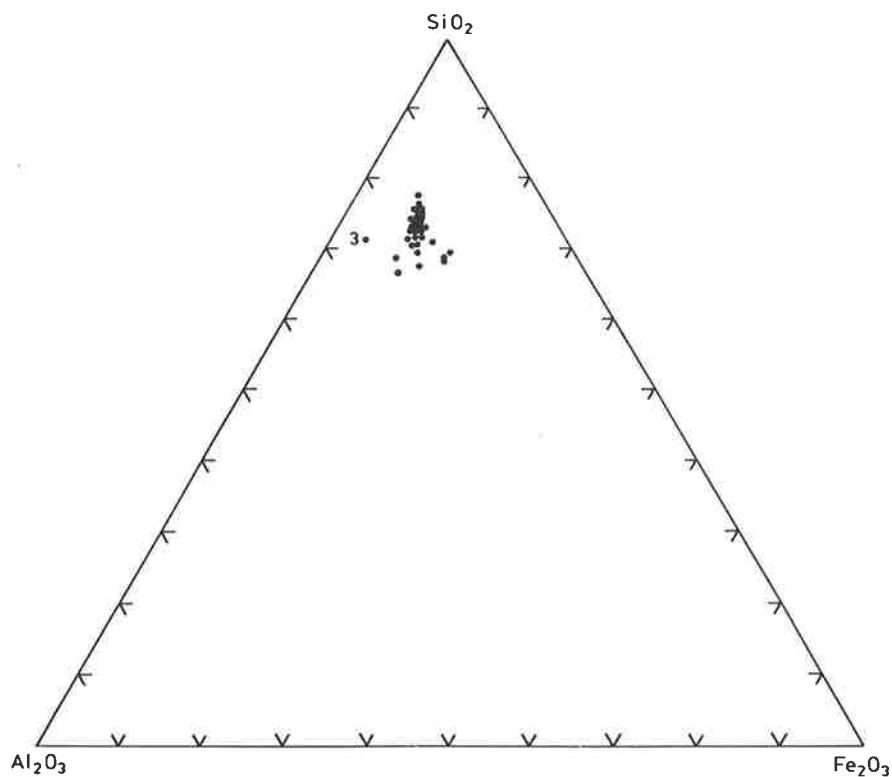


Figure 4.17 Triangular diagram of samples from the Willunga Hill borehole, illustrating their uniform chemical compositions.

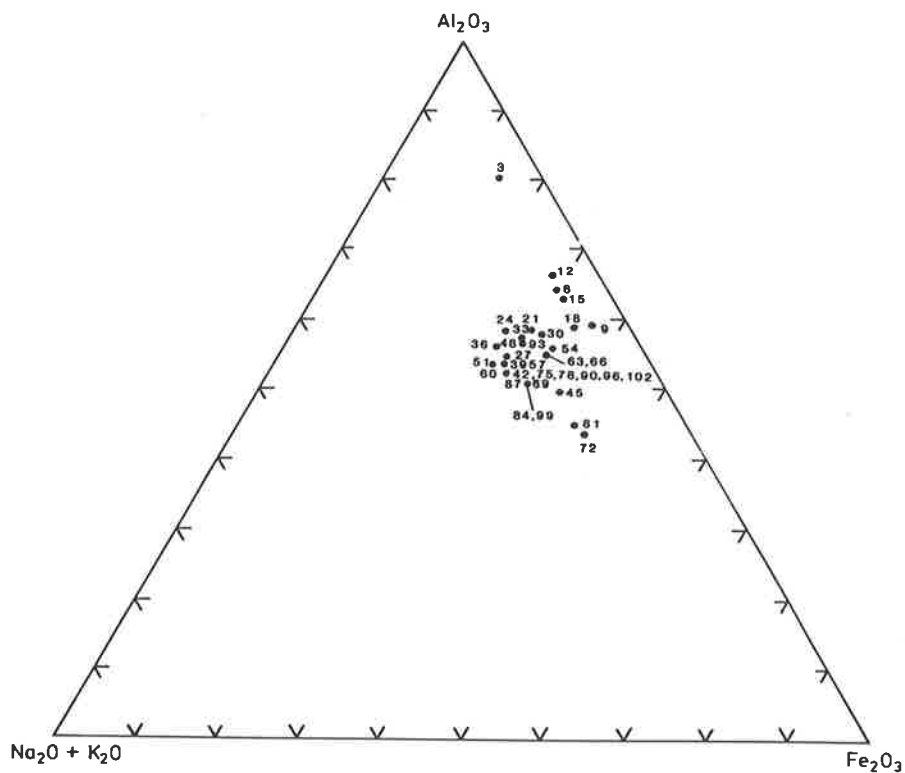


Figure 4.18 Triangular plot of Willunga Hill borehole samples illustrating depletion of bases in the upper part of the profile.

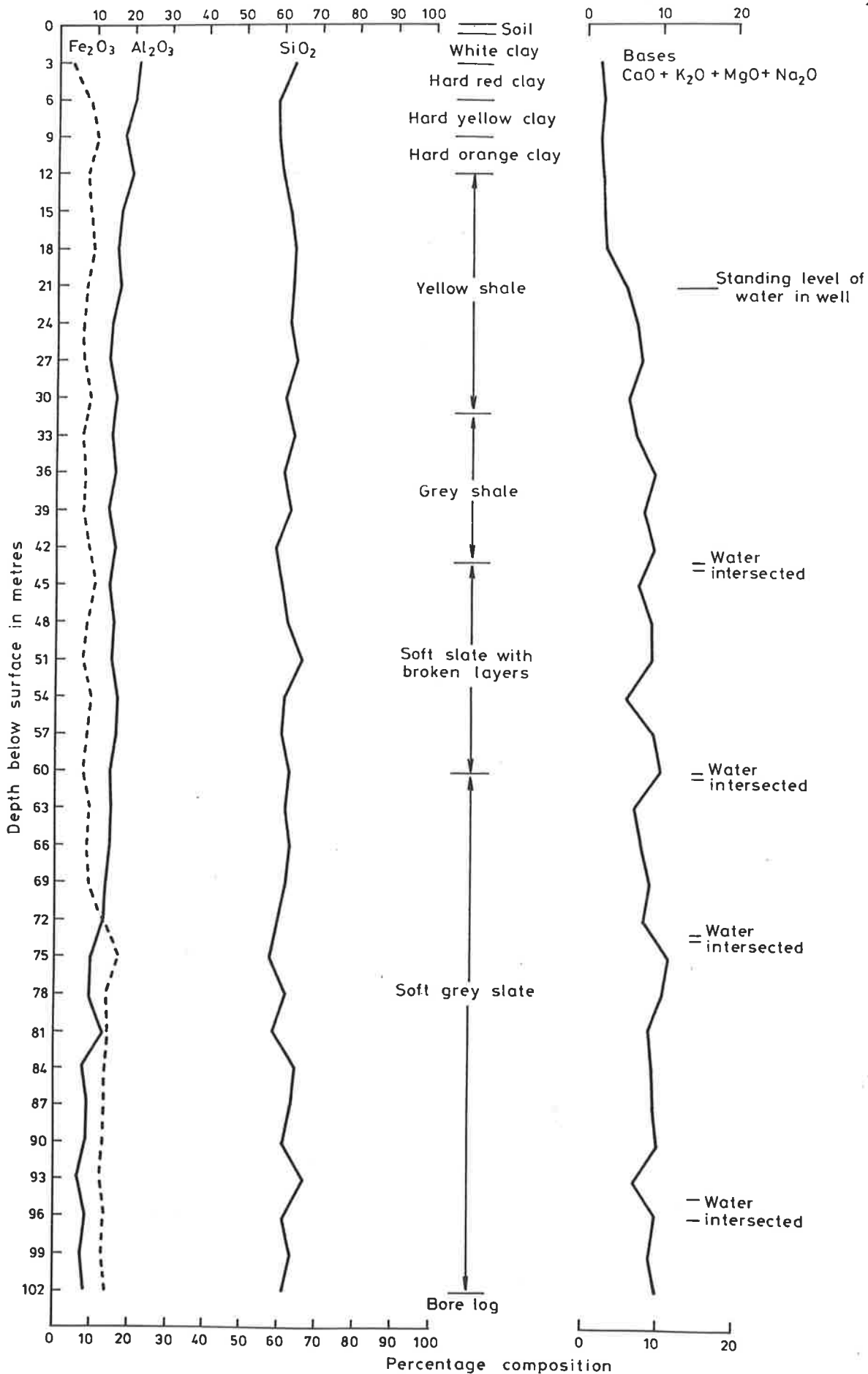


Figure 4.19 Variations of bulk chemistry down the Willunga Hill borehole.

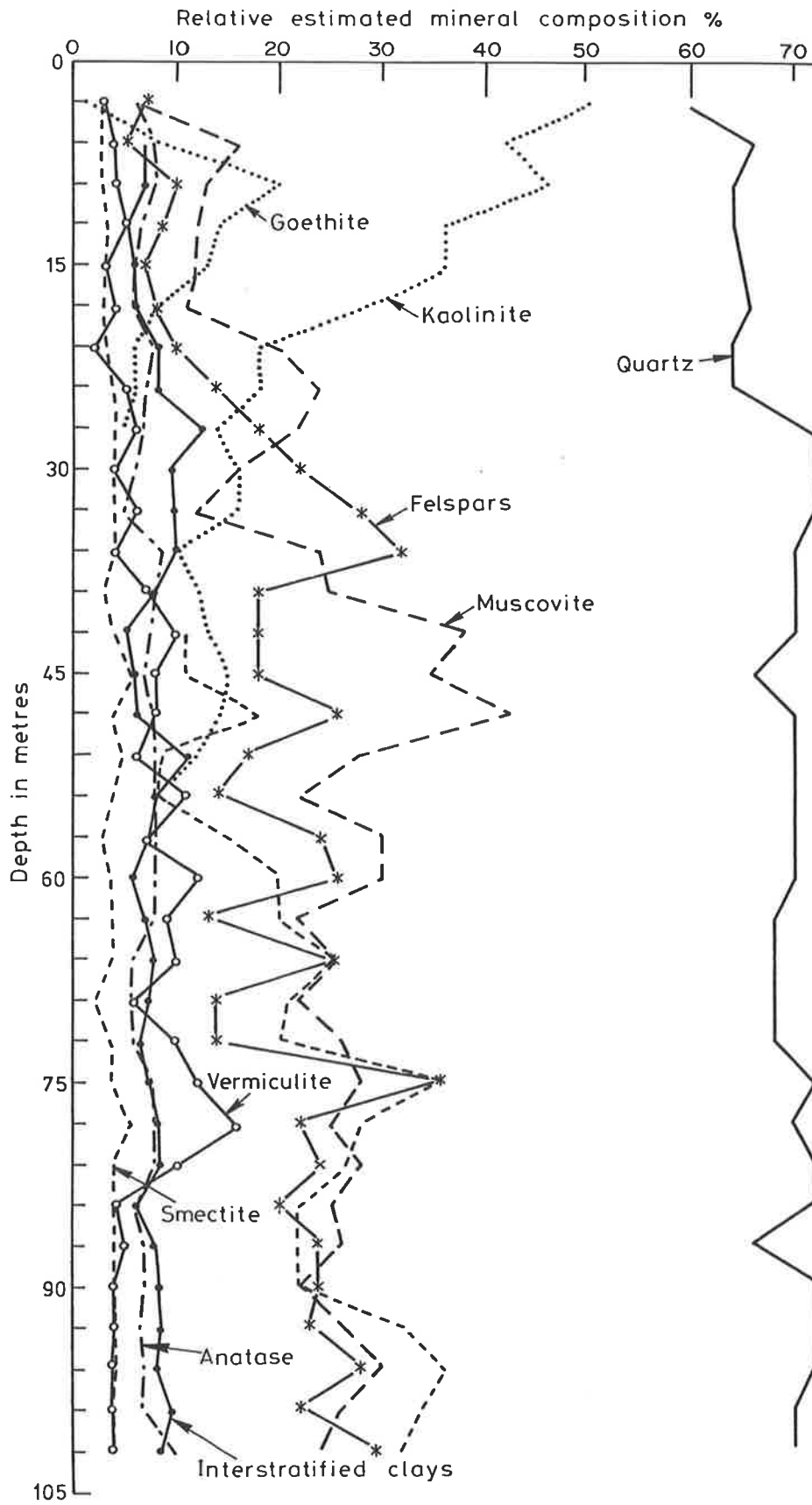


Figure 4.20 Variations in bulk mineralogy down the Willunga Hill borehole.

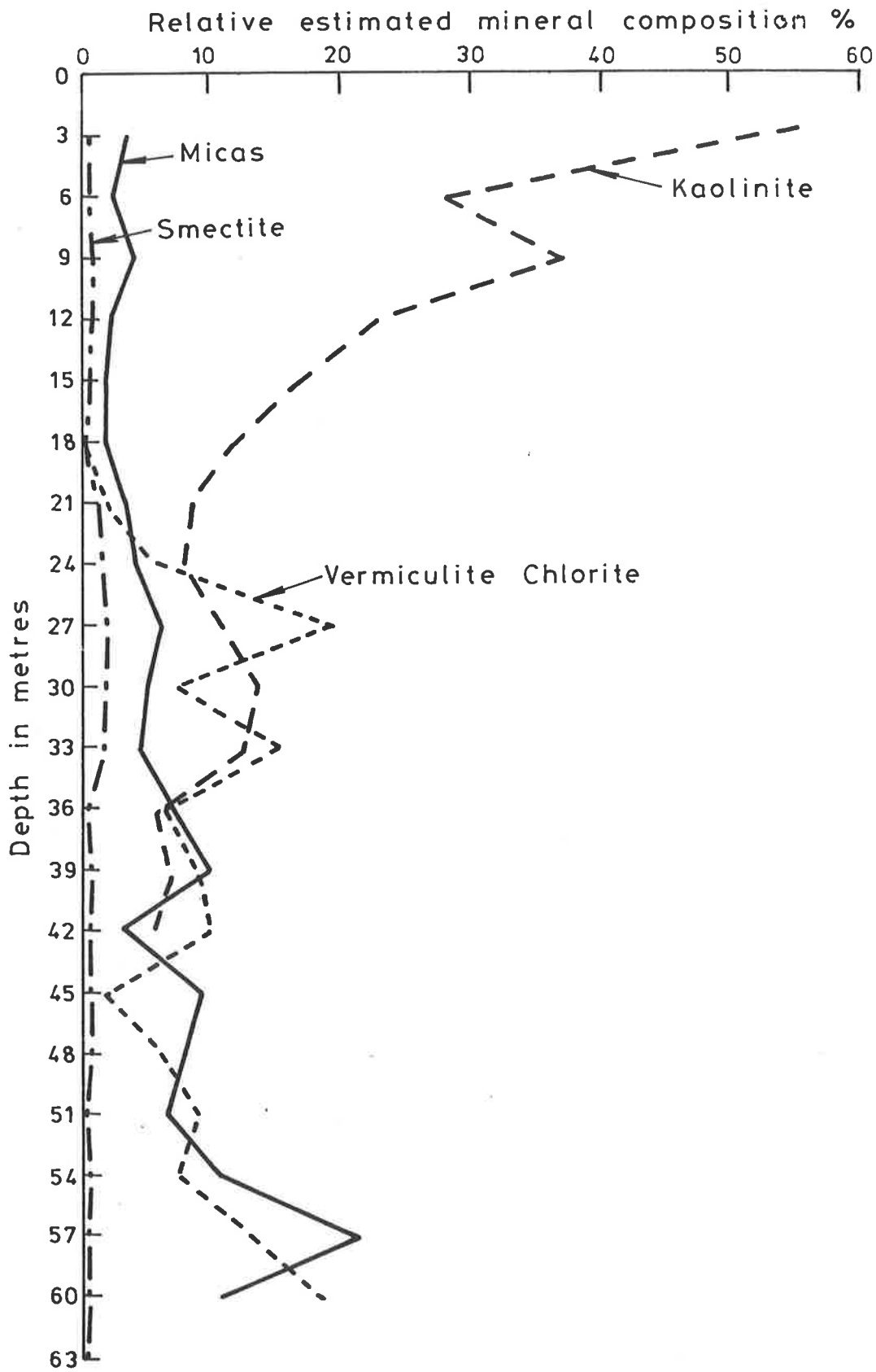


Figure 4.21 Variations in mineralogy of the <2 micron clay fraction down the Willunga Hill borehole.

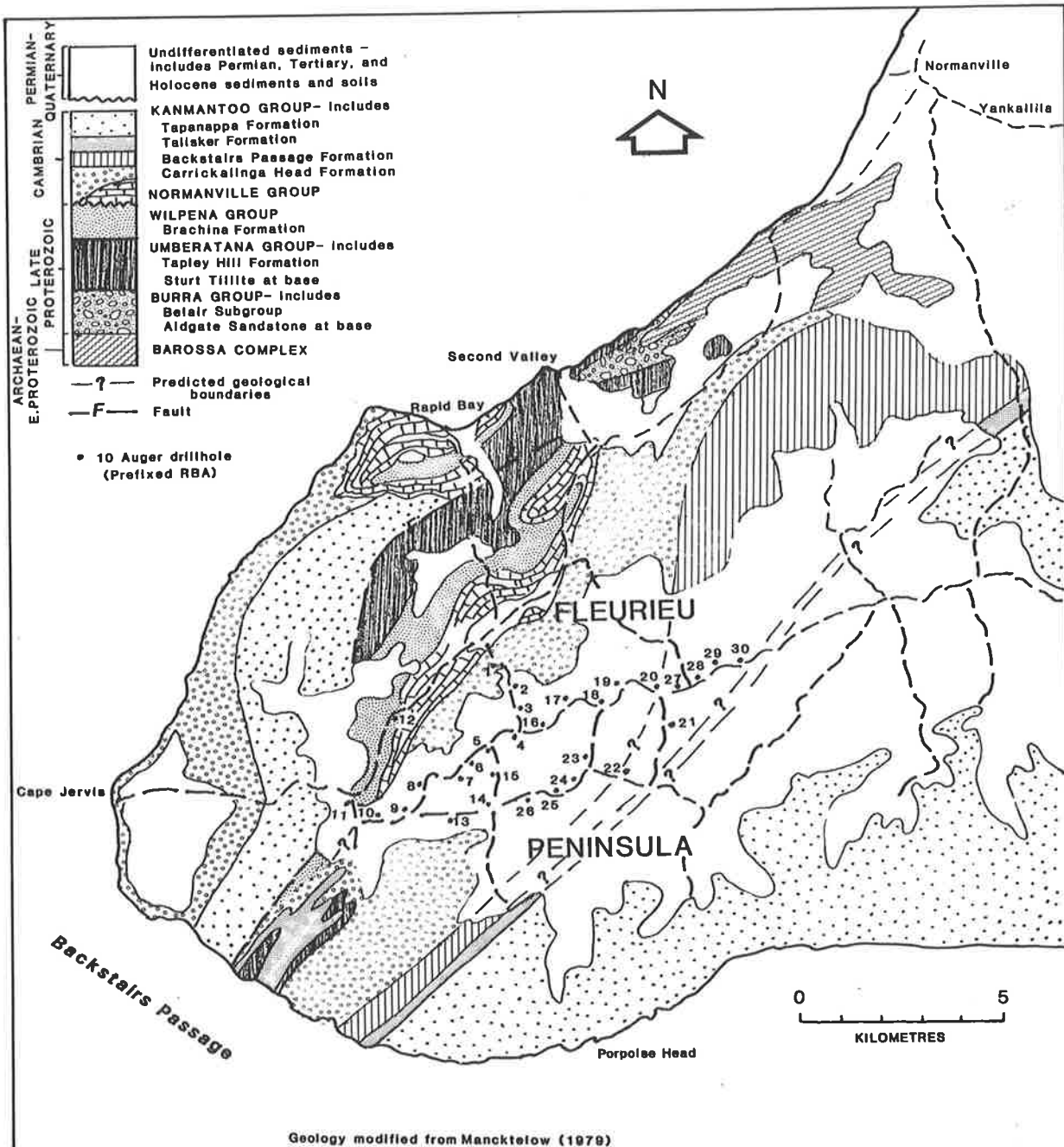
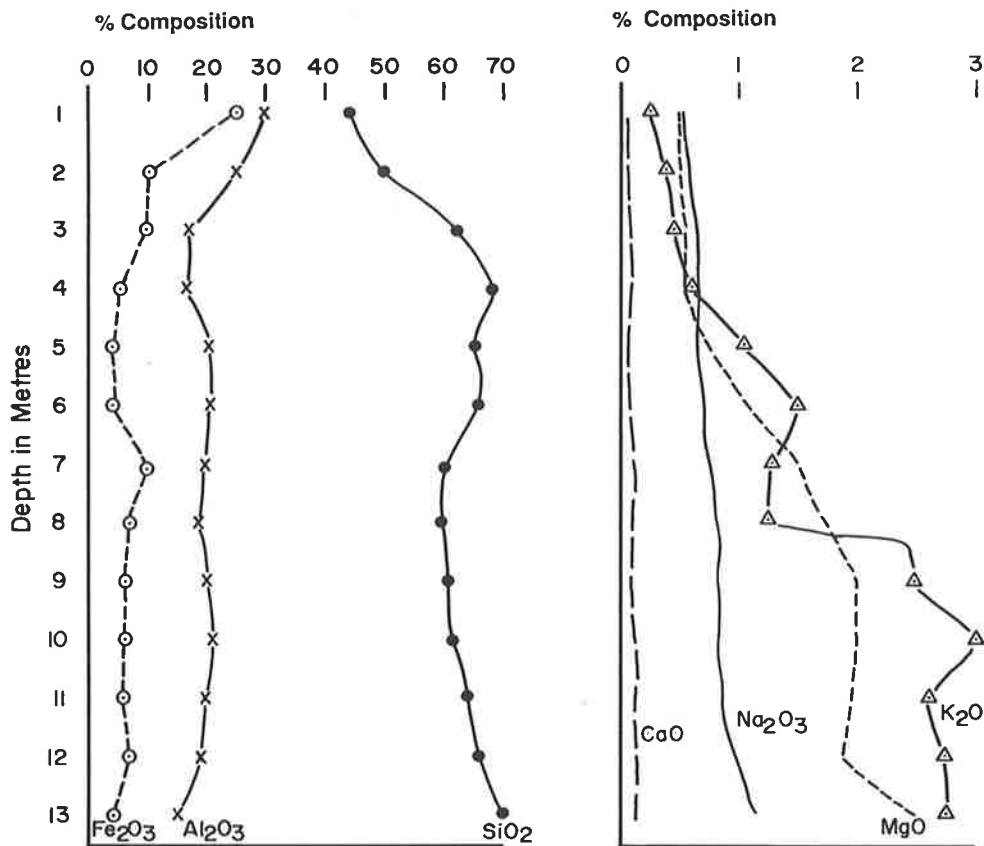


Figure 4.22 Distribution of auger holes in weathered materials on the Parawa Plateau of Fleurieu Peninsula in relationship to bedrock geology (Modified after Mancktelow, 1979).

CHEMISTRY



MINERALOGY

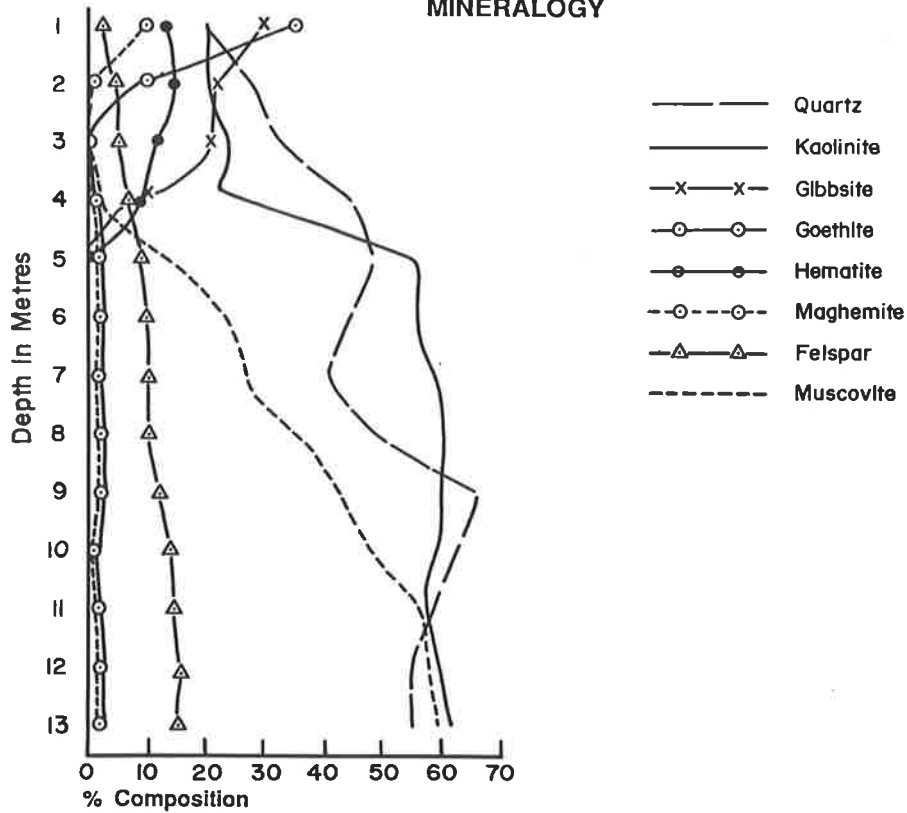


Figure 4.23 Generalised variations in chemistry and mineralogy beneath the Parawa Plateau.



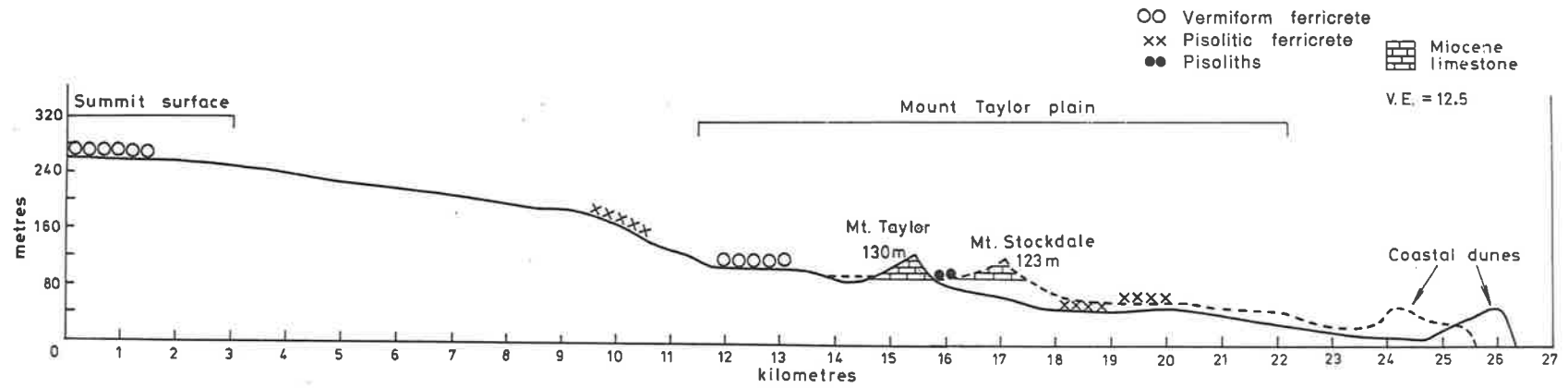
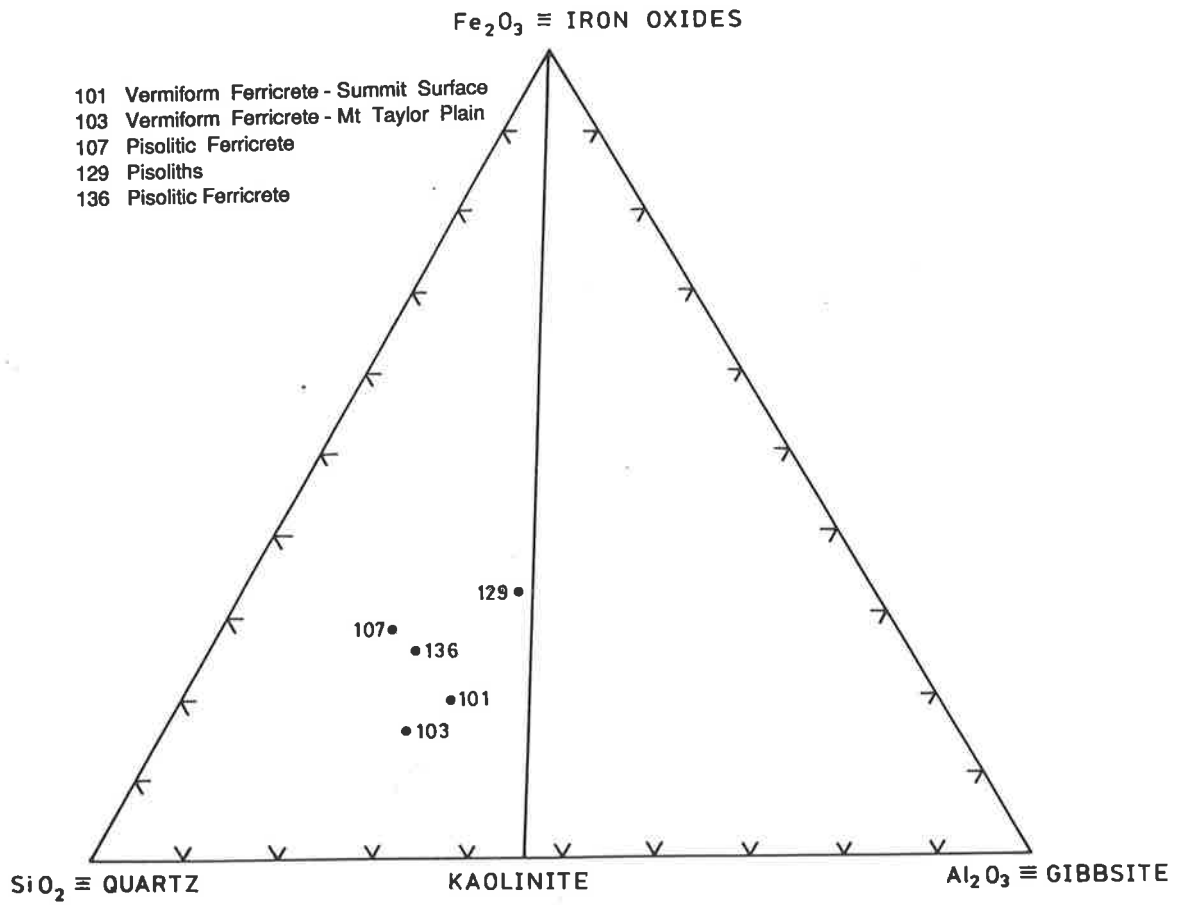


Figure 4.24 Cross section of the Mount Taylor Plain, showing its relationship to Miocene limestone.



**Figure 4.25** Triangular diagram of Mount Taylor Plain samples, with summit surface sample for comparison.

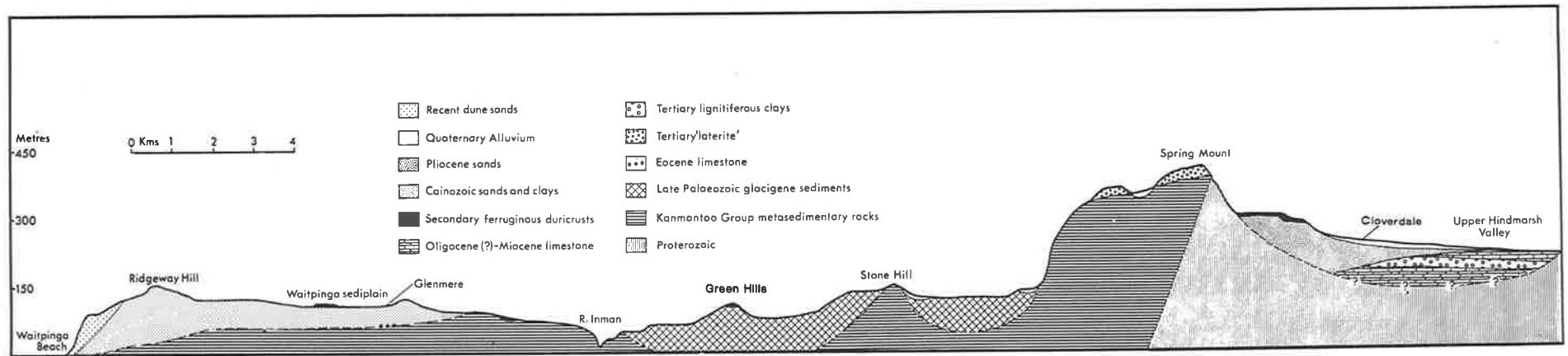


Figure 4.26 Cross section through Waitpinga, Green Hills to Upper Hindmarsh Valley (After Bourman, 1973).

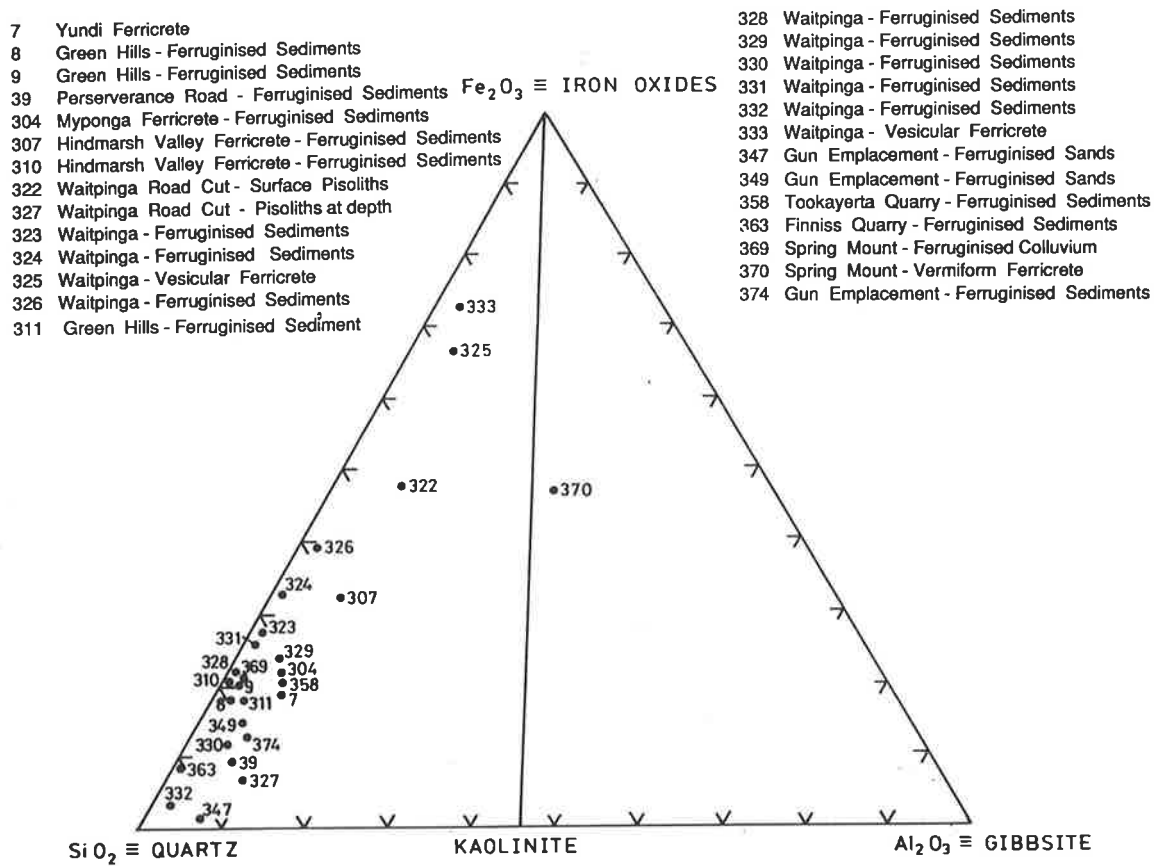


Figure 4.27 Triangular diagram of iron-impregnated sediments (clastic and organic) with samples of vermiform ferricrete (BOU 370) and pisoliths (BOU 322) for comparison.

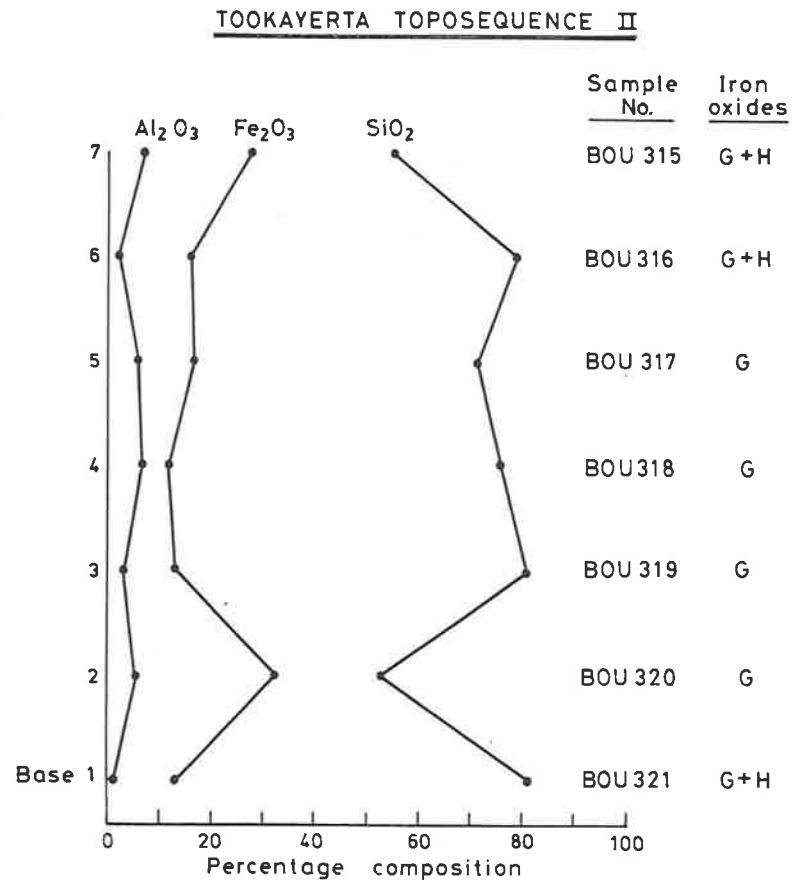
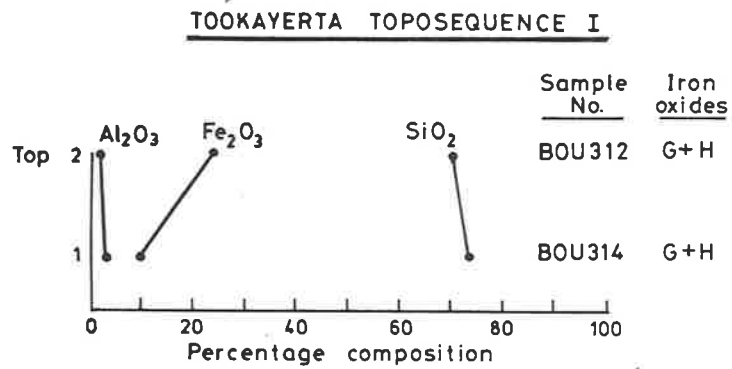


Figure 4.28 Graphs of major chemical compositions of ferricretes associated with toposequences in the Tookayerta Valley. Iron oxide mineralogy is shown also. (G=goethite; H=hematite).

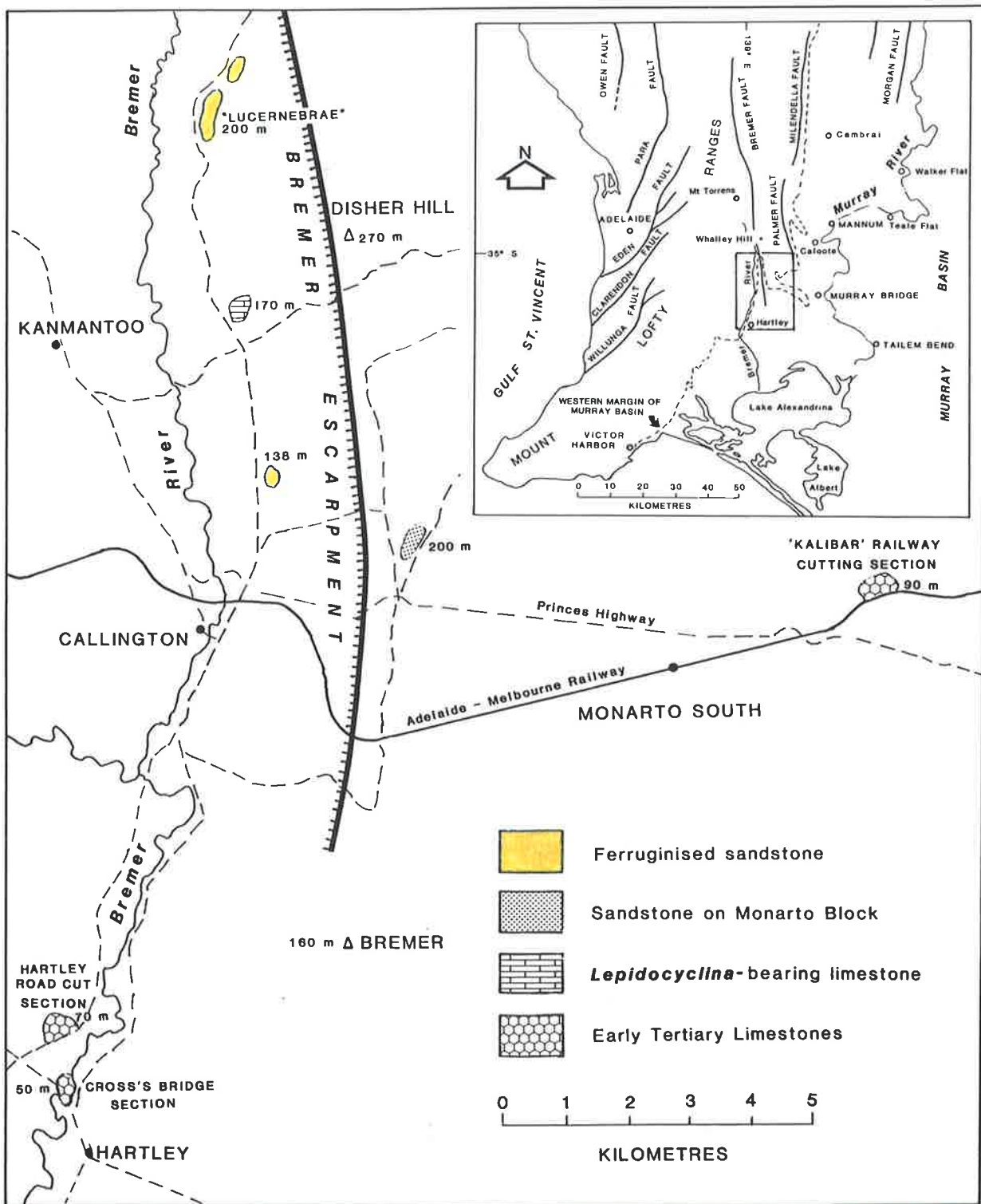


Figure 4.29 Map of Bremer Valley area showing the distribution of ferricretes in relationship to Tertiary limestones and topography.

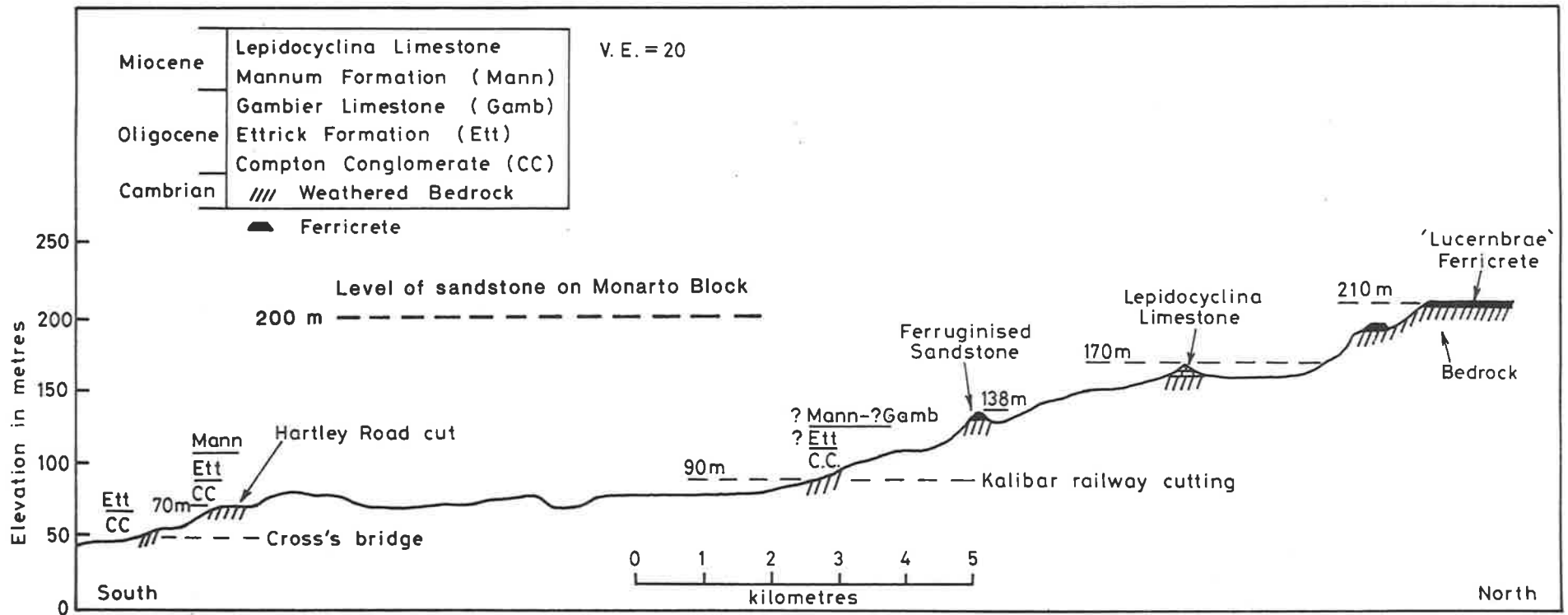


Figure 4.30 Long section through the Bremer Valley, showing the relationship of ferricretes to Tertiary limestones.

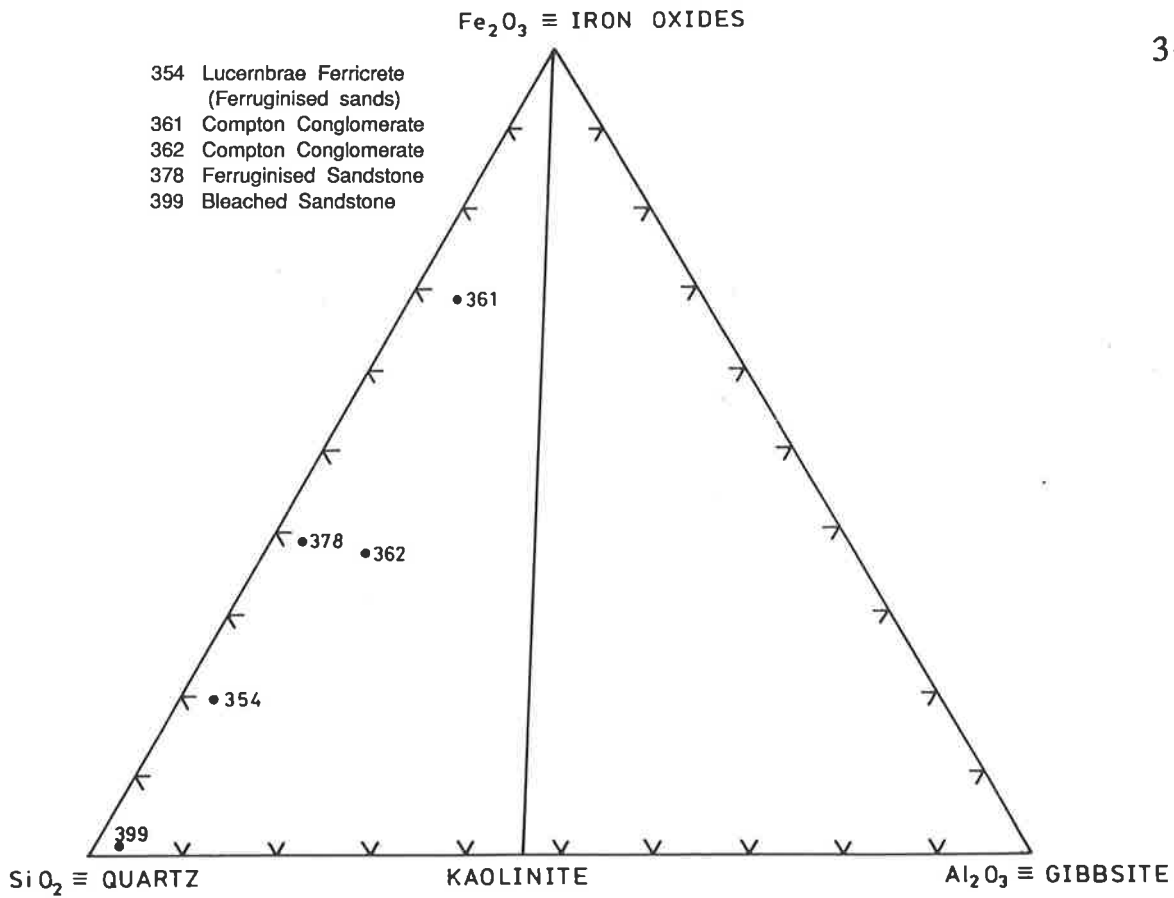


Figure 4.31 Triangular diagram of Bremer River samples.

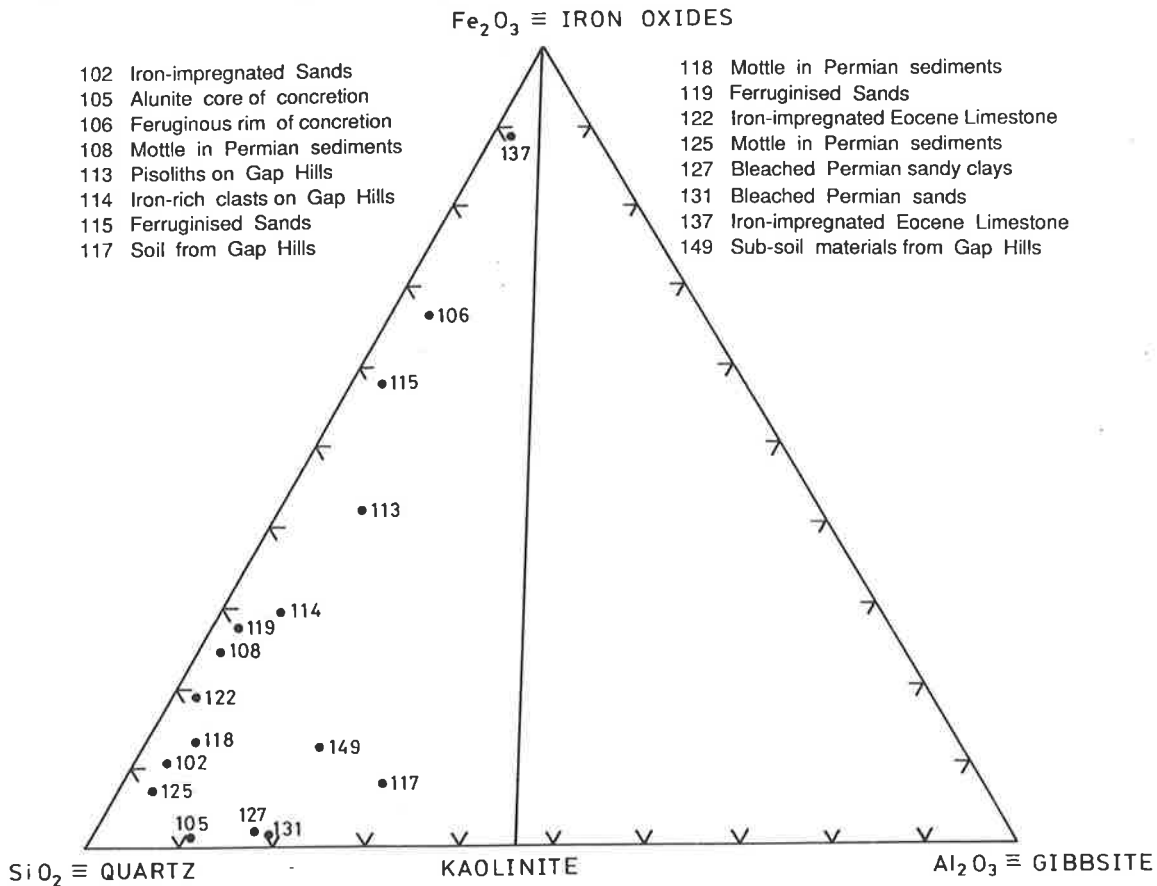


Figure 4.32 Triangular diagram of samples relevant to the timing of 'lateritisation' on Kangaroo Island.



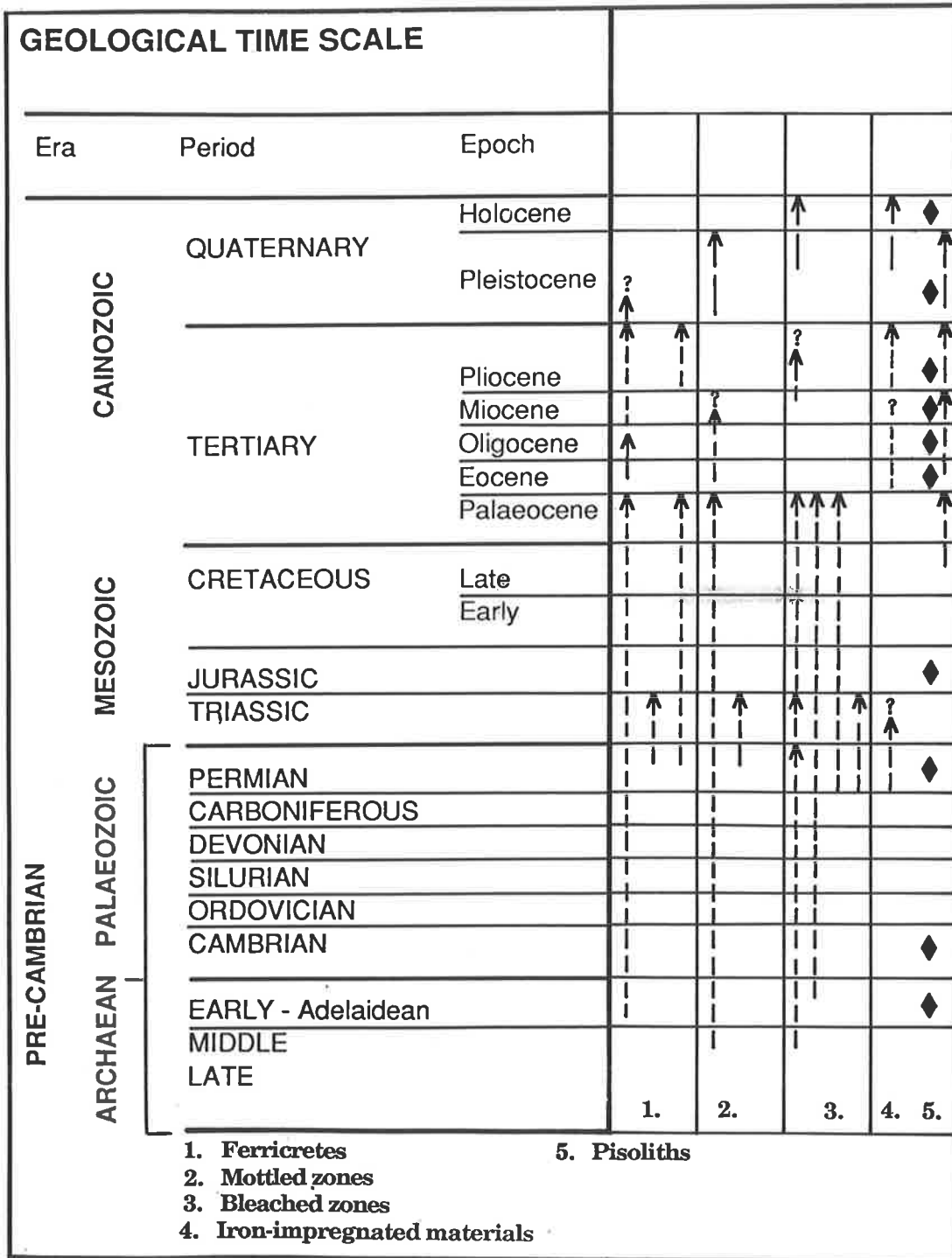


Figure 4.33 Diagram illustrating the lower ages of rocks and sediments overlain by ferricretes and pisoliths, and affected by mottling, bleaching and diffuse iron-impregnation. Where possible the upper age limits of these features are indicated by arrows.

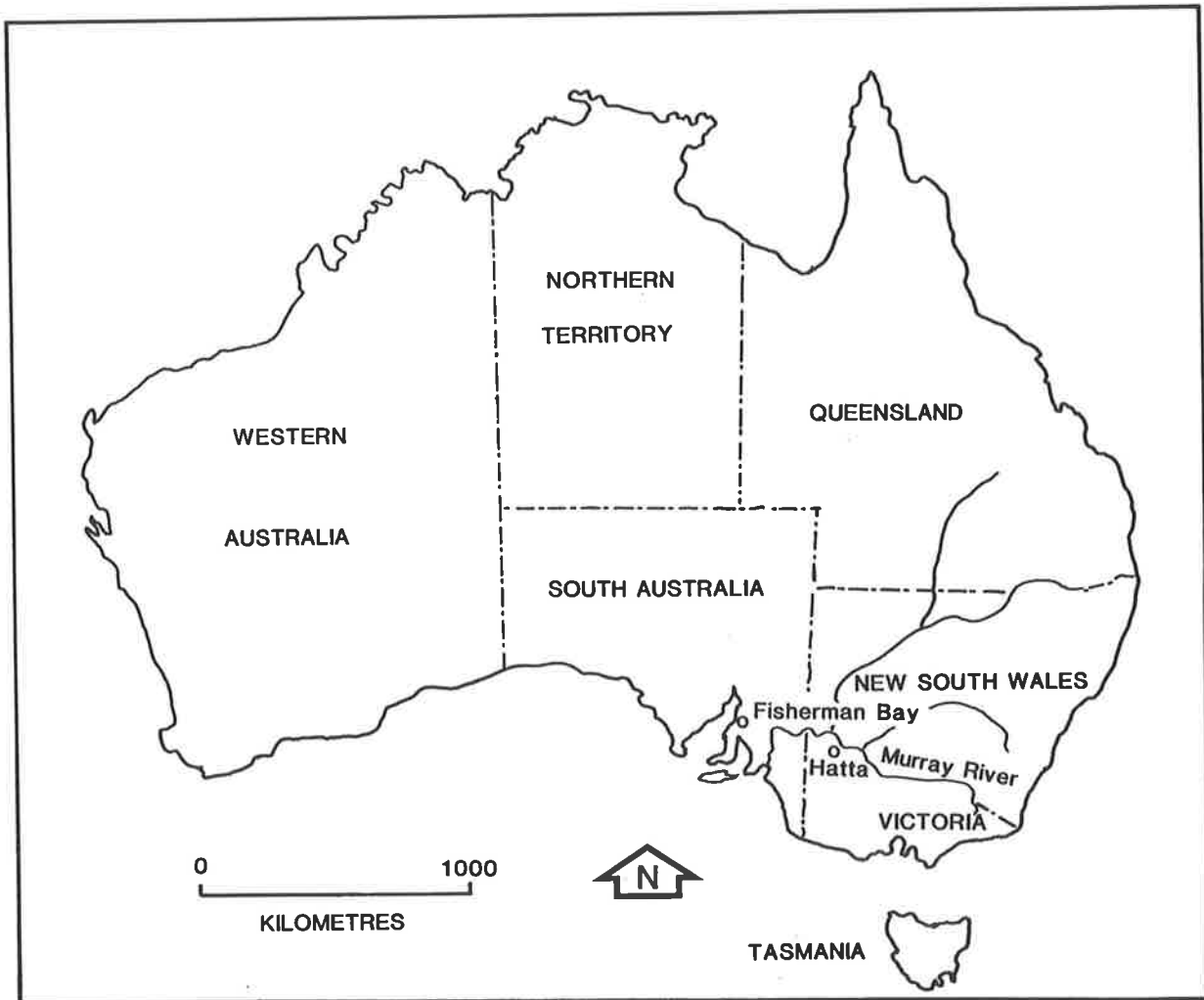


Figure 4.34 Location map of Fishermans Bay and the Hatta Lakes.

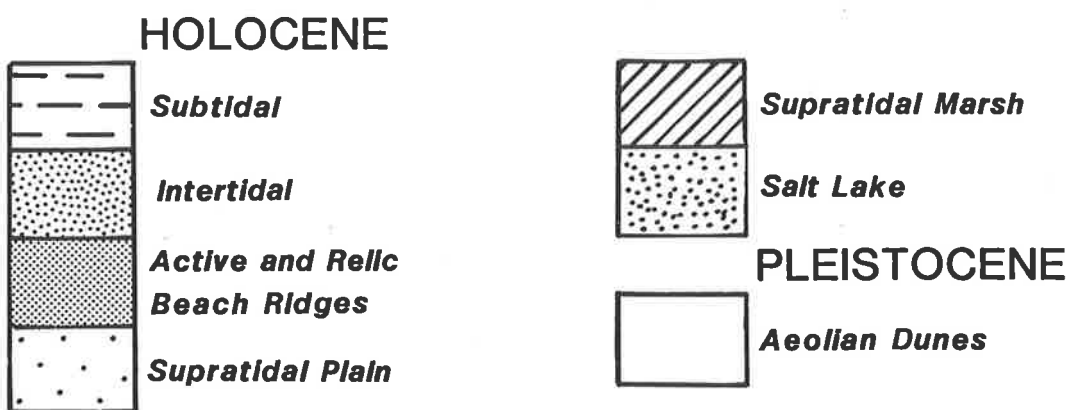
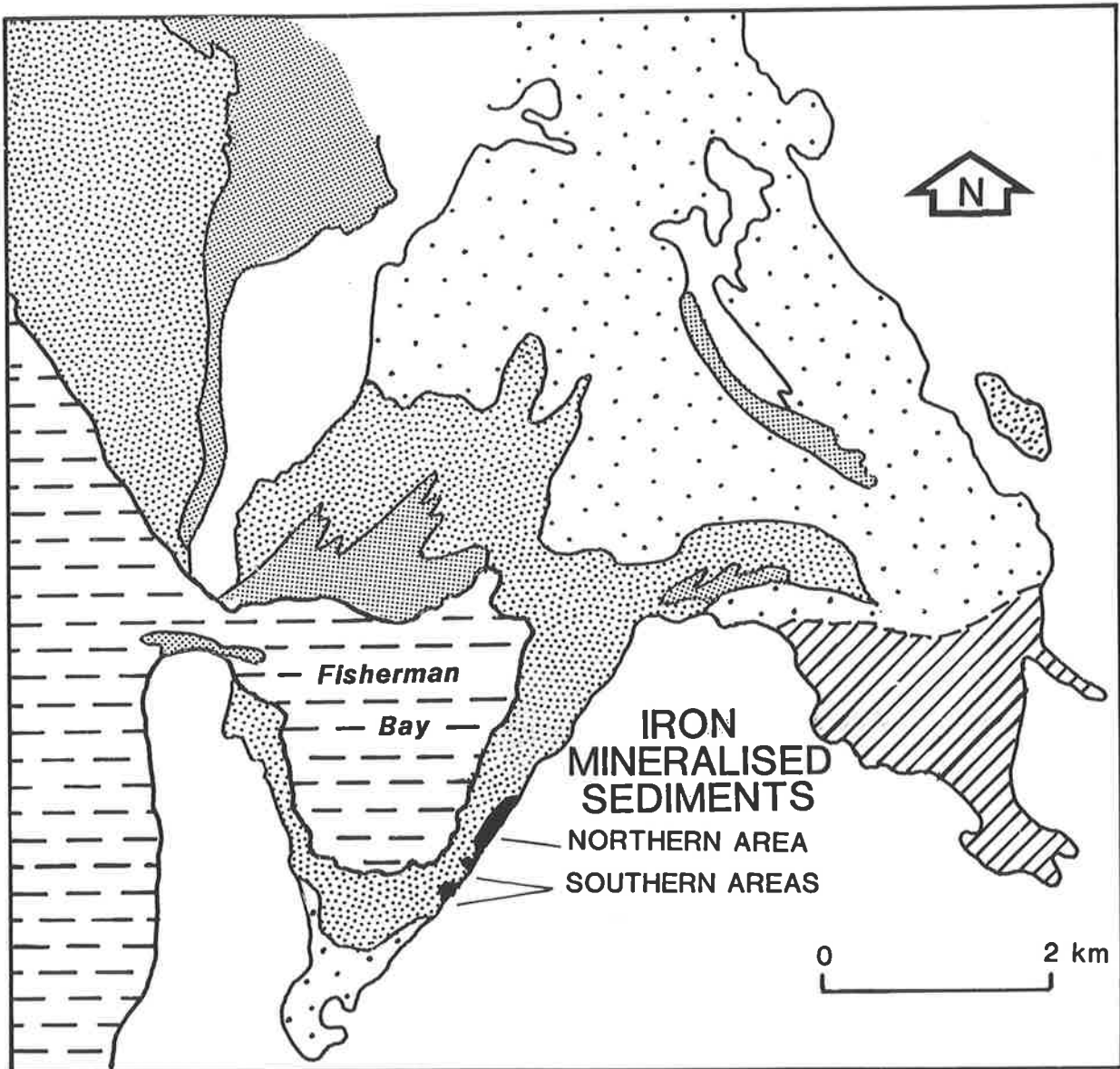


Figure 4.35 Location of iron mineralised sediments, Fisherman Bay. (After Ferguson *et al.*, 1983).

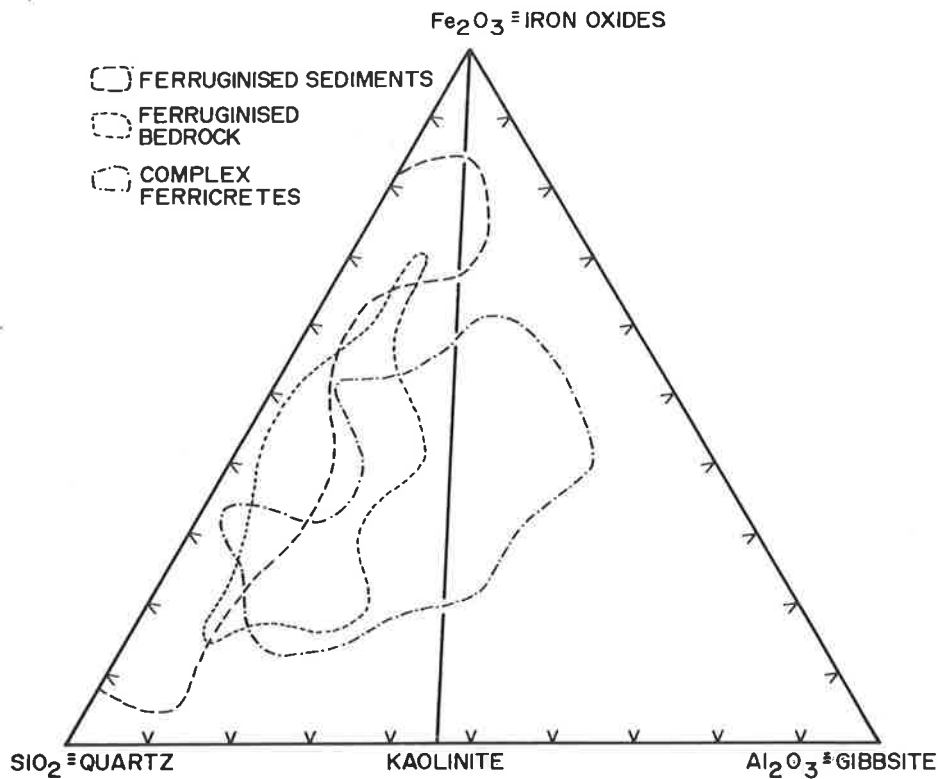


Figure 5.1 Ternary diagram showing three different categories of ferricretes.

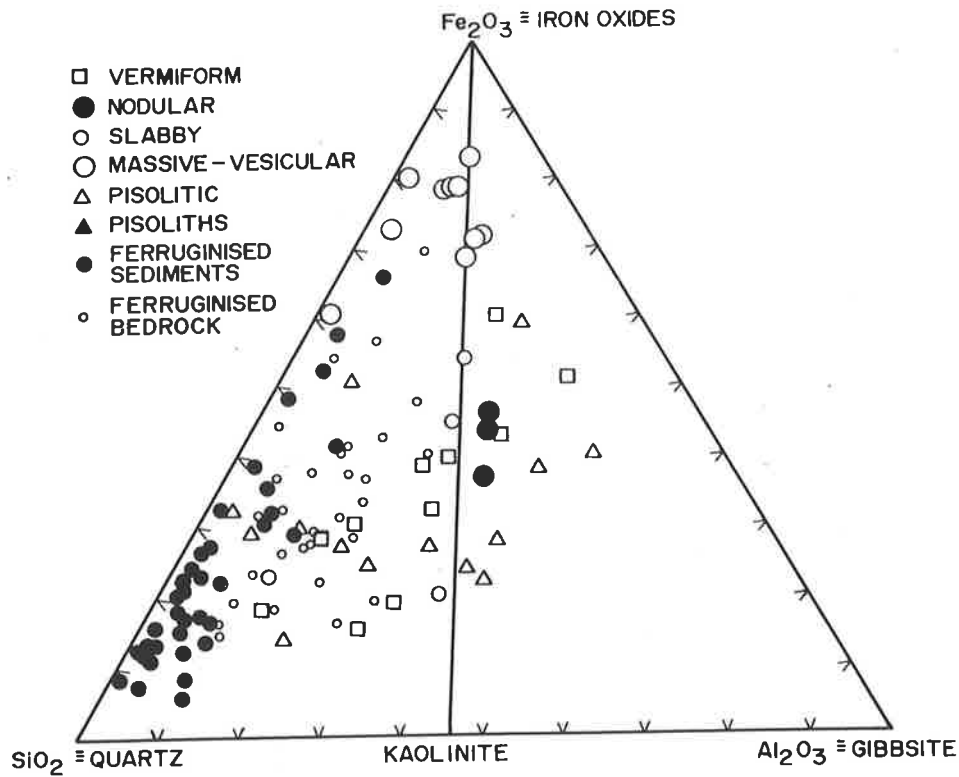


Figure 5.2 Ternary diagram of bulk chemistry of all types of ferricretes.

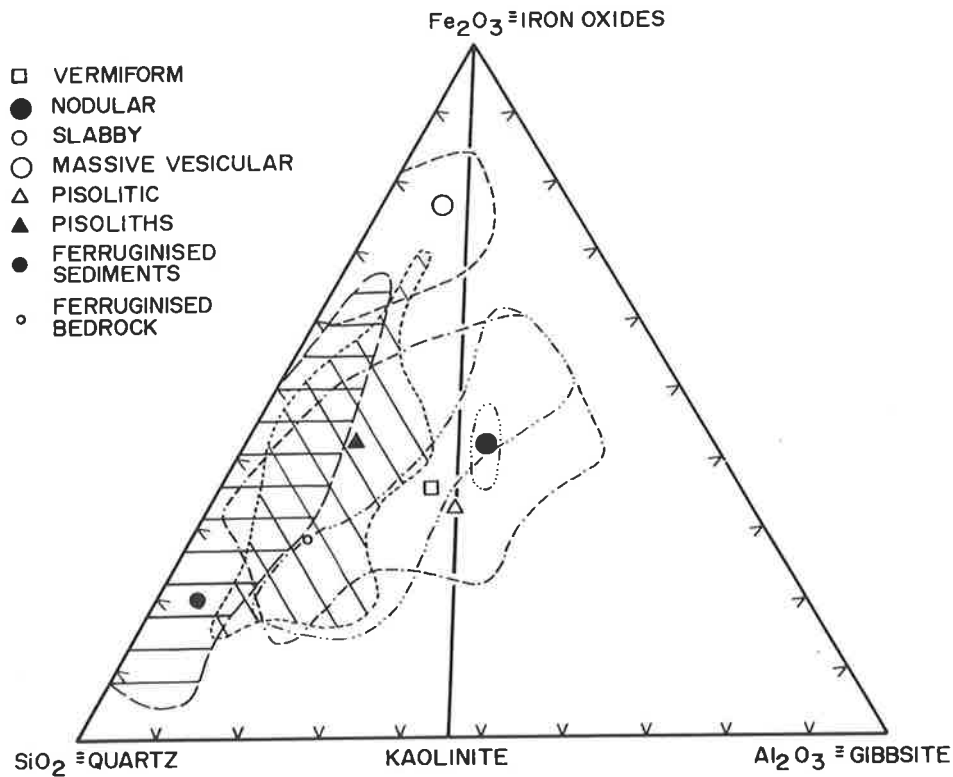


Figure 5.3 Ternary diagram showing mean plot of ferricrete types and their ranges.

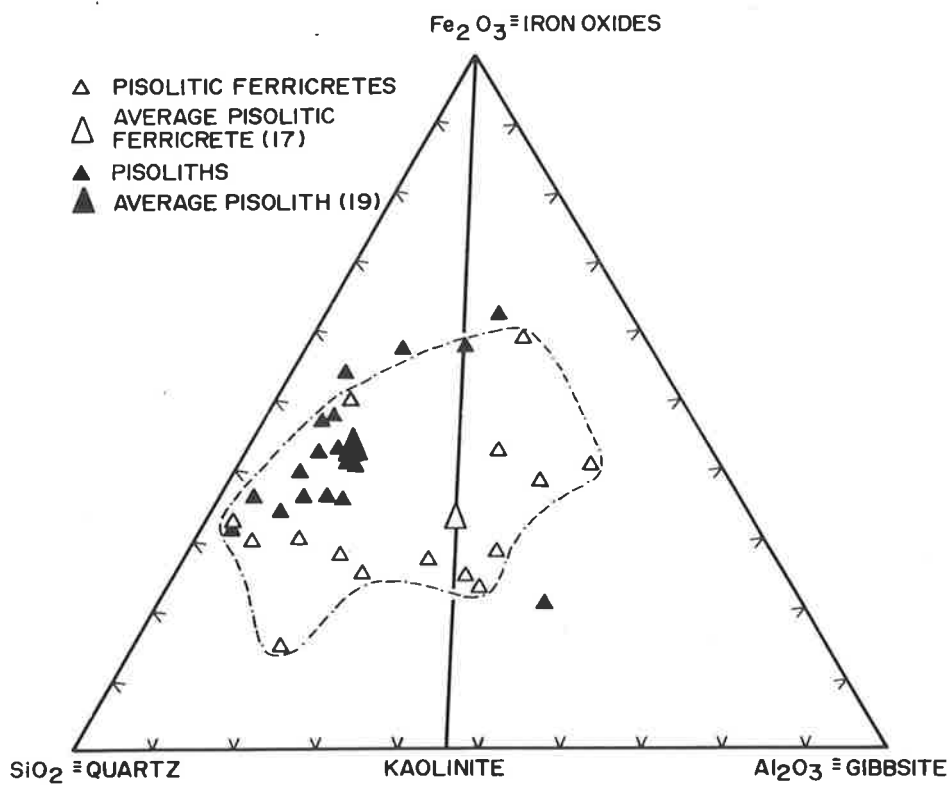


Figure 5.4 Ternary plot of pisolitic ferricretes and individual pisoliths.

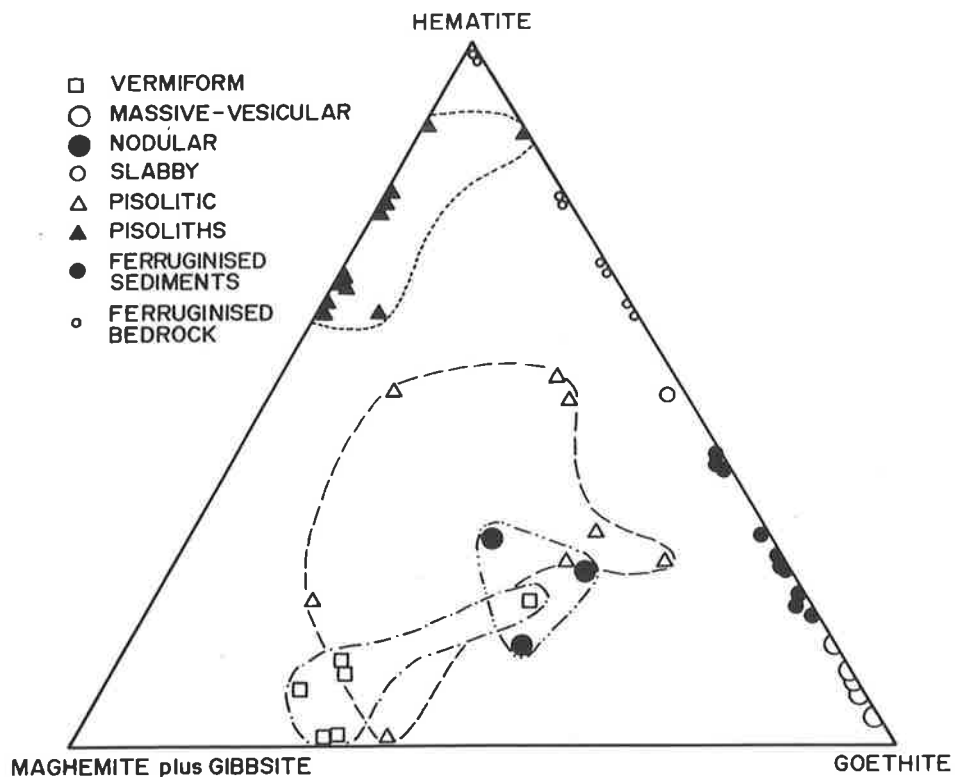


Figure 5.5 Triangular diagram showing variations in ferricrete mineralogy.

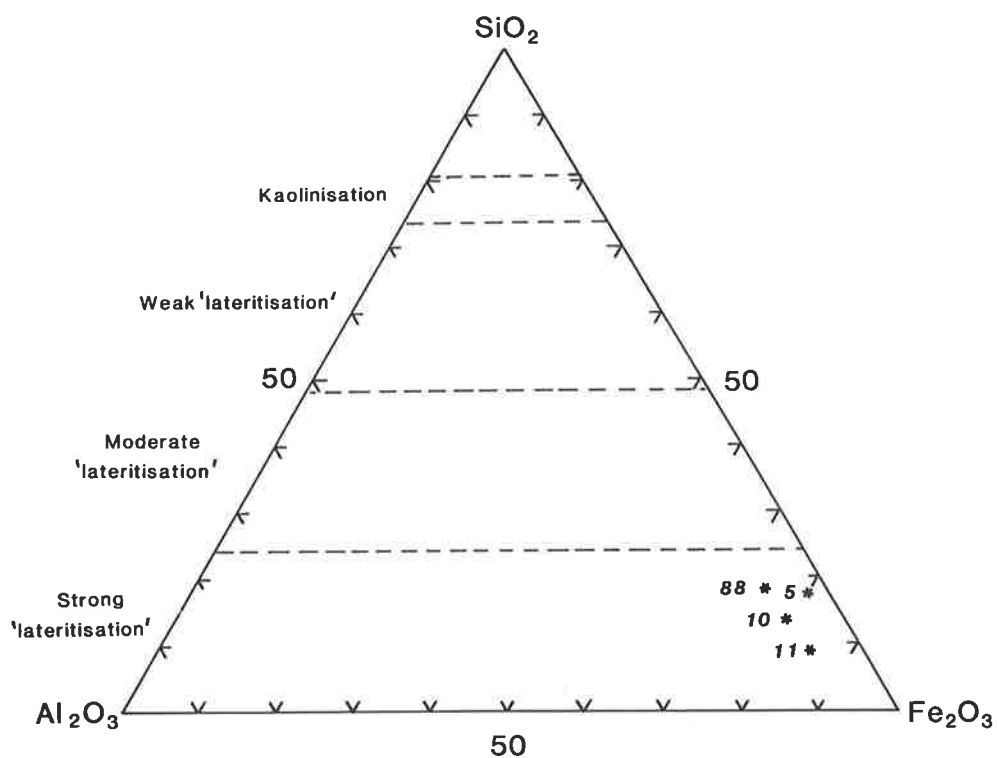


Figure 5.6 Triangular diagram of Schellmann (1981), showing different degrees of 'lateritisation'.

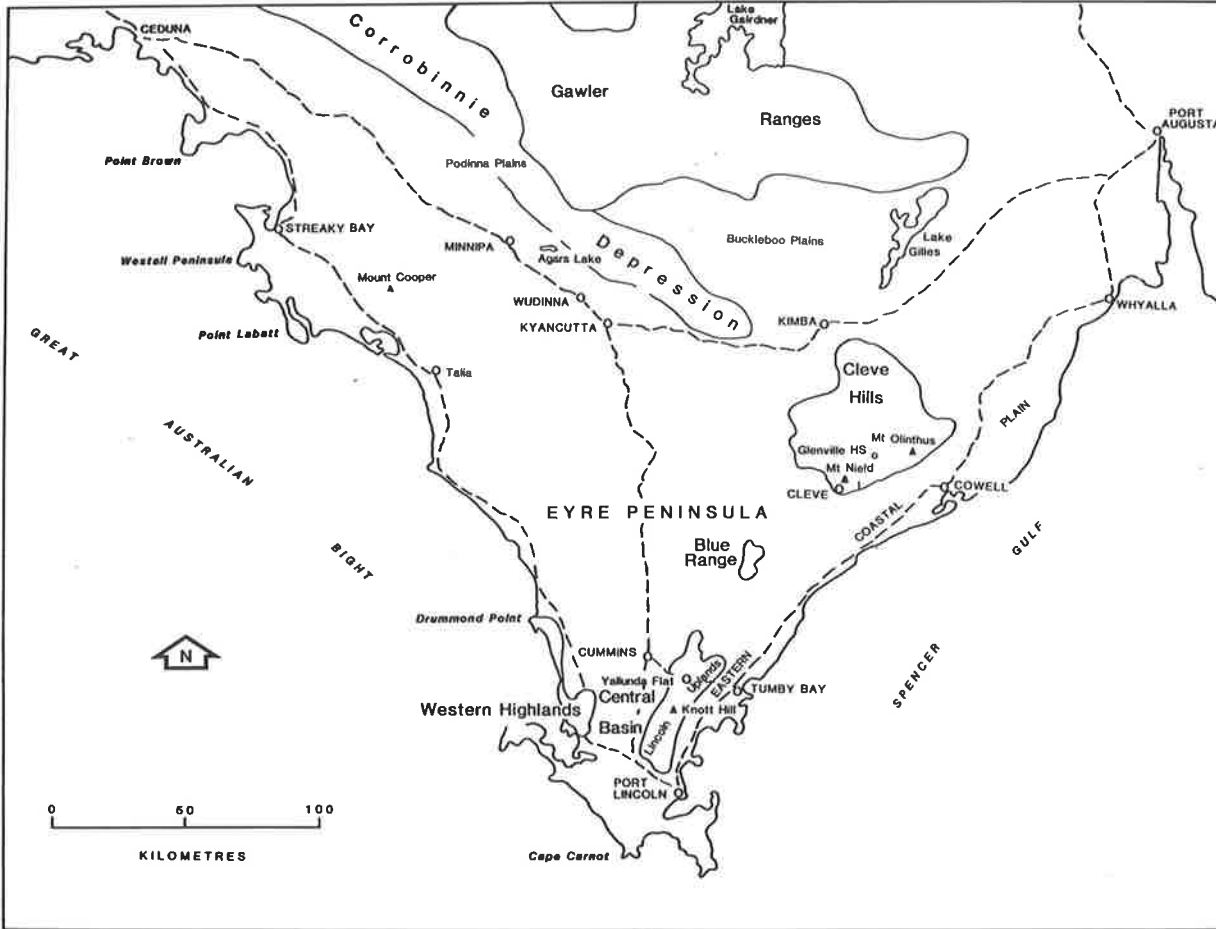


Figure 6.1 Location map of study sites on northern Eyre Peninsula.

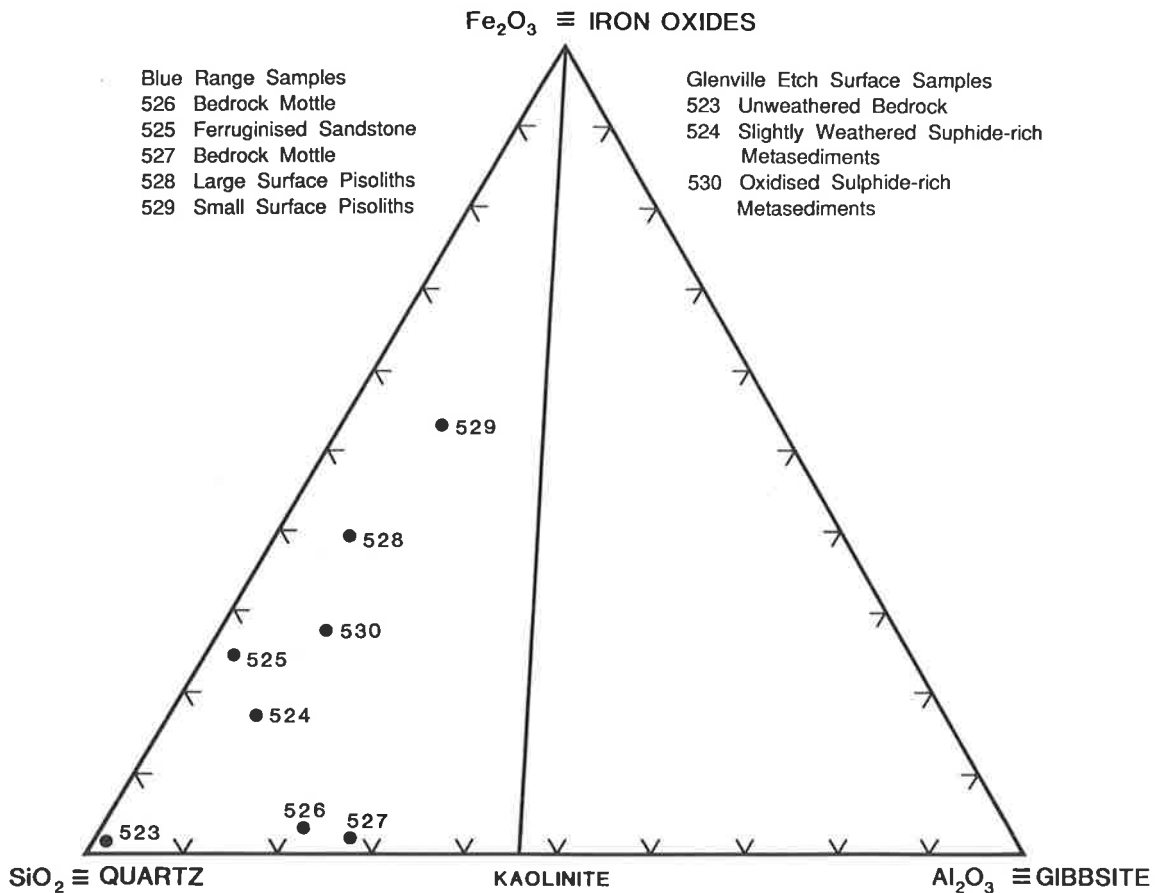
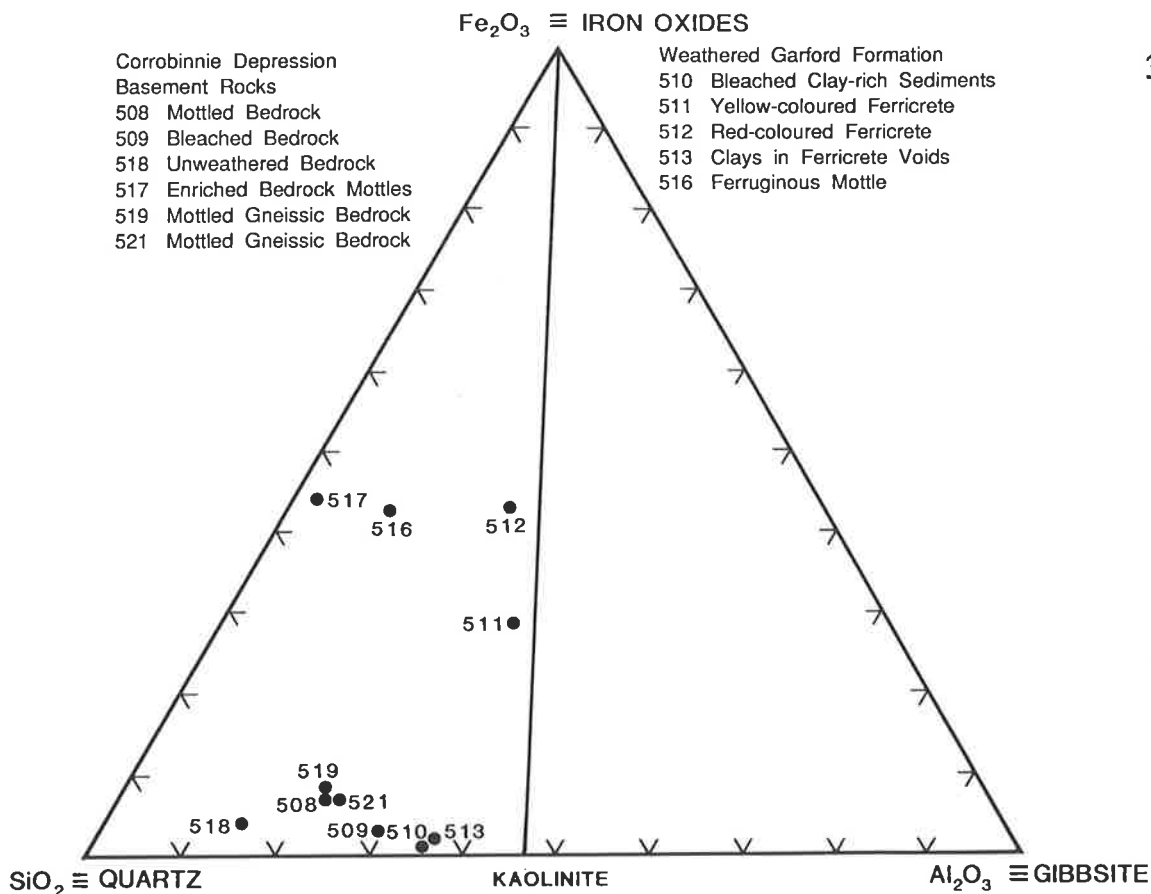
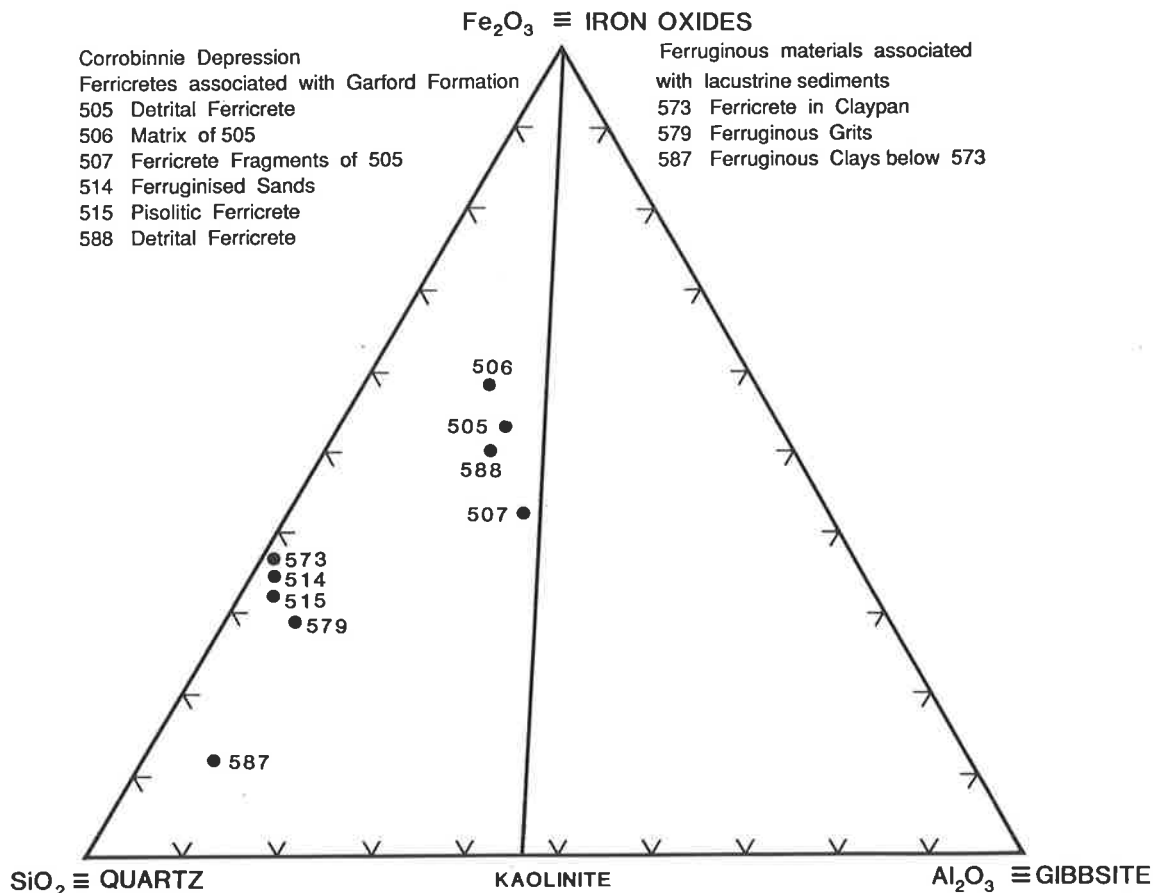


Figure 6.2 Triangular diagram of samples from the Blue Range and the so-called Glenville etch surface of Twidale *et al.* (1976).



**Figure 6.3** Triangular diagram of samples from the Corrobinnie Depression (weathered Precambrian basement rocks and Eocene Garford Formation sediments).



**Figure 6.4** Triangular diagram of pisolitic ferricretes from the Corrobinnie Depression.



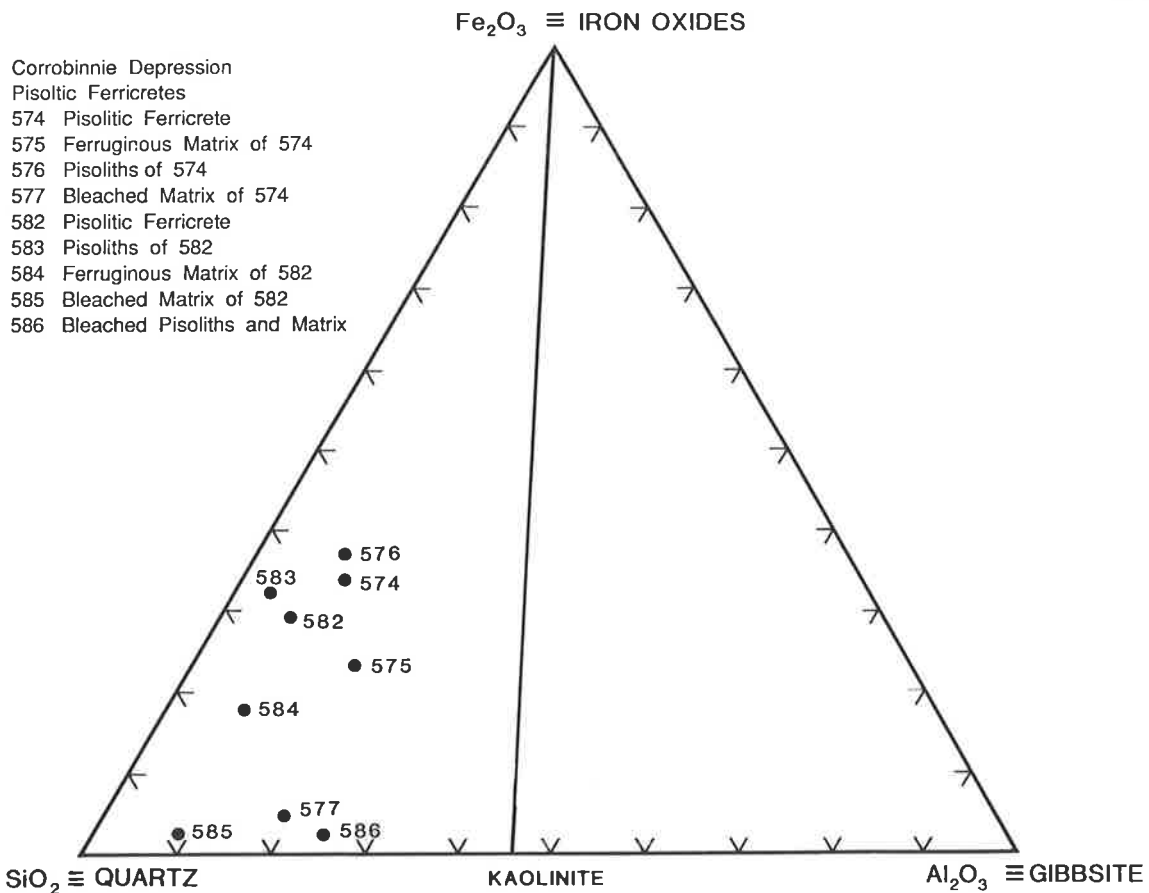


Figure 6.5 Triangular diagram of ferricretes and pisoliths from the Corrobinnie Depression.

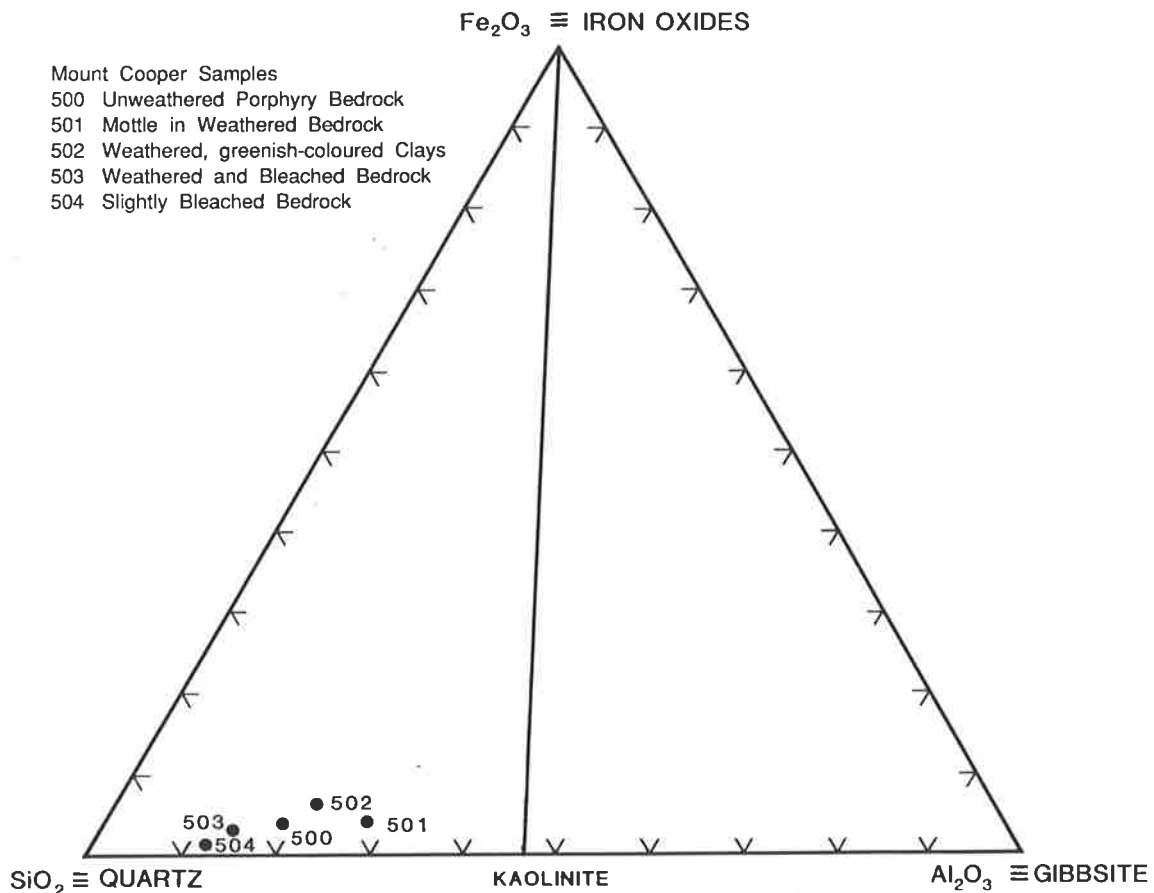


Figure 6.6 Triangular diagram of samples from Mount Cooper.

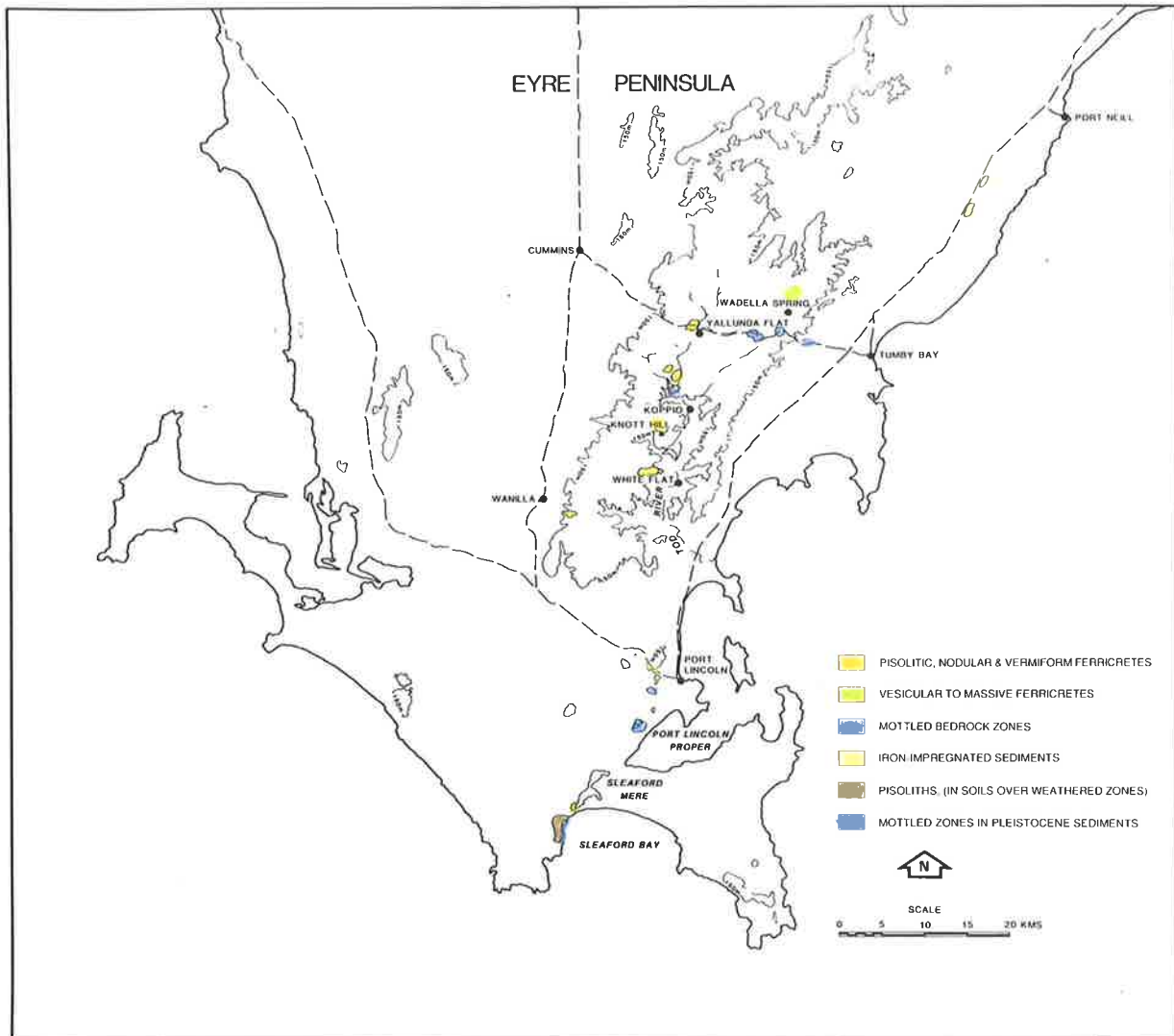


Figure 6.7 Location map of ferricrete sites studied in southern Eyre Peninsula.

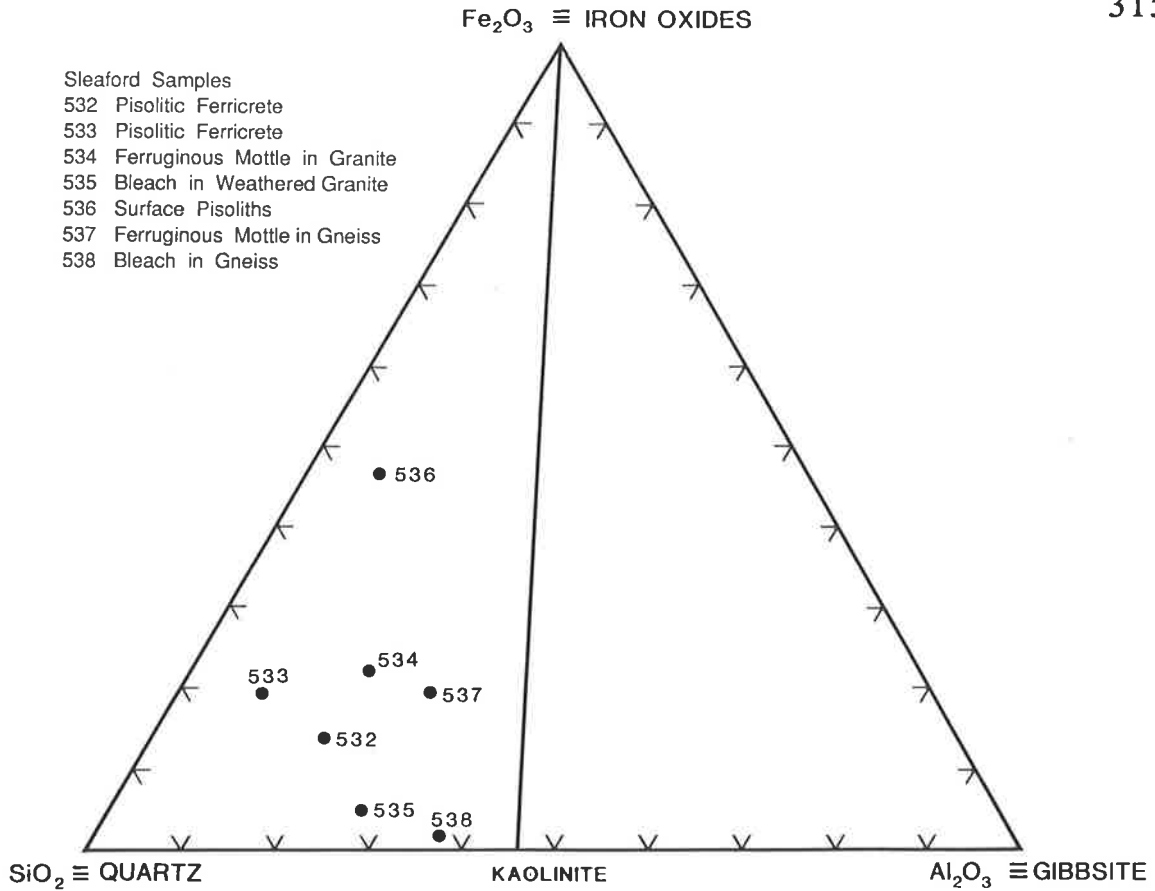


Figure 6.8 Triangular diagram of samples from the Sleaford Bay area.

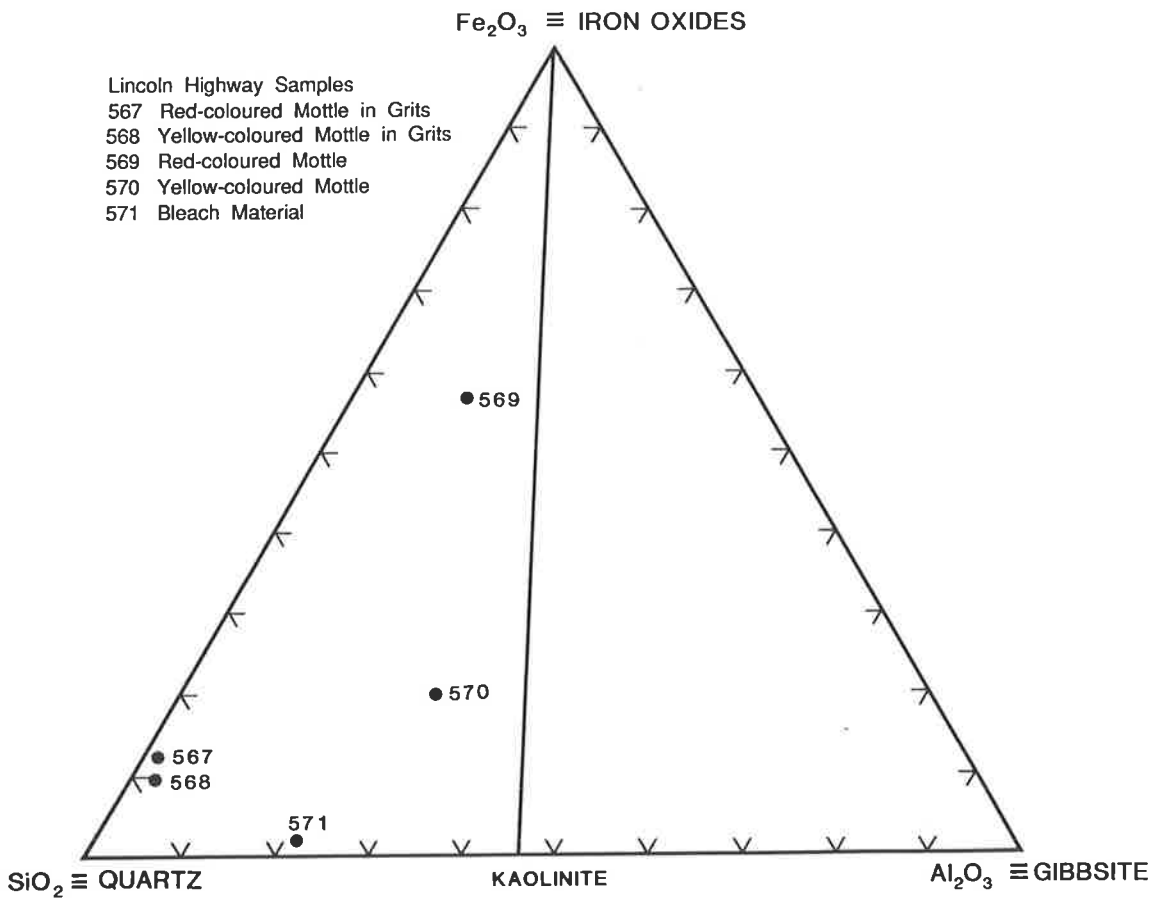


Figure 6.9 Triangular diagram of samples from the Lincoln Highway.

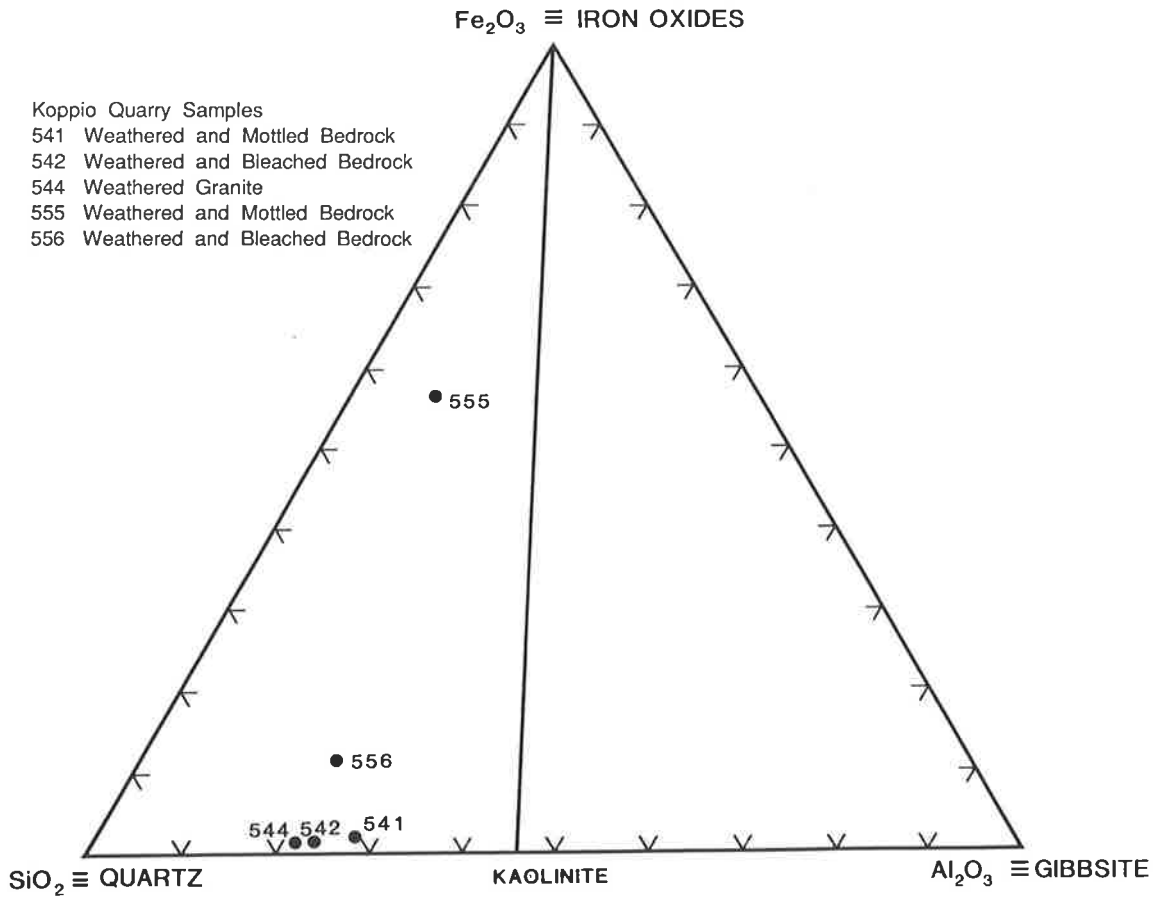


Figure 6.10 Triangular diagram of samples of weathered and mottled bedrock from the Koppio quarry site.

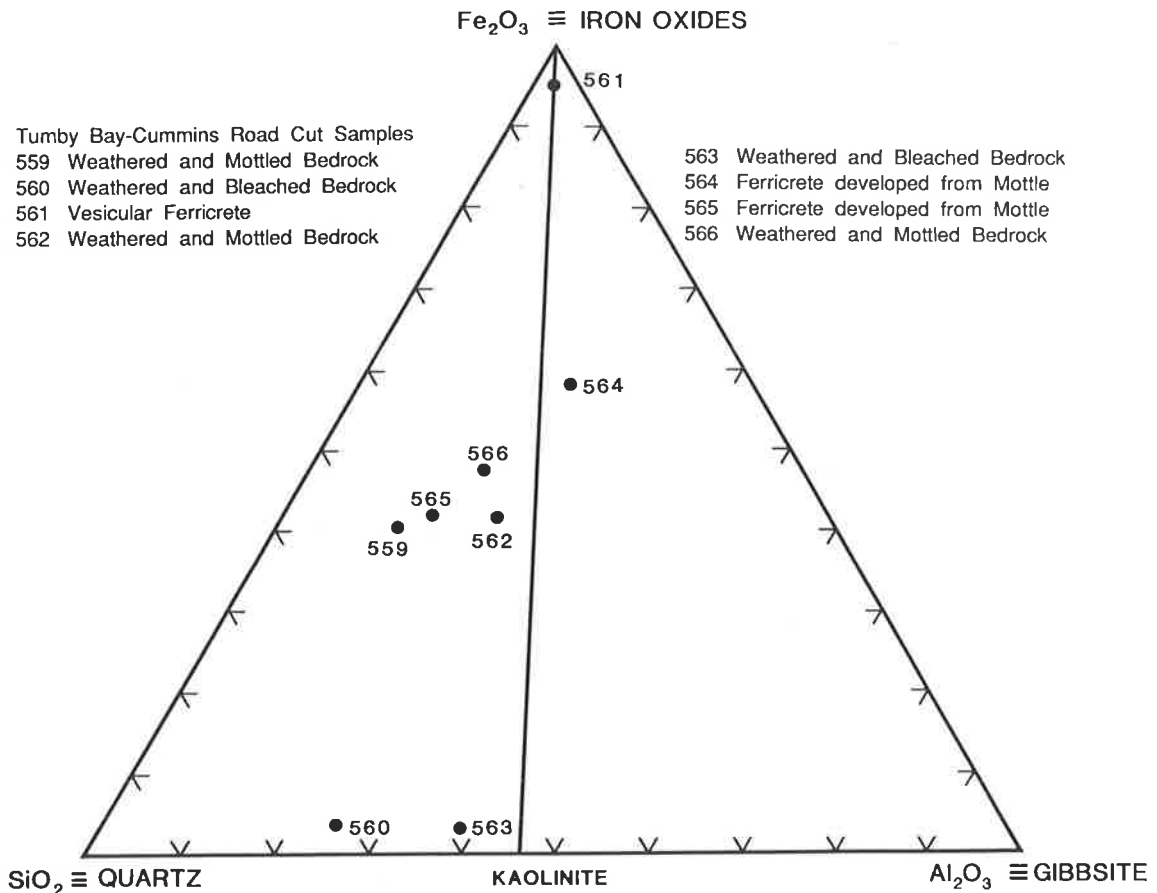


Figure 6.11 Triangular diagram of samples from road cuts on the Tumby Bay-Cummins Road.

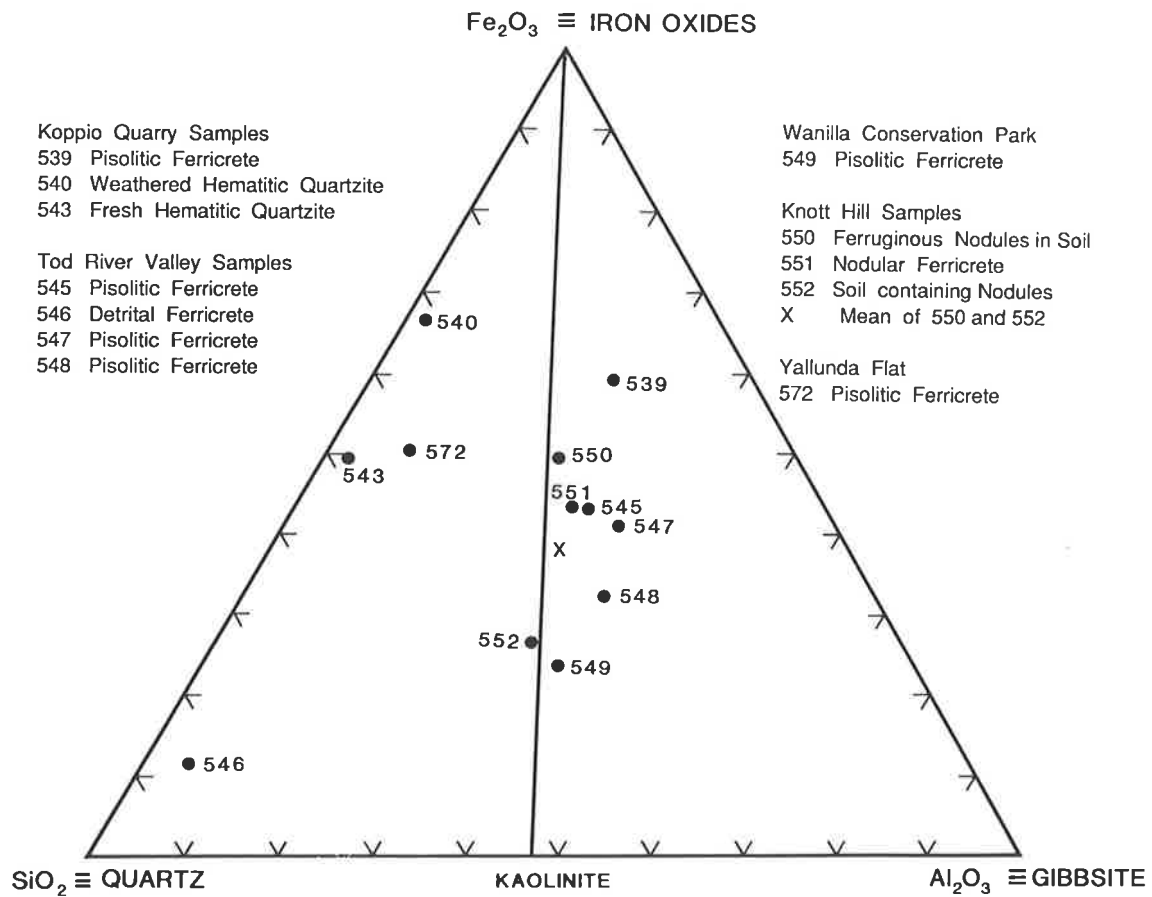


Figure 6.12 Triangular diagram of ferricrete samples from the Koppio Quarry site, Tod River Valley, Wanilla Conservation Park, Knott Hill and Yallunda Flat.

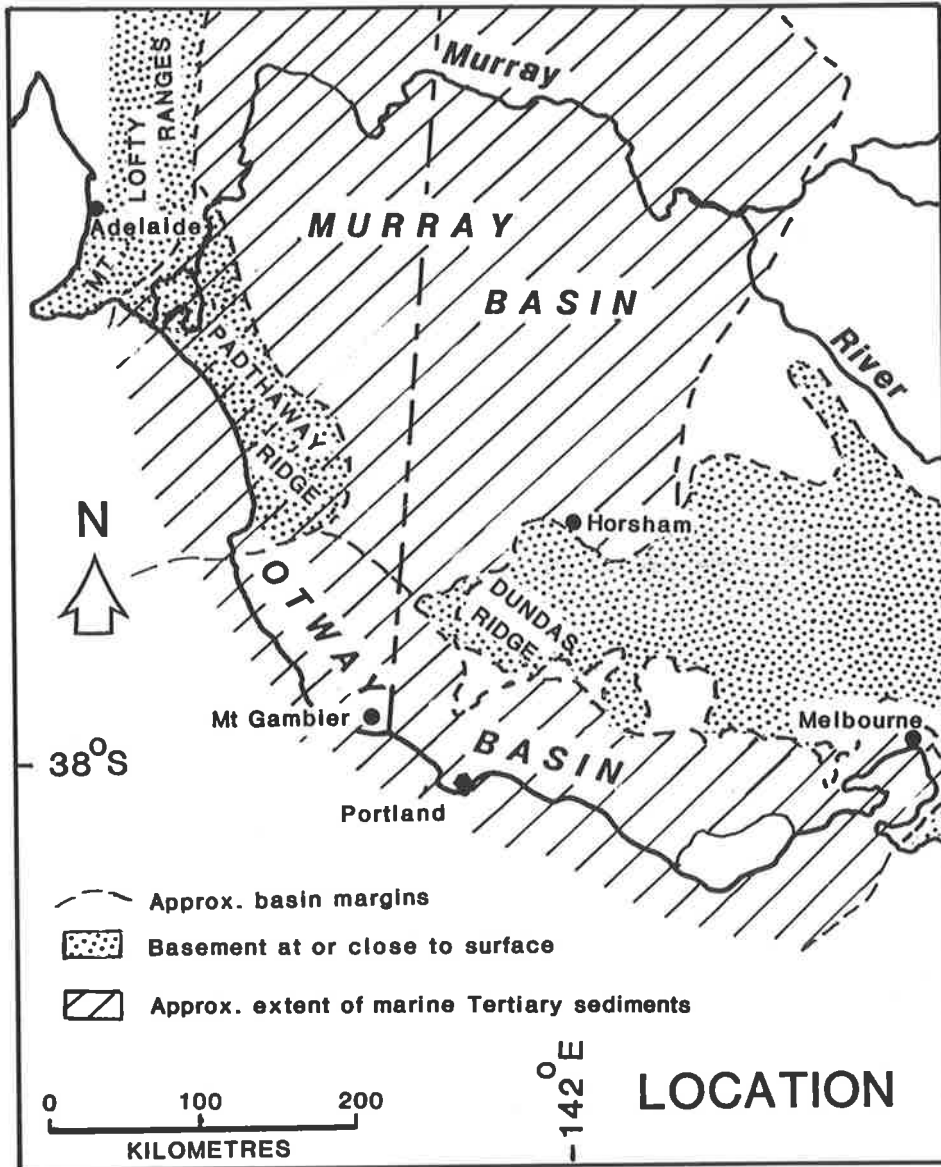


Figure 7.1 Location of the Otway Basin.

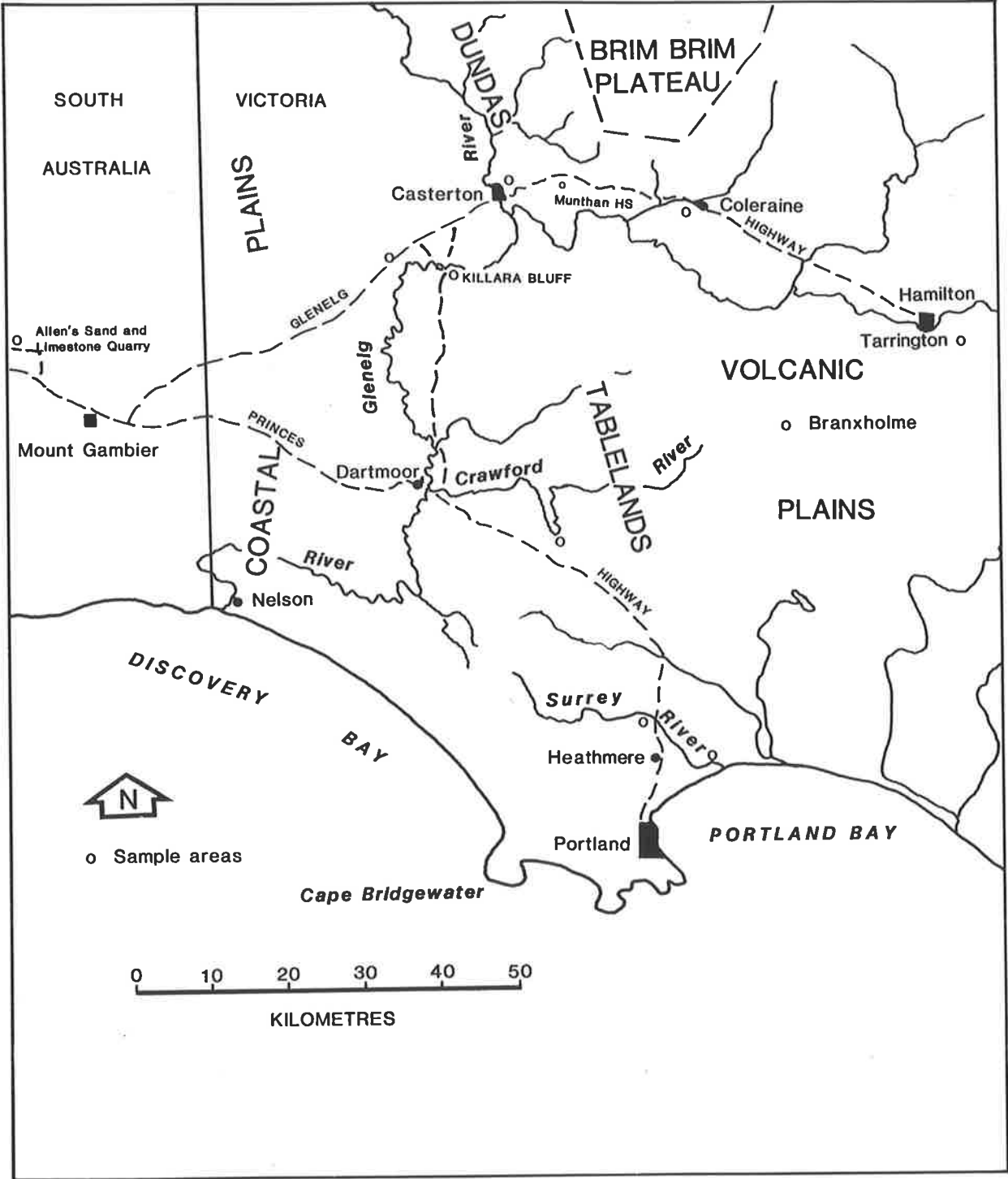


Figure 7.2 Location of sample sites in the western Otway Basin.

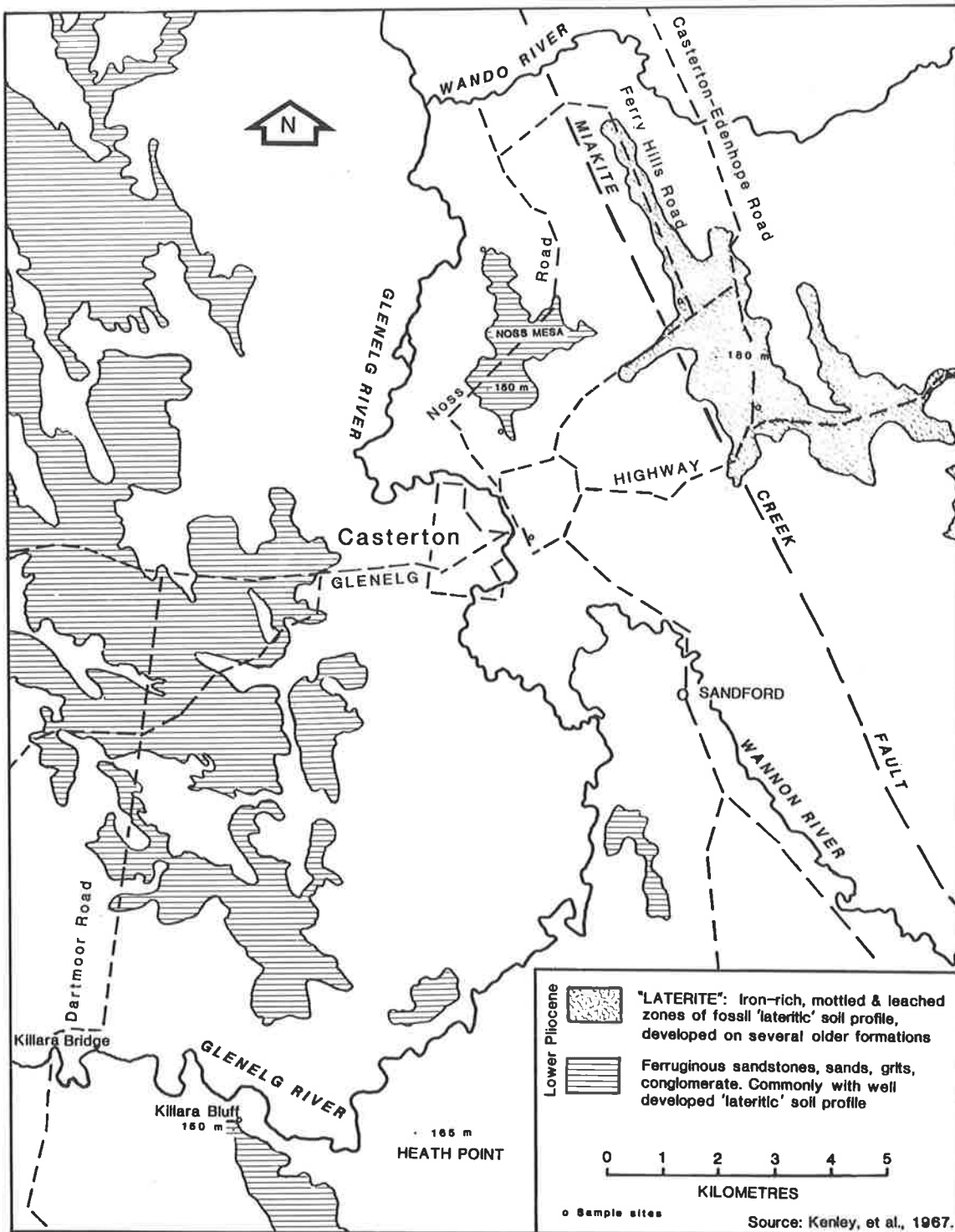


Figure 7.3 Location of sample sites in the Casterton area.



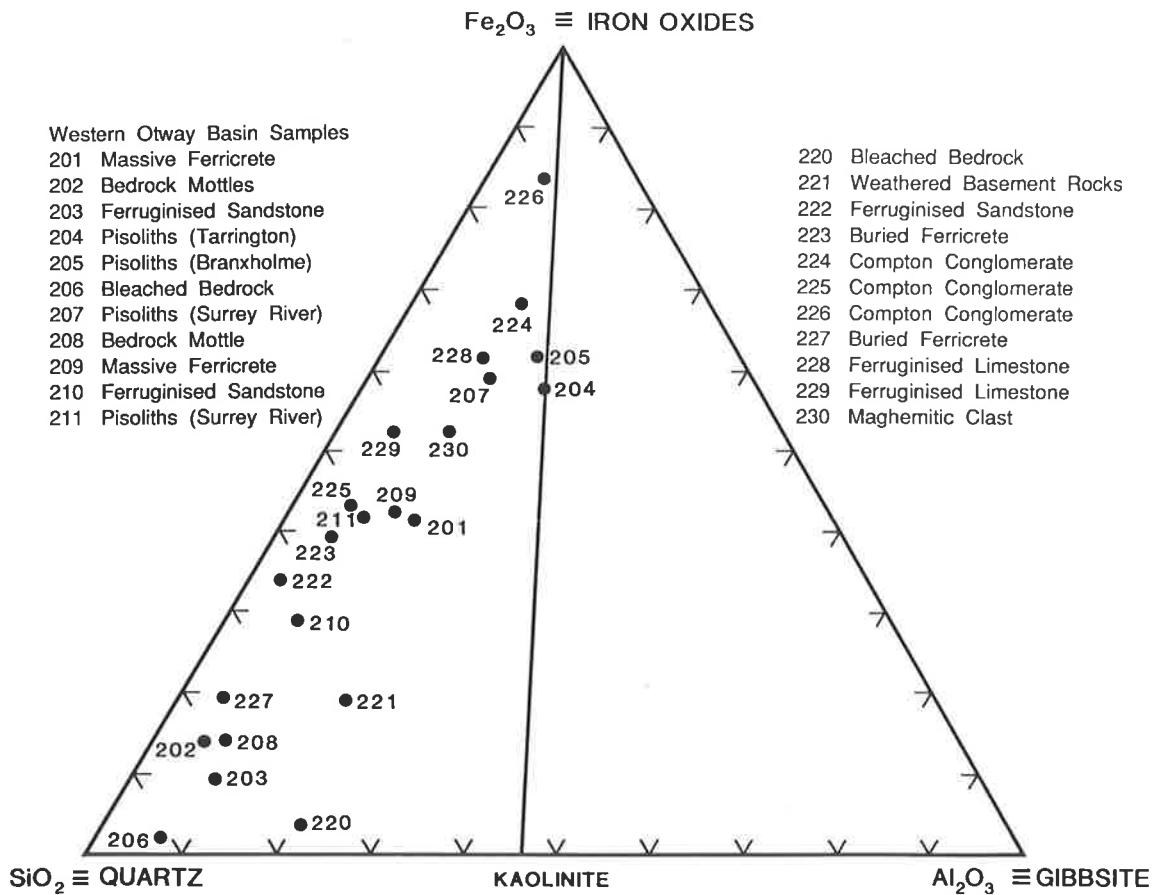


Figure 7.4 Triangular diagram of samples from the western Otway Basin.

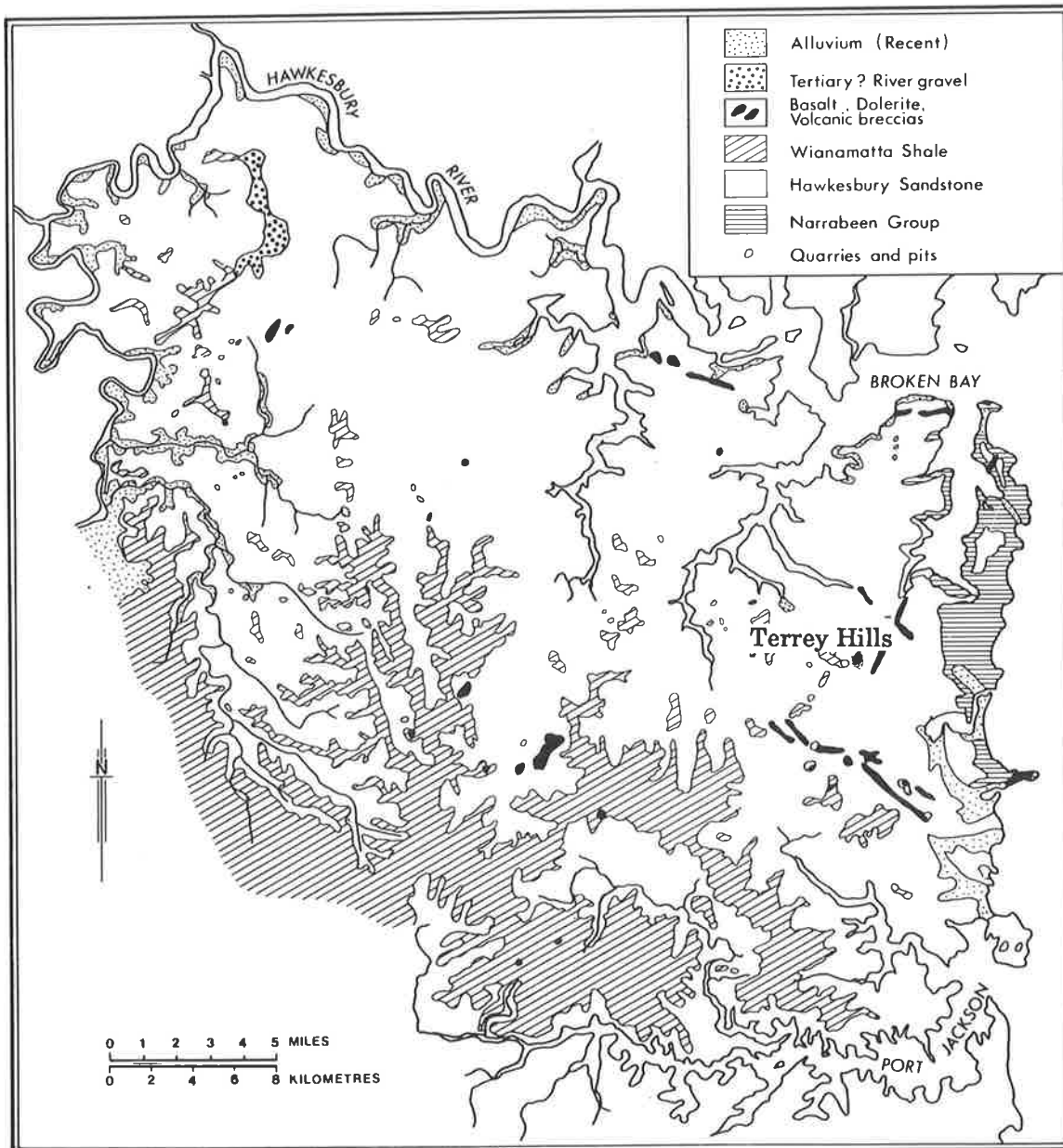


Figure 8.1 Geology of the Sydney area (After Faniran, 1971).

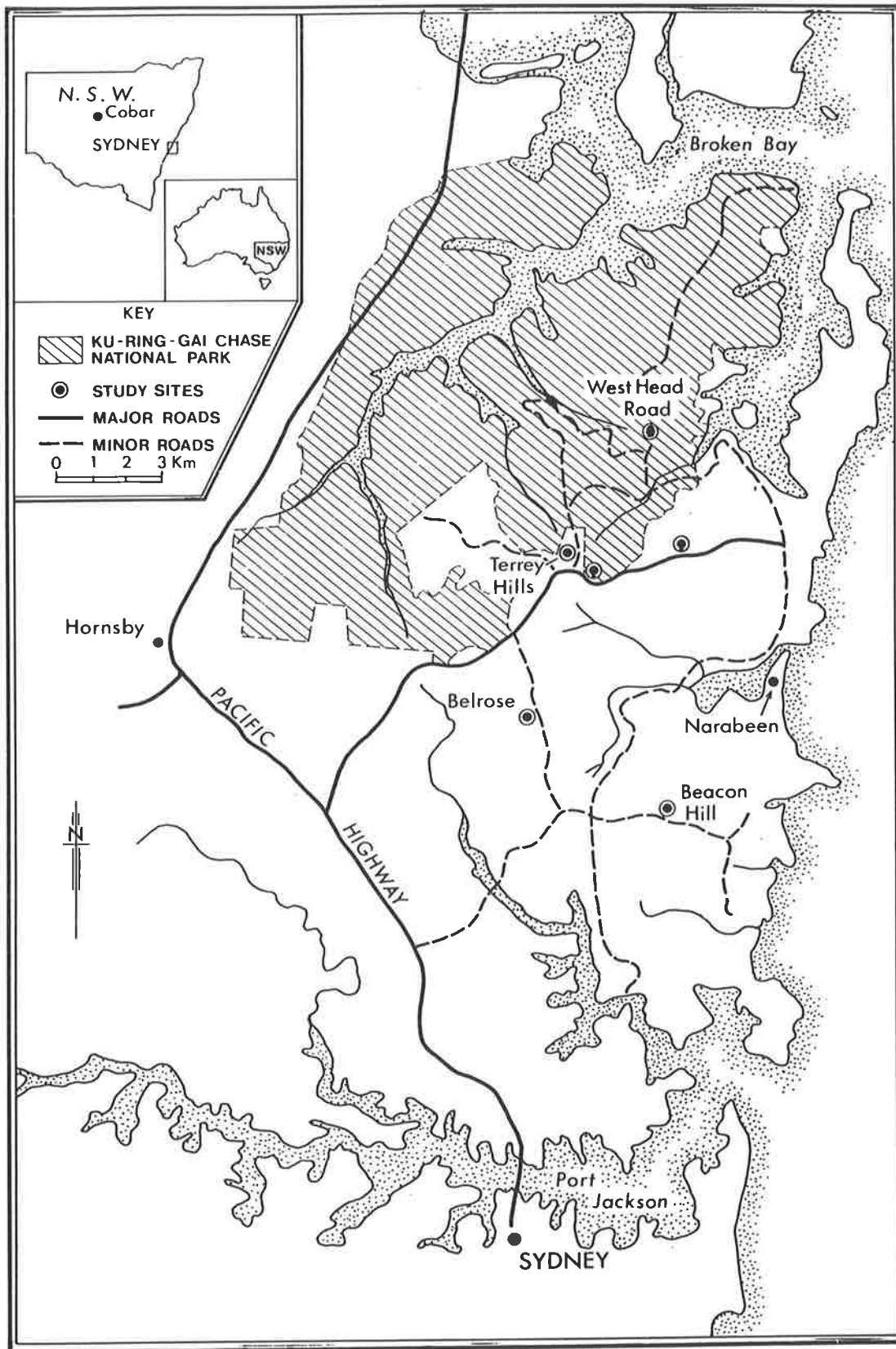


Figure 8.2 Location of study sites in the North Sydney area (After Hunt *et al.*, 1977).

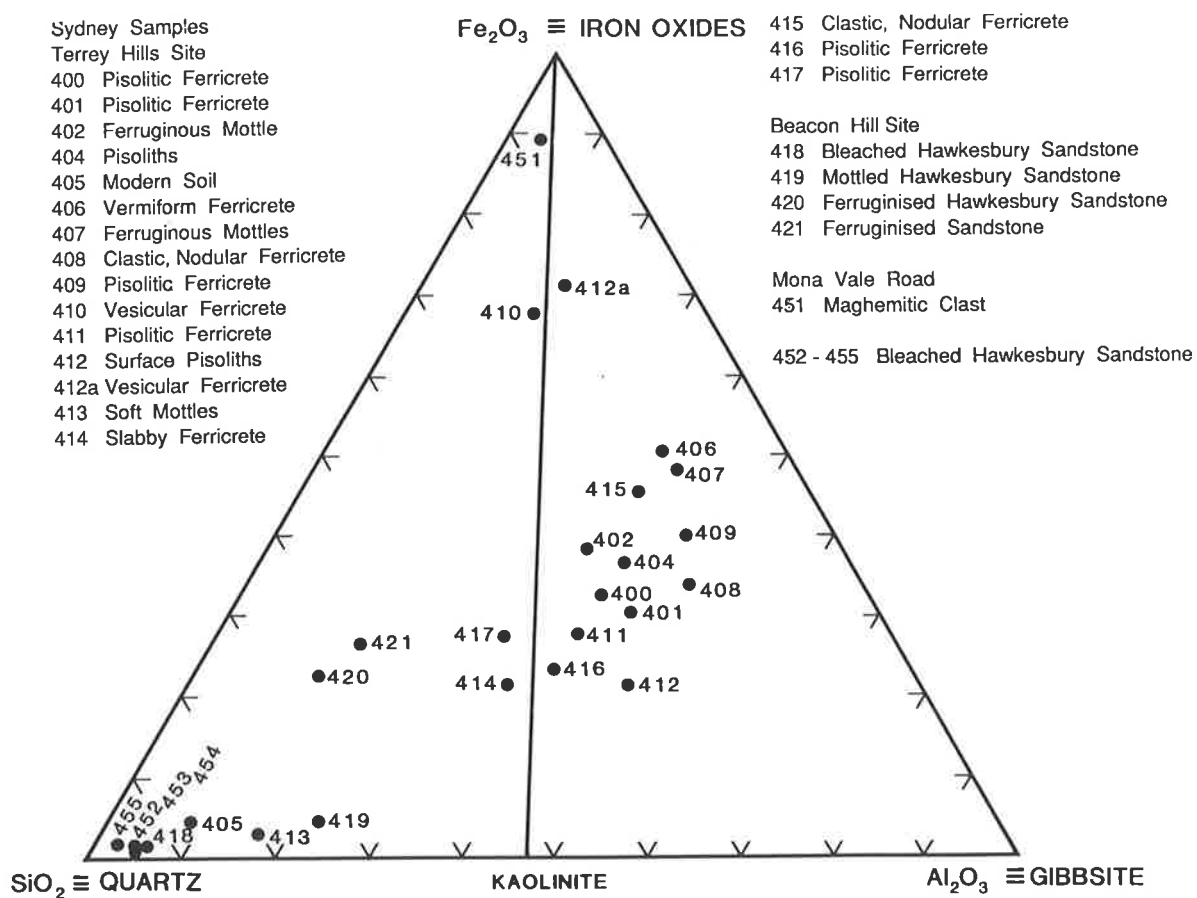


Figure 8.3 Triangular diagram of samples from the North Sydney area.

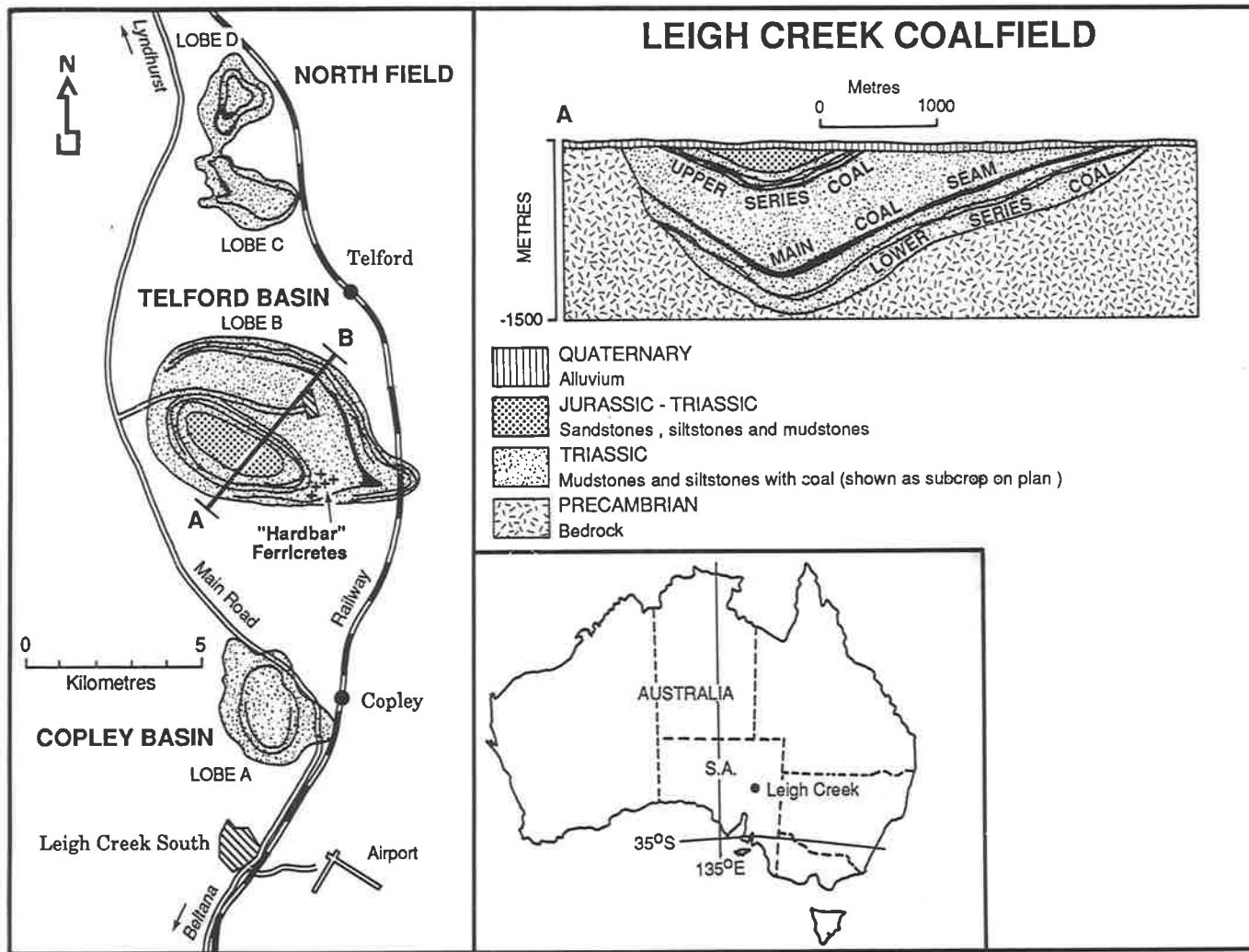


Figure 9.1 Location and geology of the Telford Basin (Source: S.A. Dept. Mines & Energy).

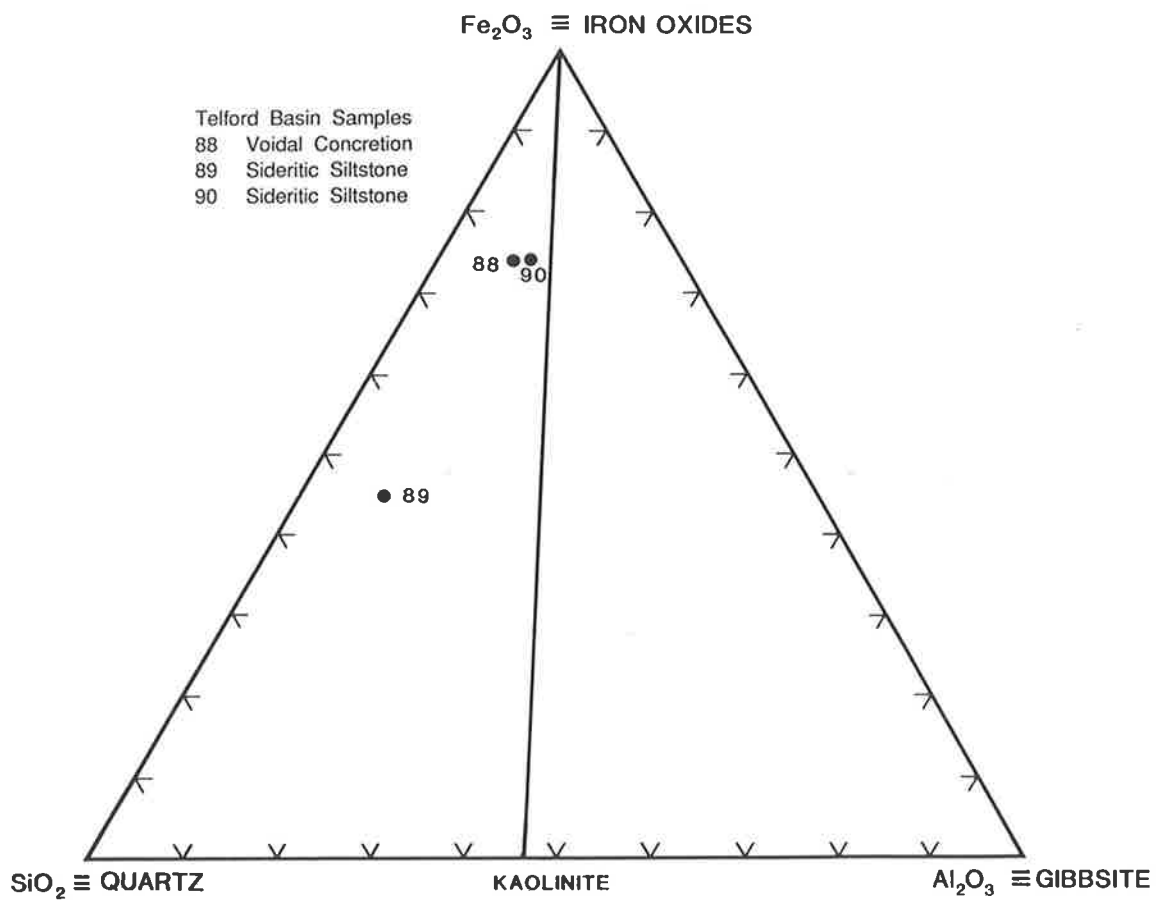
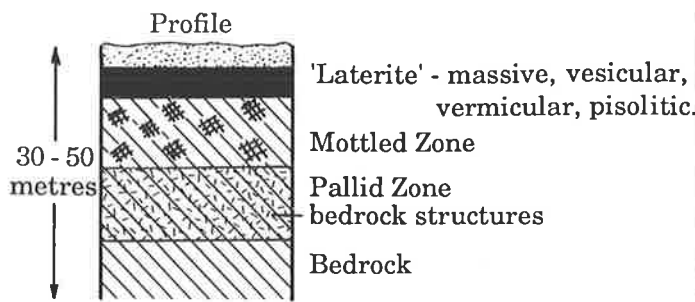


Figure 9.2 Triangular diagram of samples from the Telford Basin.



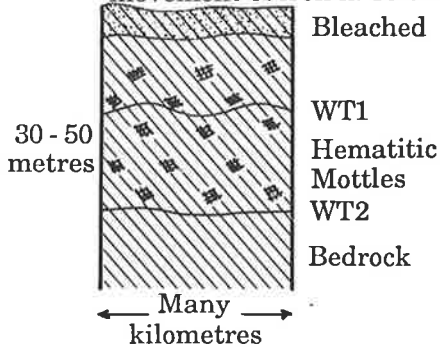
Standard 'laterite' profile developed by model of Stephens (1946) involving *in situ* isovoluminous weathering on 'peneplain' surface under humid tropical conditions. This model does not fit the reality of the South Australian situation. Instead one finds quite irregular distribution of ferricretes, bleached and mottled zones resulting from preferential weathering, depending on local topography and controlled by water flow.

I 'DEEP WEATHERING'

These examples of 'deep weathering', mottling and ferricretes have formed largely in metasedimentary rocks and sediments.

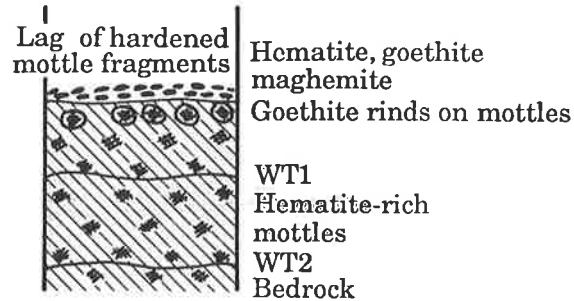
A. MOTTLED ZONE DEVELOPMENT

(1) Involves no major lateral movement of iron in solution.



LANDSCAPE DOWNWASTING

(2) Following uplift

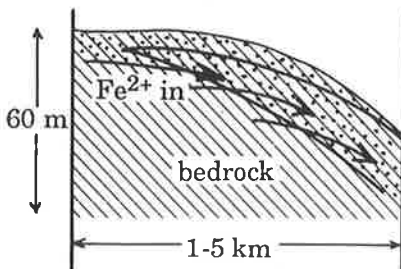


- i. Requires stability and locations away from steep slopes, but surface relief not necessarily subdued.
- ii. Water table change can be due to:
  - a. Seasonal changes
  - b. Climatic changes
  - c. Tectonic changes
- iii. Chemical weathering of bedrock under influence of water table fluctuations, leading to redistribution of iron into hematitic mottles.

- i. Slow landscape downwasting
- ii. Progressive transformation of hematite to goethite near surface.
- iii. Ferruginous lag at surface, containing hematite, goethite and maghemite.

B. BLEACHED ZONES

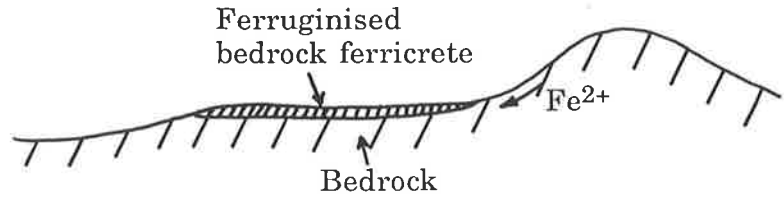
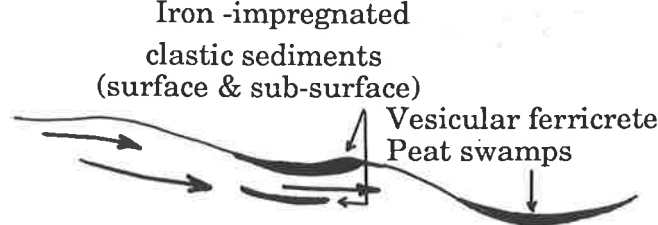
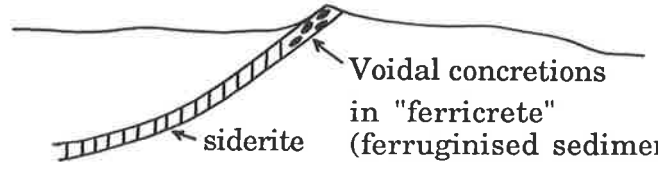
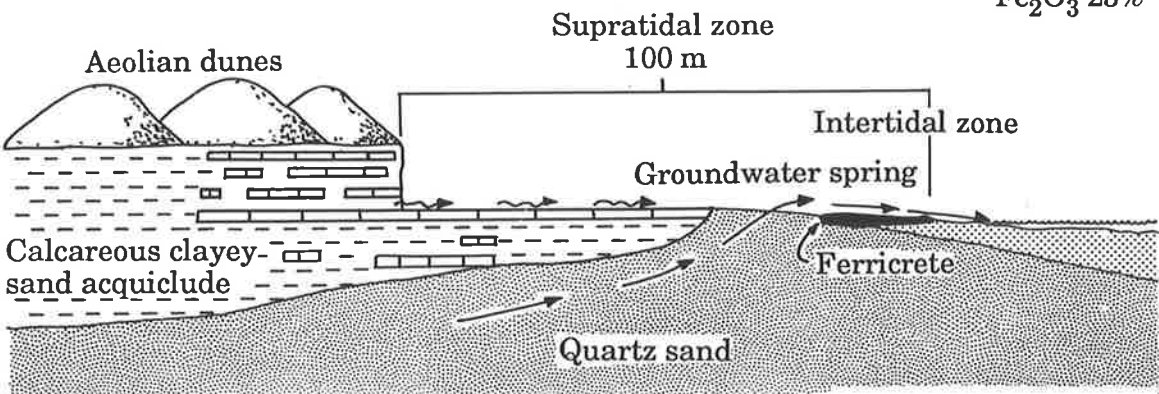
(1) Requires continuous lateral movement for evacuation of iron ( $Fe^{2+}$ ) in solution. Ideal conditions exist on margins of plateaus.



Mineralogy  
Kaolinite  
Smectite  
Quartz  
Felspar  
Illite

Figure 10.1 Sketches of 'Standard Laterite Profile' and 'Deep weathering' with the development of mottled and bleached zones.

II. FERRICRETES: SIMPLE TYPES

II. FERRICRETES: SIMPLE TYPES	Hand specimen	Mineralogy & Chemistry
<p>1. Ferruginised bedrock ferricrete</p> 	<p>Bedrock structures visible.</p>	<p>Hematite Goethite Fe<sub>2</sub>O<sub>3</sub> 17%</p>
<p>2. Iron-impregnated clastic and organic sediments (vesicular ferricrete).</p> <p>Iron-impregnated clastic sediments (surface &amp; sub-surface)</p> 	<p>(Clastic type) Sedimentary structures visible Vesicular ferricrete</p>	<p>Goethite Fe<sub>2</sub>O<sub>3</sub> 10% 3% Al-subst. Fe<sub>2</sub>O<sub>3</sub> 70% &lt;1% Al-subst</p>
<p>3. Oxidised pre-existing iron-rich sediments</p> 	<p>Voidal concretions in ferricrete Ferruginisation of sedimentary beds.</p>	<p>Goethite Lepidocrocite Hematite Fe<sub>2</sub>O<sub>3</sub> 60%</p>
<p>4. Peritidal environments</p>	<p>Massive Biscuits</p>	<p>Hematite Goethite Ferrihydrite Pyrite Rozenite Fe<sub>2</sub>O<sub>3</sub> 25%</p>
		

Continued on Fig 10.3

Figure 10.2 Sketches of simple types of ferricretes, showing their environments of formation, macro-morphology, chemistry and mineralogy.

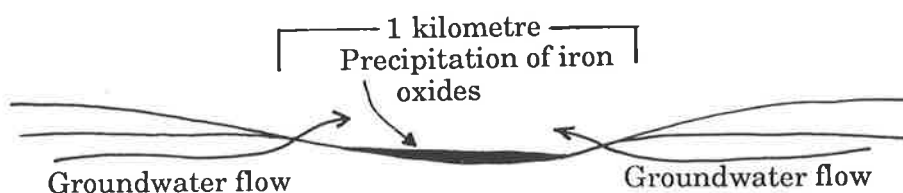


## II. FERRICRETES: SIMPLE TYPES (continued)

Hand specimen

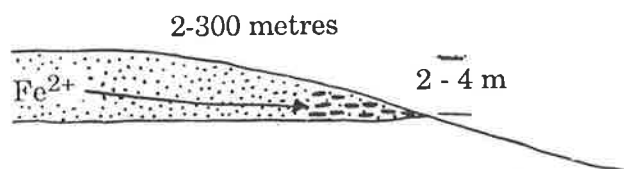
Mineralogy  
& Chemistry

### 5. Boinka environments

Platy fragments  
BiscuitsGoethite  
Hematite  
Rozenite  
Anhydrite  
 $\text{Fe}_2\text{O}_3$  25%  
V. low Al-  
subst.

## III. COMPLEX TYPES

### 1. Slabby ferricrete

Slabs separated  
by claysHematite  
GoethiteMinor gibbsite  
Kaolinite  
 $\text{Fe}_2\text{O}_3$  45%  
6% Al-subst.

### 2. Pisolitic to Nodular ferricrete Lateral physical transport to depressions

Pisoliths & nodules  
in iron-rich matrixHematite  
Goethite  
Maghemite  
Gibbsite  
 $\text{Fe}_2\text{O}_3$  35%  
Al-subst.  
up to 20%

### 3. Vermiform ferricrete - due to dissolution of pre-existing ferricretes of different types. Occurs on low angle slopes.

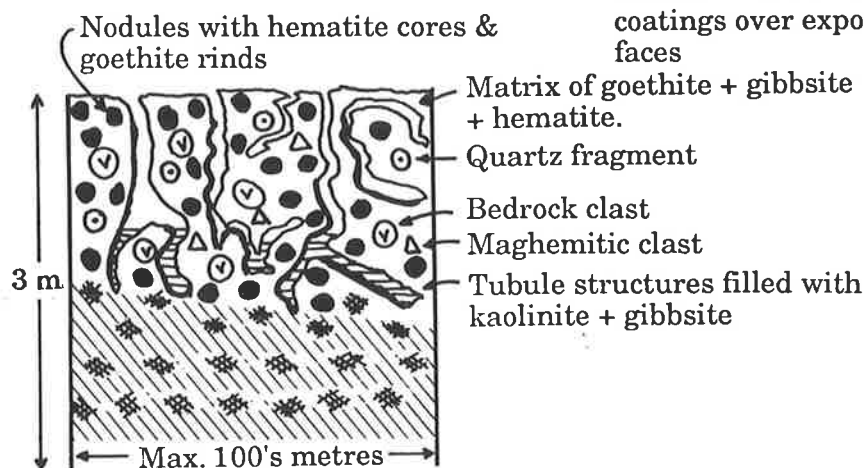
Worm-like tubules,  
clay-filled (kaolinite  
+ gibbsite). Some  
tubules filled with  
hematite. Goethite  
coatings over exposed  
facesHematite  
Goethite  
Maghemite  
Gibbsite  
Kaolinite $\text{Fe}_2\text{O}_3$  30%  
Al subst.  
up to 20%

Figure 10.3 Sketches of simple ferricretes (continued) and sketches of complex types of ferricretes, showing their environments of formation, macro-morphology, chemistry and mineralogy.

# PLATES

Plate 2.1 Reverse fault (F) near Cambrai on the eastern side of the Mount Lofty Ranges, exposed in a scarp foot valley. Shattered Cambrian metasedimentary rocks (K) on the right of the plate overlie red-brown Pleistocene conglomerates (P) on the left. Pods of light-coloured fossiliferous limestone (T) occur along the fault zone. Surface calcrete (c) occurs downslope of the fault, and may have formed from the dissolution and reprecipitation of Tertiary limestone dragged to the surface by faulting.

Plate 3.1 Oblique aerial view of Witton Bluff, south of Adelaide. Light-coloured Tertiary sediments in the lower half of the cliff are overlain by Pleistocene sediments, the base of which is marked by a zone of pronounced ferruginisation (F). Light-coloured calcareous material occurs at the surface. This stratigraphic sequence has been described as a 'laterite' profile by some workers, and boulders of 'laterite' have also been reported from within the Tertiary sediments.

Plate 3.2 Ferruginous sandstone unit of Pleistocene age, which thickens to the right of Plate 3.1. The upper and lower beds of this unit are sub-horizontal (h), but the intervening beds are contorted and convoluted (c), indicating intraformational slumping.

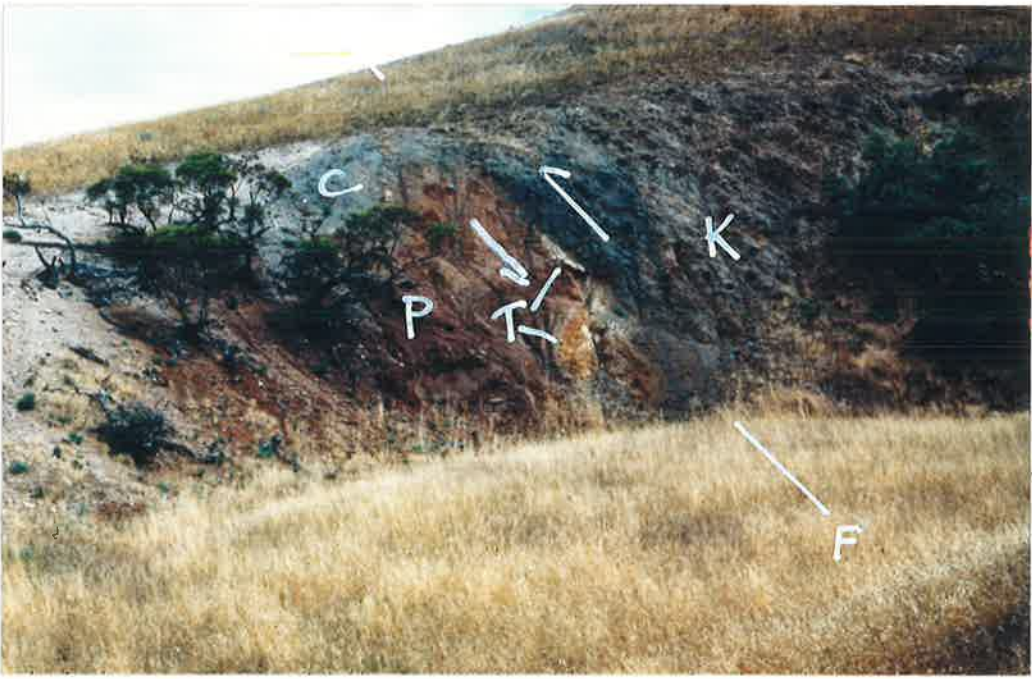


Plate 4.1 General view of the summit surface of the South Mount Lofty Ranges and the Willunga escarpment looking southeast from near Clarendon. The general elevation of the summit surface in this area varies between approximately 300 m and 420 m above sea level. This surface has been widely interpreted in the past as an uplifted 'peneplain' capped by a fossil 'laterite profile', to which it allegedly owes its preservation.

Plate 4.2 Vermiform ferricrete showing sinuous tubule structures filled with white-coloured clays that contain kaolinite and gibbsite. Clasts of ferruginised bedrock (B) and maghemite (M) are evident on the left of the sample. The yellow material comprises dominantly goethite and gibbsite, whereas the dark red material is dominated by hematite. Sample is approximately 25 cm wide.

Plate 4.3 Pisolitic ferricrete illustrating discrete pisoliths cemented in a ferruginous matrix material. Sample is approximately 10 cm wide.

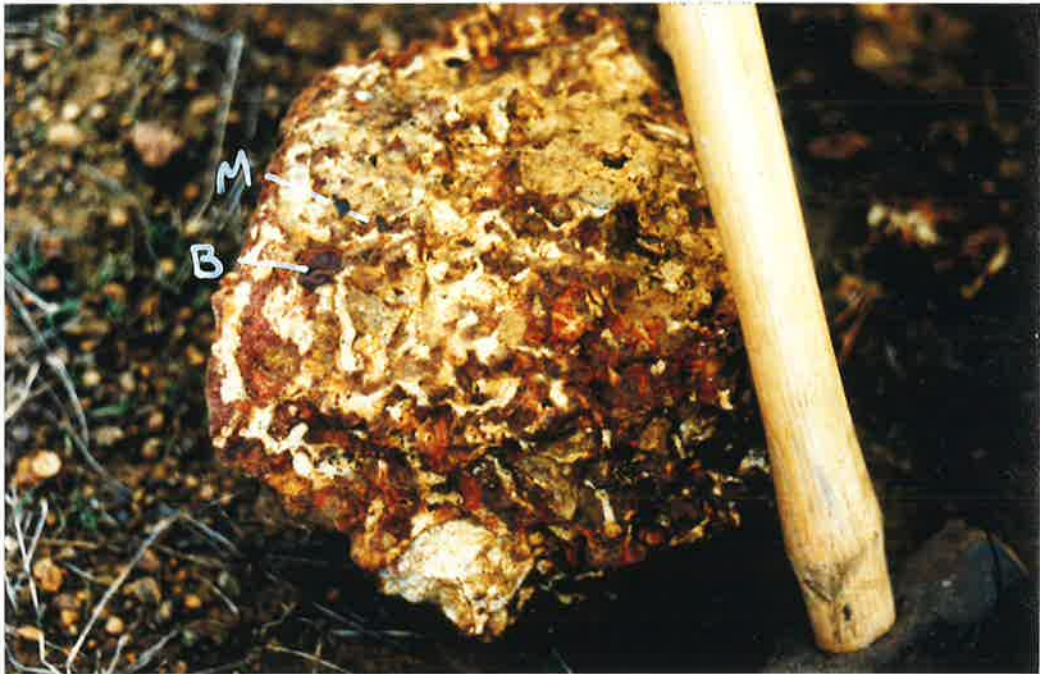


Plate 4.4 Block of nodular ferricrete, with large nodule (N) right of centre outlined by fracture. The nodules are considerably larger than pisoliths. The material comprising the nodules (goethite, quartz, gibbsite, hematite, kaolinite, anatase, smectite, interstratified clays and maghemite) is of similar composition to that of the matrix except that the matrix does not contain maghemite. Scale is 10 cm long.

Plate 4.5 Sectioned boulder of vesicular ferricrete, showing small cavities that were originally filled with clay-rich (smectitic) materials. Goethite is the dominant iron oxide present, and up to 70% of the total composition of this ferricrete consists of  $\text{Fe}_2\text{O}_3$ . Scale is 40 cm long.

Plate 4.6 Blocks of slabby ferricrete (dominantly goethite and hematite), developed in weathered Precambrian metasiltstones, separated by clay-rich material (kaolinite, smectite and interstratified clays) and exposed in road cut on Chandlers Hill. Geology hammer 35 cm long.





Plate 4.7 Block of ferricreted sandstone. A pre-existing quartzose sandy sediment has been impregnated by iron-rich waters, and lithified following the precipitation and crystallisation of the iron. Ferricretes formed by the iron oxide impregnation and induration of sediments display an iron oxide mineralogy dominated by goethite and have a total iron content of about 20%. Scale is 10 cm long.

Plate 4.8 Precambrian metasedimentary rocks variably impregnated with iron oxides (hematite and goethite), forming ferricreted bedrock. Original bedrock structures are clearly visible. This ferricrete forms a prominent ridge at about 340 m asl near Koonunga in the Mid North of the State. Although it forms a ridge it is still well below the level of higher land nearby. Hammer head is 15 cm long.

Plate 4.9 View across a sediplain, the Upper Hindmarsh Valley, from Spring Mount northwards towards Mount Cone on a similar line to the cross section shown in Figure 4.4. The horizon to the right (east) of Mount Cone carries sporadic occurrences of nodular and vesicular ferricrete at about 400 m asl. The Upper Hindmarsh Valley is approximately 210 m asl and is underlain by Oligo-Miocene limestone, above which a ferricrete formed by the ferruginisation of sands occurs above Pliocene sediments.



Plate 4.10 Small mesa sporadically capped with nodular ferricrete (e.g. scattered boulders in foreground) east of Mount Cone. This ferricrete is currently undergoing destruction, but there is no evidence that it ever completely covered the landscape. An alternative view is that different types of ferricretes developed in different and discrete parts of the landscape.

Plate 4.11 Eastward view from Mount Cone of the small mesa on the horizon, sporadically mantled with nodular ferricrete shown in Plate 4.10. Small red-brown patch at base of slope near left of plate marks position of vesicular ferricrete (V) about 15 m below the level of the nodular ferricrete (N).

Plate 4.12 Photomicrograph in transmitted plane polarised light of vermiform ferricrete from the summit surface of Kangaroo Island (BOU 101) showing small islands of clay and quartz grains, with interstitial iron oxides (goethite and hematite) and gibbsite (light yellow). The main difference between the segregations and the matrix material is that the segregations contain more iron oxides. The framework grains are similar in both the matrix and the segregations, which favours the view that iron and aluminium oxides have penetrated into pre-existing sediments. Minerals present include quartz, gibbsite, goethite, kaolinite, feldspar, hematite and anatase. Width of field 2.6 mm.

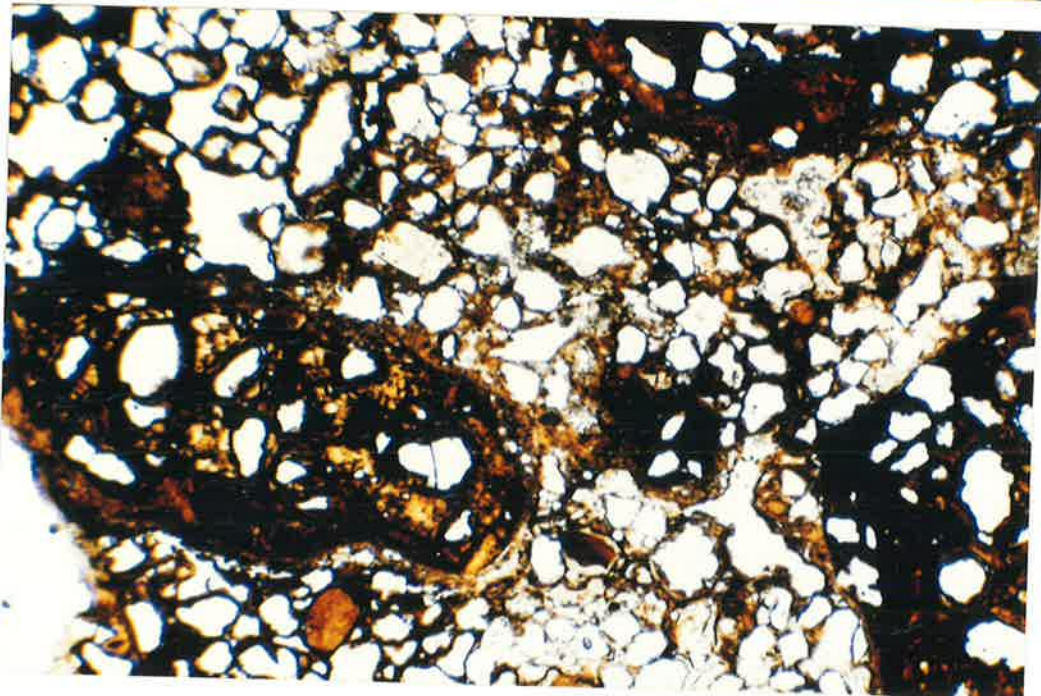
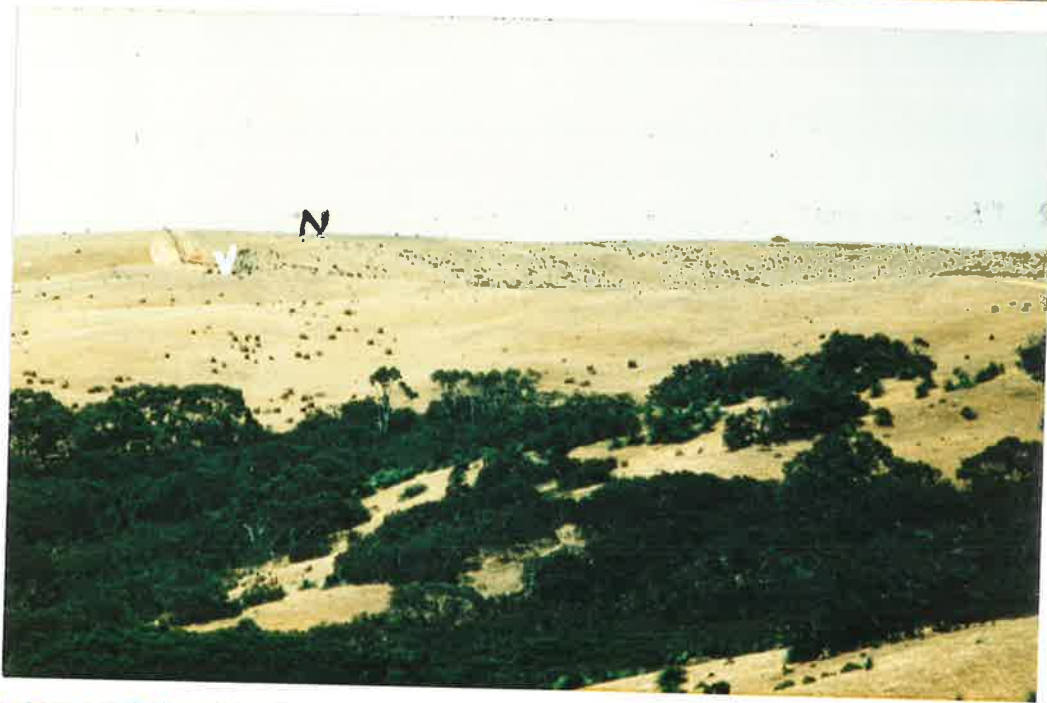
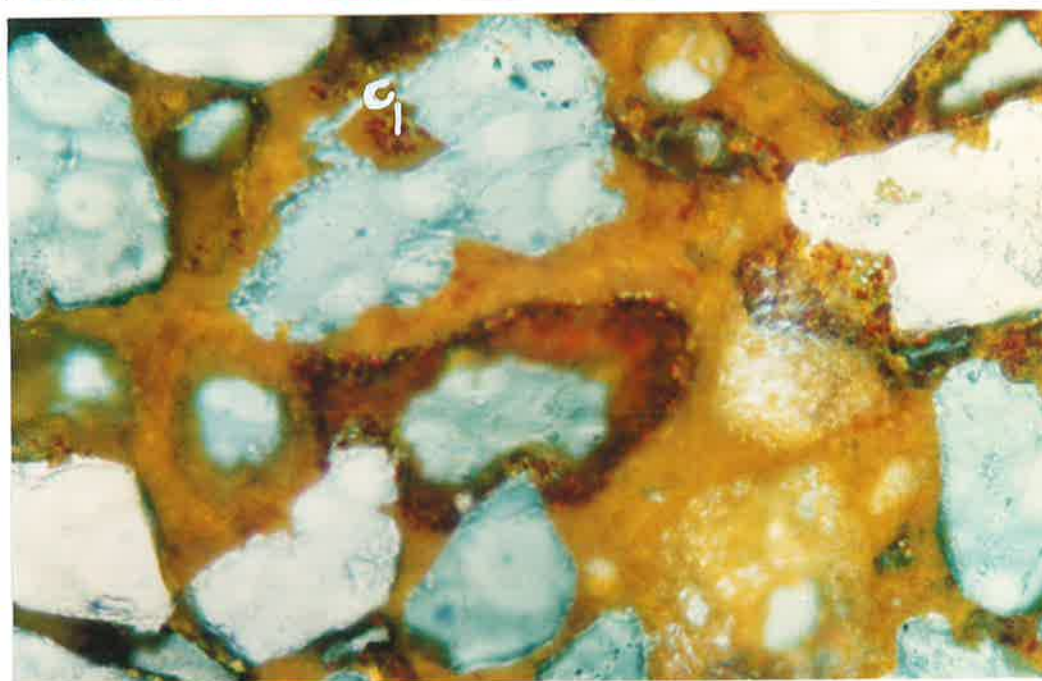
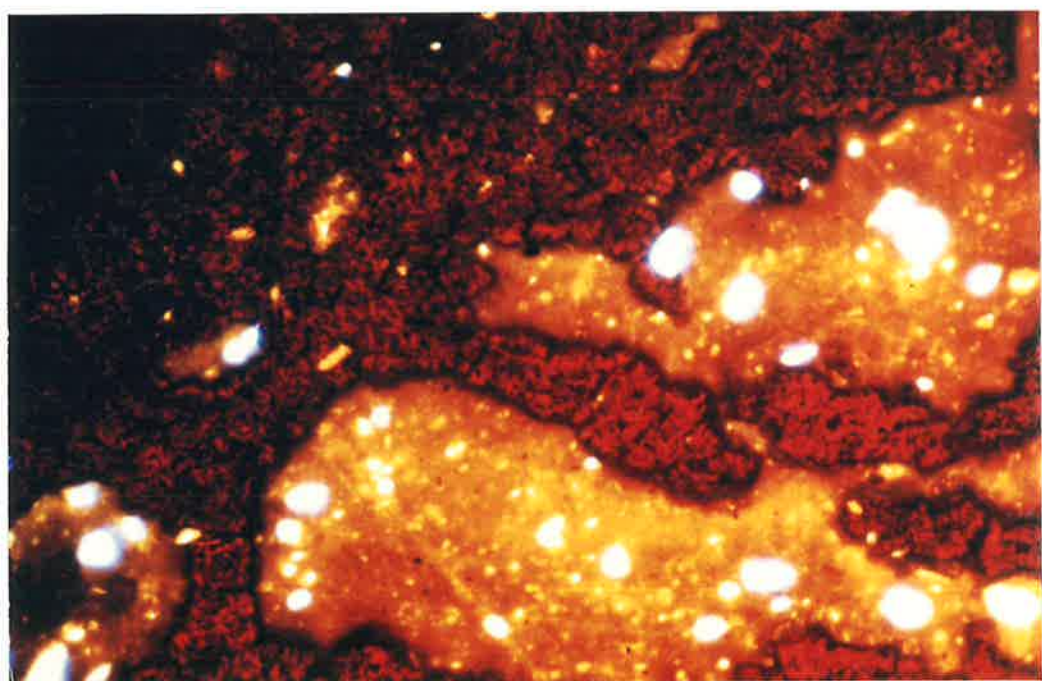
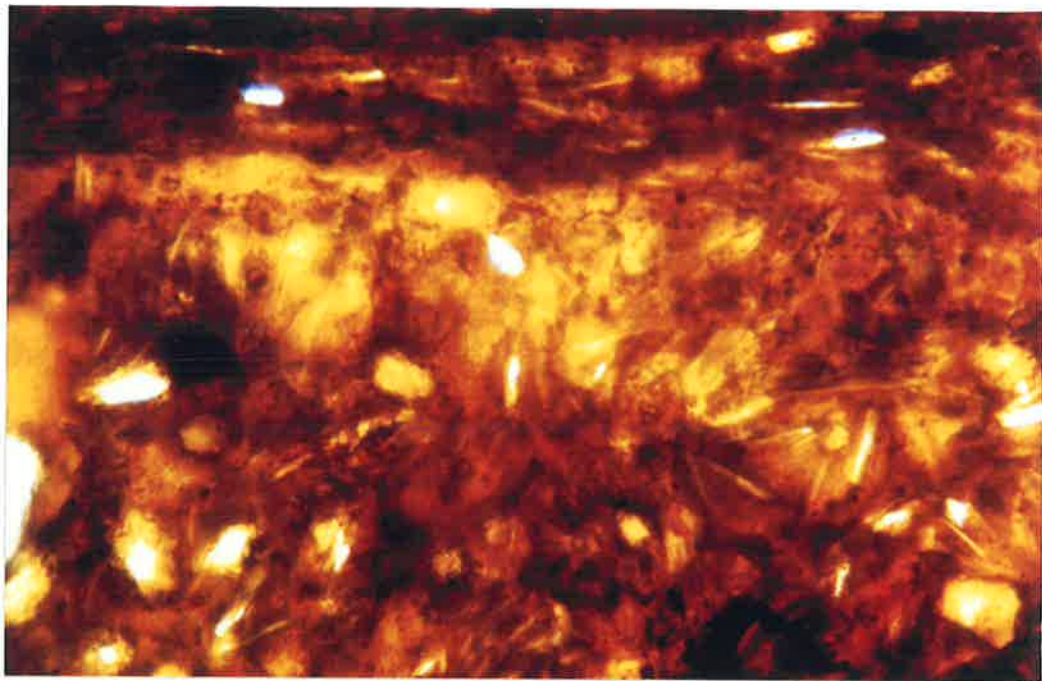


Plate 4.13 Photomicrograph of vermiform ferricrete (BOU 18) from summit surface of Fleurieu Peninsula, showing disoriented micas, or pseudomorphs after micas, which suggest that it has derived from weathered bedrock, and may represent an indurated soil. The iron oxides dominantly comprise goethite and hematite. There is a tendency for the micas to be aligned parallel to the surface coating but to be randomly dispersed elsewhere. Transmitted plane polarised light. Width of field 2.6 mm.

Plate 4.14 Photomicrograph of vermiform ferricrete (BOU 101) from Kangaroo Island, showing zones of clay kaolinite plus gibbsite) and quartz grains with rims of goethite and hematite surrounded by material composed dominantly of goethite and hematite with possible maghemite. Transmitted plane polarised light. Width of field 2.7 mm.

Plate 4.15 Photomicrograph of poorly sorted coarse sandy sediment (BOU 306), which is probably a fluvioglacial sediment of Permian age. The sub-angular quartz grains are cemented by a yellow matrix of goethite plus clay (kaolinite, smectite and interstratified clays). Very fine red hematite crystallites (c) are scattered throughout the matrix, and line voids within the matrix. Incident polarised light. Width of field 1.2 mm.



Handwritten text on the right margin, possibly a page number or reference number, including the number '9'.

Plate 4.16 Photomicrograph of quartzose sediment with complex semi-opaque matrix of hematite and clays connecting poorly sorted, angular, shard-like and embayed quartz grains, suggesting either the inheritance of such grains or their dissolution during weathering (BOU 4). Transmitted plane polarised light. Width of field 0.6 mm.

Plate 4.17 Photomicrograph of sample BOU 4, showing hematite occurring as small crystals (c) with red internal reflections in yellowish goethite plus clay matrix, cementing quartz grains (q). Some red hematite occurs in thin zones around voids (v). The angular and embayed character of the framework grains suggests that some of them have developed by the breakup of larger grains. Incident polarised light. Width of field 1.2 mm.

Plate 4.18 Photomicrograph of weathered Precambrian metasiltstone bedrock (BOU 386), showing blue-coloured quartz grains with an iron oxide matrix consisting of masses of small crystals of hematite and individual hematite crystallites in a yellowish matrix of clay and goethite. Scattered fine hematite crystallites occur throughout the matrix, in places coalescing to form aggregates. Well crystallised hematite also occurs along fractures. Polarised incident light. Width of field 0.5 mm.

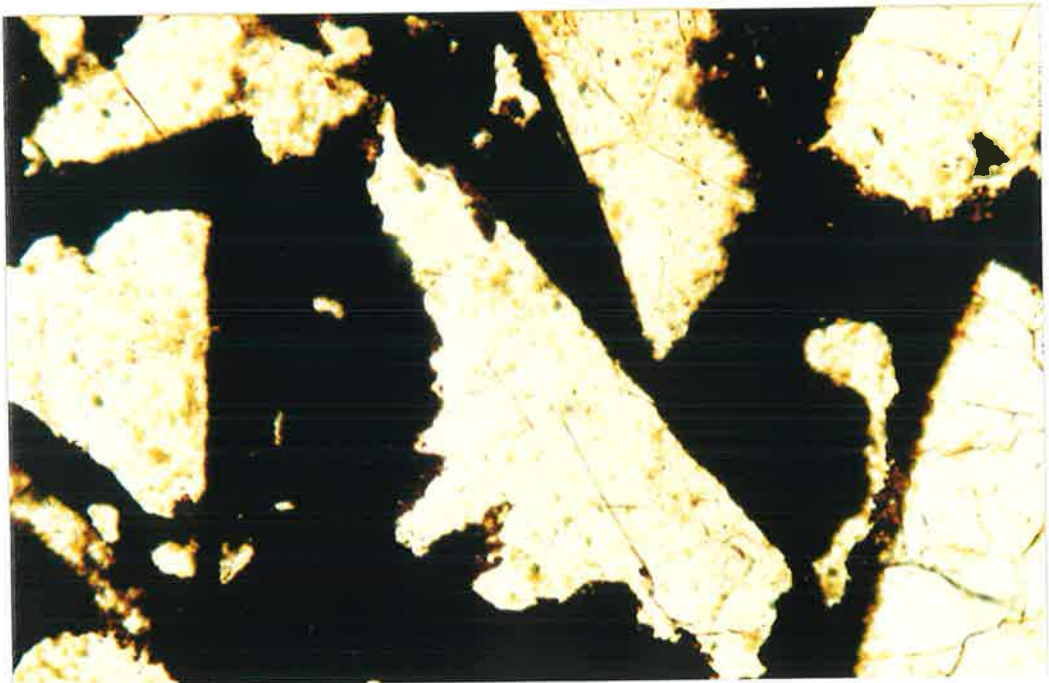
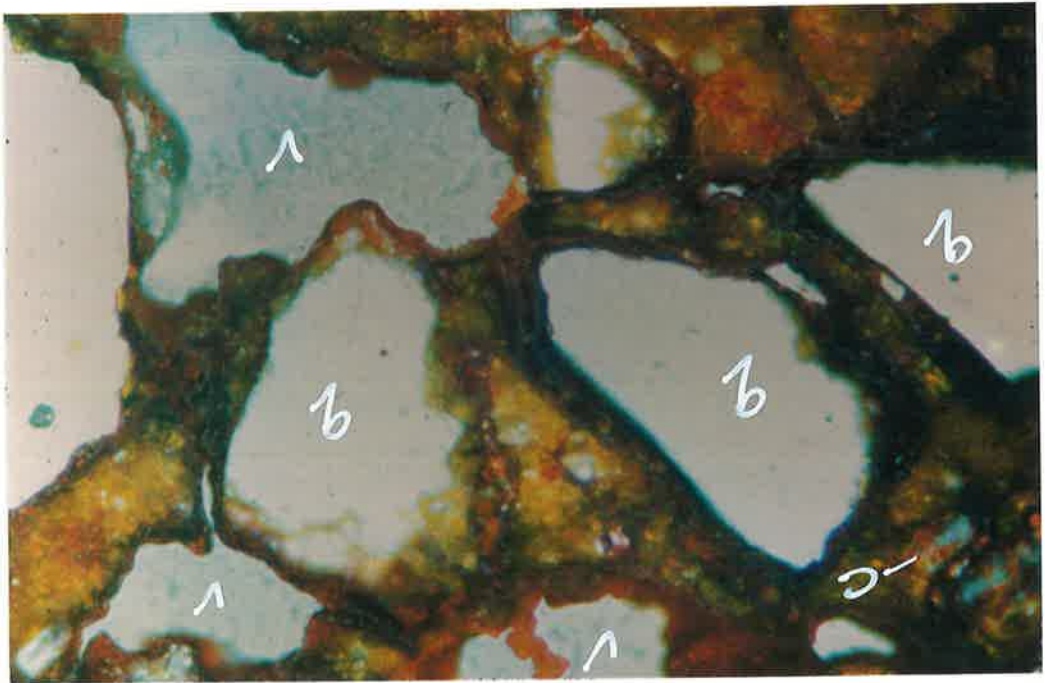
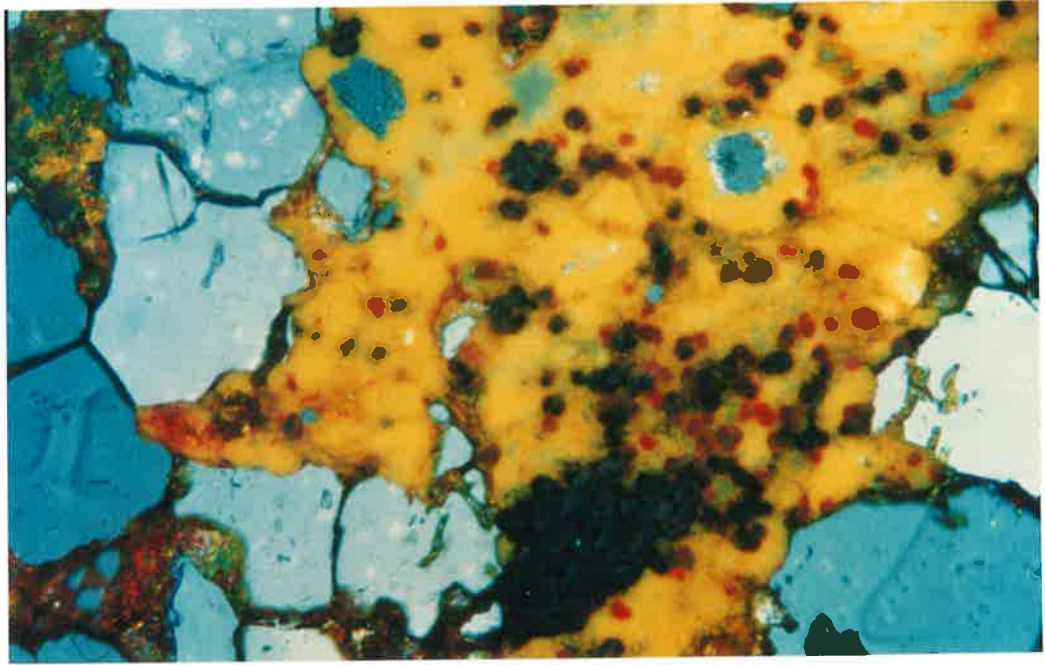




Plate 4.19 Photomicrograph of clay-rich material (kaolinite and vermiculite) (BOU 20) with scattered quartz grains impregnated by iron oxides (goethite and fine equigranular hematite crystallites). The concentration of the crystallites increases, especially along fractures, where the clay matrix appears to be replaced. Hematite appears to have formed at a later stage than the goethite. Transmitted plane polarised light. Width of field 1.4 mm.

Plate 4.20 View of bulldozer excavation on Peeralilla Hill showing ferruginous crust of vesicular ferricrete (V) and light-coloured clays (C and B) at a lower level in the section, that include calcite and barite. This deposit of ferricrete occurs on the summit surface but below the level of surrounding hills. Borehole evidence indicates that this deposit is underlain by sandy sediments. Figure provides scale.

Plate 4.21 Closer view of ferricrete at Peeralilla Hill showing rudimentary layering which dips to the south. Isolated boulders of vesicular ferricrete (V) occur in the section as do small patches of clays (kaolinite, smectite and vermiculite) (C). Geology hammer 35 cm long.

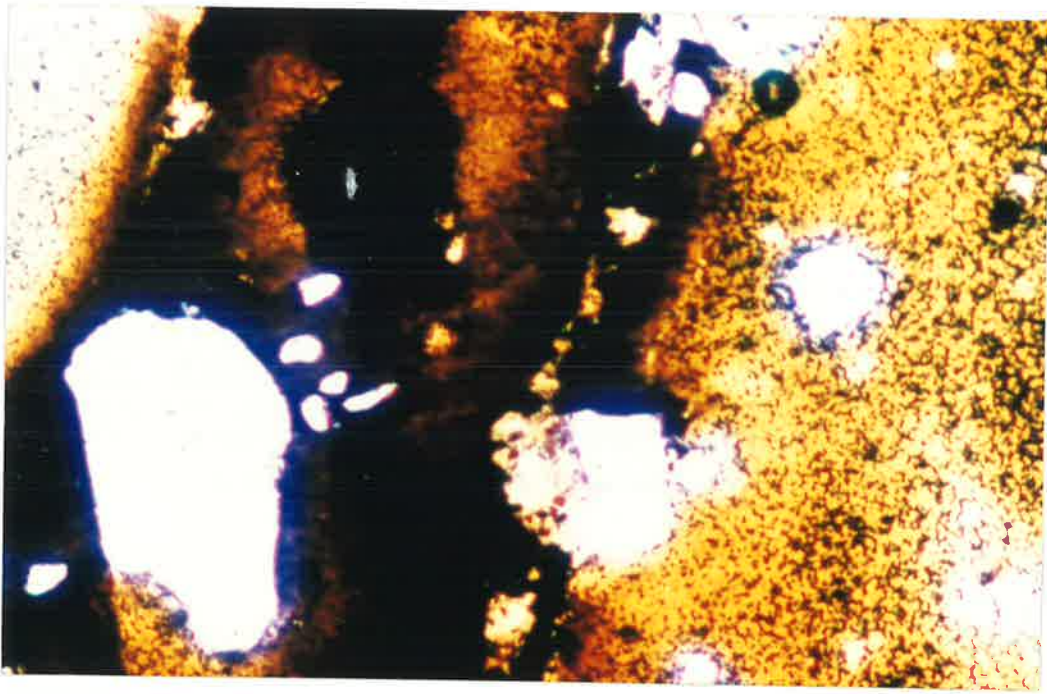


Plate 4.22 Photomicrograph of calcitic sediment (BOU 33) underlying ferricrete on Peeralilla Hill. Rounded to sub-angular quartz grains ranging from silt to sand-sized are set in a matrix of calcite, smectite and kaolinite, which coats the grains and fills cavities and fractures. Transmitted plane polarised light. Width of field 1.2 mm.

Plate 4.23 Photomicrograph of vesicular ferricrete from Mount Compass (BOU 5). Note the opaque iron oxides, the linear cavities (C) and the numerous voids. Transmitted plane polarised light. Width of field 0.5 mm.

Plate 4.24 Photomicrograph of vesicular ferricrete from Mount Compass showing presumed organic matter replaced by iron oxides, showing as cell-like structures (C). Small dark patches are hematite. Transmitted plane polarised light. Width of field 0.5 mm.

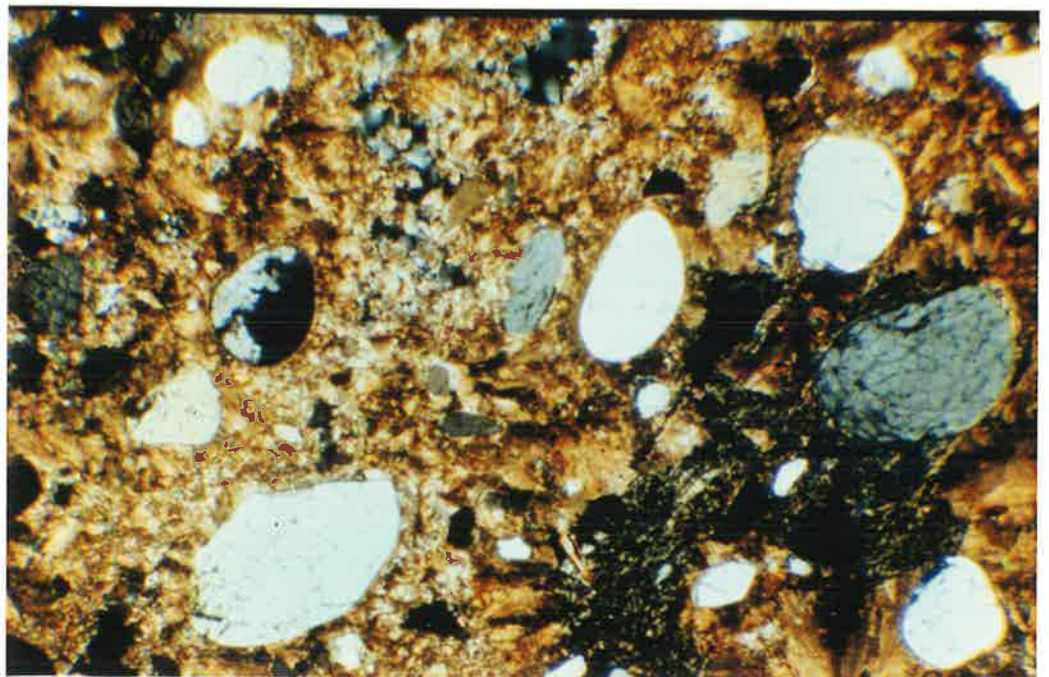
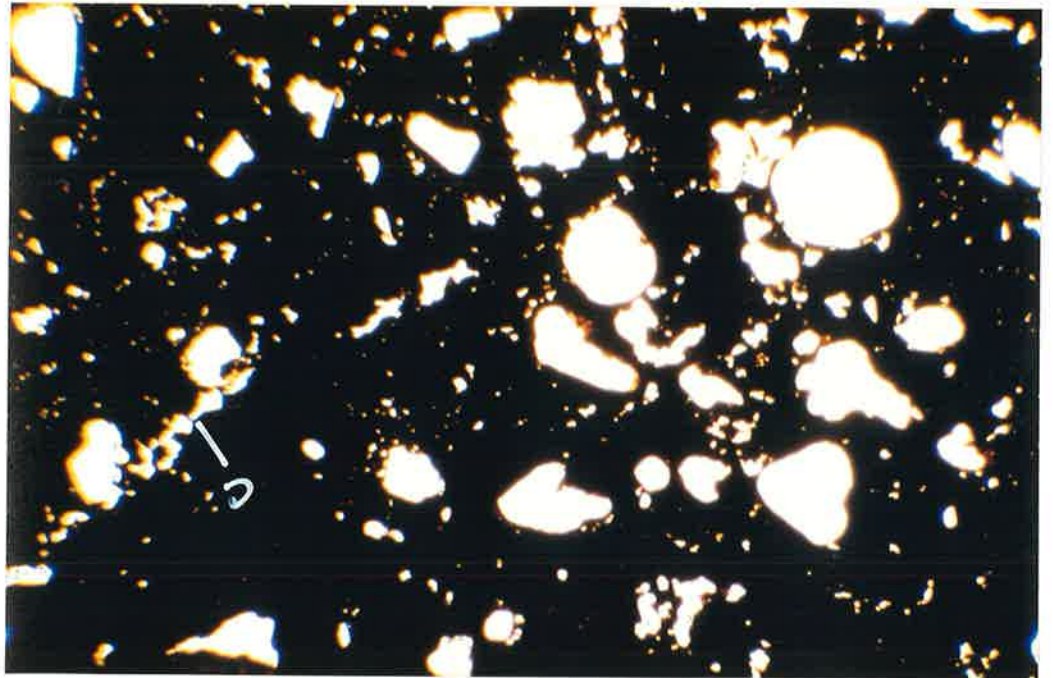
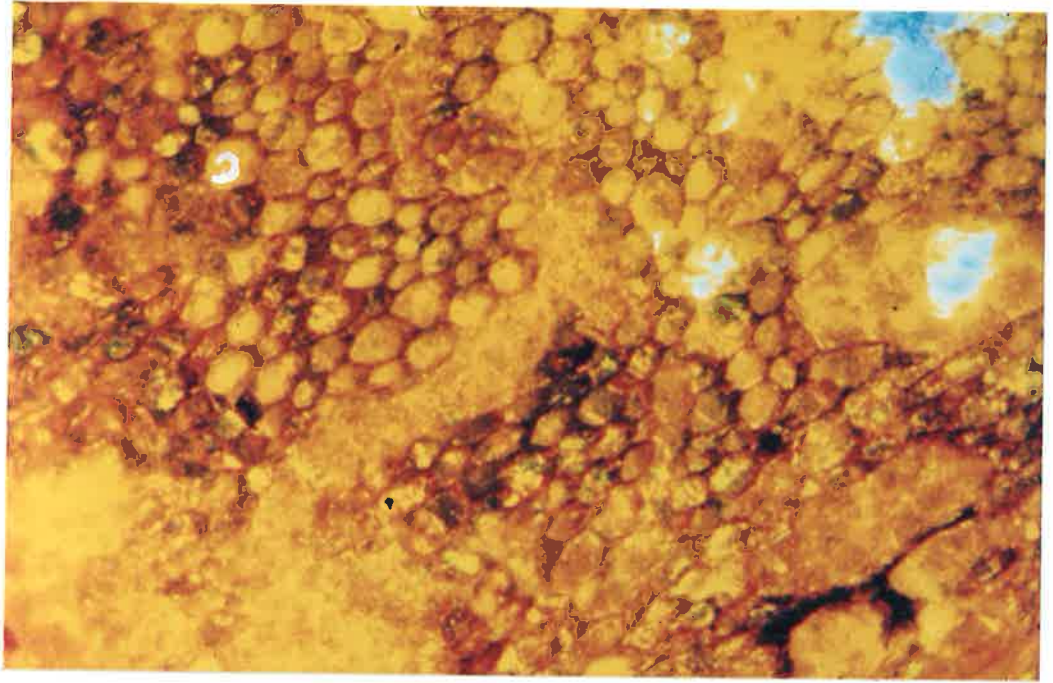
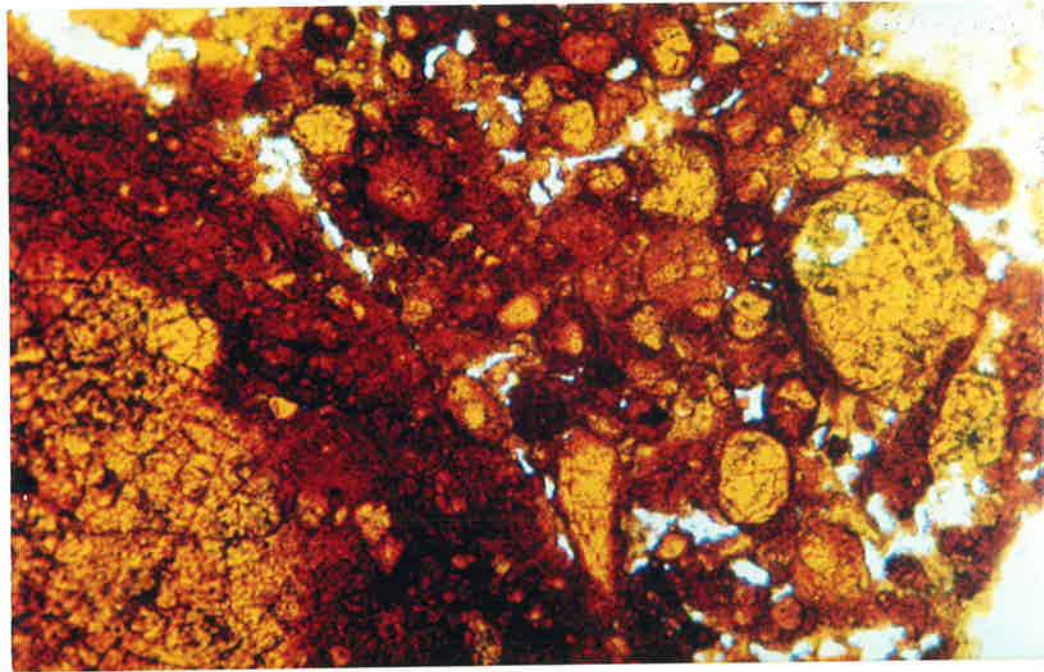
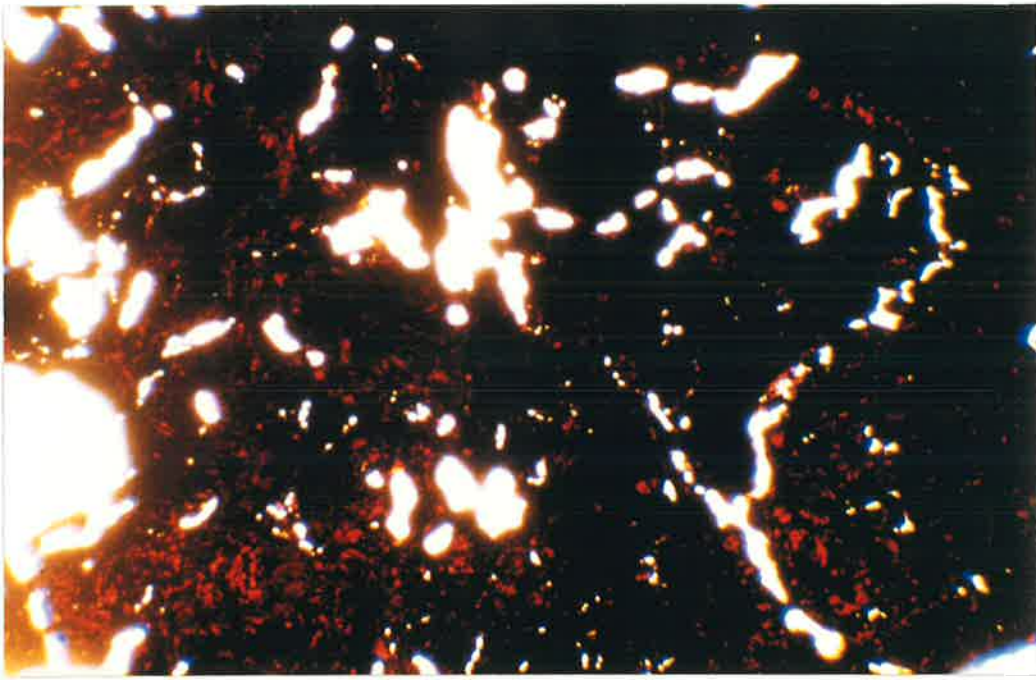


Plate 4.25 Photomicrograph of vesicular ferricrete from Peeralilla Hill (BOU 12) showing linear white voids. Small areas of 'cell-like' goethite crystals occur in places. Transmitted plane polarised light. Width of field 4 mm.

Plate 4.26 Photomicrograph of vesicular ferricrete from Peeralilla Hill, showing rounded structures which could represent former organic material. Transmitted plane polarised light. Width of field 0.6 mm.

Plate 4.27 Palaeochannel on summit surface near Mount Desert cut into weathered and iron mottled Kanmantoo Group metasedimentary rocks (K) and exposed by road construction. Irregular base of channel is marked as is the location of some of the ferruginous and variably maghemitic pisoliths (p) that occur at the base of the channel. Clasts of hematite mottles, derived from the adjacent bedrock, also occur in the channel fill, which in its upper half resembles mudflow deposits. Post is approximately 1 metre high.



1000

1000

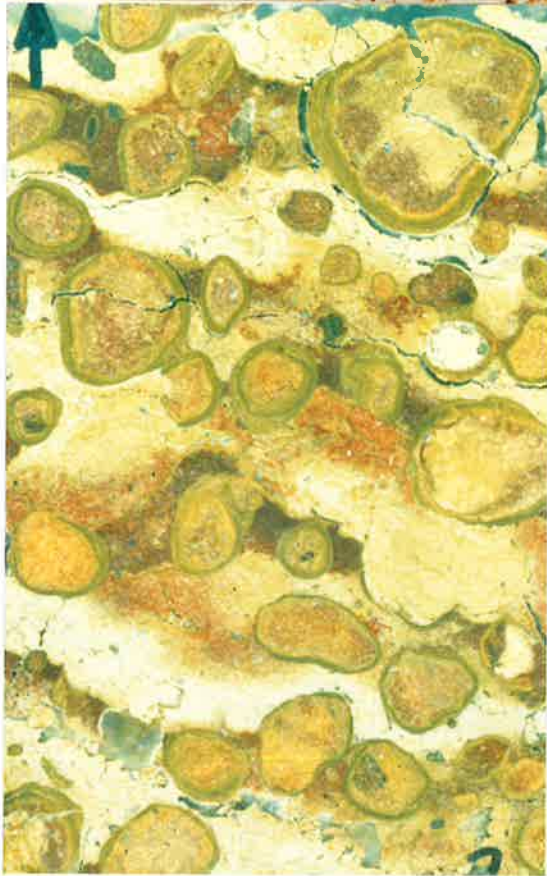
Plate 4.28 Sharp boundary between unconsolidated pisoliths with goethitic rinds occurring over weathered bedrock near Parawa. Width of field approximately 0.5 m.

Plate 4.29 Polyester-resin impregnated slab of pisolitic ferricrete from the Parawa Plateau. Note the variation in the composition of the core materials of the pisoliths. The majority of the larger clasts consist of ferruginous and hematitic bedrock, but some smaller ones have cores of maghemite. Note the complex rinds of goethite and gibbsite on some of the clasts and their crude stratification. The clasts are separated by kaolinitic clays, which in places contain later generations of iron oxides. True scale.

Plate 4.30 Hammer head marks contact of base of channel filled with ferruginous detritus of pisoliths, nodules, and mottle fragments, and underlying weathered Cambrian metasedimentary rocks.



100x



100x

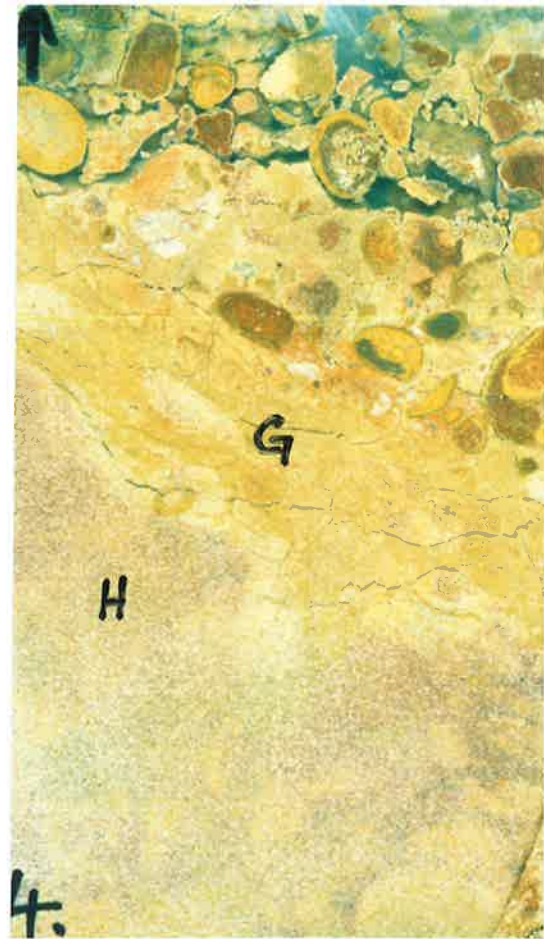
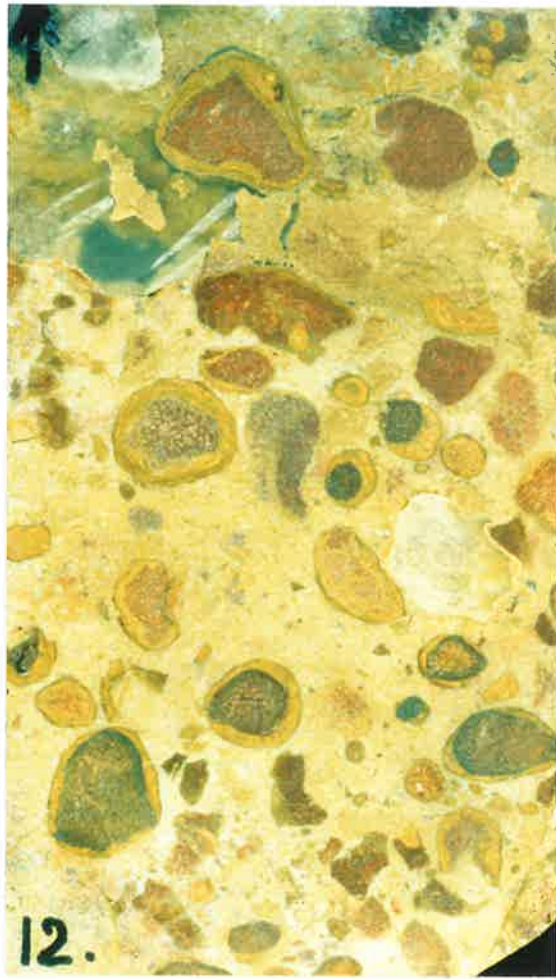
100x  
100x  
100x





Plate 4.31 Polyester-resin impregnated slab of channel fill material extracted from above the erosional contact shown in Plate 4.32. Note the similarity between the pisoliths and those from higher up on the summit surface, shown in Plate 4.29. Similar core materials of hematitic bedrock and maghemite are variably encased in rinds of goethite and gibbsite. True scale.

Plate 4.32 Polyester-resin impregnated slab of sample taken across the contact of the underlying weathered bedrock and the base of the channel fill, from the site in Plate 4.30. At the base of the slab weathered and ferruginous metasedimentary bedrock (H), containing hematite is overlain by a thin goethitic clay zone (G), which in turn is overlain by the channel fill materials that include maghemitic pisoliths with cores of various materials and complex rinds. True scale.



12. *Utricularia*  
13. *Utricularia*  
14. *Utricularia*  
15. *Utricularia*

16. *Utricularia*  
17. *Utricularia*  
18. *Utricularia*

19. *Utricularia*

Plate 4.33 Photomicrograph of sandstone (BOU 17) with a clay matrix on the right and an opaque iron oxide matrix on the left . The clay matrix has been partly replaced by iron oxides, particularly along fractures in the matrix. The iron oxide impregnation appears to be a single generation one as there are no complex layers or zones. The quartz grains are more closely packed in the area with the clay matrix, and appear to 'float within the iron oxide (dominantly goethite) matrix. Transmitted plane polarised light. Width of field 4 mm.

Plate 4.34 Section in road cut near Clarendon, showing angular unconformity with ferruginised pebbles, grits and sands of Eocene (E) age overlying weathered, bleached and partly kaolinised Precambrian metasilstones (P). Section is approximately 3 m high.

Plate 4.35 Ferruginised and cross-bedded fluvial sediments of North Maslin Sand sediments exposed in a road cutting on the south side of the Onkaparinga Gorge. Near vertical structures may represent former tree roots. Vehicle provides scale.

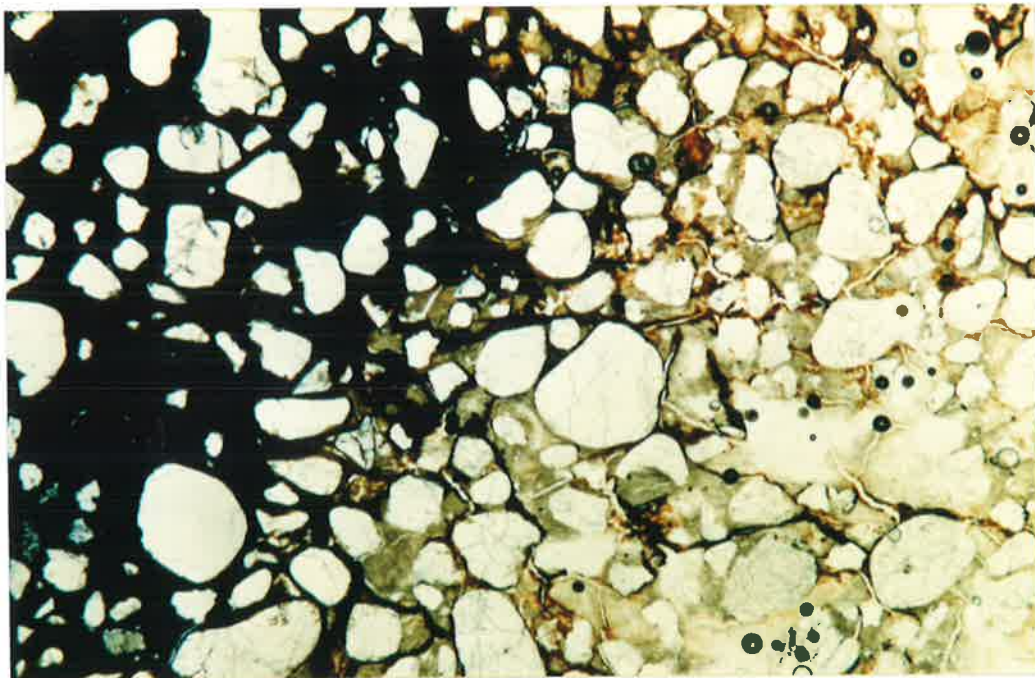


Plate 4.36 Section exposed in the Blackwood railway cutting showing partly weathered Precambrian rocks at the base, which become more intensively weathered and mottled immediately below the unconformity, which is overlain by a Tertiary sandy sediment with dense hematitic mottles and a hardened surface carapace. An ironstone gravelly duplex soil occurs at the surface.

Plate 4.37 Section in road cutting on Range Road near Willunga, excavated in Precambrian metasiltsstones with sandstone horizons. Large purplish hematitic mottles occur at the base, separated by bleached and kaolinised bedrock. Towards the surface the mottles have become isolated and smaller, with goethitic rinds. A lag of disintegrated mottles, pisoliths and bedrock fragment occurs at the surface and has been incorporated into the present ironstone gravelly duplex soil. The section has developed entirely in weathered bedrock, but irregular structures below the hammer suggest that there has been 'churning' of the upper section, perhaps due to wetting and drying effects. Geology hammer 35 cm high.

Plate 4.38 Hematitic mottles in Precambrian metasiltsstone bedrock in abandoned road cutting near Willunga Hill, but well below the summit of the hill. Figure provides scale.



Plate 4.39 Photomicrograph of ferruginised bedrock (BOU 22) illustrated in Plate 4.38, which displays a metamorphic structure, with angular embayed quartz grains and large unaltered micas. The fine-grained ground mass has been replaced by iron oxides (hematite). Transmitted plane polarised light. Width of field 3.5 mm.

Plate 4.40 Photomicrograph of coarse schistose metasediment (BOU 28) of angular quartz with an iron oxide matrix, dominantly of goethite plus clay (yellow), with scattered reddish crystals of hematite. Replaced micas and relic porphyroblasts of metamorphic minerals such as andalusite and/or staurolite also occur. Incident polarised light. Width of field 1.2 mm.

Plate 4.41 Hematitic mottled zone in weathered and bleached Precambrian bedrock, underlying hill summit at 370 m above sea level, near Kapunda, Mid North, comprising part of the pre-Tertiary Mount Herbert surface of Alley (1969). The summit of the hill lies about 70 m above the surrounding country.

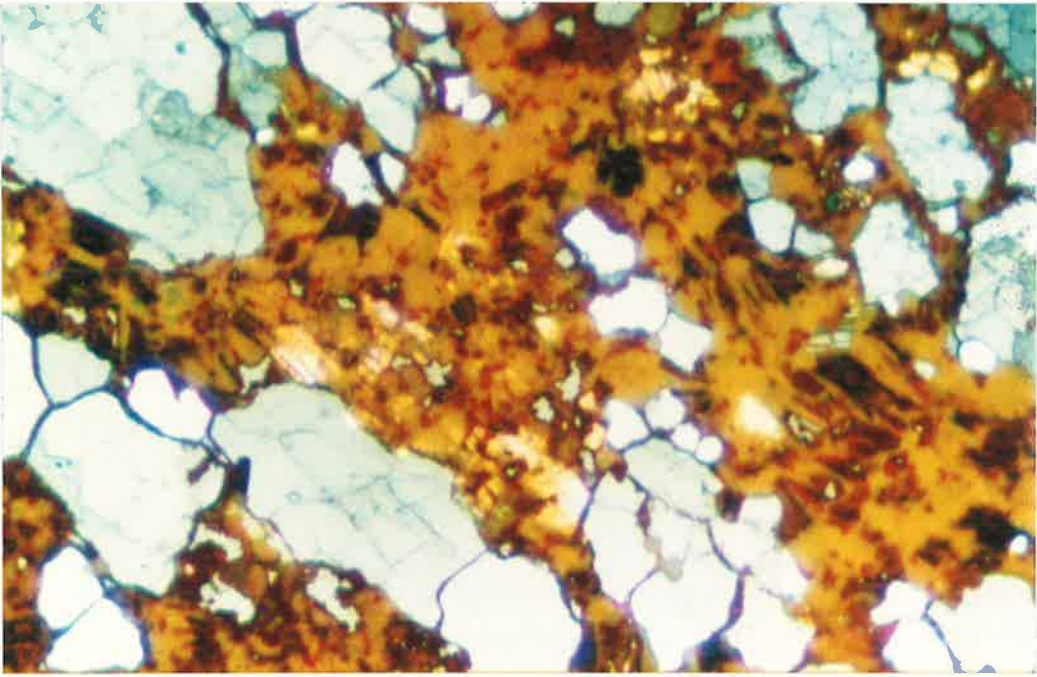
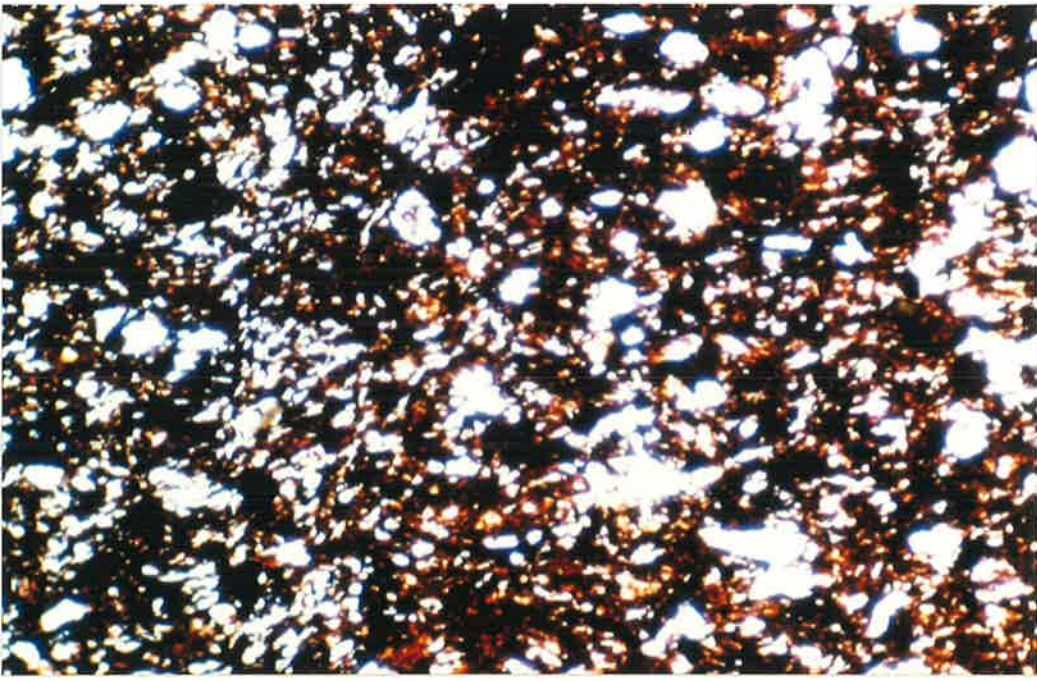




Plate 4.42 Strongly mottled zone with a crude vertical orientation in Precambrian bedrock south of Kapunda in Mid North. Mottles (dominantly hematitic) and adjacent bleached zones display a pronounced vertical orientation. Figure provides scale.

Plate 4.43 Photomicrograph of ferruginised and weathered bedrock below the mottled zone south of Kapunda, shown in Plate 4.41. In places hematite is concentrated along blue quartz grain boundaries. Kaolinite has developed from alteration of micas (M). Scattered hematite crystallites (red) forming patches (H) and zones within goethitic and clay groundmass (yellow) (BOU 389). Polarised incident light. Width of field 1.2 mm.

Plate 4.44 Coarsely mottled zone exposed in road cutting near Mount Torrens, developed in Precambrian metasiltstone, approximately 520 m above sea level. Purple coloured iron oxides are hematitic and orange-yellow colours are goethitic. Section is 3.5 m high.

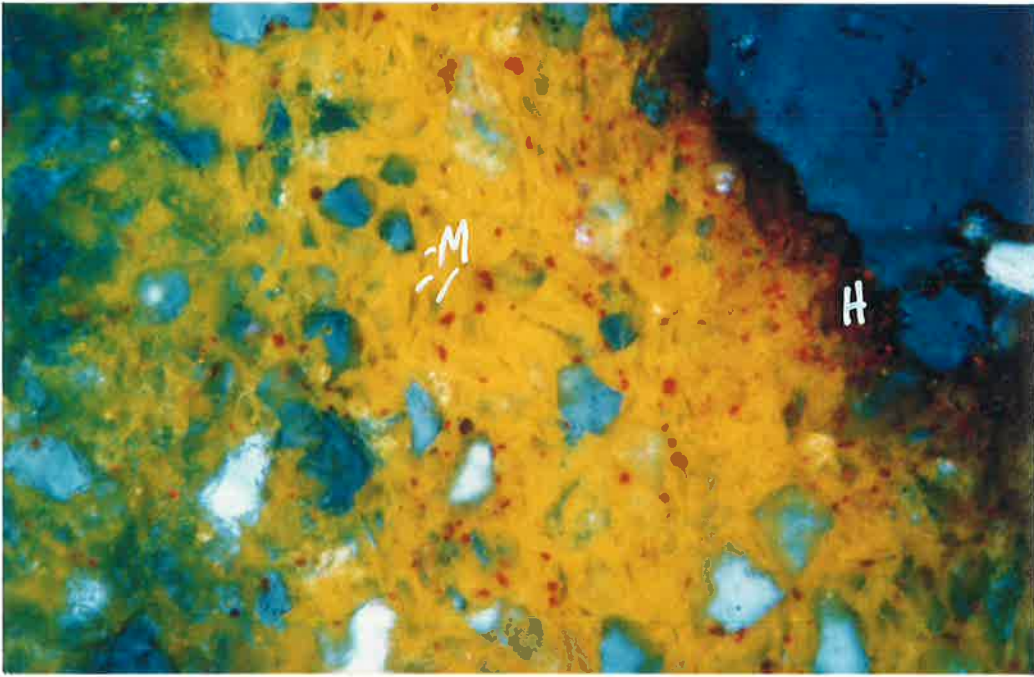


Plate 4.45 Bleached and kaolinised Precambrian Aldgate sandstone exposed by quarrying at Longwood, in the South Mount Lofty Ranges at 400 m above sea level. The depth of the section is 30 m.

Plate 4.46 View south across the Mount Taylor Plain from the summit surface of Kangaroo Island. Mount Taylor (T) is visible on the horizon in the centre of the plate, and Mount Stockdale (S) occurs on the left horizon. Compare with the section illustrated in Figure 4.24.

Plate 4.47 Photomicrograph of complex polygenetic pisolith (BOU 129). Sample collected from area intermediate between summit surface and the Mount Taylor Plain on Kangaroo Island. Earlier generation oolites and pisoliths display various cortex materials and thin gibbsitic rinds. They are cemented in a quartz-rich matrix indurated with goethite plus gibbsite, which forms the core of the subsequent generation pisolith. The rind of the large pisolith (right of photograph) consists of layers of goethite, gibbsite and possibly maghemite. Photograph in transmitted plane polarised light. Width of field 6.8 mm.

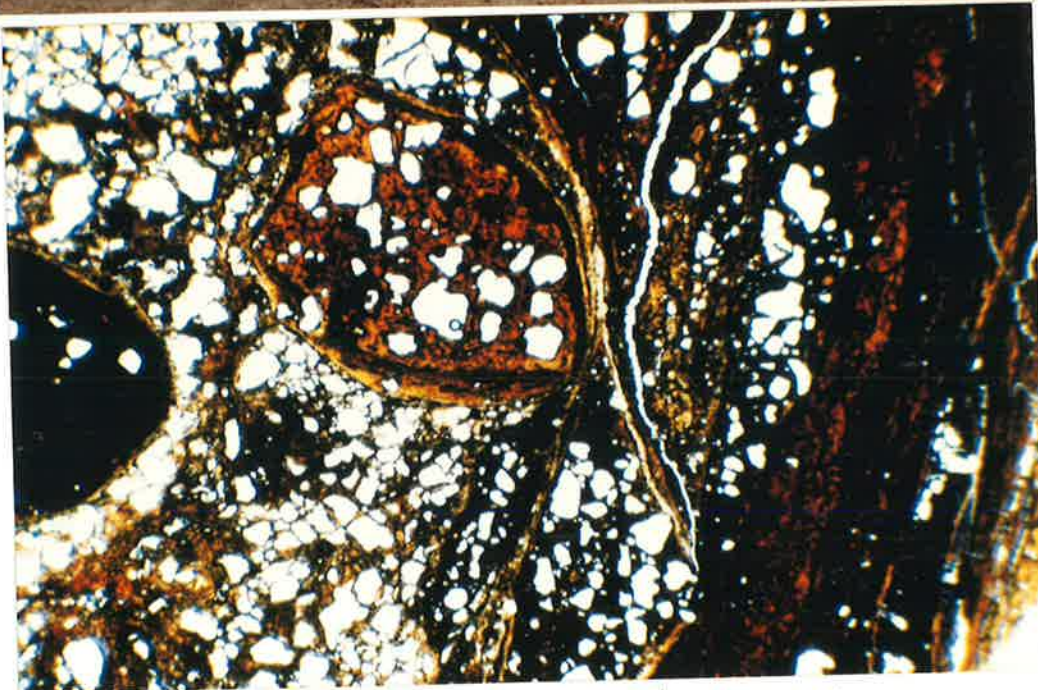
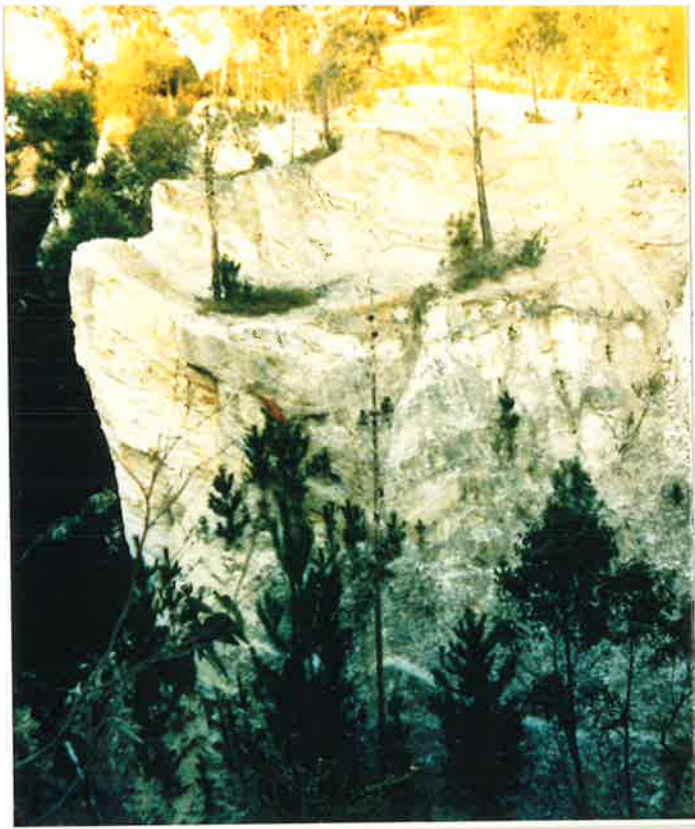


Plate 4.48 Complex goethite-rich pisoliths with quartz clasts up to grit size, in clay matrix replaced by iron oxide (hematite) (BOU 136). Oolith (O) with gibbsite plus goethite rind appears within a pisolith, illustrating a series of cycles of formation. Photograph in transmitted plane polarised light. Width of field 14.6 mm. Sample from the Mount Taylor Plain.

Plate 4.49 Photomicrograph of a sandy sediment showing quartz grains with an intergranular matrix of opaque hematite and goethite (BOU 9). The framework grains are rounded to sub-rounded with a few displaying embayed edges. The framework grains are not closely packed, which suggests that the iron oxides may have replaced pre-existing materials such as clays. The coloured skeleton grains are tourmaline (T) and some irregular intergranular voids (V) occur. Photograph in transmitted plane polarised light. Width of field 4 mm.

Plate 4.50 Photomicrograph of ferruginised quartzose sediment (BOU 8), with large rounded quartz grains and rock fragments with fine angular and smaller grains cemented with iron oxides (dominantly goethite). The matrix has developed through the coalescence of coatings around grains, infilling voids. Transmitted plane polarised light. Width of field 4 mm.

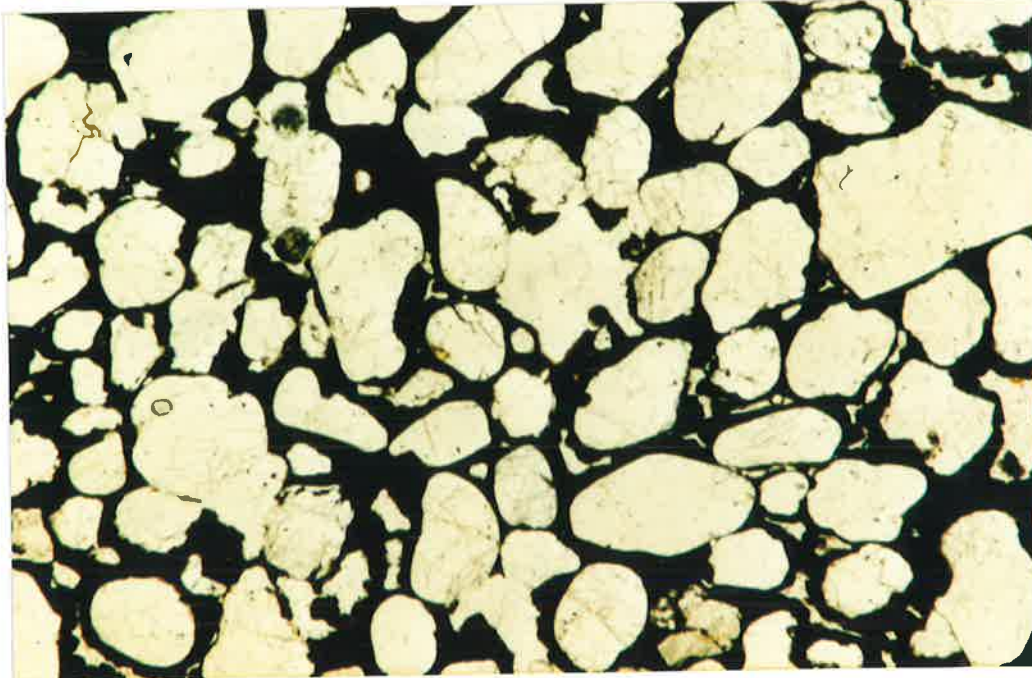
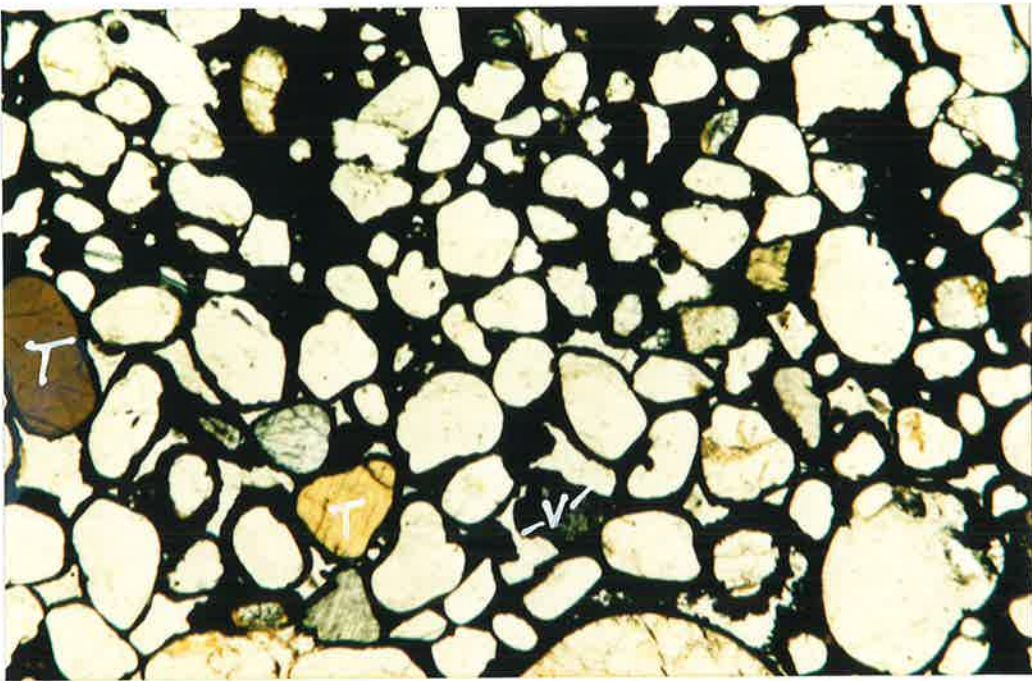
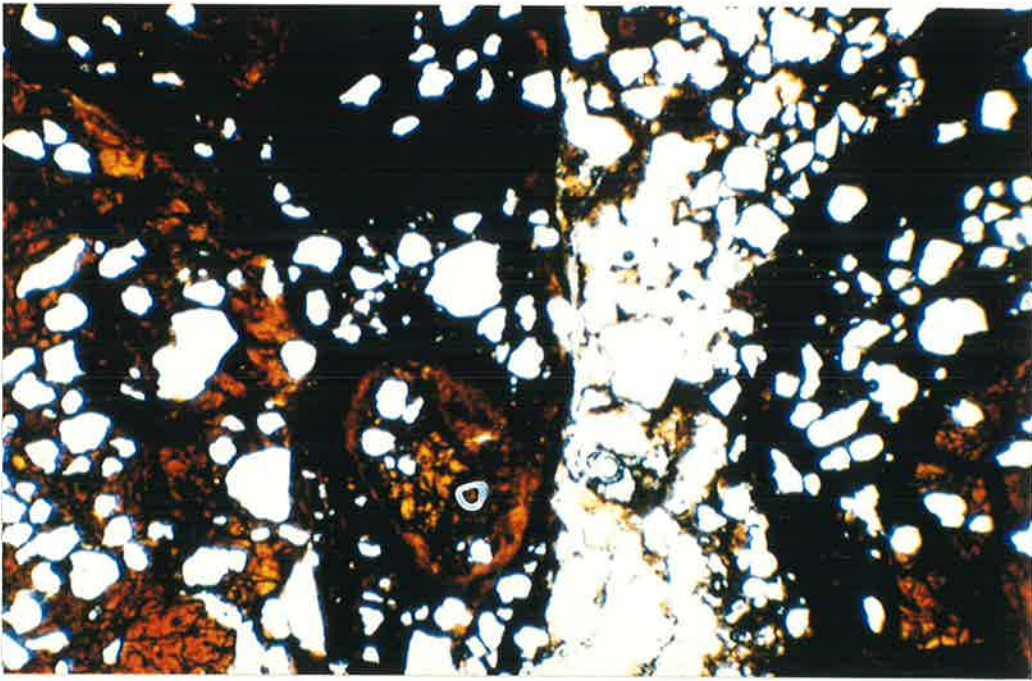


Plate 4.51 Road cutting near Yundi, with surface ferricrete dipping below the surface towards the far left of the section. The ferricrete occurs above weathered Precambrian bedrock and within a sandy unit of Permian glaciogene sediments. The height of the section is 2 m.

Plate 4.52 Photomicrograph of bedded sandy sediment (BOU 7) in which the larger quartz grains are sub-rounded and silt-sized grains angular and shard-like cemented dominantly by goethite with minor hematite. The framework grains are not closely packed but are corroded and etched, suggesting that the groundmass has replaced pre-existing matrix material, such as clays. Transmitted plane polarised light. Width of field 4 mm.

Plate 4.53 View to the northeast of the ferricrete-capped Gun Emplacement on the margin of the Eden escarpment, showing the planate nature of the surface and the pronounced breakaway on its nearest (southern) side. The Gun Emplacement stands at about 210 m above sea level and some 200 m below the level of the backing escarpment summit surface.

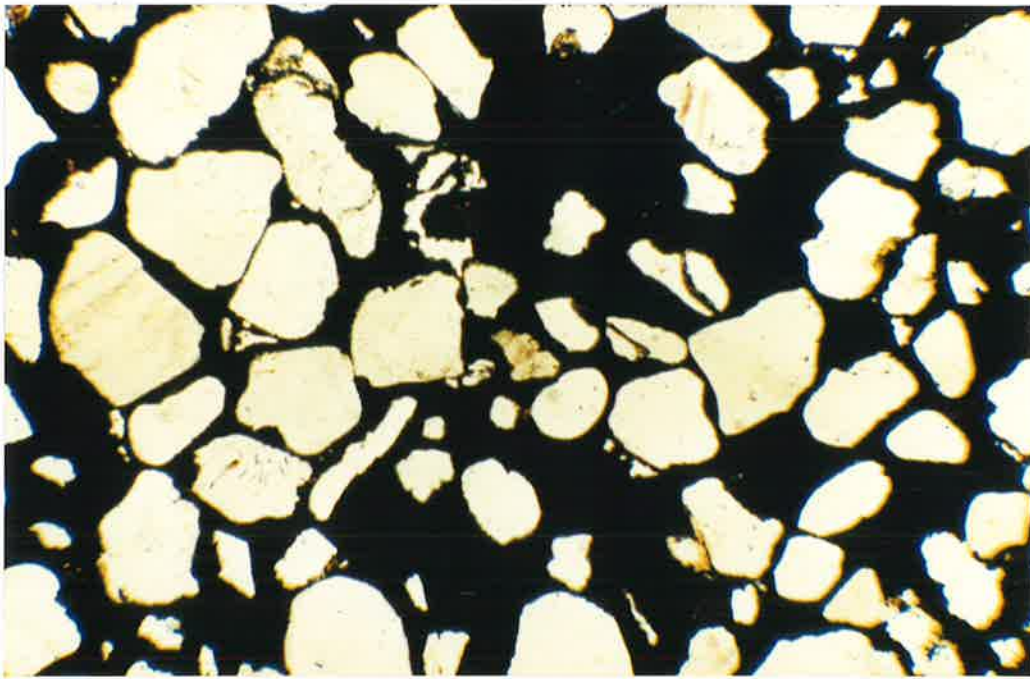




Plate 4.54 Quarry exposing variably iron-stained and bleached sandy quartzose sediments of possible Eocene age, which underlie the Gun Emplacement. It is currently possible to trace these sediments, without major discontinuity to within a short distance of the Gun Emplacement surface

Plate 4.55 Ferruginous sandy sediments underlying the Gun Emplacement occasionally contain clasts of quartz and small iron-rich pisoliths and fragments, suggesting the existence of ferruginous clasts prior to the Eocene. Goethite is the dominant iron oxide in the sands. Hammer handle 30 cm long.

Plate 4.56 Northwestern edge of Gun Emplacement showing goethite-impregnated sands with pisolith structures (P) overlain by coarse fanglomerate sediments displaying dominantly hematite-rich mottles (H). The pisoliths appear to have been transported, and in places have been subsequently bleached of iron. The overlying coarse, angular, bleached and mottled fanglomerates are typical of many similar sediments in scarp foot situations along the escarpments of the Mount Lofty Ranges and were regarded as the Kurrajong Formation by Ward (1966).

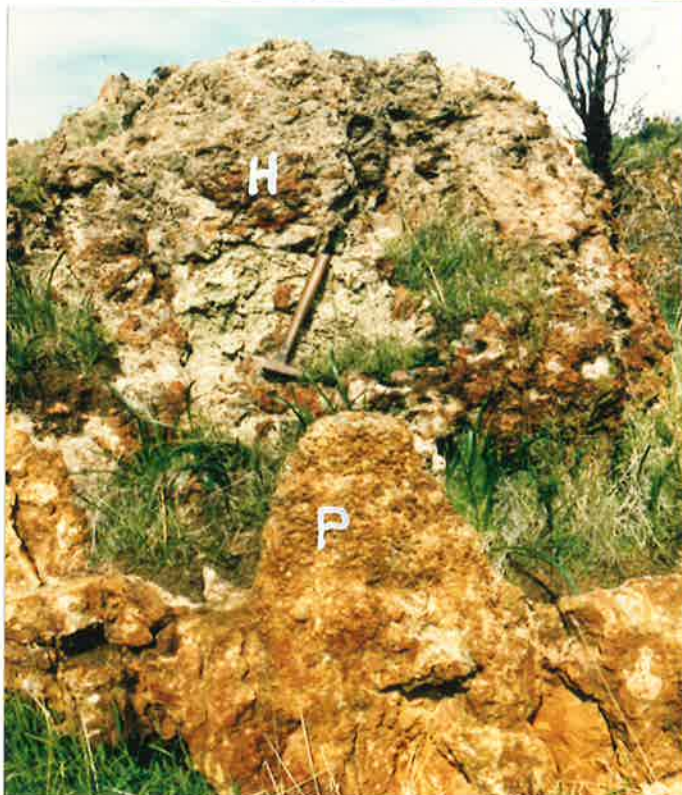


Plate 4.57 View of the Bremer scarp looking east from Mount Barker. The Murray Basin appears in the far distance. Note the planate surface above the escarpment, dipping gently to the south (right). Several marine incursions in the Tertiary penetrated into the Eastern Mount Lofty Ranges along this structure.

Plate 4.58 Bench on the Willunga escarpment at approximately 160 m asl underlain by mottled sandy sediments. Ward (1966) regarded this bench as the effect of a eustatically controlled Late Pliocene shoreline, but it is probably much older and part of its elevation is due to tectonic uplift. Sands at the surface have some shoreline characteristics, but have formed from the weathering of the pre-existing mottled sandy sediments, which may be of Early Pliocene or Miocene age.

Plate 4.59 Section approximately 4 m deep exposed in the overflow channel of the Happy Valley reservoir. Tertiary sediments with goethitic mottles are overlain by a dark grey to black Vertisol.



Plate 4.60 Road cutting on the Victor Harbor-Cape Jervis road west of the Waitpinga road, exposing bands rich in pisoliths at a depth of about 1 m in ferruginous sandy sediments of probable Pliocene age and of aeolian origin. Other pisoliths occur at the ground surface and in the upper soil mantle. The pisoliths at depth contain only goethite, whereas those at the surface have higher iron contents and contain dominantly hematite and maghemite. Geological hammer 33 cm long.

Plate 4.61 Photomicrograph of former aeolian sandy sediment (BOU 327) impregnated with iron oxides (dominantly goethite). Dense, opaque zone on right marks concentration of iron oxides forming incipient pisolith, and probably replacing pre-existing clays. Note the similarity in the framework quartz grains throughout the photograph. Transmitted plane polarised light. Width of field 4 mm.

Plate 4.62 Photomicrograph showing details of of matrix material shown in Plate 4.61, illustrating colloform structures indicating illuvial layers or clays (kaolinite and smectite) plus iron oxides in the intergranular spaces. Some quartz grains have hematite coatings and laminated goethite and clays occur in the voids. Transmitted plane polarised light. Width of field 1.2 mm.

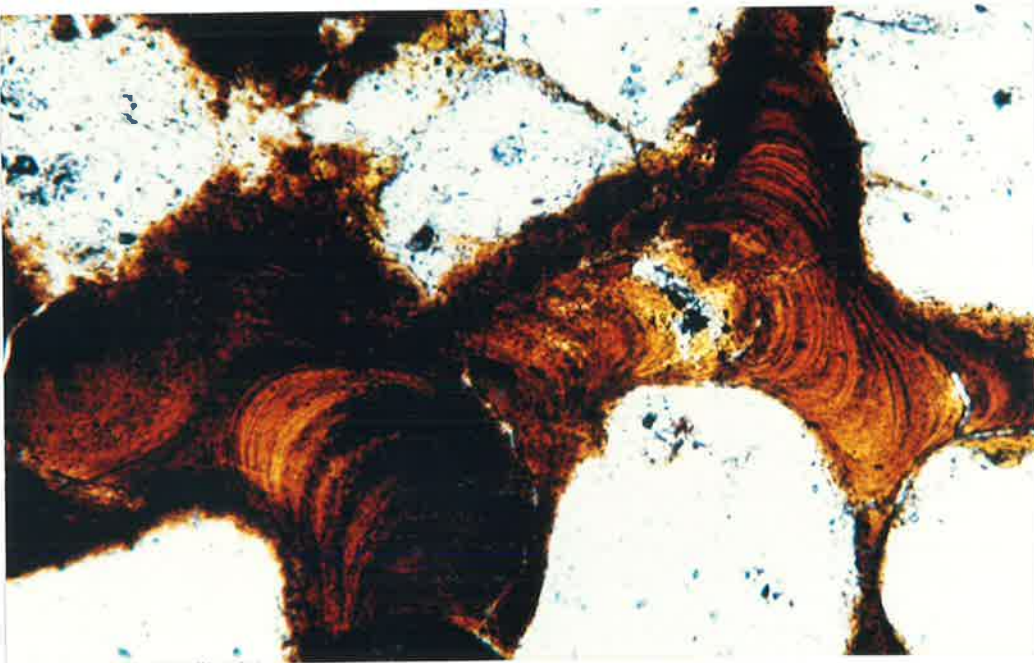
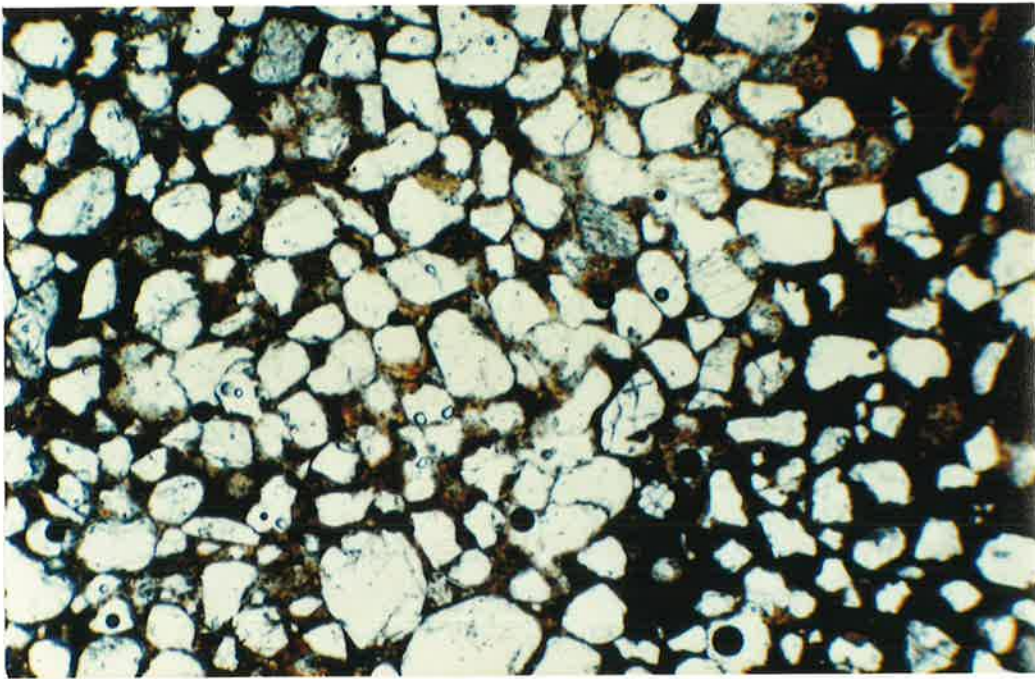


Plate 4.63 Sharp but irregular contact between the Jurassic Wisanger basalt and underlying bleached and kaolinised Permian glaciogene sediments in the Old Government Quarry, Kingscote, Kangaroo Island. Oxygen isotope analyses suggest that the kaolinisation pre-dated the extrusion of the basalt. Section approximately 20 m high.

Plate 4.64 Ferruginous mottling (dominantly hematitic) exposed in sea cliff eroded in Permian glaciogene sediments near jetty, Kingscote, Kangaroo Island. Calcium carbonate of probable Pleistocene age has penetrated into the upper section of the profile, but the mottles are still visible. Height of section 10 m.

Plate 4.65 Structure at the cliff base near the Kingscote jetty with an alunite core and a rim of iron oxides (dominantly hematite) incorporated in weathered, bleached and mottled Permian glaciogene sediments. The alunite has probably formed by the weathering of a pre-existing sulphide-rich boulder in the glaciogene sediments. The structure is approximately 1 m across.





Plate 4.66 Convolute ferricrete (F) (BOU 102) in coastal cliff at Kingscote, formed by the iron oxide-impregnation of Permian ice-contact glaciogene sediments. The sands underlying the ferricrete contain clay clasts, presumably transported in a frozen condition. The section is approximately 4 m high.

Plate 4.67 Close-up of clay clasts, immediately below the convolute ferricrete in Plate 4.66, incorporated into sandy sediments in a pro-glacial environment while still frozen. This provides evidence of the nature of the original Permian glaciogenic sediments (slumped ice-contact deposits), which were iron-impregnated at a later stage. Key provides scale.

Plate 4.68 Photomicrograph of partly ferruginised Eocene limestone (BOU 122). Dominantly shows calcite structures, with some voids (V), and small yellow patches comprise goethite. Photograph in polarised light. Width of field 18 mm.

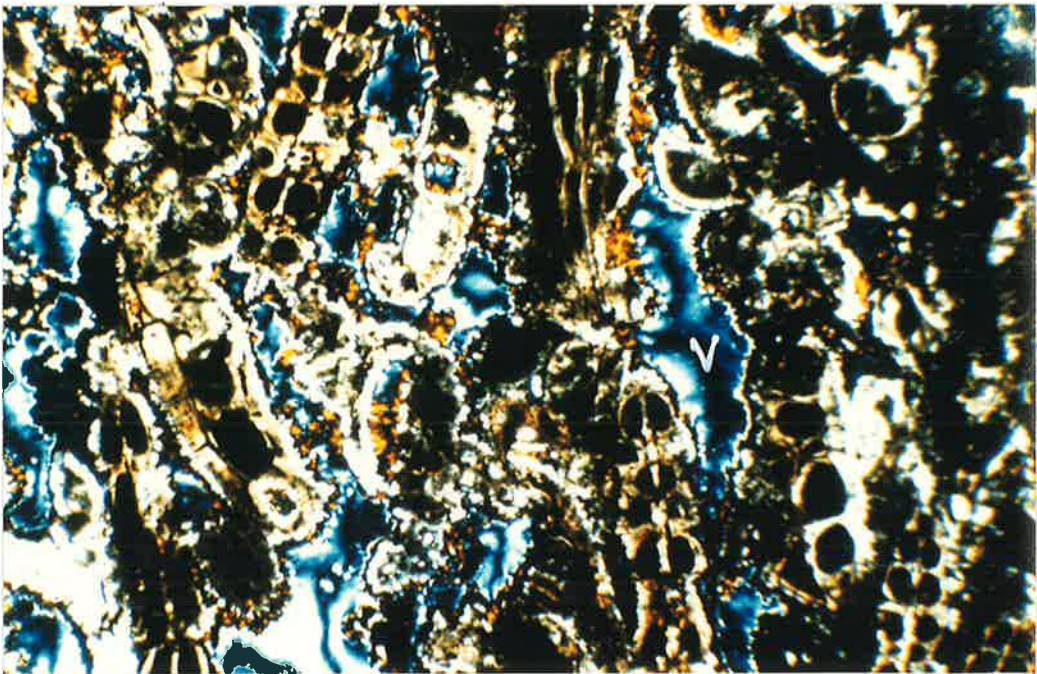
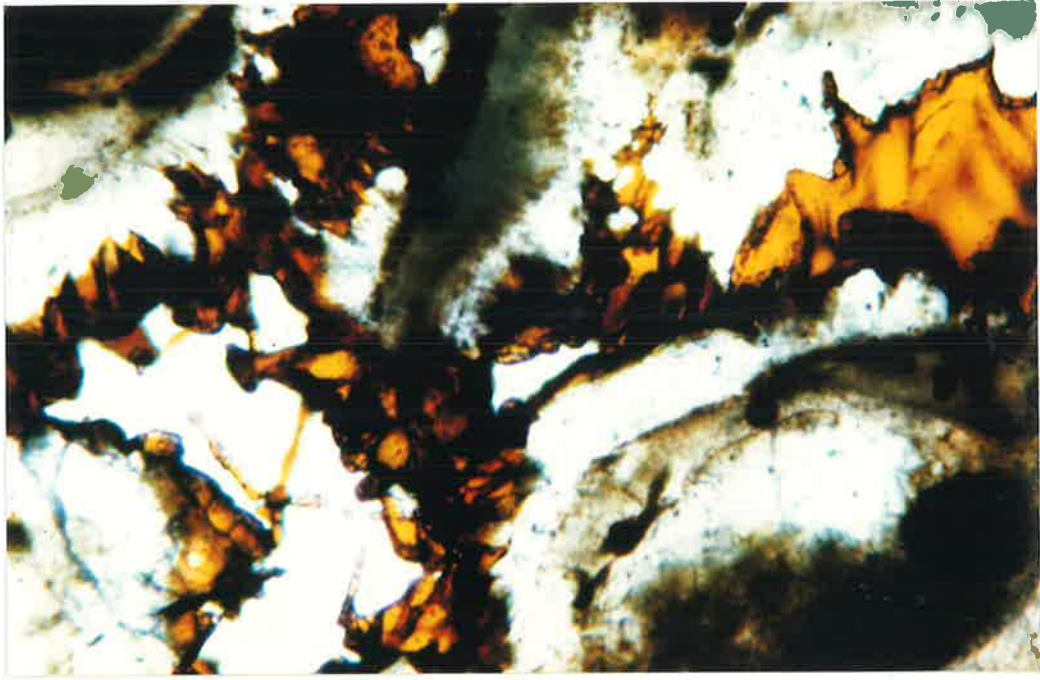


Plate 4.69 Photomicrograph of details of ferruginised Eocene limestone (BOU 122), showing infilling of voids, formed by dissolution of calcite crystals, with orange coloured goethite crystallites. Transmitted plane polarised light. Width of field 1.2 mm.

Plate 4.70 Eroding hematitic mottled zone in Pleistocene sediments at Hallett Cove, forming a lag of ferruginous clasts at the surface, which may ultimately form pisoliths. This is one of the mechanisms suggested for the initiation of pisolith formation. Scale is marked on photograph.

Plate 4.71 Section of iron-mottled Pleistocene sediments at Redbanks on the Light River, Mid North overlain by calcareous horizon. The mottles of these Pleistocene sediments are typically hematitic and contain small amounts of maghemite. The section in the right background is approximately 15 m high.



100000

Plate 4.72 Variably weathered and ferruginised Precambrian basement rocks of Brachina Formation (B) overlain by ferruginised and mottled Pliocene and Pleistocene sediments (P) at Ochre Cove (S=Seaford Formation; OC=Ochre Cove Formation; N=Ngaltinga Clay of Ward, 1966). The unconformity (U) occurs at approximately the line of the path that extends across the plate approximately two thirds of the way up the section. Height from unconformity to surface approximately 24 m.

Plate 4.73 Road cutting near 'Yorke Farm' on the Kingscote-Penneshaw road. Weakly iron-mottled (M) sandy sediments occur at the base of the section, succeeded by a carbonate-rich horizon (C) on which the modern soil with ferruginous pisoliths (P) occur.

Plate 4.74 View of ferruginised Pleistocene sediments exposed in the coastal cliffs at Redbanks, Kangaroo Island. In places the sediments comprise transported pisoliths as well as showing the impacts of *in situ* weathering. The cliffs are approximately 10 m high.



Plate 4.75 View of peritidal environment at Fishery Bay. Pleistocene sediments form the cliff and iron oxide precipitation has occurred in the foreground in calcareous and organic sediments, with iron oxides having been derived from continental ground waters emerging at the shoreline. See Figure 10.2. The cliffs are approximately 5 m high.

Plate 4.76 Spodosol with well developed pipy Bh and Bhir horizons, with a deeper Bhir horizon (placic horizon or 'coffee rock') and a pronounced bleached A2-horizon exposed in sand quarry near Mount Compass. The A12 horizon contains some organic matter,, whereas the A2 horizon is strongly bleached. The B21h contains humic matter, and the B21hir contains iron as well as humic matter. A stoneline separates these horizons from an underlying IIB22hir horizon, part of a truncated profile. In turn this is underlain by a IIB3 horizon, which contains clay lamellae. The parent material of this spodosol consists of Permian glaciogene sands, or their reworked equivalents. Photograph Dr. R.W. Fitzpatrick.

Plate 4.77 Photomicrograph of spodic horizon at Mount Compass (BOU 1). Sub-angular to sub-rounded fine sand to silt-sized quartz framework grains, with some tourmaline grains. Incomplete matrix of reddish incoherent clays. Clay-rich organic material coats the individual grains and occasionally bridges voids. Transmitted plane polarised light. Width of field 6.8 mm.

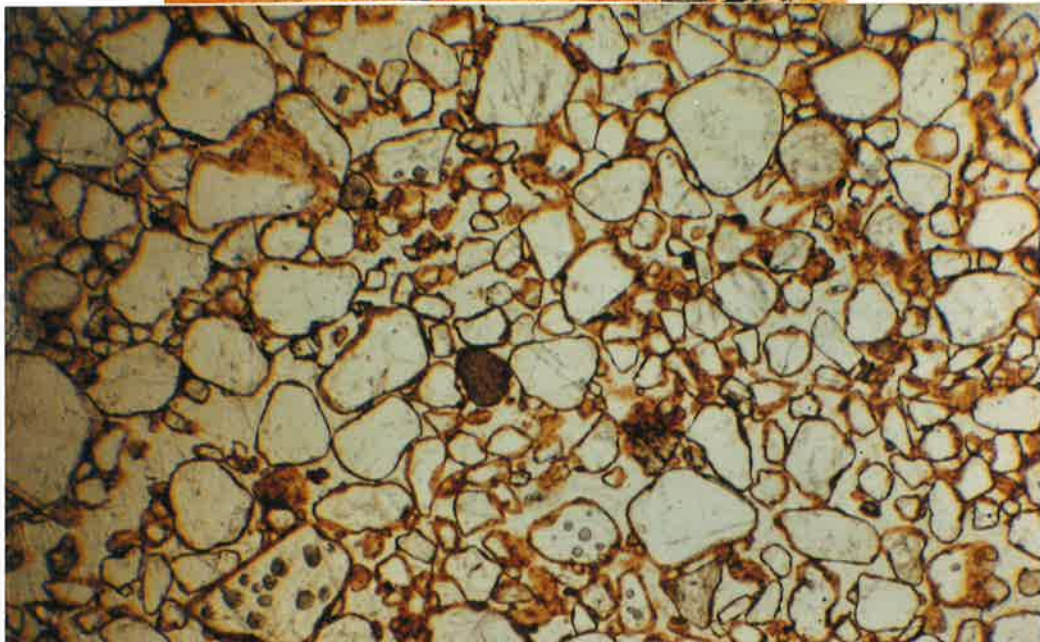
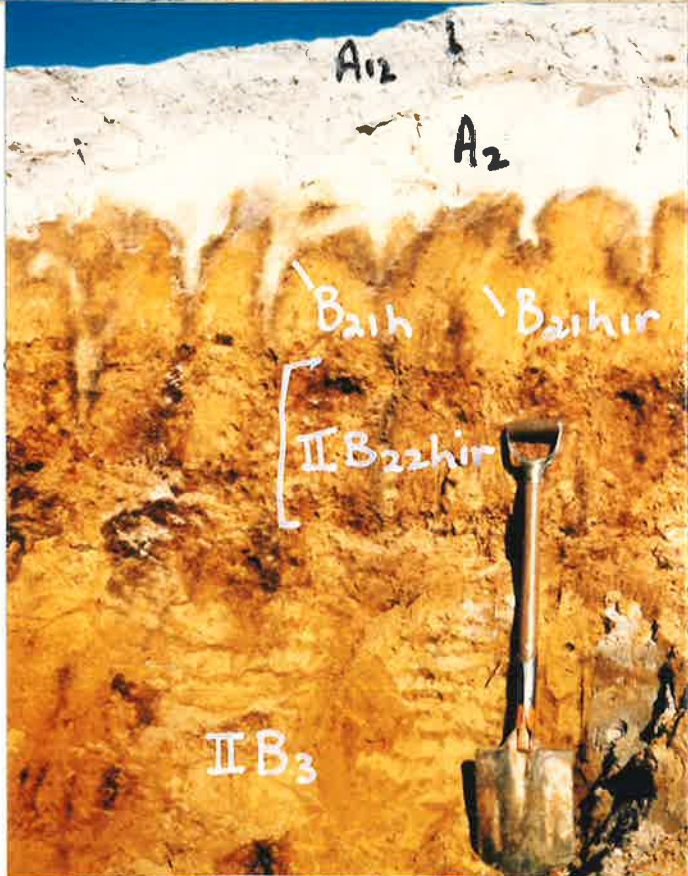




Plate 4.78 Saline seepage zone in the Middle River catchment area, Kangaroo Island. Ferrihydrite (F) has precipitated at the sites of piezometers. Posts 1 m high.

Plate 4.79 Photomicrograph of core of incipient pisolith (BOU 133) in seepage zone of Tin Hut Creek. Cellular structures reveal organic character of core material. The dominant iron oxide present is goethite. Transmitted plane polarised light. Width of field 2.6 mm.

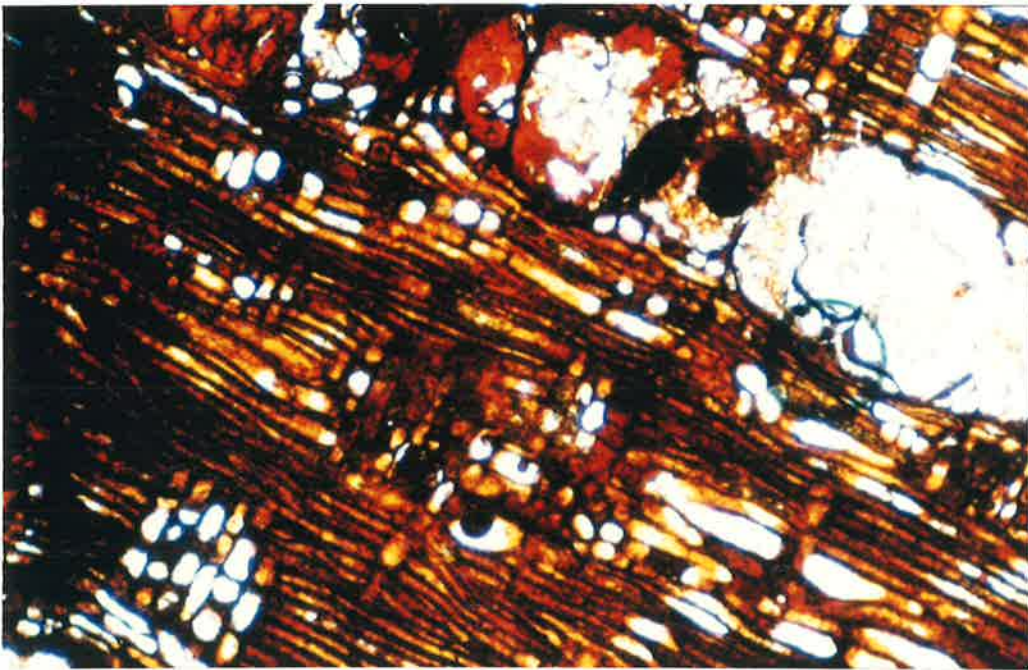


Plate 5.1 Pronounced undulating stoneline of ferruginous pisoliths at the top of the B-horizon in a soil profile near Craighburn in the Mount Lofty Ranges. Bleaching occurs at the base of the A-horizon, indicating seasonal waterlogging. The gravel layer has collapsed into a solution hollow near the centre of the photograph. Profile is 1.2 m deep.

Plate 5.2 Photomicrograph of intergranular void between skeleton quartz veins in a ferruginised sediment (BOU 9) occupied by alternating deposits of hematite (red) and goethite (yellow), forming pronounced bands. Polarised transmitted light. Width of field 0.5 mm.

Plate 5.3 Photomicrograph of portions of two complex pisoliths that contain abundant quartz and display laminar iron oxide and gibbsite rinds, set in matrix material of different character incorporating ooliths indurated by gibbsite. Transmitted plane polarised light. Width of field 6.8 mm.

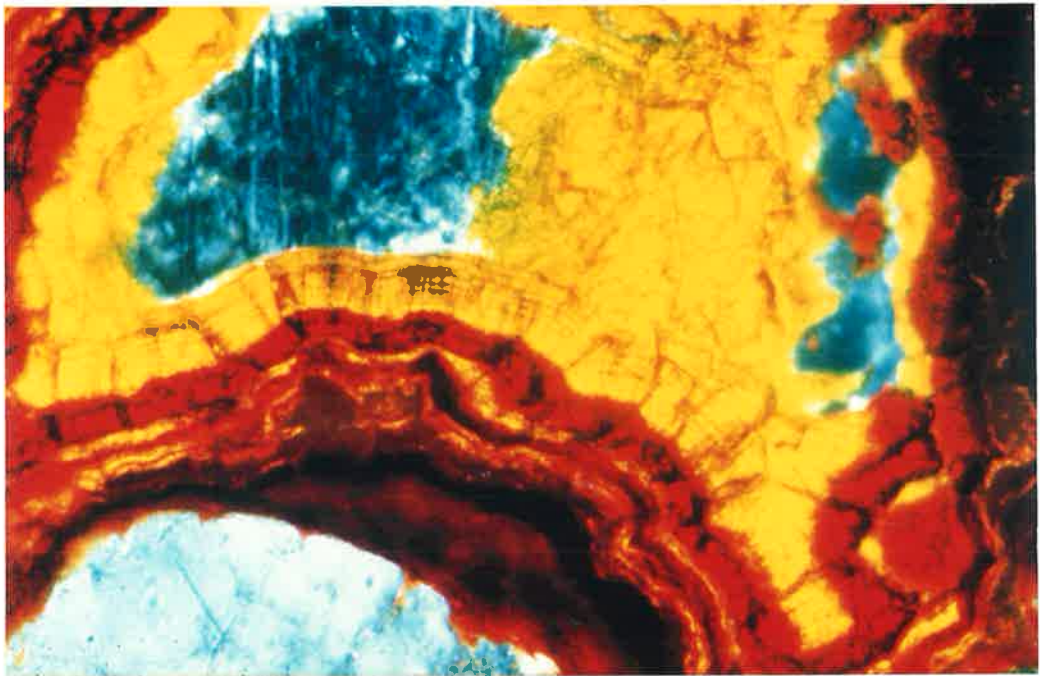
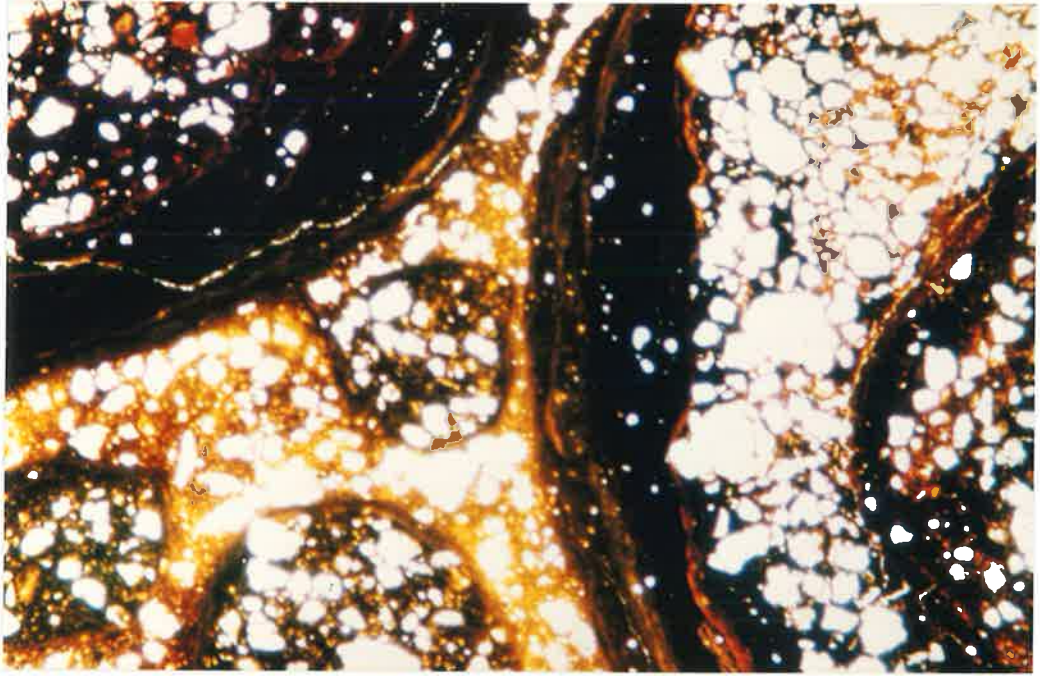


Plate 5.4 Photomicrograph of pisolith with core of ferruginised metasandstone surrounded by rind composed of quartz clasts cemented by iron oxides, illustrating the accretionary nature of this pisolith. Dominant iron oxides present are hematite and maghemite. Width of field 6.8 mm. Transmitted plane polarised light. BOU 121, Redbanks, Kangaroo Island.

Plate 5.5 Photomicrograph of pisolith (BOU 104) consisting of alternating but irregular bands rich in quartz grains and iron oxides (hematite plus maghemite). Transmitted plane polarised light. Width of field 6.8 mm.

Plate 5.6 Vermiform ferricrete in 'Laterite Quarry' near Ione, California, showing a pronounced horizontal orientation. The red material is dominantly hematitic and the light-coloured structures are composed dominantly of kaolinite with minor gibbsite. The hammer is 35 cm high.

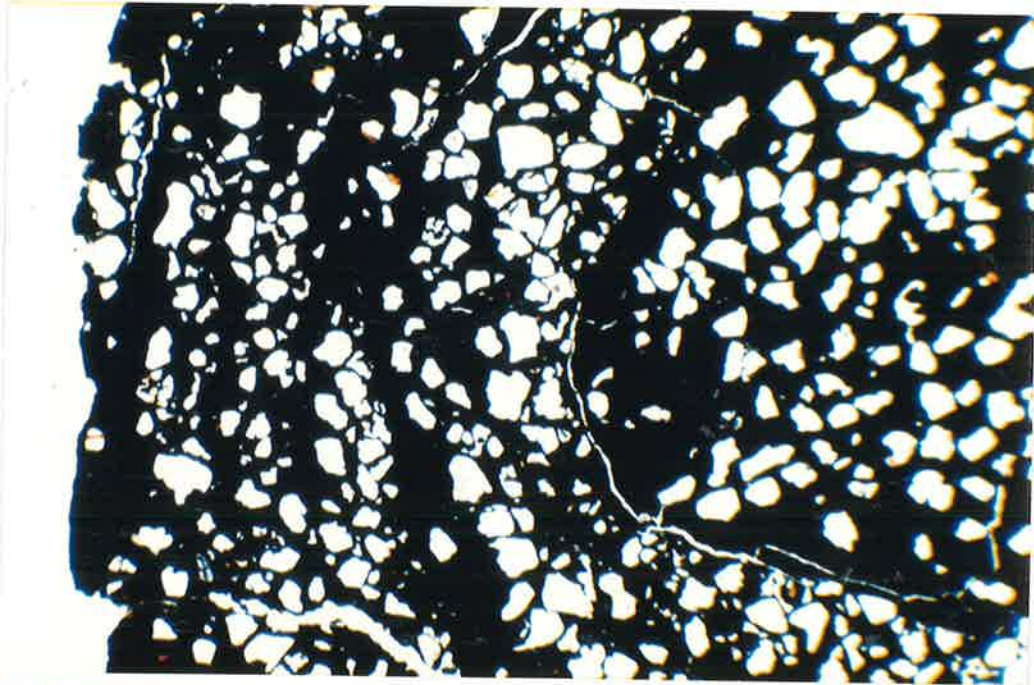


Plate 6.1 Profile showing calcareous earth (C) overlain by red soil with ferruginous pisoliths (R) and exposed by dam construction on the Blue Range, Eyre Peninsula at an elevation of approximately 250 m asl. The depth of the profile is approximately 2 m.

Plate 6.2 General northeasterly view from Mount Nield of the area mapped as the Glenville etch surface by Twidale *et al.* (1976). The highest points range up to 400 m asl.

Plate 6.3 Weathered and bleached Precambrian gneissic bedrock with coarse hematitic mottles in the Corrobinnie Depression. In the distance it is overlain by weathered and ferruginised Eocene sediments of the Garford Formation. Denser and harder iron-rich mottles (M) occur in the weathered bedrock two thirds of the way up and on the left of the plate. Hammer 35 cm long.





Plate 6.4 Closer view of hardened dense mottles shown in Plate 6.3. They stand up above the level of the surrounding bleached zones, and their disintegration has formed a lag of ferruginous clasts (L), especially on the right of the plate. The plastic bags are approximately 30 cm high.

Plate 6.5 Closer view of section exposed in the weathered and ferruginised Garford Formation sediments shown in Plate 6.3. Bleached materials occur at the base of the section and a ferricrete with weathered clays in the upper section. The section is approximately 3.5 m high.

Plate 6.6 Ferricrete crust at top of section shown in Plate 6.5, showing voids in crust, some of which are occupied by light-coloured clay-rich materials. Figure provides a scale.



Plate 6.7 Ferricrete (BOU 573) exposed in claypan near Pinjarra dam in the Corrobinnie Depression. Hammer provides scale. Photograph Dr. N.F. Alley.

Plate 6.8 Bleached weathering profile preserved on Mount Cooper, a granitic inselberg in western Eyre Peninsula. Figures provide scale. Photograph Dr. A.R. Milnes.

Plate 6.9 Coastal erosion has exposed bleached and mottled gneissic bedrock in the lowest 4 m of the coastal cliffs at Point Labatt, Eyre Peninsula. These rocks are overlain by a thin ferricrete of sedimentary origin, which in turn is overlain by calcarenites of probable Pleistocene age. These sediments comprise the greatest proportion of the 50 m high cliffs.



Plate 6.10 Weathered, bleached and iron-mottled Precambrian rocks exposed in coastal cliffs at Sleaford Bay, Eyre Peninsula. The cliffs are approximately 20 m high.

Plate 6.11 Accumulation of ferruginous pisoliths in small channel cut in weathered Precambrian basement rocks in coastal cliffs at Sleaford Bay, Eyre Peninsula. Geology hammer 35 cm long.

Plate 6.12 Surface lag of ferruginous pisoliths above weathered Precambrian bedrock at Sleaford Bay, Eyre Peninsula.



Plate 6.13 Pisolitic ferricrete overlying weathered and iron-stained basement rocks in coastal cliffs at Sleaford Bay. Note the rectangular bleaching pattern that affects both pisolitic ferricrete and the underlying weathered basement rocks. Hammer 33 cm long.

Plate 6.14 Weathered boulders of sandstone and grit on the Lincoln Highway bleached and variably stained with red (hematite) and yellow (goethite) mottles.

Plate 6.15 Quarry in light-coloured, weathered and slightly iron-stained bedrock in the Tod River valley near Koppio, Eyre Peninsula. Pisolitic ferricrete occurs downslope and to the left of the tree on the horizon, and Precambrian hematitic quartzite occurs to the far right of the tree. Geology hammer 35 cm long.





Plate 6.16 Intricately iron-stained kaolinised bedrock exposed in quarry shown in Plate 6.15 and formed under the influence of groundwaters. Height of section 2.5 m.

Plate 6.17 Mottled, bleached and weathered bedrock overlain by and impregnated with calcium carbonate, near Port Lincoln. The mottles are dominantly of hematite. Geology hammer 33 cm long.

Plate 6.18 Weathered, bleached and iron-mottled Precambrian bedrock exposed by a road cut on the Tumby Bay-Cummins road. Some of the hematite mottles are aligned along near vertical bedrock structures. Figure provides a scale.



Plate 6.19 Ferruginised channel fill material occupying palaeochannel cut in weathered and mottled basement rocks in the same area as Plate 6.18. The channel sediments are strongly ferruginised in the upper 2 m. The section is approximately 7 m deep, and illustrates the polygenetic nature of the profile.

Plate 6.20 Yellow soil containing ferricrete fragments (C) on the flank of Knott Hill. The clasts of ferricrete have derived from the disintegration of pre-existing nodular ferricrete. Note the strongly bleached A-horizon. Hammer 33 cm long.

Plate 6.21 Pisolitic ferricrete at Yallunda Flat, Eyre Peninsula. The ferricrete occurs in a relatively low point in the topography. Geology hammer 35 cm long.

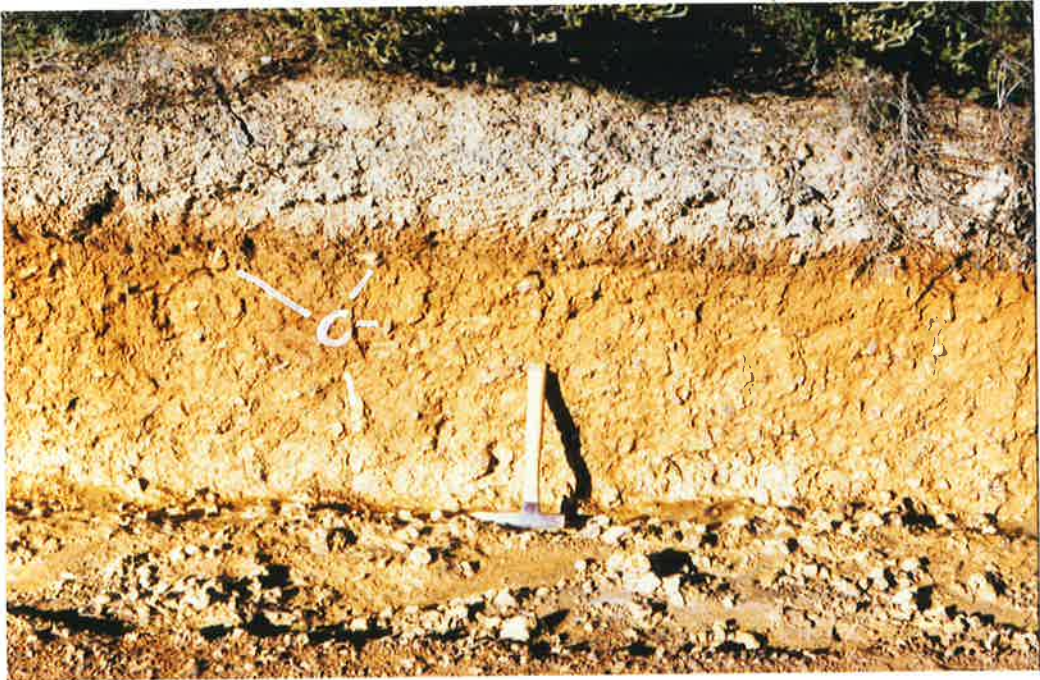


Plate 6.22 Strongly ferruginised fluvial sediments occupying palaeochannel eroded in weathered and bleached Precambrian basement rocks near Yallunda Flat. Vehicle provides scale.



Plate 7.1 Headwall of landslide on southern edge of 'Noss Mesa' at 150 m asl, near Casterton. A brown soil, 30 cm deep contains platy fragments of ferricrete and ferruginous pisoliths. An horizon of massive ferricrete forms the pronounced bluff, contains large maghemitic clasts at depth, and overlies weathered and bleached Late Cretaceous Otway Group metasediments. The section is approximately 10 m high.

Plate 7.2 Landslide headwall on the northern margin of "Noss Mesa" near Casterton, revealing bleached and mottled zone overlain by the modern soil profile. The section is 4-5 m deep.

Plate 7.3 Photomicrograph of massive ferricrete (BOU 201) shown in Plate 7.1, illustrating unsorted angular to very angular embayed and etched quartz grains set in a complex matrix of clays and iron oxides. The embayed quartz grains suggest modification by weathering processes. Photograph in polarised light. Width of field 2.9 mm.

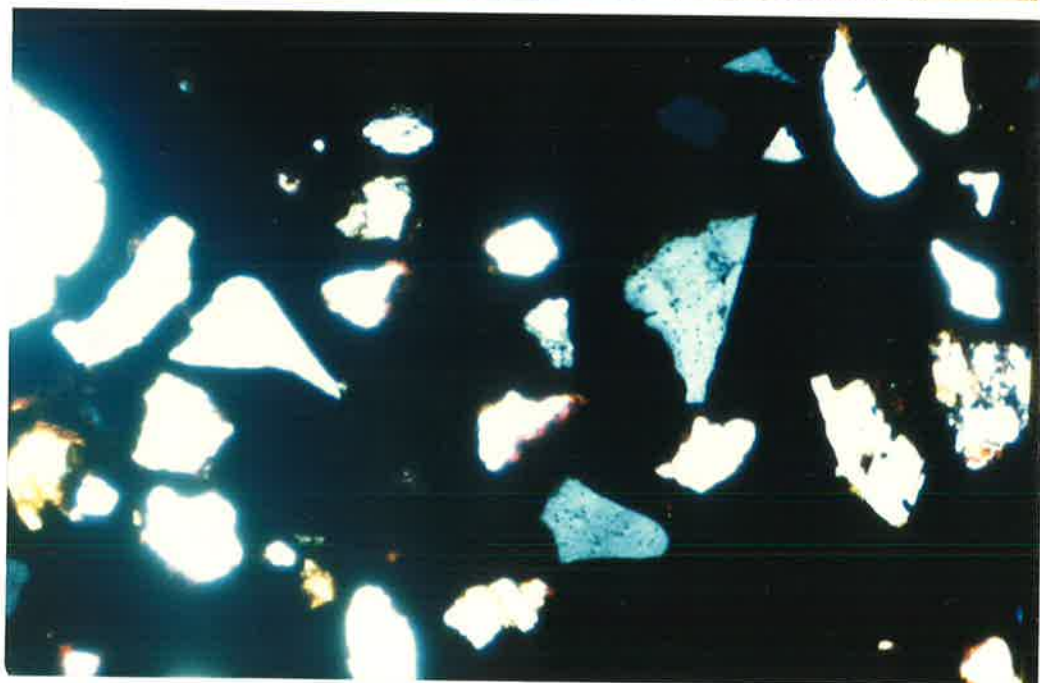




Plate 7.4 Photomicrograph of mottle (BOU 208) from the section illustrated in Plate 7.2, revealing that it is a very ill-sorted sediment consisting of medium to coarse quartz grains set in a matrix of kaolinite and iron oxides. The iron oxide is hematite and occurs as fine-grained crystals apparently replacing the kaolinite. Photograph in transmitted plane polarised light. Width of field 2.8 mm.

Plate 7.5 Section at Killara Bluff, exposed by erosion of the Glenelg River, showing bleached metasediments of the Runnymede Formation at the top of the Late Cretaceous Otway Group, overlain unconformably by 16 m of ferruginised Palaeocene fossiliferous marine sediments of the Pebble Point Formation. The section is approximately 30 m deep.

Plate 7.6 Close-up view of ferruginous rhizomorphs formed towards the base of the Pebble Point Formation shown in Plate 7.5. Geology hammer 35 cm long.

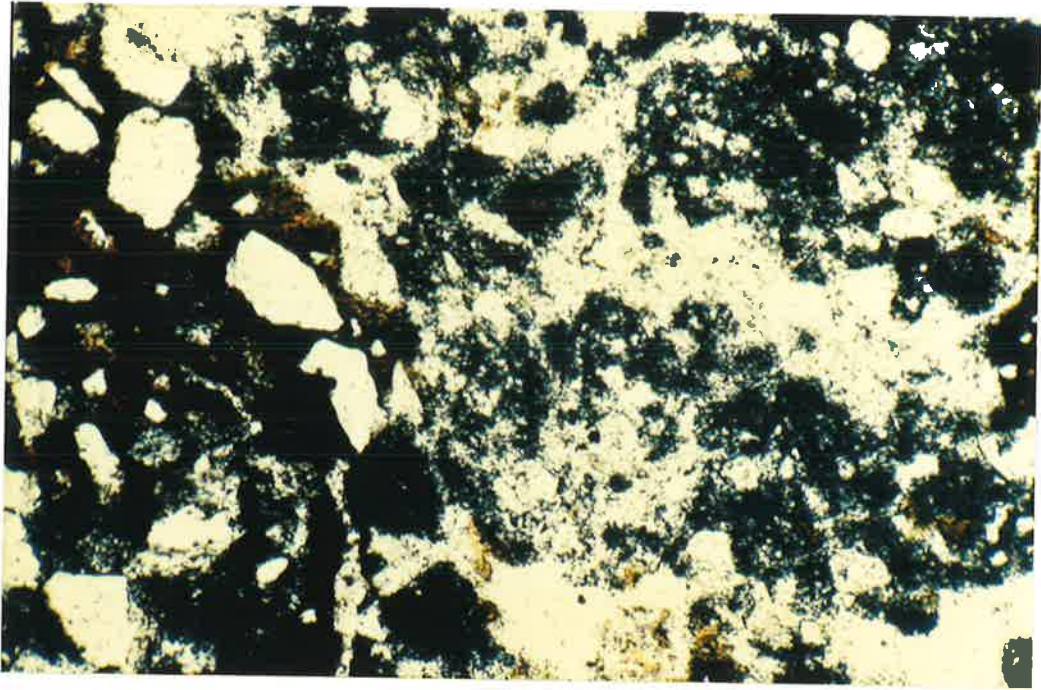


Plate 7.7 Compton Conglomerate of Oligocene age exposed in Allen's Quarry near Mount Gambier, unconformably overlying the Eocene Dilwyn Formation. The Compton Conglomerate here is approximately 0.6 m thick and consists of rounded ironstone pebbles and grits set in a goethitic matrix. Hammer 35 cm high. Photograph Dr. R.W. Fitzpatrick.

Plate 7.8 Photomicrograph of ferruginised quartzose sediment from Coleraine (BOU 210) showing angular quartz clasts and voids in an opaque ferruginous clay matrix. Transmitted polarised light. Width of field 8.9 mm.

Figure 1  
Photomicrograph of  
the matrix  
of the  
sample  
from the  
locality  
of the  
sample



Figure 2  
Photomicrograph of  
the matrix  
of the  
sample  
from the  
locality  
of the  
sample

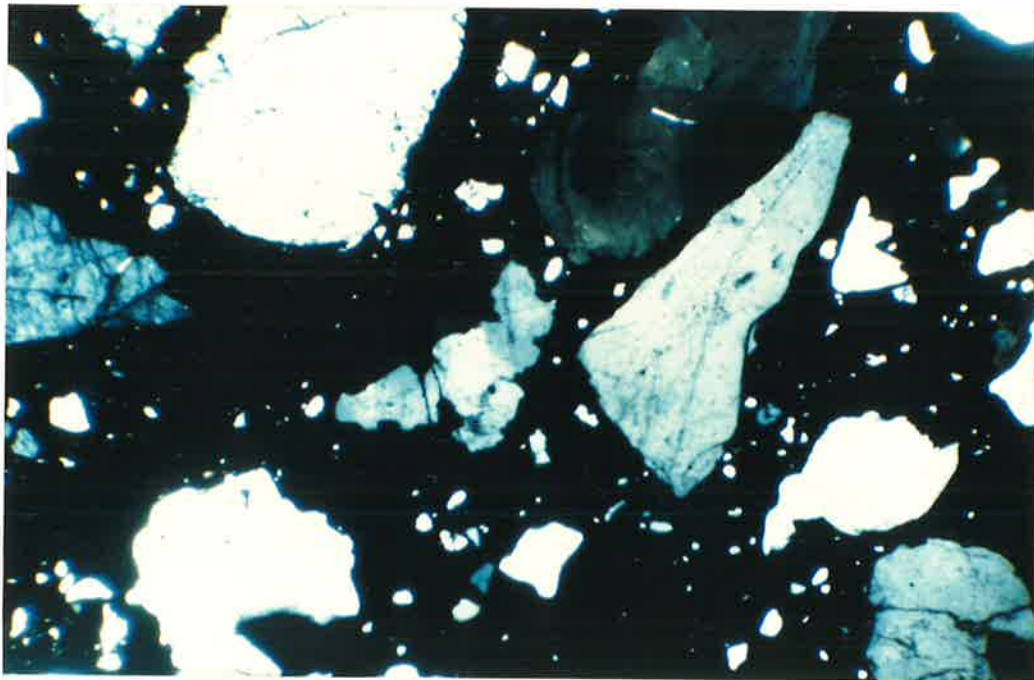


Plate 7.9 Photomicrograph of BOU 210 showing details of the matrix, with crystals of iron oxides replacing clays. Pseudomorphs of micas also occur. Transmitted plane polarised light. Width of field 2.6 mm.

Plate 7.10 Weathered zone exposed by road cut in the partly ferruginised Hamilton basalt near Branxholme, Victoria. Thin bleached zones follow bedrock joints. Magnetic ferruginous pisoliths occur at the surface and in the thin soil. Section 1.5 m high.

Plate 7.11 Photomicrograph of pisolith (BOU 204) formed from weathering and erosion of the Hamilton basalt shown in Plate 7.10. Original basalt structures are apparent, with olivine having been replaced by goethite. Lath-like structures of altered olivines and ghosts of plagioclase crystals are also apparent. Opaque patches hematite. Transmitted plane polarised light. Width of field 2.5 mm.

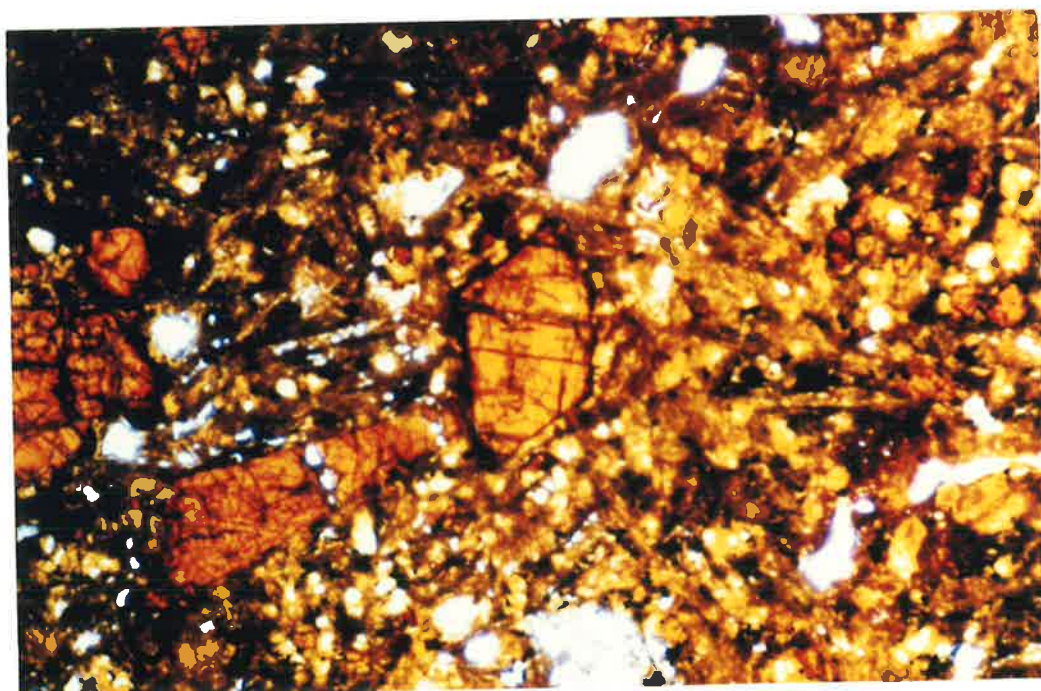
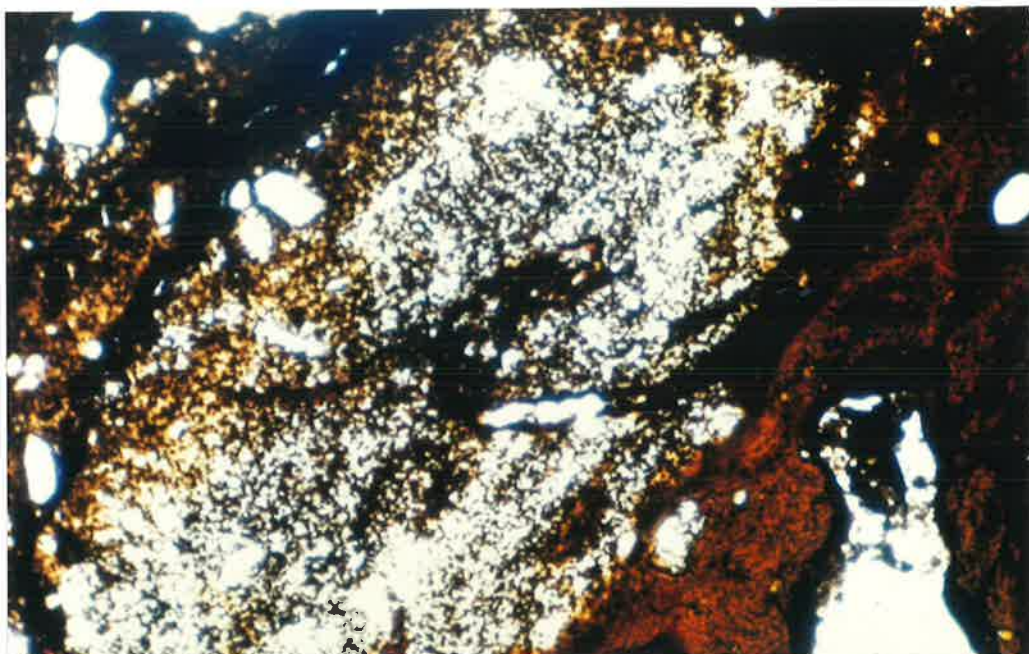


Plate 8.1 Photograph of Site 1 (most southerly exposure) at Terrey Hills quarry where hematitic pisoliths (BOU 400) with no surface rinds are overlain by hematite-rich pisoliths (BOU 401) with pronounced goethitic rinds. In turn these are overlain by a yellow earth. Hammer 35 cm long. Locations of samples are shown in the accompanying sketch. The mineralogy and chemistry of the samples are presented below.

## Sample BOU 400

**Mineralogy**

Gibbsite  
 Quartz  
 Hematite  
 Goethite  
 Anatase  
 Smectite  
 Kaolinite

**Chemistry**

Fe <sub>2</sub> O <sub>3</sub>	31.7%
SiO <sub>2</sub>	28.0%
Al <sub>2</sub> O <sub>3</sub>	37.4%
TiO <sub>2</sub>	1.7%

## Sample BOU 401

**Mineralogy**

Gibbsite  
 Quartz  
 Hematite  
 Goethite  
 Anatase  
 Kaolinite

**Chemistry**

Fe <sub>2</sub> O <sub>3</sub>	29.6%
SiO <sub>2</sub>	26.3%
Al <sub>2</sub> O <sub>3</sub>	40.5%
TiO <sub>2</sub>	1.9%

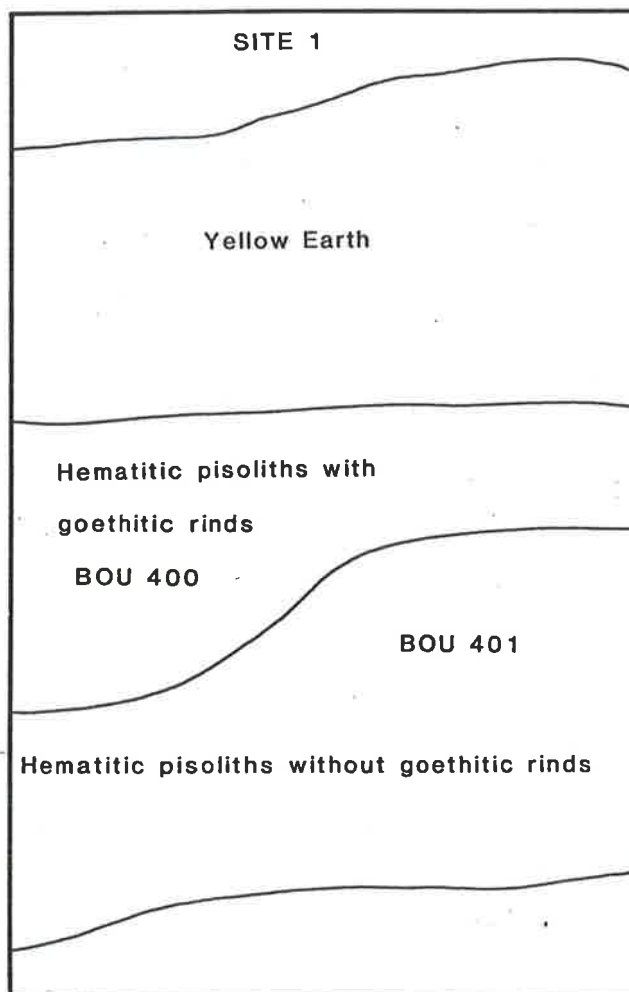




Plate 8.2 Photograph of Site 2, (immediately north of Site 1) Terrey Hills quarry, where mottled and vermiform ferricrete (BOU 403) is overlain by pisoliths (BOU 404). Hammer provides a scale.

Sample BOU 403

**Mineralogy**

Quartz  
Gibbsite  
Goethite  
Hematite  
Anatase  
Maghemite

**Chemistry**

Fe <sub>2</sub> O <sub>3</sub>	37.6%
SiO <sub>2</sub>	26.1%
Al <sub>2</sub> O <sub>3</sub>	33.2%
TiO <sub>2</sub>	1.6%

Sample BOU 404

**Mineralogy**

Gibbsite  
Quartz  
Hematite  
Goethite  
Maghemite  
Kaolinite

**Chemistry**

Fe <sub>2</sub> O <sub>3</sub>	37.2%
SiO <sub>2</sub>	22.5%
Al <sub>2</sub> O <sub>3</sub>	38.0%

Plate 8.3 Close view of mottled vermiform ferricrete at base of section shown in Plate 8.2. White areas consist of kaolinite plus gibbsite. Maghemite clast (M) near lens cap, which is 6 cm in diameter. Thin surface coating of goethite occurs over the surface to the left of the lens cap.



Plate 8.4 Photograph and sketch of section examined at Site 3 (north of Site 2) in Terrey Hills quarry. Section is approximately 1.5 m high.

Sample BOU 405 (Soil)

**Mineralogy**

Quartz  
Gibbsite  
Goethite  
Smectite  
Anatase  
Hematite  
Kaolinite

**Chemistry**

Fe<sub>2</sub>O<sub>3</sub> 4.0%  
SiO<sub>2</sub> 85.0%  
Al<sub>2</sub>O<sub>3</sub> 9.0%

Sample BOU 406 (Vermiform)

**Mineralogy**

Quartz  
Gibbsite  
Goethite  
Hematite  
Anatase  
Maghemite  
Kaolinite

**Chemistry**

Fe<sub>2</sub>O<sub>3</sub> 41.0%  
SiO<sub>2</sub> 10.7%  
Al<sub>2</sub>O<sub>3</sub> 29.0%

Sample BOU 407 (Mottles)

**Mineralogy**

Gibbsite  
Quartz  
Goethite  
Hematite  
Anatase  
Kaolinite

**Chemistry**

Fe<sub>2</sub>O<sub>3</sub> 48.0%  
SiO<sub>2</sub> 12.0%  
Al<sub>2</sub>O<sub>3</sub> 38.5

Sample BOU 408 (Nodular)

**Mineralogy**

Gibbsite  
Quartz  
Goethite  
Hematite  
Anatase  
Kaolinite  
Maghemite  
Smectite

**Chemistry**

Fe<sub>2</sub>O<sub>3</sub> 41.0%  
SiO<sub>2</sub> 17.0%  
Al<sub>2</sub>O<sub>3</sub> 38.5%

Sample BOU 409 (Pisolitic)

**Mineralogy**

Gibbsite  
Quartz  
Goethite  
Hematite  
Anatase  
Kaolinite  
Maghemite  
Smectite

**Chemistry**

Fe<sub>2</sub>O<sub>3</sub> 39.4%  
SiO<sub>2</sub> 15.2%  
Al<sub>2</sub>O<sub>3</sub> 43.6%

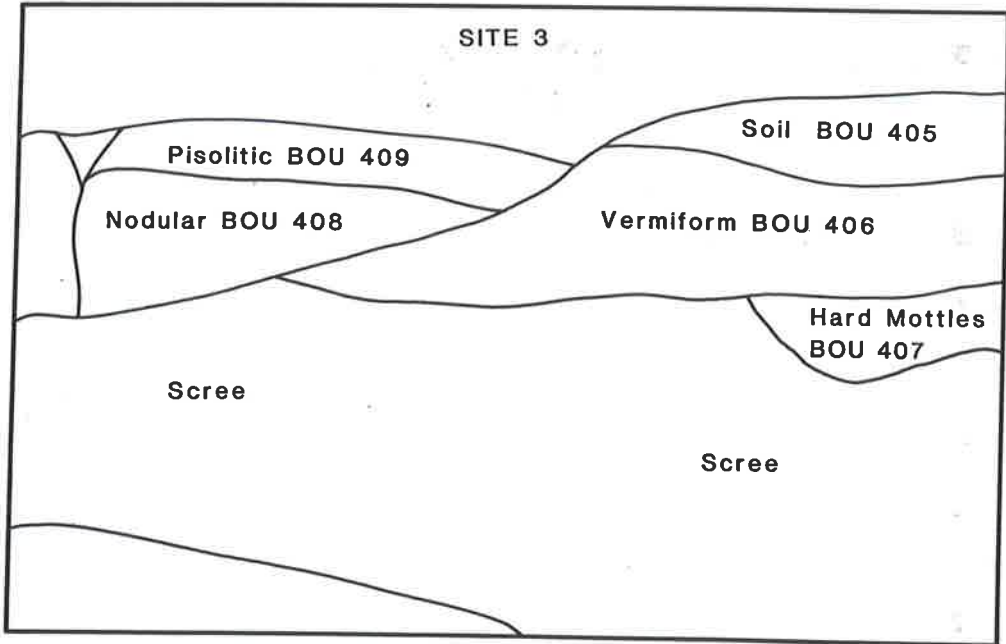


Plate 8.5 Photograph and sketch of section at Site 4 examined in the Terrey Hills quarry. The section is approximately 2 m high.

Sample BOU 410 (Vesicular)

**Mineralogy**

Goethite  
Quartz  
Kaolinite  
Hematite  
Gibbsite  
Smectite

**Chemistry**

Fe<sub>2</sub>O<sub>3</sub> 67.5%  
SiO<sub>2</sub> 17.0%  
Al<sub>2</sub>O<sub>3</sub> 14.0%

Sample BOU 411 (Pisolitic)

**Mineralogy**

Gibbsite  
Quartz  
Goethite  
Hematite  
Kaolinite  
Maghemite  
Anatase

**Chemistry**

Fe<sub>2</sub>O<sub>3</sub> 27.0%  
SiO<sub>2</sub> 13.0%  
Al<sub>2</sub>O<sub>3</sub> 38.0%

Sample BOU 412 (Pisoliths)

**Mineralogy**

Quartz  
Hematite  
Maghemite  
Gibbsite  
Corundum  
Kaolinite

**Chemistry**

Fe<sub>2</sub>O<sub>3</sub> 20.0%  
SiO<sub>2</sub> 31.0%  
Al<sub>2</sub>O<sub>3</sub> 46.0%

Sample BOU 412a (Vesicular)

**Mineralogy**

Goethite  
Gibbsite  
Hematite  
Kaolinite  
Anatase  
Quartz

**Chemistry**

Fe<sub>2</sub>O<sub>3</sub> 72.0%  
SiO<sub>2</sub> 31.0%  
Al<sub>2</sub>O<sub>3</sub> 15.0%

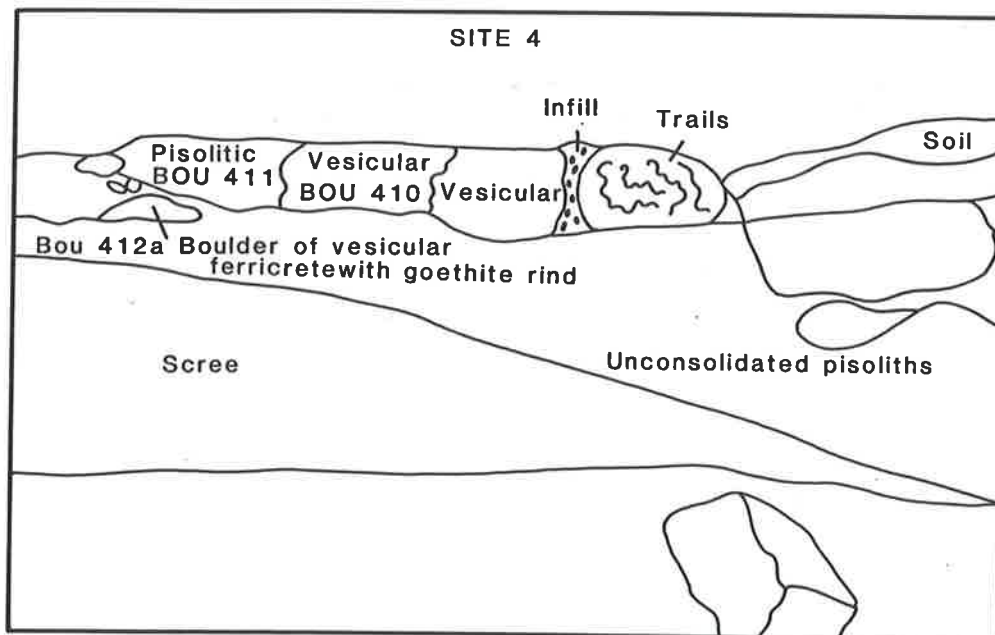


Plate 8.6 Photograph and sketch of section exposed at Site 5 in Terrey Hills quarry. Hammer 35 cm long.

Sample BOU 413 (Mottles)

**Mineralogy**

Quartz  
Kaolinite  
Hematite  
Goethite  
Smectite  
Felspar  
Anatase

**Chemistry**

Fe<sub>2</sub>O<sub>3</sub> 1.8%  
SiO<sub>2</sub> 78.8%  
Al<sub>2</sub>O<sub>3</sub> 16.4%

Sample BOU 414 (Slabby)

**Mineralogy**

Gibbsite  
Quartz  
Kaolinite  
Goethite  
Anatase  
Hematite  
Maghemite

**Chemistry**

Fe<sub>2</sub>O<sub>3</sub> 20.0%  
SiO<sub>2</sub> 44.0%  
Al<sub>2</sub>O<sub>3</sub> 34.0%

Sample BOU 415 (Nodular)

**Mineralogy**

Gibbsite  
Quartz  
Goethite  
Hematite  
Kaolinite  
Anatase  
Maghemite

**Chemistry**

Fe<sub>2</sub>O<sub>3</sub> 44.9%  
SiO<sub>2</sub> 18.0%  
Al<sub>2</sub>O<sub>3</sub> 35.0%

Sample BOU 416 (Pisolitic)

**Mineralogy**

Gibbsite  
Quartz  
Goethite  
Kaolinite  
Anatase  
Hematite  
Maghemite

**Chemistry**

Fe<sub>2</sub>O<sub>3</sub> 22.0%  
SiO<sub>2</sub> 37.0%  
Al<sub>2</sub>O<sub>3</sub> 39.0%

Sample BOU 417 (Pisolitic)

**Mineralogy**

Gibbsite  
Quartz  
Goethite  
Hematite  
Anatase  
Kaolinite

**Chemistry**

Fe<sub>2</sub>O<sub>3</sub> 26.3%  
SiO<sub>2</sub> 41.0%  
Al<sub>2</sub>O<sub>3</sub> 30.0%

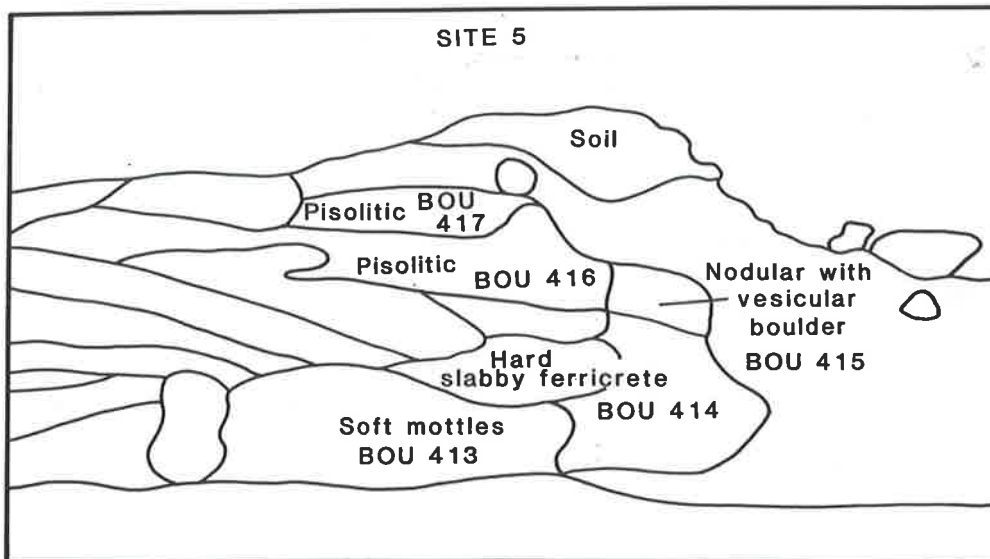




Plate 8.7 Photograph of indurated detrital ferricrete containing boulders and clasts of varying characters. For example, end of hammer handle rests on goethite-coated boulder of vesicular ferricrete (bog iron ore), which is overlain by pisolitic ferricrete. Hammer 35 cm high.

Plate 8.8 Boulder of vesicular ferricrete (V) incorporated into detrital ferricrete, which contains variety of materials, including maghemite clasts (M). Hammer handle 4 cm wide.

Plate 8.9 Irregular contact between detrital ferricrete and *in situ* Hawkesbury Sandstone exposed in road cutting on the Mona Vale road. Camera lens cap 6 cm wide is on the contact. The detrital ferricrete includes clasts of maghemite up to 3 cm in diameter.



Plate 8.10 Lenticular bedrock structures in the Hawkesbury Sandstone in road cutting in the Ku-ring-gai Chase National Park. Some bedding planes have been more intensively weathered than the surrounding sandstone. Detrital boulders (B) and bleached materials occur on the top right of the section. Section 3 m high.

Plate 8.11 Further differential and sub-surface weathering of the Hawkesbury Sandstone is illustrated in this photograph, in which one of the beds, located by hammer, has been desilicified and weathered. Coarse detritus occurs at the surface. Hammer 35 cm long.

Plate 8.12 Ferruginous and magnetic clasts lying on the ground surface in Ku-ring-gai Chase National Park. Similar clasts occur within the ferricretes of the North Sydney area, suggesting their incorporation into the ferricretes as the landscape underwent downwasting. Geology hammer 35 cm long.



Plate 8.13 Section exposed in Terrey Hills quarry illustrating modern soil overlying what appears to be an older lithified soil. Geology hammer 35 cm long.

Plate 8.14 Photomicrograph of the complex rind of a pisolith (BOU 417) incorporating zones of laminated microcrystalline brown goethite and yellowish gibbsite, lenses of quartz clasts and concentric fractures lined with opaque maghemite. The core of the pisolith on the left contains an opaque zone enriched in maghemite. Polarised incident light. Width of field 3.5 mm.

Plate 8.15 Photomicrograph of complex pisolith (BOU 417) showing details of outer zoned rind of pisolith. Yellow colour is gibbsite and red, hematite. Hematite, or possibly maghemite (dark, opaque areas) fills linear fractures. Incident polarised light. Width of field 2 mm.

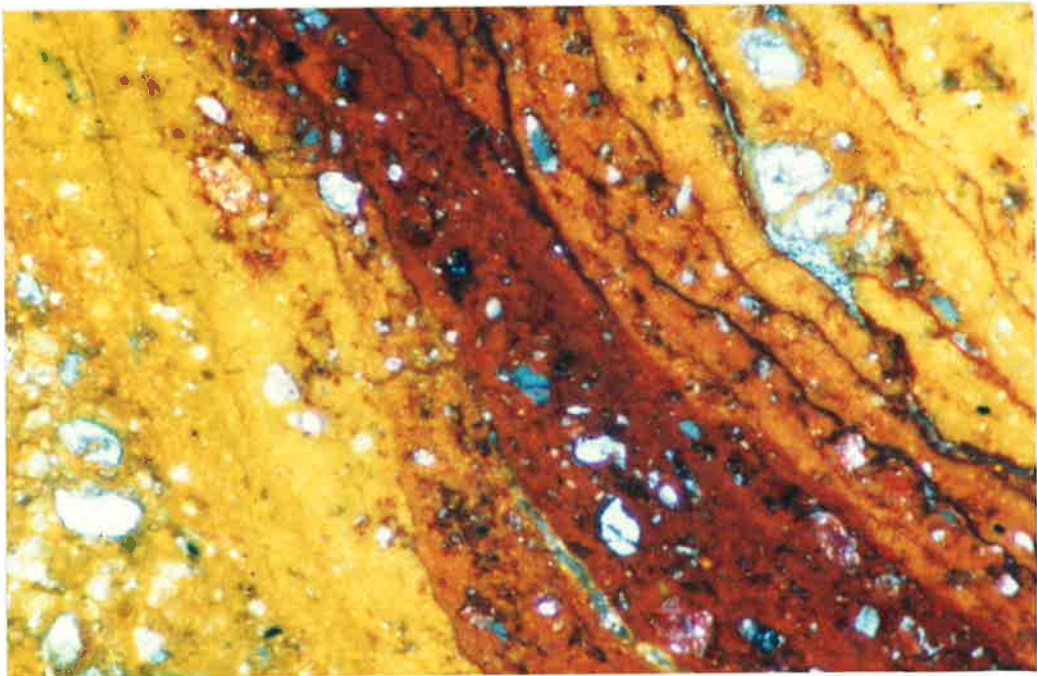
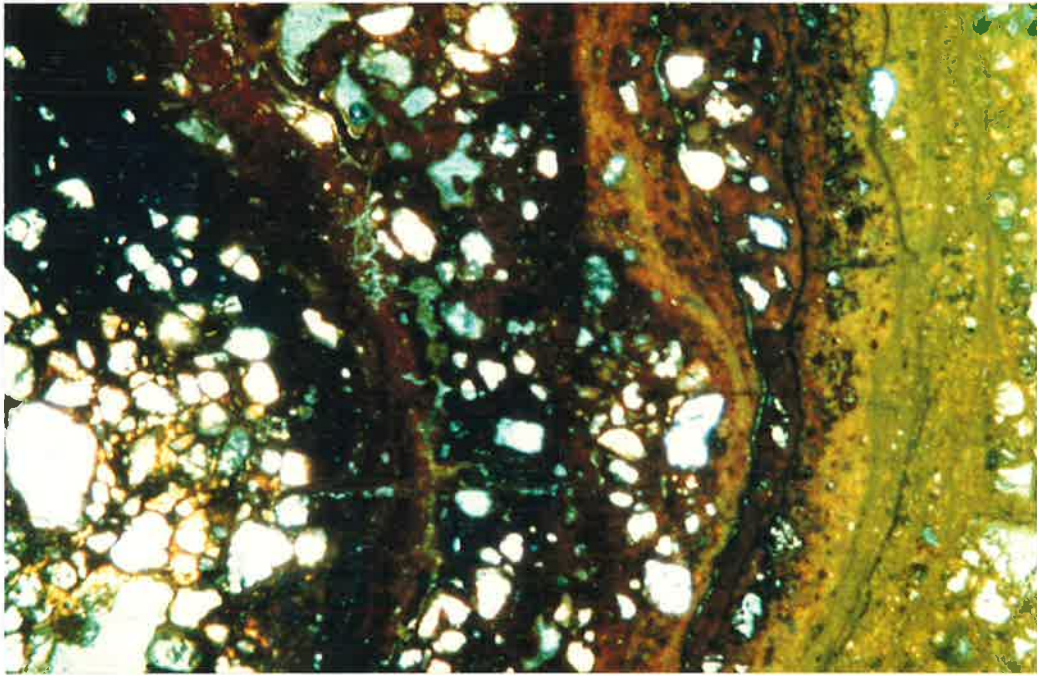


Plate 8.16 Ferrihydrite precipitated from surface water seepage in drainage ditch in Ku-ring-gai Chase National Park.





Plate 9.1 One of a series of *cuestas* formed by differential erosion of ferricrete with associated voidal concretions on the southwestern corner of the Telford Basin, Lobe B. The *cuesta* has a maximum elevation of about 10 m and extends for approximately 1 km.

Plate 9.2 Voidal concretion approximately 30 cm across showing layers dominantly of hematite (dark), goethite (yellow) and lepidocrocite (orange).

Plate 9.3 Concretion, 20 cm across, broken open to reveal a clay core. Geology hammer 4 cm wide.



Plate 9.4 *In situ* concretion broken open to reveal core closely packed with clays and gypsum.

Plate 9.5 Skin of secondary iron oxides around core of unweathered sideritic siltstone in Upper Series overburden beds. Geological hammer handle 4 cm wide.

Plate 9.6 Concretion with an outer layer of dark-coloured hematite, near centre of hammer handle (4 cm wide), an intermediate layer of yellow and orange iron oxides and an inner core of partly weathered sideritic siltstone.



# APPENDICES

## APPENDIX I:

TABLES 4.1 to 4.17

TABLE 4.1 MOUNT LOFTY RANGE PROVINCE:  
Mount Cone area

<b>CHEMISTRY</b>					
<i>SAMPLE</i>	<i>BOU</i>	<i>BOU</i>	<i>BOU</i>	<i>BOU</i>	<i>BOU</i>
	<b>301</b>	<b>303</b>	<b>423</b>	<b>424</b>	<b>302</b>
	Gneissic Bedrock	Nodular Fe/crete	Nodules of 303	Matrix of 303	Vesicular Fe/crete
Fe <sub>2</sub> O <sub>3</sub>	14.33	30.03	32.10	24.72	0.12
TiO <sub>2</sub>	0.74	0.73	0.70	0.87	0.42
CaO	0.01	0.04	0.01	0.01	0.05
K <sub>2</sub> O	6.63	0.40	0.13	0.16	0.18
SO <sub>3</sub>	0.03	0.01	0.03	0.02	0.02
P <sub>2</sub> O <sub>5</sub>	0.01	0.02	0.02	0.02	0.25
SiO <sub>2</sub>	51.8	25.2	23.0	25.1	12.26
Al <sub>2</sub> O <sub>3</sub>	20.79	26.54	26.67	31.16	11.92
MgO	0.69	0.08	0.08	0.11	0.10
Na <sub>2</sub> O	0.22	0.02	0.05	0.03	nd
<u>Ig.Loss</u>	<u>4.77</u>	<u>14.92</u>	<u>17.38</u>	<u>17.62</u>	<u>13.12</u>
<u>Total</u>	<u>100.3</u>	<u>98.0</u>	<u>100.2</u>	<u>99.77</u>	<u>99.0</u>

### MINERALOGY

In decreasing order of abundance

Mu	Gb	Gt	Gt	Gt
Qz	Qz	Qz	Qz	Hm
Hm	Gt	Gb	Gb	Qz
Gt	Hm	Hm	Hm	Kt
Fr	Mh	Kt	Kt	St
St	Kt	An	An	
Kt	Fr	St	St	
	St	Ic	Ic	
		Mh		
Magnetic reaction	N	Y	Y	N
		str		N

Qz=quartz; Hm=hematite; Gt=goethite; Kt=kaolinite;  
St=smectite; Mi=micas; An=anatase; Fr=felspar;  
Mh=maghemite; Mu=muscovite; Gb=gibbsite;  
Ic=interstratified clays; str=strong.

TABLE 4.2  
MOUNT LOFTY RANGE PROVINCE  
(Spring Mount area)

<b>CHEMISTRY</b>			
<i>SAMPLE</i>	<i>BOU</i>	<i>BOU</i>	<i>BOU</i>
	<b>370</b>	<b>366</b>	<b>309</b>
	Nodular Ferricrete	Vermiform Ferricrete	Laminated rind
Fe <sub>2</sub> O <sub>3</sub>	38.21	56.6	26.79
MnO	0.02	0.02	0.03
TiO <sub>2</sub>	0.68	0.53	0.44
CaO	0.02	0.02	0.03
K <sub>2</sub> O	0.31	0.40	0.04
SO <sub>3</sub>	0.02	0.02	0.01
P <sub>2</sub> O <sub>5</sub>	0.02	0.02	0.05
SiO <sub>2</sub>	21.66	16.2	44.33
Al <sub>2</sub> O <sub>3</sub>	23.77	21.21	12.89
MgO	0.08	0.06	0.04
Na <sub>2</sub> O	0.06	0.03	0.04
<u>Ig.Loss</u>	<u>14.44</u>	<u>4.13</u>	<u>15.20</u>
<u>Total</u>	<u>99.3</u>	<u>99.3</u>	<u>99.9</u>

### MINERALOGY

In decreasing order of abundance

Gt	Gt	Qz
Qz	Qz	Hm
Gb	Gb	Kt
Hm	Hm	Gt
Mh	Fr	
Kt	Kt	
St	St	
Fr	Ic	
Ic		

Magnetic reaction	Y	N	N
str			

Qz=quartz; Hm=hematite; Gt=goethite;  
Kt=kaolinite; St=smectite; Fr=felspar;  
Mh=maghemite; Gb=gibbsite;  
Ic=interstratified clays;str=strong.

TABLE 4.3 MOUNT LOFTY RANGE PROVINCE:  
Summit surface (Parawa & K.Island)

<b>CHEMISTRY</b>							
(Parawa Plateau area) (K.I. Summit Surface)							
SAMPLE	BOU 18	BOU 21	BOU 339	BOU 343	BOU 101	BOU 126	BOU 130
(Pisolitic to vermiform ferricretes in)							Magnetic
(various materials)							Pisoliths
Fe <sub>2</sub> O <sub>3</sub>	33.04	32.84	35.36	28.01	16.07	15.98	32.72
MnO	0.01	0.01	0.01	0.01	nd	0.01	0.01
TiO <sub>2</sub>	0.68	0.66	0.77	0.22	0.50	0.52	0.65
CaO	0.05	0.02	0.02	0.08	0.02	0.06	0.07
K <sub>2</sub> O	0.90	0.60	0.34	0.41	0.14	0.58	0.22
SO <sub>3</sub>	0.01	0.01	0.02	0.03	nd	nd	0.02
P <sub>2</sub> O <sub>5</sub>	0.02	0.02	0.02	0.25	0.02	0.03	0.02
SiO <sub>2</sub>	27.9	31.9	21.0	33.9	42.1	58.2	45.6
Al <sub>2</sub> O <sub>3</sub>	22.62	20.54	26.43	24.88	24.42	12.41	13.13
MgO	0.21	0.12	0.08	0.11	0.09	0.19	0.09
Na <sub>2</sub> O	0.08	0.04	0.03	0.05	0.03	0.10	0.02
<u>Ig.Loss</u>	<u>14.40</u>	<u>12.80</u>	<u>15.41</u>	<u>10.94</u>	<u>16.39</u>	<u>10.44</u>	<u>6.57</u>
<u>Total</u>	<u>99.9</u>	<u>99.5</u>	<u>99.5</u>	<u>98.9</u>	<u>99.8</u>	<u>98.5</u>	<u>99.1</u>

### MINERALOGY

In decreasing order of abundance

Qz	Qz	Qz	Kt	Qz	Qz	Qz
Gt	Gt	Gb	Qz	Gb	Gt	Hm
Gb	Hm	Gt	Hm	Gt	St	Mh
Mi	Gb	Hm	Gt	Kt	Kt	Gb
Hm	Kt	Kt	Mu	Fr	Gb	St
Kt	Mi	Mh	Gb	Hm	Fr	
Fr	Fr	Fr	Ic	An	An	
Vm	Mh	An	Mh		Mh	
An		Mu				
Mh		St				

Magnetic

reaction	Y	Y	Y	Y	N	Y	Y
		trace	str	sl			vstr

Qz=quartz; Hm=hematite; Gt=goethite; Kt=kaolinite; St=smectite;  
Mi=micas; An=anatase; Fr=felspar; Mh=maghemite; Mu=muscovite.  
Gb=gibbsite; Ic=interstratified clays; Vm=vermiculite; str=strong;  
sl=slight; vstr=very strong.



TABLE 4.4 MOUNT LOFTY RANGE PROVINCE:  
(Summit Surface: Iron-impregnated sediments)

<b>CHEMISTRY</b>						
<i>SAMPLE</i>	<i>BOU</i>	<i>BOU</i>	<i>BOU</i>	<i>BOU</i>	<i>BOU</i>	<i>BOU</i>
	<b>306</b>	<b>57</b>	<b>397</b>	<b>359</b>	<b>380</b>	<b>4</b>
	Glen Shera Plateau	Cut Hill	Mount Gawler	Knott Hill	Para- wirra	Humbug Scrub
Fe <sub>2</sub> O <sub>3</sub>	12.01	23.06	10.66	23.71	11.28	21.99
MnO	nd	0.01	0.01	0.01	0.01	0.01
TiO <sub>2</sub>	0.07	0.18	0.99	0.86	0.17	0.40
CaO	nd	0.01	0.13	0.09	0.01	0.05
K <sub>2</sub> O	0.03	0.02	0.50	2.52	0.08	0.87
SO <sub>3</sub>	nd		0.01	0.04	0.02	0.01
P <sub>2</sub> O <sub>5</sub>	0.01	0.01	0.04	0.19	0.06	0.02
SiO <sub>2</sub>	83.1	70.4	49.2	51.8	83.9	65.8
Al <sub>2</sub> O <sub>3</sub>	1.63	1.72	30.41	13.01	1.45	6.80
MgO	nd	0.02	0.55	0.65	0.05	0.11
Na <sub>2</sub> O	nd	0.02	0.07	0.13	0.06	0.03
ZrO		0.02				
<u>Ig.Loss</u>	<u>2.73</u>	<u>3.41</u>	<u>6.39</u>	<u>6.30</u>	<u>2.44</u>	<u>3.70</u>
<u>Total</u>	<u>99.6</u>	<u>98.9</u>	<u>99.0</u>	<u>99.3</u>	<u>99.5</u>	<u>99.8</u>

### MINERALOGY

In decreasing order of abundance

	Qz	Qz	Qz	Qz	Qz	Qz
	Gt	Hm	Gt	Hm	Gt	Hm
	St	Gt	Hm	Mu	St	Gt
	Kt	St	Kt	Gt	Hm	Mi
	Ic	Fr	Mu	Kt	Kt	Kt
	Hm	Mh	St	St	Ic	Fr
			Mh	Ic	Fr	
Magnetic reaction	N	Y	Y	N	N	N
			vvsl			

Qz=quartz; Hm=hematite; Gt=goethite; Kt=kaolinite; St=smectite;  
Mi=micas; Fr=felspar; Mu=muscovite; Mh=maghemite;  
Ic=interstratified clays; nd=not detected; vvsl=very very slight.

TABLE 4.5 MOUNT LOFTY RANGE PROVINCE:  
 Ferruginised bedrock (Mid North)  
 and Slabby Ferricretes (Chandlers Hill)

SAMPLE	CHEMISTRY					
	BOU 386 Ferruginised bedrock	BOU 20 Slabby F/crete	BOU 60 Slabby F/crete	BOU 429 Slabby F/crete	BOU 430 Matrix of 429	BOU 398 Soil above Slabby F/crete
Fe <sub>2</sub> O <sub>3</sub>	17.20	46.35	42.10	38.28	6.57	9.50
MnO	0.01	0.01	0.01	0.01	nd	0.01
TiO <sub>2</sub>	0.66	0.85	0.77	0.86	0.73	0.88
CaO	0.23	0.03	0.03	0.03	0.03	0.11
K <sub>2</sub> O	0.11	0.21	0.06	0.10	0.06	0.46
SO <sub>3</sub>	0.02	0.04		0.04	0.01	0.04
P <sub>2</sub> O <sub>5</sub>	0.75	0.02	0.03	0.02	0.01	0.03
SiO <sub>2</sub>	62.8	21.3	27.4	25.8	73.4	47.0
Al <sub>2</sub> O <sub>3</sub>	9.03	18.36	15.88	21.31	12.21	27.71
MgO	0.07	0.13	0.11	0.14	0.09	0.49
Na <sub>2</sub> O	0.12	0.06	0.36	0.10	0.05	0.11
ZrO					0.03	
Ig.Loss	<u>7.36</u>	<u>12.41</u>	<u>12.42</u>	<u>13.34</u>	<u>6.21</u>	<u>13.53</u>
Total	<u>98.4</u>	<u>99.8</u>	<u>98.9</u>	<u>100.0</u>	<u>99.3</u>	<u>99.9</u>

#### MINERALOGY

In decreasing order of abundance

Qz	Qz	Gt	Gt	Qz	Qz	
Hm	Gt	Qz	Hm	Kt	Kt	
Gt	Hm	Hm	Kt	Hm	Gt	
Kt	Kt	Kt	Qz	Gt	Ic	
Ic	Gb	Fr	Ic	St	Fr	
Fr	Fr	Ic	Gb	Ic	An	
St	Vm	Gb		Fr	Gb(?)	
Mu						
Magnetic reaction	Y vvsl	Y trace	N	N	N	N

Qz=quartz; Hm=hematite; Gt=goethite; Kt=kaolinite; St=smectite;  
 Mi=micas; An=anatase; Fr=felspar; Mh=maghemite; Mu=muscovite.  
 Gb=gibbsite; Ic=interstratified clays. Vm=vermiculite; nd=not detected;  
 vvsl=very very slight.

TABLE 4.6 MOUNT LOFTY RANGE PROVINCE:  
CHEMISTRY

SAMPLE	BOU 32 (Peeralilla Hill) (Sandy clays)	BOU 33	BOU 10 (Peeralilla (Vesicular ferricretes)	BOU 11 Hill )	BOU 12 Hill )	BOU 5&6 Mt Compass (Vesic. F/crete)
Fe <sub>2</sub> O <sub>3</sub>	2.74	9.21	67.66	69.81	n	68.49
MnO	0.02	0.01	0.10	0.23	o	0.02
TiO <sub>2</sub>	0.21	0.27	0.23	0.18	t	0.09
CaO	0.28	3.08	0.27	0.03		0.03
K <sub>2</sub> O	0.25	0.46	0.05	0.07	a	0.05
SO <sub>3</sub>	4.22	0.99	0.01	0.02	v	0.01
P <sub>2</sub> O <sub>5</sub>	nd	0.01	0.54	0.01	a	0.02
SiO <sub>2</sub>	62.0	70.7	11.7	7.69	i	15.4
Al <sub>2</sub> O <sub>3</sub>	18.52	12.66	6.13	6.76	l	1.70
MgO	0.75	0.94	0.06	0.08	a	0.01
Na <sub>2</sub> O	0.21	0.23	0.01	nd	b	nd
					l	
<u>Ig.Loss</u>	<u>11.51</u>	<u>13.38</u>	<u>13.51</u>	<u>14.61</u>	e	<u>14.11</u>
<u>Total</u>	<u>89.2</u>	<u>98.5</u>	<u>100.3</u>	<u>99.5</u>		<u>99.9</u>

### MINERALOGY

In decreasing order of abundance

	Qz	Qz	Gt	Gt	Gt	Gt
	Kt	St	Qz	Qz	Qz	Qz
	Br	Ct	Hm	Hm	Hm	
	Mi	Kt	Vm	Kt	Kt	
		Br	Kt	Vm		
Magnetic reaction	N	N	N	N	Y trace	N

Qz=quartz; Hm=hematite; Gt=goethite; Kt=kaolinite; St=smectite;  
Mi=micas; Mh=maghemite; Vm=vermiculite; Br=barite; Ct=calcite;  
nd=not detected.

TABLE 4.7 MOUNT LOFTY RANGE PROVINCE:  
(Anstey Hill iron mine)  
**CHEMISTRY**

SAMPLE	BOU	BOU	BOU	BOU	BOU	BOU
	337	340	342	338	345	350
	(Vesicular ferricretes)		(Iron-impregnated sediments)			
Fe <sub>2</sub> O <sub>3</sub>	78.73	34.67	54.26	50.91	23.50	36.76
MnO	0.21	0.12	0.14	0.09	0.28	0.09
TiO <sub>2</sub>	0.01	0.94	0.05	0.09	0.11	0.12
CaO	0.12	0.27	0.12	0.10	0.16	0.16
K <sub>2</sub> O	0.09	0.23	0.28	1.82	0.27	1.48
SO <sub>3</sub>	0.02	nd	0.01	nd	nd	0.01
P <sub>2</sub> O <sub>5</sub>	0.64	0.32	0.56	0.53	0.08	0.42
SiO <sub>2</sub>	1.83	57.1	33.8	38.7	65.2	51.4
Al <sub>2</sub> O <sub>3</sub>	0.18	0.72	0.98	2.05	4.44	2.61
MgO	0.04	0.22	0.11	0.08	0.15	0.16
Na <sub>2</sub> O	nd	0.02	0.01	nd	nd	0.06
Ig.Loss	<u>13.13</u>	<u>6.02</u>	<u>9.12</u>	<u>4.94</u>	<u>5.86</u>	<u>6.07</u>
Total	<u>95.0</u>	<u>100.2</u>	<u>99.4</u>	<u>99.3</u>	<u>100.0</u>	<u>99.3</u>

**MINERALOGY**

	In decreasing order of abundance					
	Gt	Qz	Gt	Qz	Qz	Qz
	Qz	Gt	Qz	Gt	Gt	Gt
	Ic	St	Hm	Hm	Hm	Hm
		Hm	St	Fr	Kt	Mh
		An		Ic	St	St
					Ic	Ic
						Fr
Magnetic reaction	N	N	N	N	Y	N
					vvsl	

Qz=quartz; Hm=hematite; Gt=goethite; Kt=kaolinite; St=smectite;  
An=anatase; Fr=felspar; Mh=maghemite; Ic=interstratified clays;  
nd=not detected; vvsl=very very slight.

TABLE 4.8 MOUNT LOFTY RANGE PROVINCE:  
(Summit surface:  
Vesicular Ferricretes)

SAMPLE	CHEMISTRY		
	BOU 147 (K.Island)	BOU 353 (Almanda Hill)	BOU 348 (Hill)
Fe <sub>2</sub> O <sub>3</sub>	59.3	66.67	64.10
MnO	0.02	0.02	0.02
TiO <sub>2</sub>	0.35	0.31	0.35
CaO	0.02	0.02	0.03
K <sub>2</sub> O	0.60	0.42	0.28
SO <sub>3</sub>		0.02	nd
P <sub>2</sub> O <sub>5</sub>	0.24	0.41	0.10
SiO <sub>2</sub>	13.8	10.9	11.6
Al <sub>2</sub> O <sub>3</sub>	10.76	6.84	11.25
MgO	0.17	0.12	0.15
Na <sub>2</sub> O	0.08	nd	nd
<u>Ig.Loss</u>	<u>13.92</u>	<u>12.73</u>	<u>12.34</u>
<u>Total</u>	<u>99.3</u>	<u>98.0</u>	<u>100.2</u>

#### MINERALOGY

In decreasing order of abundance

Gt	Gt	Gt
Qz	Qz	Qz
Hm	Hm	Hm
Kt	Kt	Mh
An	Ic	Kt
Fr		Ic
Mi		

Magnetic reaction	N	N	Y vstr
-------------------	---	---	-----------

Qz=quartz; Hm=hematite; Gt=goethite; Kt=kaolinite;  
St=smectite; Mi=micas; An=anatase; Fr=felspar;  
Mh=maghemite; Ic=interstratified clays;  
nd=not detected; vstr=very strong.

TABLE 4.9 MOUNT LOFTY RANGE PROVINCE:  
Summit surface palaeochannels

SAMPLE	CHEMISTRY			
	BOU 422 (Mount Bedrock Mottle)	BOU 372 Desert Hematitic Pisoliths	BOU 371 Channels) Goethitic Pisoliths	BOU 17 (Pottery Road) Ferruginised Sands
Fe <sub>2</sub> O <sub>3</sub>	29.23	50.46	35.44	12.91
MnO	0.01	0.01	0.01	.nd
TiO <sub>2</sub>	0.35	0.44	0.52	0.40
CaO	nd	nd	0.02	0.01
K <sub>2</sub> O	0.66	0.22	0.16	0.05
SO <sub>3</sub>	0.03	0.04	0.02	nd
P <sub>2</sub> O <sub>5</sub>	0.01	0.04	0.02	0.01
SiO <sub>2</sub>	58.0	36.6	39.1	72.5
Al <sub>2</sub> O <sub>3</sub>	7.28	6.68	12.85	8.0
MgO	0.15	0.09	0.06	0.06
Na <sub>2</sub> O	0.05	0.02	nd	0.06
Ig.Loss	<u>3.42</u>	<u>4.56</u>	<u>11.2</u>	<u>5.28</u>
<u>Total</u>	<u>99.2</u>	<u>99.2</u>	<u>99.4</u>	<u>99.3</u>

### MINERALOGY

In decreasing order of abundance

Qz	Qz	Qz	Qz
Hm	Hm	Gt	Gt
Kt	Mh	Hm	Hm
Mi	Gt	Kt	Kt
St	Kt	Vm	
Vm	Vm	Mh	
Magnetic reaction	N	Y str	Y vvvsl

Qz=quartz; Hm=hematite; Gt=goethite; Kt=kaolinite;  
St=smectite; Mi=micas; Mh=maghemite; Mu=muscovite;  
Vm=vermiculite; nd=not detected; v=very; sl=slight;  
str=strong.

TABLE 4.10 MOUNT LOFTY RANGE PROVINCE:  
Palaeochannels

**CHEMISTRY**

(Clarendon Road Cut)(Mt Bold)(Chapel Hill area)

SAMPLE	BOU 75	BOU 74	BOU 73	BOU 355	BOU 336	BOU 344	BOU 346
	Wthd Bedrock	Ferr.& silic. Gravels	Ferrug. Sands	Ferrug. Gravels	Wthd B/rock	Ferrug. Gravels	Ferrug. Sands
Fe <sub>2</sub> O <sub>3</sub>	1.39	4.32	2.63	n	1.05	7.85	5.60
MnO	0.01	0.01	0.01	o	nd	0.03	0.02
TiO <sub>2</sub>	1.66	0.09	0.33	t	0.61	0.32	0.18
CaO	0.03	0.01	0.05		0.05	0.02	0.01
K <sub>2</sub> O	0.86	0.07	0.17	a	0.75	0.07	0.04
SO <sub>3</sub>				v	nd	nd	nd
P <sub>2</sub> O <sub>5</sub>	0.02	0.03	0.01	a	0.02	0.03	0.01
SiO <sub>2</sub>	64.5	89.8	86.4	i	76.7	83.9	88.7
Al <sub>2</sub> O <sub>3</sub>	13.64	2.39	5.78	l	14.59	5.04	3.24
MgO	1.12	0.03	0.13	a	0.28	0.15	0.11
Na <sub>2</sub> O	1.70	0.17	0.19	b	0.09	0.10	0.01
ZrO	0.03	0.02	0.08	l			
<u>Ig.Loss</u>	<u>14.70</u>	<u>2.03</u>	<u>3.71</u>	e	<u>5.32</u>	<u>2.45</u>	<u>1.38</u>
<u>Total</u>	<u>99.7</u>	<u>99.0</u>	<u>99.5</u>		<u>99.9</u>	<u>100.0</u>	<u>99.2</u>

**MINERALOGY**

In decreasing order of abundance

Qz	Qz	Qz	Qz	Qz	Qz	Qz
Kt	St	St	Gt	Kt	St	Gt
Mi	Kt	Kt	St	Fr	Gt	St
Fr	Hm	Fr	Kt	Mu	Hm	Hm
St	Gt	Gt	Hm	St	Kt	Kt
HI	Sr(?)	Hm	Fr		Ic	Ic
					Fr	Fr
					Sr(?)	Sr(?)

Magnetic  
reaction

N N N N N N N

Qz=quartz; Hm=hematite; Gt=goethite; Kt=kaolinite; St=smectite;  
Mi=micas; An=anatase; Fr=felspar; Mh=maghemite;  
Mu=muscovite; HI=halite; Ic=interstratified clays; Sr=staurolite;  
nd=not detected.

TABLE 4.11  
MOUNT LOFTY RANGE PROVINCE:

SAMPLE	CHEMISTRY		
	BOU 56 Mottle	BOU 48 Seaford Formatn	BOU 38 Bleached sediments
Fe <sub>2</sub> O <sub>3</sub>	35.90	2.55	0.75
MnO	0.01	.nd	.nd
TiO <sub>2</sub>	0.41	0.15	0.53
CaO	0.17	0.02	0.08
K <sub>2</sub> O	0.08	0.52	0.10
SO <sub>3</sub>	nd	0.01	
P <sub>2</sub> O <sub>5</sub>	0.03	0.01	0.01
SiO <sub>2</sub>	41.6	89.3	87.8
Al <sub>2</sub> O <sub>3</sub>	10.31	2.84	6.34
MgO	1.05	0.20	0.10
Na <sub>2</sub> O	0.07	0.45	0.05
ZrO	0.02		0.03
<u>Ig.Loss</u>	<u>9.82</u>	<u>3.17</u>	<u>4.42</u>
<u>Total</u>	<u>99.5</u>	<u>99.2</u>	<u>100.2</u>

#### MINERALOGY

In decreasing order of abundance

Qz	Qz	Qz
Gt	Kt	Kt
Hm	Fr	St
Kt	Gt	Vm
Vm		An
Ic		Fr

Magnetic reaction	Y vvsl	N	N
----------------------	-----------	---	---

Qz=quartz; Hm=hematite; Gt=goethite; Kt=kaolinite;  
St=smectite; Mi=micas; An=anatase; Fr=felspar;  
Mh=magemite; Ic=interstratified clays.  
Vm=vermiculite; nd=not detected; v=very; sl=slight.



TABLE 4.12 MOUNT LOFTY RANGE PROVINCE:  
(Mottled Zones, Range Road)

<b>CHEMISTRY</b>				
<i>SAMPLE</i>	<i>BOU</i> <b>425</b>	<i>BOU</i> <b>426</b>	<i>BOU</i> <b>27</b>	<i>BOU</i> <b>428</b>
	Bleached M/siltstone	Hematitic Mottle	Hematitic Mottle	Goethitic Mottle
Fe <sub>2</sub> O <sub>3</sub>	1.93	23.01	32.80	32.25
MnO	nd	0.01	0.01	0.01
TiO <sub>2</sub>	0.80	0.77	0.65	0.66
CaO	nd	nd	0.01	0.01
K <sub>2</sub> O	0.98	1.05	0.55	0.67
SO <sub>3</sub>	0.01	0.05	0.04	0.02
P <sub>2</sub> O <sub>5</sub>	0.02	0.02	0.03	0.03
SiO <sub>2</sub>	74.8	55.2	41.7	42.7
Al <sub>2</sub> O <sub>3</sub>	14.00	12.51	13.92	14.23
MgO	0.35	0.30	0.21	0.25
Na <sub>2</sub> O	0.11	0.07	0.05	0.05
<u>Ig.Loss</u>	<u>6.16</u>	<u>6.58</u>	<u>9.19</u>	<u>9.14</u>
<u>Total</u>	<u>99.1</u>	<u>99.5</u>	<u>99.2</u>	<u>99.9</u>

### MINERALOGY

In decreasing order of abundance

Qz	Qz	Qz	Qz
Kt	Hm	Hm	Gt
St	Kt	Gt	Hm
Fr	Gt	Kt	Kt
Ic	St	Ic	St
Mu	Fr	Fr	Mu
An	Mu	An	Fr
	Ic		An
	An		

Magnetic  
reaction    N            N            N            N

Qz=quartz; Hm=hematite; Gt=goethite; Kt=kaolinite;  
St=smectite; An=anatase; Fr=felspar; Mu=muscovite;  
Ic=interstratified clays; nd=not detected.

TABLE 4.13 MOUNT LOFTY RANGE PROVINCE:  
(Bedrock Mottled Zones)  
CHEMISTRY

SAMPLE	BOU 23	BOU 19	BOU 25	BOU 31	BOU 357	BOU 28
	Willunga Hill	Ashbourne Mesa	Hawthn Farm	Bnython Hill	Sellicks Hill	Sundial Hill
Fe <sub>2</sub> O <sub>3</sub>	32.87	59.34	27.56	25.27	23.71	32.84
MnO	0.01	0.04	0.01	0.04	0.01	0.01
TiO <sub>2</sub>	0.11	0.27	0.86	0.92	0.86	0.80
CaO	0.05	0.34	0.08	0.04	0.09	0.07
K <sub>2</sub> O	0.04	0.06	0.07	1.43	2.52	0.04
SO <sub>3</sub>	0.02	0.02	0.02	0.02	0.04	0.03
P <sub>2</sub> O <sub>5</sub>	0.08	0.16	0.09	0.04	0.19	0.05
SiO <sub>2</sub>	50.6	18.1	44.6	46.0	51.8	40.9
Al <sub>2</sub> O <sub>3</sub>	5.94	7.55	14.71	18.02	13.01	15.53
MgO	0.28	0.09	0.08	0.25	0.65	0.04
Na <sub>2</sub> O	0.02	0.01	0.02	0.19	0.13	0.04
<u>Ig.Loss</u>	<u>9.23</u>	<u>12.89</u>	<u>11.20</u>	<u>7.24</u>	<u>6.30</u>	<u>9.07</u>
<u>Total</u>	<u>99.3</u>	<u>98.9</u>	<u>99.3</u>	<u>99.5</u>	<u>99.3</u>	<u>99.4</u>

#### MINERALOGY

In decreasing order of abundance

Qz	Gt	Qz	Qz	Qz	Qz
Hm	Hm	Gt	Hm	Hm	Kt
Gt	Qz	Hm	Kt	Mu	Hm
Kt	Kt	Kt	Gt	Gt	Gt
Fr		Mi	Mi	Kt	
Mi			Fr	St	
St				Ic	
Ch					
Vm					

Magnetic reaction N N N N N N

Qz=quartz; Hm=hematite; Gt=goethite; Kt=kaolinite; St=smectite;  
Mi=micas; Fr=felspar; Ic=interstratified clays; Vm=vermiculite;  
Ch=chlorite.

TABLE 4.14 MOUNT LOFTY PROVINCE: Mottled Zones.  
Mid North, Kapunda area  
**CHEMISTRY**

SAMPLE	BOU 383	BOU 384	BOU 391	BOU 54	BOU 389	BOU 388	BOU 387	BOU 390
	Ferr. B/rock	Ferr. Mottle	Bleached B/rock	Ferr. Mottle	Wthd B/rock	Ferr. Mottle	Bleached B/rock	Speckled Mottle
Fe <sub>2</sub> O <sub>3</sub>	8.17	25.95	0.60	9.09	8.53	29.54	0.67	11.38
MnO	0.01	0.01	.nd	0.01	0.01	0.01	nd	0.01
TiO <sub>2</sub>	0.91	0.88	0.98	1.23	1.09	1.12	1.42	1.35
CaO	0.01	0.06	0.01	0.11	0.03	0.07	0.10	0.03
K <sub>2</sub> O	0.33	0.25	0.28	0.56	0.20	0.08	0.34	0.13
SO <sub>3</sub>	nd	0.02	nd	nd	0.01	0.05	0.01	0.03
P <sub>2</sub> O <sub>5</sub>	0.03	0.02	0.02	0.05	0.02	0.03	0.01	0.04
SiO <sub>2</sub>	67.1	49.8	73.5	76.6	64.8	41.8	64.8	58.5
Al <sub>2</sub> O <sub>3</sub>	15.03	13.37	15.52	7.87	16.70	16.44	19.90	18.21
MgO	0.11	0.30	0.21	0.14	0.14	0.14	0.41	0.16
Na <sub>2</sub> O	0.11	0.23	0.19	0.12	0.09	0.27	0.69	0.12
Ig.Loss	<u>7.02</u>	<u>7.64</u>	<u>7.09</u>	<u>3.77</u>	<u>8.01</u>	<u>8.84</u>	<u>10.61</u>	<u>8.74</u>
Total	<u>98.8</u>	<u>98.5</u>	<u>98.4</u>	<u>99.6</u>	<u>99.6</u>	<u>98.4</u>	<u>99.0</u>	<u>98.7</u>

### MINERALOGY

In decreasing order of abundance

Qz	Qz	Qz	Qz	Qz	Qz	Qz	Qz	
Kt	Hm	Kt	Kt	Kt	Kt	Kt	Kt	
Hm	Kt	Ic	Hm	Gt	Hm	Ic	Hm	
Gt	Gt	St	Gt	Hm	Gt	Fr	Ic	
An	Fr	An	Mi	An	Fr	Mu	An	
Mu	Ic	Mi	St	St	An	St	St	
Ic	St	Fr	An	Fr	Ic	An	Mi	
Fr	Mi			Ic	St	Hl		
St	An				Mi			
Magnetic reaction	Y	N	N	N	Y	N	N	N
	vvs				vvs			

Qz=quartz; Hm=hematite; Gt=goethite; Kt=kaolinite; St=smectite;  
Ho=hollandite; Mi=micas; An=anatase; Fr=felspar; Mh=maghemite;  
Mu=muscovite; Hl=halite; Ic=interstratified clays; nd=not detected;  
v=very; sl=slight.

TABLE 4.15 MOUNT LOFTY RANGES  
Mid North - Black Hill

**CHEMISTRY**

<i>SAMPLE</i>	<i>BOU</i> <b>392</b>	<i>BOU</i> <b>394</b>	<i>BOU</i> <b>393</b>
	(Weathered Bedrock) Ferricrete		
Fe <sub>2</sub> O <sub>3</sub>	13.78	11.35	53.32
MnO	0.01	0.01	0.03
TiO <sub>2</sub>	0.38	0.35	0.23
CaO	0.03	0.07	0.28
K <sub>2</sub> O	0.41	0.47	0.69
SO <sub>3</sub>	0.03	0.02	0.09
P <sub>2</sub> O <sub>5</sub>	0.02	0.02	0.31
SiO <sub>2</sub>	69.9	72.4	34.8
Al <sub>2</sub> O <sub>3</sub>	9.11	8.95	4.46
MgO	0.14	0.18	0.19
Na <sub>2</sub> O	0.22	0.09	0.09
<u>Ig.Los</u>	<u>5.24</u>	<u>5.18</u>	<u>5.07</u>
<u>Total</u>	<u>99.2</u>	<u>99.1</u>	<u>99.5</u>

**MINERALOGY**

In decreasing order of abundance

Qz	Qz	Qz
Hm	Hm	Hm
Kt	Kt	Gt
Gt	Fr	Mi
St	St	St
Ic	Ic	

Magnetic reaction	N	N	Y vvsl
-------------------	---	---	-----------

Qz=quartz; Hm=hematite; Gt=goethite; Kt=kaolinite;  
St=smectite; Mi=micas; Fr=felspar; Mh=maghemite;  
Ic=interstratified clays; Ct=calcite; v=very; sl=slight.

TABLE 4.16

MOUNT LOFTY PROVINCE:  
(East Mt Lofty Ranges)

## CHEMISTRY

SAMPLE	BOU 356 (Whalley Hill) (Ferruginised)	BOU 367	BOU 381 (Newbury) Bedrock	BOU 382 (Summit) samples)	BOU 375 (Mount Torrens) Mottle	BOU 360 Fe/crete
Fe <sub>2</sub> O <sub>3</sub>	28.54	21.16	17.10	24.25	34.75	55.05
MnO	0.04	0.02	0.01	0.03	0.01	0.01
TiO <sub>2</sub>	0.64	0.53	0.42	0.55	0.58	0.35
CaO	0.19	0.07	0.06	0.15	0.04	0.01
K <sub>2</sub> O	1.97	0.35	0.20	0.35	0.41	0.72
SO <sub>3</sub>	0.02	0.02	0.02	0.03	0.08	0.04
P <sub>2</sub> O <sub>5</sub>	0.09	0.04	0.02	0.07	0.03	0.11
SiO <sub>2</sub>	51.2	60.1	61.9	57.2	47.7	20.9
Al <sub>2</sub> O <sub>3</sub>	8.35	9.37	13.88	11.53	9.75	11.54
MgO	0.84	0.15	0.08	0.14	0.07	0.09
Na <sub>2</sub> O	0.06	0.13	0.06	0.16	0.08	0.07
ZrO						
Ig.Loss	<u>6.97</u>	<u>7.03</u>	<u>7.05</u>	<u>4.43</u>	<u>6.46</u>	<u>11.07</u>
Total	<u>98.9</u>	<u>98.5</u>	<u>100.8</u>	<u>98.9</u>	<u>99.9</u>	<u>98.9</u>

## MINERALOGY

In decreasing order of abundance

Qz	Qz	Qz	Qz	Qz	Gt
Hm	Hm	Kt	Hm	Hm	Hm
Gt	Kt	Hm	Kt	Kt	Qz
Fr	Gt	St	St	Gt	Kt
Kt	St	Ic	An	Vm	Hm
Mu	Mu		Mu	Fr	Fr
St	Fr		Fr	An	
	Ic				

Magnetic  
reaction

N	N	Y	Y	N	N
		vvsl	vvvsl		

Qz=quartz; Hm=hematite; Gt=goethite; Kt=kaolinite; St=smectite;  
An=anatase; Fr=felspar; Mh=maghemite; Mu=muscovite; Ic=interstratified  
clays; Vm=vermiculite; v=very; sl=slight.

TABLE 4.17 MOUNT LOFTY PROVINCE

SAMPLE	CHEMISTRY			
	BOU 68 (North M.L.Ranges) Non-magnetic Pisoliths	BOU 69 Magnetic Pisoliths	BOU 341 Longwood Bleached Bedrock	BOU 395 Para Res. Hematitic Quartzite
Fe <sub>2</sub> O <sub>3</sub>	9.33	22.30	0.27	70.30
MnO	0.04	0.05	nd	0.02
TiO <sub>2</sub>	1.00	1.83	0.19	2.04
CaO	0.09	0.09	0.02	0.01
K <sub>2</sub> O	0.04	0.05	0.48	0.25
SO <sub>3</sub>			0.01	0.01
P <sub>2</sub> O <sub>5</sub>	0.04	0.04	0.01	0.03
SiO <sub>2</sub>	84.5	72.8	81.3	25.7
Al <sub>2</sub> O <sub>3</sub>	2.70	1.62	12.52	0.91
MgO	0.04	0.07	0.24	0.06
Na <sub>2</sub> O	0.01	0.03	0.21	0.07
ZrO	0.03	0.06		
Ig.Loss	<u>2.11</u>	<u>0.07</u>	<u>5.09</u>	<u>0.22</u>
Total	<u>99.9</u>	<u>99.6</u>	<u>100.3</u>	<u>99.6</u>

## MINERALOGY

In decreasing order of abundance

Qz	Qz	Qz	Hm
Hm	Hm	Kt	Il
St	Mh	St	Qz
Kt	St	Mu	Fr
An	An	Fr	Vm
		Ic	

Magnetic  
reaction NY  
vstr

N

Y  
vvsl

Qz=quartz; Hm=hematite; Gt=goethite; Kt=kaolinite;  
 St=smectite; An=anatase; Fr=felspar; Mh=maghemite;  
 Mu=muscovite; Ic=interstratified clays; Vm=vermiculite;  
 Il=ilmenite; nd=not detected; v=very; sl=slight; str=strong.

APPENDIX II:  
TABLES 4.18 to 4.19.

TABLE 4.18

## WILLUNGA HILL BOREHOLE ANALYSES

Sample	Depth	CHEMISTRY											Ign Loss	Total
		Fe <sub>2</sub> O <sub>3</sub>	MnO	TiO <sub>2</sub>	CaO	K <sub>2</sub> O	SO <sub>3</sub>	P <sub>2</sub> O <sub>5</sub>	SiO <sub>2</sub>	Al <sub>2</sub> O <sub>3</sub>	MgO	Na <sub>2</sub> O		
Bou														
970	3 m	3.85	nd	1.67	0.03	1.16	nd	0.01	62.9	21.19	0.40	0.06	8.82	100.1
971	6 m	9.18	nd	1.68	0.01	1.63	0.02	0.04	58.1	20.09	0.46	0.15	8.97	100.3
972	9 m	10.83	nd	2.02	0.02	1.20	0.01	0.15	59.1	17.42	0.36	0.18	8.75	100.0
973	12 m	8.38	nd	1.46	0.02	1.43	0.02	0.21	60.0	19.50	0.40	0.20	8.09	99.7
974	15 m	8.29	0.01	1.79	0.04	1.47	nd	0.27	62.3	16.79	0.44	0.25	8.06	99.7
975	18 m	9.09	0.01	1.95	0.04	1.50	0.08	0.24	63.7	15.31	0.76	0.27	7.07	100.0
976	21 m	7.70	0.01	1.65	0.08	2.70	0.02	0.09	63.3	15.50	1.89	0.65	6.44	100.1
977	24 m	6.91	0.02	1.48	0.13	2.84	0.01	0.13	62.3	14.82	2.74	1.45	6.85	100.2
978	27 m	6.95	0.02	1.36	0.19	2.36	nd	0.02	64.4	13.41	3.53	1.16	5.31	98.7
979	30 m	9.01	0.05	1.69	0.11	2.54	0.01	0.09	60.8	15.97	2.17	0.73	6.74	99.9
980	33 m	6.93	0.02	1.64	0.21	2.10	nd	0.01	63.3	14.54	3.20	1.45	6.85	100.2
981	36 m	7.45	0.03	1.45	0.12	3.70	nd	0.05	60.7	15.60	3.91	1.32	5.83	100.1
982	39 m	7.16	0.03	1.40	0.11	2.94	0.09	0.07	62.7	13.61	3.79	1.52	7.11	100.5
983	42 m	8.97	0.13	1.39	0.08	4.20	nd	0.16	58.7	15.97	4.05	1.05	4.97	99.6
984	45 m	10.49	0.03	1.45	0.17	2.46	nd	0.19	60.1	14.21	3.30	1.32	6.54	100.2
985	48 m	8.13	0.06	1.35	0.10	3.54	nd	0.12	61.9	15.01	4.03	1.05	4.76	100.0
986	51 m	7.12	0.03	1.28	0.12	3.15	nd	0.10	65.7	14.07	3.98	1.58	3.38	100.2
987	54 m	9.21	0.02	1.45	0.11	2.25	0.01	0.15	61.0	16.02	2.42	0.91	5.96	99.6
988	57 m	8.47	0.03	1.39	0.18	3.11	nd	0.16	60.1	15.15	4.45	1.57	4.85	99.4
989	60 m	7.59	0.03	1.43	0.18	3.23	nd	0.19	62.4	14.62	4.63	2.14	3.39	99.8
990	63 m	9.05	0.03	1.38	0.19	2.35	0.10	0.14	61.1	15.07	3.30	1.09	6.30	100.8
991	66 m	8.33	0.02	1.31	0.20	2.51	0.01	0.14	62.0	14.78	3.80	1.29	4.80	99.2
992	69 m	8.92	0.03	1.26	0.20	2.74	nd	0.19	61.1	13.53	4.20	1.59	5.54	99.3
993	72 m	13.01	0.02	1.23	0.24	2.65	0.04	0.26	59.4	13.12	3.94	1.32	4.51	99.7
994	75 m	9.17	0.04	1.70	0.28	2.76	0.10	0.20	57.4	16.11	6.05	2.31	3.86	99.9
995	78 m	8.20	0.03	1.44	0.28	2.56	0.08	0.19	61.3	13.72	5.46	1.97	4.24	99.5
996	81 m	12.91	0.03	1.15	0.23	2.74	0.05	0.17	58.4	13.86	4.34	1.46	3.95	99.3
997	84 m	7.74	0.03	1.20	0.27	2.99	nd	0.19	64.4	13.52	4.49	1.60	3.17	99.6
998	87 m	8.10	0.03	1.26	0.27	2.94	0.04	0.20	63.4	13.84	4.68	1.62	3.62	99.7
999	90 m	8.07	0.03	1.33	0.28	2.82	nd	0.19	61.6	13.69	5.03	1.78	4.61	99.4
250	93 m	6.38	0.02	1.45	0.03	1.93	0.02	0.03	66.4	12.94	3.09	1.77	5.45	99.5
251	96 m	8.22	0.04	1.47	0.29	2.79	0.05	0.20	62.0	13.75	5.18	1.70	3.63	99.3
252	99 m	7.58	0.03	1.43	0.13	2.69	0.01	0.09	63.5	13.27	4.80	1.47	4.75	99.7
253	102 m	8.05	0.03	1.44	0.30	2.57	0.06	0.19	61.1	14.51	5.08	1.96	3.81	99.2



TABLE 4.19 WILLUNGA HILL BOREHOLE ANALYSES

SAMPLE		$\frac{\text{Fe}_2\text{O}_3}{\text{TiO}_2}$	$\frac{\text{Fe}_2\text{O}_3}{\text{Al}_2\text{O}_3}$	$\frac{\text{SiO}_2}{\text{Al}_2\text{O}_3}$	$\frac{\text{K}_2\text{O}}{\text{Al}_2\text{O}_3}$
BOU	Depth				
970	3 m	2.31	0.18	2.97	0.05
971	6 m	5.46	0.46	2.89	0.08
972	9 m	5.36	1.61	3.39	0.07
973	12 m	5.74	0.43	3.08	0.07
974	15 m	4.63	0.49	3.71	0.09
975	18 m	4.66	0.59	4.16	0.10
976	21 m	4.67	0.50	4.08	0.17
977	24 m	4.67	0.47	4.20	0.19
978	27 m	5.11	0.52	4.80	0.18
979	30 m	5.33	0.56	3.81	0.16
980	33 m	4.22	0.48	4.35	0.14
981	36 m	5.14	0.48	3.89	0.24
982	39 m	5.11	0.53	4.61	0.22
983	42 m	6.45	0.56	3.68	0.26
984	45 m	7.23	0.74	4.23	0.17
985	48 m	6.02	0.54	4.12	0.24
986	51 m	5.56	0.51	4.67	0.22
987	54 m	6.35	0.57	3.81	0.14
988	57 m	6.09	0.56	3.97	0.21
989	60 m	5.31	0.52	4.27	0.22
990	63 m	6.56	0.60	4.05	0.16
991	66 m	6.36	0.56	4.19	0.17
992	69 m	6.01	0.66	4.52	0.20
993	72 m	10.58	0.99	4.53	0.20
994	75 m	5.39	0.57	3.56	0.17
995	78 m	5.69	0.60	4.47	0.19
996	81 m	11.22	0.93	4.21	0.20
997	84 m	6.45	0.57	4.76	0.22
998	87 m	6.43	0.58	4.58	0.21
999	90 m	6.07	0.59	4.50	0.21
250	93 m	4.40	0.49	5.13	0.15
251	96 m	5.59	0.60	4.51	0.20
252	99 m	5.30	0.57	4.79	0.20
253	102 m	5.59	0.55	4.21	0.18

APPENDIX III:  
TABLES 4.20 to 4.50.

TABLE 4.20 PARAWA PLATEAU - UNWEATHERED BEDROCK ANALYSES

## CHEMISTRY

<i>Sample</i>	<i>Fe<sub>2</sub>O<sub>3</sub></i>	<i>MnO</i>	<i>TiO<sub>2</sub></i>	<i>CaO</i>	<i>K<sub>2</sub>O</i>	<i>P<sub>2</sub>O<sub>5</sub></i>	<i>SiO<sub>2</sub></i>	<i>Al<sub>2</sub>O<sub>3</sub></i>	<i>MgO</i>	<i>Na<sub>2</sub>O</i>	<i>ZrO</i>	<i>Loss</i>	<i>Total</i>
64 Backstairs Passage Fm	2.57	0.03	0.24	0.57	3.56	0.06	77.7	10.52	0.70	2.41	0.02	0.90	99.3
78 Carricka- linga Fm	3.82	0.01	0.50	0.79	2.46	0.17	74.1	11.45	1.29	2.91	0.03	1.54	99.1
79 Tapanappa Fm	4.81	0.05	0.55	1.21	2.69	0.05	71.8	11.11	1.85	2.00	0.04	2.19	98.4
80 Hay Flat	2.44	0.03	0.40	0.96	1.70	0.16	76.7	10.44	0.64	3.68	0.03	1.98	99.2

The mineralogy of these samples is dominated by quartz, muscovite and low plagioclase feldspars.

TABLE 4.21 PARAWA PLATEAU BORE HOLE ANALYSES  
Borehole RBA-1 (315 m asl) (Sited over weathered Carrickalinga Head Formation rocks)

CHEMISTRY															
Sample	Depth	Fe <sub>2</sub> O <sub>3</sub>	MnO	TiO <sub>2</sub>	CaO	K <sub>2</sub> O	SO <sub>3</sub>	P <sub>2</sub> O <sub>5</sub>	SiO <sub>2</sub>	Al <sub>2</sub> O <sub>3</sub>	MgO	Na <sub>2</sub> O	ZrO	Loss	Total
Bou	in m.														
600	0-1	5.98	0.01	0.67	2.43	0.90	0.11	0.03	62.0	15.72	0.28	0.08	0.04	11.48	99.7
601	1-2	5.19	0.01	0.75	0.28	1.10	0.02	0.01	67.6	16.89	0.21	0.06	0.05	7.53	99.7
602	2-3	4.90	0.01	0.73	0.10	1.51	nd	0.02	68.8	16.31	0.27	0.08	0.04	6.57	99.3
603	3-4	5.20	0.01	0.79	0.04	1.35	0.01	0.02	68.8	15.92	0.39	0.09	0.06	6.62	99.3
604	4-5	6.20	0.01	0.76	0.05	1.83	nd	0.03	65.6	17.19	0.49	0.13	0.04	7.04	99.4
605	5-6	6.18	0.02	0.77	0.03	2.45	0.02	0.02	64.4	17.68	0.73	0.14	0.03	6.77	99.2
606	6-7	5.48	0.02	0.74	0.05	1.53	0.02	0.02	66.1	17.19	0.45	0.18	0.04	7.35	99.2
607	7-8	5.45	0.01	0.82	0.03	2.52	0.01	0.02	63.0	19.56	0.52	0.20	0.03	7.13	99.3
608	8-9	5.56	0.02	0.82	0.03	2.60	0.02	0.02	62.2	19.56	0.64	0.29	0.03	7.15	98.9

MINERALOGY														
Sample	Depth	Qz	Kt	Gb	Gt & Hm	Mh	Mu	St	Ic	Vm	An	Fr		
Bou	in m													
600	0-1	230	150	nd	15	10	55	30	25	nd	nd	nd		
601	1-2	230	190	nd	15	nd	75	30	15	nd	nd	nd		
602	2-3	110	250	nd	10	nd	130	25	10	nd	nd	nd		
603	3-4	180	200	nd	20	nd	90	20	20	nd	nd	nd		
604	4-5	150	160	nd	15	nd	130	35	15	nd	nd	nd		
605	5-6	230	120	nd	15	nd	180	20	10	nd	nd	nd		
606	6-7	230	110	nd	15	nd	90	15	15	nd	nd	nd		
607	7-8	140	115	nd	20	nd	185	25	15	nd	nd	nd		
608	8-9	150	140	nd	10	nd	200	20	10	nd	nd	nd		

Qz=quartz; Kt=kaolinite; Gb=gibbsite; Gt=goethite; Hm=hematite; Mh=maghemite; Mu=muscovite; St=smectite; Ic= interstratified clays; Vm=vermiculite; An=anatase; Fr=felspar. nd= not detected.

TABLE 4.22 PARAWA PLATEAU BORE HOLE ANALYSES  
Borehole RBA-2 (330 m asl) (Sited over weathered Carrickalinga Head Formation rocks)

CHEMISTRY															
Sample	Depth	Fe <sub>2</sub> O <sub>3</sub>	MnO	TiO <sub>2</sub>	CaO	K <sub>2</sub> O	SO <sub>3</sub>	P <sub>2</sub> O <sub>5</sub>	SiO <sub>2</sub>	Al <sub>2</sub> O <sub>3</sub>	MgO	Na <sub>2</sub> O	ZrO	Loss	Total
609	0-1	18.26	0.01	0.93	0.07	0.37	0.02	0.02	36.6	27.23	0.26	0.12	0.0	15.65	99.6
610	1-2	8.48	0.01	1.03	0.05	0.79	0.01	0.03	47.4	27.57	0.32	0.06	0.05	13.39	99.2
611	2-3	12.21	0.01	0.96	0.03	1.12	0.02	0.04	51.6	23.03	0.25	0.06	0.05	10.49	99.9
612	3-4	4.25	0.01	1.21	0.21	1.70	0.02	0.06	60.9	21.27	0.31	0.52	0.07	8.22	98.8
613	4-5	2.58	nd	1.16	0.01	1.90	0.01	0.03	66.2	19.79	0.32	0.05	0.05	6.96	99.1
614	5-6	2.85	0.01	0.93	0.01	1.53	0.01	0.05	69.5	18.09	0.25	0.05	0.05	6.56	99.9
615	6-7	5.17	nd	0.92	0.02	0.95	0.02	0.06	67.1	18.29	0.18	0.12	0.05	7.41	100.3
616	7-8	6.30	0.01	0.84	0.03	0.96	0.02	0.06	65.9	17.83	0.16	0.02	0.05	7.41	99.6
617	8-9	9.19	0.01	0.75	0.01	0.90	0.02	0.04	65.7	16.03	0.16	0.02	0.05	6.93	99.8
618	9-10	6.07	0.01	0.80	0.01	1.22	0.01	0.04	66.9	17.54	0.20	0.04	0.05	6.85	99.7
619	10-11	6.14	0.01	0.79	0.02	1.51	nd	0.03	64.1	19.10	0.28	0.07	0.04	7.44	99.5
620	11-12	9.47	0.01	0.78	0.02	1.60	0.01	0.04	61.4	18.62	0.27	0.12	0.04	7.27	99.7
621	12-13	10.13	0.01	0.80	0.02	1.69	0.02	0.05	60.6	18.71	0.26	0.10	0.04	7.18	99.6
622	13-14	9.26	0.01	0.83	0.02	1.79	0.01	0.05	61.0	19.08	0.26	0.10	0.04	7.17	99.6

MINERALOGY														
Sample	Depth	Qz	Kt	Gb	Gt & Hm	Mh	Mu	St	Ic	Vm	An	Fr		
609	0-1	40	70	170	100	100	tr	20	15		10	20		
610	1-2	50	140	80	80	60		10	15		15	20		
611	2-3	60	150	35	60	60		50	10		10	30		
612	3-4	40	190		25		90	15	10		15	30		
613	4-5	100	160		15		90	15	10		15	35		
614	5-6	70	200		10		90	25	10		10	30		
615	6-7	180	160		25		160	25	20		10	20		
616	7-8	100	130		15	15	60	25	25		10	35		
617	8-9	100	130		20	20	50	20	25		10	35		
618	9-10	80	180		15	15	80	25	25		10	40		
619	10-11	150	160		20		140	20	20		10	30		
620	11-12	120	170		20	20	160	20	20		10	35		
621	12-13	140	140		20	20	130	20	20		10	30		
622	13-14	140	140		25	25	140	25	20		10	35		

Qz=quartz; Kt=kaolinite; Gb=gibbsite; Gt=goethite; Hm=hematite; Mh=maghemite; Mu=muscovite; St=smectite; Ic= interstratified clays; Vm=vermiculite; An=anatase; Fr=felspar; tr= trace.

TABLE 4.23 PARAWA PLATEAU BORE HOLE ANALYSES  
Borehole RBA-3 (330 m asl) (Carrickalinga Head Formation)

Sample	Depth	CHEMISTRY												Ign Loss	Total
		Fe <sub>2</sub> O <sub>3</sub>	MnO	TiO <sub>2</sub>	CaO	K <sub>2</sub> O	SO <sub>3</sub>	P <sub>2</sub> O <sub>5</sub>	SiO <sub>2</sub>	Al <sub>2</sub> O <sub>3</sub>	MgO	Na <sub>2</sub> O	ZrO		
Bou	in m.														
623	0-1	26.59	0.01	0.84	0.23	0.26	0.02	0.03	40.6	19.30	0.26	0.24	0.05	10.67	99.0
624	1-2	14.96	0.01	1.07	0.07	0.30	0.02	0.02	42.1	25.70	0.32	0.29	0.05	14.40	99.1
625	2-3	10.00	nd	1.18	0.03	0.36	0.01	0.02	53.4	22.00	0.25	0.22	0.06	11.93	99.3
626	3-4	12.92	0.01	1.13	0.09	0.37	0.03	0.02	49.5	22.40	0.31	0.23	0.06	12.30	98.1
627	4-5	10.08	0.01	0.98	0.46	0.59	0.15	0.04	58.5	19.10	0.32	0.42	0.05	9.22	99.8
628	5-6	1.77	0.01	0.88	0.02	2.10	0.04	0.06	64.1	22.10	0.25	0.52	0.04	7.67	99.7
629	6-7	1.26	0.01	0.88	0.02	1.36	0.03	0.06	69.6	18.80	0.18	0.23	0.05	6.69	99.1
630	7-8	1.49	0.01	0.95	0.02	1.59	0.01	0.04	67.1	20.20	0.16	0.26	0.06	7.40	99.2
631	8-9	6.97	0.01	0.83	0.01	1.62	nd	0.04	63.6	18.50	0.16	0.27	0.04	6.87	98.9
632	9-10	5.96	0.01	0.86	0.01	1.88	0.01	0.03	63.5	19.70	0.20	0.28	0.03	6.90	99.3
633	10-11	6.17	0.01	0.82	0.02	1.74	0.06	0.04	63.6	19.00	0.28	0.27	0.04	7.02	98.9

Sample	Depth	MINERALOGY											
		Qz	Kt	Gb	Gt &	Hm	Mh	Mu	St	Ic	Vm	An	Fr
Bou	in m												
623	0-1	150	40	110	65	100	50		10	15		10	
624	1-2	80	100	170	40	70		10	15	20		15	30
625	2-3	90	180	45	100	100		20	15	20		15	20
626	3-4	160	120	60	80	80		15	20	15		15	15
627	4-5	160	280	25	50	50		70	15	15		10	
628	5-6	230	240					150	30	15		10	
629	6-7	160	230					180	30	20		10	
631	8-9	220	280		60	80		290	15	10		10	15
632	9-10	220	330		40	40		220	25	20		10	15
633	10-11	170	210		40	40		150	30	20		10	

Qz=quartz; Kt=kaolinite; Gb=gibbsite; Gt=goethite; Hm=hematite; Mh=maghemite; Mu=muscovite; St=smectite; Ic= interstratified clays; Vm=vermiculite; An=anatase; Fr=felspar; tr= trace.

TABLE 4.24 PARAWA PLATEAU BORE HOLE ANALYSES  
Borehole RBA-4 (330 m asl) (Carrickalinga Head Formation)

Sample	Depth	CHEMISTRY												Loss	Total
		Fe <sub>2</sub> O <sub>3</sub>	MnO	TiO <sub>2</sub>	CaO	K <sub>2</sub> O	SO <sub>3</sub>	P <sub>2</sub> O <sub>5</sub>	SiO <sub>2</sub>	Al <sub>2</sub> O <sub>3</sub>	MgO	Na <sub>2</sub> O	ZrO		
Bou	in m.														
634	0-1	23.42	0.01	0.93	0.10	0.33	0.03	0.03	42.8	19.89	0.28	0.13	0.05	10.94	98.9
635	1-2	9.58	0.01	1.18	0.06	0.28	0.01	0.02	50.6	23.61	0.36	0.08	0.06	13.57	99.4
636	2-3	7.96	nd	1.18	0.04	0.22	0.02	0.02	63.2	16.64	0.23	0.05	0.07	9.27	98.9
637	3-4	5.85	nd	1.14	0.05	0.29	0.02	0.01	67.1	16.10	0.20	0.11	0.06	8.69	99.6
638	4-5	1.67	nd	0.84	0.03	1.20	0.01	0.03	65.7	21.42	0.25	0.11	0.04	8.32	99.7
639	5-6	1.38	0.01	0.84	0.03	1.58	0.01	0.09	65.6	21.48	0.26	0.11	0.04	8.03	99.5
640	6-7	2.67	0.01	0.89	0.05	1.33	0.02	0.07	65.9	19.34	0.25	0.15	0.04	7.52	98.2
641	7-8	9.77	0.01	0.85	0.03	1.27	0.01	0.11	60.3	18.13	0.22	0.08	0.03	8.03	98.9
642	8-9	8.08	0.01	0.83	0.03	2.54	0.01	0.13	59.7	19.71	0.37	0.12	0.03	7.45	99.0
643	9-10	6.54	0.01	0.87	0.03	2.94	0.01	0.12	59.5	21.09	0.45	0.18	0.02	7.55	99.3
644	10-11	5.52	0.23	0.83	0.03	1.75	0.01	0.07	65.1	18.24	0.40	0.11	0.03	7.02	99.3
645	11-12	5.48	0.02	0.79	0.04	1.84	0.01	0.05	67.1	16.78	0.78	0.11	0.04	6.49	99.5

Sample	Depth	MINERALOGY											
		Qz	Kt	Gb	Gt &	Hm	Mh	Mu	St	Ic	Vm	An	Fr
Bou	in m												
634	0-1	190	60	100	100	80	50		10	20		10	25
635	1-2	200	90	60	40	60			10	20		20	20
636	2-3	210	110		20	30			20	30		20	20
637	3-4	220	100	10	15	20		15	25	15		15	15
638	4-5	210	300					90	25	10		10	10
639	5-6	160	200					90	10	10		10	
640	6-7	230	270					90	25	10		10	
641	7-8	180	190		15	15		95	20	10		5	
642	8-9	180	120		15	15		140	15	10		5	
643	9-10	180	160		10	10		280	15	10		5	
644	10-11	220	200		10	10		190	15	10		5	
645	11-12	230	180		5	5		160	15	10		5	

Qz=quartz; Kt=kaolinite; Gb=gibbsite; Gt=goethite; Hm=hematite; Mh=maghemite; Mu=muscovite; St=smectite; Vm=vermiculite; An=anatase; Fr=felspar; tr= trace; nd= not detected.

TABLE 4.25 PARAWA PLATEAU BORE HOLE ANALYSES  
Borehole RBA-5 (335 m asl) (Sited over weathered Carrickalinga Head Formation rocks).

CHEMISTRY															
Sample	Depth	Fe <sub>2</sub> O <sub>3</sub>	MnO	TiO <sub>2</sub>	CaO	K <sub>2</sub> O	SO <sub>3</sub>	P <sub>2</sub> O <sub>5</sub>	SiO <sub>2</sub>	Al <sub>2</sub> O <sub>3</sub>	MgO	Na <sub>2</sub> O	ZrO	Loss	Total
BOU	in m.														
646	0-1	21.21	0.01	0.77	0.14	0.32	0.02	0.03	48.7	16.80	0.25	0.74	0.05	10.95	100.0
647	1-2	7.76	nd	0.80	0.05	0.49	0.02	0.08	56.8	21.79	0.27	0.53	0.05	11.03	99.7
648	2-3	3.60	0.01	0.76	0.03	0.57	0.01	0.04	62.8	21.28	0.25	0.11	0.05	9.98	99.5
649	3-4	1.78	nd	0.77	0.04	0.94	0.02	0.03	68.2	19.37	0.19	0.06	0.06	7.83	99.2
650	4-5	3.09	0.01	0.90	0.05	0.97	0.03	0.15	69.7	16.99	0.32	0.25	0.06	7.23	99.8
651	5-6	4.33	0.01	0.82	0.03	1.48	0.01	0.08	68.0	17.05	0.61	0.06	0.06	6.96	99.4
652	6-7	4.90	0.02	0.74	0.03	1.83	0.01	0.07	68.8	15.71	1.00	0.08	0.05	6.52	98.8
653	7-8	5.27	0.03	0.75	0.03	2.23	0.01	0.05	69.4	15.06	1.20	0.10	0.06	5.90	100.1
654	8-9	4.58	0.03	0.85	0.03	2.30	0.01	0.05	69.0	15.87	0.94	0.09	0.07	6.04	99.9
655	9-10	4.44	0.03	0.82	0.04	2.56	0.02	0.06	67.9	16.52	1.03	0.15	0.05	6.03	99.6
656	10-11	4.38	0.03	0.71	0.03	2.32	0.01	0.11	70.7	15.06	1.06	0.11	0.05	5.47	100.1
657	11-12	3.59	0.02	0.78	0.04	2.27	0.02	0.13	70.9	15.44	0.93	0.14	0.06	5.56	99.9
658	12-13	4.44	0.03	0.88	0.05	2.50	0.01	0.08	69.7	15.45	1.19	0.16	0.07	5.47	100.0
MINERALOGY															
Sample	Depth	Qz	Kt	Gb	Gt & Hm	Mh	Mu	St	Ic	Vm	An	Fr			
BOU	in m														
646	0-1	200	90	35	100 120	20		10	20		10				
647	1-2	140	200	15	70 60		20	20	20		10				
648	2-3	220	200		10		30	25	25		5				
649	3-4	160	290				70	25	20		10				
650	4-5	230	210		10		60	35	10		10	10			
651	5-6	230	250				100	35	15		10	10			
652	6-7	190	220				130	30	15		5				
653	7-8	230	160		15		125	30							
654	8-9	240	180				150	30	10		5				
655	9-10	170	180		5		160	30	25		5	40			
656	10-11	170	170		5		140	30	20		5	30			
657	11-12	220	150				120	25	20		10	40			
658	12-13	160	190				150	30	20		5	35			

Qz=quartz; Kt=kaolinite; Gb=gibbsite; Gt=goethite; Hm=hematite; Mh=maghemite; Mu=muscovite; St=smectite; Ic= interstratified clays; Vm=vermiculite; An=anatase; Fr=felspar; tr= trace; nd= not detected.

TABLE 4.26 PARAWA PLATEAU BORE HOLE ANALYSES  
Borehole RBA-6 (342 m asl) (Sited over weathered Carrickalinga Head Formation rocks)

CHEMISTRY															
Sample	Depth	Fe <sub>2</sub> O <sub>3</sub>	MnO	TiO <sub>2</sub>	CaO	K <sub>2</sub> O	SO <sub>3</sub>	P <sub>2</sub> O <sub>5</sub>	SiO <sub>2</sub>	Al <sub>2</sub> O <sub>3</sub>	MgO	Na <sub>2</sub> O	ZrO	Loss	Total
BOU	in m.														
659	0-1	26.54	0.01	0.85	0.09	0.32	0.03	0.03	42.5	18.48	0.24	0.11	0.06	9.47	98.7
660	1-2	12.71	0.01	1.07	0.07	0.31	0.06	0.02	51.1	21.65	0.29	0.07	0.06	11.84	99.3
661	2-3	5.36	0.01	0.99	0.04	0.70	0.02	0.02	60.6	20.99	0.28	0.07	0.05	9.92	99.1
662	3-4	1.94	nd	0.78	0.03	1.22	0.01	0.04	69.4	18.12	0.24	0.11	0.04	6.95	98.9
663	4-5	1.93	0.02	0.84	0.03	1.30	0.01	0.03	69.1	18.13	0.27	0.12	0.05	7.11	98.9
664	5-6	1.75	0.01	0.82	0.04	1.08	0.01	0.04	67.1	19.71	0.25	0.14	0.04	8.32	99.3
665	6-7	1.52	nd	0.82	0.03	1.61	0.01	0.05	67.3	19.90	0.32	0.11	0.04	7.51	99.2
666	7-8	2.80	0.01	0.82	0.03	1.47	0.01	0.06	66.9	18.06	0.30	0.11	0.04	8.68	99.3
667	8-9	9.94	0.02	0.77	0.03	1.75	0.01	0.08	63.7	15.65	0.60	0.08	0.05	6.71	99.4
668	9-10	8.38	0.02	0.77	0.03	2.04	0.28	0.09	64.4	15.59	0.99	0.08	0.05	6.32	99.0
669	10-11	6.99	0.02	0.78	0.72	1.71	0.01	0.10	65.2	16.28	0.73	0.10	0.05	7.00	99.7
670	11-12	5.41	0.03	0.80	0.03	1.97	0.01	0.07	67.3	16.25	1.00	0.07	0.05	6.29	99.3
671	12-13	5.32	0.03	0.80	0.04	2.33	0.02	0.05	66.9	16.34	1.23	0.08	0.05	6.00	99.2
MINERALOGY															
Sample	Depth	Qz	Kt	Gb	Gt & Hm	Mh	Mu	St	Ic	Vm	An	Fr			
BOU	in m														
659	0-1	210	55	110	90 120	40			20		10	25			
660	1-2	120	120	40	90 80		15		15		10	15			
661	2-3	240	160		15		35	10	15		10	5			
662	3-4	160	190				80	25	20		10				
663	4-5	230	180				110	20	20		15				
664	5-6	220	170				80	30	20		10				
665	6-7	240	160				120	25	20		15				
666	7-8	210	150				140	40	10		10				
667	8-9	200	110		40		160	30	20		10				
668	9-10	250	110		35		200	40	10		10				
669	10-11	230	110		20		130	30	10		5				
670	11-12	190	110		20		140	25	15		10				
671	12-13	170	120		15		200	30	10		10				

Qz=quartz; Kt=kaolinite; Gb=gibbsite; Gt=goethite; Hm=hematite; Mh=maghemite; Mu=muscovite; St=smectite; Ic= interstratified clays; Vm=vermiculite; An=anatase; Fr=felspar; tr= trace; nd= not detected.

TABLE 4.27 PARAWA PLATEAU BORE HOLE ANALYSES  
Borehole RBA-7 (335 m asl) (Sited over Carrickalinga Head Formation rocks)

CHEMISTRY															
Sample	Depth	FeO <sub>3</sub>	MnO	TiO <sub>2</sub>	CaO	K <sub>2</sub> O	SO <sub>3</sub>	P <sub>2</sub> O <sub>5</sub>	SiO <sub>2</sub>	Al <sub>2</sub> O <sub>3</sub>	MgO	Na <sub>2</sub> O	ZrO	Loss	Total
Bou	in m.														
672	0-1	18.38	0.03	0.88	0.48	0.28	0.08	0.03	51.4	16.03	0.25	0.18	0.05	10.42	98.5
673	1-2	11.73	0.01	0.95	0.16	0.50	0.03	0.03	56.1	18.92	0.25	0.09	0.05	10.61	99.4
674	2-3	6.03	0.01	0.80	0.04	1.71	0.03	0.10	63.1	19.08	0.44	0.10	0.04	8.42	99.9
675	3-4	5.06	0.02	0.65	0.04	1.63	0.03	0.17	67.1	16.55	0.54	0.13	0.04	7.17	99.1
676	4-5	5.74	0.02	0.71	0.05	2.16	0.02	0.15	65.9	16.46	0.82	0.14	0.04	6.58	98.8
677	5-6	6.80	0.03	0.77	0.07	2.96	0.02	0.06	63.0	17.30	1.44	0.18	0.03	6.69	99.4
678	6-7	5.52	0.04	0.75	0.09	3.02	0.02	0.04	65.1	16.94	1.62	0.26	0.03	6.14	99.6
679	7-8	5.80	0.04	0.67	0.15	3.02	0.02	0.03	66.4	15.51	1.85	0.39	0.04	5.24	99.2
680	8-9	6.12	0.03	0.71	0.23	3.19	0.02	0.06	67.0	15.00	1.78	0.59	0.04	4.89	99.7
681	9-10	6.12	0.06	0.74	0.36	2.95	0.01	0.05	67.4	14.65	1.73	0.85	0.05	4.52	99.5
682	10-11	5.59	0.04	0.74	0.46	2.79	0.02	0.05	68.1	14.60	1.76	1.01	0.05	4.27	99.5
683	11-12	5.90	0.04	0.72	0.48	2.95	0.02	0.08	66.6	15.05	1.90	0.94	0.04	4.43	99.2
684	12-13	6.94	0.05	0.73	0.38	3.89	0.01	0.09	63.3	16.47	2.33	0.83	0.03	4.79	99.8

MINERALOGY													
Sample	Depth	Qz	Kt	Gb	Gt & Hm	Mh	Mu	St	Ic	Vm	An	Fr	
Bou	in m												
672	0-1	200	80	10	90 120	30	15	15		15	5	15	
673	1-2	250	100		10 70	5		10	10	8	10	10	
674	2-3	210	160		15		130	25	5		5	10	
675	3-4	230	120		5		80	25	5		5		
676	4-5	210	135		10		160	30	10		10	10	
677	5-6	150	120		10		240	30	5	5	5		
678	6-7	200	110		10		250	35	10		5		
679	7-8	220	110		15		220	35	10		5	40	
680	8-9	230	90		15		240	35	5		5	40	
681	9-10	210	90		15		240	30	5		5	35	
682	10-11	220	90		15		250	35	5		10	50	
683	11-12	180	80		15		260	30	5		5	50	
684	12-13	190	50		20		270	35	10		5	50	

Qz=quartz; Kt=kaolinite; Gb=gibbsite; Gt=goethite; Hm=hematite; Mh=maghemite; Mu=muscovite; St=smectite; Ic= interstratified clays; Vm=vermiculite; An=anatase; Fr=felspar; tr= trace; nd= not detected.

TABLE 4.28 PARAWA PLATEAU BORE HOLE ANALYSES  
Borehole RBA-8 (345 m asl) (Sited over weathered Carrickalinga Head Formation rocks)

CHEMISTRY															
Sample	Depth	Fe <sub>2</sub> O <sub>3</sub>	MnO	TiO <sub>2</sub>	CaO	K <sub>2</sub> O	SO <sub>3</sub>	P <sub>2</sub> O <sub>5</sub>	SiO <sub>2</sub>	Al <sub>2</sub> O <sub>3</sub>	MgO	Na <sub>2</sub> O	ZrO	Loss	Total
Bou	in m.														
685	0-1	16.22	0.01	0.96	0.11	0.33	0.03	0.03	40.0	25.39	0.40	0.14	0.04	14.17	97.8
686	1-2	10.42	0.01	1.04	0.09	0.30	0.01	0.02	52.2	22.69	0.37	0.10	0.05	12.15	99.5
687	2-3	5.53	0.01	1.07	0.14	0.26	0.03	0.01	62.4	19.01	0.30	0.11	0.06	10.03	99.0
688	3-4	10.74	0.01	0.98	0.05	0.28	0.01	0.02	68.3	18.22	0.20	0.07	0.05	7.42	98.2
690	5-6	1.81	0.01	0.90	0.03	0.95	0.01	0.05	69.3	17.89	0.20	0.07	0.07	7.28	98.6
691	6-7	1.61	0.01	0.91	0.03	1.58	0.01	0.08	66.9	20.53	0.32	0.14	0.06	7.30	99.5
692	7-8	2.87	0.01	0.83	0.03	1.64	0.02	0.06	68.2	18.13	0.51	0.14	0.06	6.80	99.3
693	8-9	5.11	0.02	0.78	0.03	1.80	0.01	0.11	67.0	17.17	0.76	0.11	0.05	6.40	99.4
694	9-10	6.66	0.02	0.82	0.03	1.85	0.01	0.13	65.9	16.40	0.83	0.11	0.06	6.38	99.2
695	10-11	6.53	0.02	0.81	0.04	1.90	0.02	0.11	66.0	16.18	0.94	0.12	0.05	6.36	99.1
696	11-12	6.64	0.03	0.75	0.03	2.45	0.02	0.12	65.8	15.92	1.22	0.16	0.04	5.85	99.0

MINERALOGY													
Sample	Depth	Qz	Kt	Gb	Gt & Hm	Mh	Mu	St	Ic	Vm	An	Fr	
Bou	in m												
685	0-1	100	100	190	150 60	15			5		15	30	
686	1-2	140	100	25	100 80			25	15		15		
687	2-3	160	135		100 60			20	5		15		
688	3-4	250	110		100 70		10	25	10		10		
689	4-5	280	280		10		120	30			10	25	
690	5-6	250	180				74	30	10		15		
691	6-7	210	300				190	35	15		15		
692	7-8	230	180				130	30	20		15		
693	8-9	240	280		20		270	30	15				
694	9-10	330	280		15		220	30	10		10		
695	10-11	230	135		15		120	30	10		5		
696	11-12	220	260		20		260	30	10		10		

Qz=quartz; Kt=kaolinite; Gb=gibbsite; Gt=goethite; Hm=hematite; Mh=maghemite; Mu=muscovite; St=smectite; Ic= interstratified clays; Vm=vermiculite; An=anatase; Fr=felspar; tr= trace; nd= not detected.

TABLE 4.29 PARAWA PLATEAU BORE HOLE ANALYSES  
Borehole RBA-9 (350 m asl) (Sited over Carrickalinga Head Formation rocks)

		CHEMISTRY													
Sample	Depth	Fe <sub>2</sub> O <sub>3</sub>	MnO	TiO <sub>2</sub>	CaO	K <sub>2</sub> O	SO <sub>3</sub>	P <sub>2</sub> O <sub>5</sub>	SiO <sub>2</sub>	Al <sub>2</sub> O <sub>3</sub>	MgO	Na <sub>2</sub> O	ZrO	Loss	Total
Bou	in m.														
697	0-1	13.56	0.01	0.80	0.88	0.26	0.02	0.02	47.5	22.84	0.31	0.05	0.04	14.27	98.9
698	1-2	15.14	nd	0.78	0.14	0.19	0.02	0.02	49.9	21.31	0.20	0.03	0.04	11.54	99.3
699	2-3	3.79	nd	1.58	0.09	0.35	0.01	0.01	79.0	9.81	0.11	0.07	0.06	4.98	99.9
700	3-4	1.30	nd	0.69	nd	1.20	0.02	0.02	56.2	29.43	0.20	0.06	0.02	10.47	99.6
701	4-5	1.59	nd	0.95	0.03	1.82	0.02	0.02	61.4	25.73	0.27	0.11	0.03	8.08	100.0
702	5-6	1.00	0.01	0.85	0.01	1.46	0.02	0.02	63.2	24.34	0.20	0.06	0.04	8.29	99.5
703	6-7	0.69	nd	0.81	0.03	1.60	0.02	0.02	65.2	23.17	0.24	0.06	0.04	7.60	99.5
704	7-8	0.77	0.01	0.76	0.23	1.45	0.03	0.03	67.2	19.69	0.21	0.12	0.04	9.94	100.5
705	8-9	0.41	nd	0.81	0.02	0.83	0.04	0.04	69.6	20.36	0.12	0.04	0.05	7.08	99.4
706	9-10	0.63	nd	0.84	0.01	1.76	0.02	0.02	69.6	19.80	0.21	0.05	0.05	6.87	99.8
707	10-11	0.56	nd	0.82	0.02	1.65	0.03	0.03	68.1	21.40	0.25	0.06	0.04	6.85	99.8
708	11-12	0.73	nd	0.90	0.02	1.52	0.03	0.03	69.8	20.11	0.23	0.06	0.06	6.62	100.1
709	12-13	3.30	0.01	0.87	0.02	1.30	0.03	0.03	68.8	18.52	0.20	0.05	0.05	6.60	99.8

#### MINERALOGY

Sample	Depth	Qz	Kt	Gb	Gt & Hm	Mh	Mu	St	Ic	Ve	An	Fr
Bou	in m											
697	0-1	130	40	120	50 50	10		20	10		10	
698	1-2	130	55	80	50 60			20	10		10	
699	2-3	170	70	15	15		10	30	10		20	
700	3-4	140	250		100 70		75	20	10		10	
701	4-5	100	260				75	20	10		5	
702	5-6	120	280				110	30	10		10	
703	6-7	100	280				110	20	10		5	
704	7-8	100	260				100	30	10		5	
705	8-9	130	270				60	35	5		5	
706	9-10	160	270				130	25	5		5	
707	10-11	170	270				120	25	5		5	
708	11-12	140	280		10		150	30	5		5	
709	12-13	160	280				130	30	5		5	

Qz=quartz; Kt=kaolinite; Gb=gibbsite; Gt=goethite; Hm=hematite; Mh=maghemite; Mu=muscovite; St=smectite; Ic= interstratified clays; Vm=vermiculite; An=anatase; Fr=felspar; tr= trace; nd= not detected.

TABLE 4.30 PARAWA PLATEAU BORE HOLE ANALYSES  
Borehole RBA-10 (342 m asl) (Sited over weathered Carrickalinga Head Formation rocks)

		CHEMISTRY													
Sample	Depth	Fe <sub>2</sub> O <sub>3</sub>	MnO	TiO <sub>2</sub>	CaO	K <sub>2</sub> O	SO <sub>3</sub>	P <sub>2</sub> O <sub>5</sub>	SiO <sub>2</sub>	Al <sub>2</sub> O <sub>3</sub>	MgO	Na <sub>2</sub> O	ZrO	Loss	Total
Bou	in m.														
710	0-1	17.12	0.02	0.89	0.48	0.93	0.06	0.02	49.0	18.57	0.29	0.17	0.04	11.46	99.1
711	1-2	9.37	0.01	1.16	0.04	1.80	0.04	0.02	56.8	22.37	0.28	0.29	0.03	8.49	100.7
712	2-3	11.59	0.02	0.89	0.01	1.07	0.03	0.01	57.4	20.01	0.19	0.20	0.03	8.33	99.7
713	3-4	2.66	0.01	0.92	0.04	1.92	0.07	0.02	58.3	25.90	0.34	0.35	0.02	8.98	99.5
714	4-5	5.89	0.01	0.87	0.02	1.37	0.01	0.01	55.0	24.19	0.24	0.26	0.02	10.99	98.9
715	5-6	3.13	0.02	0.83	0.04	1.38	0.02	0.02	56.5	27.01	0.28	0.38	0.02	10.05	99.4
716	6-7	6.02	0.02	0.78	0.03	1.70	0.01	0.02	57.6	23.82	0.27	0.25	0.02	8.81	99.4
717	7-8	5.19	0.02	0.81	0.03	2.51	0.02	0.03	57.7	24.63	0.30	0.30	0.02	7.82	99.4
718	8-9	10.73	0.02	0.80	0.03	2.30	0.02	0.04	55.8	21.46	0.30	0.28	0.02	7.71	99.5
719	9-10	9.42	0.02	0.78	0.03	2.40	0.02	0.03	56.2	21.99	0.29	0.33	0.02	7.66	99.2
720	10-11	9.39	0.18	0.79	0.03	2.41	0.01	0.03	56.9	21.74	0.29	0.33	0.02	7.15	99.3
721	11-12	10.04	0.02	0.76	0.03	1.80	0.02	0.04	58.9	19.57	0.27	0.23	0.02	7.51	99.2

#### MINERALOGY

Sample	Depth	Qz	Kt	Gb	Gt & Hm	Mh	Mu	St	Ic	Vm	An	Fr
Bou	in m											
710	0-1	180	100	20	60 160	35	40	20	20		15	35
711	1-2	200	220		50 50		220	20	20	15	20	
712	2-3	180	200		70 60		80	20	20		10	10
713	3-4	160	250				200	20	20		10	
714	4-5	130	220		20		100	30	20		10	
715	5-6	200	200				150	30	20		10	
716	6-7	180	230		20		110	30	20	10	10	5
717	7-8	140	280		20		220	20	20	5	5	
718	8-9	160	150		40 40		140	20	15		5	
719	9-10	170	240		40 40		220	30	20		5	
720	10-11	220	150		40 30		170	20	20		5	
721	11-12	180	240		40 30		200	30	15		5	

Qz=quartz; Kt=kaolinite; Gb=gibbsite; Gt=goethite; Hm=hematite; Mh=maghemite; Mu=muscovite; St=smectite; Ic= interstratified clays; Vm=vermiculite; An=anatase; Fr=felspar; tr= trace; nd= not detected.



TABLE 4.31 PARAWA PLATEAU BORE HOLE ANALYSES  
Borehole RBA-11 (340 m asl) (Sited over Brachina Formation rocks)

CHEMISTRY														Ign	Total
Sample	Depth	Fe <sub>2</sub> O <sub>3</sub>	MnO	TiO <sub>2</sub>	CaO	K <sub>2</sub> O	SO <sub>3</sub>	P <sub>2</sub> O <sub>5</sub>	SiO <sub>2</sub>	Al <sub>2</sub> O <sub>3</sub>	MgO	Na <sub>2</sub> O	ZrO	Loss	Total
Bou	in m.														
722	0-1	6.14	0.01	0.87	0.19	0.83	0.01	0.02	54.0	24.92	0.33	0.12	0.04	11.71	99.2
723	1-2	4.17	0.01	0.88	0.82	1.16	0.02	0.02	60.8	22.70	0.26	0.34	0.04	9.26	100.5
724	2-3	5.25	0.01	0.83	0.04	1.40	0.05	0.03	63.5	20.69	0.26	0.14	0.03	7.73	100.1
725	3-4	6.53	0.01	0.83	0.03	1.42	0.01	0.04	63.4	19.56	0.23	0.15	0.03	7.18	99.4
726	4-5	4.91	0.01	0.84	0.06	1.63	0.01	0.05	63.2	21.12	0.28	0.19	0.03	7.52	99.9
727	5-6	5.85	0.01	0.80	0.58	1.71	0.04	0.04	62.0	20.56	0.65	0.17	0.03	7.30	99.7
728	6-7	6.58	0.01	0.84	0.04	1.72	0.01	0.03	62.4	20.58	0.28	0.20	0.03	7.40	100.1
729	7-8	6.02	0.01	0.82	0.06	1.62	0.01	0.04	63.5	19.92	0.27	0.19	0.03	7.37	99.9
730	8-9	6.97	0.01	0.84	0.07	1.20	0.01	0.02	64.7	18.74	0.23	0.13	0.03	7.39	100.3
731	9-10	6.86	0.01	0.84	0.09	1.09	0.02	0.02	64.3	18.74	0.23	0.13	0.04	7.49	99.9
732	10-11	6.34	0.01	0.84	0.06	1.36	0.01	0.03	64.6	18.93	0.24	0.16	0.04	7.22	99.8
733	11-12	6.77	0.01	0.85	0.09	1.45	0.01	0.03	63.5	19.18	0.24	0.16	0.03	7.20	100.0
734	12-13	6.38	0.01	0.86	0.05	1.75	nd	0.03	64.1	18.78	0.27	0.16	0.03	6.84	99.6

**MINERALOGY**

Sample	Depth	Qz	Kt	Gb	Gt & Hm	Mh	Mu	St	Ic	Vm	An	Fr
Bou	in m											
722	0-1	120	230	10	15		65	10	10	15	5	
723	1-2	160	230	5	15		90	20	10	10	10	
724	2-3	140	190		15		80	20	10	10	5	
725	3-4	150	220		20		120	25	10	5	5	
726	4-5	200	240		15		170	30	10		10	
727	5-6	100	180		15		100	30	10		5	
728	6-7	100	180		25		140	20	10		5	
729	7-8	170	200		25		130	20	10		10	
730	8-9	100	140		20		60	25	10	10	5	
731	9-10	200	200		20		130	20	10	5	5	
732	10-11	150	200		20		130	30	15	5	5	5
733	11-12	150	220		20		140	30	15		5	
734	12-13	120	180		25		160	20	10		10	

Qz=quartz; Kt=kaolinite; Gb=gibbsite; Gt=goethite; Hm=hematite; Mh=maghemite; Mu=muscovite; St=smectite; Ic= interstratified clays; Vm=vermiculite; An=anatase; Fr=felspar; tr= trace; nd= not detected.

TABLE 4.32 PARAWA PLATEAU BORE HOLE ANALYSES  
Borehole RBA-12 (300 m asl) (Sited over weathered Brachina Formation rocks)

CHEMISTRY														Loss	Total
Sample	Depth	Fe <sub>2</sub> O <sub>3</sub>	MnO	TiO <sub>2</sub>	CaO	K <sub>2</sub> O	SO <sub>3</sub>	P <sub>2</sub> O <sub>5</sub>	SiO <sub>2</sub>	Al <sub>2</sub> O <sub>3</sub>	MgO	Na <sub>2</sub> O	ZrO	Loss	Total
Bou	in m.														
735	0-1	9.66	0.03	0.90	2.20	2.85	0.07	0.06	51.6	21.19	0.95	0.28	0.02	9.29	99.1
736	1-2	6.86	0.04	0.87	0.02	4.46	0.01	0.02	56.4	22.57	1.79	0.28	0.02	6.13	99.5
737	2-3	7.12	0.06	0.79	0.68	3.80	0.02	0.02	60.6	17.96	2.53	1.30	0.02	4.54	99.4
738	3-4	6.62	0.05	0.78	0.49	4.28	0.01	0.03	60.7	18.80	2.45	1.31	0.02	4.35	99.4
739	4-5	6.45	0.04	0.80	0.33	4.42	0.08	0.04	58.9	19.86	2.09	1.42	0.03	4.75	99.2
740	5-6	6.49	0.05	0.76	0.76	3.94	0.06	0.04	60.5	18.70	2.52	1.61	0.03	4.24	99.7
741	6-7	5.43	0.05	0.73	0.78	3.20	0.07	0.03	64.9	16.53	2.02	1.39	0.03	3.85	99.0
742	7-8	5.18	0.05	0.70	0.75	2.89	0.01	0.02	67.6	15.62	1.90	1.26	0.04	3.77	99.8
743	8-9	5.05	0.04	0.69	0.75	2.92	0.01	0.02	67.9	15.50	1.86	1.21	0.03	3.76	99.7
744	9-10	5.14	0.04	0.77	0.49	3.63	0.01	0.03	64.8	17.50	1.83	1.13	0.03	4.13	99.5

**MINERALOGY**

Sample	Depth	Qz	Kt	Gb	Gt & Hm	Mh	Mu	St	Ic	Vm	An	Fr
BOU	in m											
735	0-1	220	140		20		250	20	10		5	10
736	1-2	190	100		15		250	20	5		5	5
737	2-3	150	50		5		200	25	10	5	5	40
738	3-4	160	40		5		220	30	5	5	5	45
739	4-5	170	50		5		210	30	5		5	50
740	5-6	150	35		5		220	30	5		10	50
741	6-7	140	40		10		160	35	5	5	10	45
742	7-8	140	60				200	30			5	45
743	8-9	200	50				220	35	10		5	50
744	9-10	180	60				220	30	10		5	50

Qz=quartz; Kt=kaolinite; Gb=gibbsite; Gt=goethite; Hm=hematite; Mh=maghemite; Mu=muscovite; St=smectite; Ic= interstratified clays; Vm=vermiculite; An=anatase; Fr=felspar; tr= trace; nd= not detected.

TABLE 4.33 PARAWA PLATEAU BORE HOLE ANALYSES  
Borehole RBA-13 (342 m asl) (Sited over weathered Brachina Formation rocks)

CHEMISTRY														Ign	Total
Sample	Depth	Fe <sub>2</sub> O <sub>3</sub>	MnO	TiO <sub>2</sub>	CaO	K <sub>2</sub> O	SO <sub>3</sub>	P <sub>2</sub> O <sub>5</sub>	SiO <sub>2</sub>	Al <sub>2</sub> O <sub>3</sub>	MgO	Na <sub>2</sub> O	ZrO	Loss	
Bou	in m.														
745	0-1	11.57	0.02	1.12	0.08	0.33	0.01	0.02	50.3	27.12	0.40	0.14	0.04	8.10	99.3
746	1-2	13.75	0.01	1.01	0.07	0.28	0.01	0.02	54.9	20.10	0.28	0.08	0.05	8.78	99.3
747	2-3	5.69	nd	1.11	0.04	0.27	0.01	0.02	65.5	17.71	0.25	0.12	0.05	8.24	99.0
748	3-4	4.19	0.01	1.15	0.04	0.29	0.02	0.05	70.3	16.15	0.21	0.10	0.05	8.01	100.6
749	4-5	2.17	0.01	0.89	0.02	0.75	0.01	0.01	66.6	20.02	0.17	0.10	0.03	8.57	99.4
750	5-6	1.38	0.01	0.78	0.02	1.38	0.01	0.03	62.1	24.96	0.17	0.13	0.03	8.44	99.4
751	6-7	0.89	0.01	0.75	0.02	1.81	0.01	0.05	61.0	24.99	0.21	0.25	0.02	9.54	99.6
752	7-8	1.00	0.01	0.83	0.02	2.09	0.01	0.04	62.5	23.32	0.23	0.26	0.02	8.86	99.2
753	8-9	0.61	0.01	0.81	0.02	2.26	0.01	0.10	62.4	23.99	0.25	0.25	0.02	8.76	99.5
754	9-10	1.25	0.01	0.89	0.03	2.13	0.01	0.08	62.8	22.80	0.25	0.21	0.03	8.89	99.4
755	10-11	1.25	0.02	0.87	0.02	1.77	0.01	0.07	62.8	22.02	0.24	0.21	0.03	9.89	99.2
756	11-12	3.74	0.02	0.81	0.02	1.97	nd	0.13	59.1	20.69	0.43	0.18	0.03	11.76	98.9
756	12-13	5.66	0.03	0.75	0.03	2.12	nd	0.14	56.6	18.77	0.84	0.17	0.03	14.75	99.9
MINERALOGY															
Sample	Depth	Qz	Kt	Gb	Gt & Hm	Mh	Mu	St	Ic	Vm	An	Fr			
BOU	in m														
745	0-1	110	80	110	20	10	5	5	15		15				
746	1-2	210	80	45	50	50		5	20		15				
747	2-3	220	110		20		10	30	10		15	20			
748	3-4	210	100		15			25	10		15	30			
749	4-5	250	230		10			60	35	10	10				
750	5-6	130	330					130	25	15	10				
751	6-7	100	290					140	15	10	10				
752	7-8	180	280					140	20	10	10	10			
753	8-9	160	300					170	20	10	10				
754	9-10	230	310					160	30	10	10				
755	10-11	240	220					140	30	15	10				
756	11-12	160	210		5			160	25	15	10				
757	12-13	250	150		10			130	20	10	10				

Qz=quartz; Kt=kaolinite; Gb=gibbsite; Gt=goethite; Hm=hematite; Mh=maghemite; Mu=muscovite; St=smectite; Ic= interstratified clays; Vm=vermiculite; An=anatase; Fr=felspar; tr= trace; nd= not detected.

TABLE 4.34 PARAWA PLATEAU BORE HOLE ANALYSES  
Borehole RBA-14 (348 m asl) (Sited over weathered Carrickalinga Head Formation rocks)

CHEMISTRY														Ign	Total
Sample	Depth	Fe <sub>2</sub> O <sub>3</sub>	MnO	TiO <sub>2</sub>	CaO	K <sub>2</sub> O	SO <sub>3</sub>	P <sub>2</sub> O <sub>5</sub>	SiO <sub>2</sub>	Al <sub>2</sub> O <sub>3</sub>	MgO	Na <sub>2</sub> O	ZrO	Loss	
BOU	in m.														
757	0-1	24.86	0.01	0.85	0.16	0.50	0.01	0.03	46.9	16.81	0.20	0.09	0.05	9.16	99.6
758	1-2	20.45	0.01	0.89	0.09	0.38	0.02	0.05	45.4	21.45	0.19	0.03	0.05	10.86	99.9
759	2-3	11.82	0.01	0.93	0.09	0.99	0.13	0.05	56.9	19.57	0.22	0.28	0.04	8.04	99.1
760	3-4	6.77	0.01	1.02	0.02	1.59	0.01	0.03	58.7	22.61	0.21	0.16	0.03	8.21	99.4
761	4-5	7.29	0.02	0.95	0.01	2.07	0.01	0.01	58.9	21.83	0.21	0.27	0.03	7.46	99.1
762	5-6	7.17	0.02	0.94	0.02	1.93	0.01	0.02	59.7	21.89	0.21	0.18	0.03	7.52	99.6
763	6-7	10.20	0.02	0.87	0.03	2.22	nd	0.02	57.9	20.98	0.22	0.24	0.03	6.98	99.7
764	7-8	4.47	0.02	0.94	0.04	1.80	nd	0.01	61.5	22.70	0.21	0.20	0.03	7.50	99.4
765	8-9	6.79	0.02	0.89	0.01	1.59	0.01	0.02	60.4	21.57	0.18	0.13	0.03	7.61	99.3
766	9-10	9.98	0.02	0.83	0.02	0.84	0.02	0.03	59.8	20.02	0.11	0.07	0.04	7.95	99.7
767	10-11	12.82	0.02	0.79	0.02	0.79	0.02	0.06	58.8	18.86	0.12	0.08	0.04	8.00	100.4
768	11-12	8.54	0.02	0.84	0.03	0.85	0.02	0.05	61.7	19.93	0.12	0.08	0.04	7.88	100.1
769	12-13	9.12	0.02	0.81	0.02	1.29	0.01	0.05	61.4	19.42	0.14	0.16	0.03	7.29	99.8
MINERALOGY															
Sample	Depth	Qz	Kt	Gb	Gt & Hm	Mh	Mu	St	Ic	Vm	An	Fr			
Bou	in m														
757	0-1	100	45	40	40	70	25		10		10				
758	1-2	50	110	40	60	70	15		10		10				
759	2-3	220	210	15	50	50		60	20		10				
760	3-4	210	230		40	40		100	20		10				
761	4-5	90	240		20	20		140	20		10				
762	5-6	100	260		15	15		190	25		10	10			
763	6-7	100	240		20	20		200	20		10				
764	7-8	70	250		20			100	30		10				
765	8-9	100	260		30	30		110	25		10	15			
766	9-10	80	270		60	35		40	20		10	10			
767	10-11	80	280		65	50		60	20		10	10			
768	11-12	110	270		55	40		80	20		10				
769	12-13	90	230		50	50		85	20		10				

Qz=quartz; Kt=kaolinite; Gb=gibbsite; Gt=goethite; Hm=hematite; Mh=maghemite; Mu=muscovite; St=smectite; Ic= interstratified clays; Vm=vermiculite; An=anatase; Fr=felspar; tr= trace; nd= not detected.

TABLE 4.34 PARAWA PLATEAU BORE HOLE ANALYSES  
Borehole RBA-15 (312 m asl) (Sited over weathered Carrickalinga Head Formation rocks)

Sample	Depth	CHEMISTRY											Ign Loss	Total	
		Fe <sub>2</sub> O <sub>3</sub>	MnO	TiO <sub>2</sub>	CaO	K <sub>2</sub> O	SO <sub>3</sub>	P <sub>2</sub> O <sub>5</sub>	SiO <sub>2</sub>	Al <sub>2</sub> O <sub>3</sub>	MgO	Na <sub>2</sub> O			ZrO
BOU	in m.														
770	0-1	10.17	0.02	0.77	0.09	1.52	0.06	0.03	48.1	24.8	1.03	0.14	0.02	12.86	99.6
771	1-2	5.60	0.02	0.82	0.19	2.50	0.03	0.01	57.7	21.56	0.98	0.55	0.03	9.39	99.4
772	2-3	6.54	0.05	0.84	0.08	2.72	nd	0.01	63.7	16.93	1.71	0.24	0.04	6.30	99.2
773	3-4	7.44	0.05	0.82	0.23	2.54	0.03	0.02	62.8	17.19	1.39	0.46	0.04	6.56	99.6
774	4-5	5.76	0.05	0.79	0.28	2.34	0.01	0.03	63.7	17.37	1.47	0.32	0.03	6.79	99.4
775	5-6	5.50	0.05	0.86	0.14	2.20	0.01	0.04	63.4	18.03	1.75	0.45	0.04	6.77	99.2
776	6-7	5.40	0.05	0.79	0.09	2.05	0.01	0.05	65.3	17.32	1.59	0.41	0.04	6.58	99.7
777	7-8	5.56	0.06	0.76	0.09	1.90	0.01	0.05	66.3	16.46	1.74	0.25	0.04	6.36	99.6
778	8-9	4.74	0.05	0.79	0.14	1.98	nd	0.03	67.0	16.39	1.70	0.27	0.03	6.35	99.5
779	9-10	6.21	0.06	0.82	0.14	3.41	0.01	0.06	62.9	17.66	2.21	0.41	0.03	5.50	99.4
780	10-11	6.32	0.05	0.81	0.14	3.42	0.02	0.06	63.7	17.17	2.31	0.87	0.03	5.06	100.0
781	11-12	5.86	0.06	0.79	0.19	2.94	0.01	0.05	65.0	16.65	2.10	0.84	0.03	5.41	99.9
782	12-13	6.04	0.06	0.81	0.18	3.36	0.01	0.04	62.7	17.77	2.28	0.75	0.03	5.38	99.4
Sample	Depth	MINERALOGY											Fr	Total	
		Qz	Kt	Gb	Gt	& Hm	Mh	Mu	St	Ic	Vm	An			
BOU	in m														
770	0-1	150	100	15	25	30		55	15	15		10	10		
771	1-2	150	210					250	10	20		10	25		
772	2-3	170	150		10			150	35	20		10	20		
773	3-4	150	250		25			210	35	20		10	30		
774	4-5	200	140					130	30	20		10	50		
775	5-6	90	200		10			170	15	5		10	50		
776	6-7	200	160		5			140	35	10		10	40		
777	7-8	250	170		5			170	40	10		10	40		
778	8-9	200	210		10			190	35	10		10	10		
779	9-10	190	200		10			180	30	10		10	10		
780	10-11	200	170		10			200	45	10		10	50		
781	11-12	170	200		15			200	40	10		10	60		
782	12-13	90	210		20			200	40	10		10	60		

Qz=quartz; Kt=kaolinite; Gb=gibbsite; Gt=goethite; Hm=hematite; Mh=maghemite; Mu=muscovite; St=smectite; Ic= interstratified clays; Vm=vermiculite; An=anatase; Fr=felspar; tr= trace; nd= not detected.

TABLE 4.35 PARAWA PLATEAU BORE HOLE ANALYSES  
Borehole RBA-16 (323 m asl) (Sited over weathered Carrickalinga Head Formation rocks)

Sample	Depth	CHEMISTRY											Ign Loss	Total	
		Fe <sub>2</sub> O <sub>3</sub>	MnO	TiO <sub>2</sub>	CaO	K <sub>2</sub> O	SO <sub>3</sub>	P <sub>2</sub> O <sub>5</sub>	SiO <sub>2</sub>	Al <sub>2</sub> O <sub>3</sub>	MgO	Na <sub>2</sub> O			ZrO
BOU	in m.														
783	0-1	20.91	0.01	0.79	0.19	0.62	0.04	0.03	51.6	15.45	0.27	0.09	0.04	8.99	99.0
784	1-2	11.98	0.01	0.92	0.03	1.33	0.03	0.04	58.0	18.31	0.30	0.07	0.03	7.96	99.0
785	2-3	2.96	nd	0.62	0.02	1.52	0.01	0.05	75.9	13.26	0.25	0.07	0.03	4.70	99.4
786	3-4	7.19	0.01	0.79	0.22	1.89	0.14	0.14	67.6	16.41	0.66	0.29	0.03	5.60	100.9
787	4-5	4.61	0.01	0.74	0.56	1.14	0.06	0.06	70.0	15.52	0.23	0.12	0.04	6.41	99.5
788	5-6	6.71	0.01	0.76	0.01	1.56	0.02	0.03	65.4	17.77	0.26	0.14	0.04	6.58	99.3
789	6-7	3.24	0.01	0.80	0.02	1.59	0.02	0.03	67.3	19.09	0.28	0.12	0.04	6.93	99.5
790	7-8	2.37	0.01	0.77	0.02	1.26	0.01	0.05	68.2	18.79	0.23	0.09	0.04	7.27	99.1
791	8-9	2.90	0.01	0.82	0.02	1.14	0.01	0.05	68.0	18.96	0.20	0.07	0.03	7.40	99.6
792	9-10	6.71	0.01	0.83	0.02	1.20	0.01	0.04	65.3	17.73	0.22	0.07	0.03	7.42	99.6
793	10-11	5.43	0.01	0.81	0.02	1.30	0.01	0.04	66.5	17.67	0.23	0.07	0.04	7.13	99.3
794	11-12	3.99	0.01	0.77	0.07	1.03	0.02	0.04	67.7	16.83	0.19	0.07	0.04	7.44	99.2
795	12-13	5.00	0.02	0.74	0.02	1.27	0.02	0.08	67.1	17.57	0.25	0.11	0.04	6.98	99.2
Sample	Depth	MINERALOGY											Fr	Total	
		Qz	Kt	Gb	Gt	& Hm	Mh	Mu	St	Ic	Vm	An			
Bou	in m														
783	0-1	230	110	25	70	180	25		10	10	5	5			
784	1-2	300	260	15	60	40		80	20	20			10		
785	2-3	290	140		15			55	30	20	5	10			
786	3-4	200	280		50	30		220	30	15		10			
787	4-5	230	190		20			60	35	15		10			
788	5-6	200	290		30			190	20	10		10			
789	6-7	170	290		20			130	50	10		10	15		
790	7-8	210	220		10			80	30	10		10	10		
791	8-9	240	200		20			100	30	10		10	10		
792	9-10	220	190		15			90	25	10		10	10		
793	10-11	160	230		20			130	30	20		10	10		
794	11-12	190	200		15			70	40	20		10	10		
795	12-13	150	250		20			100	30	15		10	10		

Qz=quartz; Kt=kaolinite; Gb=gibbsite; Gt=goethite; Hm=hematite; Mh=maghemite; Mu=muscovite; St=smectite; Ic= interstratified clays; Vm=vermiculite; An=anatase; Fr=felspar; tr= trace; nd= not detected.

TABLE 4.37 PARAWA PLATEAU BORE HOLE ANALYSES  
Borehole RBA-17 (328 m asl) Sited over weathered Carrickalinga Head Formation rocks)

CHEMISTRY														Ign	Total
Sample	Depth	Fe <sub>2</sub> O <sub>3</sub>	MnO	TiO <sub>2</sub>	CaO	K <sub>2</sub> O	SO <sub>3</sub>	P <sub>2</sub> O <sub>5</sub>	SiO <sub>2</sub>	Al <sub>2</sub> O <sub>3</sub>	MgO	Na <sub>2</sub> O	ZrO	Loss	
Bou	in m.														
796	0-1	21.77	0.01	0.89	0.29	0.33	0.03	0.03	42.5	21.30	0.26	0.24	0.05	12.73	100.4
797	1-2	21.36	0.01	0.88	0.03	0.39	0.02	0.02	42.9	21.20	0.20	0.08	0.04	12.34	99.5
798	2-3	11.04	0.01	0.88	0.03	0.39	0.02	0.05	58.6	18.74	0.19	0.09	0.03	8.75	99.3
799	3-4	17.34	0.02	0.91	0.02	0.79	0.02	0.07	50.3	19.47	0.16	0.12	0.03	9.51	98.8
800	4-5	9.68	0.02	0.90	0.02	1.52	0.01	0.04	59.9	19.38	0.24	0.18	0.03	7.40	99.3
801	5-6	7.37	0.02	0.85	0.02	1.13	0.01	0.03	62.1	19.18	0.19	0.13	0.03	8.00	99.1
802	6-7	5.60	0.01	0.81	0.02	0.79	0.02	0.03	64.2	19.20	0.17	0.30	0.03	8.28	99.5
803	7-8	6.11	0.01	0.85	0.02	0.88	0.01	0.03	64.5	18.37	0.18	0.09	0.04	7.73	99.1
804	8-9	6.25	0.01	0.85	0.02	1.11	0.01	0.03	65.7	17.41	0.19	0.10	0.04	7.27	99.8
805	9-10	8.02	0.02	0.86	0.02	1.36	0.02	0.05	62.5	18.38	0.21	0.15	0.03	7.53	99.2
806	10-11	7.69	0.02	0.86	0.02	1.41	0.01	0.06	63.2	18.68	0.22	0.16	0.03	7.32	99.1
808	12-13	7.13	0.02	0.85	0.02	1.49	0.02	0.07	64.3	17.92	0.22	0.34	0.03	6.78	99.2
MINERALOGY															
Sample	Depth	Qz	Kt	Gb	Gt & Hm	Mh	Mu	St	Ic	Vm	An	Fr			
Bou	in m														
796	0-1	200	60	200	140	140	25	10	10	15	10	40			
797	1-2	170	100	90	150	100		10	10	10	10	20			
798	2-3	220	200	10	100	70		60	20	10	15	10			
799	3-4	170	170		120	110		50	20	10		15	10		
800	4-5	230	230		60	50		150	15		10	10			
801	5-6	220	170		60	50		80	25	10	5	10	10		
802	6-7	220	200		20			60	25	10		10	10		
803	7-8	210	280		20			130	30	10		10	10		
804	8-9	210	160		20			70	30	10	5	10	10		
805	9-10	200	250		20			140	25	10		10	10		
806	10-11	200	140		20			80	40	10		10	10		
807	11-12	180	250		25			190	45	10		10	10		
808	12-13	180	240		30			180	30	10		10	10		

Qz=quartz; Kt=kaolinite; Gb=gibbsite; Gt=goethite; Hm=hematite; Mh=maghemite; Mu=muscovite; St=smectite; Ic= interstratified clays; Vm=vermiculite; An=anatase; Fr=felspar; tr= trace; nd= not detected.

TABLE 4.38 PARAWA PLATEAU BORE HOLE ANALYSES  
Borehole RBA-18 (318 m asl) (Sited over weathered Carrickalinga Head Formation rocks)

CHEMISTRY														Ign	Total
Sample	Depth	Fe <sub>2</sub> O <sub>3</sub>	MnO	TiO <sub>2</sub>	CaO	K <sub>2</sub> O	SO <sub>3</sub>	P <sub>2</sub> O <sub>5</sub>	SiO <sub>2</sub>	Al <sub>2</sub> O <sub>3</sub>	MgO	Na <sub>2</sub> O	ZrO	Loss	
Bou	in m.														
809	0-1	12.71	0.02	0.89	3.84	0.92	0.18	0.04	44.5	22.54	0.43	0.14	0.03	13.84	100.1
810	1-2	6.38	0.01	0.93	0.60	1.52	0.09	0.04	52.6	24.46	0.20	0.20	0.03	9.84	96.9
811	2-3	3.29	0.02	0.99	0.10	2.03	0.04	0.03	59.6	24.01	0.23	0.23	0.03	7.74	98.7
812	3-4	2.08	0.02	0.94	0.05	2.12	0.04	0.03	62.2	24.07	0.27	0.27	0.02	7.90	99.9
813	4-5	2.34	0.02	0.89	0.03	2.34	0.03	0.02	61.4	24.55	0.25	0.25	0.02	7.19	99.4
814	5-6	2.68	0.02	0.88	0.08	2.16	0.06	0.03	61.8	23.07	0.24	0.24	0.03	7.94	99.3
815	6-7	4.00	0.02	0.93	0.08	1.64	0.04	0.03	57.4	25.88	0.23	0.23	0.03	9.66	100.3
816	7-8	2.75	0.01	0.74	0.03	1.24	0.03	0.03	67.2	19.93	0.19	0.19	0.02	6.96	99.4
817	8-9	4.27	0.02	0.87	0.09	1.47	0.04	0.05	62.8	21.52	0.21	0.21	0.02	7.83	99.4
MINERALOGY															
Sample	Depth	Qz	Kt	Gb	Gt & Hm	Mh	Mu	St	Ic	Vm	An	Fr			
Bou	in m														
809	0-1	160	200	10	80	60		80	20	10		10	10		
810	1-2	100	210		25			140	25	10		10	10		
811	2-3	100	190					150	20	15		5	10		
812	3-4	100	230					190	25	5		5	10		
813	4-5	90	180					160	25	5	5	10	10		
814	5-6	150	150					140	30	5		10	10		
815	6-7	150	170		10			110	25			10	10		
816	7-8	190	110		10			60	25	10	5	5	10		
817	8-9	170	150		10			90	20	5		5	10		

Qz=quartz; Kt=kaolinite; Gb=gibbsite; Gt=goethite; Hm=hematite; Mh=maghemite; Mu=muscovite; St=smectite; Ic= interstratified clays; Vm=vermiculite; An=anatase; Fr=felspar; tr= trace; nd= not detected.

TABLE 4.39 PARAWA PLATEAU BORE HOLE ANALYSES  
Borehole RBA-19 (325 m asl) (Sited over weathered Carrickalinga Head Formation rocks)

Sample	Depth	CHEMISTRY												Ign Loss	Total
		Fe <sub>2</sub> O <sub>3</sub>	MnO	TiO <sub>2</sub>	CaO	K <sub>2</sub> O	SO <sub>3</sub>	P <sub>2</sub> O <sub>5</sub>	SiO <sub>2</sub>	Al <sub>2</sub> O <sub>3</sub>	MgO	Na <sub>2</sub> O	ZrO		
BOU	in m.														
818	0-1	12.15	0.01	0.79	0.29	0.64	0.11	0.04	60.3	18.86	0.32	0.12	0.04	5.48	99.2
819	1-2	10.86	0.01	0.97	0.17	0.26	0.08	0.03	56.1	20.43	0.28	0.08	0.04	9.86	99.2
820	2-3	5.15	nd	1.12	0.04	0.25	0.05	0.02	59.5	19.01	0.22	0.07	0.05	10.60	96.1
821	3-4	2.26	nd	1.11	0.05	0.23	0.05	0.02	69.3	18.26	0.22	0.13	0.04	9.90	101.6
822	4-5	1.43	nd	1.19	0.05	0.55	0.11	0.02	72.7	13.35	0.15	0.15	0.04	9.25	99.0
823	5-6	1.22	0.01	0.94	0.03	1.65	0.08	0.02	64.3	22.34	0.21	0.27	0.03	8.50	99.6
824	6-7	1.47	0.02	0.82	0.07	2.09	0.08	0.08	62.6	23.02	0.25	0.26	0.03	8.49	99.3
825	7-8	1.09	0.02	0.89	0.04	2.30	0.07	0.08	63.7	22.36	0.28	0.28	0.03	7.81	99.0
826	8-9	2.62	0.01	0.85	0.10	2.21	0.08	0.07	62.2	22.51	0.29	0.29	0.03	8.00	99.3
827	9-10	6.31	0.03	0.87	0.04	2.15	0.08	0.08	60.5	20.85	0.25	0.25	0.03	7.62	99.1
828	10-11	7.01	0.03	0.85	0.08	2.15	0.07	0.08	60.1	20.02	0.24	0.28	0.03	7.80	98.7
829	11-12	7.63	0.04	0.85	0.04	2.11	0.07	0.08	58.5	20.19	0.32	0.35	0.03	7.71	97.9
830	12-13	7.73	0.04	0.84	0.06	2.35	0.04	0.11	59.0	19.98	0.77	0.05	0.02	8.11	99.1

Sample	Depth	MINERALOGY											
		Qz	Kt	Gb	Gt &	Hm	Mh	Mu	St	Ic	Vm	An	Fr
Bou	in m												
818	0-1	200	70	90	70	70	10	40	20	10	5	5	20
819	1-2	150	80	30	60	40	5		20	15		5	30
820	2-3	150	110		10				20	15		5	25
821	3-4	230	120						35	20		10	30
822	4-5	200	140						40	35		10	25
823	5-6	150	220						145	25		15	20
824	6-7	200	240						190	25		10	20
825	7-8	200	200						200	20		10	10
826	8-9	170	250						220	25		10	15
827	9-10	190	200		5	10			190	20		10	10
828	10-11	160	140		15	10			170	20		10	10
829	11-12	210	150		20	10			200	20		10	10
830	12-13	150	135		20	10			200	20		10	10

Qz=quartz; Kt=kaolinite; Gb=gibbsite; Gt=goethite; Hm=hematite; Mh=maghemite; Mu=muscovite; St=smectite; Ic= interstratified clays; Vm=vermiculite; An=anatase; Fr=felspar; tr= trace; nd= not detected.

TABLE 4.40 PARAWA PLATEAU BORE HOLE ANALYSES  
Borehole RBA-20 (330 m asl) (Sited over weathered Carrickalinga Head Formation rocks, overlain by 4m of quartzose sands)

Sample	Depth	CHEMISTRY												Ign Loss	Total
		Fe <sub>2</sub> O <sub>3</sub>	MnO	TiO <sub>2</sub>	CaO	K <sub>2</sub> O	SO <sub>3</sub>	P <sub>2</sub> O <sub>5</sub>	SiO <sub>2</sub>	Al <sub>2</sub> O <sub>3</sub>	MgO	Na <sub>2</sub> O	ZrO		
Bou	in m.														
831	0-1	10.70	0.01	0.83	1.24	0.20	0.06	0.02	58.2	16.85	0.19	0.07	0.04	10.66	99.1
832	1-2	3.98	0.03	0.69	0.03	0.12	nd	0.01	78.8	10.05	0.11	0.02	0.02	5.60	99.5
833	2-3	3.56	nd	0.36	0.01	0.05	nd	0.01	87.3	4.75	0.04	nd	0.02	3.20	96.3
834	3-4	1.58	nd	0.24	0.01	0.04	nd	0.01	92.0	3.09	0.03	nd	0.01	1.96	99.0
835	4-5	0.93	nd	1.33	0.01	0.14	nd	0.01	89.5	4.99	0.41	0.01	0.05	2.34	99.7
836	5-6	2.17	0.01	1.05	0.01	1.15	nd	0.02	66.2	20.67	0.19	0.10	0.04	8.13	99.6
837	6-7	1.98	0.01	0.96	0.01	1.15	nd	0.07	67.2	20.36	0.21	0.08	0.03	7.68	99.7
838	7-8	2.88	0.01	0.93	0.01	1.57	nd	0.06	65.8	20.38	0.23	0.16	0.03	7.81	99.9
839	8-9	5.97	0.02	0.84	0.02	1.76	nd	0.09	62.7	19.96	0.37	0.16	0.03	7.57	99.5
840	9-10	6.39	0.02	0.87	0.04	1.50	0.01	0.21	63.0	18.78	0.61	0.13	0.03	7.72	99.3
841	10-11	3.99	0.03	0.88	0.07	1.28	nd	0.15	68.7	15.97	0.71	0.15	0.03	6.72	98.7
842	11-12	6.75	0.02	0.82	0.05	1.89	nd	0.18	63.8	17.59	1.01	0.11	0.03	7.22	99.8
843	12-13	6.19	0.04	0.80	0.06	2.00	nd	0.14	64.7	17.02	1.40	0.13	0.03	6.93	99.4

Sample	Depth	MINERALOGY											
		Qz	Kt	Gb	Gt &	Hm	Mh	Mu	St	Ic	Vm	An	Fr
Bou	in m												
831	0-1	150	40	70	60	30	10		20	20		10	
832	1-2	200	35	10		5			30	20	5	10	
833	2-3	230	25						30	20	5		10
834	3-4	250	30						30	20			
835	4-5	230	40						35	20		10	10
836	5-6	140	170						90	20		15	10
837	6-7	140	180						120	25		10	10
838	7-8	140	140						90	20		10	10
839	8-9	120	90			15			120	15		10	10
840	9-10	120	110			10			110	25	5	10	10
841	10-11	110	60			10			70	20		10	10
842	11-12	120	80			10			80	20		10	10
843	12-13	140	60						60	20		10	10

Qz=quartz; Kt=kaolinite; Gb=gibbsite; Gt=goethite; Hm=hematite; Mh=maghemite; Mu=muscovite; St=smectite; Ic= interstratified clays; Vm=vermiculite; nd= not detected.

TABLE 4.41 PARAWA PLATEAU BORE HOLE ANALYSES  
Borehole RBA-21 (323 m asl) ( Sited over weathered Backstairs Passage Formation rocks)

CHEMISTRY														Ign	Total
Sample	Depth	Fe <sub>2</sub> O <sub>3</sub>	MnO	TiO <sub>2</sub>	CaO	K <sub>2</sub> O	SO <sub>3</sub>	P <sub>2</sub> O <sub>5</sub>	SiO <sub>2</sub>	Al <sub>2</sub> O <sub>3</sub>	MgO	Na <sub>2</sub> O	ZrO	Loss	
BOU	in m.														
844	0-1	17.68	0.01	1.02	0.03	0.20	0.01	0.02	50.7	18.26	0.15	0.09	0.05	11.04	99.3
845	1-2	11.78	0.01	1.10	0.02	0.50	0.01	0.01	55.7	21.31	0.18	0.07	0.05	8.04	99.8
846	2-3	1.40	nd	0.90	0.01	1.05	0.01	0.01	67.3	20.51	0.20	0.05	0.05	7.75	96.3
847	3-4	1.07	0.01	0.95	0.01	1.09	0.01	0.01	68.3	20.04	0.20	0.10	0.05	7.40	99.2
848	4-5	4.25	nd	0.93	0.01	0.97	0.01	0.02	63.6	20.81	0.18	0.07	0.04	8.16	99.1
849	5-6	5.16	0.01	0.90	0.01	0.91	0.02	0.01	65.2	19.17	0.18	0.24	0.05	7.63	99.5
850	6-7	6.44	0.01	0.85	0.01	0.93	0.02	0.01	64.9	18.03	0.18	0.07	0.05	7.17	98.7
851	7-8	7.12	0.01	0.86	0.02	1.03	0.02	0.02	66.3	16.79	0.16	0.06	0.05	6.63	99.1
852	8-9	2.56	0.01	0.72	nd	1.05	nd	0.02	66.8	20.14	0.16	0.06	0.05	7.56	99.1
853	9-10	2.46	nd	0.80	0.01	1.30	0.01	0.01	67.1	19.58	0.20	0.05	0.04	6.60	99.3
854	10-11	1.73	0.01	0.81	0.01	1.50	nd	0.01	69.3	19.4	0.22	0.05	0.04	6.60	99.3
855	11-12	2.08	0.01	0.80	0.01	1.54	0.01	0.01	69.9	18.63	0.25	0.06	0.05	6.51	99.9
856	12-13	2.61	nd	0.81	0.01	1.28	0.01	0.02	69.3	18.32	0.21	0.09	0.05	6.73	99.4

MINERALOGY													
Sample	Depth	Qz	Kt	Gb	Gt &	Hm	Mh	Mu	St	Ic	Vm	An	Fr
BOU	in m												
844	0-1	120	75	170	110	80	5		25	20		15	20
845	1-2	180	80	190	110	90		10	20	20	10	15	20
846	2-3	250	220	55				25	15	20		10	15
847	3-4	170	280	10				45	20	20		10	10
848	4-5	230	270		20			50	25	20		10	10
849	5-6	250	250		20			50	25	20		10	10
850	6-7	230	240		30			50	25	20		10	10
851	7-8	250	260					80	20	15		10	10
852	8-9	230	210		10			60	20	15		10	10
853	9-10	220	250		5			90	25	25		10	10
854	10-11	200	250		5			110	30	25		10	10
855	11-12	230	250		5			130	35	25		10	10
856	12-13	260	250					140	35	30		10	10

Qz=quartz; Kt=kaolinite; Gb=gibbsite; Gt=goethite; Hm=hematite; Mh=maghemite;  
Mu=muscovite; St=smectite; Ic= interstratified clays; Vm=vermiculite; An=anatase; Fr=felspar;  
tr= trace; nd= not detected.

TABLE 4.42 PARAWA PLATEAU BORE HOLE ANALYSES  
Borehole RBA-22 (280 m asl) (Sited over weathered Backstairs Passage Formation rocks)

CHEMISTRY														Ign	Total
Sample	Depth	Fe <sub>2</sub> O <sub>3</sub>	MnO	TiO <sub>2</sub>	CaO	K <sub>2</sub> O	SO <sub>3</sub>	P <sub>2</sub> O <sub>5</sub>	SiO <sub>2</sub>	Al <sub>2</sub> O <sub>3</sub>	MgO	Na <sub>2</sub> O	ZrO	Loss	
Bou	in m.														
857	0-1	7.11	0.03	0.77	1.92	0.67	0.14	0.04	60.1	13.81	0.35	0.17	0.03	14.21	99.4
858	1-2	8.80	0.02	0.92	0.21	0.95	0.05	0.03	62.1	17.23	0.39	0.18	0.04	9.47	100.4
859	2-3	9.59	0.01	0.83	0.09	0.81	0.06	0.03	56.4	19.84	0.35	0.27	0.03	10.74	99.1
860	3-4	8.56	0.02	0.83	0.07	1.17	0.05	0.04	58.4	20.49	0.29	0.18	0.03	9.38	99.5
861	4-5	10.2	0.03	0.85	0.10	1.85	0.05	0.12	58.3	19.57	0.53	0.26	0.03	8.28	100.2
862	5-6	9.31	0.03	0.77	0.07	2.08	0.11	0.19	57.6	18.36	0.61	0.34	0.02	7.58	97.1
863	6-7	7.51	0.04	0.81	0.04	2.00	0.03	0.18	60.2	20.31	0.74	0.21	0.03	7.73	99.8
864	7-8	7.33	0.05	0.82	0.08	2.24	0.02	0.20	57.8	19.96	1.25	0.24	0.02	7.95	98.0
865	8-9	7.78	0.05	0.83	0.07	2.39	0.04	0.18	58.6	20.36	1.19	0.28	0.02	7.72	99.5
866	9-10	7.50	0.05	0.79	0.07	2.38	0.03	0.19	58.2	20.62	1.11	0.26	0.02	7.87	99.5
867	10-11	8.07	0.06	0.82	0.07	2.63	0.05	0.27	59.5	19.27	1.40	0.31	0.02	7.19	99.7
868	11-12	7.60	0.06	0.83	0.07	2.95	0.03	0.22	59.4	19.65	1.47	0.33	0.02	6.94	99.6
869	12-13	7.85	0.06	0.86	0.08	2.63	0.04	0.20	58.9	19.18	1.47	0.28	0.02	7.23	98.8

MINERALOGY													
Sample	Depth	Qz	Kt	Gb	Gt &	Hm	Mh	Mu	St	Ic	Vm	An	Fr
Bou	in m												
857	0-1	150	60	5	40	20	tr	30	20	20		10	10
858	1-2	120	70		30	30		30	20	20	5	10	20
859	2-3	130	80		40	30		20	40	20	5	10	20
860	3-4	160	140		40	40		80	20	10		10	5
861	4-5	220	120		70	40		110	20	20		10	5
862	5-6	140	160		60	40		170	25	20		10	20
863	6-7	210	190		60	40		150	25	10		10	15
864	7-8	160	140					140	20	40		10	5
865	8-9	160	160		10			150	20	60		10	10
866	9-10	160	160		10			150	20	60		10	10
867	10-11	210	120		15			170	30	100		10	15
868	11-12	140	110		10			180	35	70		10	5
869	12-13	210	150		10			160	20	60		10	5

Qz=quartz; Kt=kaolinite; Gb=gibbsite; Gt=goethite; Hm=hematite; Mh=maghemite; Mu=muscovite;  
St=smectite; Ic= interstratified clays; Vm=vermiculite; An=anatase; Fr=felspar;  
tr= trace; nd= not detected.

TABLE 4.43 PARAWA PLATEAU BORE HOLE ANALYSES  
Borehole RBA-23 (300 m asl) (Sited over weathered Carrickalinga Head Formation rocks)

CHEMISTRY														Ign	Total
Sample	Depth	Fe <sub>2</sub> O <sub>3</sub>	MnO	TiO <sub>2</sub>	CaO	K <sub>2</sub> O	SO <sub>3</sub>	P <sub>2</sub> O <sub>5</sub>	SiO <sub>2</sub>	Al <sub>2</sub> O <sub>3</sub>	MgO	Na <sub>2</sub> O	ZrO	Loss	
Bou	in m.														
870	0-1	8.50	0.03	0.80	1.74	0.95	0.10	0.02	54.5	20.48	0.32	0.17	0.03	11.89	99.5
871	1-2	7.71	0.03	0.85	0.19	1.63	0.03	0.02	58.9	20.33	0.36	0.21	0.03	9.46	99.8
872	2-3	7.23	0.04	0.85	0.13	1.79	0.02	0.03	61.2	18.90	0.73	0.35	0.03	8.25	99.6
873	3-4	7.02	0.04	0.84	0.03	2.00	0.01	0.04	61.7	18.38	1.06	0.23	0.03	8.25	99.6
874	4-5	6.80	0.05	0.84	0.02	2.41	0.01	0.05	63.0	17.81	1.23	0.17	0.03	7.11	99.5
875	5-6	6.63	0.05	0.85	0.04	2.77	nd	0.05	63.0	18.14	1.54	0.20	0.03	6.00	99.3
876	6-7	6.66	0.05	0.83	0.01	2.79	0.01	0.05	61.9	17.91	1.57	0.18	0.03	7.62	99.6
877	7-8	6.52	0.05	0.85	0.02	2.83	0.01	0.06	62.2	18.17	1.57	0.27	0.03	7.01	99.6
878	8-9	6.59	0.05	0.83	0.03	2.97	nd	0.06	62.4	17.66	1.61	0.26	0.03	7.10	99.6
879	9-10	6.49	0.06	0.83	0.03	2.95	0.01	0.07	62.3	17.95	1.88	0.23	0.03	6.80	99.6
880	10-11	6.42	0.06	0.85	0.03	2.82	0.01	0.06	63.8	17.99	1.88	0.20	0.03	6.00	100.2
881	11-12	6.66	0.06	0.83	0.04	3.04	nd	0.07	62.3	17.92	1.96	0.21	0.03	6.52	99.6
882	12-13	6.62	0.06	0.84	0.04	3.31	0.01	0.07	62.0	17.88	2.05	0.25	0.03	6.58	99.7

MINERALOGY														
Sample	Depth	Qz	Kt	Gb	Gt & Hm	Mh	Mu	St	Ic	Vm	An	Fr		
Bou	in m													
870	0-1	180	220	5	15		80	20	10		10	10		
871	1-2	220	200		10		130	25			10	5		
872	2-3	170	230		10		120	30	15		10	5		
873	3-4	220	180		5		90	20	10		10	10		
874	4-5	170	160				140	30	15		10	15		
875	5-6	230	170		5		190	25			10	10		
876	6-7	160	130		5		130	25			10	15		
877	7-8	220	140				160	25			10	15		
878	8-9	190	140		5		180	20	5		10	10		
879	9-10	220	120				160	30			10	10		
880	10-11	120	170		5		200	30			10	10		
881	11-12	120	160		5		230	20	10		10	10		
882	12-13	120	140		5		260	20			10	10		

Qz=quartz; Kt=kaolinite; Gb=gibbsite; Gt=goethite; Hm=hematite; Mh=maghemite; Mu=muscovite; St=smectite; Ic= interstratified clays; Vm=vermiculite; An=anatase; Fr=felspar; tr= trace; nd= not detected.

TABLE 4.44 PARAWA PLATEAU BORE HOLE ANALYSES  
Borehole RBA-24 (325 m asl) (Sited over weathered Carrickalinga Head Formation rocks)

CHEMISTRY														Ign	Total
Sample	Depth	Fe <sub>2</sub> O <sub>3</sub>	MnO	TiO <sub>2</sub>	CaO	K <sub>2</sub> O	SO <sub>3</sub>	P <sub>2</sub> O <sub>5</sub>	SiO <sub>2</sub>	Al <sub>2</sub> O <sub>3</sub>	MgO	Na <sub>2</sub> O	ZrO	Loss	
Bou	in m.														
883	0-1	24.69	0.01	0.86	0.11	0.46	0.03	0.03	38.0	21.53	0.27	0.19	0.05	13.24	99.5
884	1-2	6.85	nd	0.90	0.02	0.81	0.01	0.01	56.6	22.69	0.23	0.07	0.05	11.41	99.7
885	2-3	2.88	nd	0.91	0.01	1.08	nd	0.01	64.0	21.52	0.21	0.06	0.05	8.79	99.5
886	3-4	3.77	0.01	0.90	0.01	1.04	0.01	0.01	62.0	21.79	0.20	0.04	0.04	9.40	99.2
887	4-5	3.58	0.01	0.86	0.01	1.20	0.01	0.01	63.0	21.84	0.20	0.07	0.03	8.64	99.5
888	5-6	3.39	nd	0.79	0.01	1.41	0.01	0.01	64.2	21.08	0.25	0.05	0.03	8.31	99.5
889	6-7	3.05	0.01	0.76	0.01	1.57	0.01	0.01	65.7	19.93	0.27	0.06	0.03	7.75	99.2
890	7-8	3.23	nd	0.72	0.02	1.34	0.01	0.01	66.4	19.50	0.23	0.07	0.03	7.76	99.3
891	8-9	1.68	nd	0.78	0.01	0.81	0.01	0.01	65.8	20.95	0.17	0.07	0.03	8.75	99.1
892	9-10	1.66	0.01	0.63	0.01	0.91	0.01	0.01	69.2	18.91	0.18	0.13	0.03	7.06	99.0
893	10-11	2.07	0.01	0.55	0.01	0.80	nd	0.01	70.3	19.91	0.16	0.13	0.03	7.06	99.0
894	11-12	3.19	0.01	0.57	0.01	1.04	0.02	0.01	69.8	17.73	0.20	0.11	0.03	6.71	99.4
895	12-13	4.02	0.01	0.62	0.01	1.22	nd	0.02	67.9	18.26	0.22	0.08	0.03	6.99	99.4

MINERALOGY														
Sample	Depth	Qz	Kt	Gb	Gt & Hm	Mh	Mu	St	Ic	Vm	An	Fr		
Bou	in m													
883	0-1	170	70	160	120	130	25	20	10	15	10	15		
884	1-2	110	220	50	15		35	20	10	5	10	10		
885	2-3	180	250		15		50	15	10	5	10	15		
886	3-4	160	260		15		50	15			10	10		
887	4-5	130	260		20		80	25	15		10	15		
888	5-6	130	260		15		100	30			10	15		
889	6-7	150	250		15		130	30	20		10	15		
890	7-8	240	240		10		100	30	10		10	15		
891	8-9	240	250		10		40	15	10		10	20		
892	9-10	240	260		5		80	15			10	15		
893	10-11	190	260		5		60	35	20		10	15		
894	11-12	240	250		15		100	20	5		10	15		
895	12-13	220	260		5		110	25			10	15		

Qz=quartz; Kt=kaolinite; Gb=gibbsite; Gt=goethite; Hm=hematite; Mh=maghemite; Mu=muscovite; St=smectite; Ic= interstratified clays; Vm=vermiculite; An=anatase; Fr=felspar; tr= trace;

TABLE 4.45 PARAWA PLATEAU BORE HOLE ANALYSES  
Borehole RBA-25 (329 m asl) (Sited over weathered Carrickalinga Head Formation rocks)

CHEMISTRY														Ign Loss	Total
Sample	Depth	Fe <sub>2</sub> O <sub>3</sub>	MnO	TiO <sub>2</sub>	CaO	K <sub>2</sub> O	SO <sub>3</sub>	P <sub>2</sub> O <sub>5</sub>	SiO <sub>2</sub>	Al <sub>2</sub> O <sub>3</sub>	MgO	Na <sub>2</sub> O	ZrO		
BOU	in m.														
896	0-1	13.42	0.01	0.94	0.07	0.30	0.02	0.02	45.6	24.21	0.26	0.13	0.04	14.28	99.3
897	1-2	7.46	nd	0.95	0.02	0.22	0.01	0.01	61.6	18.43	0.22	0.03	0.04	10.34	99.3
898	2-3	2.46	nd	1.18	0.01	0.24	0.02	0.01	72.7	15.76	0.10	0.05	0.06	7.23	99.8
899	3-4	2.31	nd	0.86	0.01	0.28	0.02	0.01	65.7	21.44	0.09	0.05	0.06	8.98	99.8
900	4-5	1.33	nd	0.94	0.02	0.35	0.01	0.02	69.3	19.51	0.09	0.03	0.08	8.16	99.8
901	5-6	0.53	nd	1.02	0.01	0.47	nd	0.02	70.2	19.67	0.11	0.08	0.15	7.71	100.0
902	6-7	2.82	nd	0.98	0.01	0.54	nd	0.02	68.7	18.85	0.13	0.04	0.09	7.76	99.9
903	7-8	7.49	0.01	0.95	0.01	0.67	0.01	0.03	64.2	18.23	0.13	0.05	0.09	7.70	99.6
904	8-9	8.15	nd	0.93	0.01	0.71	0.01	0.03	63.1	18.37	0.14	0.05	0.08	7.87	99.5
905	9-10	5.36	0.01	0.96	0.01	0.82	0.01	0.02	65.4	18.63	0.24	0.07	0.09	7.83	99.5
906	10-11	5.42	0.01	0.95	0.01	0.99	0.01	0.02	66.1	17.88	0.43	0.08	0.09	7.13	99.1
907	11-12	4.43	0.01	0.91	0.01	1.30	0.01	0.02	68.3	16.85	0.63	0.08	0.10	6.78	99.4
908	12-13	5.18	0.02	0.92	0.02	1.57	0.01	0.03	66.8	17.04	0.87	0.09	0.08	7.09	99.7
MINERALOGY															
Sample	Depth	Qz	Kt	Gb	Gt &	Hm	Mh	Mu	St	Ic	Vm	An	Fr		
Bou	in m														
896	0-1	170	75	210	70	70	10		15			10	20		
897	1-2	180	80	75		15			20			10	15		
898	2-3	230	200					10	30	5		10	15		
899	3-4	170	230					10	30	10		10	10		
900	4-5	130	250					15	30	15		10	10		
901	5-6	260	260					20	20	15		10			
902	6-7	200	260					30	25	10		10	5		
903	7-8	220	250		tr	40		40	25				10		
904	8-9	230	260			20		45	20	10		10	5		
905	9-10	160	220			10		40	30	10		10	5		
906	10-11	230	250			10		80	30	10		10	10		
907	11-12	200	220			5		65	25	15		10	5		
908	12-13	190	230			5		110	30			10	10		

Qz=quartz; Kt=kaolinite; Gb=gibbsite; Gt=goethite; Hm=hematite; Mh=maghemite; Mu=muscovite; St=smectite; Ic= interstratified clays; Vm=vermiculite; An=anatase; Fr=felspar; tr= trace; nd= not detected.

TABLE 4.46 PARAWA PLATEAU BORE HOLE ANALYSES  
Borehole RBA-26 (342 m asl) (Sited over weathered Carrickalinga Head Formation rocks)

CHEMISTRY														Ign Loss	Total
Sample	Depth	Fe <sub>2</sub> O <sub>3</sub>	MnO	TiO <sub>2</sub>	CaO	K <sub>2</sub> O	SO <sub>3</sub>	P <sub>2</sub> O <sub>5</sub>	SiO <sub>2</sub>	Al <sub>2</sub> O <sub>3</sub>	MgO	Na <sub>2</sub> O	ZrO		
BOU	in m.														
909	0-1	14.02	0.01	1.03	0.08	0.89	0.02	0.03	46.6	23.34	0.31	0.10	0.04	12.92	99.4
910	1-2	8.75	0.02	1.09	0.03	1.48	0.02	0.03	52.9	24.13	0.35	0.09	0.04	10.81	99.7
911	2-3	5.78	0.02	1.00	0.03	1.59	0.01	0.02	59.5	20.89	0.30	0.18	0.04	10.44	99.5
912	3-4	9.30	0.02	0.96	0.02	1.72	0.01	0.02	59.1	19.42	0.32	0.08	0.04	8.31	99.3
913	4-5	3.26	0.01	0.82	0.02	1.40	0.02	0.05	65.7	19.67	0.25	0.01	0.06	8.09	99.4
914	5-6	3.07	0.01	0.65	0.02	1.46	0.01	0.06	67.7	18.78	0.27	0.07	0.15	7.37	99.5
915	6-7	4.89	0.01	0.88	0.02	1.15	0.02	0.06	67.3	17.07	0.22	0.08	0.01	7.26	99.1
916	7-8	6.58	0.01	0.76	0.01	1.19	0.01	0.03	67.1	16.32	0.23	0.05	0.08	7.11	99.5
917	8-9	6.80	0.01	0.71	0.02	1.62	0.01	0.02	64.5	16.84	0.25	0.06	0.03	8.52	99.4
918	9-10	7.22	0.01	0.74	0.01	1.84	0.02	0.03	64.4	17.21	0.30	0.10	0.03	7.32	99.2
919	10-11	7.80	0.01	0.79	0.02	1.60	0.01	0.04	64.3	16.76	0.27	0.08	0.05	7.41	99.1
920	11-12	6.73	0.01	0.57	0.01	1.23	0.01	0.02	67.4	15.26	0.22	0.14	0.04	7.53	99.2
921	12-13	6.43	0.02	0.84	0.01	1.75	0.01	0.03	65.9	17.04	0.32	0.06	0.05	6.70	99.2
MINERALOGY															
Sample	Depth	Qz	Kt	Gb	Gt &	Hm	Mh	Mu	St	Ic	Vm	An	Fr		
Bou	in m														
909	0-1	120	150	65	110	80	5	25	20	15		15	20		
910	1-2	150	220	20		30		80	10	10		10	20		
911	2-3	140	200			20		80	20			10	20		
912	3-4	170	170			40		110	10			10	20		
913	4-5	250	250			10		120	20	10		10	20		
914	5-6	250	260			10		120	20			10	30		
915	6-7	230	200					80	25	10		10	20		
916	7-8	230	170			20		60	20	10		10	20		
917	8-9	240	150			20		90	35	10		10	10		
918	9-10	210	180			25		130	25	10		10	10		
919	10-11	220	140			25		100	40	20		10	15		
920	11-12	250	180			25		90	30	10		10	5		
921	12-13	200	160			15		100	25	20		10	60		

Qz=quartz; Kt=kaolinite; Gb=gibbsite; Gt=goethite; Hm=hematite; Mh=maghemite; Mu=muscovite; St=smectite; Ic= interstratified clays; Vm=vermiculite; An=anatase; Fr=felspar; tr= trace; nd= not detected.



TABLE 4.47 PARAWA PLATEAU BORE HOLE ANALYSES  
Borehole RBA-27 (322 m asl) (Sited over weathered Backstairs Passage Formation rocks)

CHEMISTRY														Ign	Total
Sample	Depth	Fe <sub>2</sub> O <sub>3</sub>	MnO	TiO <sub>2</sub>	CaO	K <sub>2</sub> O	SO <sub>3</sub>	P <sub>2</sub> O <sub>5</sub>	SiO <sub>2</sub>	Al <sub>2</sub> O <sub>3</sub>	MgO	Na <sub>2</sub> O	ZrO	Loss	
Bou	in m.														
922	0-1	9.69	0.01	0.73	1.06	0.97	0.13	0.05	52.5	20.88	0.36	0.11	0.03	12.89	99.4
923	1-2	4.12	0.01	0.86	0.07	1.29	0.03	0.03	62.0	21.36	0.26	0.13	0.03	9.05	99.2
924	2-3	2.16	0.01	0.89	0.11	2.22	0.02	0.07	61.1	23.95	0.31	0.25	0.02	8.62	99.7
925	3-4	2.36	0.01	0.85	0.05	2.57	0.02	0.05	65.1	20.34	0.34	0.16	0.02	6.95	98.8
926	4-5	1.98	0.01	1.04	0.10	2.49	0.01	0.11	57.0	26.26	0.36	0.22	0.03	9.15	98.8
927	5-6	3.66	0.02	0.76	0.08	2.14	0.02	0.11	67.5	17.62	0.53	0.14	0.03	6.24	98.9
928	6-7	6.28	0.03	0.76	0.05	2.43	0.02	0.14	64.6	16.99	1.14	0.39	0.04	6.56	99.4
929	7-8	5.18	0.03	0.89	0.04	1.81	0.02	0.12	67.0	16.58	0.95	0.26	0.07	6.65	99.6
930	8-9	5.55	0.03	0.85	0.04	1.76	0.01	0.14	67.0	16.25	0.83	0.11	0.06	6.64	99.3
931	9-10	5.71	0.02	0.87	0.06	1.82	0.01	0.15	69.2	17.01	0.86	0.11	0.06	3.31	99.2
MINERALOGY															
Sample	Depth	Qz	Kt	Gb	Gt	& Hm	Mh	Mu	St	Ic	Vm	An	Fr		
Bou	in m														
922	0-1	170	130		15		5	25	20	20		10	15		
923	1-2	140	230		15			100	25	10		10	10		
924	2-3	140	270					170	20	10		10	5		
925	3-4	230	150					160	25	10		10	10		
926	4-5	100	300					180	30	10		10	5		
927	5-6	140	220					190	30	10		10	10		
928	6-7	180	140		10			150	20	10		10	5		
929	7-8	190	190		10			120	25	10		10	10		
930	8-9	150	210		10			160	25	15		10	5		
931	9-10	230	160		5			130	30	10		10	10		

Qz=quartz; Kt=kaolinite; Gb=gibbsite; Gt=goethite; Hm=hematite; Mh=maghemite; Mu=muscovite; St=smectite; Ic= interstratified clays; Vm=vermiculite; An=anatase; Fr=felspar; tr= trace; nd= not detected.

TABLE 4.47 PARAWA PLATEAU BORE HOLE ANALYSES  
Borehole RBA-28 (332 m asl) (Sited over weathered Backstairs Passage Formation rocks)

CHEMISTRY														Ign	Total
Sample	Depth	Fe <sub>2</sub> O <sub>3</sub>	MnO	TiO <sub>2</sub>	CaO	K <sub>2</sub> O	SO <sub>3</sub>	P <sub>2</sub> O <sub>5</sub>	SiO <sub>2</sub>	Al <sub>2</sub> O <sub>3</sub>	MgO	Na <sub>2</sub> O	ZrO	Loss	
Bou	in m.														
932	0-1	17.97	0.01	0.85	0.91	0.23	0.05	0.03	45.6	19.53	0.26	0.09	0.05	13.61	99.3
933	1-2	16.57	0.01	0.90	0.10	0.26	0.02	0.02	46.8	21.36	0.25	0.04	0.05	12.85	99.2
934	2-3	9.81	0.01	0.84	0.14	0.34	0.02	0.02	66.7	15.35	0.18	0.02	0.07	6.03	99.5
935	3-4	5.90	0.01	0.97	0.07	0.49	0.02	0.06	65.2	18.00	0.23	0.05	0.08	8.30	99.4
936	4-5	4.21	0.01	0.93	0.09	0.68	0.02	0.08	69.3	16.17	0.21	0.05	0.09	7.37	99.2
937	5-6	3.55	0.01	0.93	0.03	0.88	0.01	0.07	69.9	16.54	0.23	0.07	0.09	6.96	99.3
938	6-7	3.12	0.01	0.95	0.04	0.87	0.01	0.08	70.5	16.29	0.22	0.13	0.09	6.78	99.1
939	7-8	4.51	0.01	0.93	0.03	0.92	0.01	0.08	69.8	16.21	0.19	0.06	0.09	6.56	99.4
940	8-9	4.80	0.01	0.95	0.03	0.83	nd	0.13	68.4	16.78	0.22	0.02	0.09	7.19	99.5
941	9-10	5.21	0.01	0.90	0.03	0.86	0.02	0.08	68.1	16.67	0.22	0.05	0.09	6.94	99.9
942	10-11	5.14	0.01	0.88	0.05	0.82	0.01	0.16	68.2	16.64	0.22	0.05	0.09	7.01	99.7
943	11-12	4.97	0.01	0.87	0.03	0.91	0.03	0.17	68.4	16.74	0.21	0.05	0.09	6.72	99.2
MINERALOGY															
Sample	Depth	Qz	Kt	Gb	Gt	& Hm	Mh	Mu	St	Ic	Vm	An	Fr		
Bou	in m														
932	0-1	200	40	140	110	80	10	15		10		10	20		
933	1-2	200	90	120	160	80		20	10	10		10	10		
934	2-3	240	150	5	100	40		10	30	15		10	10		
935	3-4	220	170			15		10	15	10		10	10		
936	4-5	250	180			10		30	35	15		10	15		
937	5-6	240	170			10		40	25	15		10	10		
938	6-7	260	160			15		50	30	15		10	10		
939	7-8	230	190			12		70	25	10		10	15		
940	8-9	260	190			15		60	20			10	10		
941	9-10	250	200			20		60	30	20		10	5		
942	10-11	210	160			25		50	30	25		10	5		
943	11-12	180	200			25		80	30	20		10	5		

Qz=quartz; Kt=kaolinite; Gb=gibbsite; Gt=goethite; Hm=hematite; Mh=maghemite; Mu=muscovite; St=smectite; Ic= interstratified clays; Vm=vermiculite; An=anatase; Fr=felspar; tr= trace; nd= not detected.

TABLE 4.48 PARAWA PLATEAU BORE HOLE ANALYSES  
Borehole RBA-29 (330 m asl)(Sited over weathered Backstairs Passage Formation rocks)

CHEMISTRY														Ign	Total
Sample	Depth	Fe <sub>2</sub> O <sub>3</sub>	MnO	TiO <sub>2</sub>	CaO	K <sub>2</sub> O	SO <sub>3</sub>	P <sub>2</sub> O <sub>5</sub>	SiO <sub>2</sub>	Al <sub>2</sub> O <sub>3</sub>	MgO	Na <sub>2</sub> O	ZrO	Loss	
BOU	in m.														
944	0-1	33.07	0.01	0.76	0.19	0.46	0.05	0.03	41.0	15.66	0.14	0.13	0.05	8.68	100.2
945	1-2	27.46	0.01	0.90	0.04	0.84	0.04	0.02	41.9	18.31	0.16	0.06	0.04	9.62	99.4
946	2-3	11.02	0.01	1.06	0.02	1.28	0.02	0.02	62.0	17.10	0.21	0.08	0.05	7.07	99.9
947	3-4	10.06	nd	0.97	0.02	1.40	nd	0.02	64.1	16.13	0.24	0.07	0.05	6.53	99.6
948	4-5	7.11	0.01	0.95	0.01	1.57	nd	0.01	66.0	17.38	0.29	0.06	0.04	6.33	99.8
949	5-6	5.70	0.01	0.90	0.02	1.80	nd	0.02	65.8	18.64	0.27	0.07	0.05	6.28	99.6
950	6-7	7.15	0.01	0.87	0.02	1.73	0.01	0.01	66.0	16.94	0.26	0.06	0.05	6.57	99.7
951	7-8	5.59	0.01	0.86	0.01	1.45	nd	0.02	65.4	18.67	0.22	0.05	0.04	7.03	99.4
952	8-9	7.98	0.01	0.85	0.02	1.22	nd	0.02	63.6	18.07	0.18	0.07	0.04	7.35	99.4
953	9-10	10.08	0.01	0.85	0.06	1.16	0.03	0.03	62.5	17.74	0.18	0.05	0.04	7.25	100.0
954	10-11	7.98	nd	0.82	0.01	1.51	nd	0.04	63.7	18.19	0.23	0.04	0.04	7.03	99.6
955	11-12	7.61	0.01	0.84	0.02	1.70	nd	0.05	63.7	18.47	0.23	0.06	0.05	6.75	99.5
956	12-13	8.02	nd	0.84	0.05	1.59	0.03	0.06	63.9	17.80	0.22	0.05	0.05	6.72	99.3
MINERALOGY															
Sample	Depth	Qz	Kt	Gb	Gt &	Hm	Mh	Mu	St	Ic	Vm	An	Fr		
Bou	in m														
944	0-1	90	30	50	70	100	25				15	5	15		
945	1-2	80	75	30	70	80		40	10	10		5	20		
946	2-3	100	160		50	40		50	20	10		5	15		
947	3-4	200	200		40	30		50	20	10		10	15		
948	4-5	150	200		30	20		70	15		10	10	10		
949	5-6	240	140			20		70	25	15		10	5		
950	6-7	150	210			15		170	20	10		10	5		
951	7-8	180	140			20		100	25	10		10	15		
952	8-9	100	120			20		60	15	10		10	5		
953	9-10	120	220			30		70	15	15		10	15		
954	10-11	100	120			20		70	20	10		10	15		
955	11-12	150	200			20		110	25	10		10	5		
956	12-13	120	190			20		90	20	15			5		

Qz=quartz; Kt=kaolinite; Gb=gibbsite; Gt=goethite; Hm=hematite; Mh=maghemite; Mu=muscovite; St=smectite; Ic= interstratified clays; Vm=vermiculite; An=anatase; Fr=felspar; tr= trace; nd= not detected.

TABLE 4.50 PARAWA PLATEAU BORE HOLE ANALYSES  
Borehole RBA-30 (332 m asl) (Sited over weathered Backstairs Passage Formation rocks)

CHEMISTRY														Ign	Total
Sample	Depth	Fe <sub>2</sub> O <sub>3</sub>	MnO	TiO <sub>2</sub>	CaO	K <sub>2</sub> O	SO <sub>3</sub>	P <sub>2</sub> O <sub>5</sub>	SiO <sub>2</sub>	Al <sub>2</sub> O <sub>3</sub>	MgO	Na <sub>2</sub> O	ZrO	Loss	
Bou	in m.														
957	0-1	10.90	0.01	0.79	1.54	0.75	0.10	0.06	54.5	18.70	0.23	0.11	0.04	12.15	99.9
958	1-2	9.60	0.02	0.76	0.05	1.71	0.01	0.04	58.0	19.61	0.25	0.23	0.02	8.82	99.1
959	2-3	9.56	0.02	0.85	0.07	1.62	0.02	0.04	59.3	19.02	0.24	0.16	0.03	8.33	99.3
960	3-4	7.54	0.02	0.86	0.04	1.28	0.01	0.04	61.2	19.39	0.21	0.19	0.02	8.52	99.3
961	4-5	8.49	0.02	0.85	0.11	1.86	0.02	0.06	59.0	20.00	0.44	0.17	0.02	8.30	99.3
962	5-6	8.34	0.03	0.83	0.02	2.89	nd	0.04	58.5	20.26	0.80	0.27	0.02	7.25	99.3
963	6-7	8.01	0.04	0.86	0.02	2.29	0.01	0.05	58.1	20.80	0.88	0.22	0.02	7.98	99.3
964	7-8	7.55	0.05	0.85	0.22	2.40	0.02	0.05	59.5	19.98	1.05	0.23	0.03	7.58	99.5
965	8-9	7.40	0.06	0.85	0.03	3.23	0.01	0.06	59.8	19.44	1.66	0.22	0.03	6.64	99.4
966	9-10	7.09	0.06	0.81	0.03	3.25	0.01	0.07	61.4	18.40	1.84	0.20	0.03	6.22	99.4
967	10-11	6.26	0.06	0.78	0.03	2.52	0.01	0.06	65.2	16.32	1.88	0.09	0.04	5.97	99.2
968	11-12	6.18	0.07	0.78	0.03	2.67	nd	0.06	66.0	15.58	1.96	0.11	0.03	5.47	98.9
969	12-13	6.68	0.07	0.82	0.04	3.42	0.01	0.06	61.8	17.81	2.22	0.16	0.03	5.91	99.0
MINERALOGY															
Sample	Depth	Qz	Kt	Gb	Gt &	Hm	Mh	Mu	St	Ic	Vm	An	Fr		
Bou	in m														
957	0-1	150	90	5	40	40		50	20	10		10	15		
958	1-2	130	90		80	40		130	25	10		10	5		
959	2-3	200	90			20		130	20			10	10		
960	3-4	190	110			20		90	20	10		10	5		
961	4-5	150	130			15		150	20			10	10		
962	5-6	100	120			15		180	20			10	5		
963	6-7	150	220			5		190	25	10		10	5		
964	7-8	150	180			5		200	20	10		10	15		
965	8-9	200	160			5		190	20	10		10	10		
966	9-10	160	150			5		190	25	10		10	5		
967	10-11	140	160					130	20	10		10	5		
968	11-12	200	170					170	25	10		10	10		
969	12-13	190	160					200	25	10			5		

Qz=quartz; Kt=kaolinite; Gb=gibbsite; Gt=goethite; Hm=hematite; Mh=maghemite; Mu=muscovite; St=smectite; Ic= interstratified clays; Vm=vermiculite; An=anatase; Fr=felspar; tr= trace; nd= not detected.

APPENDIX IV:  
TABLES 4.51 to 4.71.

TABLE 4.51 MOUNT LOFTY RANGE PROVINCE:  
Mount Taylor Plain area

SAMPLE	CHEMISTRY						
	Mt Tay. Plain	Summit surface					
	BOU	BOU	BOU	BOU	BOU	BOU	BOU
	103	101	143	129	136	107	116
	(Vermiform) (Ferricretes)	(Weathered) Bedrock		(Pisolitic Ferricretes)			Pisoliths C. Borda
Fe <sub>2</sub> O <sub>3</sub>	14.00	16.07	n	27.21	21.57	23.47	26.42
MnO	0.01	nd	o	0.01	0.01	0.01	0.07
TiO <sub>2</sub>	0.46	0.50	t	0.60	0.42	0.53	0.54
CaO	0.03	0.02		0.02	0.10	0.09	0.10
K <sub>2</sub> O	0.34	0.14	a	0.16	0.23	0.35	0.30
SO <sub>3</sub>	nd	nd	v	0.01	nd	0.01	nd
P <sub>2</sub> O <sub>5</sub>	0.02	0.02	a	0.02	0.02	0.02	0.03
SiO <sub>2</sub>	52.6	42.1	i	31.1	44.4	45.4	50.4
Al <sub>2</sub> O <sub>3</sub>	24.67	24.42	l	25.23	19.77	16.47	11.55
MgO	0.14	0.09	a	0.11	0.16	0.13	0.07
Na <sub>2</sub> O	0.04	0.03	b	nd	0.09	0.03	0.05
<u>Ig.Loss</u>	<u>6.77</u>	<u>16.39</u>	<u>l</u>	<u>14.60</u>	<u>12.51</u>	<u>12.77</u>	<u>9.84</u>
<u>Total</u>	<u>99.0</u>	<u>99.8</u>	<u>e</u>	<u>99.1</u>	<u>99.3</u>	<u>99.3</u>	<u>99.4</u>

### MINERALOGY

In decreasing order of abundance

	Qz	Qz	Qz	Qz	Qz	Qz	Qz
	Gb	Gb	Fr	Gb	Gt	Gt	Gt
	Gt	Gt	Kt	Hm	Gb	Gb	Hm
	Kt	Kt	Mu	Gt	St	Kt	Gb
	Hm	Fr	St	Kt	Kt	Fr	Kt
	An	Hm	Ic	St	Hm	Hm	Fr
		An		Vm			Mh
				Mi			
				An			
				Mh			
Magnetic reaction	N	Y vsl	N	Y	Y	Y	Y str

Qz=quartz; Hm=hematite; Gt=goethite; Kt=kaolinite; St=smectite; Mi=micas;  
An=anatase; Fr=felspar; Mh=maghemite; Mu=muscovite; Gb=gibbsite;  
Ic=interstratified clays; Vm=vermiculite; nd=not detected; v=very; sl=slight;  
str=strong.

TABLE 4.52  
MOUNT LOFTY RANGE PROVINCE:  
Green Hills area

**CHEMISTRY**

<i>Sample</i>	<i>BOU</i>	<i>BOU</i>	<i>BOU</i>
	<b>9</b>	<b>8</b>	<b>311</b>
(Ferruginised quartzose sediments)			
Fe <sub>2</sub> O <sub>3</sub>	19.14	16.79	17.12
MnO	0.02	0.01	0.01
TiO <sub>2</sub>	0.26	0.32	0.07
CaO	0.07	0.03	0.03
K <sub>2</sub> O	0.07	0.03	0.03
SO <sub>3</sub>	0.01	nd	nd
P <sub>2</sub> O <sub>5</sub>	0.02	0.01	0.20
SiO <sub>2</sub>	73.5	74.0	74.4
Al <sub>2</sub> O <sub>3</sub>	2.64	4.02	3.17
MgO	0.05	0.06	0.05
Na <sub>2</sub> O	0.04	0.02	0.04
<u>Ig.Loss</u>	<u>3.44</u>	<u>4.03</u>	<u>3.96</u>
<u>Total</u>	<u>99.3</u>	<u>99.3</u>	<u>99.5</u>

**MINERALOGY**

In decreasing order of abundance

	Qz	Qz	Qz
	Gt	Gt	Gt
	Hm	Hm	Hm
	St	Kt	St
		St	Kt
		Fr	Fr
			Ic
Magnetic reaction	Y	N	Y
	vvsl		vvvsl

Qz=quartz; Hm=hematite; Gt=goethite;  
Kt=kaolinite; St=smectite;; Fr=felspar;  
Mh=maghemite; Ic=interstratified clays;  
nd=not detected; v=very; sl=slight.

TABLE 4.53 MOUNT LOFTY RANGE PROVINCE:  
(Waitpinga Creek area)

CHEMISTRY						
SAMPLE	BOU	BOU	BOU	BOU	BOU	BOU
	311	323	324	325	326	328
(Ferruginised quartzose clastic sediments)						
Fe <sub>2</sub> O <sub>3</sub>	17.12	24.71	30.82	57.24	35.08	16.41
MnO	0.01	0.07	0.03	0.03	0.01	11.56
TiO <sub>2</sub>	0.07	0.29	0.05	0.23	0.12	0.12
CaO	0.03	0.09	0.08	0.07	0.03	0.05
K <sub>2</sub> O	0.44	0.24	0.30	0.26	0.32	1.13
SO <sub>3</sub>	nd	nd	nd	nd	0.01	0.04
P <sub>2</sub> O <sub>5</sub>	0.20	0.20	0.20	0.29	0.04	0.16
SiO <sub>2</sub>	74.4	66.4	61.7	24.6	53.5	60.3
Al <sub>2</sub> O <sub>3</sub>	3.17	2.20	1.11	4.88	2.59	1.28
MgO	0.05	0.12	0.04	0.11	0.07	0.06
Na <sub>2</sub> O	0.04	0.03	nd	0.03	0.03	0.12
<u>Ig.Loss</u>	<u>3.96</u>	<u>5.06</u>	<u>5.36</u>	<u>11.77</u>	<u>7.06</u>	<u>5.57</u>
<u>Total</u>	<u>99.5</u>	<u>99.4</u>	<u>99.7</u>	<u>99.5</u>	<u>98.9</u>	<u>96.8</u>

#### MINERALOGY

	In decreasing order of abundance					
	Qz	Qz	Qz	Gt	Qz	Qz
	Gt	Gt	Gt	Qz	Gt	Gt
	Hm	St	Fr	Ic	Fr	St
	St	Hm	St	Fr	St	Ho
	Kt	Kt				Fr
	Fr	Ic				
	Ic	Fr				
Magnetic reaction	Y	Y	N	N	N	N
	vvvsl	vvsl				

Qz=quartz; Hm=hematite; Gt=goethite; Kt=kaolinite; St=smectite;  
Fr=felspar; Mh=maghemite; Ic=interstratified clays; Ho=hollandite;  
nd=not detected; v=very; sl=slight.

TABLE 4.54 MOUNT LOFTY PROVINCE  
(Waitpinga Beach area)

Sample	CHEMISTRY				
	BOU 329 (Ferruginised clastic sediments)	BOU 330	BOU 331	BOU 332	BOU 333 Vesicular Ferricrete
Fe <sub>2</sub> O <sub>3</sub>	22.98	10.65	22.60	2.30	64.03
MnO	0.04	0.07	4.75	7.83	0.06
TiO <sub>2</sub>	0.29	4.30	0.71	0.44	0.15
CaO	0.02	0.06	0.05	0.04	0.09
K <sub>2</sub> O	0.36	0.11	0.31	0.49	0.06
SO <sub>3</sub>	0.01	0.03	0.01	0.06	nd
P <sub>2</sub> O <sub>5</sub>	0.11	0.37	0.15	0.05	0.51
SiO <sub>2</sub>	65.8	69.3	63.7	80.38	21.2
Al <sub>2</sub> O <sub>3</sub>	4.13	3.77	1.36	2.34	2.67
MgO	0.09	0.07	0.06	0.03	0.13
Na <sub>2</sub> O	nd	0.02	0.03	0.08	nd
<u>Ig.Loss</u>	<u>5.84</u>	<u>3.80</u>	<u>3.93</u>	<u>3.20</u>	<u>10.71</u>
<u>Total</u>	<u>99.7</u>	<u>96.6</u>	<u>97.7</u>	<u>97.2</u>	<u>99.6</u>

### MINERALOGY

In decreasing order of abundance

Gt	Qz	Qz	Qz	Gt
Qz	Gt	Gt	St	Qz
Kt	Zr	Hm	Ho	St
St	Fr	Ho	Hm	Kt
Fr	Hm	St	Ic	
	Kt			
	St			
Magnetic reaction	N	Y vvsl	N	Y vvvsl
				N

Qz=quartz; Hm=hematite; Gt=goethite; Kt=kaolinite;  
St=smectite; Ho=hollandite; Fr=felspar; Mh=maghemite;  
Zr=zircon; Ic=interstratified clays; nd=not detected;  
v=very; sl=slight.

TABLE 4.55 MOUNT LOFTY PROVINCE

<b>CHEMISTRY</b>					
(Iron oxide impregnated sediments)					
<i>Sample</i>	<i>BOU</i>	<i>BOU</i>	<i>BOU</i>	<i>BOU</i>	<i>BOU</i>
	<b>369</b>	<b>307</b>	<b>310</b>	<b>304</b>	<b>7</b>
	(Ferruginised) (Conglomerate) (Spring Mt)	(Ferruginised sands) (U.Hindmarsh) (Valley)	(Myponga) (Basin)		Ferruginised glacigene sediments (Yundi)
Fe <sub>2</sub> O <sub>3</sub>	19.76	28.82	21.73	21.05	15.75
MnO	0.01	0.01	0.01	0.01	0.01
TiO <sub>2</sub>	0.22	0.36	0.07	0.19	0.18
CaO	0.02	0.02	0.03	0.03	0.03
K <sub>2</sub> O	0.08	0.06	0.07	0.62	0.10
SO <sub>3</sub>	0.01	nd	0.02	0.01	nd
P <sub>2</sub> O <sub>5</sub>	0.01	0.05	0.06	0.03	0.03
SiO <sub>2</sub>	72.6	54.0	72.4	67.0	70.6
Al <sub>2</sub> O <sub>3</sub>	3.00	7.41	1.61	5.84	7.62
MgO	0.03	0.04	0.02	0.03	0.03
Na <sub>2</sub> O	nd	nd	nd	nd	nd
<u>Ig.Loss</u>	<u>4.01</u>	<u>8.53</u>	<u>3.46</u>	<u>5.39</u>	<u>5.16</u>
<u>Total</u>	<u>99.8</u>	<u>99.3</u>	<u>99.5</u>	<u>100.2</u>	<u>99.5</u>

**MINERALOGY**

In decreasing order of abundance

Qz	Qz	Qz	Qz	Qz
Gt	Gt	Gt	Gt	Hm
Hm	Hm	Hm	Kt	Gt
St	Kt	St	Hm	Kt
Kt	St	Kt	Fr	
Ic	Fr	Ic	St	
		Fr		

Magnetic  
reaction

N	N	Y	Y	N
		vvvsl	vvvsl	

Qz=quartz; Hm=hematite; Gt=goethite; Kt=kaolinite;  
 St=smectite; Fr=felspar; Mh=maghemite;  
 Ic=interstratified clays; nd=not detected; v=very; sl=slight.



TABLE 4.56 TOOKAYERTA TOPOSEQUENCES  
(Ferruginous quartzose clastic sediments)

Sample	CHEMISTRY								
	<i>Toposequence No 1.</i>		<i>Toposequence No 2.</i>						<b>Base</b> BOU
	<b>Top</b> BOU 312	<b>Base</b> BOU 314	<b>Top</b> BOU 315	BOU 316	BOU 317	BOU 318	BOU 319	BOU 320	
Fe <sub>2</sub> O <sub>3</sub>	23.46	9.02	27.94	15.29	16.5	11.78	12.64	32.63	13.34
MnO	nd	nd	0.01	0.01	0.01	nd	0.03	0.02	0.02
TiO <sub>2</sub>	0.08	0.14	0.31	0.05	0.19	0.16	0.11	0.20	0.16
CaO	0.01	0.03	0.02	nd	0.03	0.02	0.11	0.02	0.15
K <sub>2</sub> O	0.07	0.09	0.39	0.03	0.75	0.43	0.08	0.58	0.06
SO <sub>3</sub>	0.03	0.01	0.01	nd	nd	0.01	nd	0.01	0.01
P <sub>2</sub> O <sub>5</sub>	0.83	0.07	0.17	0.04	0.05	0.05	0.07	0.33	0.24
SiO <sub>2</sub>	70.2	73.3	55.9	79.3	71.3	75.7	80.3	53.7	80.9
Al <sub>2</sub> O <sub>3</sub>	1.63	2.54	7.1	1.7	5.82	6.44	3.00	5.44	1.79
MgO	0.02	0.05	0.10	nd	0.07	0.04	0.03	0.06	0.01
Na <sub>2</sub> O	0.01	nd	0.03	nd	0.03	0.06	0.02	0.02	nd
Ig.Loss	3.69	14.34	7.51	3.23	4.87	5.26	3.48	6.42	2.81
Total	100.0	99.6	99.5	99.7	99.6	100.0	99.9	99.4	99.5

#### MINERALOGY

In decreasing order of abundance

	Qz	Qz	Qz	Qz	Qz	Qz	Qz	Qz	Qz
	Gt	Gt	Gt	Gt	Gt	Gt	Gt	Gt	Gt
	Hm	Hm	Kt	St	Kt	St	St	Kt	St
	Kt	St	Hm	Hm	Fr	Kt	Kt	Hm	Fr
	St	Kt	St	Kt	St	Ic	Fr	Fr	Kt
	Fr	Ic	Ic	Ic	Ic	Fr		St	Hm
		Fr	Fr	Fr		Hm			
Magnetic reaction	N	N	N	N	N	N	Y sl	N	Y vsl

Qz=quartz; Hm=hematite; Gt=goethite; Kt=kaolinite; St=smectite; Fr=felspar; Ic=interstratified clays; nd=not detected; v=very; s=slight.

TABLE 4.57  
MOUNT LOFTY PROVINCE  
(Ferruginised glaciogene sediments)

Sample	CHEMISTRY	
	BOU	BOU
	358	363
	Tookayerta	Finniss
	Quarry	Quarry
Fe <sub>2</sub> O <sub>3</sub>	21.04	8.19
MnO	0.01	0.01
TiO <sub>2</sub>	0.09	0.05
CaO	0.02	0.02
K <sub>2</sub> O	1.14	0.07
SO <sub>3</sub>	0.01	nd
P <sub>2</sub> O <sub>5</sub>	0.79	0.08
SiO <sub>2</sub>	66.7	87.7
Al <sub>2</sub> O <sub>3</sub>	4.08	0.88
MgO	0.06	0.05
Na <sub>2</sub> O	0.11	0.03
<u>Ig.Loss</u>	<u>5.05</u>	<u>2.33</u>
<u>Total</u>	<u>99.1</u>	<u>99.4</u>

#### MINERALOGY

In decreasing order of abundance

Qz	Qz
Gt	Gt
Fr	St
Kt	Kt
St	Hm
Ic	Fr
	Ic
Magnetic reaction	N
	N

Qz=quartz; Hm=hematite;  
Gt=goethite; Kt=kaolinite;  
St=smectite; Fr=felspar;  
Ic=interstratified clays;  
nd=not detected.

TABLE 4.58 MOUNT LOFTY PROVINCE  
(Gun Emplacement)  
Ferruginised sediments  
**CHEMISTRY**

Sample	BOU 347 (Mottled Sands)	BOU 349 (Mottled Sands)	BOU 373 (Pisolitic Ferricrete)	BOU 374 Hematitic Mottle	BOU 39 Ferruginised sediments with pisoliths Perserverance Rd
Fe <sub>2</sub> O <sub>3</sub>	1.85	13.14	n	12.34	8.03
MnO	nd	0.01	o	0.01	nd
TiO <sub>2</sub>	0.30	0.41	t	0.41	0.66
CaO	0.05	0.29		0.28	0.08
K <sub>2</sub> O	0.10	0.45	a	0.45	0.21
SO <sub>3</sub>	nd	0.02	v	0.02	
P <sub>2</sub> O <sub>5</sub>	0.01	0.02	a	0.02	0.01
SiO <sub>2</sub>	85.7	73.1	i	73.1	78.6
Al <sub>2</sub> O <sub>3</sub>	6.21	5.90	l	5.90	6.09
MgO	0.14	0.32	a	0.32	0.15
Na <sub>2</sub> O	0.04	0.11	b	0.11	0.04
ZrO			l		0.08
Ig.Loss	<u>4.20</u>	<u>6.09</u>	<u>e</u>	<u>6.09</u>	<u>5.49</u>
Total	<u>98.6</u>	<u>99.9</u>		<u>99.1</u>	<u>99.4</u>

### MINERALOGY

In decreasing order of abundance

Qz	Qz	Qz	Qz	Qz
St	Kt	Gt	Hm	Kt
Kt	Fr	Hm	Gt	St
Ic	St	St	Kt	Hm
Gt	Gt	Kt	St	Mh
Hm	Ic	Fr	Ic	Fr
			Fr	An

Magnetic reaction N N N Y Y  
trace trace

Qz=quartz; Hm=hematite; Gt=goethite; Kt=kaolinite;  
St=smectite; An=anatase; Fr=felspar; Mh=maghemite;  
Ic=interstratified clays.

TABLE 4.59 MOUNT LOFTY PROVINCE  
(Bremer Valley)  
**CHEMISTRY**

Sample	BOU 354 Ferrug. sands 'Lucernbrae'	BOU 399 Bleached sandstone Monarto Block	BOU 378 Ferrug. quartzose sediments	BOU 362 (Compton Cross's Bridge	BOU 361 Conglomerate) Hartley Road Cut
Fe <sub>2</sub> O <sub>3</sub>	18.23	0.50	36.03	33.07	57.37
MnO	.01	nd	0.10	0.22	0.15
TiO <sub>2</sub>	0.24	0.34	0.16	0.43	0.15
CaO	0.08	0.04	0.08	0.18	0.14
K <sub>2</sub> O	0.22	0.03	0.44	0.48	0.68
SO <sub>3</sub>	0.02	nd	0.02	0.01	0.03
P <sub>2</sub> O <sub>5</sub>	0.25	nd	0.18	0.13	0.34
SiO <sub>2</sub>	71.9	89.2	52.2	45.0	20.9
Al <sub>2</sub> O <sub>3</sub>	3.54	4.51	3.29	9.82	4.20
MgO	0.14	0.03	0.21	0.38	1.22
Na <sub>2</sub> O	0.03	0.01	0.08	0.21	0.04
Ig.Loss	<u>5.15</u>	<u>3.36</u>	<u>6.23</u>	<u>9.45</u>	<u>13.21</u>
Total	<u>99.8</u>	<u>98.0</u>	<u>99.0</u>	<u>99.3</u>	<u>98.8</u>

**MINERALOGY**

In decreasing order of abundance

Qz	Qz	Qz	Qz	Gt
Gt	St	Gt	Gt	Qz
Hm	Kt	Hm	Kt	Mu
St	Ic	Fr	Mu	St
Kt	An	St	St	
Ic			An	
			Fr	

Magnetic

reaction N N N N N

Qz=quartz; Hm=hematite; Gt=goethite; Kt=kaolinite;  
St=smectite; An=anatase; Fr=felspar; Mu=muscovite;  
Ic=interstratified clays.

TABLE 4.60 MOUNT LOFTY PROVINCE  
(Mottled sediments)

Sample	CHEMISTRY		
	BOU 2 (Willunga Mottled sands)	BOU 14 Scarp) Mottled Conglom	BOU 368 Happy Valley Mottled sands
Fe <sub>2</sub> O <sub>3</sub>	6.17	5.16	15.33
MnO	nd	nd	0.01
TiO <sub>2</sub>	0.14	0.78	0.75
CaO	0.04	0.12	0.06
K <sub>2</sub> O	0.44	2.48	0.13
SO <sub>3</sub>	0.01	nd	0.02
P <sub>2</sub> O <sub>5</sub>	0.01	0.02	0.02
SiO <sub>2</sub>	88.2	72.1	71.8
Al <sub>2</sub> O <sub>3</sub>	2.95	12.10	4.52
MgO	0.07	0.67	0.12
Na <sub>2</sub> O	0.04	0.34	0.07
Ig.Loss	2.75	5.67	5.73
Total	99.9	99.4	98.6

#### MINERALOGY

In decreasing order of abundance

Qz	Qz	Qz
Fr	Fr	Gt
Mi	Mi	Hm
Hm	Hm	St
Gt	Gt	Fr
		Kt
		Ic

Magnetic  
reaction

N	N	N
---	---	---

Qz=quartz; Hm=hematite; Gt=goethite;  
Kt=kaolinite; St=smectite; Mi=micas;  
Fr=felspar; Ic=interstratified clays;  
nd=not detected.

TABLE 4.61 MOUNT LOFTY RANGE PROVINCE:  
CHEMISTRY

Sample	BOU 322 (Waitpinga Road) (Pisoliths) Surface	BOU 327 At depth	BOU 113 (Gap Pisoliths)	BOU 114 Hills Ferrug. sediments	BOU 117 Soil	BOU 149 Surface) Subsoil	BOU 104 Cape Borda Pisoliths
Fe <sub>2</sub> O <sub>3</sub>	44.88	5.35	39.83	26.65	6.55	6.64	32.47
MnO	0.01	nd	0.02	0.01	0.01	0.03	0.01
TiO <sub>2</sub>	0.44	0.33	0.72	2.82	0.90	0.50	0.51
CaO	0.05	0.06	0.11	0.06	0.27	30.24	0.19
K <sub>2</sub> O	0.07	0.09	0.39	0.13	0.61	0.54	0.62
SO <sub>3</sub>	0.01	nd	0.02	0.14	nd		0.02
P <sub>2</sub> O <sub>5</sub>	0.03	0.01	0.05	nd	0.01	0.05	0.03
SiO <sub>2</sub>	41.7	75.5	45.0	57.4	53.2	36.8	44.5
Al <sub>2</sub> O <sub>3</sub>	7.96	9.05	9.08	5.59	23.23	10.16	14.14
MgO	0.06	0.16	0.11	0.04	0.48	1.67	0.22
Na <sub>2</sub> O	0.01	0.25	0.11	0.05	0.15	1.12	0.09
Ig.Loss	<u>3.85</u>	<u>8.23</u>	<u>3.70</u>	<u>6.06</u>	<u>13.86</u>	<u>8.92</u>	<u>6.66</u>
Total	99.1	99.0	99.1	99.0	99.3	99.5	99.2

### MINERALOGY

In decreasing order of abundance

	Qz	Qz	Qz	Qz	Qz	Gt	Qz
	Hm	Gt	Ht	Hm	Kt	Qz	Hm
	Mh	Hm	Mh	An	Gt	Fr	Fr
	Kt	Kt	Fr	Fr	Fr	Kt	Mh
	St	St	Kt	Kt	Mh	St	Kt
	Ic	Gb					
Magnetic reaction	Y vstr	N	Y str	Y vvvsl	N	N	Y str

Qz=quartz; Hm=hematite; Gt=goethite; Kt=kaolinite; St=smectite; An=anatase;  
Fr=felspar; Mh=maghemite; Gb=gibbsite; Ic=interstratified clays;

**TABLE 4.62:  
STRATIGRAPHY OF WEATHERED, FERRUGINISED AND BLEACHED  
MATERIALS**

*HOLOCENE*

Modern beach sand, Goolwa (F)  
Modern stream channel, Kangaroo Island (F)  
Mid-Holocene estuarine sediments - Breckan Sand (F)  
St Kilda Formation (F)  
Fisherman Bay, peritidal sediments (SF)

*PLEISTOCENE*

Christies Beach Formation (F)  
Adare Clay (F)  
Glanville Formation (F)  
Boinkas of Murray Basin (SF)  
Taringa Formation (M)  
Kurrajong Formation (SM)  
Ochre Cove Formation (SM)  
Seaford Formation (M)  
Hindmarsh Clay (M)  
Burnham Limestone (Base of Pleistocene)

*PLIOCENE*

Hallett Cove Sandstone (SF)  
Sands Green Hills area, Waitpinga Drainage Basin (FC).  
Eleanor Sand of Kangaroo Island (FC)  
Ferruginous sands in Barossa Valley (F)  
Bremer Valley ferruginised clastic sediments (FC)  
Happy Valley ferruginous sands (FC)

*MIOCENE*

Ferruginised sands in Bremer Valley, 'Lucernbrae', Upper Hindmarsh Valley,  
Myponga Basin (FC).  
Terrestrial sands in Barossa Valley (FC)

*OLIGOCENE*

Compton Conglomerate and equivalents in Murray and Otway Basins

*EOCENE*

North Maslin Sands  
Palao-channel fills in Ranges (BL, F and FC)  
Limestone, Kingscote, K.I. (F)  
Garford Formation in palaeochannels, Eyre Peninsula (BL, F, M, FC)

*MESOZOIC*

Jurassic Basalt on Kangaroo Island (SW)  
Triassic sediments in Telford Basin (F, FC)

*PALAEOZOIC*

Permian glacial sediments, Fleurieu Peninsula, Kangaroo Island (M, BL, F, FC).

*CAMBRIAN*

Metasediments (BL, M).

*PRECAMBRIAN*

Metasediments and igneous rocks (BL, M)

(F=ferruginised; SF= strongly ferruginised; M= mottled; SM= strongly mottled;  
Bl=bleached; FC= ferricrete; SW= slightly weathered.)

TABLE 4.63

MOUNT LOFTY RANGE PROVINCE  
Kangaroo Island - Kingscote Cliffs

SAMPLE	CHEMISTRY						
	BOU 131 Bleached Sandstone	BOU 127 Bleached sandy clays	BOU 108 Mottle	BOU 118 Mottle	BOU 125 Mottle	BOU 106 Ferrug. Rim of Boulder	BOU 105 Weathered Core of Boulder
Fe <sub>2</sub> O <sub>3</sub>	2.24	1.97	22.78	12.64	6.56	56.58	0.30
MnO	0.02	0.01	0.31	0.17	0.01	0.31	0.01
TiO <sub>2</sub>	1.00	0.70	0.11	0.20	0.39	0.21	0.01
CaO	0.20	0.06	0.06	0.05	0.13	0.05	0.02
K <sub>2</sub> O	0.52	1.95	1.24	1.78	0.39	0.61	9.71
SO <sub>3</sub>	0.01	0.02	0.03	0.01	0.01	0.05	9.33
P <sub>2</sub> O <sub>5</sub>	0.02	0.05	0.06	0.04	nd	0.17	0.13
SiO <sub>2</sub>	71.6	67.6	68.1	75.9	83.4	25.0	4.3
Al <sub>2</sub> O <sub>3</sub>	15.62	17.92	2.66	4.75	4.00	3.75	36.1
MgO	0.52	0.54	0.20	0.24	0.20	0.54	0.05
Na <sub>2</sub> O	0.18	1.06	0.33	0.50	0.10	0.66	0.74
<u>Ig.Loss</u>	<u>7.50</u>	<u>7.75</u>	<u>4.06</u>	<u>3.32</u>	<u>4.17</u>	<u>11.56</u>	<u>37.68</u>
<u>Total</u>	<u>99.9</u>	<u>99.6</u>	<u>99.9</u>	<u>99.6</u>	<u>99.3</u>	<u>99.5</u>	<u>98.4</u>

MINERALOGY

In decreasing order of abundance

Qz	Qz	Qz	Qz	Qz	Qz	Al
Kt	Kt	Hm	Fr	St	Gt	Qz
St	St	Gt	Gt	Fr	Hm	Kt
Fr	Fr	Fr	Kt	Hm	Fr	
Mi	Mi	Kt	Hl	Kt	Kt	
An			Mi	Gt	Hl	

Magnetic reaction	N	N	Y vvsl	Y vvsl	Y sl	Y vvvsl	N
----------------------	---	---	-----------	-----------	---------	------------	---

Qz=quartz; Hm=hematite; Gt=goethite; Kt=kaolinite; St=smectite; Mi=micas;  
An=anatase; Fr=felspar; Mh=maghemite; Hl=halite; Ic=interstratified clays;  
nd=not detected; v=very; sl=slight.



TABLE 4.64 MOUNT LOFTY RANGE PROVINCE:  
Kangaroo Island: Kingscote Cliffs

SAMPLE	CHEMISTRY				
	BOU 119 Iron- rich Boulder	BOU 115 Slumped Iron Mass	BOU 102 Iron- impreg. sands	BOU 122 (Iron-impreg) Eocene Limestone	BOU 137
Fe <sub>2</sub> O <sub>3</sub>	25.38	46.89	10.74	10.52	73.39
MnO	0.19	1.36	0.09	nd	0.05
TiO <sub>2</sub>	0.09	0.14	0.10	nd	0.13
CaO	0.03	2.64	0.04	45.95	0.45
K <sub>2</sub> O	0.87	0.78	0.97	0.02	0.31
SO <sub>3</sub>	0.04	0.25	0.01	0.28	0.03
P <sub>2</sub> O <sub>5</sub>	0.10	0.23	0.05	0.23	0.89
SiO <sub>2</sub>	64.9	31.1	81.0	1.40	9.0
Al <sub>2</sub> O <sub>3</sub>	2.54	2.94	3.07	0.35	1.57
MgO	0.27	1.13	0.11	0.83	1.19
Na <sub>2</sub> O	0.42	0.35	0.04	nd	0.09
Ig.Loss	<u>4.83</u>	<u>11.31</u>	<u>3.33</u>	<u>39.66</u>	<u>13.46</u>
Total	<u>99.7</u>	<u>99.1</u>	<u>99.8</u>	<u>99.2</u>	<u>100.6</u>

#### MINERALOGY

In decreasing order of abundance

Qz	Qz	Qz	Ct	Gt
Gt	Gt	Gt	Gt	Qz
Hm	Hm	Fr	St	St
Kt	Fr	Hm		
Fr	Al	Kt		
Mi	Kt			
Hl				

Magnetic reaction	Y	N	Y	N	N
	vs		sl		

Qz=quartz; Hm=hematite; Gt=goethite; Kt=kaolinite;  
St=smectite; Mi=micas; Fr=felspar; Al=alunite;  
Hl=halite; Ct=calcite; nd=not detected; v=very; sl=slight.

TABLE 4.65

MOUNT LOFTY PROVINCE  
 Ferruginous mottles from Pleistocene  
 Sediments in scarp foot positions

SAMPLE	CHEMISTRY						
	BOU 53	BOU 39	BOU 58	BOU 70	BOU 71	BOU 72	BOU 364
Fe <sub>2</sub> O <sub>3</sub>	25.52	8.03	7.66	12.20	10.96	10.77	16.41
MnO	0.01	nd	0.01	0.02	0.01	0.01	0.01
TiO <sub>2</sub>	0.71	0.66	0.49	0.67	0.78	0.69	0.83
CaO	0.11	0.08	0.10	0.29	0.26	0.27	0.17
K <sub>2</sub> O	0.53	0.21	0.36	2.29	1.72	1.43	2.11
SO <sub>3</sub>	0.02					0.01	
P <sub>2</sub> O <sub>5</sub>	0.04	0.01	0.01	0.04	0.02	0.02	0.06
SiO <sub>2</sub>	57.4	78.6	79.3	68.3	70.1	72.1	63.7
Al <sub>2</sub> O <sub>3</sub>	7.73	6.09	6.11	8.55	8.84	7.82	8.77
MgO	0.29	0.15	0.29	1.04	0.56	0.51	1.13
Na <sub>2</sub> O	0.19	0.04	0.12	0.63	1.76	1.15	0.89
ZrO	0.03	0.10	0.02	0.03	0.03		
<u>Ig.Loss</u>	<u>6.83</u>	<u>4.42</u>	<u>4.80</u>	<u>5.37</u>	<u>3.92</u>	<u>4.64</u>	<u>5.35</u>
<u>Total</u>	<u>99.4</u>	<u>99.4</u>	<u>99.4</u>	<u>99.4</u>	<u>99.0</u>	<u>99.4</u>	<u>99.4</u>

### MINERALOGY

In decreasing order of abundance

Qz	Qz	Qz	Qz	Qz	Qz	Qz
Hm	Kt	St	Mi	Fr	Fr	Hm
Gt	St	Kt	Fr	Mi	Mi	Mh
Kt	Hm	Hm	Hm	St	Kt	Fr
Fr	Mh	Gt	St	Hm	Hm	Mu
An	Fr	Fr	Mh	Mh	Mh	Gt
Mh	An					St
						Kt
						Ic

Magnetic  
 reaction

Y	Y	Y	Y	Y	Y	Y
	trace					str

Qz=quartz; Hm=hematite; Gt=goethite; Kt=kaolinite; St=smectite; Ho=hollandite;  
 Mi=micas; An=anatase; Fr=felspar; Mh=maghemite; Ic=interstratified clays;  
 nd=not detected; str=strong.

TABLE 4.66 MOUNT LOFTY RANGE PROVINCE:  
Iron-mottled and bleached  
Pleistocene sediments  
**CHEMISTRY**

SAMPLE	BOU 41 Mottle (Hallett Cove)	BOU 40 Bleach	BOU 44 Mottle (Redbanks, Mid-North)	BOU 43 Bleach	BOU 59 Surface	BOU 42 Mottle Bow Hill
Fe <sub>2</sub> O <sub>3</sub>	9.87	0.94	8.00	1.54	3.39	41.31
MnO	0.01	nd	0.01	0.01	0.01	0.18
TiO <sub>2</sub>	0.33	0.42	0.08	0.84	0.72	0.13
CaO	0.09	0.10	0.05	0.07	0.05	0.07
K <sub>2</sub> O	0.79	0.87	1.14	0.90	1.02	0.60
SO <sub>3</sub>	0.01	0.01	nd	0.17		0.01
P <sub>2</sub> O <sub>5</sub>	0.06	0.01	0.07	0.01	0.03	0.02
SiO <sub>2</sub>	77.7	87.6	70.5	80.3	71.1	45.8
Al <sub>2</sub> O <sub>3</sub>	5.10	5.45	10.65	7.95	8.43	2.93
MgO	0.37	0.29	0.65	0.51	0.69	0.26
Na <sub>2</sub> O	0.20	0.28	0.79	1.71	1.35	0.20
ZrO			0.02		0.04	
Ig.Loss	<u>5.02</u>	<u>3.77</u>	<u>7.63</u>	<u>6.07</u>	<u>12.87</u>	<u>8.16</u>
Total	<u>99.6</u>	<u>99.7</u>	<u>100.3</u>	<u>100.1</u>	<u>99.7</u>	<u>99.7</u>

**MINERALOGY**

In decreasing order of abundance

Qz	Qz	Qz	Qz	Qz	Qz
Fr	Kt	Fr	St	Kt	Gt
Hm	Fr	Hm	Kt	Mu	Fr
Kt	Mi	Mu	Mi	St	Hm
Mh	An	St	Fr	Fr	Kt
		Kt	An	An	Mi
		Gt		HI	
		An			
		Mh			

Magnetic reaction Y trace N Y sl N N Y vvsl

Qz=quartz; Hm=hematite; Gt=goethite; Kt=kaolinite; St=smectite;  
Mi=micas; Fr=felspar; An=anatase; Mh=maghemite; Mu=muscovite;  
HI=halite; nd=not detected; v=very; sl=slight.

TABLE 4.67 MOUNT LOFTY PROVINCE:  
Ochre Cove/Ochre Point

SAMPLE	CHEMISTRY			
	BOU 365 Ferrug. Bedrock	BOU 51 Ferrug. Sands	BOU 50 Ferrug. Lime- stone	BOU 49 Ferrug. Sands
Fe <sub>2</sub> O <sub>3</sub>	24.22	10.85	8.34	14.05
MnO	0.02	0.01	0.02	0.01
TiO <sub>2</sub>	0.87	0.06	0.13	0.12
CaO	0.01	0.08	0.07	0.06
K <sub>2</sub> O	3.31	0.23	0.41	0.53
SO <sub>3</sub>	0.12	0.01	0.01	0.02
P <sub>2</sub> O <sub>5</sub>	0.05	0.02	0.08	0.01
SiO <sub>2</sub>	49.4	72.8	82.1	79.3
Al <sub>2</sub> O <sub>3</sub>	13.17	0.96	1.82	1.30
MgO	0.97	0.06	0.21	0.35
Na <sub>2</sub> O	0.60	0.17	0.14	0.31
<u>Ig.Loss</u>	<u>6.93</u>	<u>13.91</u>	<u>5.85</u>	<u>3.75</u>
<u>Total</u>	<u>99.7</u>	<u>99.2</u>	<u>99.2</u>	<u>99.8</u>

#### MINERALOGY

In decreasing order of abundance

Qz	Qz	Qz	Qz
Hm	Gt	Gt	Gt
Mu	Fr	Fr	Fr
Gt	St	St	St
Kt	Kt	Kt	Kt
Ic		Ic	Ic

Magnetic reaction N	Y vvvsl	Y vvsl	Y vvsl
------------------------	------------	-----------	-----------

Qz=quartz; Hm=hematite; Gt=goethite; Kt=kaolinite;  
St=smectite; Fr=felspar; Mh=maghemite; Mu=muscovite;  
Ic=interstratified clays; nd=not detected; v=very; sl=slight.

TABLE 4.68 MOUNT LOFTY PROVINCE  
(Ochre Cove/Ochre Point area)

SAMPLE	CHEMISTRY			
	BOU 48 Mottle (Seaford Formation)	BOU 46 Mottle (Ochre Cove Formatn)	BOU 45 Bleach	BOU 334 Pisoliths
Fe <sub>2</sub> O <sub>3</sub>	2.55	7.54	1.66	28.67
MnO	nd	nd	nd	0.01
TiO <sub>2</sub>	0.15	0.32	0.12	0.65
CaO	0.02	0.07	0.01	0.13
K <sub>2</sub> O	0.52	0.32	0.10	0.21
SO <sub>3</sub>	0.01	0.01	nd	0.01
P <sub>2</sub> O <sub>5</sub>	0.01	0.03	0.01	0.17
SiO <sub>2</sub>	89.3	86.2	95.8	59.6
Al <sub>2</sub> O <sub>3</sub>	2.84	1.50	0.48	3.73
MgO	0.20	0.22	0.04	0.12
Na <sub>2</sub> O	0.45	0.23	0.13	0.13
<u>Ig. Loss</u>	<u>3.17</u>	<u>3.03</u>	<u>0.93</u>	<u>5.73</u>
<u>Total</u>	<u>99.2</u>	<u>99.5</u>	<u>99.3</u>	<u>99.2</u>

#### MINERALOGY

In decreasing order of abundance

Qz	Qz	Qz	Qz
Kt	Fr	Fr	Hm
Fr	Kt		Gt
Gt	Gt		St
			Ic
			Mh

Magnetic reaction    N            N            N            Y

Qz=quartz; Hm=hematite; Gt=goethite; Kt=kaolinite;  
St=smectite; Fr=felspar; Mh=maghemite;  
Ic=interstratified clays; nd=not detected.

TABLE 4.69

MOUNT LOFTY PROVINCE:  
Kangaroo Island-Pleistocene sediments

SAMPLE	CHEMISTRY							
	BOU 112 (Road Mottle	BOU 111 cut near Calc. zone	BOU 110 Yorke (Pisoliths) Surface	BOU 148 Farm) B-hor.	BOU 123 (Redbanks) Mottle	BOU 139 Bleach	BOU 132 (Redbanks) Mottle	BOU 121 Buried Pisoliths
Fe <sub>2</sub> O <sub>3</sub>	6.05	3.01	32.26	15.71	2.89	1.12	7.68	33.77
MnO	0.01	nd	0.01	0.01	0.01	nd	nd	0.01
TiO <sub>2</sub>	0.54	0.29	0.73	0.68	0.30	0.38	0.66	0.48
CaO	0.19	29.73	0.12	0.06	0.06	0.05	0.06	0.12
K <sub>2</sub> O	0.28	0.66	0.42	0.34	0.82	1.24	1.00	0.52
SO <sub>3</sub>	0.01	0.22	0.02		0.01	0.01	0.05	0.02
P <sub>2</sub> O <sub>5</sub>	0.37	nd	0.03	0.02	0.01	0.01	0.02	0.03
SiO <sub>2</sub>	70.8	26.9	54.1	58.0	86.7	88.8	77.4	56.0
Al <sub>2</sub> O <sub>3</sub>	11.77	9.1	8.23	14.24	4.41	5.16	5.60	3.90
MgO	0.37	1.19	0.09	0.11	0.01	0.25	0.35	0.14
Na <sub>2</sub> O	0.60	0.11	0.13	0.04	0.25	1.61	1.47	0.53
ZrO				0.05				
<u>Ig.Loss</u>	<u>9.06</u>	<u>28.84</u>	<u>3.41</u>	<u>10.20</u>	<u>3.43</u>	<u>2.24</u>	<u>5.39</u>	<u>4.03</u>
<u>Total</u>	<u>99.6</u>	<u>99.5</u>	<u>99.6</u>	<u>99.5</u>	<u>99.9</u>	<u>100.8</u>	<u>99.4</u>	<u>99.6</u>

MINERALOGY

In decreasing order of abundance

Qz	Ct	Qz	Qz	Qz	Qz	Qz	Qz
Gt	Qz	Hm	Gt	St	St	St	Hm
Kt	Kt	Mh	Gb	Fr	Fr	Gt	Mh
Hm	Fr	Kt	Mi	Mi	Kt	Fr	
An	Kt	St	Kt	Kt	Fr	St	
		Gb	An		Hm	An	
		St	Mi		Mh		
			Fr				
			Hm				

Magnetic reaction Y N Y Y N N Y Y  
 vvvw str vstr vvsl vstr

Qz=quartz; Hm=hematite; Gt=goethite; Kt=kaolinite; St=smectite; Mi=micas;  
 An=anatase; Fr=felspar; Mh=maghemite; Ct=calcite; Gb=gibbsite;  
 Ic=interstratified clays; nd=not detected; v=very; w=weak; str=strong; sl=slight.

TABLE 4.70 BASINS MARGINAL TO THE MOUNT LOFTY PROVINCE:  
Iron impregnated Holocene sediments

Sample	CHEMISTRY						
	BOU 84 (Fisherman	BOU 85 Bay)	BOU 86 Bay)	BOU 61 (Boinkas of	BOU 65 Murray	BOU 66 Basin)	BOU 67 Basin)
Fe <sub>2</sub> O <sub>3</sub>	22.71	36.15	8.49	8.04	28.46	24.17	31.94
MnO	0.44	0.02	0.01	0.01	0.06	0.01	0.03
TiO <sub>2</sub>	0.11	0.38	0.59	0.37	0.13	0.10	0.10
CaO	4.23	0.06	0.13	0.07	0.09	0.07	0.15
K <sub>2</sub> O	0.76	0.74	1.15	0.89	0.27	0.20	0.22
P <sub>2</sub> O <sub>5</sub>	0.04	0.01	0.02	0.04	0.03	0.19	0.02
SiO <sub>2</sub>	32.2	46.1	71.9	82.7	62.0	67.7	62.1
Al <sub>2</sub> O <sub>3</sub>	1.66	4.89	7.69	2.01	1.75	1.41	0.96
MgO	1.78	0.60	0.88	0.23	0.19	0.15	0.16
Na <sub>2</sub> O	4.06	0.87	1.10	1.21	0.24	0.17	0.32
ZrO	0.01	0.02	0.04	0.06	0.02	0.13	0.01
Ig.Loss	<u>26.79</u>	<u>5.39</u>	<u>8.37</u>	<u>4.05</u>	<u>6.56</u>	<u>5.44</u>	<u>3.52</u>
<b>Total</b>	<u>94.76</u>	<u>99.8</u>	<u>100.4</u>	<u>99.7</u>	<u>99.8</u>	<u>99.6</u>	<u>99.5</u>

#### MINERALOGY

In decreasing order of abundance

Qz	Qz	Qz	Qz	Qz	Qz	Qz
Gy	Hm	Hm	Hm	Gt	Gt	Hm
Fh	Gt	Kt	Jr	Fr	Hm	St
Arg	Kt	St	St	Hm	St	Fr
Pr	Fr	Mi	Mu	Mi	Kt	Gt
HI	St	Fr	HI	St	Ic	HI
St	Ic	An	Fr		Fr	
Kt	Rz		Rz			
	Ah		Ah			

Magnetic  
reaction

N	N	N	N	N	N	N
---	---	---	---	---	---	---

Qz=quartz; Hm=hematite; Gt=goethite; Kt=kaolinite; St=smectite; Ho=hollandite;  
Mi=micas; An=anatase; Fr=felspar; Mh=maghemite; Mu=muscovite; HI=halite;  
Ic=interstratified clays; Jr=jarosite; Gy=gypsum; Fh=ferrihydrite; Arg=aragonite  
Pr=Pyrite; Rz=rozenite; Ah=anhydrite; nd=not detected.

TABLE 4.71 MOUNT LOFTY PROVINCE:  
Recent iron mobility

Sample	CHEMISTRY					
	BOU 1 (Mt Compass) Coffee Rock	BOU 16 Geode	BOU 140 Bleached Bedrock	BOU 141 Seepage Zone 1m	BOU 142 Iron Sludge	BOU 133 Incipient Pisoliths
Fe <sub>2</sub> O <sub>3</sub>	0.63	47.26	1.48	5.60	28.97	21.78
MnO	.nd	0.01	0.01	.nd	0.04	0.01
TiO <sub>2</sub>	0.10	0.28	0.42	0.78	0.30	0.36
CaO	0.01	0.02	0.01	0.02	0.33	0.10
K <sub>2</sub> O	0.05	0.10	1.93	0.85	0.47	0.56
SO <sub>3</sub>	.nd	0.02	0.01	.nd	0.04	0.01
P <sub>2</sub> O <sub>5</sub>	.nd	0.05	0.03	0.03	0.06	0.02
SiO <sub>2</sub>	94.3	38.5	76.4	58.3	40.9	50.2
Al <sub>2</sub> O <sub>3</sub>	1.72	3.96	14.16	22.19	5.58	7.90
MgO	0.01	0.03	0.24	0.28	0.44	0.14
Na <sub>2</sub> O	0.03	.nd	0.20	0.08	1.19	0.54
Ig.Loss	<u>2.75</u>	<u>9.34</u>	<u>4.99</u>	<u>11.13</u>	<u>21.59</u>	<u>17.81</u>
Total	<u>99.6</u>	<u>99.6</u>	<u>99.9</u>	<u>99.3</u>	<u>99.9</u>	<u>99.4</u>

#### MINERALOGY

In decreasing order of abundance

Qz	Qz	Qz	Qz	Qz	Qz
Fr	Gt	Kt	Kt	Fh	Gt
Kt	Hm	Mi	Gb	Kt	Fr
	Kt	Fr	Fr	St	Kt
	Mi	St	St	Fr	St
		Vm	Mi		Vm
			An		

Magnetic

reaction	Y	Y	N	N	Y	N
	vvs	vsl			vsl	

Qz=quartz; Hm=hematite; Gt=goethite; Kt=kaolinite; St=smectite;  
Mi=micas; An=anatase; Fr=felspar; Mh=maghemite; Gb=gibbsite;  
Vm=vermiculite; Fh=ferrihydrite; nd=not detected; v=very; sl=slight.



APPENDIX V:  
TABLES 5.1 to 5.3

TABLE 5.1 CLASSIFICATION OF FERRICRETES

- I SIMPLE FERRICRETES
1. Ferricreted bedrock
  2. Ferricreted sediments
    - a. Ferruginised clastic, quartzose sediments including blocks of reworked ferricrete (Detrital ferricrete)
    - b. Ferruginised organic sediments displaying a *massive to vesicular* fabric (bog iron ores)
    - c. Ferricretes formed by *in situ* weathering of iron-rich sediments containing siderite, glauconite and pyrite. Some of these ferricretes contain voidal concretions.
- II COMPLEX AND COMPOSITE FERRICRETES
1. Pisolitic ferricretes in which pisoliths are important constituents.
  2. Nodular ferricretes
  3. Slabby ferricretes
  4. Vermiform ferricretes

TABLE 5.2 Mean chemical analyses (XRF) of major ferricrete types

	Vermiform (9)	Nodular (3)	Slabby (4)	Massive- Vesicular (11)	Pisolitic (17)	Ferr. B/Rock (39)	Ferr. Sediments (55)
Fe <sub>2</sub> O <sub>3</sub>	30.4	34.6	46.4	65.6	27.1	25.5	18.8
MnO	0.01	0.02	0.01	0.01	0.01	0.02	0.32
TiO <sub>2</sub>	0.59	0.76	0.85	0.23	0.93	0.63	0.50
CaO	0.04	0.02	0.03	0.06	0.02	0.10	0.06
K <sub>2</sub> O	0.41	0.30	0.21	0.15	0.14	0.61	0.30
P <sub>2</sub> O <sub>5</sub>	0.05	0.02	0.02	0.38	0.03	0.09	0.11
SiO <sub>2</sub>	33.0	23.3	21.3	13.6	34.5	51.1	69.9
Al <sub>2</sub> O <sub>3</sub>	22.9	25.0	18.4	6.55	22.0	12.7	4.49
MgO	0.11	0.06	0.13	0.07	0.09	0.28	0.10
Na <sub>2</sub> O	0.05	0.04	0.06	0.01	0.09	0.21	0.09
ZrO	0.05	0.01	12.1	12.6	13.9	8.0	5.1
<u>Ig.Loss</u>	<u>11.90</u>	<u>14.8</u>	<u>12.1</u>	<u>12.6</u>	<u>13.9</u>	<u>8.0</u>	<u>5.1</u>
<u>Total</u>	<u>99.5</u>	<u>98.9</u>	<u>99.7</u>	<u>99.5</u>	<u>98.9</u>	<u>99.3</u>	<u>99.8</u>

TABLE 5.3

<i>Sample</i>	<b>CHEMISTRY</b>					
	<i>BOU</i> <b>29</b> Pisoliths (Mt Barker area)	<i>BOU</i> <b>30</b> Matrix	<i>Ione</i> <b>7</b> Vermiform Fe/crete	<i>Ione</i> <b>9</b> Pisolitic Fe/crete	<i>BOU</i> <b>213</b> (Vermiform Fe/crete) Robertson	<i>BOU</i> <b>215</b> Nowra
Fe <sub>2</sub> O <sub>3</sub>	37.3	27.04	35.1	25.85	32.1	32.96
MnO	0.02	0.01	0.05	0.01	0.01	0.01
TiO <sub>2</sub>	0.78	0.86	1.30	1.67	0.99	0.41
CaO	0.07	0.14	0.09	0.06	0.01	nd
K <sub>2</sub> O	0.13	0.47	0.09	0.02	0.20	0.40
P <sub>2</sub> O <sub>5</sub>	0.05	0.04	0.19	0.21	0.02	0.03
SiO <sub>2</sub>	40.9	54.8	26.8	14.3	60.4	60.1
Al <sub>2</sub> O <sub>3</sub>	13.28	18.99	22.92	21.67	17.18	15.71
MgO	0.10	0.28	0.08	0.07	0.06	0.07
Na <sub>2</sub> O	0.01	0.13	0.10	0.06	0.06	0.02
ZrO			0.02	0.03	0.01	
<u>Ig.Loss</u>	<u>6.46</u>	<u>17.98</u>	<u>11.90</u>	<u>19.99</u>	<u>9.67</u>	<u>9.44</u>
<u>Total</u>	<u>99.1</u>	<u>100.7</u>	<u>98.7</u>	<u>98.7</u>	<u>99.5</u>	<u>99.3</u>

**MINERALOGY**

In decreasing order of abundance

Qz	Qz	Hm	Gb	Qz	Qz
Hm	Kt	Kt	Hm	Gt	Gt
Mh	Fr	Qz	Kt	Kt	Gb
Kt	Mi	Vm	Gt	Hm	Hm
Gb	Gt	Gb	Qz	Gb	Vm
Gt		St	An	Fr	St
		An	Mh	St	Kt
					Mi

Magnetic

reaction	Y	N	N	Y	Y	Y
	vstr				vvsl	vvsl

Qz=quartz; Hm=hematite; Gt=goethite; Kt=kaolinite; St=smectite;  
 Mi=micas; An=anatase; Fr=felspar; Mh=maghemite; Gb=gibbsite;  
 Vm= vermiculite; nd=not detected; v=very; str=strong; sl=slight.

APPENDIX VI:  
TABLES 6.1 to 6.18

TABLE 6.1 EYRE PENINSULA SAMPLES  
(Blue Range)

<i>Sample</i>	<b>CHEMISTRY</b>				
	<i>BOU</i> <b>526</b> Bedrock Mottle	<i>BOU</i> <b>527</b> Bedrock Mottle	<i>BOU</i> <b>525</b> Ferrug SStone	<i>BOU</i> <b>528</b> Large Pisol- iths	<i>BOU</i> <b>529</b> Small Pisol- iths
Fe <sub>2</sub> O <sub>3</sub>	2.14	1.75	22.59	37.78	48.18
MnO	0.01	0.01	0.01	0.02	0.02
CaO	0.17	0.49	0.08	0.05	0.10
K <sub>2</sub> O	2.56	0.05	0.04	0.21	0.21
P <sub>2</sub> O <sub>5</sub>	0.04	0.06	0.03	0.06	0.06
SiO <sub>2</sub>	66.5	62.8	67.3	49.7	32.5
Al <sub>2</sub> O <sub>3</sub>	19.11	23.98	3.13	7.81	9.73
MgO	1.01	0.87	0.07	0.08	0.10
Na <sub>2</sub> O	0.12	0.29	0.01	0.07	0.04
ZrO	0.04	0.02	0.02	0.04	0.05
<u>Ig.Loss</u>	<u>7.60</u>	<u>7.02</u>	<u>5.82</u>	<u>2.70</u>	<u>6.20</u>
<u>Total</u>	<u>100.0</u>	<u>99.9</u>	<u>99.2</u>	<u>99.0</u>	<u>97.8</u>

### MINERALOGY

In decreasing order of abundance

Qz	Kt	Qz	Qz	Hm
Kt	Qz	Gt	Hm	Qz
Mi	Mi	Hm	Mh	Mh
St	An	St	Kt	Kt
Fr	St	Kt	An	An
Gt		Ic		St
An				

Magnetic

reaction N

N

N

Y  
vstr

Y  
vstr

Qz=quartz; Hm=hematite; Gt=goethite; Kt=kaolinite;  
St=smectite; Mi=micas; An=anatase; Fr=felspar;  
Mh=maghemite; Ic=interstratified clays; v=very; str=strong.

TABLE 6.2 EYRE PENINSULA  
(Glenville Etch Surface')

Sample	CHEMISTRY		
	BOU 523 Oxidised Pyritic Bedrock	BOU 524 Slightly weathered Pyritic Bedrock	BOU 530 Unweathered Bedrock
Fe <sub>2</sub> O <sub>3</sub>	23.7	14.33	0.48
MnO	0.01	0.01	nd
TiO <sub>2</sub>	0.01	0.49	0.09
CaO	0.09	0.08	0.02
K <sub>2</sub> O	0.03	0.65	0.44
P <sub>2</sub> O <sub>5</sub>	0.04	0.05	0.02
SiO <sub>2</sub>	52.0	66.5	96.4
Al <sub>2</sub> O <sub>3</sub>	9.93	8.78	1.30
MgO	0.29	0.31	nd
Na <sub>2</sub> O	0.12	0.17	0.03
ZrO	nd	0.01	nd
Ig.Loss	10.97	7.57	1.11
Total	97.3	98.9	9.9

### MINERALOGY

In decreasing order of abundance

Qz	Qz	Qz
Gt	Kt	Fr
Kt	Hm	St
St	St	Kt
Pt	Fr	Ic
	An	Gg(?)
	Gt	

Magnetic  
reaction Y N N  
vww

Qz=quartz; Hm=hematite; Gt=goethite;  
Kt=kaolinite; St=smectite; An=anatase;  
Fr=felspar; Ic=interstratified clays;  
Gg=griegite; Pt=pyrite; V=very; w=weak.

TABLE 6.3

EYRE PENINSULA SAMPLES  
(Corrobinnie Depression-Unweathered,  
bleached & mottled gneissic bedrock)

Sample	CHEMISTRY					
	BOU 508 Mottled Bedrock	BOU 509 Bleached Bedrock	BOU 518 Unweathd Bedrock	BOU 519 Mottled Gneiss	BOU 521 Mottled Gneiss	BOU 517 Enriched Mottles
Fe <sub>2</sub> O <sub>3</sub>	4.93	1.79	3.75	1.25	5.28	41.55
MnO	0.02	0.02	0.06	nd	nd	0.01
TiO <sub>2</sub>	0.55	1.44	0.51	0.26	0.72	0.07
CaO	0.03	0.02	1.19	0.65	0.06	0.36
K <sub>2</sub> O	1.13	1.48	5.36	3.81	0.34	0.07
P <sub>2</sub> O <sub>5</sub>	0.02	0.02	0.08	0.06	0.01	0.03
SiO <sub>2</sub>	54.2	54.3	71.96	74.3	62.6	49.8
Al <sub>2</sub> O <sub>3</sub>	17.05	23.84	12.87	12.94	20.10	2.34
MgO	1.04	0.75	0.46	1.67	0.52	0.07
Na <sub>2</sub> O	2.07	1.27	2.24	0.12	0.17	0.11
ZrO	0.02	0.04	0.06	0.03	0.03	0.01
Ig.Loss	<u>18.70</u>	<u>15.57</u>	<u>0.74</u>	<u>4.47</u>	<u>9.95</u>	<u>3.78</u>
<u>Total</u>	<u>99.7</u>	<u>100.5</u>	<u>99.3</u>	<u>99.5</u>	<u>99.3</u>	<u>98.2</u>

MINERALOGY

In decreasing order of abundance

Qz	Kt	Qz	Qz	Qz	Qz
Kt	Qz	Fr	Mi	Kt	Hm
Mi	Mi	Mi	Fr	Hm	Kt
Hl	Fr	St	St	Mi	St
Ic	An		Kt	St	
St	Hl		Hm	Ic	
Hm			Gt		
Gt					

Magnetic  
reaction

N	N	Y	N	Y	Y
---	---	---	---	---	---

Qz=quartz; Hm=hematite; Gt=goethite; Kt=kaolinite;  
St=smectite; Mi=micas; An=anatase; Fr=felspar; Hh=maghemite;  
Hl=halite; Ct=calcite; Ic=interstratified clays; nd=not detected.

TABLE 6.4

EYRE PENINSULA  
(Corrobinnie Depression:  
Garford Formation-bleached  
and mottled materials)

<i>Sample</i>	<b>CHEMISTRY</b>				
	<i>BOU</i> <b>510</b> Bleached clays	<i>BOU</i> <b>511</b> Yellow cellular crust	<i>BOU</i> <b>512</b> Red cellular crust	<i>BOU</i> <b>513</b> Clays in voids in crust	<i>BOU</i> <b>516</b> Ferrug. Mottle
Fe <sub>2</sub> O <sub>3</sub>	1.00	24.82	35.70	1.26	37.15
MnO	nd	0.01	0.01	nd	0.01
TiO <sub>2</sub>	0.91	0.63	0.55	1.38	0.75
CaO	0.06	0.04	0.03	0.04	0.01
K <sub>2</sub> O	0.18	0.11	0.08	0.33	0.07
P <sub>2</sub> O <sub>5</sub>	0.01	0.03	0.02	0.03	0.03
SiO <sub>2</sub>	52.2	35.3	28.63	50.3	42.5
Al <sub>2</sub> O <sub>3</sub>	28.1	28.11	20.76	29.13	10.05
MgO	0.72	0.47	0.33	0.21	0.08
Na <sub>2</sub> O	1.70	1.27	0.64	0.82	0.23
ZrO	0.05	0.04	0.04	0.05	0.04
<u>Ig.Loss</u>	<u>14.92</u>	<u>15.65</u>	<u>13.44</u>	<u>16.22</u>	<u>7.32</u>
<u>Total</u>	<u>99.9</u>	<u>99.7</u>	<u>100.2</u>	<u>99.7</u>	<u>98.3</u>

**MINERALOGY**

In decreasing order of abundance

Kt	Gt	Hm	Kt	Hm
Qz	Kt	Kt	Qz	Qz
Mi	Qz	Qz	Hl	Kt
St	Ic	Hl	Ic	An
Hl	Fr	Gt	St	St
Ic	Hl		Fr	Vm
An				

Magnetic  
reaction

N	N	N	N	N
---	---	---	---	---

Qz=quartz; Hm=hematite; Gt=goethite; Kt=kaolinite;  
St=smectite; Mi=micas; An=anatase; Fr=felspar;  
Mu=muscovite; Hl=halite; Vm=vermiculite;  
Ic= interstratified clays; nd=not detected.



TABLE 6.5

EYRE PENINSULA SAMPLES  
(Corrobinnie Depression:  
Ferricretes on Garford Formation)

Sample	CHEMISTRY					
	BOU 514 Ferrug. sands	BOU 515 Pisolitic ferricrete	BOU 505 Fragmental ferricrete	BOU 506 Matrix BOU 505	BOU 507 Fragments BOU 505	BOU 588 Fragmental ferricrete
Fe <sub>2</sub> O <sub>3</sub>	32.32	30.13	46.66	50.71	35.47	43.86
MnO	0.01	0.01	0.01	0.01	0.01	0.01
TiO <sub>2</sub>	0.17	0.25	0.59	0.54	0.60	0.49
CaO	0.10	0.12	0.21	0.27	0.19	0.28
K <sub>2</sub> O	0.04	0.06	0.09	0.13	0.10	0.05
P <sub>2</sub> O <sub>5</sub>	0.02	0.03	0.03	0.03	0.19	0.04
SiO <sub>2</sub>	60.4	60.2	24.53	23.9	28.1	27.6
Al <sub>2</sub> O <sub>3</sub>	1.77	2.99	16.03	11.79	21.27	15.47
MgO	0.09	0.10	0.18	0.19	0.02	0.17
Na <sub>2</sub> O	0.05	0.05	0.12	0.17	0.18	0.18
ZrO	0.02	0.02	0.04	0.04	0.03	0.04
Ig.Loss	<u>3.69</u>	<u>4.29</u>	<u>10.98</u>	<u>5.8</u>	<u>2.37</u>	<u>11.00</u>
<u>Total</u>	<u>98.7</u>	<u>98.2</u>	<u>99.5</u>	<u>98.8</u>	<u>98.5</u>	<u>99.2</u>

MINERALOGY

In decreasing order of abundance

Fr	Qz	Hm	Hm	Hm	Hm
Qz	Hm	Gt	Qz	Kt	Qz
Mi	Gt	Qz	Kt	Qz	Gt
Tr	Kt	Kt	Gt	Gt	Kt
St	St	St	An	An	St
	Hl	Vm		Vm	
		Mi			
		An			
		Mh			

Magnetic  
reaction

Y	Y	Y	N	Y	Y
		w			vw

Qz=quartz; Hm=hematite; Gt=goethite; Kt=kaolinite; St=smectite;  
Mi=micas; An=anatase; Fr=felspar; Mh=maghemite; Hl=halite;  
Vm=vermiculite; Tr=tourmaline; nd=not detected; v=very; w=weak.

TABLE 6.6 EYRE PENINSULA  
(Corrobinnie Depression:  
Lacustrine Ferricretes)

SAMPLE	CHEMISTRY		
	BOU 573 Ferricrete in Claypan	BOU 587 Ferrug. seds under BOU 573	BOU 579 Ferrug. Grits
Fe <sub>2</sub> O <sub>3</sub>	31.84	8.52	23.86
MnO	0.01	nd	0.01
TiO <sub>2</sub>	0.10	0.24	0.08
CaO	0.06	0.03	0.03
K <sub>2</sub> O	0.93	1.37	3.92
P <sub>2</sub> O <sub>5</sub>	0.10	0.02	0.04
SiO <sub>2</sub>	56.5	66.4	53.8
Al <sub>2</sub> O <sub>3</sub>	1.82	6.26	6.60
MgO	0.03	1.55	0.01
Na <sub>2</sub> O	0.17	3.22	0.76
ZrO	0.06	0.02	0.01
<u>Ig.Loss</u>	<u>7.3</u>	<u>9.02</u>	<u>10.01</u>
<u>Total</u>	<u>98.9</u>	<u>98.9</u>	<u>99.2</u>

#### MINERALOGY

In decreasing order of abundance

Qz	Qz	Qz
Hm	Hm	Jr
Jr	Hl	Hm
Alt	Alt	Fr
An	Jr	Alt
St	St	
	Mi	
	An	
	Fr	
	N-Jr	

Magnetic  
reaction Y  
sl

N N

Qz=quartz; Hm=hematite; St=smectite; Mi=micas;  
An=anatase; Fr=felspar; Alt=alunite; Hl=halite;  
Jr= jarosite; N-Jr=natro-jarosite; nd=not detected;  
sl=slight.

TABLE 6.7 EYRE PENINSULA SAMPLES  
(Corrobinnie Depression:  
Pisolitic ferricretes)

Sample	CHEMISTRY					
	BOU 582 Pisolitic ferricrete	BOU 583 Pisoliths of 582	BOU 584 Matrix of 582	BOU 574 Pisolitic ferricrete	BOU 575 Matrix of 574	BOU 585 Bleached matrix of 582
Fe <sub>2</sub> O <sub>3</sub>	26.72	29.70	15.99	30.26	19.94	2.00
MnO	0.01	0.01	0.01	0.01	nd	nd
TiO <sub>2</sub>	1.23	1.24	0.68	1.68	0.69	1.04
CaO	0.16	0.06	0.10	0.24	0.31	0.26
K <sub>2</sub> O	0.22	0.90	0.31	0.10	0.41	0.36
P <sub>2</sub> O <sub>5</sub>	0.03	0.03	0.02	0.02	0.02	0.02
SiO <sub>2</sub>	57.5	60.6	66.7	49.2	51.3	80.7
Al <sub>2</sub> O <sub>3</sub>	6.49	3.53	6.60	9.36	14.74	7.97
MgO	0.20	0.10	0.21	0.12	0.42	0.33
Na <sub>2</sub> O	0.19	0.10	0.20	0.15	0.14	0.16
ZrO	0.06	0.05	0.04	0.08	0.03	0.06
<u>Ig.Loss</u>	<u>6.18</u>	<u>3.53</u>	<u>7.81</u>	<u>7.06</u>	<u>11.48</u>	<u>6.58</u>
<u>Total</u>	<u>99.0</u>	<u>99.1</u>	<u>98.7</u>	<u>98.3</u>	<u>99.4</u>	<u>99.4</u>

#### MINERALOGY

In decreasing order of abundance

Qz	Qz	Qz	Qu	Qz	Qz
Hm	Hm	Gt	Hm	Kt	Kt
Gt	Mh	Hm	Kt	Gt	Fr
Kt	Kt	Kt	Mh	Hm	An
Fr	Fr	St	An	An	Mi
Mh	An	Fr		Ic	St
An	St	An			Vm
St	Gt				

Magnetic  
reaction

Y	Y	N	Y str	N	N
---	---	---	----------	---	---

Qz=quartz; Hm=hematite; Gt=goethite; Kt=kaolinite; St=smectite;  
Mi=micas; An=anatase; Fr=felspar; Mh=maghemite; Vm=vermiculite;  
Ic=interstratified clays; nd=not detected; str=strong.

TABLE 6.8 EYRE PENINSULA  
(Corrobinnie Depression:  
Pisolitic Ferricretes)

Sample	CHEMISTRY		
	BOU 576 Pisoliths from 574	BOU 577 Bleached matrix of BOU 574	BOU 586 Bleached material with nodules
Fe <sub>2</sub> O <sub>3</sub>	32.12	4.11	1.75
MnO	0.01	nd	nd
TiO <sub>2</sub>	1.76	0.97	0.81
CaO	0.22	0.32	0.21
K <sub>2</sub> O	0.11	0.36	0.43
P <sub>2</sub> O <sub>5</sub>	0.03	0.01	0.01
SiO <sub>2</sub>	47.8	65.1	61.0
Al <sub>2</sub> O <sub>3</sub>	8.56	16.54	20.32
MgO	0.14	0.42	0.84
Na <sub>2</sub> O	0.11	0.23	0.34
ZrO	0.07	0.47	0.03
Ig.Loss	<u>7.3</u>	<u>11.60</u>	<u>14.52</u>
Total	<u>98.3</u>	<u>100.2</u>	<u>100.3</u>

#### MINERALOGY

In decreasing order of abundance

Qz	Qz	Qz
Hm	Kt	Kt
Gt	An	Mi
Kt	Mi	St
Mh	St	An
An	Fr	
St		
Fr		

Magnetic  
reaction    Y            N            N

Qz=quartz; Hm=hematite; Gt=goethite; Kt=kaolinite;  
St=smectite; Mi=micas; An=anatase; Fr=felspar;  
Mh=maghemite; nd=not detected.

TABLE 6.9 EYRE PENINSULA SAMPLES  
(Weathering on Mt Cooper)

SAMPLE	CHEMISTRY				
	BOU 500	BOU 501	BOU 502	BOU 503	BOU 504
	Unweathered bedrock- porphyry	Weathered mottle	Weathered greenish material	Weathered, bleached bedrock	Slightly bleached bedrock
Fe <sub>2</sub> O <sub>3</sub>	3.65	3.58	4.55	1.26	3.72
MnO	0.11	0.01	0.02	0.01	0.02
TiO <sub>2</sub>	0.81	0.65	0.57	0.41	0.37
CaO	1.56	0.10	1.58	0.21	0.13
K <sub>2</sub> O	5.81	0.06	2.14	2.52	4.00
P <sub>2</sub> O <sub>5</sub>	0.29	0.01	0.01	0.01	0.01
SiO <sub>2</sub>	65.2	55.2	58.43	77.8	74.9
Al <sub>2</sub> O <sub>3</sub>	15.79	21.84	17.34	10.78	11.76
MgO	0.77	0.20	0.73	0.16	0.13
Na <sub>2</sub> O	4.43	0.05	1.05	3.20	3.79
ZrO	0.08	0.11	0.05	0.06	0.06
Ig.Loss	0.79	16.85	13.21	3.00	6.73
Total	99.3	98.7	99.7	99.4	100.0

#### MINERALOGY

In decreasing order of abundance

Fr	Qz	Qz	Qz	Qz
Qz	Kt	Fr	Fr	Fr
Mi	St	Kt	St	St
Tr	Ic	St	Kt	Mi
St	St	Ct		Gt
	Mi			

Magnetic

reaction	Y	N	N	N	Y
	w				vw

Qz=quartz; Gt=goethite; Kt=kaolinite; St=smectite;  
Mi=micas; Fr=felspar; Ct=calcite; Tr=tourmaline.  
Ic=interstratified clays; nd=not detected; v=very; w=weak.

TABLE 6.10 EYRE PENINSULA SAMPLES  
(Sleaford area: Mottled bedrock)

SAMPLE	CHEMISTRY			
	BOU 534 Mottle in granite	BOU 535 Bleach in granite	BOU 537 Mottle in gneiss	BOU 538 Bleach in gneiss
Fe <sub>2</sub> O <sub>3</sub>	19.44	4.12	16.95	1.00
MnO	0.01	nd	nd	nd
TiO <sub>2</sub>	0.64	1.35	0.80	0.94
CaO	0.07	0.07	0.34	0.28
K <sub>2</sub> O	0.42	0.68	0.46	0.79
P <sub>2</sub> O <sub>5</sub>	0.19	0.18	0.05	0.04
SiO <sub>2</sub>	51.3	57.1	46.3	49.3
Al <sub>2</sub> O <sub>3</sub>	16.60	22.92	23.41	29.31
MgO	0.47	0.49	0.58	0.72
Na <sub>2</sub> O	1.24	1.42	0.39	0.69
ZrO	0.08	0.09	0.04	0.03
<u>Ig.Loss</u>	<u>9.27</u>	<u>10.24</u>	<u>10.31</u>	<u>16.50</u>
<u>Total</u>	<u>99.7</u>	<u>99.6</u>	<u>98.7</u>	<u>99.6</u>

#### MINERALOGY

In decreasing order of abundance

Qz	Qz	Kt	Kt
Kt	Kt	Qz	Qz
Hm	Fr	Hm	Mu
Mi	Mi	Mi	Hl
Hl	Hl	Fr	St
Gt	An	An	An
Fr	St	Ic	

Magnetic  
reaction N N N N

Qz=quartz; Hm=hematite; Gt=goethite; Kt=kaolinite;  
St=smectite; Mi=micas; An=anatase; Fr=felspar;  
Mu=muscovite; Hl=halite; Ic=interstratified clays;  
nd=not detected.

TABLE 6.11 EYRE PENINSULA SAMPLES  
(Sleaford area: Pisoliths and  
pisolitic ferricrete)

SAMPLE	CHEMISTRY		
	BOU 536 Surface pisoliths	BOU 532 Pisolitic ferricrete	BOU 533 Pisolitic ferricrete
Fe <sub>2</sub> O <sub>3</sub>	43.69	13.11	18.71
MnO	0.02	0.01	0.02
TiO <sub>2</sub>	0.46	0.63	0.63
CaO	0.15	0.17	0.03
K <sub>2</sub> O	0.37	0.42	0.51
P <sub>2</sub> O <sub>5</sub>	0.04	0.04	0.05
SiO <sub>2</sub>	43.2	62.3	67.2
Al <sub>2</sub> O <sub>3</sub>	7.43	17.29	8.66
MgO	0.22	0.27	0.10
Na <sub>2</sub> O	0.19	0.14	0.08
ZrO	0.04	0.05	0.05
<u>Ig.Loss</u>	<u>2.84</u>	<u>5.11</u>	<u>3.18</u>
<u>Total</u>	<u>98.7</u>	<u>99.5</u>	<u>99.2</u>

#### MINERALOGY

In decreasing order of abundance

Qz	Qz	Kt
Hm	Kt	Qz
Mh	Hm	Hm
Kt	Gt	Mi
Fr	St	Fr
An	Mh	An
	An	
	Gb	

Magnetic

reaction	Y	Y	N
	str		

Qz=quartz; Hm=hematite; Gt=goethite; Kt=kaolinite;  
St=smectite; Mi=micas; An=anatase; Fr=felspar;  
Mh=maghemite; Gb=gibbsite; str=strong.

TABLE 6.12 EYRE PENINSULA SAMPLES  
(Mottled materials)

SAMPLE	CHEMISTRY				
	BOU 567 Red Mottle in grits	BOU 568 Yellow Mottle in grits	BOU 569 Red Mottle	BOU 570 Yellow Mottle	BOU 571 Bleached Material
Fe <sub>2</sub> O <sub>3</sub>	11.64	8.69	47.32	16.54	1.38
MnO	nd	0.03	0.02	0.03	0.02
TiO <sub>2</sub>	0.37	0.24	0.11	1.73	1.29
CaO	0.07	0.10	0.10	0.06	0.03
K <sub>2</sub> O	0.02	0.06	0.06	0.10	0.15
P <sub>2</sub> O <sub>5</sub>	0.02	0.02	0.06	0.02	0.02
SiO <sub>2</sub>	84.1	85.6	25.8	42.0	65.7
Al <sub>2</sub> O <sub>3</sub>	1.32	2.49	11.37	21.38	18.66
MgO	0.05	0.10	0.31	0.44	0.39
Na <sub>2</sub> O	nd	0.04	0.80	1.37	1.13
ZrO	0.02	0.02	0.02	0.07	0.05
Ig.Loss	<u>2.19</u>	<u>2.76</u>	<u>12.75</u>	<u>15.64</u>	<u>10.85</u>
Total	<u>99.7</u>	<u>100.1</u>	<u>98.3</u>	<u>99.3</u>	<u>99.7</u>

### MINERALOGY

In decreasing order of abundance

Qz	Qz	Gt	Kt	Kt
Hm	Gt	Hm	Gt	Qz
Gt	Kt	Qz	Qz	St
Kt	St	Kt	Fr	Hl
St	Vm	Hl	Hl	An
Mh	Hm	Mh		

Magnetic reaction Y vvs1 N Y vsl N N

Qz=quartz; Hm=hematite; Gt=goethite; Kt=kaolinite;  
St=smectite; An=anatase; Fr=felspar; Mh=maghemite;  
Hl=halite; Vm=vermiculite; nd=not detected; v=very; sl=slight.



TABLE 6.13 EYRE PENINSULA SAMPLES

(Koppio Quarry: Weathered (Flinders Highway)  
and mottled bedrock)

SAMPLE	CHEMISTRY				
	BOU 544 Weathered Granite	BOU 542 Weathered Br-bleach	BOU 541 Mottled Bedrock	BOU 555 Mottled Bedrock	BOU 556 Bleached Bedrock
Fe <sub>2</sub> O <sub>3</sub>	0.61	0.72	1.91	50.65	3.18
MnO	nd	0.02	nd	0.02	nd
TiO <sub>2</sub>	0.14	0.71	0.88	0.45	0.54
CaO	0.03	0.02	0.01	0.89	66.16
K <sub>2</sub> O	0.84	0.23	0.18	0.91	0.77
P <sub>2</sub> O <sub>5</sub>	0.04	0.05	0.03	0.02	0.02
SiO <sub>2</sub>	71.4	68.4	63.5	30.5	18.5
Al <sub>2</sub> O <sub>3</sub>	19.48	21.15	23.85	8.02	5.66
MgO	0.08	0.09	0.05	0.12	1.27
Na <sub>2</sub> O	0.11	0.15	0.11	0.11	0.14
ZrO	0.01	0.09	0.08	0.02	0.02
<u>Ig.Loss</u>	<u>7.20</u>	<u>8.58</u>	<u>9.49</u>	<u>6.73</u>	<u>36.70</u>
<u>Total</u>	<u>100.0</u>	<u>100.2</u>	<u>100.1</u>	<u>98.5</u>	<u>97.6</u>

## MINERALOGY

In decreasing order of abundance

Qz	Kt	Kt	Hm	Ct
Kt	Qz	Qz	Qz	Qz
Mu	St	St	Gt	Mi
St	Mu	Hm	Mi	St
	An	An	Kt	Kt
		Ct		

Magnetic  
reaction N N N N NQz=quartz; Hm=hematite; Gt=goethite; Kt=kaolinite;  
St=smectite; Mi=micas; An=anatase; Mu=muscovite.  
Ct=calcite; nd=not detected.

TABLE 6.14 EYRE PENINSULA SAMPLES  
(Mottled zones: Tumby Bay-  
Cummins road cuts)

SAMPLE	CHEMISTRY				
	BOU 559 Mottled Bedrock	BOU 560 Bleached Bedrock	BOU 561 Bog iron ore	BOU 562 Mottled Bedrock	BOU 563 Bleached Bedrock
Fe <sub>2</sub> O <sub>3</sub>	35.65	2.39	78.59	33.22	2.10
MnO	0.01	0.01	0.05	0.02	0.01
TiO <sub>2</sub>	0.68	1.66	0.02	0.48	0.99
CaO	0.06	0.09	0.05	nd	nd
K <sub>2</sub> O	1.32	3.01	0.02	0.03	0.05
P <sub>2</sub> O <sub>5</sub>	0.03	0.02	1.16	0.03	0.01
SiO <sub>2</sub>	41.7	63.9	1.7	29.8	48.50
Al <sub>2</sub> O <sub>3</sub>	11.50	21.64	1.80	19.85	31.76
MgO	0.25	0.51	0.02	0.06	0.11
Na <sub>2</sub> O	0.26	0.15	0.06	0.33	0.58
ZrO	0.03	0.04	nd	0.02	0.04
Ig.Loss	<u>7.08</u>	<u>7.86</u>	<u>14.05</u>	<u>13.58</u>	<u>15.64</u>
<u>Total</u>	<u>99.1</u>	<u>99.7</u>	<u>97.5</u>	<u>97.4</u>	<u>99.8</u>

### MINERALOGY

In decreasing order of abundance

Qz	Qz	Gt	Gt	Kt
Hm	Mi	Hm	Hm	Vm
Gt	Kt	Ic	Kt	Hl
Kt	An		Qz	An
Mi	St			Qz
St				
An				

Magnetic  
reaction N N N N N

Qz=quartz; Hm=hematite; Gt=goethite; Kt=kaolinite;  
St=smectite; Mi=micas; An=anatase; Hl=halite;  
Vm=vermiculite; Ic=interstratified clays; nd=not detected.

TABLE 6.15  
 EYRE PENINSULA SAMPLES  
 (Weathered profile: Tumbay Bay-  
 Cummins Road cut, near tower)

SAMPLE	CHEMISTRY		
	BOU 566 Mottled Bedrock	BOU 565 Ferricrete	BOU 564 Ferricrete
Fe <sub>2</sub> O <sub>3</sub>	40.93	36.72	47.73
MnO	0.01	0.02	0.04
TiO <sub>2</sub>	0.45	0.18	1.33
CaO	0.08	0.18	0.03
K <sub>2</sub> O	0.67	0.05	0.04
P <sub>2</sub> O <sub>5</sub>	0.02	0.05	0.03
SiO <sub>2</sub>	29.1	37.9	15.8
Al <sub>2</sub> O <sub>3</sub>	16.44	14.21	18.59
MgO	0.23	0.06	0.05
Na <sub>2</sub> O	0.30	0.03	0.06
ZrO	0.01	0.01	0.03
Ig.Loss	<u>10.27</u>	<u>9.99</u>	<u>13.38</u>
<u>Total</u>	<u>98.5</u>	<u>99.3</u>	<u>97.1</u>

#### MINERALOGY

In decreasing order of abundance

Hm	Hm	Gt
Qz	Qz	Hm
Kt	Gt	Kt
Gt	Kt	Qz
Mi	Vm	
An		

Magnetic  
 reaction N N N

Qz=quartz; Hm=hematite; Gt=goethite;  
 Kt=kaolinite; Mi=micas; An=anatase;  
 Vm=vermiculite.

TABLE 6.16  
EYRE PENINSULA SAMPLES  
(Koppio Quarry area)

SAMPLE	CHEMISTRY		
	BOU 539 Pisolitic ferricrete	BOU 540 Hematitic quartzite (weathered)	BOU 543 Hematitic quartzite (fresh)
Fe <sub>2</sub> O <sub>3</sub>	51.70	60.69	47.06
MnO	0.03	0.04	0.02
TiO <sub>2</sub>	1.26	0.10	0.07
CaO	0.05	0.03	0.03
K <sub>2</sub> O	0.05	0.03	0.02
P <sub>2</sub> O <sub>5</sub>	0.06	0.29	0.41
SiO <sub>2</sub>	13.0	30.0	46.48
Al <sub>2</sub> O <sub>3</sub>	22.60	2.19	2.21
MgO	0.04	0.04	0.03
Na <sub>2</sub> O	0.06	0.08	0.04
ZrO	0.02	nd	0.02
<u>Ig.Loss</u>	<u>9.08</u>	<u>4.99</u>	<u>3.30</u>
<u>Total</u>	<u>97.9</u>	<u>98.5</u>	<u>99.7</u>

#### MINERALOGY

In decreasing order of abundance

Hm	Hm	Hm
Mh	Qz	Qz
Gb	Gt	Gt
Hl	Mh	Kt
Qz	Kt	St
Bm	Vm	An
Vm		

Magnetic  
reaction Y Y Y  
vstr

Qz=quartz; Hm=hematite; Gt=goethite;  
Kt=kaolinite; St=smectite; An=anatase;  
Mh=maghemite; Gb=gibbsite; Hl=halite;  
Vm=vermiculite; Bm=boemite; nd=not detected;  
v=very; str=strong.

TABLE 6.17 EYRE PENINSULA SAMPLES  
(Ferricretes in Tod River  
Valley area)

SAMPLE	CHEMISTRY				
	BOU 545 Pisolitic F/crete	BOU 546 Pisolitic F/crete	BOU 547 Pisolitic F/crete	BOU 548 Pisolitic F/crete	BOU 549 Pisolitic F/crete Vanilla CP.
Fe <sub>2</sub> O <sub>3</sub>	35.21	10.24	32.21	25.55	19.37
MnO	0.01	0.01	0.02	0.01	0.01
TiO <sub>2</sub>	1.05	0.90	0.95	0.82	0.69
CaO	0.02	0.05	0.01	0.01	0.01
K <sub>2</sub> O	0.04	0.10	0.01	0.03	0.05
P <sub>2</sub> O <sub>5</sub>	0.04	0.02	0.02	0.02	0.03
SiO <sub>2</sub>	21.33	79.1	19.1	22.9	31.39
Al <sub>2</sub> O <sub>3</sub>	25.49	6.15	28.72	30.88	29.04
MgO	0.05	0.09	0.04	0.03	0.03
Na <sub>2</sub> O	0.01	0.04	0.02	0.04	0.03
ZrO	0.03	0.03	0.02	0.02	0.04
Ig.Loss	<u>15.75</u>	<u>2.80</u>	<u>17.43</u>	<u>19.12</u>	<u>18.49</u>
Total	<u>99.0</u>	<u>99.5</u>	<u>98.5</u>	<u>99.4</u>	<u>99.1</u>

### MINERALOGY

In decreasing order of abundance

Gt	Qz	Gb	Gt	Gb
Gb	Hm	Qz	Qz	Qz
Qz	Kt	Hm	Gb	Hm
Hm	St	Gt	Hm	Gt
Kt	An	Kt	An	Kt
An	Mh	An	St	An
		Mh		Bm
				St
				Mh

Magnetic  
reaction

N	Y	Y	N	Y
				sl

Qz=quartz; Hm=hematite; Gt=goethite; Kt=kaolinite;  
St=smectite; An=anatase; Mh=maghemite; Gb=gibbsite;  
Bm=boemite; sl=slight.

TABLE 6.18 EYRE PENINSULA SAMPLES  
(Knott Hill & Yallunda Flat)

CHEMISTRY				
SAMPLE	BOU 551	BOU 550	BOU 552	BOU 572
	Nodular ferricrete	Nodules in soil	Soil with nodules	Pisolitic ferricrete
Fe <sub>2</sub> O <sub>3</sub>	35.63	41.43	21.01	45.32
MnO	0.04	0.03	0.04	0.04
TiO <sub>2</sub>	0.88	1.05	1.36	0.54
CaO	0.01	0.02	0.06	0.05
K <sub>2</sub> O	0.19	0.05	0.23	0.27
P <sub>2</sub> O <sub>5</sub>	0.02	0.03	0.02	0.03
SiO <sub>2</sub>	22.05	21.9	32.8	36.2
Al <sub>2</sub> O <sub>3</sub>	24.79	22.1	28.04	8.52
MgO	0.02	0.03	0.12	0.08
Na <sub>2</sub> O	0.04	0.06	0.10	0.04
ZrO	0.01	0.01	0.02	0.03
<u>Ig.Loss</u>	<u>15.03</u>	<u>12.22</u>	<u>13.95</u>	<u>7.39</u>
<u>Total</u>	<u>98.7</u>	<u>98.9</u>	<u>97.8</u>	<u>98.5</u>

#### MINERALOGY

In decreasing order of abundance

Gt	Kt	Gt	Hm
Hm	Gt	Kt	Qz
Qz	Hm	Qz	Gt
Gb	Qz	Hm	Kt
Kt	An	Ic	Gb
An		An	An
			Fr
			Mh

Magnetic reaction	N	N	N	Y

Qz=quartz; Hm=hematite; Gt=goethite; Kt=kaolinite;  
An=anatase; Fr=felspar; Mh=maghemite;  
Ic=interstratified clays; Gb=gibbsite.

APPENDIX VII:  
TABLES 7.1 to 7.4

TABLE 7.1 WESTERN OTWAY BASIN SAMPLES

SAMPLE	CHEMISTRY			
	BOU 222 Ferrug. Sandstone	BOU 221 Weathered Basement	BOU 220 (Bleached) (Bedrock)	BOU 206
Fe <sub>2</sub> O <sub>3</sub>	31.54	14.62	2.83	0.94
MnO	0.06	0.02	0.01	0.01
TiO <sub>2</sub>	0.08	0.74	0.87	0.95
CaO	0.07	0.07	0.07	0.03
K <sub>2</sub> O	0.04	2.68	2.96	0.35
P <sub>2</sub> O <sub>5</sub>	0.16	0.26	0.03	0.01
SiO <sub>2</sub>	57.1	53.2	63.0	88.1
Al <sub>2</sub> O <sub>3</sub>	2.93	15.15	17.56	6.47
MgO	0.06	0.98	0.91	0.16
Na <sub>2</sub> O	nd	1.68	1.55	0.06
ZrO	0.04	0.02	0.03	
<u>Ig.Loss</u>	<u>7.17</u>	<u>10.39</u>	<u>9.69</u>	<u>2.73</u>
<u>Total</u>	<u>99.2</u>	<u>99.8</u>	<u>99.5</u>	<u>99.8</u>

## MINERALOGY

In decreasing order of abundance

Qz	Qz	Qz	Qz
Gt	Fr	Fr	St
Hm	Gt	Mi	Kt
St	Mi	Kt	Fr
	Vm	St	Mi
	St	Ic	Ic
	Ic		An
	Kt		

Magnetic  
reaction Y N N N  
vvs1

Qz=quartz; Hm=hematite; Gt=goethite; Kt=kaolinite;  
St=smectite; Mi=micas; An=anatase; Fr=felspar;  
Mh=maghemite; Mu=muscovite; Gb=gibbsite; Alt=alunite;  
Hl=halite; Ct=calcite; Vm=vermiculite;  
Im=ilmenite; Ic=interstratified clays; nd=not detected;  
v=very; sl=slight.



TABLE 7.2 WESTERN OTWAY BASIN SAMPLES

SAMPLE	CHEMISTRY						
	(Noss Mesa - Casterton)			Coleraine	Noss	(Killara Bluff)	
	BOU	BOU	BOU	BOU	BOU	BOU	BOU
	201	202	208	209	230	228	229
	F/crete	(Bedrock)	(Mottles)	F/crete	Magnetic Clasts	(Pebble Point Fm)	(Ferr. Limestone)
Fe <sub>2</sub> O <sub>3</sub>	35.26	12.86	6.42	36.39	50.94	48.56	44.90
MnO	0.04	0.01	0.01	0.04	0.03	0.06	0.03
TiO <sub>2</sub>	0.67	0.32	1.02	1.78	0.43	0.40	0.41
CaO	0.11	0.03	0.06	0.04	0.03	0.01	0.02
K <sub>2</sub> O	0.25	0.21	0.23	0.19	0.07	0.52	0.28
SO <sub>3</sub>	0.03	nd	nd	0.02			
P <sub>2</sub> O <sub>5</sub>	0.09	0.03	0.01	0.21	0.08	0.83	0.47
SiO <sub>2</sub>	39.2	75.7	72.4	40.9	33.9	22.9	36.0
Al <sub>2</sub> O <sub>3</sub>	12.36	5.26	12.45	10.24	10.46	8.68	4.39
MgO	0.22	0.13	0.21	0.11	0.05	0.51	0.17
Na <sub>2</sub> O	0.03	0.07	0.06	.01	0.02	0.10	0.02
ZrO					0.06	0.03	0.06
Ig. Loss	<u>9.94</u>	<u>4.57</u>	<u>6.69</u>	<u>8.63</u>	<u>2.70</u>	<u>16.45</u>	<u>12.17</u>
Total	<u>99.2</u>	<u>99.2</u>	<u>99.5</u>	<u>99.5</u>	<u>98.8</u>	<u>99.1</u>	<u>98.9</u>

## MINERALOGY

In decreasing order of abundance

Qz	Qz	Qz	Qz	Hm	Gt	Gt
Hm	Gt	Hm	Gt	Qz	Qz	Qz
Gt	Hm	Gt	Hm	Mh	Kt	Fr
Kt	Kt	Kt	Kt	St	Vm	Kt
St	St	An	An	Vm	Fr	
Ic	Ic	St			Mi	
Vm	Fr					
Mi						
An						

Magnetic  
reaction

N	N	N	N	Y	N	Y
				vvstr		vvvw

Qz=quartz; Hm=hematite; Gt=goethite; Kt=kaolinite; St=smectite;  
 Mi=micas; An=anatase; Fr=felspar; Mh=maghemite; Mu=muscovite.  
 Gb=gibbsite; Alt=alunite; Hl=halite; Ct=calcite; Vm=vermiculite;  
 Im=ilmenite; Ic=interstratified clays; nd=not detected; v=very; str=strong;  
 w=weak.

TABLE 7.3 WESTERN OTWAY BASIN SAMPLES

SAMPLE	CHEMISTRY						
	BOU 224 (Compton Conglomerate) (Mount Gambier)	BOU 225 (Crawford)	BOU 226 (River)	BOU 223 (Casterton) (Bridge)	BOU 227 (Ferricrete)	BOU 210 (Ferrug. Sediments) (Coleraine)	BOU 203 (Cawkers Creek)
Fe <sub>2</sub> O <sub>3</sub>	53.57	39.47	65.10	33.44	17.91	26.89	7.44
MnO	0.14	0.06	0.26	0.04	0.03	0.01	.nd
SiO <sub>2</sub>	0.20	0.53	0.16	0.25	0.28	0.44	0.44
CaO	0.89	0.10	1.88	0.04	0.06	0.03	0.10
K <sub>2</sub> O	0.91	0.25	0.20	0.32	0.34	0.16	0.14
SO <sub>3</sub>						0.01	nd
P <sub>2</sub> O <sub>5</sub>	1.17	0.11	0.92	0.21	0.13	0.02	0.02
SiO <sub>2</sub>	16.0	47.7	7.3	49.4	69.1	58.8	74.1
Al <sub>2</sub> O <sub>3</sub>	8.88	6.09	4.39	5.51	4.33	7.26	8.41
MgO	1.41	0.08	1.49	0.14	0.22	0.09	0.10
Na <sub>2</sub> O	0.10	0.06	0.12	0.11	0.20	0.10	0.04
ZrO	0.02	0.05	0.02	0.02	0.04		
Ig.Loss	<u>15.92</u>	<u>4.71</u>	<u>16.45</u>	<u>9.13</u>	<u>6.68</u>	<u>5.54</u>	<u>8.68</u>
Total	<u>99.2</u>	<u>99.2</u>	<u>98.3</u>	<u>99.1</u>	<u>99.3</u>	<u>99.3</u>	<u>99.5</u>

## MINERALOGY

In decreasing order of abundance

Gt	Qz	Gt	Qz	Qz	Qz	Qz
Qz	Hm	Qz	Gt	Gt	Hm	Gt
Mi	Mh	Ct	Gb	Fr	Gt	Kt
Kt	Fr	Kt	Kt	Kt	Kt	Mi
Ic		Vm	St	Mi	St	St
				St	Vm	Ic
				Vm		

Magnetic  
reaction

N	Y	N	Y	N	N	N
	str		vvvsl			

Qz=quartz; Hm=hematite; Gt=goethite; Kt=kaolinite; St=smectite;  
 Mi=micas; An=anatase; Fr=felspar; Mh=maghemite; Mu=muscovite.  
 Gb=gibbsite; Alt=alunite; Hl=halite; Ct=calcite; Vm=vermiculite;  
 Im=ilmenite; Ic=interstratified clays; nd=not detected; str=strong; v=very;  
 sl=slight.

TABLE 7.4 WESTERN OTWAY BASIN SAMPLES  
(PISOLITHS)

SAMPLE	CHEMISTRY			
	BOU 204	BOU 205	BOU 207	BOU 211
	Tarington Branhholme (Surrey River)			
Fe <sub>2</sub> O <sub>3</sub>	48.63	56.61	54.99	35.6
MnO	0.03	0.03	0.03	0.04
TiO <sub>2</sub>	1.69	1.61	0.57	0.29
CaO	0.06	0.03	0.03	0.05
K <sub>2</sub> O	0.07	0.03	0.11	0.05
SO <sub>3</sub>	0.02	0.05	0.03	nd
P <sub>2</sub> O <sub>5</sub>	0.05	0.04	0.15	0.16
SiO <sub>2</sub>	19.4	14.7	25.6	44.6
Al <sub>2</sub> O <sub>3</sub>	16.21	19.63	11.77	7.74
MgO	0.13	0.04	0.07	0.10
Na <sub>2</sub> O	0.06	0.02	nd	nd
ZrO				0.04
<u>Ig.Loss</u>	<u>12.87</u>	<u>6.73</u>	<u>5.8</u>	<u>10.61</u>
<u>Total</u>	<u>99.2</u>	<u>99.5</u>	<u>99.2</u>	<u>99.2</u>

#### MINERALOGY

In decreasing order of abundance

Hm	Hm	Hm	Qz
Gt	Mh	Qz	Hm
Qz	Gt	Mh	Gt
Kt	Qz	Gt	Mh
Mh	Kt	Gb	Fr
Im	Im	Kt	Vm
Mi	Fr	Fr	St
St	Vm	An	An

Magnetic reaction	Y	Y	Y	Y
	str	str	str	str

Qz=quartz; Hm=hematite; Gt=goethite; Kt=kaolinite;  
St=smectite; Mi=micas; An=anatase; Fr=felspar;  
Mh=maghemite; Mu=muscovite; Gb=gibbsite; Alt=alunite;  
Hl=halite; Ct=calcite; Vm=vermiculite; Im=ilmenite;  
Ic=interstratified clays; nd=not detected; str=strong.

APPENDIX VIII:  
TABLES 8.1 to 8.4

TABLE 8.1

## SYDNEY SAMPLES

SAMPLE	CHEMISTRY						
	BOU 400 (Pisoliths)	BOU 401	BOU 403 Mottle	BOU 404 Pisoliths	BOU 405 Soil	BOU 406 Vermiform	BOU 407 Mottle
Fe <sub>2</sub> O <sub>3</sub>	25.58	23.58	30.98	30.29	3.61	41.02	37.79
MnO	0.01	0.01	0.01	nd	0.01	0.01	0.01
TiO <sub>2</sub>	1.36	1.55	1.31	1.60	1.01	0.99	0.87
CaO	nd	nd	nd	nd	0.01	0.02	nd
K <sub>2</sub> O	0.06	0.08	0.05	0.05	0.13	0.06	0.03
SO <sub>3</sub>	0.03	0.03	0.03	0.02	0.01		0.03
P <sub>2</sub> O <sub>5</sub>	0.03	0.03	0.04	0.03	0.02	0.04	0.04
SiO <sub>2</sub>	22.8	21.0	21.6	18.3	79.9	10.7	9.4
Al <sub>2</sub> O <sub>3</sub>	30.17	32.32	27.33	30.85	8.50	28.96	30.10
MgO	0.06	0.10	0.06	0.06	0.12	0.03	0.05
Na <sub>2</sub> O	0.02	0.09	0.05	0.05	0.04	0.02	0.05
ZrO	0.09	0.09	0.09	0.12	0.09	0.05	
<u>Ig.Loss</u>	<u>19.3</u>	<u>20.28</u>	<u>17.58</u>	<u>18.62</u>	<u>6.11</u>	<u>17.76</u>	<u>21.9</u>
<u>Total</u>	<u>99.4</u>	<u>99.1</u>	<u>99.1</u>	<u>100.0</u>	<u>99.5</u>	<u>99.6</u>	<u>100.3</u>

## MINERALOGY

In decreasing order of abundance

	Gb	Gb	Gb	Gb	Qz	Hm	Gb
	Qz	Qz	Qz	Qz	Gb	Gb	Hm
	Hm	Hm	Gt	Hm	St	Qz	Gt
	Gt	Gt	Hm	Gt	Kt	Gt	Qz
	Kt	Kt	Kt	An	An	Kt	Kt
	An	An	An	Mh	Gt	Mh	An
	Vm	Vm	Mh	Kt	Mi	Vm	Ic
		St	Vm	Vm	Hm		
Magnetic reaction	Y vw	Y  401a- pisoliths Y 401b- matrix N	Y	Y vstr	N  pisoliths in soil Y	Y vstr	Y w

Qz=quartz; Hm=hematite; Gt=goethite; Kt=kaolinite; St=smectite;  
 Mi=micas; An=anatase; Mh=maghemite; Gb=gibbsite; Vm=vermiculite;  
 Ic= interstratified clays; nd=not detected; v=very; str=strong; w=weak.

TABLE 8.2

## SYDNEY SAMPLES

SAMPLE	CHEMISTRY						
	BOU 408 Nodular Fe/crete	BOU 409 Pisolitic Fe/crete	BOU 410 Vesicular Fe/crete	BOU 411 Pisolitic Fe/crete	BOU 412 Pisoliths	BOU 412a Vesicular Fe/crete	BOU 413 Soft Mottles
Fe <sub>2</sub> O <sub>3</sub>	22.75	31.27	57.54	21.93	19.00	64.05	1.68
MnO	0.01	0.01	0.03	0.01	0.01	0.02	nd
TiO <sub>2</sub>	1.34	1.14	0.40	0.91	0.84	0.50	1.37
CaO	0.01	nd	0.02	nd	nd	nd	nd
K <sub>2</sub> O	0.05	0.07	0.25	0.06	0.02	0.20	0.14
SO <sub>3</sub>	0.03	0.02	0.03	0.02	0.03	0.07	0.02
P <sub>2</sub> O <sub>5</sub>	0.04	0.03	0.15	0.02	0.02	0.10	0.03
SiO <sub>2</sub>	13.46	12.1	14.3	26.5	28.5	11.6	73.5
Al <sub>2</sub> O <sub>3</sub>	31.72	34.59	12.24	30.40	42.81	13.07	15.31
MgO	0.07	0.06	0.04	0.05	0.03	0.05	0.05
Na <sub>2</sub> O	0.01	0.06	0.04	0.02	0.03	0.03	0.02
ZrO		0.07	0.03				
<u>Ig.Loss</u>	<u>20.2</u>	<u>20.64</u>	<u>14.71</u>	<u>19.57</u>	<u>7.40</u>	<u>10.79</u>	<u>6.70</u>
<u>Total</u>	<u>99.7</u>	<u>100.0</u>	<u>99.8</u>	<u>99.5</u>	<u>98.7</u>	<u>100.5</u>	<u>98.8</u>

## MINERALOGY

In decreasing order of abundance

Gb	Gb	Gt	Gb	Qz	Gt	Qz
Hm	Hm	Qz	Qz	Hm	Hm	Kt
Qz	Qz	Hm	Gt	Crn	Qz	St
Gt	Gt	Gb	Hm	Mh	Gb	An
Kt	Kt	Kt	Kt	Gb	Kt	Ic
Mh	Mh	Ic	St	Kt	An	Fr
An	An	Mh	An	Vm		An
Vm	Vm					Hm

Magnetic  
reaction

Y Y N Y Y N N

w str

411a-  
pisoliths  
Y(sl)  
411b  
matrix N

Qz=quartz; Hm=hematite; Gt=goethite; Kt=kaolinite; St=smectite; Mi=micas;  
An=anatase; Fr=felspar; Mh=maghemite; Gb=gibbsite; Vm=vermiculite;  
Crn=corundum; Ic=interstratified clays; nd=not detected; str=strong; w=weak.

TABLE 8.3

## SYDNEY SAMPLES

SAMPLE	CHEMISTRY						
	BOU 414 Slabby Fe/crete	BOU 415 Nodular Fe/crete	BOU 416 Pisolitic Fe/crete	BOU 417 Pisolitic Fe/crete	BOU 418 Bleached HSS	BOU 419 Mottled HSS	BOU 420 Ferrug. Sandst.
Fe <sub>2</sub> O <sub>3</sub>	16.66	37.05	17.78	21.93	0.19	4.22	19.97
MnO	0.01	0.01	0.01	0.10	nd	nd	0.01
TiO <sub>2</sub>	1.33	0.77	0.99	1.04	0.86	0.65	0.73
CaO	nd	nd	nd	nd	nd	nd	nd
K <sub>2</sub> O	0.16	0.13	0.03	0.05	0.70	1.40	0.29
SO <sub>3</sub>	0.02	0.05	0.02	0.02	0.01	0.03	0.02
P <sub>2</sub> O <sub>5</sub>	0.03	0.04	0.02	0.02	0.02	0.07	0.04
SiO <sub>2</sub>	37.0	14.8	30.0	34.3	89.7	66.1	57.5
Al <sub>2</sub> O <sub>3</sub>	28.71	28.99	31.10	24.89	5.88	19.22	11.59
MgO	0.06	0.04	0.04	0.04	0.04	0.14	0.04
Na <sub>2</sub> O	0.05	0.04	nd	0.04	0.03	0.02	0.04
ZrO	0.06	0.05	0.08	0.09	0.04	0.04	0.05
<u>Ig.Loss</u>	<u>15.78</u>	<u>17.66</u>	<u>19.79</u>	<u>16.67</u>	<u>1.85</u>	<u>7.06</u>	<u>9.46</u>
<u>Total</u>	<u>99.86</u>	<u>99.62</u>	<u>99.9</u>	<u>99.1</u>	<u>99.3</u>	<u>98.9</u>	<u>99.7</u>

## MINERALOGY

In decreasing order of abundance

	Gb	Gb	Gb	Qz	Qz	Qz	Qz
	Qz	Qz	Qz	Gb	Kt	Kt	Gt
	Kt	Hm	Gt	Gt	St	Hm	Gb
	Hm	Gt	Hm	Hm	Mi	Gt	Hm
	Gt	Kt	Kt	Kt	An	St	Kt
	Mh	An	St	St	Fr	An	St
	An	Mh	Mh	An			Ic
	Vm		An				
			Ic				
Magnetic reaction	Y sl	Y vstr	Y 416a- pisoliths Y 416b- matrix N	Y sl	N	N	N

Qz=quartz; Hm=hematite; Gt=goethite; Kt=kaolinite; St=smectite; Mi=micas; An=anatase; Mh=maghemite; Gb=gibbsite; Vm=vermiculite; Ic=interstratified clays; nd=not detected; sl=slight; v=very; str=strong; sl= slight.

TABLE 8.4 SYDNEY SAMPLES

SAMPLE	CHEMISTRY					
	BOU 421 Ferrug. sandst.	BOU 451 Maghem. clast	BOU 452 ( Hawkesbury	BOU 453	BOU 454 Sandstone	BOU 455
Fe <sub>2</sub> O <sub>3</sub>	22.59	83.61	0.32	1.41	0.48	1.39
MnO	0.01	0.03	nd	nd	nd	nd
TiO <sub>2</sub>	0.49	0.52	0.49	0.01	0.14	0.08
CaO	nd	0.01	0.01	0.01	0.12	0.03
K <sub>2</sub> O	0.19	0.08	0.20	0.86	0.65	0.35
SO <sub>3</sub>	0.02	0.03				
P <sub>2</sub> O <sub>5</sub>	0.03	0.03	0.02	0.02	0.02	0.01
SiO <sub>2</sub>	50.6	3.00	92.4	90.9	92.6	93.6
Al <sub>2</sub> O <sub>3</sub>	14.06	6.26	4.12	4.30	4.87	2.83
MgO	0.05	0.03	0.01	0.02	0.03	0.04
Na <sub>2</sub> O	nd	nd	nd	nd	0.03	0.19
ZrO	0.04	0.03	0.03	0.01	0.01	0.01
<u>Ig.Loss</u>	<u>10.39</u>	<u>4.58</u>	<u>2.52</u>	<u>2.00</u>	<u>1.62</u>	<u>0.98</u>
<u>Total</u>	<u>98.5</u>	<u>98.2</u>	<u>100.1</u>	<u>99.6</u>	<u>100.5</u>	<u>99.5</u>

## MINERALOGY

In decreasing order of abundance

Gt	Mh	Qz	Qz	Qz	Qz
Qz	Hm	Kt	St	Kt	Kt
Gb	Qz	St	Kt	St	St
Hm	Vm	Mi	Mi	Mi	Mi
Kt	Ic	An	Fr	Ic	Ic
An	Mi			Fr	Fr
Fr					
St					
Ic					

Magnetic reaction	Y	Y	N	N	N	N
	w	vvstr				

Qz=quartz; Hm=hematite; Gt=goethite; Kt=kaolinite; St=smectite; Mi=micas;  
An=anatase; Fr=felspar; Mh=maghemite; Mu=muscovite; Gb=gibbsite;  
Vm=vermiculite; Ic=interstratified clays; nd=not detected; w=weak; v=very;  
str=strong.



APPENDIX IX:  
TABLE 9.1

TABLE 9.1 TELFORD BASIN SAMPLES

SAMPLE	CHEMISTRY		
	BOU 88 Voidal Conc.	BOU 89 Sideritic Siltstone	BOU 90 Sideritic Siltstone
Fe <sub>2</sub> O <sub>3</sub>	61.75	31.08	51.54
MnO	0.31	0.21	0.30
TiO <sub>2</sub>	0.48	0.46	0.37
CaO	0.08	0.48	0.18
K <sub>2</sub> O	0.46	0.46	0.62
P <sub>2</sub> O <sub>5</sub>	1.85	0.25	1.09
SiO <sub>2</sub>	14.71	32.7	12.0
Al <sub>2</sub> O <sub>3</sub>	6.70	5.91	6.72
MgO	0.12	3.43	0.32
Na <sub>2</sub> O	0.33	0.20	0.37
ZrO	0.04	0.01	
Ig.Loss	<u>12.30</u>	<u>24.62</u>	<u>26.4</u>
Total	<u>99.3</u>	<u>99.8</u>	<u>99.9</u>

**MINERALOGY**

In decreasing order of abundance

Gt	Sd	Sd
Lp	Qz	Qz
Qz	Pt	Kt
Hm	Kt	Pt
Kt	Mu	Mu
St	An	Fr
Mu	Cd(?)	Cd(?)

Magnetic  
reaction

N            N            N

Qz=quartz; Hm=hematite; Gt=goethite;  
 Kt=kaolinite; Fr=felspar; Mh=maghemite;  
 Mu=muscovite; St=smectite; Sd=siderite;  
 Pt=pyrite; Cd=crandellite; An=anatase;  
 Ic= randomly interstratified clays;  
 Lp=lepidocrocite.

## REFERENCES

- ABELE, C., KENLEY, P.R., HOLDGATE, G. & RIPPER, D. (1976): Otway Basin. in, J. G. Douglas and J. A. Ferguson (Eds), *Geology of Victoria. Geol. Soc. Aust. Spec. Pub. No. 5*, 528pp.
- AITCHISON, G.S., SPRIGG, R.C. & COCHRANE, G.W. (1954): The soils and geology of Adelaide and suburbs. *Bull. Geol. Surv. S. Aust.* 32: 126 pp.
- ALEVA, G.J.J. (1983): Suggestions for a systematic structural and textural description of lateritic rocks. In: *Lateritisation Processes*, A.J. Melfi and A. Carvalho (Eds): *Proceedings of Second International Seminar on Lateritisation Processes*, Sao Paulo, Brazil. pp. 443-454.
- ALEXANDER, L.T. & CADY, J.G. (1962): Genesis and hardening of Laterite. *U.S. Dept. Agr. Tech. Bull.*
- ALLEY, N.F. (1969): The Cainozoic History of the Mid North of South Australia. Unpub. M.A. Thesis, University of Adelaide.
- ALLEY, N.F. (1973): Landsurface development in the Mid-North of South Australia. *Trans. R. Soc. S. Aust.* 97: 1-17.
- ALLEY, N.F. (1977): Age and origin of laterite and silcrete duricrusts and their relationship to episodic tectonism in the Mid-North of South Australia. *J. geol. Soc. Aust.* 24: 107-116.
- ALLEY, N.F. (1978): Discussion: Age and origin of laterite and silcrete duricrusts and their relationship to episodic tectonism in the Mid-North of South Australia. Reply. *J. geol. Soc. Aust.* 24: 423-425.
- ALLEY, N.F. & BOURMAN, R.P. (1984): Sedimentology and origin of Late Palaeozoic glaciogene deposits at Cape Jervis, South Australia. *Trans. R. Soc. S. Aust.* 108: 63-75.
- AMBROST, J.P., NAHON, D. & HERBILLON, A.J. (1986): The epigenetic replacement of kaolinite by hematite in laterite - petrographic evidence and the mechanisms involved. *Geoderma*, 37: 283-294.
- ANAND, R.R. & GILKES, R.J. (1987): The association of maghemite and corundum in Darling Range Laterites, Western Australia. *Aust. J. Soil Res.* 35: 303-311.
- BANERJEE, S.K. & MOSKOWITZ, B.M. (1985): Ferrimagnetic properties of magnetite. Ch2 in, *Magnetite Biomineralization and Magnetoreception in Organisms*. KIRSCHVINK, J.L., JONES, D.S. & MACFADDEN, B.J. [Eds] Plenum Press. New York.
- BANERJI, P.K. (1981): Laterization processes: what do we know about them? *Bulletin of the International Geological Correlation Programme. Nature and Resources.* 17(3): 21-25.
- BARNETT, S. (1978): Late Tertiary sediments on Eyre Peninsula. *Quart. geol. Notes Geol. Surv. S. Aust.* 67: 2-4.
- BARKER, S. (1986): The evolution of the South Australian Environment. Ch 1 in, *A Land Transformed*, C. Nance and D.L. Speight (Eds), pp. 1-28.
- BASEDOW, H. (1904) Note on Tertiary exposures in the Happy Valley District, with descriptions of a new specimen of *Septifer*. *Trans. R. Soc. S. Aust.* 28: 248-252.

- BAUER, F.H. (1959): The regional geography of Kangaroo Island. Ph.D. Thesis Aust. Natl. Univ. Canberra (unpubl.).
- BEADLE, N.C.W. & BURGESS, A. (1953): A further note on laterites. *Aust. J. Sci.* 15: 170-171.
- BENBOW, M.C. & PITT, G.M. (1978): The Garford Formation. *Quart. Geol. Notes, geol. Surv. S. Aust.* 68: 8-15.
- BENSON, W.N. (1906): Petrographical notes on certain Precambrian rocks of the Mount Lofty Ranges with special reference to the geology of the Houghton district. *Trans. R. Soc. S. Aust.* 33: 101-140.
- BENSON, W.N. (1911): Notes descriptive of a stereogram of the Mount Lofty ranges. *Trans. R. Soc. S. Aust.* 35: 103-111.
- BINKS, P.J. & HOOPER, G.J. (1984): Uranium in Tertiary palaeochannels "West Coast Area", South Australia. *Bull. & Proc. Min. and Met.* 289: 271-275.
- BIRD, M.J. (in prep.): An oxygen- and hydrogen-isotope study of laterites and deep weathering. Ph.D. Thesis, A.N.U.
- BOURMAN, R.P. (1969): Landform Studies near Victor Harbour. B.A. (Hons) Thesis, Univ. Adelaide (unpubl.).
- BOURMAN, R.P. (1973): Geomorphic evolution of southeastern Fleurieu Peninsula. M.A. Thesis Univ. Adelaide (unpubl.).
- BOURMAN, R.P. (1987): A review of controversial issues related to the Late Palaeozoic glaciation of southern South Australia. *International Geomorphology Part II*. V. Gardiner (Ed). John Wiley & Sons. pp 725-742.
- BOURMAN, R.P. & LINDSAY, J.M. (1973): Implications of fossiliferous Eocene marine sediments underlying part of the Waitpinga drainage basin, Fleurieu Peninsula. *Search* 4: 7.
- BOURMAN, R.P. & MILNES, A.R. (1985): Gibber Plains. *Austr. Geogr.* 16(3): 229-232.
- BOURMAN, R.P. & HARVEY, N. (1986): Landforms, Ch. 4 In, A Land Transformed, C. Nance and D.L. Speight (Eds), pp. 78-125.
- BOURMAN, R.P., MILNES, A.R. & OADES, J.M. (1987): Investigations of ferricretes and related surficial ferruginous materials in parts of southern and eastern Australia. *Z. Geomorph. N.F. Suppl.-Bd.* 64: 1-24.
- BOURMAN, R.P. & LINDSAY, J.M. (1989): Timing, extent and character of Late Cainozoic faulting on the eastern margin of the Mount Lofty Ranges, South Australia. *Trans. R. Soc. S. Aust.* (in press).
- BOURMAN, R.P. & LINDSAY, J.M. (1973): Implications of fossiliferous Eocene marine sediments underlying part of the Waitpinga drainage basin, Fleurieu Peninsula. *Search* 4: 7.
- BOURNE, J.A. (1974): Chronology of denudation of Northern Eyre Peninsula. M.A. Thesis University of Adelaide (Unpub.).
- BOURNE, J.A., TWIDALE, C.R. & SMITH, D.M. (1974): The Corrobinnie Depression, Eyre Peninsula, South Australia. *Trans. R. Soc. S. Aust.* 98: 139-152.

- BREWER, R. (1964): *Fabric and mineral analysis of soils*. Wiley, New York. 470 pp.
- BRINDLEY, G.W. & BROWN, G. (Eds) (1980): *Crystal structures of clay minerals and their X-ray identification*. Mineralogical Society, London. 495 pp.
- BROCK, E.J. (1964): The denudation chronology of Fleurieu Peninsula. M.A. Thesis, University of Adelaide (unpub.) 176 pp.
- BROCK, E.J. (1971): The denudation chronology of the Fleurieu Peninsula, South Australia. *Trans. R. Soc. S. Aust.* 95: 85-94.
- BRYAN, W.H. (1939): The red earth residuals and their significance in Southeastern Queensland. *Proc. R. Soc. Qld.* 50(4): 21-32.
- BUCHANAN, F. (1807): A journey from Madras through the countries of Mysore, Canara, and Malabar. East India Company, London.
- BURGESS, A. & BEADLE, N.C.W. (1952): The laterites of the Sydney district. *Aust. J. Sci.* 14: 161-162.
- BUTT, C.R.M. (1982): Weathering and the Australian landscape. In, *Geochemical Exploration in Deeply Weathered Terrain*. (Ed. R.E. Smith) *CSIRO Inst. Energy & Earth Res.* pp 9-18.
- CAMPANA, B. (1955): The Geology of the Gawler Military Sheet. *Rep. Invest. geol. Surv. S. Aust.* 4: 24pp.
- CAMPANA, B. & WILSON, R.B. (1955) The Geology of the Jervis and Yankalilla Military Sheets. *Rep. Invest. Geol. Surv. S. Aust.* 3: 1-24.
- CAMPBELL, J.M. (1917): Laterite, its origin, structure and minerals. *Mineralogical Magazine.* 17: 67-77, 120-128, 171-179, 220-229.
- CENT, J. & BREWER, R. (1971): Preparation of thin sections of soil materials using synthetic resins. CSIRO Division of Soils Tech. Pap. 7.
- CHAPPELL, J. (1967): Recognising fossil strand lines from grain size analysis. *Jour. Sed. Petr.* 37: 157-165.
- CHARTRES, C.J. (1983): The pedogenesis of desert loam soils in the Barrier Range, western New South Wales. II, Weathering and soil formation. *Aust. J. Soil Res.*, 21: 1-13.
- CHILDS, C.W., WARD, W.T. & WELLS, N. (1972): Rattling iron concretions from the Waikato coal measures. *N.Z. Jour. Geol. & Geophys.* 17(1): 93-101.
- CHRISTIAN, G.S. & STEWART, G.A. (1946): Survey of the Katherine-Darwin Region. C.S.I.R.O., *Land Research Series*, No. 1.
- CONNAH, T.H. & HUBBLE, G.D. (1960): Laterites in Queensland. *J. geol. Soc. Aust.* 7: 373-386.
- COOK, P.J., COLWELL, J.B., FIRMAN, J.B., LINDSAY, J.M., SCHWEBEL, D.A. & von der BORCH, C.C. (1976): The Late Cainozoic sequence of southeast South Australia and Pleistocene sea-level changes. *BMR Jour. Aust. Geol. & Geophys.* 2: 81-88.
- COOPER, B.J. (1986): A record of Ordovician conodonts from the Warburton

Basin, South Australia. *Quart. Geol. Notes, geol. Surv. S. Aust.* 100: 8-14.

COVENTRY, R.J., TAYLOR, R.M. & FITZPATRICK, R.W. (1983): Pedological significance of the gravels in some red and grey earths of central North Queensland. *Aust. J. Soil Res.* 21: 219-240.

CRAWFORD, A.R. (1959): Geology of the Encounter Military Sheet, Explanatory Notes (unpub.).

CRAWFORD, A.R. (1965): The geology of Yorke Peninsula. *Bull. Geol. Surv. S. Aust.* 39: 1-96.

CROCKER, R.L. (1946): Post-Miocene climatic and geologic history and its significance in relation to the genesis of the major soil types of South Australia. *C.S.I.R. Bull.* No. 193, 56 pp.

DAILY, B. & MILNES, A.R. (1971): Stratigraphic notes on Lower Cambrian fossiliferous metasediments between Campbell Creek and Tunkalilla Beach in the type section of the Kanmantoo Group, Fleurieu Peninsula, South Australia. *Trans. R. Soc. S. Aust.* 95(4): 199-214.

DAILY, B., TWIDALE, C.R. & MILNES, A.R. (1974): The age of the lateritized summit surface on Kangaroo Island and adjacent regions of South Australia. *J. geol. Soc. Aust.* 21: 387-392.

DAILY, B., FIRMAN, J.B., FORBES, B.G. & LINDSAY, J.M. (1976): Geology. In: TWIDALE, C.R., TYLER, M.J. and WEBB, B.P. (Eds): Natural History of the Adelaide Region. *R. Soc. S. Aust.* p.5-42.

DAILY, B., MILNES, A.R., TWIDALE, C.R. & BOURNE, J.A. (1979): Geology and geomorphology. In: TYLER, M.J., TWIDALE, C.R. and LING, D. (Eds): Natural History of Kangaroo Island. *R. Soc. S. Aust.* p.1-38.

DAVID, EDGEWORTH T.W. (1887): Origin of the laterite in the New England District of New South Wales. *Aust. Assoc. Adv. Sci.* 1: 233-241.

DAVIS, W.M. (1909): *Geographical Essays*. Ginn, Boston. 777p.

DAVIS, W.M. (1920): Physiographic relations of laterite. *Geol. Mag.* 57: 429-431.

de SWARDT, A.M.J. (1964): Lateritization and landscape development in parts of equatorial Africa. *Z. Geomorph.* 8: 313-333.

du BOIS, C.G.B. & JEFFREY, P.G. (1955): The composition and origin of the laterites of the Entebbe Peninsula, Uganda. *Col. Geol. Min. Res.* 5: 387-408.

EYLES, V.A. (1952): The composition and origin of the Antrim laterites and bauxites. *Memoirs of the Geological Survey*. Government of Northern Ireland, Belfast. 90 pp.

EVANS, R.C. (1964): *Introduction to Crystal Chemistry*. University Press, Cambridge. (Second Ed.).

FANIRAN, A. (1969): A deeply-weathered surface and its destruction: a geomorphological study of duricrusts in the Northern Sydney District. Unpub. Ph.D. Thesis, University of Sydney, 464 pp.

FANIRAN, A. (1970): Maghemite in the Sydney duricrusts. *Am. Miner.* 55: 925-933.

- FANIRAN, A. (1971): The parent materials of Sydney laterites. *J. geol. Soc. Aust.* 18: 159-164.
- FENNER, C. (1930): The major structural and physiographic features of South Australia. *Trans. R. Soc. S. Aust.* 54: 1-36.
- FENNER, C. (1931): *South Australia-a geographical study*. Whitcombe and Tombs, Melbourne.
- FENNER, C. (1939): The significance of the topography of Anstey Hill, South Australia. *Trans. R. Soc. S. Aust.* 63(1): 79-87.
- FERGUSON, J., BURNE, R.V. & CHAMBERS, L.A. (1984): Iron mineralisation of peritidal carbonate sediments by continental groundwaters, Fisherman Bay, South Australia. *Sedimentary Geology*. 34: 41-57.
- FERMOR, L.L. (1911): What is Laterite? *Geological Magazine*.(V) 8: 454-462, 507-516, 559-566.
- FIRMAN, J.B. (1967a): Late Cainozoic stratigraphic units in South Australia. *Quart. Geol. Notes, geol. Surv. S. Aust.* 22: 4-8.
- FIRMAN, J.B. (1967b): Stratigraphy of Late Cainozoic deposits in South Australia. *Trans. Roy. Soc. S. Aust.* 91: 165-180.
- FIRMAN, J.B. (1976): Laterite: palaeosols in the laterite profile. In: Abstracts 25th Int. Geol. Congr., Sydney, 1976. Vol. 2, p. 495.
- FIRMAN, J.B. (1981): Regional stratigraphy of the regolith on the southwest margin of the Great Australian Basin province, South Australia. S.A. Dept. Mines and Energy. Rept. Bk. 81/40.
- FIRMAN, J.B. & LINDSAY, J.M. (1976): The Cainozoic. In Chapter 1 of Natural History of the Adelaide area. [C.R. Twidale, M.J. Tyler and B.P. Webb (Eds)] *Trans. R. Soc. S. Aust.*
- FITZPATRICK, R.W. (1987): Iron compounds as indicators of pedogenic processes: examples from the Southern Hemisphere with particular reference to Australia and South Africa. Chapter 13, In: *Iron in Soil and Clay Minerals*. D. Reidel Pub. Co. Dordrecht: Holland/Boston: U.S.A.
- FITZPATRICK, R.W. & SCHWERTMANN, U. (1982): Al-substituted goethite - an indicator of pedogenic and other weathering environments in South Africa. *Geoderma*. 27: 335-347.
- FITZPATRICK, R.W., TAYLOR, R.M., SCHWERTMANN, U. and CHILDS, C.W. (1985): Occurrence and properties of lepidocrocite in some soils of New Zealand, South Africa and Australia. *Aust. Jour. Soil Res.* 23: 543-567.
- FORBES, B.G. (1980): Adelaide 1:50000 Map Sheet. Geol. Surv. S. Aust.
- FORREST, G.J. (1969): Geomorphological evolution of the Bremer Valley. Unpub. B.A. Hons thesis, University of Adelaide.
- FRANCIS, G, and SEGNIT, E.R. (1981): Lepidocrocite from Iron Monarch, South Australia. *Aust. Mineral.* 36: 187-188.
- FRANKEL, R.B., BLAKEMORE, R.P. & WOLTE, R.S. (1979): Magnetite in freshwater magnetotactic bacteria. *Science* 203: 1355-1356.



FURNESS, L.J., WATERHOUSE, J.D. & EDWARDS, D.R. (1981): The hydrology of the Hindmarsh Tiers and Myponga Basins. *Geol.Surv. S. Aust. Rep. of Investigations* 53, 39 pp.

GARDNER, L. R. (1970): A chemical model for the origin of gibbsite from kaolinite. *Am. Miner.* 55: 1380-1389.

GENTILLI, J. (1972): *Australian Climatic Patterns*. Nelson, Melbourne. 285 pp.

GIBBONS, F.R. & DOWNES, R.G. (1964) A Study of the Land in Southwestern Victoria. Soil Cons. Authority, Vic., 269pp.

GIBBONS, F.R. & GILL, E.D. (1964): Terrains and soils of the basaltic plains of Far-Western Victoria. *Proc. Roy. Soc. Vic.* 77: 387-395.

GIBSON, A.A. (1963): Final geological report on Happy Valley Tunnels Project. *Geol. Surv. S. Aust.* (Unpub. Report).

GILKES, R.J., SCHOLZ, G. & DIMMOCK, G.M. (1973): Lateritic deep weathering of granite. *Jour. Soil Sci.* 24(4): 523-536.

GILL, E.D. (1958): Dating of Cainozoic non-marine rocks in Australia. *A.N.Z.A.A.S. Adelaide Congress, Abstracts of Lectures and Papers.* 4pp.

GILL, E.D. (1964): Rocks contiguous with the basaltic cuirass of Western Victoria. *Proc. R. Soc. Vic.* 77(2): 331-335.

GLAESSNER, M.F. (1953a): Conditions of Tertiary sedimentation in southern Australia. *Trans. R. Soc. S. Aust.* 76: 141-146.

GLAESSNER, M.F. (1953b): Some problems of Tertiary geology in southern Australia. *J. Proc. Roy. Soc. N.S.W.* 87: 31-45.

GLAESSNER, M.F. (1955): Contributions on Tertiary Stratigraphy and Palaeontology. In : Campana, B. (1955): *Geology of the Gawler Military Sheet. Rep. Invest. geol. Surv. S. Aust.* 4: 24pp.

GLAESSNER, M.F. and WADE, M. (1958): The St Vincent Basin. In: GLAESSNER, M.F. and PARKIN, L.W. (Eds): *The Geology of South Australia. J. geol. Soc. Aust.* 5(2): 115-126.

GUNN, R.H. (1985): Shallow groundwaters in weathered volcanic, granitic and sedimentary rocks in relation to dryland salinity in Southern New South Wales. *Aust. Jour. Soil Res.* 23: 355-371.

HALLSWORTH, E.G. & COSTIN, A.B. (1953): Studies in pedogenesis in New South Wales. IV. The ironstone soils. *J. Soil Sci.* 4:24-47.

HARRIS, W.K. (1964): Mesozoic sediments of the Poldia Basin, Eyre Peninsula. *Quart. geol. Notes, geol. Surv. S. Aust.*, 12: 6

HARRIS, W.K. (1979): Streaky Bay town water supply. Palynology of a carbonaceous clay from FOR-20A. S.A. Dept Mines and Energy. Rept. Bk. 79/91.

HARRIS, W.K. & OLLIVER, J.G. (1964): The age of the Tertiary sands at Rowland Flat, Barossa Valley. *Quart. Geol. Notes, geol. Surv. S. Aust.* 13: 1-2.

- HARRIS, W.K. & MCGOWRAN, B. (1971): Permian and reworked Devonian micro-fossils from the Troubridge Basin. *Quart. Geol. Notes, geol. Surv. S. Aust.* 40: 5-11.
- HARTLEY, R. (1981): A study of the causes, mechanisms and consequences of non-irrigated salinity on Kangaroo Island, South Australia. M.Eng.Sci. University of N.S.W. unpub.
- HEATH, G.R. (1962): Peeralilla Hill iron deposit. *Mining Review S.A. Geol. Surv.* 116: 20-22.
- HEMMING, E. (1968); On laterite and latosols. *Professional Geographer.* 20: 238-241.
- HERBILLON, A.J. & NAHON, D. (1987): Laterites and Laterization processes. Chapter 22, In: *Iron in Soil and Clay Minerals*. D. Reidel Pub. Co. Dordrecht: Holland/Boston: U.S.A.
- HILLS, E.S. (1934): Tertiary freshwater fishes from Southern Queensland. *Mem. Quid Mus.* 10(4): 171.
- HOLLAND, T.H. (1903): On the constitution, origin and dehydration of Laterite. *Geological Magazine.* (IV) 10: 59-69.
- d'HOORE, J. (1954): Essai de classification des zones d'accumulation de sesquioxides libres sur de bases genetiques. *Sols. afr.* 3: 66-80.
- HORWITZ, R.C. (1960): Geologie de la region de Mount Compass (feuille Milang) Australie meridionale. *Eclog. Geol. Helv.* 53: 211-264.
- HORWITZ, R.C. (1961): The Geology of the Wakefield Military Sheet. *Rept. Invest. Geol. Surv. S. Aust.* 18: 1-32.
- HORWITZ, R.C. & DAILY, B. (1958): Yorke Peninsula. In: GLAESSNER, M.F. and PARKIN, L.W. (Eds): *The Geology of South Australia.* *J. geol. Soc. Aust.* 5(2): 46-60.
- HOS, D.P.C. (1977): Palynological Report on three samples from the Late Triassic of the Telford Basin, Leigh Creek. *Geol. Surv. S. Aust. Rept. Bk. No.* 77/83 (unpub.)
- HOS, D.P.C. (1978): Stratigraphy and palynology of Leigh Creek No. 13 Borehole. *Geol. Surv. S. Aust. Rept Bk No.* 78/61 (unpub.).
- HOSSFELD, P.S. (1949): The significance of the occurrence of fossil fruits in the Barossa Senkungsfeld, South Australia. *Trans. Roy. Soc. S. Aust.* 72(2): 252-258.
- HOWCHIN, W. (1931): The dead rivers of South Australia. Part I, Western group. *Trans. R. Soc. S. Aust.* 55: 113-135.
- HOWCHIN, W. (1933): The dead rivers of South Australia. Part II, The eastern group. *Trans. Roy. Soc. S. Aust.* 55: 113-135.
- HSU, P.H. (1977): Aluminium oxides and oxyhydroxides. - In J.B. DIXON & S.B. WEED (eds): *Minerals in Soil Environments*, p 93-143.- Soil Sci. Soc. Amer., Madison.

- HUNT, P.A., MITCHELL, P.B. & PATON, T.R. (1977): "Laterite profiles" and 'lateritic ironstones' on the Hawkesbury Sandstone, Australia. *Geoderma* 19: 105-121.
- HURLBUT, C.S. (1959): *Dana's Manual of Mineralogy*. John Wiley, New York.
- HUTTON, J.T. (1976): Laterite and silcrete - are they related? A geochemical consideration. *Abstr. Int. geol. Congr.* 25: 502-503.
- IDNURM, M. & SENIOR, B.R. (1978): Palaeomagnetic ages of Late Cretaceous and Tertiary weathered profiles in the Eromanga Basin, Queensland. *Palaeogeog. Paleoclim. Palaeoecol.* 24: 267-277.
- JESSUP, R.W. (1960): The stony tableland soils of the southeastern portion of the Australian arid zone and their evolutionary history. *Jour. Soil Sci.* 11: 188-197.
- JOHNS, R.K. (1961a): Geology and mineral resources of southern Eyre Peninsula. *Geol. Surv. S. Aust. Bull.* 37.
- JOHNS, R.K. (1961b): The geology of the Mobilong military sheet (Explanation of the Geological Map). *Rep. Invest. geol. Surv. S. Aust.* 17.
- JOHNSON, P.D. (1976): Stratigraphy and Engineering Geology of the Monarto Designated area. *S.A. Dept Mines and Energy, Rept Bk No. 76/107.*
- KEELING, J.L. (1983): Low alkali shale investigation Rapid Bay - Delamere area. Results of auger drilling 1983. *S.A. Dept Mines and Energy, Geol. Surv., Rept. Bk. No. 83/90.*
- KEELING, J.L. (1985): Low alkali shale investigation in the Rapid Bay - Delamere area. *Min. Res. Rev.* 155: 38-43.
- KENLEY, P.R. (1951): Marine Eocene sediments near Casterton, Victoria. *Aust. Jour. Sci.* 14: 9-92.
- KENLEY, P.R. (1971): Cainozoic Geology of the Eastern Part of the Gambier Embayment, Southwestern Victoria. in H.Wopfner and J.G.Douglas(eds), The Otway Basin of Southeastern Australia. Special Bulletin, *Geol. Survs. S. Aust., Vic.* pp 89-153.
- KENLEY, P.R. (1975): Geology and Geomorphology of Southwestern Victoria. A.I.H.S. Symposium, Horsham. *Geol. Surv. Vic.*
- KENLEY, P.R., SPENCER-JONES, D. & CARTER, A.N. (1967): Casterton geological map, scale 1:63360. *Geol. Surv. Vic.*
- KENNEDY, W.Q., 1962, Some theoretical factors in geomorphological analysis. *Geol. Mag.* 99: 304-312.
- KING, L.C. (1962): *The Morphology of the Earth*. (Oliver and Boyd: Edinburgh)
- KING, L.C. (1976): Planation remnants upon high lands. *Z.Geomorph.* 20: 133-148.
- KIRSCHVINK, J.L., JONES, D.S. & MACFADDEN, B.J. (Eds) (1985): *Magnetite Biomineralization and Magnetoreception in Organisms* . Plenum Press. New York.

- KLEEMAN, A.W. & WHITE, A.J.R. (1956): The structural petrology of portion of the eastern Mount Lofty Ranges. *J. geol. Soc. Aust.* 3: 17-31.
- LAMPLUGH, G.W. (1902): Calcrete. *Geol. Mag.* 9: 575.
- LANG, D. (1965): Data of the geomorphology and soils of the Yundi area, S.A. C.S.I.R.O. Div. Report 3/65.
- LAWRENCE, J.R. & TAYLOR, H.P. (1971): Deuterium and oxygen-18 correlation: Clay minerals and hydroxides in Quaternary Soils compared to meteoric waters. *Geochim. et Cosmochim. Acta.* 35: 993-1003.
- LINDSAY, J.M. (1969): Cainozoic foraminifera and stratigraphy of the Adelaide Plains Sub-basin, South Australia. *Geol. Surv. S. Aust. Bull.* No. 42.
- LINDSAY, J.M. (1986): New record and tectonic implication of a high level *Lepidocyclina*-bearing limestone, Bremer Valley, Eastern Mount Lofty Ranges. *Dept. Mines and Energy, Geological Survey.* DME 222/86.(unpub.)
- LINDSAY, J.M. & GILES, S.D. (1973): Notes on the *Lepidocyclina* Zone in Morgan Limestone along the Murray River, South Australia. *Quart. Geol. Notes, geol. Surv. S. Aust.* 45: 1-7.
- LINDSAY, J.M. & WILLIAMS, A.J. (1977): Oligocene marine transgression at Hartley and Monarto, southwestern margin of the Murray Basin. *Quart. Geol. Notes, geol. Surv. S. Aust.* 64: 9-16
- LONG, J.V.P. (1977): Electron probe microanalysis. Chapter 6, in: J.Zussman (Ed.) *Physical Methods in Determinative Mineralogy.* Academic Press, London. Second Ed.
- LUDBROOK, N.H. (1961): Stratigraphy of the Murray Basin in South Australia. *Geol. Surv. S. Aust. Bull.* No. 36.
- LUDBROOK, N.H. (1967): Permian deposits of South Australia and their fauna. *Trans. R. Soc. S. Aust.* 91: 65-75.
- LUDBROOK, N.H. (1969): Tertiary Period. In: PARKIN, L.W.(Ed): Handbook of the Geology of South Australia. *J. geol. Soc. Aust.* 5(2): 172-203.
- LUDBROOK, N.H. (1980): *A guide to the geology and mineral resources of South Australia.* S.A. Dept. Mines and Energy. Adelaide.
- LUDBROOK, N.H. (1983): Molluscan faunas on the Early Pleistocene Point Ellen Formation and Burnham Limestone, South Australia. *Trans. R. Soc. S. Aust.* 107: 37-50.
- MACHADO, A. de Barros (1983a): Termitic remains in some bauxites. *Proceedings Second International Seminar on Lateritisation Processes,* Sao Paulo (Eds: A.J. Melfi & A. Carvalho). pp 251-256.
- MACHADO, A. de Barros (1983b): The contribution of termites to the formation of laterites. *Proceedings Second International Seminar on Lateritisation Processes,* Sao Paulo (Eds: A.J. Melfi & A. Carvalho). pp 261-270.
- MACLAREN, M. (1906): On the origin of certain laterites. *Geological Magazine.*(V) 4: 536-547.
- McFARLANE, M.J. (1971): Lateritisation and landscape development in Kyagwe, Uganda. *Quart. J. geol. Soc. Lond.* 126: 501-539.

- McFARLANE, M.J. (1976): *Laterite and landscape*. Academic Press, London.
- McFARLANE, M.F. (1983): Laterites. In: GOUDIE, A. & PYE, K.(Eds): *Chemical Sediments and Geomorphology*. Academic Press, London. p. 7-58.
- McFARLANE, M.F. (1987): Proceedings Laterite Workshop, 1st International Geomorphological Conference. *Z. Geomorph. N.F. Suppl.-Bd.* 64
- McFARLANE, M.F. & SOMBROEK, W.G. (1984): Information exchange for earth scientists working in laterite areas. Annual Report, International Soil Museum, Wageningen, The Netherlands, pp. 14 - 20.
- McFARLANE, M.F. & HEYDEMAN, M.T. (in press): Some aspects of kaolinite dissolution by a laterite-indigenous micro-organism. *Geo. Eco. Trop.*
- McGOWRAN, B. (1978): Early Tertiary foraminiferal biostratigraphy in southern Australia: a progress report. In: BELFORD, D.J. & SCHEIBNEROVA, V.(Eds): *The Crespin Volume: Essays in honour of Irene Crespin. Bur. Miner. Res. Aust. Bull.* No. 192: 83-95.
- McGOWRAN, B. (1979a): The Tertiary of Australia: foraminiferal overview. *Marine Micropal.* 4: 235-264.
- McGOWRAN, B. (1979b): Comments on Early Tertiary tectonism and lateritization. *Geol. Mag.* 116: 227-230.
- McGOWRAN, B., RUTLAND, R.W.R. & TWIDALE, C.R. (1978): Discussion: Age and origin of laterite and silcrete duricrusts and their relationship to episodic tectonism in the Mid-North of South Australia. *J. geol. Soc. Aust.* 24: 421-425.
- MACLAREN, M. (1906): On the origin of certain laterites. *Geol. Mag.* 5: 536-547.
- MACUMBER, P.G. (1983): Interactions between groundwaters and surface systems in northern Victoria. Ph.D.Thesis, University of Melbourne (unpubl.).
- MAIGNEN, R. (1966): Review of research on laterites. *UNESCO Natural Resources Research IV*, 148 pp.
- MAJOR, R.B. & VITOLS, V. (1973): The geology of Vennachar and Borda 1:50000 map areas, K.I. *Min. Resour. Rev S. Aust.* 134: 38 - 51.
- MANCKTELOW, N.S. (1979): The structure and metamorphism of the Southern Adelaide Fold Belt. Ph.D. Thesis, Uni. of Adel. (unpubl.).
- MANN, A.W. & OLLIER, C.D. (1985): Chemical diffusion and ferricrete formation. *Soils and Geomorphology, Catena Supplement.* 6: 151-157.
- MARBUT, C.F. (1932): Morphology of laterites. *Proc. and Pap. Sec. Int. Cong. Soil Sci. Comm.* 5: 72-80.
- MARKER, M.E. (1959): Soil erosion in relation to the development of landforms in the Dundas area of Western Victoria, Australia. *Proc. R. Soc. Vic.* 71(11): 125-136.
- MAUD, R.R. (1972): Geology, geomorphology and soils of Central County Hindmarsh (Mount Compass-Milang), South Australia. *CSIRO Aust. Soils Publ.* No. 29.

- MAWSON, D. (1907a): Geological features of part of Eyre Peninsula. *Trans. R. Soc. S. Aust.* 31: 71-76.
- MAWSON, D. (1907b): The Wadella Springs and associated bog-iron ore deposits. *Trans. R. Soc. S. Aust.* 31: 77-78.
- MAWSON, D. (1953): The Willunga Basin. Introductory and historical notes. *Trans. R. Soc. S. Aust.* 76: 108-113.
- MAY, R.I. & BOURMAN, R.P. (1984): Coastal landslumping in Pleistocene sediments at Sellicks Beach, South Australia. *Trans. R. Soc. S. Aust.* 108(1&2): 85-94.
- MELFI, A.J. & CARVALHO, A. (1983): Lateritisation Processes. Proceedings *Second International Seminar on Lateritisation Processes*. Instituto Astronomico e Geofisico, University of Sao Paulo, Brazil. 590 pp.
- MILES, K.R. (1952): Geology and underground water resources of the Adelaide Plains area. *Bull. Geol. Surv. S. Aust.* 27: 1-257.
- MILLS, K.J. (1965): The structural petrology of the Milendella area of South Australia. Unpub. Ph.D. Thesis, University of Adelaide.
- MILNES, A.R. & BOURMAN, R.P. (1972): A Late Palaeozoic glaciated granite surface at Port Elliot, South Australia. *Trans. R. Soc. S. Aust.* 95: 149-155.
- MILNES, A.R., COMPSTON, W. & DAILY, B. (1977): Pre- to syn-tectonic emplacement of Early Palaeozoic granites in south-eastern South Australia. *J. geol. Soc. Aust.* 24: 87-106.
- MILNES, A.R., COOPER, B.J. & COOPER, J.A. (1982): The Jurassic Wisanger Basalt of Kangaroo Island, South Australia. *Trans. R. Soc. S. Aust.* 106: 1-13.
- MILNES, A.R., LUDBROOK, N.H., LINDSAY, J.M. & COOPER, B.J. (1983): The succession of marine Cainozoic sediments on Kangaroo Island, South Australia. *Trans. Roy. Soc. S. Aust.* 107: 1-35.
- MILNES, A.R., R.P. BOURMAN & K.H. NORTHCOTE (1985): Field relationships of ferricretes and weathered zones in southern South Australia: a contribution to 'laterite' studies in Australia. *Aust. J. Soil Res.* 23: 441-465.
- MILNES, A.R., R.P. BOURMAN & R.W. FITZPATRICK (1987): Petrology and mineralogy of 'laterites' in southern and eastern Australia and South Africa. *Chemical Geology.* 60: 237-250.
- MILNES, A.R. & LUDBROOK, N.H. (1986): Provenance of microfossils in aeolian calcarenites and calcretes in southern South Australia. *Aust. Jour. Earth Sci.* 33: 145-159.
- MILNES, A.R. & FARMER, V.C. (1987): Micromorphological and analytical studies of the fine matrix of an Australian humus iron podzol. (In press).
- MOORE, A.W., ISBELL, R.F. & NORTHCOTE, K.H. (1983): Classification and mapping of Australian soils. In: *Soils: An Australian Viewpoint*. CSIRO, Melbourne/Academic Press, London. p. 253-266.
- MULLER, J. & BOQUIER, G. (1986): Dissolution of kaolinites and accumulation of iron oxides in lateritic-ferruginous nodules: mineralogical and microstructural transformations. *Geoderma*, 37: 113-136.

- MURRAY-WALLACE, C.V. (1983): Underground gasification of inaccessible Leigh Creek Coal Measures - A preliminary evaluation of the geological structure of the Telford Basin. *S.A. Dept Mines & Energy*. Rept Bk No. 83/84 (unpub.) 46 pp.
- NAHON, D., JANOT, C., KARPOFF, A.M., PAQUET, H., & TARDY, Y. (1977): Mineralogy, petrography and structures of iron crusts (ferricretes) developed on sandstones in the western part of Senegal. *Geoderma*, 19: 263-277.
- NORRISH, K. & HUTTON, J.T. (1969): An accurate x-ray spectrographic method for the analysis of a wide range of geological samples. *Geochim. Cosmochim. Acta*. 33: 431.
- NORRISH, K. & PICKERING, J.G. (1983): Clay minerals. Chapter 22. pp. 281-308 *In: Soils: an Australian Viewpoint*. Division of Soils, C.S.I.R.O. (Academic Press, Melbourne).
- NORRISH, K. & TAYLOR, R.M. (1961): The isomorphous replacement of iron by aluminium in soil goethites. *Jour. Soil Sci.* 12(3): 294-306.
- NORTHCOTE, K.H. (1946): A fossil soil from Kangaroo Island, South Australia. *Trans. R. Soc. S. Aust.* 70: 294-296.
- NORTHCOTE, K.H. (1976): Soils. In Natural History of the Adelaide Region. C.R. Twidale, M.J. Tyler and B.P. Webb (Eds). *R. Soc S. Aust.*
- NORTHCOTE, K.H. (1979): Soils. In: TYLER, M.J., TWIDALE, C.R. and LING, D. (Eds), Natural History of Kangaroo Island. *R. Soc. S. Aust.*
- NORTHCOTE, K.H. & TUCKER, B.M. (1948): A soil survey of the Hundred of Seddon and part of the Hundred of MacGillivray, Kangaroo Island, South Australia. *C.S.I.R. Aust. Bull.* No. 233.
- NORTHCOTE, K.H., HUBBLE, G.D., ISBELL, R.F., THOMPSON, C.H. & BETTENAY, E. (1975): *A Description of Australian Soils*, CSIRO Aust: Melbourne.
- OADES, J.M. and TIPPING, E. (1988): Hydrous oxides and humic substances. In: Humic Substances III. Interactions with Metals, Minerals and Organic Chemicals. P.McArthy, M.H.D. Hayes, R.L. Malcolm and R.S. Swift (Eds). Wiley, Chichester.
- OGURA, Y. (1987): Proceedings of an International Seminar on Laterite. Oct 14-17, 1985, Tokyo, Japan. *Chemical Geology*. 60: 1-396.
- OLLIER, C.D., CHAN, R.A., CRAIG, M.A. & GIBSON, D.L. (1988): Aspects of landscape history and regolith in the Kalgoorlie region, Western Australia. *B.M.R. Jour. Aust. Geol. & Geophys.* 10: 309-321.
- OLLIVER, J.G. (1964): Auger boring of Happy Valley sand deposit. *S. Aust. Min. Rev.* 121: 136-140.
- OLLIVER, J.G. & WEIR, L.J. (1967): The construction sand industry in the Adelaide metropolitan area. *Geol. Surv. S. Aust. Rept Invest.* No. 30.
- OLLIVER, J.G. and NICHOL, D. (1975): Longwood Clay Deposits. *Mineral Resour. Rev. S. Aust.* 142: 119-132.

- PARKER, A.J., FANNING, C.M. & FLINT, R.B. (1985): Chapter 2, Geology. Natural History of Eyre Peninsula (Eds. C.R. Twidale, M.J. Tyler & M. Davies). *R. Soc. S. Aust.* pp. 21-46.
- PARKIN, L.W. (1953): The Leigh Creek Coalfield. *Bull. Geol. Surv. S. Aust.* 31, 74 pp.
- PATON, T.R. & WILLIAMS, M.A.J. (1972): The concept of laterite. *Annals Assoc. Amer. Geogr.* 62: 42-56.
- PENDLETON, R.L. & SHARASUVANA, S. (1946): Analysis of some Siamese laterites. *Soil Science* 423-440.
- PETTIJOHN, F.J. (1959): *Sedimentary Rocks*. Harper and Row, New York.
- PLAYFORD, P.E. (1954): Observations on Laterite in Western Australia. *Aust. Jour. Sci.* 17: 11-14.
- PLAYFORD, G. & DETMANN, M.E. (1965): Rhaeto-Liassic microfossils from the Leigh Creek Coal Measures, South Australia. *Senckenbergiana Lethaea* 46: 127-181.
- PLUMB, K.A. & GOSTIN, V.A. (1973): Origin of Australian bauxite deposits. *Record, B.M.R.* 156: 71 pp.
- POSTMA, D. (1982): Pyrite and siderite formation in brackish and freshwater swamp sediments. *Am. Jour. Sci.* 282: 1151-1183.
- POSTMA, D. (1983): Pyrite and siderite oxidation in swamp sediments. *Jour. Soil Sci.* 34: 163-182.
- PREISS, W. (1987): The Adelaide Geosyncline: Late Proterozoic Stratigraphy, Sedimentation, Palaeontology and Tectonics. *S.A. Dept. Mines and Energy. Bull.* 53.
- PRESCOTT, J.A. (1931): The soils of Australia in relation to vegetation and climate. *C.S.I.R. Aust. Bull.* No. 31.
- PRESCOTT, J.A. (1934): The composition of some ironstone gravels from Australian soils. *Trans. Roy. Soc. S. Aust.* 58: 10-13.
- PRESCOTT, J.A. & PENDLETON, R.L. (1952): Laterite and lateritic soils. *Comm. Bur. Soil Sci. Tech. Comm.* No. 47.
- PULLAN, R.A. (1967): A morphological classification of lateritic ironstones and ferruginised rocks in Northern Nigeria. *Nigerian Jour. Sci.* 1(2): 161-174.
- RAISON, R.J. (1979): Modification of the soil environment by vegetation fires with particular reference to nitrogen transformations: a review. *Plant and Soil.* 51: 53-108.
- RAMBERG, I.B. (1969): Lepidocrocite at Rossvatn. North Norway, and examples of pseudomorphism after pyrite cubes. *Norsk Geol. Tidsskr.* 49: 251-256.
- RIX, C.E. & HUTTON, J.T. (1953): A soil survey of the Hundred of Kuitpo in the Mount Lofty Ranges of South Australia. *S. Aust. Land Tax Bull.* No. 1.
- ROBERTSON, R.S. (1974): Extremely weathered cut material on the South East Freeway. *Quart. Geol. Notes, geol. Surv. S. Aust.* 52: 9-12.



- SCHELLMANN, W. (1981): Considerations on the definition and classification of laterites. In, *Proceedings of the International Seminar on Lateritisation Processes*, Trivandrum, India. A.A. Balkema, Rotterdam. pp.1-10.
- SCHULZE, D.G. (1984): The influence of aluminium on iron oxides. Unit cell dimensions of Al-substituted goethite and estimation of Al from them. *Clays and Clay Minerals* 32(11): 36-44.
- SCHMIDT, P.W. & EMBLETON, B.J.J. (1976): Palaeomagnetic results from sediments of the Perth Basin, Western Australia and their bearing on the timing of regional lateritization. *Palaeogeog. Palaeoclimat. Palaeoecol.* 19: 257-273.
- SCHMIDT, P.W., CURRY, D.T. & OLLIER, C.D. (1976): Sub-basaltic weathering, damsites, palaeomagnetism and the age of lateritization. *J. geol. Soc. Aust.* 23: 367-370.
- SCHWERTMANN, U. (1985): The effect of pedogenic environments on iron oxide minerals.-In: *Advances in Soil Science*, Vol.1, p.172-196. Springer Verlag, New York.
- SCHWERTMANN, U. & TAYLOR, R.M. (1979): Natural and synthetic poorly crystallised lepidocrocite. *Clay Min.* 14: 285-293.
- SCHWERTMANN, U. & TAYLOR, R.M. (1987): Iron oxides. In (Eds J.B. Dixon and S.B. Weed) *Minerals in Soil Environments. Soil Sci. Soc. Am.*, Madison, Wisc.
- SENKAYI, A.L., DIXON, J.B. & HOSSNER, B.R. (1986): Todorokite, goethite and hematite alteration products of siderite in east Texas lignite overburden. *Soil Science* 142(4): 36-42.
- SEGNIT, R.W. (1937): Geology of the northern part of the Hundred of Macclesfield. *Geol. Surv. S. Aust. Bull.No.* 16.
- SEGUIN, M. (1966): Instability of FeCO<sub>3</sub> in air. *Am. Jour. Sci.* 264: 562-568.
- SHEARD, M. (1983): Volcanoes. In: *Natural History of the South East*. M.J. Tyler, C.R. Twidale, J.K. Ling and J.W. Holmes (Eds). *Roy. Soc S. Aust.*
- SIMPSON, E.S. (1912): Notes on laterite in Western Australia. *Geol. Mag.* 5: 399-406.
- SIVARAJASINGHAM, S., ALEXANDER, L.T., CADY, J.G. & CLINE, M.G. (1962): Laterite. *Advances in Agronomy.* 14: 1-60.
- SPRIGG, R.C. (1942): The geology of the Eden-Moana Fault Block. *Trans. R. Soc. S. Aust.* 66(2): 185-214.
- SPRIGG, R.C. (1945): Some aspects of the geomorphology of portion of the Mount Lofty Ranges. *Trans. Roy. Soc. S. Aust.* 69: 277-302.
- SPRIGG, R.C. (1946): Reconnaissance geological survey of portion of the western escarpment of the Mount Lofty Ranges. *Trans. R. Soc. S. Aust.* 70: 313-347.
- SPRIGG, R.C. (1961): Oil and gas possibilities of the St.Vincent Gulf Graben. *A.A.A.P. Bull.* (Melbourne Conference)

- SPRIGG, R.C. & WILSON, R.B. (1954): Echunga Map Sheet. Geological Atlas of South Australia, 1:63 360 series. *Geol. Surv. S. Aust.*
- STANDARD, J.C. (1969): Hawkesbury Sandstone. In: Sydney Basin. Geology of New South Wales. *Jour. geol. Soc. Aust.* 16: 406-415.
- STEPHENS, C.G. (1946): Pedogenesis following dissection of lateritic regions in southern Australia. *C.S.I.R. Bull.* No. 206.
- STEPHENS, C.G. (1971): Laterite and silcrete in Australia. *Geoderma*, 5: 5- 52.
- STUART, W.J. (1970): The Cainozoic stratigraphy of the southeastern coastal area of Yorke Peninsula, South Australia. *Trans. R. Soc. S. Aust.* 94: 151-178.
- TARDY, Y. & NAHON, D. (1985): Geochemistry of laterites, stability of Al-goethite, A-hematite and Fe(III)-Kaolinite in bauxites and ferricretes: an approach to the mechanism of concretion formation. *Am. Jour. Sci.* 285: 865-903.
- TATE, R. (1879): The anniversary address of the President. *Trans. phil. Soc. S. Aust.* 2: xxxix-lxxv.
- TAYLOR, R.M. (1987): The iron oxide group of minerals. Ch 2, p. 129-201, In, *Chemistry of Clays and Clay Minerals*. A.C.D. Newman (Ed.) Mineralogical Society of London. Monograph No. 6. Longman.
- TAYLOR, R.M. & SCHWERTMANN, U. (1974): Maghemite in soils and its origin, Parts I and II. *Clay Minerals*. 10: 289-310.
- TEALE, E.O. (1918): Soil survey and Forest physiography of Kuitpo. *Dept. For. Univ. Adelaide Bull.* 6.
- TEPPER, J.G.O. (1879): Introduction to the cliffs and rocks at Ardrossan, Yorke's Peninsula. *Trans. R. Soc. S. Aust.* 2: 71-79.
- THOMSON, B.P. (1969): The Kanmantoo Group and Early Palaeozoic tectonics. In Parkin, L.W. (Ed.), Handbook of South Australian Geology. *Geol. Surv. S. Aust.* pp. 97-108.
- THOMSON, B.P. & HORWITZ, R.C. (1961): The geology of the Milang Military Sheet. *Geol. Surv. S. Aust.* (unpub.)
- THORP, J. (1941): Influence of environment on soil formation. *Soil Sci. Soc. Am.* 6: 39-46.
- TOWE, K.M. & MOENCH, T.T. (1981): Electron-optical characterization of bacterial magnetite. *Earth Planet. Sci. Lett.* 52: 213-220.
- TOWNSEND, I.J. (1979): The correlation and depositional history of the Leigh Creek coal measures. *Quart. Geol. Notes. Geol. Surv. S. Aust.* 70: 5-10.
- TRENDALL, A.F. (1962): The formation of apparent peneplains by a process of combined lateritisation and surface wash. *Z. Geomorph. (NS)* 6: 183 -197.
- TWIDALE, C.R. (1968): *Geomorphology with special reference to Australia*. (Nelson: Melbourne.)
- TWIDALE, C.R. (1976a): Geomorphological evolution. In: TWIDALE, C.R., TYLER, M.J. & WEBB, B.P.(Eds): Natural history of the Adelaide region. *R. Soc. S. Aust.* Adelaide. p.43-59.

- TWIDALE, C.R. (1976b): On the survival of palaeoforms. *Am. J. Sci.* 276: 77-95.
- TWIDALE, C.R. (1978): L.C.King's "Planation remnants upon high lands": Discussion. *Z. Geomorph. N.F.* 22: 118-122.
- TWIDALE, C.R. (1983): Australian laterites and silcretes: ages and significance. *Rev. Geol. Dynam. Geogt. Phys.* 24: 35-45.
- TWIDALE, C.R., DAILY, B. & FIRMAN, J.B. (1967): Eustatic and climatic history of the Adelaide area: a discussion. *Jour. Geol.* 75: 237-242.
- TWIDALE, C.R. & BOURNE, J.A. (1975a): Geomorphological evolution of part of the eastern Mount Lofty Ranges, South Australia. *Trans. R. Soc. S. Aust.* 99: 197-209.
- TWIDALE, C.R. & BOURNE, J.A. (1975b): Episodic exposure of inselbergs. *Geol. Soc. Amer. Bull.* 86: 1473-1481.
- TWIDALE, C.R., BOURNE, J.A. & SMITH, D.M. (1976): Age and origin of palaeosurfaces on Eyre Peninsula and the southern Gawler Ranges, South Australia. *Z. Geomorph.* 20: 28-55.
- VAIL, P.R. & HARDENBOL, J. (1979): Sea-level changes during the Tertiary. *Oceanus.* 22: 71-79.
- VAIL, P.R. & MITCHUM, R.M. (1979): Global cycles of relative changes of sea level from seismic stratigraphy. In: Watkins, J.S., Montadert, L. and Dickerson, P.W.(Eds), Geological and geophysical investigations of continental margins. *Mem. Am. Assoc. Pet. Geol.* 29: 469.
- VAIL, P.R., MITCHUM, R.M. & THOMPSON, S. (1977): Seismic stratigraphy and global changes of sea level, Part 4: Global cycles of relative changes of sea level.. In: Payton, C.E.(Ed.) Seismic stratigraphy - applications to hydrocarbon exploration. *Mem. Amer. Assoc. Petrol. Geol.* 26: 83-97.
- WALKER, M.M., KIRSCHVINK, J.L., PERRY, Anjanette & DIZON, A.E. (1985): Detection, extraction and characterization of biogenic magnetite. Ch5 in, *Magnetite Biomineralization and Magnetoreception in Organisms* . KIRSCHVINK, J.L., JONES, D.S. & MACFADDEN, B.J. [Eds] Plenum Press. New York.
- WALKER, P.H. (1960): A soil survey of the county of Cumberland Sydney Region, New South Wales. *Bull. Soil Surv. Unit Dept. Agric., N.S.W.*
- WALTHER, J. (1899): Bericht über die Resultate einer Reise nach Ostindien im Winter 1888-89. *Verh. Gesellsch. Erdk.* 16: 318-328.
- WALTHER, J. (1915): Laterit in West Australien. *Zeits. Deuts. Geol. Gessellsch.* 67B: 113-140.
- WARD, W.T. (1965): Eustatic and climatic history of the Adelaide area. *Jour. Geol.* 73(4): 592-602.
- WARD, W.T. (1966): Geology, geomorphology and soils of the southwestern part of County Adelaide, South Australia. *C.S.I.R.O. Aust. Soil Publ.* 23.
- WARD, W.T. (1967): The Adelaide area: a reply. *Jour. Geol.* 75(3): 351-357.

- WARD, W.T. (1968): Pliocene sea levels. *In: Glenie, R.C., Schofield, J.C. and Ward, W.T. Palaeogeog. Palaeoclim. Palaeocol.* 5: 141-163.
- WHITE, D.A. (1954): Observations on Laterites in the Northern Territory. *Aust. Jour. Sci.* 17: 14-17.
- WHITEHOUSE, F.W. (1940): Studies in the late geological history of Queensland. *Papers Univ. Qld. Dept. Geol.*, Vol 2, No. 1.
- WHITTEN, G.F. (1962): Metallurgical testing of Peeralilla Hill laterite. *Mining Rev. Geol. Surv. S. Aust.* 117: 89-90.
- WOOLNOUGH, W.G. (1927): The duricrust of Australia. *J. Proc. R. Soc. N.S.W.* 61: 24-53.
- WOOLNOUGH, W.G. (1942): Geological extrapolation and pseudo-abyssal sediments. *Bull. Amer. Assoc. Petroleum Geol.* 26: 7655-792.
- WOPFNER, H. (1964): Permian-Jurassic history of the western Great Artesian Basin. *Trans. R. Soc. S. Aust.* 98: 1-12.
- WOPFNER, H. (1970): Permian palaeogeography and depositional environment of the Arckaringa Basin, South Australia. *Second Gondwana Symposium, South Africa.* pp. 273-291.
- WOPFNER, H. (1972a): Maghemite from Cainozoic sediments at Hallett Cove. *Quart. Geol. Notes, geol. Surv. S. Aust.* 43: 5-8.
- WOPFNER, H. (1972b): Depositional history and tectonics of South Australian sedimentary basins. *Min. Resour. Rev. S. Aust.* 133: 32-50.
- WOPFNER, H. (1974): Post-Eocene history and stratigraphy of northeastern South Australia. *Trans. R. Soc. S. Aust.* 98-8.
- WOPFNER, H. & DOUGLAS, J.G. (Eds) (1971): The Otway Basin of South Australia. Special Bulletin, *Geol. Surv. S. Aust.*, Vict. 451 pp.
- YEH, H. & SAVIN, S.M. (1976): The extent of oxygen isotope exchange between clay minerals and sea water. *Geochim. et Cosmochim. Acta.* 40: 743-748.
- ZUSSMAN, J. (Ed.). (1977): *Physical Methods in Determinative Mineralogy.* Academic Press, London (Second Ed.). 72 pp.